

Studies towards the Organocatalytic ‘Dialled In’ Synthesis of Chiral, Non-Racemic Aziridines, and Amino Acids, Containing Multiple Isotopic Labels

Sean Thurston

A thesis submitted in part fulfilment of the requirements for the degree of Doctor of Philosophy



School of Chemistry

University of East Anglia

September 2012

Supervised by Dr Sean Patrick Bew

© This copy of the thesis has been supplied on the condition that anyone who consults it is understood to recognize that its copyright rests with the author and that no quotation from the thesis, nor any information derived there from, may be published without the prior written consent of the author, in accordance with UK Copyright Law. In addition, any quotation or extract must include full attribution.

Declaration

The research contained in this thesis is, to the best of my knowledge, original, except where due reference is made.

Sean Thurston

Acknowledgements

First, thanks need to be made to everyone (friends, family, and colleagues) who has put up with me throughout this process; special thanks to Zoe and my parents for all of their help and support. Thanks to Sunil for his multitude of advice (and for calming me down on several occasions), and to all members of the Bew group (past and present) for the same. Finally, thanks to the EPSRC, UEA, and Dr Sean Bew for providing the lab facilities.

Abstract

Within this thesis, a highly effective one-pot methodology (based around the use of the organocatalyst pyridinium triflate) has been developed for the highly *cis*-selective synthesis of *N*-aryl 3-aryl-aziridine-2-carboxylates as racemates in yields of up to 80 %. This methodology has been extended by the use of a highly acidic C2 symmetric 3,3'-anthracenyl functionalised BINOL triflylphosphoramidate organocatalyst, which allows for the formation of the desired *cis*- *N*-aryl 3-aryl-aziridine-2-carboxylates in an effective and highly enantioselective manner (affording the desired materials in yields of up to 81 %, and *e.e.s* of >99 %).

Utilising the methodology developed within the first part of the thesis, *enantio*- and isotopically enriched *cis*- *N*-aryl 3-aryl-aziridine-2-carboxylates have been synthesised in a regioselective manner; with deuterium selectively introduced at the C2, and/or C3 positions of the aziridine ring with generally >90 % isotopic enrichment. Further to this, these aziridines have been submitted to ring opening methodologies in order to produce enantiomerically enriched α -amino acid derivatives bearing regioselectively introduced deuterium labels (with generally >90 % isotopic enrichment), in yields of up to 97 %, and *e.e.s* of up to 97 %,.

Finally, these methods have been combined in order to synthesise 5 target molecules consisting of functionalised enantioenriched α -amino acid derivatives bearing multiple isotopic labels including deuterium, ^{15}N , and ^{18}O , in what has become known as the 'Dialled In' methodology.

List of Abbreviations

$^1\text{H-NMR}$	Proton Nuclear Magnetic Resonance Spectroscopy
$^{13}\text{C-NMR}$	Carbon Nuclear Magnetic Resonance Spectroscopy
ACDC	Asymmetric Counterion Directed Catalysis
Anth	Anthracene
Ar	Aromatic
ATR	Attenuated Total Reflection
BINOL	1,1'-binaphthol
CAN	Cerium Ammonium Nitrate
CD	Circular Dichroism Spectrometry
d	Doublet
DCE	1,2-dichloroethane
DCM	Dimethylformamide
DMF	Dichloromethane
DMSO	Dimethyl sulfoxide
DNA	Deoxyribonucleic acid
EDA	Ethyl diazoacetate
EDA- <i>d</i>	α -deuterated ethyl diazoacetate
<i>e.e.</i>	Enantiomeric Excess
ESI	Electrospray Ionisation
FT-IR	Fourier Transform Infrared Spectroscopy
H/D	Hydrogen/Deuterium
HOMO	Highest Occupied Molecular Orbital
HPLC	High Pressure (Performance) Liquid Chromatography
HRMS	High Resolution Mass Spectroscopy
Hz	Hertz
$^i\text{PrDA}$	<i>iso</i> -propyl diazoacetate
$^i\text{PrDA-}d$	α -deuterated <i>iso</i> -propyl diazoacetate
KIE	Kinetic Isotope Effect
LUMO	Lowest Unoccupied Molecular Orbital
M	Molarity
m	Multiplet
MHz	Megahertz
MO	Molecular Orbital

MS	Mass Spectroscopy
NIST	National Institute of Standards and Technology
p-TSA	<i>para</i> -toluene sulfonic acid
PET	Petroleum (refers to the fraction that boils between 40 °C – 60 °C unless otherwise stated)
PyTf (PyTf- <i>h</i>)	pyridinium triflate <i>h</i> -form
PyTf- <i>d</i>	pyridinium triflate <i>d</i> -form
<i>rac</i> -	Racemic
RT	Room Temperature
s	Singlet
S _N	Nucleophilic Substitution
SOMO	Singularly Occupied Molecular Orbital
t	Triplet
^t BDA	<i>tert</i> -butyl diazoacetate
^t BDA- <i>d</i>	α -deuterated <i>tert</i> -butyl diazoacetate
Tf	Trifluoromethylsulfonyl
TFA	Trifluoroacetic acid
TS	Transition state
VAPOL	Vaulted biphenanthrol
VCD	Vibrational Circular Dichroism Spectroscopy
UV	Ultraviolet
ZPE	Zero Point Energy

A Note on Terminology

Throughout this thesis, the several non-standard prefixes are given to novel aziridines according to the following convention:

- *rac*- (a racemic aziridine).
- *cis*- (an enantiomerically enriched aziridine in which the protons/deuterons at the C2 and C3 positions are orientated in a *cis*- relationship. *i.e.* they are on the same face of the molecule).
- *trans*- (an enantiomerically enriched aziridine in which the protons/deuterons at the C2 and C3 positions are orientated in a *trans*- relationship. *i.e.* they are on opposite faces of the molecule).

Contents:

Section 1: Introduction	1
Chapter 1: Deuterium and Labelled Compounds	1
1.1: Deuterium: Origins and Early History	1
1.2: Industrial production of Deuterium	2
1.3: Properties of Deuterium, Deuterium Oxide, & the Deuteron	3
1.4: Deuterium and the Kinetic Isotope Effect	5
1.5: Synthesis of Deuterated Compounds	8
1.5.1: Introduction	8
1.5.2: Pre, and Mid Synthesis Incorporation	9
1.5.3: Post Synthesis Methods	11
1.5.3.1: Acid Catalysed H/D Exchange	11
1.5.3.2: Base Catalysed H/D Exchange	14
1.5.3.3: Heterogeneous Metal Catalysed H/D Exchange	16
1.5.3.4: Homogeneous Metal Catalysed H/D Exchange	20
1.5.3.4.1: Iridium (II) catalytic systems	21
1.5.3.4.2: Iridium (I) catalytic systems	24
1.5.3.4.3: Rhodium based catalytic systems	29
1.6: Applications of Deuteration and the Kinetic Isotope Effect in Mechanism and Metabolism Studies	32
1.7: Labelling of Molecules for Pharmaceutical Effect	34
Chapter 2: Organocatalysis	37
2.1: Organocatalysis: A Brief Early History	37
2.2: Organocatalysis: General Activation Mechanisms & Selected Examples	41
2.2.1: Introduction	41
2.2.2: Enamine Catalysis	41
2.2.3: Iminium Catalysis	48
2.2.4: Hydrogen Bonding Catalysis	52
2.2.5: SOMO Catalysis	56
2.2.6: Counterion Catalysis	60
2.3: Organocatalysis: Chiral Brønsted Acid Catalysts	62
Chapter 3: Aziridines & Aziridination	72
3.1: Aziridines: Introduction	72

3.2: Aziridines: An Overview of General Synthesis Methods	73
3.3: Aziridination: Aziridination with Alkyl Diazoacetates	78
3.3.1: Introduction	78
3.3.2: Lewis Acid Catalysis	79
3.3.3: Brønsted Acid Catalysis	84
3.4: Aziridines: Utilisation in Synthesis	89
3.4.1: Introduction	89
3.4.2: Reactivity and Activation	89
3.4.3: Ring Opening Reactions	91
Section 2: Results and Discussion	97
Chapter 4: Pyridinium Triflate Catalysed Aziridination Reactions, the One-Pot Method, and Asymmetric Aziridinations	97
4.1: Pyridinium Triflate Catalysed Aziridination Methods	97
4.1.1: Introduction	97
4.1.2: Development of the One-pot Procedure	97
4.2: One-pot Asymmetric Aziridinations	103
4.2.1: Introduction	103
4.2.2: Synthesis of aziridines <i>cis</i> -(309) to <i>cis</i> -(317)	105
4.2.3: Synthesis of bis-aziridines <i>cis</i> -(318) and <i>cis</i> -(319)	109
4.2.4: Hypothesis upon the Enantioselectivity of the Asymmetric One-pot Aziridination Reaction	111
4.3: Development of a Flow Reactor Based Aziridination Procedure	114
4.3.1: Introduction and Advantages	114
4.3.2: Chemical Basis for the Flow System	115
4.3.3: Sourcing and Set-up of the Reactor	116
4.3.4: Synthesis of a Racemic Aziridine via a Flow Chemistry Procedure	117
4.3.5: Suggestions for Future Work	119
Chapter 5: Studies towards the Synthesis of C2-deuterated Aziridines	121
5.1: Development of Deuteration Techniques	121
5.1.1: Introduction	121
5.1.2: Deuteration of Ethyl diazoacetate	121
5.1.3: Initial Aziridination Reactions	124

5.1.4: Attempted Deuteration of Pyridinium Triflate	130
5.1.5: Test Aziridination to form <i>rac</i> -(342) Catalysed by Deuterated Pyridinium Triflate (345)	132
5.1.6: Determination of a Potential Primary Kinetic Isotope Effect	133
5.1.7: Initial Development of Asymmetric Deuterated Aziridination Reactions and the Synthesis of <i>cis</i> -(350)	136
5.2: Asymmetric Synthesis of C2-deuterated Aziridines	141
5.2.1: Introduction	141
5.2.2: Synthesis of <i>cis</i> -(350) to <i>cis</i> -(359), <i>cis</i> -(363), and <i>cis</i> -(367) to <i>cis</i> -(370)	142
5.2.3: Summary and Conclusions	152
Chapter 6: Studies towards the Synthesis of C3- and C2-, C3-deuterated Aziridines	154
6.1: Synthesis of Deuterated Aldehydes	154
6.1.1: Introduction	154
6.1.2: Morpholinoacetonitrile Methodology	155
6.1.3: Further Comments	156
6.2: Asymmetric Synthesis of C2-deuterated Aziridines	156
6.2.1: Introduction	156
6.2.2: Synthesis of aziridines <i>cis</i> -(383) to <i>cis</i> -(388), and <i>cis</i> -(392) to <i>cis</i> -(393), and <i>cis</i> -(398) to <i>cis</i> -(399)	157
6.2.3: General Remarks	164
6.3: Asymmetric Synthesis of C2-, C3- deuterated Aziridines	165
6.3.1: Introduction	165
6.3.2: Synthesis of aziridines <i>cis</i> -(401) to <i>cis</i> -(408)	165
6.4: Conclusions upon the Synthesis of C2- and C2-, C3-di-deuterated Aziridines, and the overall 'Dialled in' Methodology	170
Chapter 7: Studies towards the 'Dialled in' Synthesis of Deuterated α-amino acid Derivatives	172
7.1: Synthesis of Deuterated α -amino acids	172
7.1.1: Introduction	172
7.1.2: Syntheses of (409) to (428)	172
7.1.3: Summary and Conclusions	186

7.2: 'Dialled in' Asymmetric Syntheses of α -amino acid Derivatives containing Multiple Isotopic Labels	188
7.2.1: Introduction	188
7.2.2: 'Dialled in' syntheses of (429) to (433)	189
Chapter 8: Spectroscopic and Computational Investigations	194
8.1: Introduction	194
8.2: Determination of a Chiral Intermediate Utilising Circular Dichroism Techniques	194
8.3: Attempted Determination of the Absolute Stereochemistry of cis-(351) and cis-(358) via VCD and Computational Methods	199
8.4: Conclusions and Future Work	202
Section 3: Experimental	203
9.1: Detailed general procedures	203
9.2: Synthesis of C2-, C3-proteo Aziridines	205
9.3: Synthesis of C2-deutero Aziridines	217
9.4: Synthesis of C3-deutero Aziridines	232
9.5: Synthesis of C2-, C3-di-deutero Aziridines	242
9.6: Synthesis of C2-, or C3-deutero, and C2-, C3-di-deutero Amino Acids	250
9.7: Synthesis of Deuterated ^{15}N and ^{18}O containing Aziridines, and Amino Acids/Alcohols	269
9.8: Synthesis of C2-deutero aziridines rac-(336), and rac-(341) to rac-(344)	277
9.9: Synthesis of Starting Materials	282
9.10: Appendix	
9.10.1: Appendix 1: COSY and HSQC Correlation Spectra for compound rac-(324)	299
9.10.2: Appendix 2: Crystal Structure Data for compound rac-(342)	303
9.10.3: Appendix 3: Percentage Composition and Rate Calculation Data for the syntheses of rac-(342) catalysed by PyTf-h (279), or PyTf-d (345)	310
9.10.4: Appendix 4: ^1H -NMR and ^{13}C -NMR spectra; and HRMS spectrum for compound cis-(350)	312
9.10.5: Appendix 5: Crystal Structure Data for compound cis-(356)	315

9.10.6: Appendix 6: <i>¹H-NMR and ¹³C-NMR spectra; and COSY, and HSQC Correlation spectra for compound (410)</i>	322
9.10.7: Appendix 7: <i>Summary of the 'Dialled in' Methodology</i>	328
9.10.8: Appendix 8: <i>¹H-NMR and ¹³C-NMR spectra; HSQC and ¹⁵N- ¹H- HMBC Correlation spectra for compound (429)</i>	329
9.10.9: Appendix 9: <i>VCD predictions for both cis-enantiomers of compounds cis-(351) and cis-(358); and sample Gaussian Input File for cis-(351), Conformer 1</i>	334
Section 4: Bibliography	340

Section 1: Introduction

Chapter 1: Deuterium and Labelled Compounds

1.1: Deuterium: Origins and Early History

Deuterium is one of three isotopes of hydrogen, containing one proton and one neutron within its nucleus. Much rarer than so called 'light hydrogen' (protium), deuterium in its natural abundance exists at ~ 0.015 %.¹ Most deuterium in existence is contained in the form HOD (with D being deuterium), as partially enriched water. It is believed that the vast majority of deuterium in existence today was formed around 10 minutes after the Big Bang, and has remained fairly constant since.¹

The existence of deuterium was originally suspected after the discovery of irregularities during the determination of the mass of hydrogen. The research group of Aston *et al* in Cambridge had developed the first mass spectrograph, publishing the designs in 1919.² With this new instrumentation, the group determined the atomic weight of hydrogen, and therefore recorded the mass of a single hydrogen nucleus. Also around this time, W. Noyes of the University of Illinois determined the average atomic weight of two hydrogen atoms (*i.e.* one hydrogen molecule). The results of these two groups were inconsistent, and were interpreted by some as evidence for the existence of a heavier isotope of hydrogen.³ After this, direct evidence of the existence of deuterium was supplied by a study of the atomic spectrum of hydrogen; with a line being shown which was consistent with a hydrogen atom of mass two. This work by Urey, Brickwedde, and Murphy, was carried out in 1931 at Columbia University. After showing the existence of this new isotope by atomic spectroscopy, they distilled liquid hydrogen near to the triple point in order to isolate a sample.⁴ However, this experiment led to a much smaller amount of deuterium than they expected. Urey (in collaboration with Washburn) went on to obtain deuterated water (enriched by 'a few percent')⁴ by electrolytic distillation in late 1931.⁵ By 1933, G. N. Lewis had improved upon the electrolytic method, producing essentially pure heavy water *via* successive concentrations.⁶

Once it became evident that this new isotope could be isolated and potentially used, debate began as to what it should be named, and how nomenclature would change to accommodate it. One suggested method was devised by Professor R. W. Wood, who suggested that the new isotope should be named bar-hydrogen, and given the symbol H.⁷ However, this was disregarded due to the potential difficulty in naming more complex molecules containing the new isotope. Thus the method settled on by the community was that suggested by Urey *et al*; namely that the new isotope should be referred to as deuterium (from the Greek *deuteros*, meaning second), and that the most abundant isotope

should be referred to as protium (from *protius*, meaning first).⁸ The symbol settled on for deuterium was also coined by Urey *et al* originally being H², before becoming the now more commonly recognised ²H (or D).

It is also worthy of note the lengths to which researchers were willing to go in order to gain a grasp of the new isotope; some resorting to drinking heavy water in order to note its effects (and taste).⁹

1.2: Industrial Production of Deuterium

As discussed above, the initial method for obtaining deuterium in a pure form involved the distillation of liquid hydrogen at near to its triple point (this being the point at which a compound exists in all three states simultaneously).⁴ However, this was problematic not only due to the inherent dangers of holding hydrogen at its triple point, but also due to the low yield of the process. This was improved somewhat by the method of repeated hydrolytic concentrations, developed by Lewis *et al*;⁶ and by 1934 Norsk Hydro had entered into a collaboration with the physicist Leif Trondstad (of the Norwegian Institute of Technology) to industrially produce heavy water utilizing the hydrolysis equipment from their Haber-Bosch process plant. By the end of 1935, the plant was producing 99 % pure heavy water in kilogram scales.¹⁰

During the Second World War, development of heavy water production was seen as an important area by the Allies, due to the potential uses of heavy water as a moderator for nuclear fission. Research in the USA and Canada led to the development of a catalytic exchange process (the Trail process) for the enrichment of water from 0.015 % D (natural abundance) through to 2.3 %, followed by electrolysis to produce 99.8 % enriched water. This system involved the use of both Pd/C and Ni/Al catalysis in a stepwise process.¹¹

A modified version of the Trail process, known as the Dual Temperature Sulfide Process has been used in modern times for the production of heavy water. By using hydrogen sulfide as an exchange material, a metal catalyst is no longer required within the enrichment system. Liquid HOD is passed through an exchange unit (containing hydrogen sulfide), and deuterium is exchanged with protium from hydrogen sulfide to produce HSD and water. The mono-deuterated hydrogen sulfide is then passed over further mono-deuterated water at low temperature, enriching the water as it does, and reproducing hydrogen sulfide. This process has the advantage of not requiring a catalyst, and also allows the hydrogen sulfide to be contained within a closed system. By combining three cycles of exchange, the modern Bruce Plant in Ontario is capable of producing enrichment from natural abundance (0.015 %) to 25 %. This is then taken to 99.85 % *via* distillation (Figure 1).¹⁰

However, due to overproduction (the plant was capable of producing 700 tonnes of deuterium oxide a year, requiring 340 000 tonnes of feed water to produce one tonne of deuterium oxide) the plant was decommissioned in 1997; after stocks were deemed sufficient for the foreseeable future.¹²

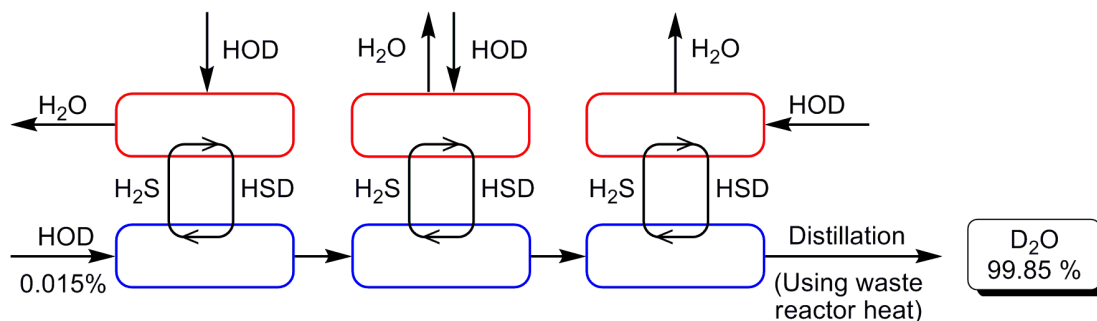


Figure 1: Modern Production of D₂O (Dual Temperature Sulfide Process)

1.3: Properties of Deuterium, Deuterium Oxide, & the Deuteron

Being an isotope of hydrogen, the deuterium nucleus (the deuteron) contains one proton, and one neutron. Therefore, the deuteron has a mass of 2.014 u, whereas the proton (standard hydrogen nucleus) has a mass of 1.007 u, making the ratio $m_d/m_p = 1.99901$ *i.e.* a deuteron has roughly twice the mass of a proton.¹³

This difference in mass has several consequences upon the properties of deuterated compounds. The most notable of these for chemists being the potential difference in the force constant (which can be related to the bond energy) of C-H and C-D bonds.¹⁴ This potential difference comes about due to an alteration in Zero Point Energy (ZPE being the lowest possible energy within a quantum mechanical system, *i.e.* the ground state energy) caused by the difference in mass between protium and deuterium (ZPE is related to vibrational frequency, which in turn is related to the masses involved within the bond, See Figure 3, Equation 3, within 1.4: *Deuterium and the Kinetic Isotope Effect*).

This property gives rise to the Kinetic Isotope Effect, and a detailed treatment can be found below. Although the difference in ZPE between isotopes can be observed in all elements, the difference in relative mass between deuterium and hydrogen is the largest observed, and therefore the subsequent effects are the most significant.

When present in compounds such as deuterium oxide, subtle differences can be observed compared to the non-deuterated version of the compound. For example, deuterium oxide has a density that is approximately one tenth higher than that of water (the density of deuterium oxide is 1.107 g/mL at 25 °C, compared to 1.0 g/mL for water) with a boiling point of 101.4 °C, and a melting point of 3.8 °C.^{15,16} One notable practical difference between water and deuterium oxide comes from the viscosity of deuterium

oxide. Being more viscous than water (deuterium oxide has a viscosity of 1.245 relative to water at 20 °C)¹⁷ makes deuterium oxide hygroscopic;¹⁸ meaning that when handling and working with heavy water, anhydrous conditions should be observed to prevent effective ‘dilution’ of deuterium oxide with water.⁴ It is worth noting that in general, the physical and chemical properties of a deuterated material are essentially the same as those of the *proteo* equivalent.

The main property of the deuterium nucleus of interest to organic chemistry is the nuclear spin, which is denoted as I . This is due to the relationship between a nucleus’ spin properties and NMR spectroscopy. In order to be active in NMR a nucleus must have net spin. This is a property derived from the contents of the nucleus, and thus can be predicted roughly using the following rules. A nucleus with an odd mass number will, in general, have a half integral spin ($I = 1/2$). A nucleus with an even mass number and an odd charge number will, in general, have an integer spin ($I = 1$). Finally, a nucleus with an even mass number and an even charge number will have zero spin ($I = 0$, NMR inactive). Deuterium has an even mass number (2), and an odd charge number (one proton within the nucleus); therefore $I_{(2H)} = 1$. This integer spin has the effect of generating three spin energy levels when the nucleus is placed within a magnetic field (as $\Delta m_i = 1$, $m_i = 1, 0, -1$).¹⁹ The effect of these three energy levels is shown in spin-spin coupling. For example, a proton adjacent to a deuteron can experience three distinct spins from the deuteron. Thus three energy levels are experienced by the proton within its excited spin state, giving rise to a triplet signal in the proton NMR.

Within ¹³C-NMR, another property of the deuteron can be seen. ¹³C-NMR is generally acquired as a proton decoupled spectra. This involves saturating the spin of the ¹H nuclei within the molecule, thus removing any coupling. This is possible as the resonant frequency of ¹³C- and ¹H-nuclei are sufficiently different. However, decoupling for ¹H does not decouple ²H from ¹³C-NMR. This is due to the differing magnetogyric ratios of ¹H and ²H. Magnetogyric ratio (γ) arises from the spin of the nucleus, and is a differing property for each. This property can be related through to the frequency of the NMR transition through the equation shown below (Figure 2); and thus can affect the decoupling frequency required for each nucleus. This effect is seen in standard ¹H-decoupled ¹³C-NMR using CDCl₃. The carbon signal from CDCl₃ is clearly split by the adjacent deuteron, despite the ¹H-decoupling (this also demonstrates the effect of $I = 1$, as the C signal is split into three lines of equal intensity).

Nucleus	Magnetogyric Ratio $\gamma \cdot 10^7 / \text{rad s}^{-1} \text{ T}^{-1}$	Spin Quantum Number (I)
^1H	26.7522	$1/2$
^2H	4.1065	1
^{13}C	6.7262	$1/2$
^{14}N	1.9331	1
^{15}N	-2.7116	$1/2$

$$\nu = (\gamma / 2\pi)B$$

Where:

ν = frequency of the NMR transition

γ = magnetogyric ratio

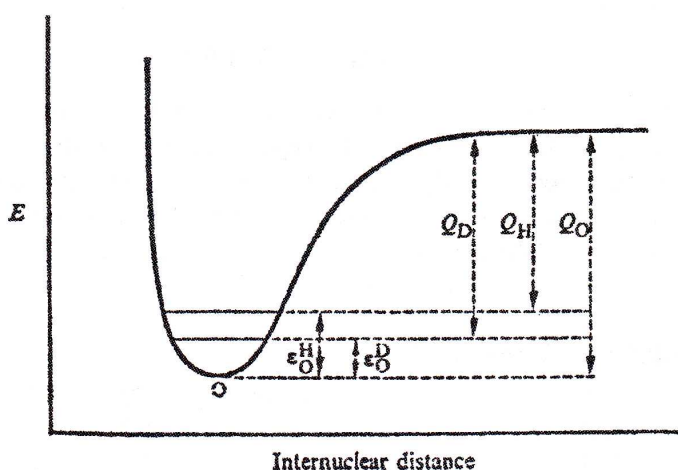
B = applied magnetic field

Figure 2: Properties of some Common Nuclei

1.4: Deuterium and the Kinetic Isotope Effect

As noted above, deuterium and protium bonds can be shown to differ in their force constants. This effect often leads to changes in the kinetics observed within a reaction (*i.e.* rate changes within the reaction). Generally termed the Kinetic Isotope Effect (KIE), the magnitude of this effect can be derived utilising the following equation: $\text{KIE} = k_{\text{H}}/k_{\text{D}}$ where k_{H} and k_{D} are the reaction rate constants for the *proteo* and *deutero* forms of the reaction respectively.²⁰ For the purposes of this treatment, KIE will be split into two parts: primary (1°) KIE, and secondary (2°) KIE. Primary KIEs arise from the direct breaking, or formation, of a bond to, or from, deuterium (*e.g.* dissociation of DCl); whereas 2° KIEs arise when deuterium is present, but remote from the reaction centre (*e.g.* enzymatic *N*-demethylation where N-CD_3 is present, compared to N-CH_3).

The simplest case to consider to demonstrate primary KIE is that of the dissociation of a chemical bond X-H, or X-D, where X is simply an undefined bonding partner. The bonding can be represented by a potential energy surface, with the intermolecular bonding distance determined by the lowest point of the surface (Figure 3). The bonding of both X-H and X-D can be represented with the same surface, as the surface is unchanged by isotopic substitution. This is due to *inter*- and *intra*- molecular forces relying upon attraction and repulsion effects between nuclei and electrons; not upon the mass (*i.e.* nuclei and electrons can be treated separately, the Born-Oppenheimer approximation).



$$\nu = \frac{1}{2\pi} \cdot \sqrt{\left(\frac{k}{\mu}\right)}$$

Equation 1

$$k = \mu(2\pi \cdot \nu)^2$$

Equation 2

$$E_0 = \frac{1}{2} h \nu$$

Equation 3

E_0^H = Zero Point Energy for X - H

E_0^D = Zero Point Energy for X - D

Figure 3: The relationship between ZPE²¹ and mass; and related equations

This approach (based upon classical mechanics) suggests that since the two bonds share the same potential energy surface, they should share the same dissociation energy; and in fact, that the relative rates of dissociation should only differ depending on the frequency of the bond. From classical mechanics, we can relate the frequency (ν) of vibration of chemical bonds to the force constant (k , related to the strength) of the bond, and the reduced mass of the system (μ). The equations demonstrating this relationship are shown above (Figure 3, Equations 1 & 2). However, changes in dissociation energy related to frequency do not account for the extent of the rate changes noted with the KIE. Therefore another effect must be involved.

From quantum mechanics it can be demonstrated that in reality the lowest point of any harmonic oscillator (*i.e.* the chemical bond) is not at the lowest point of the potential energy curve. The lowest actual point lies at the minimum plus the Zero Point Energy (ZPE) of the system. The ZPE can be represented by Equation 3 (Shown in Figure 3) where ν is the frequency of the oscillator.

As shown in Equations 1 and 2 (shown in Figure 3) above, we can relate frequency to the mass of the system. Thus X-D has a lower ZPE than that of X-H (again, where X is an undefined bonding partner), and therefore higher dissociation energy. This effect is large enough to account for the variations involved within the primary KIE.

In general, the size of the primary KIE can vary between 1 and 16.²² This variation is observed in both polar and free radical processes.²² For example, the values calculated for the bromination of acetone and nitromethane; and the acid base behaviour of nitroethane are 7.7, 6.5, and 10 respectively.²³⁻²⁵ An example of the KIE in free radical reactions is the reaction of $\text{CH}_3\cdot$ with H_2 and D_2 ; the reaction being three times faster with H_2 at 182 °C (relating to a KIE of 4-5 at 25 °C).²⁶

Secondary KIE, as stated above, are effects upon a reaction which take place where deuterium is remote from the bond being broken. The primary area of study into these effects involves their presence within S_N2 type reaction processes where deuterium is α - to the reaction centre. Although the focus of KIE investigations has been to probe these S_N2 reactions more fully, the work has also led to several accepted theories of what causes secondary KIE.

As secondary KIE are effects which arise in reactions where deuterium is remote from the bond being broken, the rate change must come about as a result of differences within the transition state of the reaction, brought about by the presence of deuterium. Several research groups including those of Jensen and Poirier have looked into this, and determined that, like the primary KIE, secondary KIE arises from changes in the ZPE. These differences in ZPE are widely believed to be caused by changes in vibrational frequencies during the transition state.^{27,28}

Although it is accepted that changes in vibrational frequencies are responsible for the change in ZPE of the transition state, the type of vibrational change responsible is a matter of some debate.²⁹⁻³² However, despite debate upon the exact nature of these vibrational changes, several correlations have been drawn from experimental data.

It has been demonstrated that the degree of separation between the leaving group, and the entering group within the transition state of an S_N2 reaction will affect the degree and even the direction of the secondary KIE. This so-called 'looseness' of the transition state affects the energy of the out of plane bending motion of the α -hydrogen (or deuterium). If a transition state has a so called 'loose' transition state (*i.e.* a larger distance between the entering and leaving groups), the difference in the energy of vibrational motions within the transition state will be the same, or lower than the starting material. Therefore, 'loose' transition states tend to lead to 'normal' secondary KIE, thus, $k_H/k_D > 1$, thus, the rate of reaction is slower with the *deutero* starting material than the *proteo* (Figure 4). *Vice versa*, a 'tight' transition state will lead to high energy out of plane H bending (see Figure 4), leading to an increased ZPE. This has the effect of reducing the difference between the activation energy of the *proteo* and *deutero* reactions, thus reducing the secondary KIE. In some cases, this can be to the extent that the KIE becomes inverse *i.e.* $k_H/k_D < 1$, a rate increase is seen upon deuterium substitution (Figure 4).

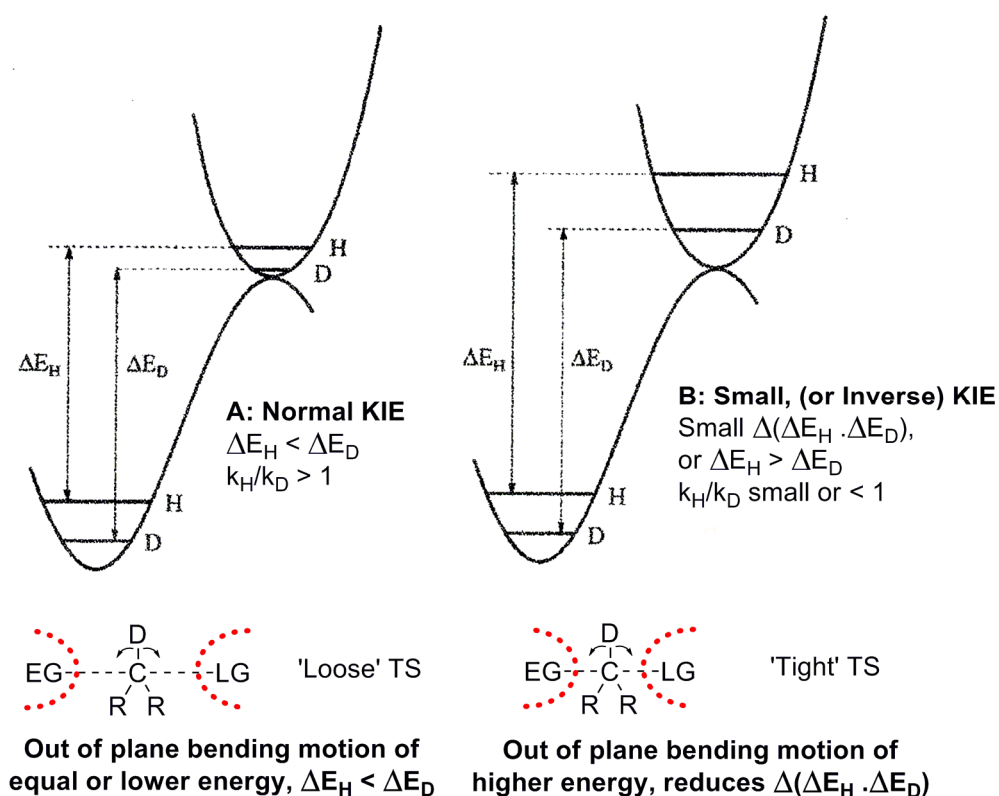


Figure 4: The α -secondary KIE and 'looseness' of the S_N2 Transition State

Recent work by Wolfe and Kim³² suggested that in reality, the C-H stretching frequency is of greater importance in examples where inverse secondary KIE is observed. This, if established, would have had implications for the assignment of transition state structure by KIE effects. However, work by Poirier *et al* has shown that although the contribution to KIE from stretching vibrations is significant for small uncomplicated substrates (*i.e.* the transfer of a methyl group), the contribution from bending vibrations greatly outweighs this effect in larger or more complicated systems (*i.e.* ethyl groups or higher).³⁰ In practice, measurements of secondary KIE within reactions have been used to probe the structure or geometry of various transition states (not only S_N2), both in theory, and in experiment. For example, Houk *et al* have utilised secondary KIE to interpret calculated geometries of the transition state of the Cope rearrangement.³³

1.5.1: Synthesis of Deuterated Compounds: Introduction

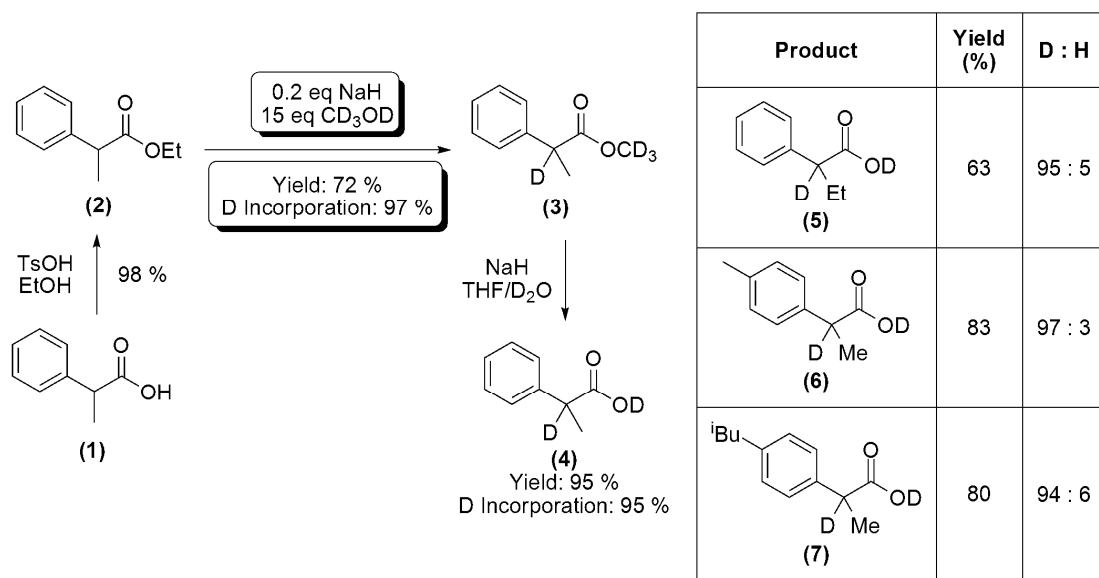
When considering the deuteration of organic compounds, there are two approaches which must be taken into account; these being pre-synthetic and post-synthetic incorporation. Both have potential advantages and disadvantages. For example, using a pre-deuterated starting material has the advantage of simplicity, as several deuterated substrates are available commercially.³⁴ However, introducing isotopic enrichment early in a synthesis can lead to loss of the isotope during subsequent reactions (*i.e.* through exchange processes with solvents or reagents, or through low yielding reactions within an

ongoing synthesis). It is for this reason that pharmaceutical process laboratories tend to lean towards incorporating deuterium at a late stage, or ideally as the last step, in a synthetic sequence.

1.5.2: Synthesis of Deuterated Compounds: Pre, and Mid Synthesis Incorporation

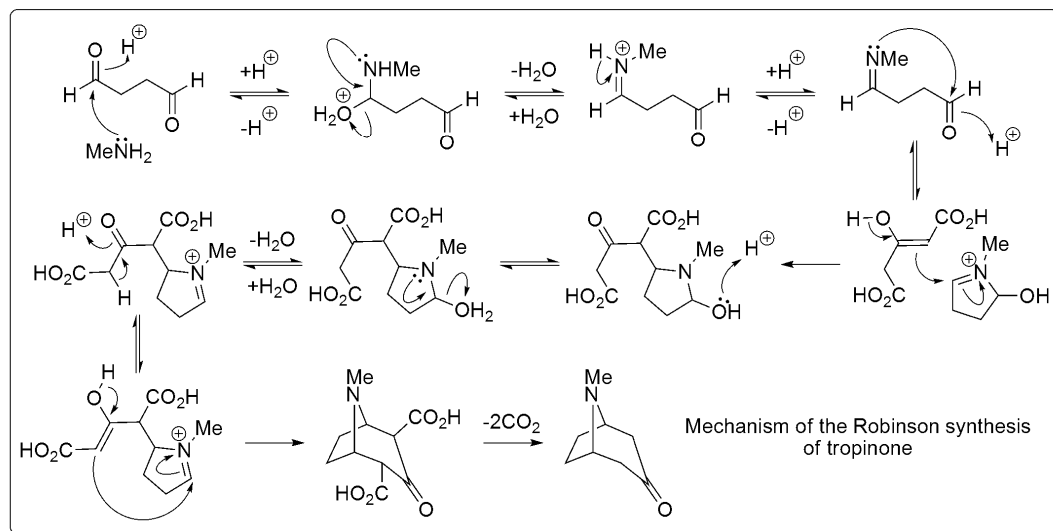
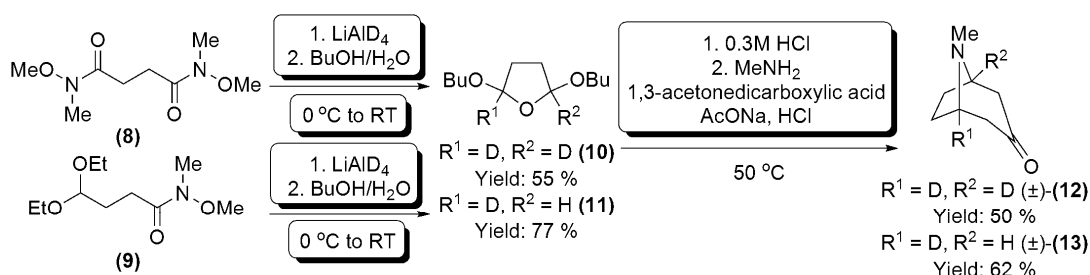
The frequently used methods for incorporating deuterium during an organic synthesis follow established synthesis procedures. For this examination the procedures can be split into acid-base methods, reduction methods, and hydrogenation methods.

The simplest method for incorporating deuterium into organic substrates is *via* simple base catalysed exchange of enolisable or base labile positions. A good example of this is the work of Eames *et al*, and their investigations into the production of various α -deuterated profens (2-aryl propionic acids, Scheme 1). Utilising 15 equivalents of d_4 -methanol, and a catalytic amount of base, the desired esterified starting material (*i.e.* (2)) underwent α -H/D exchange *via* an intermediate enolate to give the deuterated product (*i.e.* (3) and subsequently (4)) in >95 % deuterium incorporation.³⁵



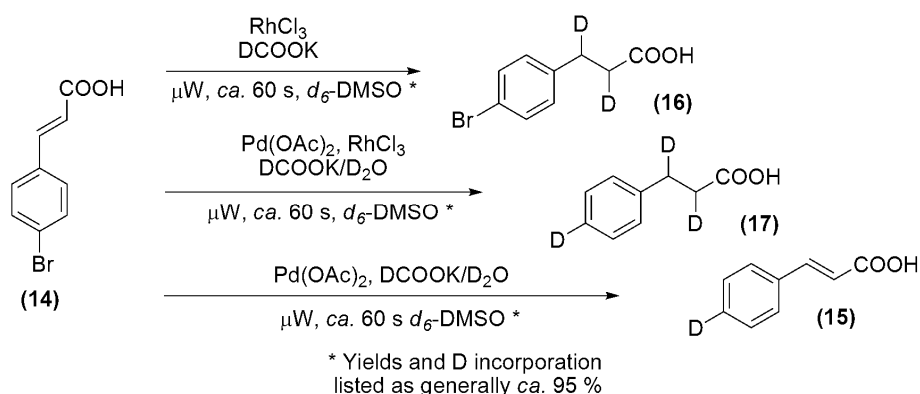
Scheme 1: Synthesis of 2-deutero-2-phenyl propionic acid (4), and related materials by Eames *et al*

Moving on, an interesting example of reduction methods being utilised in order to selectively introduce deuterium was recently published by Lebreton *et al*.³⁶ The group were attempting to synthesise deuterated tropinone species (12) and (13) (shown in Scheme 2). In order to facilitate this, it was decided to synthesise deuterated 2,5-dialkoxytetrahydrofuran species (10) and (11) (*via* reductive deuteration of (8) or (9) with lithium aluminium deuteride, followed by cyclisation; yielding (10) in 55 %, and (11) in 77 %) as an intermediate step before undertaking the classical Robinson synthesis of tropinones, affording (12) in 50 % yield, and (13) in 62 % yield (Scheme 2).



Scheme 2: Synthesis of deuterated tropinones (12) and (13) by Lebreton *et al*, and the Robinson synthesis of tropinone

The work of Jones *et al* concerned with the transfer deuteration of double bonds is a good example of a reductive hydrogenation technique.³⁷ By treating *para*-bromocinnamic acid (14) with palladium or rhodium based catalysts under microwave conditions, >95 % deuterium incorporation could be achieved regioselectively in either the 7- position (15), 2-, 3- positions (16), or 2-, 3-, and 7- positions (17) (Scheme 3). The deuterium source for these reactions was a combined mixture of potassium deuterioformate in deuterium oxide. However, potassium deuterioformate in water was also successful; suggesting the deuterium source within the reaction is the formate itself.



Scheme 3: Transfer hydrogenation and catalytic dehalogenation reactions, incorporating deuterium, by Jones *et al*

As mentioned above, these examples are representative of the general methods used in order to incorporate deuterium within a synthesis. However, there is significant scope to adapt synthetic methods in order to incorporate deuterium, and as the breadth of organic synthesis is so large, this is not covered in greater detail here.³⁸⁻⁴³

1.5.3: Synthesis of Deuterated Compounds: Post Synthesis Methods

For the purposes of this examination, the methods for incorporating deuterium into organic molecules in a general and potentially post synthetic manner can be split into four categories: acid mediated exchange, base mediated exchange, heterogeneous metal catalysed exchange, and homogeneous metal catalysed exchange. Each of these areas will be examined in turn.

1.5.3.1: Synthesis of Deuterated Compounds: Post Synthesis Methods – Acid Catalysed H/D Exchange

The main class of acid catalysed H/D exchange reactions in common use are the High Temperature Dilute Acid (HTDA) reactions developed by the group of Werstiuk *et al.* Initially, the procedure involved treatment of the desired substrate with dilute acetic acid in deuterium oxide, at temperatures above or around 250 °C. This was followed by a second exchange reaction with 10 % DCl in D₂O. This method has been applied to the exchange reactions of benzene derivatives, allowing for exchange of only the aromatic protons of benzene, biphenyl, 1,2-dimethylbenzene, and 1,3-dimethylbenzene. The deuterium incorporation levels achieved ranged from 88 % for benzene, through to 98 % for 1,2-dimethyl benzene (Figure 7).⁴⁴ Further to this work, Werstiuk *et al* have applied HTDA methods to polycyclic aromatics (such as: anthracene, phenanthrene, pyrene, and 1,2'-binaphthyl),⁴⁵ anilines, phenols,⁴⁶ and alkenes.⁴⁷

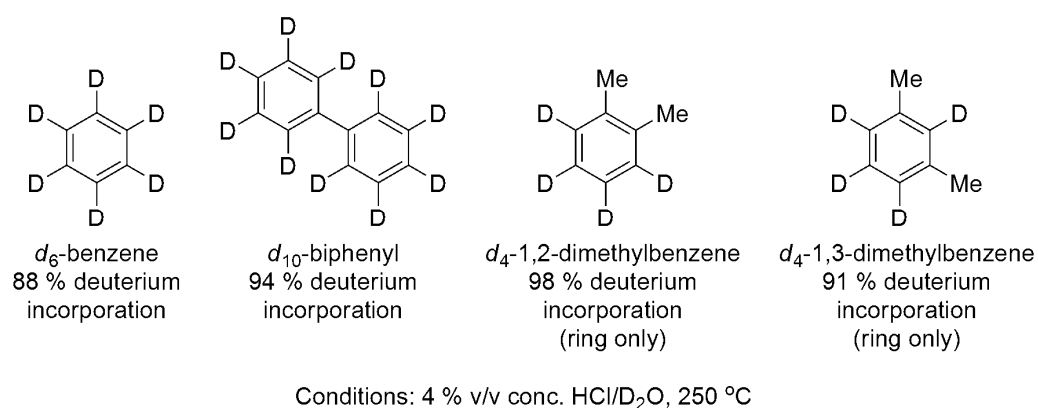
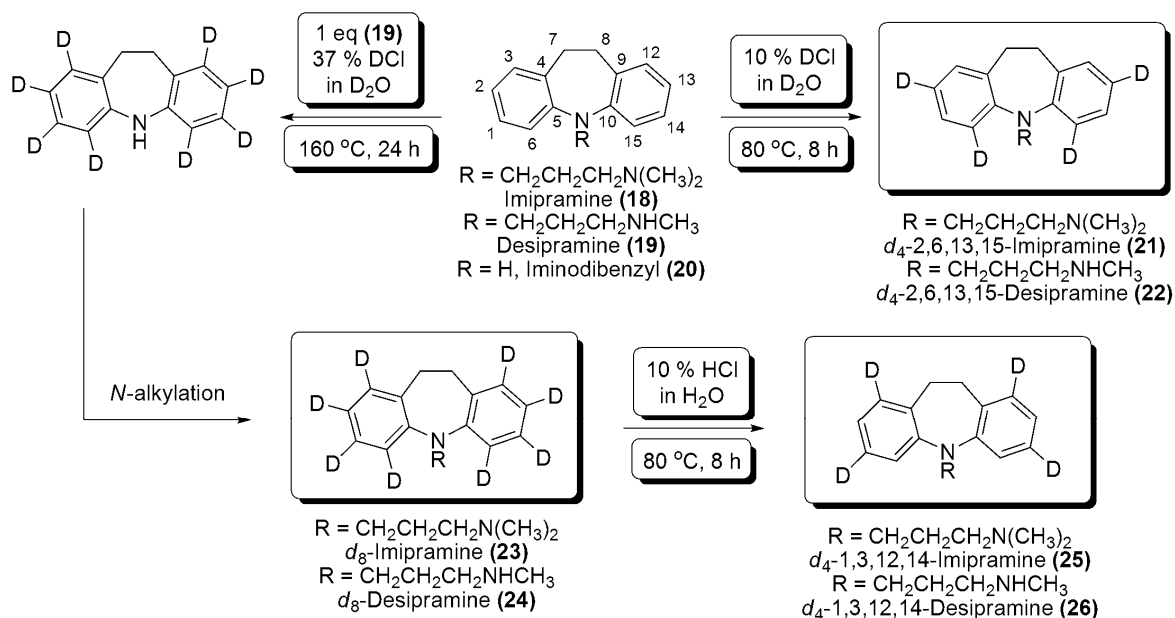


Figure 7: Initial application of the HTDA H/D exchange methodology of Werstiuk *et al*

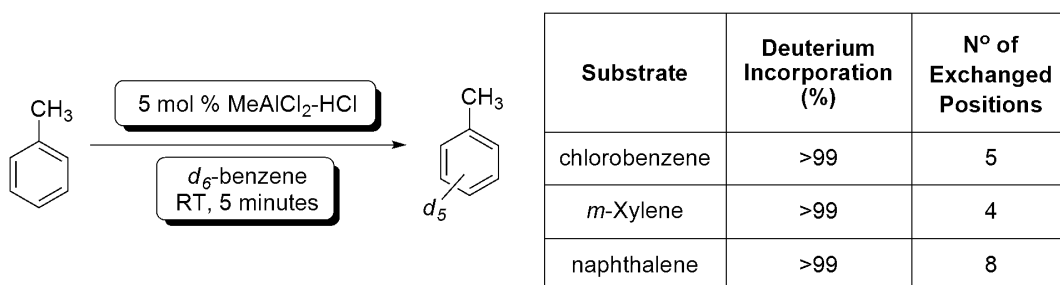
HTDA procedures have also been utilised in a more selective manner in order to produce deuterated aromatics. For example, Sasaki *et al* have utilised 10 % DCl in D₂O to

produce selectively deuterated antidepressants imipramine (**18**), and desipramine (**19**).^{48,49} Selective d_4 -deuteration of (**18**) at the 2-, 6-, 13-, and 15- positions (producing (**21**)) was achieved by simple HTDA methods (Scheme 4). Deuterium incorporation levels were good, reported as >95 % at all desired positions; d_8 - (**23**), and d_4 -1,3,12,14- (**25**) imipramine were also synthesised *via* HTDA methods with good deuterium incorporation of 88 % and 95 % respectively (Scheme 4).



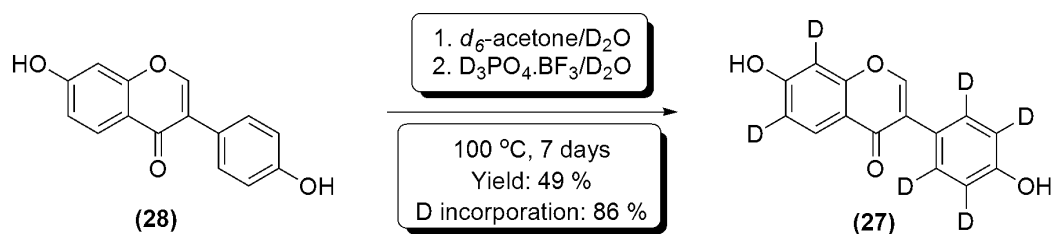
Scheme 4: Selective deuteration of imipramine (18**) and desipramine (**19**)**

Moving on from the HTDA methodology, Lewis acids have been utilised in combination with Brønsted acids for H/D exchange. For example, early work in this area carried out by Garnett *et al* utilised methyl aluminium chloride, or ethyl aluminium chloride as the catalyst (in *ca.* 5 % loading), with deuterated benzene as the deuterium source (Scheme 5). Deuterium incorporation from this reaction was good, with reported values of >95 %; however, the reaction required extremely strict anhydrous conditions be maintained, in addition to requiring the use of pyrophoric Lewis acids.^{50,51}



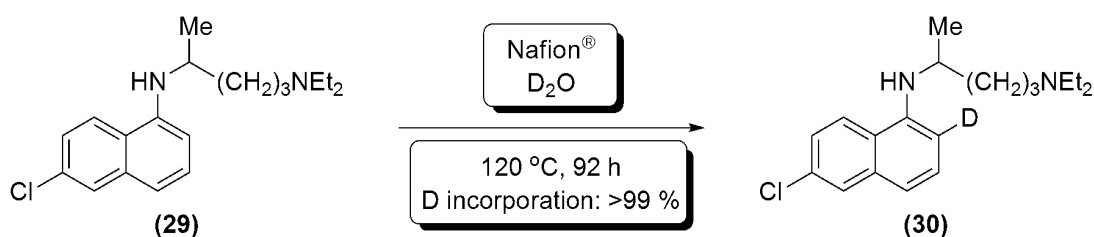
Scheme 5: Deuteration of aromatic substrates with a mixed Brønsted/Lewis acid catalyst carried out by Garnett *et al*

More recently, Wahala *et al* have utilised boron trifluoride : phosphoric acid complex in D₂O for the synthesis of *d*₆-daidzein (**27**) (Scheme 6). Interest in this compound is due to its potential as an anti-cancer drug. The synthesis of (**27**) was carried out at 100 °C, with the reaction time being ~7 days. This procedure yielded the *d*₆- product, with an isotopic incorporation of 86 % (Scheme 6).⁵²



Scheme 6: Synthesis of *d*₆-daidzein (**27**) carried out by Wahala *et al*

Attempts have also been made to make use of acidic polymer resins in order to catalyse H/D exchange reactions. Foremost among these is the work on Nafion[®]. Nafion[®] has been used to selectively introduce deuterium into the 3-position of the antimalarial chloroquine (**29**) in >99 % incorporation (Scheme 7).⁵³ However, recent work utilising polymer bound acids under supercritical water conditions have shown improvements compared to the aforementioned method.⁵⁴



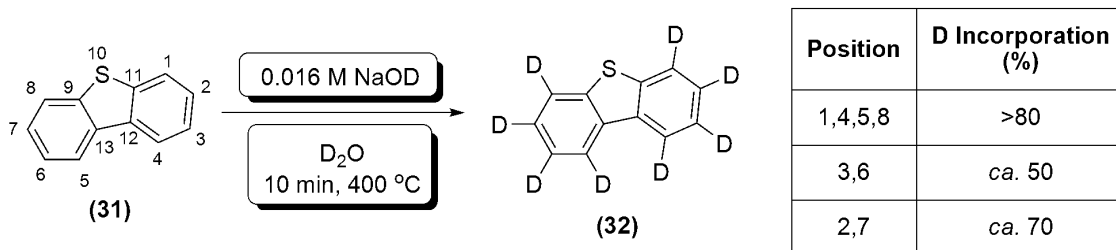
Scheme 7: Synthesis of 3-deuteriochloroquine (**30**) utilising Nafion[®] as the catalyst

In general, HTDA, polymer supported, and Lewis acid catalysed procedures have all shown potential for the incorporation of deuterium into compounds. However, there are various issues with these methodologies. Mainly, the harsh reaction conditions required in order to achieve a good level of deuterium incorporation (*i.e.* temperatures ranging from 120 °C to 300 °C, in the presence of strong acids), and also the inability to selectively introduce deuterium at specific positions (*i.e.* most of the reactions introduce deuterium into multiple, rather than distinct, positions). Therefore, this area of H/D exchange is not seeing as much interest in recent years; although some work concerned with increasing the selectivity of these methods is still being carried out.⁵⁵

1.5.3.2: Synthesis of Deuterated Compounds: Post Synthesis Methods – Base Catalysed H/D Exchange

Recent developments in base catalysed exchange reactions are characterised by the development of supercritical exchange; relying upon the physical properties of supercritical water or supercritical deuterium oxide. At, or close to the triple point, the dissociation constant of water is much greater than at room temperature. This in turn leads to a much higher concentration of the deuterioxide anion than is present below the triple point. Also, under supercritical conditions ($T > 375\text{ }^{\circ}\text{C}$, $P > 218\text{ bar}$), water will solubilise most organic substrates. The use of supercritical exchange in organic substrates has seen significant interest, and is the subject of several patents.^{56,57}

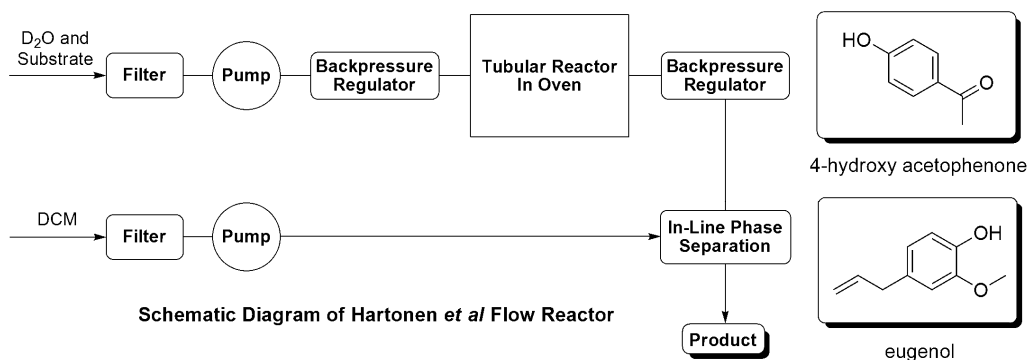
Experimentally, the groups of Junk and Evilia have demonstrated the use of supercritical water combined with small amounts of base in order to perform deuteration of organic substrates. For example, dibenzothiophene (**31**) was deuterated by Evilia *et al* with an average of 70 % deuterium incorporation at all ring positions (Scheme 8). Aliphatic substrates (*i.e.* 2-methyl pentane) also underwent deuteration, although incorporation was low, and reaction conditions were harsh (20 % deuterium incorporation at methyl positions, 0.16 M KOD, D_2O , 150 min, $380\text{ }^{\circ}\text{C}$).⁵⁸ The protocol employed by Junk *et al* was similar; substrates being treated with small amounts of sodium deuterioxide solution in deuterium oxide at high temperatures (*ca.* $400\text{ }^{\circ}\text{C}$). However, Junk *et al* tended to use extended reaction times from 1 – 24 h.⁵⁹



Scheme 8: Supercritical exchange protocol employed by Evilia *et al*

Although supercritical exchange can be considered a general procedure, several functionalities are incompatible with the high temperature conditions required for exchange to occur. For example, the method has been shown to be unsuitable for ethers, ketals, acetals, nitriles, and aryl azo compounds.⁶⁰ Also, the high temperatures and pressures involved are inherently hazardous. The hazards of synthesising deuterated molecules at such high temperatures and pressures to the chemist are significant (*i.e.* failure of equipment at high pressure, leading to injury). Potentially, these hazards could be reduced by the use of flow chemistry, as reactions are carried out on a much smaller scale, reducing the severity of any such failure of equipment.

To this end, the work of Hartonen *et al* is of interest. Hartonen demonstrated a supercritical flow type system, which allowed for the deuteration of both eugenol, and 4-hydroxyacetophenone.⁶¹ This method had several advantages over the traditional batch type supercritical deuteration reactions. For example, the contact time at high temperature was reduced to around 4 minutes, allowing for less temperature degradation of the substrates. One disadvantage of this procedure however, was that a range of deuteration products were noted (*i.e.* $d_0, d_1, d_2 \dots etc$); although increasing the reaction temperature did lead to a bias towards higher levels of deuterium incorporation (Figure 8).



Substrate	Contact Time (min)	Temperature (°C)	Isotopic Distribution (%)												
			d_0	d_1	d_2	d_3	d_4	d_5	d_6	d_7	d_8	d_9	d_{10}	d_{11}	d_{12}
Eugenol	4	250	46	44	9	1	0	0	0	0	0	0	0	0	0
	2	300	19	61	17	3	0	0	0	0	0	0	0	0	0
	4	300	6	58	30	6	0	0	0	0	0	0	0	0	0
	2	350	0	17	48	31	4	0	0	0	0	0	0	0	0
	4	350	0	4	33	51	12	0	0	0	0	0	0	0	0
4-hydroxy acetophenone	1	250	8	22	35	25	8	2	0	0	0	-	-	-	-
	2	250	1	9	28	36	21	4	1	0	0	-	-	-	-
	1	300	0	0	2	16	39	34	8	1	0	-	-	-	-
	2	300	0	0	0	1	19	62	17	1	0	-	-	-	-
	1	350	0	0	0	0	4	74	20	2	0	-	-	-	-
	2	350	0	0	0	0	2	82	15	1	0	-	-	-	-

Figure 8: Isotopic Exchange Under Flow Conditions; demonstrated by Hartonen *et al*

In summary, the use of base catalysed exchange, and in particular utilising supercritical water, is disadvantaged by the need for high reaction temperatures (these typically being *ca.* 400 °C), high reaction pressures (typically >218 bar), and the subsequent need for specialised equipment. The requirement of high temperatures also precludes the use of this method with certain substrates (*i.e.* ethers, ketals, acetals, nitriles, and aryl azo compounds). However, these disadvantages have been overcome to a degree by the use of flow chemistry. Flow chemistry allows both a reduction in contact time at high temperature, and the use of small reaction vessels (thus reducing the danger inherent

with high pressures). Despite this, flow chemistry methods still show disadvantages; primary among these being the generation of a range of deuterated products (*i.e.* d_0 , d_1 , d_2 ...etc), as opposed to generation of a discrete deuterated material.

1.5.3.3: Synthesis of Deuterated Compounds: Post Synthesis Methods – Heterogeneous Metal Catalysed H/D Exchange

The development of heterogeneous metal catalysis for hydrogen/deuterium exchange reactions has primarily focused upon palladium and platinum based catalyst systems. Investigations were first carried out by Garnett *et al* in the 1960s,⁶² and the area has seen significant research interest since.

The mechanism of H/D exchange for both platinum and palladium systems with D_2O has been studied extensively; concluding that palladium favours an associative exchange mechanism,⁶³ whereas platinum preferentially undergoes a dissociative π -complex mechanism (Figure 9).

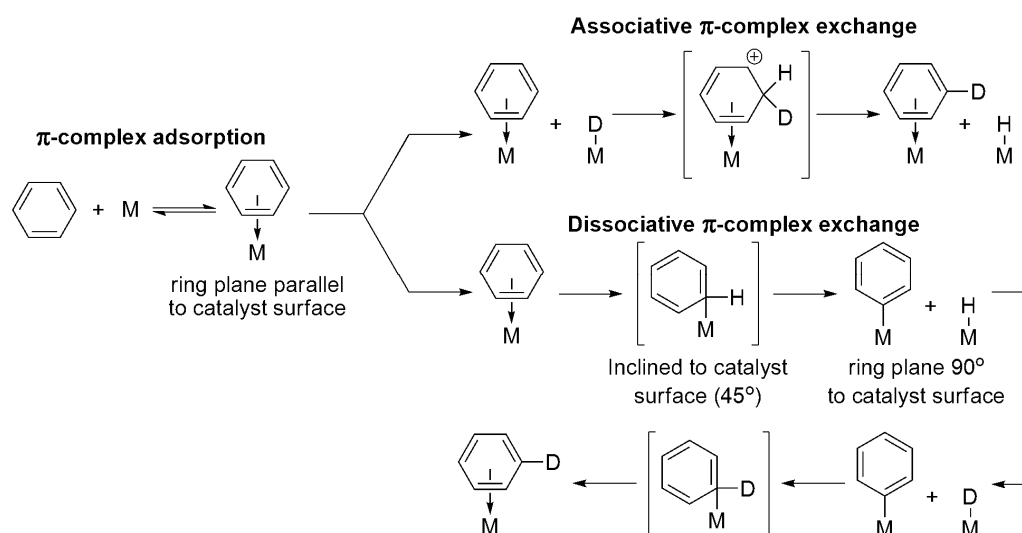


Figure 9: Associative, and dissociative, heterogeneous metal catalysed hydrogen exchange mechanisms

The difference between these mechanisms is small, and can be demonstrated if the deuteration of a general aromatic substrate is considered. Thus, both mechanisms rely upon initial π -complex adsorption of the aromatic substrate to the metal surface. At this point, the aromatic ring is parallel to the metal, and in the case of the associative mechanism, is attacked by a previously chemisorbed deuteron (from the dissociative chemisorption of D_2O or deuterium gas). In the case of the dissociative mechanism, it is believed that the aromatic forms a σ -bond with the metal, rotating through 90° to do so. The carbon-metal bond then undergoes a dissociative attack by a chemisorbed deuteron, and the substrate returns to the original π -bonded state.⁶⁴ Experimentally, palladium containing catalyst

systems have a higher affinity for H/D exchange at aliphatic hydrogen, whereas platinum based catalyst systems have a higher affinity for H/D exchange upon the aromatic itself.⁶⁵

With respect to the experimental application of heterogeneous palladium and platinum catalysts for hydrogen exchange; activation of the catalysts is generally required in order for the system to be effective. There are several general methods of catalyst activation which can be applied; these being hydrothermal activation, hydrogenation, or self-activation (reduction of the surface with an organic molecule *e.g.* benzene).⁶⁶ Each of these activation methods, and examples of their experimental application, are detailed below.

Hydrothermal activation of heterogeneous metal catalysts, for hydrogen/deuterium exchange reactions, relies upon the increase in the rate of dissociation of water (or D₂O) at elevated temperature and pressure (typically 250 °C, 4-5 MPa).⁶⁷ This effect allows the heterogeneous metal catalyst (generally systems based upon Pd(0) or Pt(0)) to undergo oxidative addition into the H-OH (or D-OD) bond, generating a Pd(II) or Pt(II) intermediate species. This intermediate species then undergoes dissociation to form the active ⁺M-H (⁺M-D) cation (Figure 10).

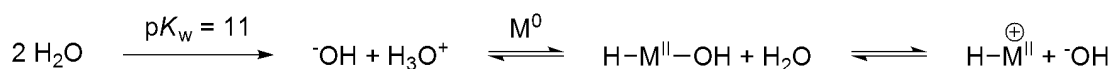
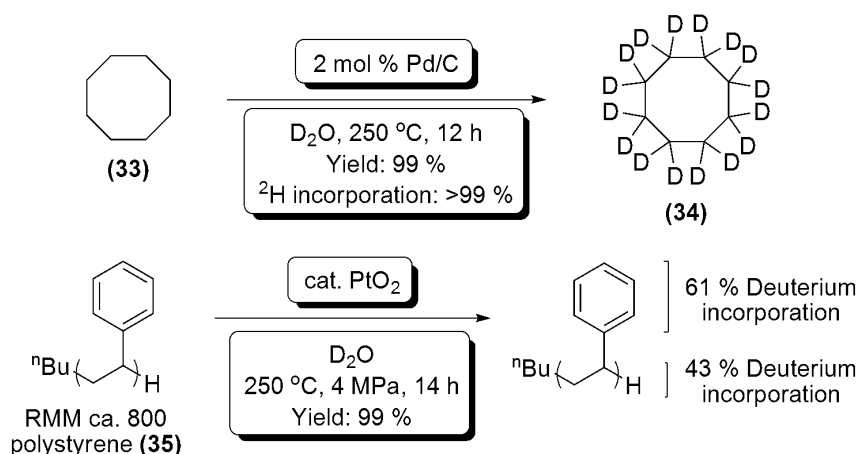


Figure 10: Generation of an active ⁺M-H (or ⁺M-D) species for hydrogen/deuterium exchange

An example of this in use is the work of Schaaf *et al.*, who demonstrated the use of palladium on carbon and D₂O to deuterate aliphatic hydrocarbons with >95 % incorporation.⁶⁸ These reactions required high temperatures in order to allow for activation of the catalyst; namely up to 290 °C. Similar to this is the work of Oshima *et al.*, who showed that full deuteration of cyclooctane (**33**) was achieved by treatment with 2 mol % Pd/C and D₂O for 12 hours. Again, this reaction required high temperature (250 °C) to allow for activation of the palladium on carbon catalyst (Scheme 10).⁶⁹



Scheme 10: Hydrothermal activation of Pd or Pt based catalysts for H/D exchange

Similar reactions utilising heterogeneous platinum based catalysts under hydrothermal conditions have also been studied; however, platinum based catalysts show a higher affinity for exchange of aromatic hydrogen over aliphatic. For example, Matsubara *et al* have demonstrated the use of platinum (IV) oxide under hydrothermal conditions for the deuteration of various substrates,⁷⁰ including polystyrene (**35**), giving a high degree of deuterium incorporation upon the aromatic rings (Scheme 10).⁷¹

The second general method of catalyst activation is treatment of the catalyst with hydrogen (or deuterium) prior to the reaction. Recently however, Hirota and Sajiki have developed a method for the *in situ* activation of the heterogeneous metal catalyst species (in this case, palladium, or platinum, on carbon).⁷²

Initially, the hydrogen/deuterium exchange reaction of diphenylmethane (**36**) at room temperature with 10 % by weight Pd/C in D₂O was attempted. No exchange was observed, as would be expected with the unreduced (inactive form) metal catalyst. When H₂ gas was placed over the reaction (*ca.* 0.45 eq vs. substrate), adsorption of the *in situ* formed D₂ allowed for 95 % deuteration of the benzylic position after 3 days. This procedure proved to be generally applicable, giving generally good deuterium incorporation of between 40 and 99 % selectively at benzylic positions (Figure 11).

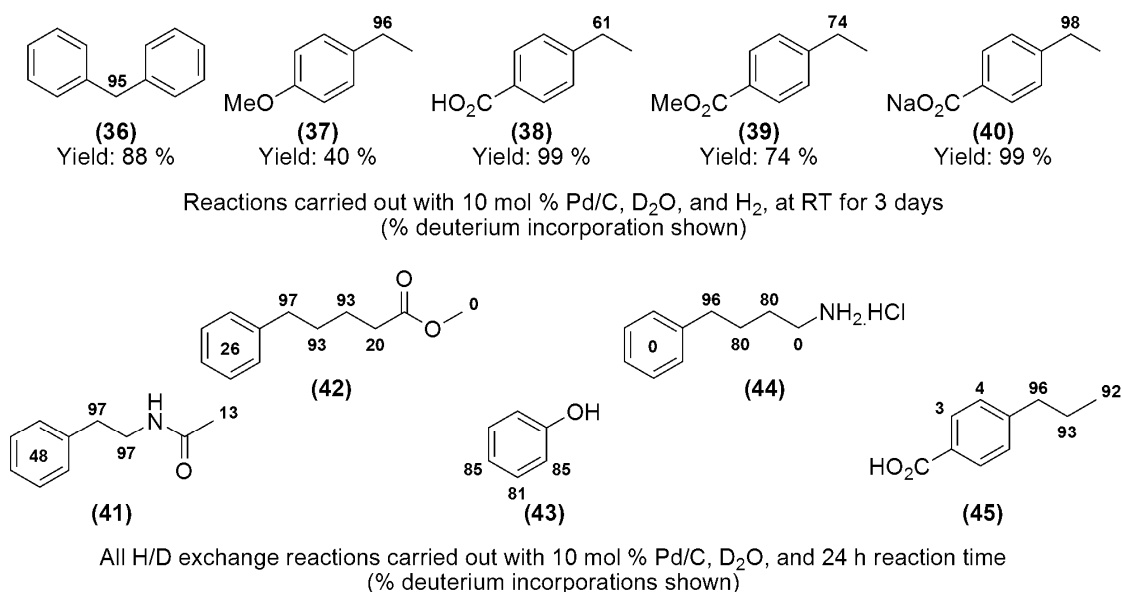


Figure 11: Deuteration of the aliphatic positions of various substrates utilising 10 mol % Pd/C and D₂O; by Sajiki *et al*

Sajiki *et al* also carried out a broad study on the applicability of this procedure to substrates bearing various functionalities. Utilising 10 mol % Pd/C, and D₂O, it was found that the system tolerated amides (**41**), esters (**42**), phenols (**43**), amines (**44**), and acids (**45**) (Figure 11); allowing for deuterium incorporation of, in general, >70 %. However, the reaction was limited to substituted benzene derivatives.⁷³

Further development of this method was carried out utilising platinum on carbon as the heterogeneous metal catalyst. Due to the selectivity of platinum for promoting exchange at aromatic positions, Pt/C allowed for introduction of deuterium into the aromatic ring positions of substituted benzene derivatives in up to 98 % (Figure 12).⁶⁵

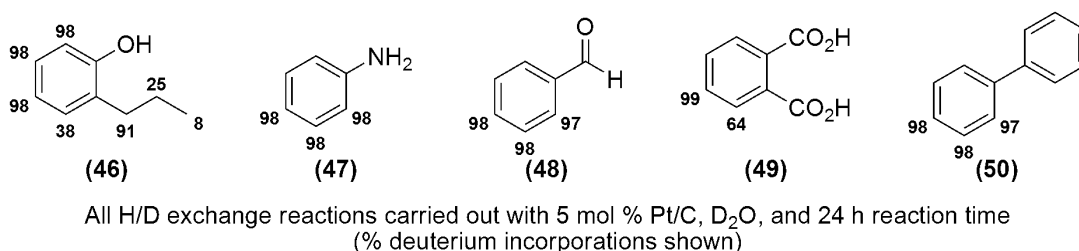
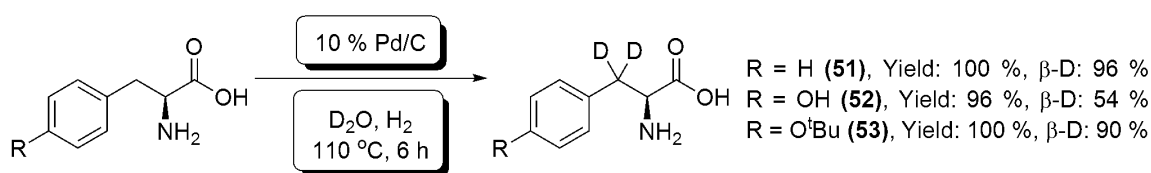


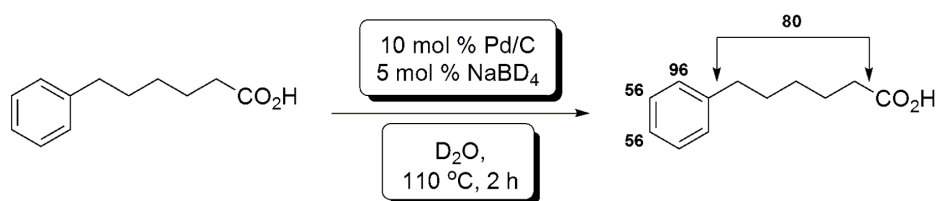
Figure 12: Deuteration of various aromatic substrates utilising 5 mol % Pt/C and D₂O; by Sajiki *et al*

Sajiki *et al* have also applied this exchange system successfully to the deuteration of (*S*)-phenylalanine (**51**) in the β-position, affording 98 % deuterium incorporation. However, an elevated reaction temperature of 110 °C was required (Scheme 11). Despite the high temperature, no racemisation of the starting material occurred during the reaction. These conditions were also successful in obtaining deuterated tyrosine derivatives (Scheme 11, (**52**) and (**53**)).⁷⁴



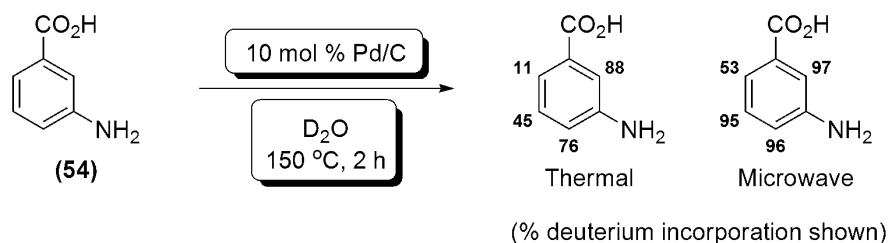
Scheme 11: Deuteration of (*S*)-phenylalanine (51**), (*S*)-tyrosine (**52**), and (*S*)-4-*tert*-butoxyphenylalanine (**53**) utilising 10 mol % Pd/C in D₂O; by Sajiki *et al***

Also recently, the work of Derdau and Atzrodt of Sanofi-Aventis has demonstrated that by utilising sodium borodeuteride to activate the heterogeneous metal catalyst by reduction, the need for an H₂ atmosphere as detailed in the previous paragraphs could be eliminated. This is advantageous due to the hazards of H₂ within a laboratory. It was shown that H/D exchange could proceed with good deuteration (*c.a.* 70 %) of various benzene derived substrates with as little as 5 mol % sodium borodeuteride (Scheme 12).⁷⁵



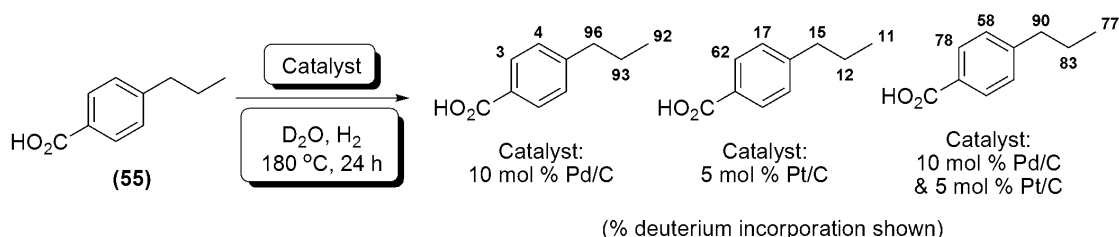
Scheme 12: Deuteration of phenylbutyric acid (54**) utilising heterogeneous metal catalysed hydrogen deuterium exchange; by Derdau and Atzrodt**

Further to this, experiments utilising microwave heating have resulted in an increase in deuterium uptake at shorter reaction times.⁷⁶ For example, the H/D exchange reaction of 3-aminobenzoic acid (**54**) was carried out under both thermal, and microwave conditions at 150 °C. After 2 hours, the microwave mediated reaction showed increased deuterium incorporation, with an average incorporation of 85 % over the four aromatic positions, compared to 55 % for the thermal reaction (Scheme 13).



Scheme 13: Thermal, and microwave mediated H/D exchange reaction of 3-aminobenzoic acid (54**) utilising 10 mol % Pd/C**

As a final note on heterogeneous palladium and platinum based catalytic systems for H/D exchange; it has been noted by Sajiki *et al* that utilising a mixed palladium and platinum on carbon catalyst can lead to a synergistic effect; increasing deuteration levels, and also allowing for deuteration of both aliphatic and aromatic positions (Scheme 14).⁷⁷

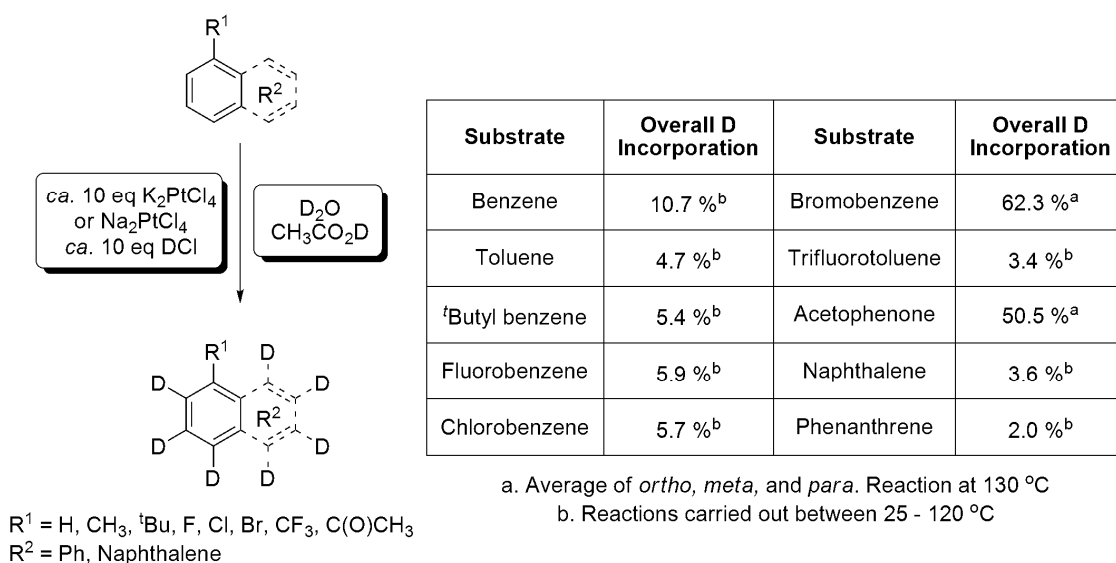


Scheme 14: Increased deuterium incorporation within 4-propyl benzoic acid (55**) upon the use of a mixed palladium/platinum on carbon catalyst, in D₂O; by Sajiki *et al***

1.5.3.4: Synthesis of Deuterated Compounds: Post Synthesis Methods – Homogeneous Metal Catalysed H/ D Exchange

The application of homogeneous metal catalysed exchange was developed around 1960, one such example of this being the work of Garnett *et al*, who demonstrated that aromatic systems (*i.e.* bromobenzene, nitrobenzene, naphthalene, and acetophenone) underwent H/D exchange after treatment with a sodium (or potassium) chloroplatinite/deuterium oxide system modified by the addition of *ca.* 10 equivalents of hydrochloric acid. The acid was required in order to prevent precipitation of the metal catalyst. This system showed deuterium incorporation ranging from 8.5 % up to 90 %, with reaction times ranging from 2 to 10 h at 130 °C.^{78,79} Selected results are shown below

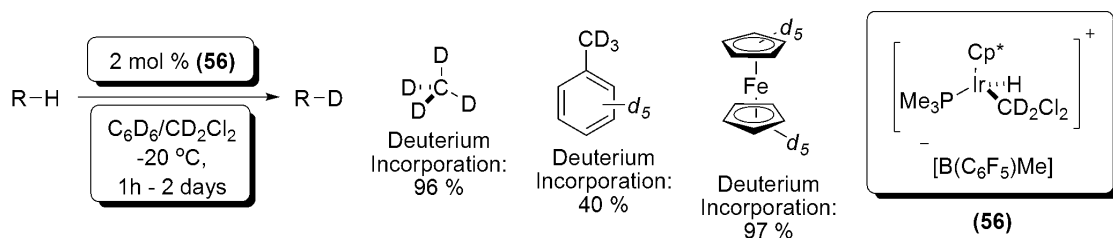
(Scheme 15). It is also worthy of note that, strictly speaking, sodium or potassium chloroplatinite are not true catalysts, due to the stoichiometric amounts required.



Scheme 15: Deuteration of aromatic substrates utilising a sodium, or potassium chloroplatinite system; by Garnett *et al*

1.5.3.4.1: Homogeneous Metal Catalysed H/D Exchange – Iridium (II) catalytic systems

Today, the area which is of most interest in homogeneous metal catalysed H/D exchange is that based upon iridium (I) and (II) catalysts. Within Ir(II) catalysed H/D exchange chemistry, particularly of note is the work of Bergman *et al*, who developed a methodology utilising [Cp*(PMe₃)IrH(CD₂Cl₂)] [B(C₆F₅)Me] (**56**) in low temperature H/D exchange. This system removed the requirement for the addition of mineral and organic acids which had been commonplace within the work of Garnett discussed previously (and within later work concerned with halide salts of Iridium).⁸⁰ Utilising *d*₆-benzene as the deuterium source, 2 mol % (**56**) allowed for deuteration of aromatic and aliphatic substrates in levels of between 40 – 97 % (Scheme 16).⁸¹



Scheme 16: Hydrogen/deuterium exchange reactions of methane, toluene, and ferrocene, catalysed by (56**); by Bergman *et al***

However, (**56**) was shown to decompose readily (*via* an ‘unknown mechanism’)⁸¹ at temperatures above -20 °C, producing the trihydride species [Cp*(PMe₃)IrH₃]⁺. Therefore, [Cp*(PMe₃)IrCl₂] (**57**) was synthesised as an air stable catalyst specifically for homogeneous hydrogen/deuterium exchange reactions. (**57**) was shown to be an active

exchange catalyst; with deuterium incorporation being demonstrated with highly water soluble organic materials (**58**) – (**63**), utilising D₂O as the deuterium source (Figure 13).

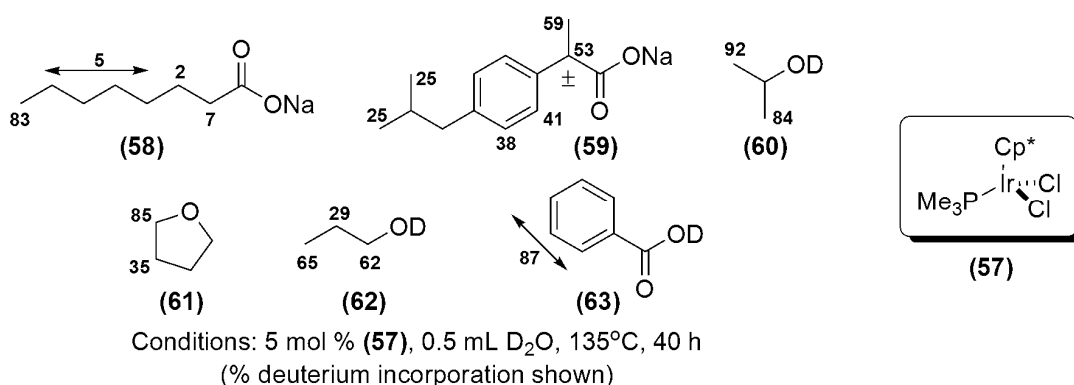


Figure 13: H/D exchange reactions of substrates (58**) to (**63**), catalysed by 5 mol % (**57**)**

However, despite successfully catalysing the incorporation of deuterium, (**57**) proved vulnerable to decomposition by disproportionation (Figure 14).⁸² In fact, no further deuterium exchange was observed when reaction times were over 40 h at 135 °C. This was shown to be due to the formation of $[\text{Cp}^*(\text{PMe}_3)_2\text{IrCl}][\text{Cl}]$ (**64**) and $[\text{Cp}^*\text{IrCl}_2]_2$ (**65**), driven by the formation of the ionic species (**64**), due to the polar nature of the solvent. Interestingly, (**64**) proved to be catalytically active for deuterium exchange (albeit to a low level); however a 1:1 mixture of (**64**) and (**65**), *i.e.* the decomposition product of (**57**), was inactive. This placed a limit of 40 h on reaction times, and thus a limitation on the catalyst.

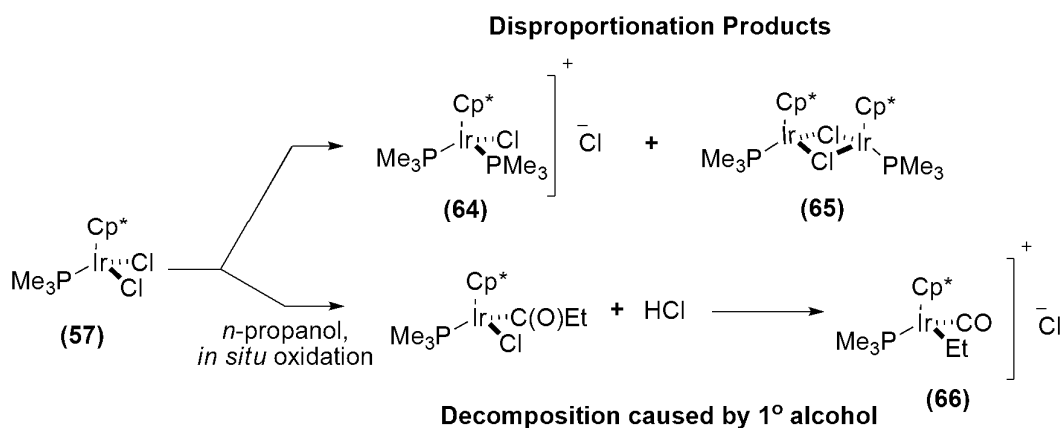


Figure 14: Decomposition pathways of (57**)**

Unfortunately, when utilised in the H/D exchange reactions of primary alcohols *e.g.* *n*-propanol, (**57**) decomposed to form $[\text{Cp}^*(\text{PMe}_3)\text{Ir}(\text{CO})(\text{Et})][\text{Cl}]$ (**66**). This was hypothesised to be due to the *in situ* oxidation of the substrate alcohol to the corresponding aldehyde; which could then undergo C-H activation to form an acyl complex with the catalyst (Figure 14). From this point, facile decarbonylation of the ligand would form the observed product (**66**).

Hoping to improve upon (**56**), and (**57**), and eliminate the disproportionation issue, Bergman *et al* synthesised a series of iridium based catalysts incorporating chelating Cp*-phosphine bridged ligands (Figure 15). However, only (**71**) and (**72**) proved active in deuterium exchange reactions; deuterating diethyl ether to 33 % and 40 % respectively (compared to the value of 36 % for the previous catalyst (**57**)).⁸² As well as showing no significant improvement in activity compared to (**57**), (**71**) and (**72**) also underwent decomposition. Unfortunately, the decomposition products could not be identified readily as they appeared to be non-active in both ³¹P- and ¹H-NMR.

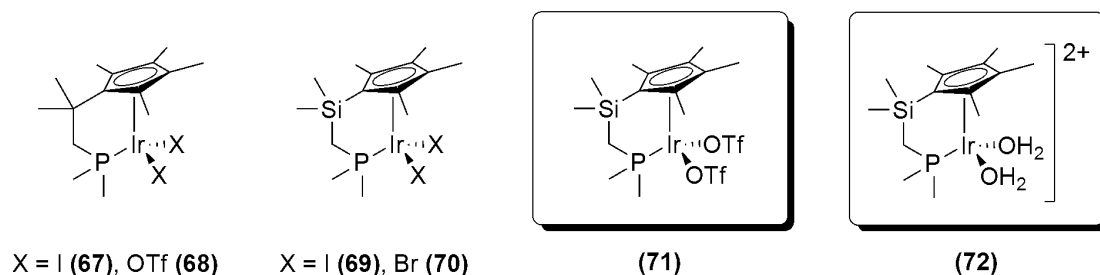


Figure 15: Cp*-phosphine bridged catalysts synthesised by Bergman *et al* for hydrogen/deuterium exchange reactions

Further to their work on water soluble catalysts for exchange, Bergman *et al* also applied a previously synthesised C-H activation catalyst to the issue of hydrogen/deuterium exchange reactions, which allowed the use of non-aqueous conditions.⁸³ This catalyst was the trihydride species [Cp*(PMe₃)Ir(H₃)OTf] (**73**).⁸⁴ Initially, *d*₁-methanol was used as the deuterium source; however, a test deuteration of benzene utilising *d*₁-methanol and (**73**) showed no deuterium incorporation. Switching the deuterium source to *d*₄-methanol interestingly did show deuterium exchange into benzene of 95 %. This result suggesting that the deuterium source in the reaction came from C-D bond activation followed by transfer. Further to this, switching to *d*₆-acetone as the deuterium source increased incorporation levels further still (99 % D incorporation into benzene at 135 °C). Screening of (**73**) (utilising *d*₆-acetone) with a broad range of substrates showed a tolerance for functionality; with successful substrates including 2,6-dimethylpyridine, *N*-phenylacetamide, methyl benzoate, and ferrocene (Figure 16).

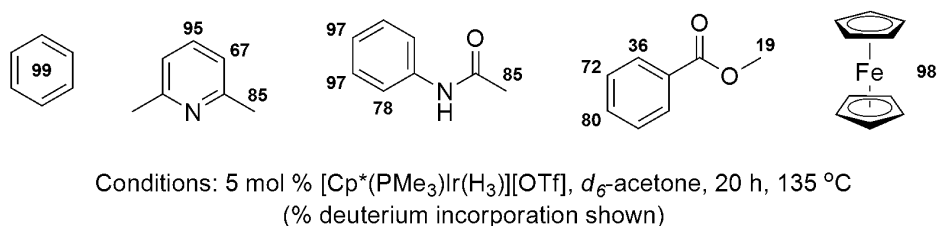


Figure 16: H/D exchange with substrates bearing differing functionality, utilising (73**), and *d*₆-acetone; by Bergman *et al***

Having taken note of the work of Bergman *et al*, Peris *et al* developed a further catalytic method for deuterium exchange, utilising iridium(II) based species, bearing *N*-heterocyclic carbene ligands.⁸⁵ The pro-catalyst iridium halide species (**74**) was treated with silver triflate in solution to generate the active species (**75**) (Figure 17), which could then utilise either *d*₄-methanol, or *d*₆-acetone as a deuterium source (*d*₄-methanol afforded greater deuterium incorporation with shorter reaction times) (Figure 17).

Interestingly, no decomposition of (**75**) was observed during the deuteration of 2-propanol; unlike the deuteration reactions of primary and secondary alcohols attempted by Bergman *et al*, utilising (**57**), which resulted in decomposition of the catalyst or the substrate (See Figure 14).

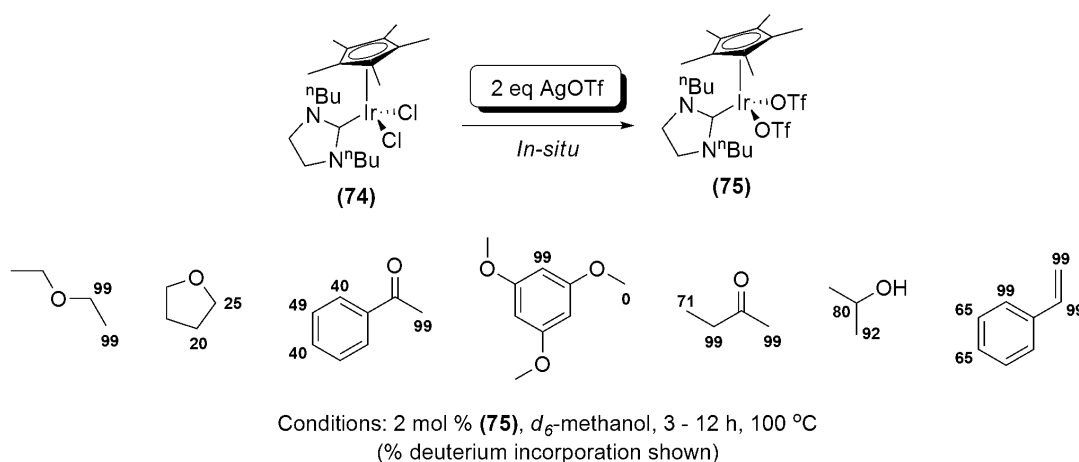


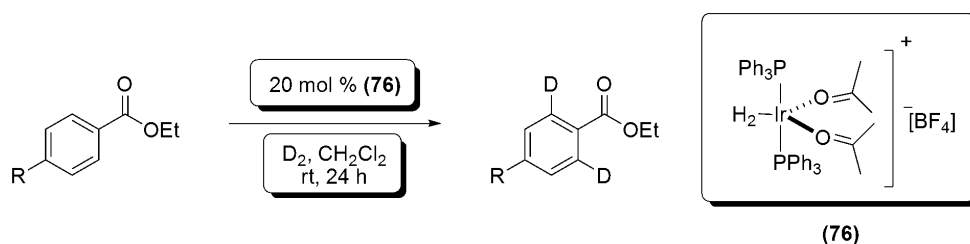
Figure 17: Selected results for H/D exchange reactions using (75**); carried out by Peris *et al***

In summary, while Ir(II) catalysts have shown potential for H/D exchange, and in general, high deuterium incorporation (*i.e.* 98 % deuteration of ferrocene utilising 5 mol % (**73**)); methods tend to rely upon high reaction temperatures (90 °C – 135 °C within the examples given), and do not allow much selectivity when introducing deuterium into molecules. They also tend to rely upon either difficult to synthesise catalysts, or catalysts which are unstable (*i.e.* (**56**), or (**57**)), and thus difficult to use in a robust synthetic procedure.

1.5.3.4.2: Homogeneous Metal Catalysed H/D Exchange – Iridium (I) catalytic systems

The development of the now ‘state of the art’ of homogeneous metal based catalysis for hydrogen/deuterium exchange reactions (*i.e.* systems utilising iridium(I) catalysts)⁸⁶, began with the observation by Heys *et al* that [(PPh₃)₂IrH₂(Me₂CO)₂]BF₄ (**76**) could catalyse the incorporation of deuterium into various heteroatom containing organic compounds. For example, treatment of *tert*-butoxybenzene with 2.5 mol % (**76**) under 1 atm of D₂, gave selective deuteration at the 2-, and 6- positions with overall 90 %

incorporation.⁸⁷ Further work by Heys *et al* expanded upon this study, hoping to gain an understanding of the scale of the observed *ortho*- directing effect (Scheme 17).⁸⁸

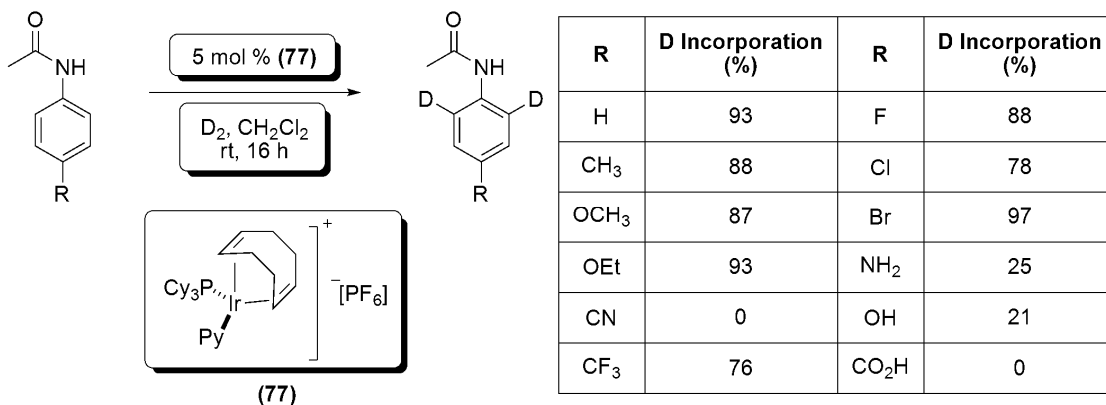


R	mol D/mol (<i>ortho</i> -)	mol D/mol (<i>meta</i> -)	R	mol D/mol (<i>ortho</i> -)	mol D/mol (<i>meta</i> -)
OH	1.9	0	F	1.5	0
OMe	1.8	0	Cl	1.8	0
^t Bu	1.4	0	Br	1.6	0
OC(O)Me	1.4	0	NO ₂	1.0	0.4

Scheme 17: Deuteration of aromatic substrates catalyzed by 20 mol % (76)

As shown in Scheme 17, the observed *ortho*- directing effect was found to be relatively ‘stronger’ than the directing effects of the *R*- substituents at the *para*-position relative to the carbonyl group; with deuterium incorporation occurring at the *ortho*- position relative to the carbonyl (as opposed to the *meta*- position relative to the carbonyl *i.e.* the *ortho*- position relative to the range of directing groups).

Seeking to improve on this procedure, Hesk *et al* utilised Crabtree’s catalyst⁸⁹ [(cod)Ir(PCy₃)(Py)]PF₆ (**77**) in order to facilitate deuteration of substituted acetanilides in dichloromethane, with D₂ as the deuterium source (Scheme 18). It was observed that the reaction was relatively insensitive to substituent effects, affording generally high deuterium incorporation (between 70 % and 90 %), and that the regioselectivity of the reaction was high (with deuteration only being seen at the *ortho*- position of the aromatic, relative to the carbonyl substituent). A few exceptions to this were observed, including OH substituted acetanilides, which underwent deuteration to a poor level of only 21 % (attributed to low solubility in the reaction solvent), and *para*-cyano substituted acetanilides, which underwent no appreciable deuteration (presumably due to coordination of the -CN group to the metal centre of the catalyst).⁹⁰



Scheme 18: Hydrogen/deuterium exchange reactions of substituted acetanilides utilising 5 mol % (77); by Heys *et al*

The selectivity of the Ir(I) based systems towards incorporation of deuterium in the *ortho*- position relative to carbonyl functionalities was first rationalised by Heys *et al*. Their work demonstrated that (76) selectively catalysed hydrogen exchange three bonds away from the directing heteroatom, whereas Crabtree's catalyst (77) showed selectivity four bonds away (See Figure 18 and Schemes 17 & 18).

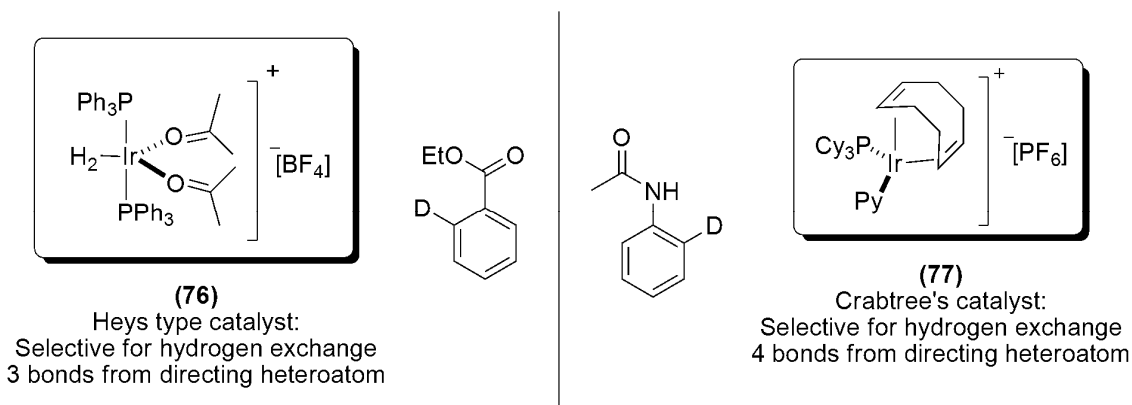


Figure 18: Structures of (76) and (77); and the regioselectivity of their hydrogen/deuterium exchange reactions

The rationale forwarded by Heys *et al* for this effect was based upon the formation of two different metallacycle species within the catalytic cycle, depending upon the catalyst employed; these being a 6-membered cycle when (77) was employed, and a 5-membered cycle when (76) was employed. To prove this, Heys *et al* employed two catalysts with differing stereochemistry about their metal centres, [Ir(cod)(PPh₃)₂][BF₄] (78) and [Ir(cod)(dppe)]PF₆ (79), and compared the regioselectivity observed when each catalyst was utilised within the deuteration of ethyl 1-naphthoate (80).

It was believed that by introducing two bulky phosphine ligands (in the case of (78)), *trans*-stereochemistry around the metal centre would be preferential; meaning that if the 5-membered metallacycle was formed, the substrate would be in a differing plane to the large triphenylphosphine ligands. Whereas, in order to form the 6-membered

metallacycle, *cis*-stereochemistry of the triphenylphosphine ligands would be required, which is disfavoured by sterics. Therefore preferential formation of the 5-membered metallacycle would lead to selectivity three bonds away from the directing heteroatom (Figure 19). In the case of **(79)**, the bidentate phosphine ligand would form *cis*-stereochemistry around the metal centre (due to the tethered nature of each phosphine), and the reduced size of the phosphine would reduce the steric hindrance to the formation of a 6-membered metallacycle; thereby allowing deuteration at the position four bonds away from the directing group (Figure 19).

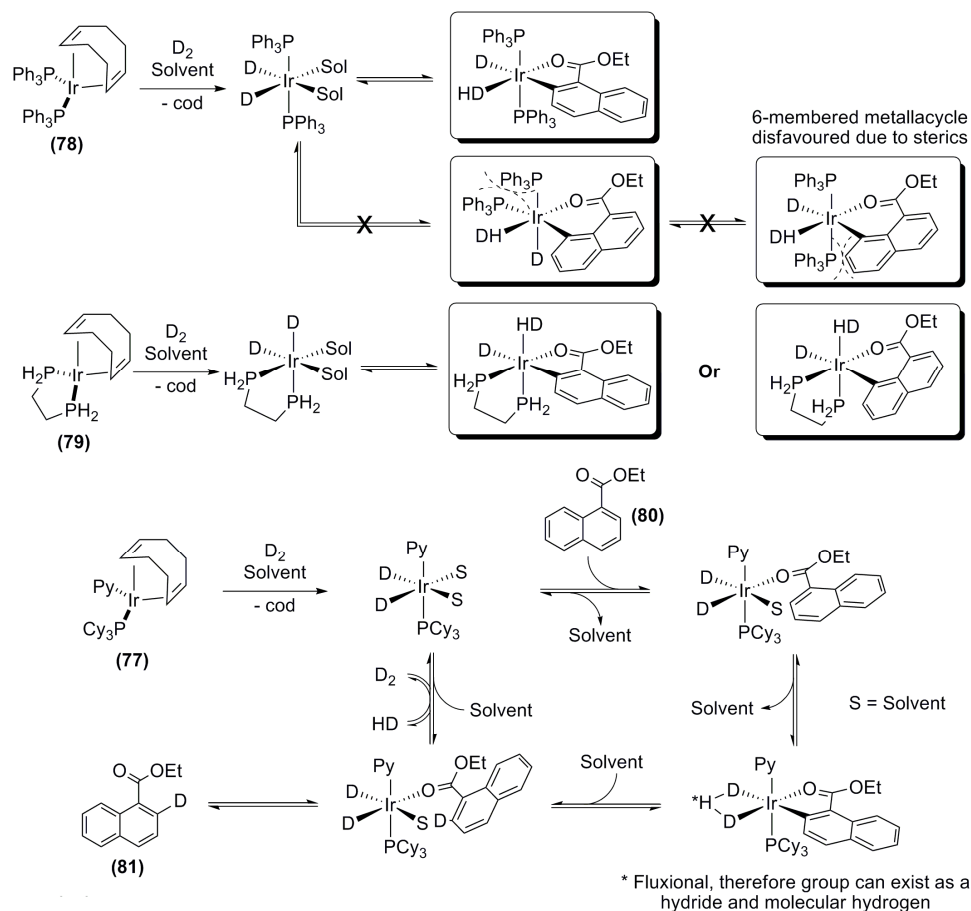


Figure 19: Mechanistic rationale for *ortho*-exchange and general catalytic cycle for **(77), **(78)**, & **(79)****

This rationale was found to be correct, as with **(78)**, deuterium was incorporated selectively at the C2 position of ethyl 1-naphthoate (90 % D incorporation, **(81)**), whereas with **(79)**, 54 % incorporation was seen at C2, and 35 % at C8 (Figure 20). Therefore, it was concluded that the relative steric bulk, and orientation of the ligands about the metal centre is the cause for the selectivity of the exchange reactions detailed.⁹¹

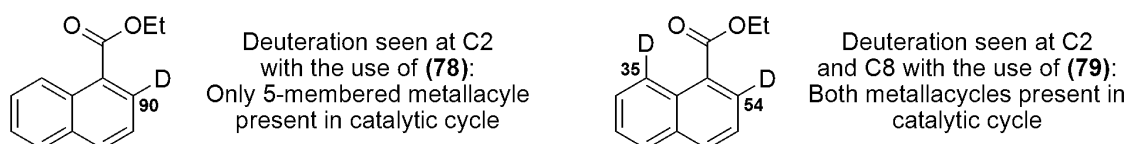


Figure 20: Deuteration of ethyl 1-naphthoate utilising **(78), or **(79)** and D₂; by Heys *et al***

Although these catalysts (*i.e.* the Crabtree, and Heys types) allow for a broad range of exchange reactions, they do have some disadvantages *i.e.*: high catalyst loading (some examples require equimolar loading or higher), and difficulty in removal of the catalyst from the crude material (due to high loading). Some progress has been made towards reducing these problems by the development of a polymer bound form of **(77)**, **(82)**. The use of a polymer bound catalyst allows purification by simple filtration; as opposed to the difficult chromatographic separation of a large amount of homogeneous catalyst. **(82)** was produced by treatment of Crabtree's catalyst **(77)** with commercially available polystyrene bound triphenylphosphine. Displacement of both the cyclooctadiene, and pyridine ligands leads to formation of the polymer bound species. **(82)** is stable at -20 °C for up to 2 months, and shows similar activity to the free catalyst (Figure 21).^{86,92}

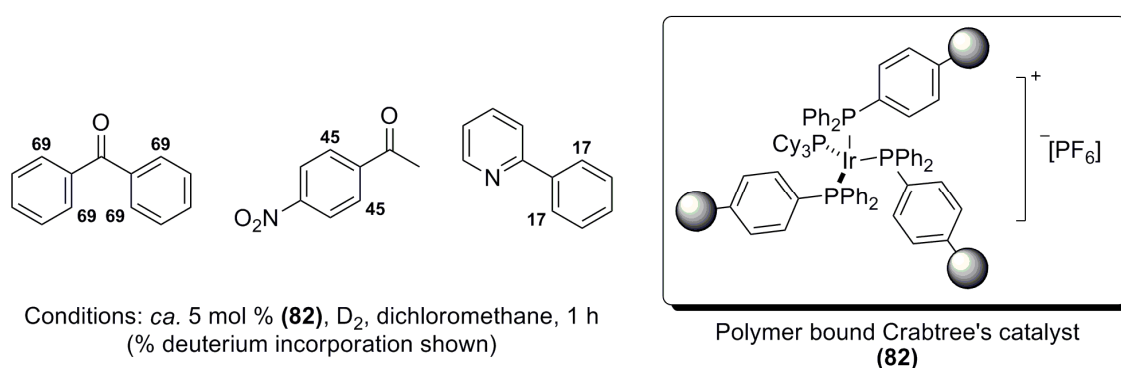
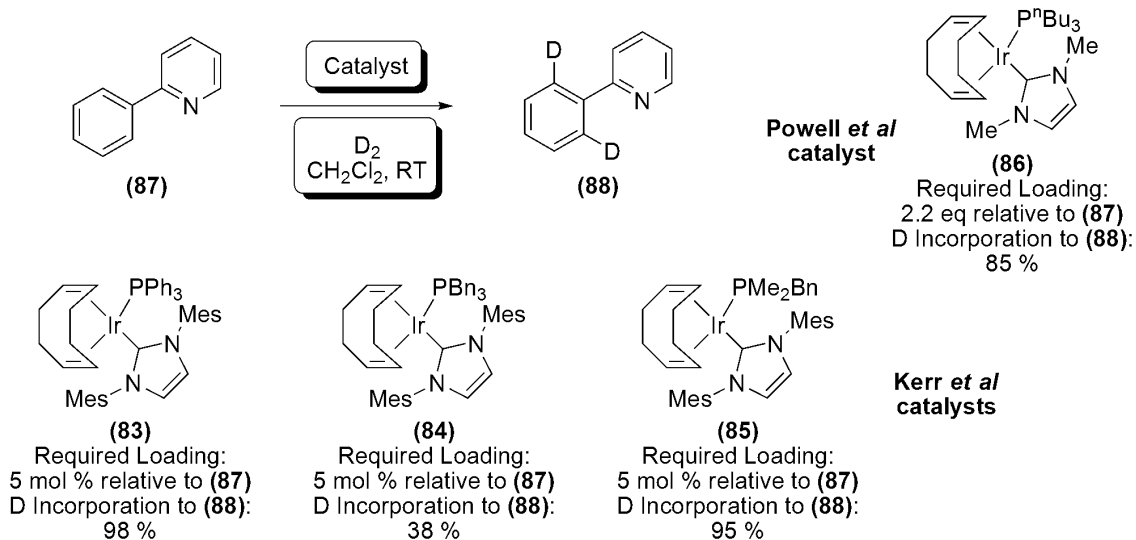


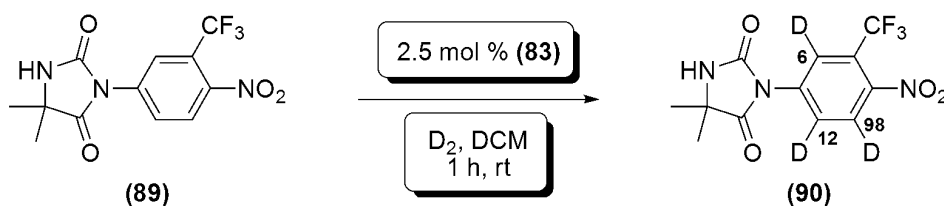
Figure 21: H/D exchange reactions catalysed by polymer bound Crabtree's catalyst (82)

Further to the work of Heys *et al*, the groups of both Kerr and Powell have investigated the use of carbene ligands to produce an Ir(I) H/D exchange catalyst with higher stability, and hopefully increased activity. In the case of Kerr *et al*, the carbene chosen was 1,3-*bis*(2,4,6-trimethylphenyl)imidazole-2-ylidene (IMes), and the phosphine ligands chosen were triphenyl (catalyst **(83)**), tribenzyl (catalyst **(84)**), and dimethylbenzyl (catalyst **(85)**).⁹³ In the case of Powell *et al*, the system was based upon *bis*-methylimidazole-2-ylidene, with an *n*-butylphosphine ligand (catalyst **(86)**).⁹⁴ Both systems showed high activity for H/D exchange reactions, however, a direct comparison reveals that the Powell system requires a loading of 2.2 equivalents of the catalytic species (technically not a true 'catalyst' due to the required stoichiometric loading), whereas, the Kerr systems only require 5 mol % loading. Also, a direct comparison of deuterium incorporation levels with the same substrate shows that, in general, the Kerr system was more effective (Scheme 19).



Scheme 19: Direct comparison of the carbene catalysts produced by Powell *et al*, and Kerr *et al*

Not only did the carbene catalysts show good reactivity, they were also air stable, making them more attractive to work with in a laboratory environment. Kerr *et al* went on to demonstrate the effectiveness of their system by performing deuteration of the Sanofi-Aventis drug nilutamide. Treating nilutamide (89) with 2.5 mol % of (83), and D₂ gas in DCM gave, in the majority, selective single deuteration of 98 % in 1 hour at room temperature (Scheme 20).⁹⁵



Scheme 20: Deuteration of nilutamide (89) utilising 2.5 mol % (83), and D₂; by Kerr *et al*

1.5.3.4.3: Homogeneous Metal Catalysed H/D Exchange - Rhodium based catalytic systems

The use of rhodium based homogeneous H/D exchange catalysts was first reported by Garnett *et al*, utilising rhodium trichloride (no stoichiometry given) to catalyse isotopic hydrogen exchange in simple aromatic systems (*i.e.* benzene, and toluene), with no major selectivity (Figure 22). However, it was shown that the reactions were much slower than with the corresponding chloroplatinite (Scheme 15) or iridium based systems.^{96,97}

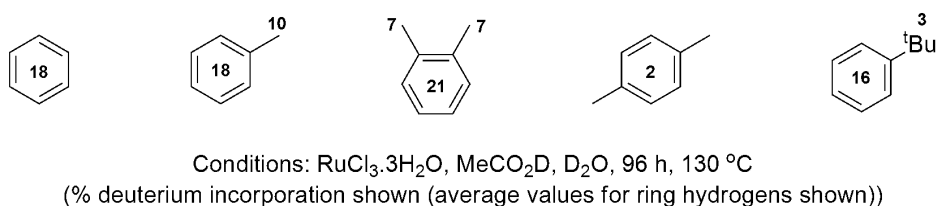
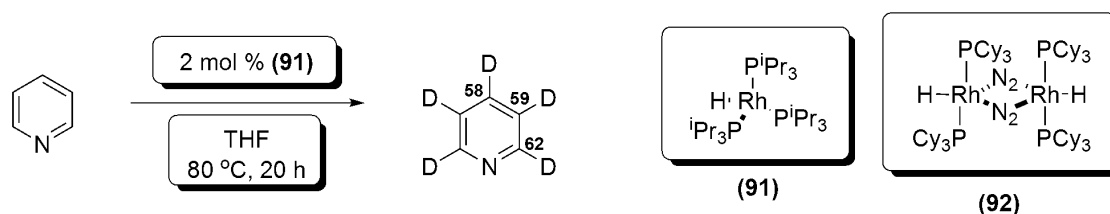


Figure 22: H/D exchange reactions catalysed by rhodium trichloride; by Garnett *et al*

Soon after this report, Otsuka *et al* published their work on the isolation of two rhodium based H/D exchange catalysts. These being $\text{RhH}[\text{P}(\text{iPr})_3]_3$ (**91**), and the dimeric species $\text{Rh}_2\text{H}_2(\mu\text{N}_2)[\text{P}(\text{Cy})_3]_4$ (**92**). These were shown to catalyse incorporation of deuterium in a relatively non-selective manner over simple ring systems (*i.e.* benzene, toluene, anisole, and pyridine (Scheme 21)).⁹⁸



Scheme 21: Deuteration of pyridine utilising 2 mol % (91); by Otsuka *et al*

The mechanism for the exchange cycle that was proposed involved oxidative addition of D_2O to the metal centre, followed by reductive elimination of partially deuterated water to produce (**93**). The substrate is then added to the metal centre by oxidative addition, and finally, the deuterated substrate is expelled *via* reductive elimination. This regenerates the active catalyst ready for the addition of a second molecule of D_2O (Figure 23).

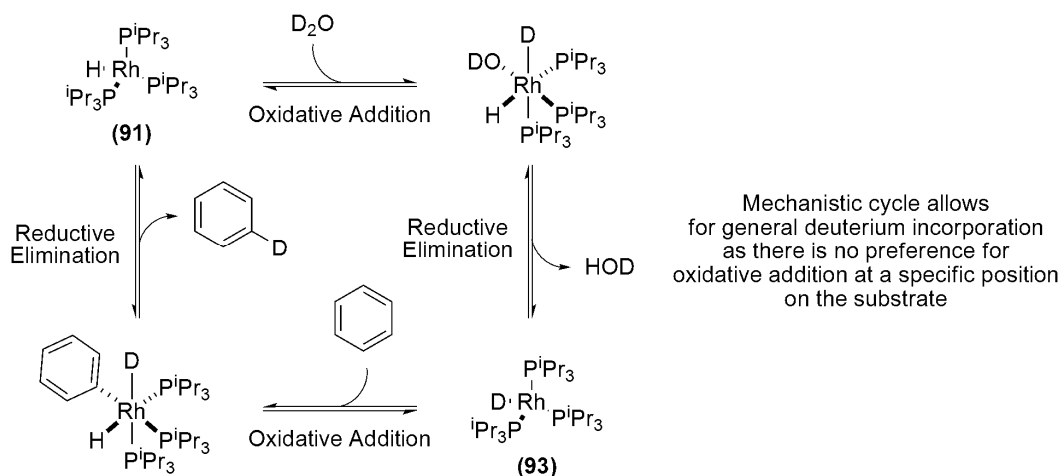


Figure 23: Proposed catalytic cycle for the deuteration of simple ring systems by (91); proposed Otsuka *et al*

More recently, Brookhart *et al* demonstrated that a rhodium based system $[\text{Cp}^*\text{Rh}(\text{CH}_2\text{CHSi}(\text{CH}_3)_3)_2]$ (**94**) was active in catalysing H/D exchange from d_6 -benzene to aromatic and aliphatic systems. These included aniline, ferrocene, di-*tert*-butyl ether, and cyclopentene (Figure 24).

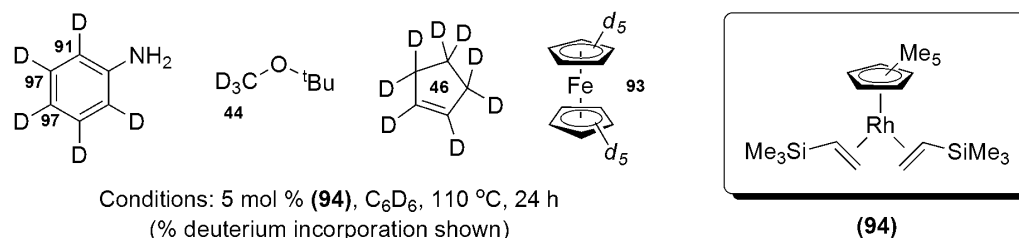


Figure 24: Deuteration of aromatic and aliphatic substrates catalysed by (94); by Brookhart *et al*

This method is interesting as it appears to occur *via* a ‘shuttle’ process, in which deuterium is first transferred to the silyl ligands of **(94)**, then transferred to the substrate after C-H activation (Figure 25). Evidence for this process was provided by monitoring the ¹H-NMR signals related to the vinyl silane ligands, while the catalyst was heated at 78 °C in a deuterated solvent (in this case, *d*₆-benzene). A significant reduction in the ¹H-NMR signals for the silane ligands was observed after 4 hours. The signals for the silane ligands were then noted to increase in intensity when a substrate was added, and heating was continued for a further week.⁹⁹

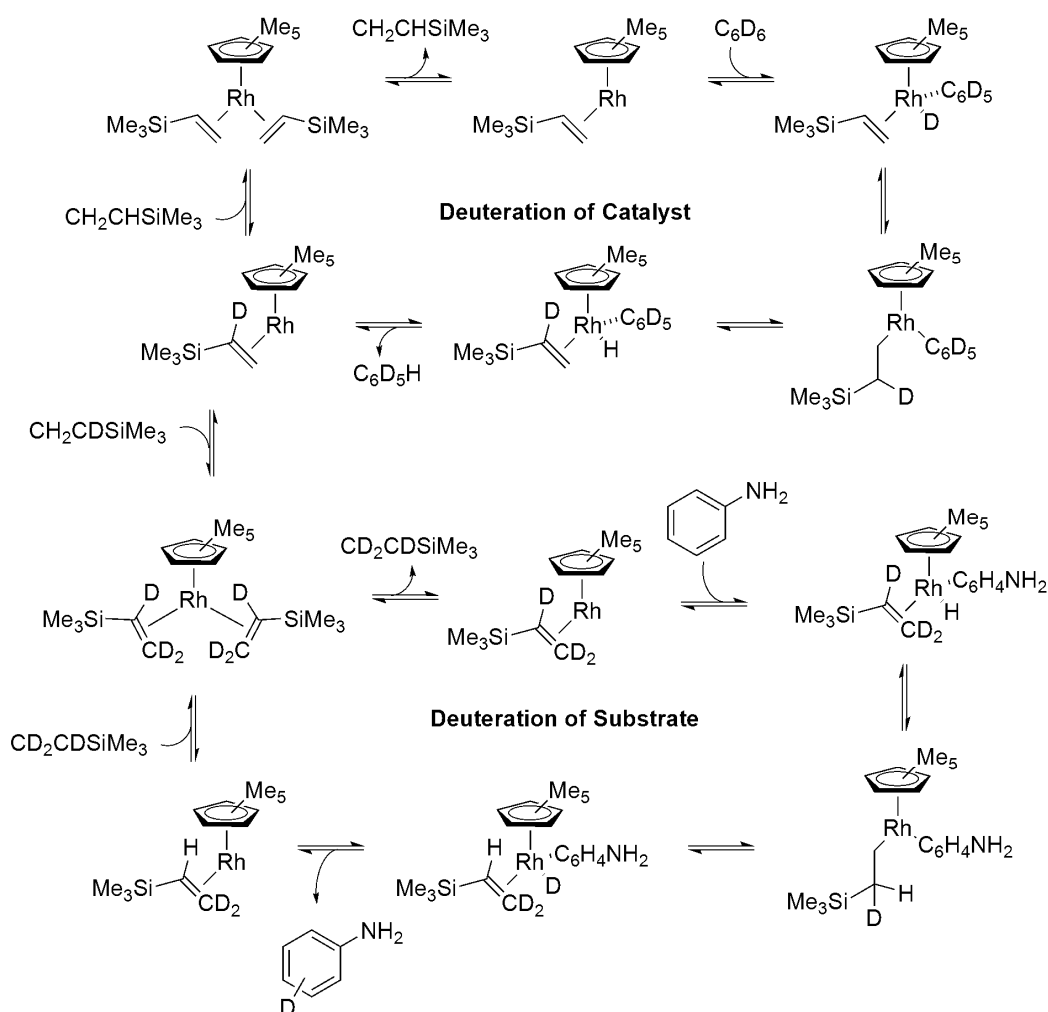


Figure 25: Proposed ‘shuttle’ process for the deuteration of aromatic and aliphatic systems catalysed by (94); by Brookhart *et al*

As a final note, there are many differing metal centred catalysts in the literature which have shown potential for H/D exchange;¹⁰⁰⁻¹⁰⁵ however, in the majority these have not been developed for the synthetic production of deuterated substrates, and are much less widely discussed within the literature. Therefore these are not explored in more detail here.

In summary, metal based homogeneous catalysis of hydrogen/deuterium exchange is potentially the most widely researched form of deuterium incorporation reaction. Of these catalysts, Ir(I) based systems are currently the 'state of the art', as generally they allow for regioselective introduction of deuterium, due to the *ortho*-exchange effect. Ir(I) systems also allow for high levels of deuterium incorporation (*i.e.* >70 %), and do not require the high reaction temperatures, and specialised equipment, utilised in HTDA, or supercritical exchange procedures. However, these metal based catalysis systems tend to utilise D₂ or deuterated solvents as the deuterium source; both of which are expensive, and carry environmental concerns when compared to the use of D₂O.

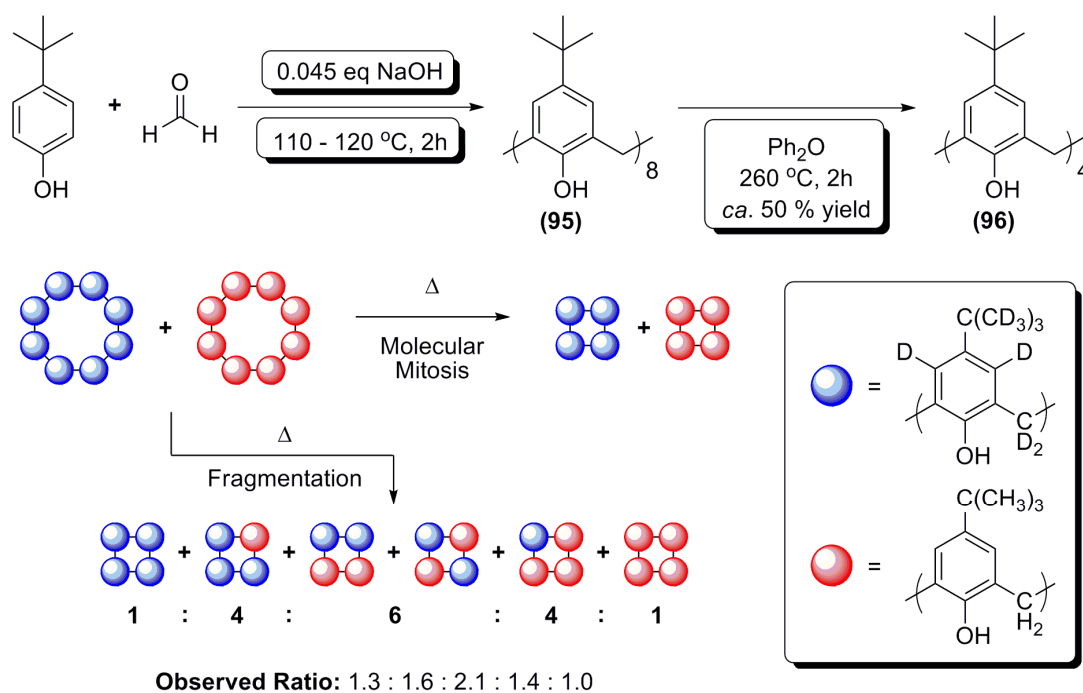
1.6: Applications of Deuteration and the Kinetic Isotope Effect in Mechanism and Metabolism Studies

Deuterium labelling has proven an invaluable tool in the study and elucidation of reaction mechanism and the metabolism of synthetic and natural compounds *in vivo*. Several representative examples of the potential uses of deuterium in this manner are discussed below.

Deuterium labelling has found significant use within synthetic chemistry for the elucidation of reaction mechanisms. For example, the synthesis of *para-tert*-butylcalix[4]arenes developed by Gutsche *et al* has been investigated utilising deuterated substrates in order to track the course of the reaction. The reaction involves the pyrolysis of a precursor mixture formed from the condensation of *tert*-butyl phenol and formaldehyde, catalysed by sodium hydroxide (Scheme 22). This mixture contains predominantly *para-tert*-butylcalix[8]arene (**95**), and therefore it was postulated that *para-tert*-butylcalix[4]arene (**96**) could be formed from this *via* a fragmentation recombination reaction, or *via* a pinching of the *para-tert*-butylcalix[8]arene, followed by separation into two *para-tert*-butylcalix[4]arene moieties (the molecular mitosis pathway).

A mechanistic study was devised to test these two pathways; involving use of a 1:1 mixture of fully deuterated *para-tert*-butylcalix[8]arene and fully *proteo-para-tert*-butylcalix[8]arene. By undertaking the pyrolysis reaction with this mixture, if molecular mitosis was the only pathway, the resulting products would be either fully *proteo*- or fully *deutero-para-tert*-butylcalix[4]arene; whereas if fragmentation was occurring, scrambling of the labels would ensue, forming a range of partially deuterated *para-tert*-

butylcalix[4]arenes. If only fragmentation was occurring, the ratio of products would be a predictable quantity, as shown in Scheme 22.



i.e.: Both pathways are in effect to some extent

Scheme 22: Modified Zinke procedure for the synthesis of *para-tert*-butylcalix[4]arene, and mechanistic study; by Gutsche *et al*

Gutsche *et al* found that the ratios of deuterated and *proteo-para-tert*-butylcalix[4]arenes produced suggested that neither fragmentation nor molecular mitosis were the only pathway in effect; and in reality, both pathways occur to a certain extent.¹⁰⁶

In order to utilise deuterium labelling within *in vivo* metabolism studies, reliable techniques are required for the identification of deuterated metabolites within complex mixtures. In practice, this is facilitated by the use of labelled compounds differing from the parent compound by at least two mass units. This has the effect that when the compound is dosed as a 1:1 mixture with the parent molecule, two characteristic mass ions are seen within the mass spectrum; each with the same isotopic splitting pattern, and a mass difference of at least two. This technique allows metabolites of the substrate to be easily identified within complex mixtures, as this characteristic motif is carried throughout.

An example of this in use is the study of the metabolism of benzylamine in rats carried out by Mutlib *et al*. By dosing a 1:1 mixture of natural abundance and d_7 -benzylamine, or natural abundance and d_2 -benzylamine, they were able to follow the metabolism through a rat model (Figure 26). By sampling bile, blood, and urine with MS, ^{13}C , and $^1\text{H-NMR}$, the metabolites formed at various stages were structurally assigned, and the pathways by which they were formed, traced. This was possible due to the ability to

determine loss of the deuterium labels, corresponding to loss of hydrogen within the parent molecule, and also structural assignment by NMR, and MS-MS techniques. The group has published various facets of their work in a series of papers.¹⁰⁷⁻¹¹⁰

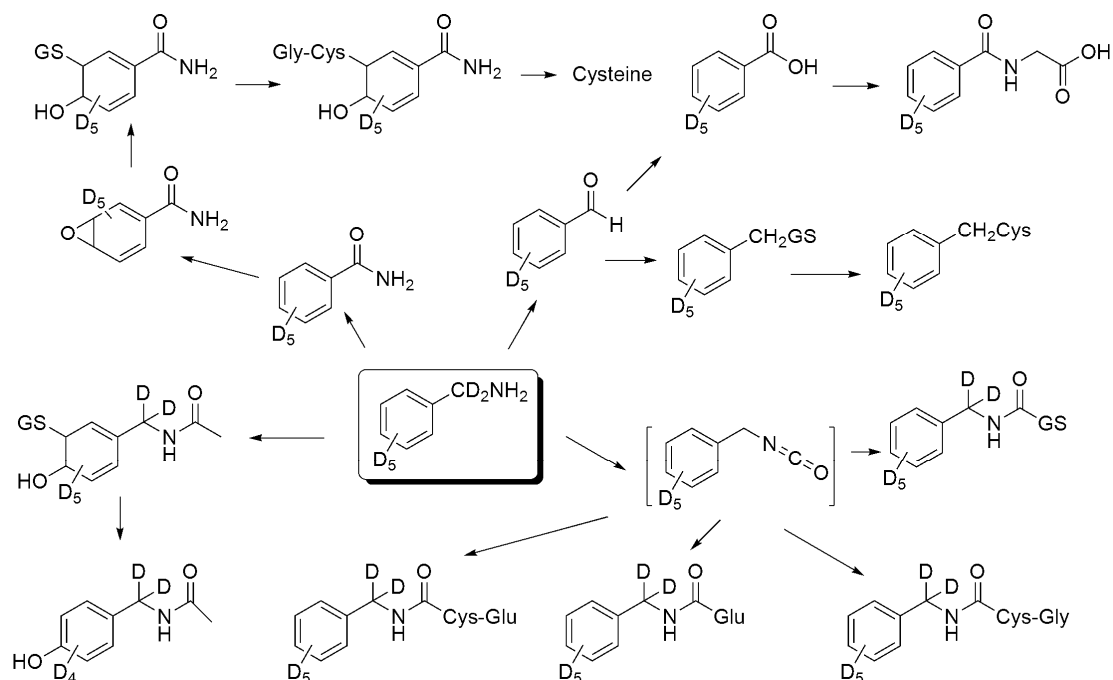
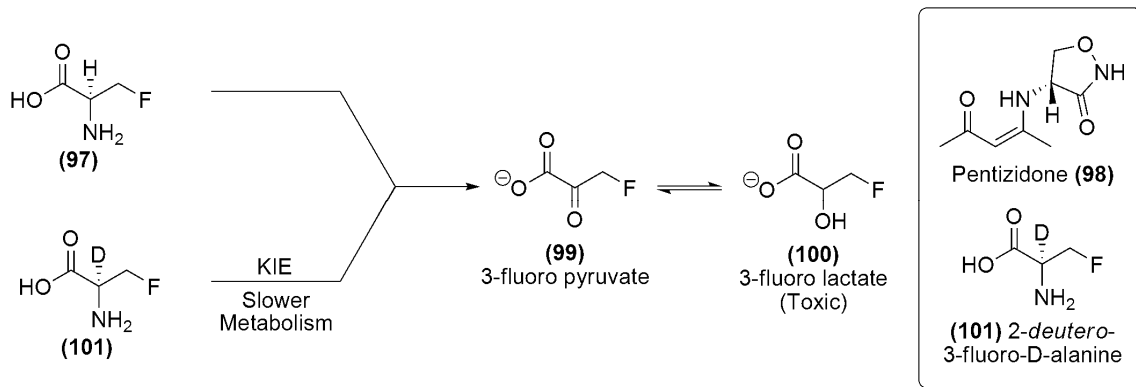


Figure 26: The rat metabolism routes of benzylamine elucidated by Mutlib *et al*

1.7: Labelling of Molecules for Pharmaceutical Effect

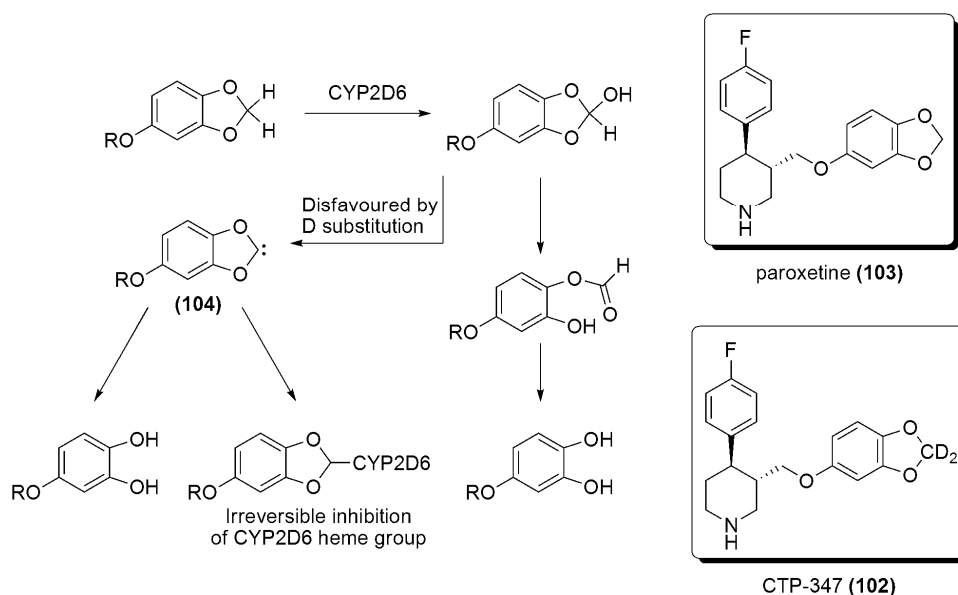
Potentially, the introduction of deuterium into a pharmaceutical molecule can convey several benefits. The two main examples of this being: extended half life within the body (due to reduced metabolism rates *via* kinetic isotope effects), and the potential to alter (or disfavour) metabolism routes, again *via* kinetic isotope effects.

An interesting example of a reduction in metabolism rate *via* deuteration is that of the Merck antibacterial combination MK0641/MK0642 (consisting of 2-*proteo*-3-fluoro-D-alanine (**97**) in combination with pentizidone (**98**)). (**97**) had shown low acute toxicity *in vitro*. However during metabolism by D-amino acid oxidase (DAO) *in vivo* 3-fluoro pyruvate (**99**) was seen to be produced. Unfortunately, (**99**) was found to be in equilibrium with 3-fluoro lactate (**100**) (Scheme 23); which has been shown to cause myelin vacuolation within the brain. In order to slow metabolism of (**97**), and allow clearance of the metabolic (**99**) produced to keep the levels of (**100**) below the concentrations implicated in myelin vacuolation, it was decided to deuterate (**97**) at the α -position, thus producing 2-*deutero*-3-fluoro-D-alanine (**101**) (Scheme 23). Initial clinical trial results proved promising,¹¹¹ with a kinetic isotope effect of 2.8 relative to DAO *in vitro*.



Scheme 23: Initial metabolism of (97) and (101), demonstrating slowed metabolism of (101) to toxic 3-fluoro lactate (100)

A more recent example of deuteration being used to disfavour a metabolism route is that of selectively deuterated paroxetine (CTP-347) (102), for which Concert Pharmaceuticals have been awarded a patent.¹¹² Initially, research interest in standard paroxetine (103) was due to its potential use as a treatment for hot flushes. However, during metabolism of (103) a metabolite structure (104) (Scheme 24) was formed which can cause irreversible inhibition of CYP2D6. This P450 cytochrome is responsible for metabolism of many drugs; therefore patients taking certain drugs could not use paroxetine (103) due to build up of toxic metabolites. The metabolism of paroxetine (103) involves cleavage of the dioxymethylene bridge contained within the molecule. As this cleavage is an enzymatic oxidative process, it was believed that replacing the dioxymethylene group with a *deutero*-dioxymethylene group, the rate of formation of (104) would be reduced, due to a kinetic isotope effect slowing the oxidative process (Scheme 24).



Scheme 24: Proposed Mechanism for Inhibition of CYP2D6 by (104), a metabolite of paroxetine (103)

Indeed, CTP-347 (**102**) was found to exhibit greatly reduced inhibition of CYP2D6 when compared to paroxetine.¹¹² When submitted to clinical trials, phase I results indicated that the use of CTP-347 (**102**) substantially preserved the enzyme's (CYP2D6) activity in patients.¹¹³

Various other examples of deuterated pharmaceuticals have arisen in the last 15 years, with research interest within the last 5 years growing significantly. Areas of research include pain medication (deuterated (\pm)-*cis*-tramadol (**105**),¹¹⁴ Sepracor Inc.), and HIV protease inhibitors (deuterated atazanavir (CTP-518, (**106**)),¹¹⁵⁻¹¹⁷ and darunavir (**107**),¹¹⁸ Concert Pharmaceuticals) (Figure 27).

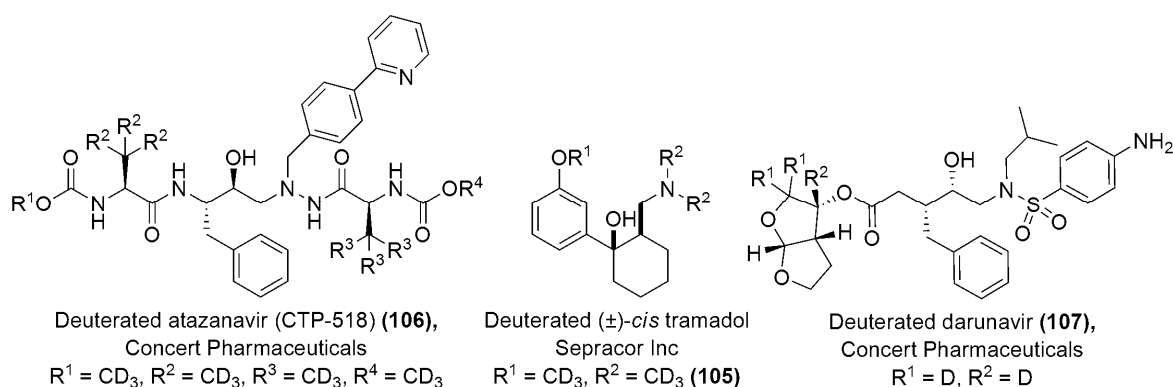


Figure 27: Structures of the deuterated pharmaceuticals (105), (106), and (107)

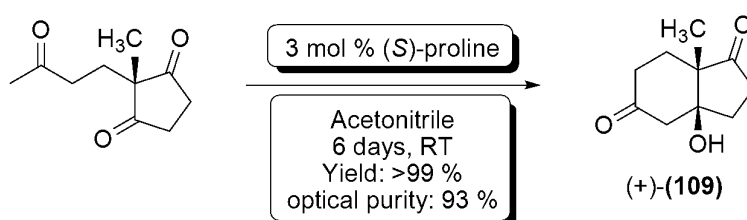
Due to the current interest in the area of deuterated compounds and the potential benefits of deuterated pharmaceuticals; the author believes it is only a matter of time before one or more of these potentially advantageous compounds pass clinical trials, and become readily available on the market. However, there are several patent issues related to the production of deuterated pharmaceuticals. For example, does changing a single nucleus from protium to a deuteron upon a patented molecule constitute a departure from the patent? Therefore, pharmaceutical companies have become much more wary of the isotopic constitution of their patented molecules in order to ensure maximum protection. Despite these issues, the possibility of developing tailored deuteration in order to induce pharmaceutical effects within molecules will be sure to affect the course of pharmaceutical development for years to come.

Chapter 2: Organocatalysis

2.1 Organocatalysis: A Brief Early History

As a topic, the field of organocatalysis is concerned with the use of organic molecules as catalysts to either allow reaction, or to induce stereoselectivity within a reaction. The definition of an organocatalyst being: "...catalysts (usually small organic molecules) with low molecular weights (<1000g/mol) where a metal is not part of the active principle".¹¹⁹

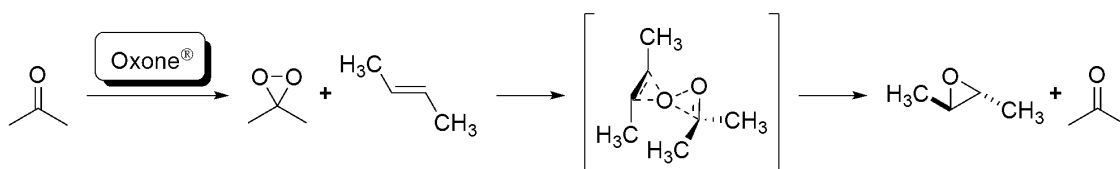
The most well known early example of organocatalysis is the use of (*S*)-proline (**108**) by Hajos *et al* in 1974 to catalyse the formation of the optically active symmetric diketone (**109**) via an asymmetric aldol cyclisation (Scheme 25).¹²⁰



Scheme 25: Organocatalytic asymmetric aldol reaction of symmetric diketone species (109**) utilising 3 mol % (*S*)-proline (**108**); by Hajos *et al***

Despite the high stereoselectivity and excellent yield achieved by Hajos *et al* within the reaction detailed above, the general use of organocatalysis in synthesis was not seen within the literature until the mid 1990s; when a series of papers were independently published by Denmark *et al*, Shi *et al*, and Yang *et al*; concerned with the use of chiral ketones as catalysts for the epoxidation of *trans*-alkenes.

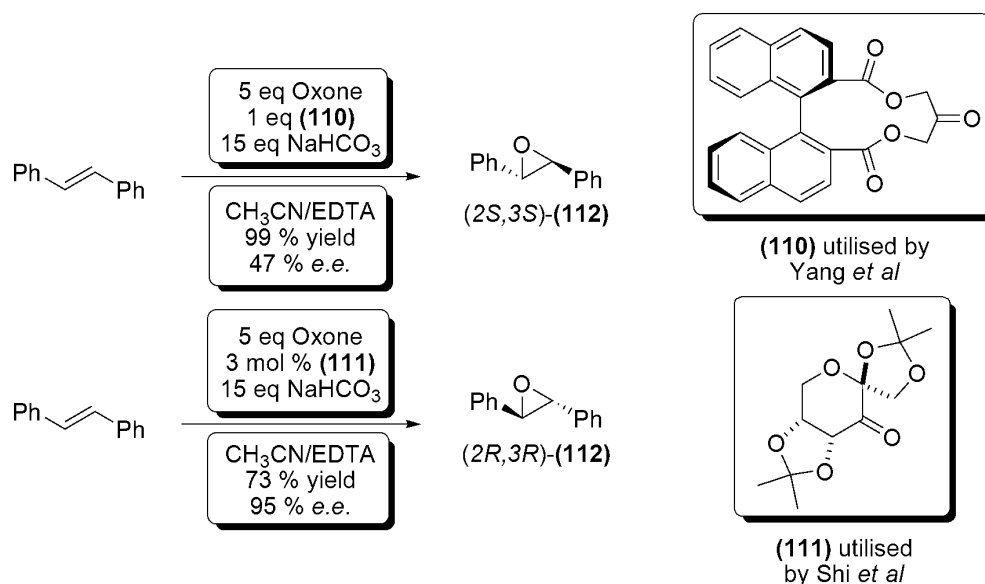
The mechanism of these epoxidation reactions involves oxidation of the catalyst ketone with Oxone[®], producing a reactive dioxirane species. This species subsequently oxidises the substrate alkene, producing the desired epoxide, and regenerating the ketone catalyst (Scheme 26).¹²¹ The proposed spiro transition state allows for both retention of the configuration of the alkene starting material, and provides some explanation as to the enantioselectivity observed when chiral ketones are utilised.¹²²



Scheme 26: Proposed spiro transition state within the epoxidation of alkenes catalysed by the formation of an intermediate dioxirane species; by Houk *et al*

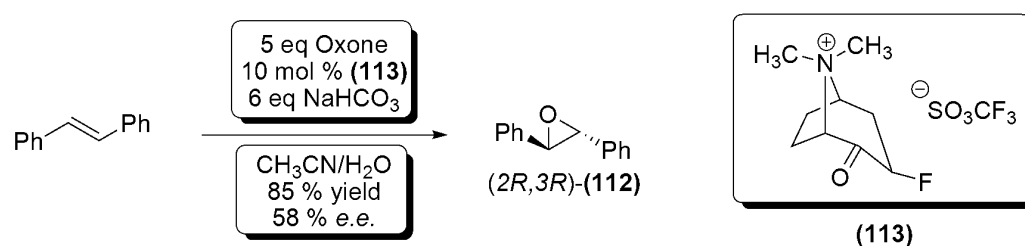
The initial papers by the groups of Yang *et al* and Shi *et al* reported *e.e.*'s ranging from 5 – 87 %, and 70 – 95 % respectively for a range of substrate *trans*-alkenes. Both

groups relied upon the use of chiral ketones as catalysts; with Yang *et al* utilising the C₂-symmetric ketone (**110**), and Shi *et al* utilising a fructose derived ketone (**111**). Direct comparison of the two reports within the synthesis of *trans*-stilbene oxide (**112**) shows that both methods were effective, generating moderate to excellent *e.e.*s, and good yields (Scheme 27).^{122,123}



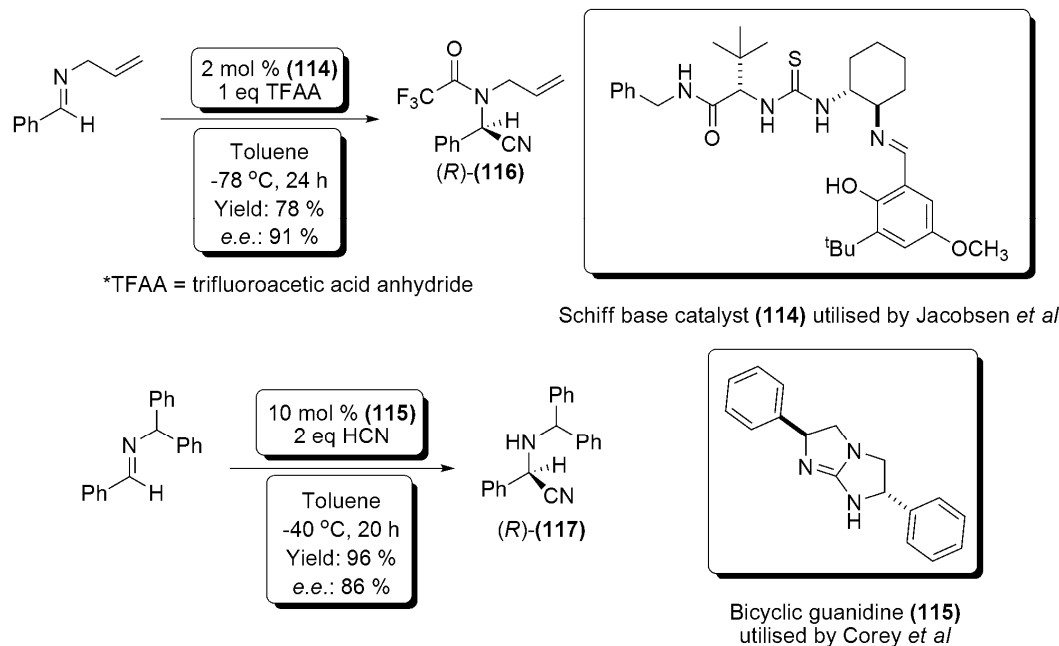
Scheme 27: Syntheses of *trans*-stilbene oxide (112**) utilising 1 equivalent (**110**) or 3 equivalents (**111**), proceeding *via* a dioxirane intermediate; by Yang *et al* and Shi *et al***

However, these reactions by Yang *et al* and Shi *et al* were not truly catalytic, due to the stoichiometric loading of (**110**) and (**111**) required; whereas, Denmark *et al* reported the formation of (*R,R*)-**(112)**, in 85 % yield, and 58 % *e.e.*, catalysed by 10 mol % of the fluoroketone species (**113**), again with *trans*-stilbene as the substrate (Scheme 28).¹²⁴



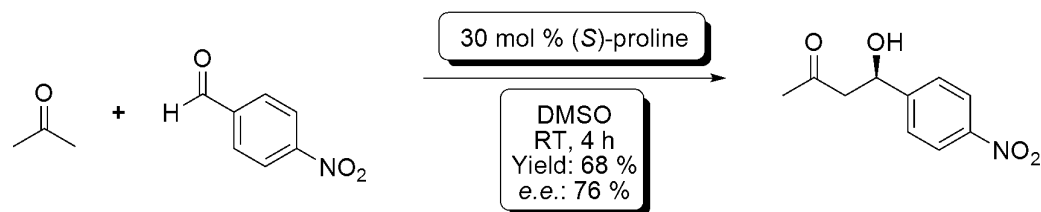
Scheme 28: Synthesis of (*R,R*)-(112)** catalysed by 10 mol % (**113**); by Denmark *et al***

Further to these initial reactions, Corey *et al* and Jacobsen *et al* independently published the first examples of catalysts which utilised a hydrogen bonding activation mechanism. These Schiff base catalysts (**(114)** Jacobsen *et al*; **(115)** Corey *et al*, Scheme 29) were employed in asymmetric Strecker type reactions. Both catalysts and methods performed well, forming their desired products (**(116)** and **(117)**) with high yields (80 – 96 % for Corey, 65 – 92 % for Jacobsen), and *e.e.*'s (50 – 88 % for Corey, 70 – 91 % for Jacobsen). The successful initial catalyst structures are shown below (Scheme 29).^{125,126}



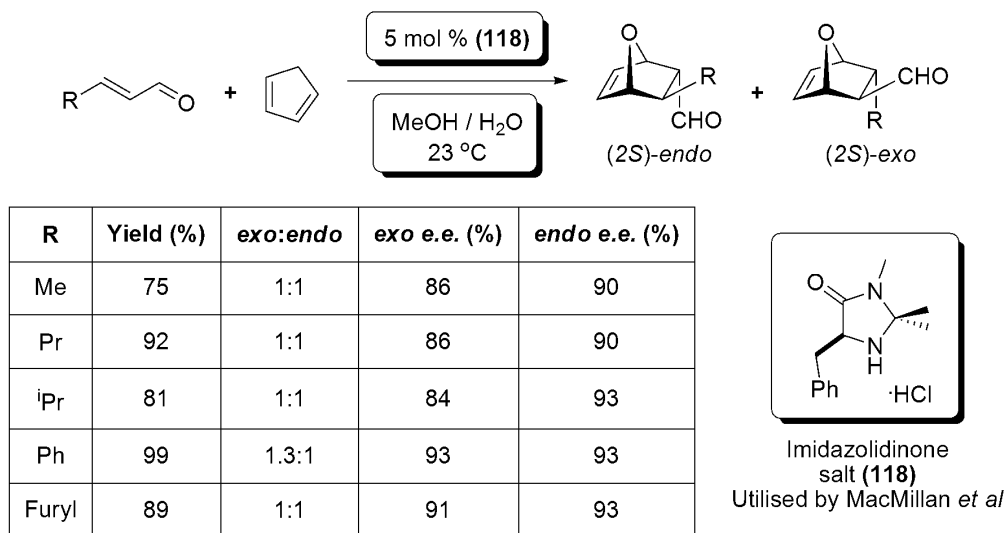
Scheme 29: Catalysts and examples of asymmetric Strecker type syntheses independently developed by Corey *et al* and Jacobsen *et al*

The two ‘landmark’ publications which saw organocatalysis begin to be widely utilised were published in 2000. The work of List *et al* was the first of these ‘landmark’ papers, and contained the first use of (*S*)-proline (**108**) as a catalyst for asymmetric aldol reactions (Scheme 30).¹²⁷ This publication is significant in the development of organocatalysis, as it demonstrates the wider use of the methodology proposed by Hajos *et al*; *i.e.* utilising (*S*)-proline as a catalyst for asymmetric aldol reactions (see Scheme 25).



Scheme 30: List *et al* example of the first asymmetric cross aldol reaction utilising catalytic (*S*)-proline

The second ‘landmark’ publication was by MacMillan research group, and concerned iminium catalysis of asymmetric Diels-Alder reactions.¹²⁸ The catalyst system was a chiral imidazolidinone salt (**118**), designed to mimic Lewis acid catalysis. (**118**), when reacted with α,β -unsaturated aldehydes, gave optically active iminium ions, which were utilised as effective dieneophiles, and afforded chiral non-racemic products (Scheme 31). For example, but-2-ene-1-al was treated with 5 mol % (**118**), and cyclopentadiene, in methanol / water at 23 °C for 16 hours, affording a 1:1 mixture of the (*2S*)-*exo* and (*2S*)-*endo* products in 75 % yield, and 86 % (*exo*) and 90 % (*endo*) *e.e.* respectively.



Scheme 31: Initial asymmetric Diels-Alder reactions, catalysed by 5 mol % (118) by MacMillan *et al*

This paper also demonstrated the advantages of organocatalytic methods; as wet solvent, relatively inexpensive catalysts, and aerobic conditions could all be used, and still afford the desired product in high yields and with excellent stereochemical control. As well as this, the term organocatalysis was coined within the text; introducing for the first time this potential new area into the literature.

It was from this point onwards that organocatalysis became widely researched; with a large number of groups interested in exploiting the potential chemistry, and new developments within this field. This can be graphically demonstrated by considering the number of papers reported utilising ‘organocatalysis’ as a key word appearing in the literature. A basic Scifinder[®] search for the key word ‘organocatalysis’ shows that since 2000 until the present day (Dec 2011), over 4000 papers have been published related to organocatalysis.

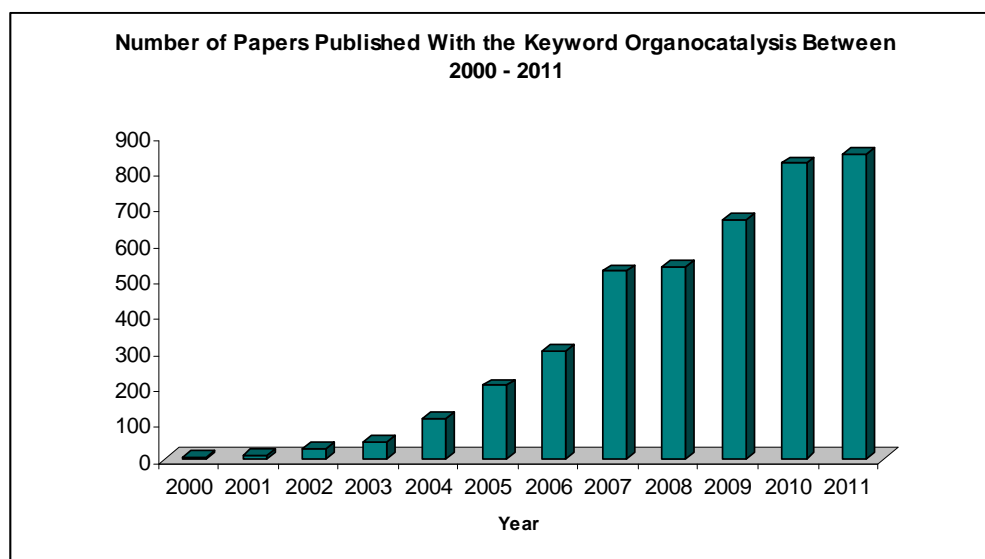


Figure 25: Graph showing the number of papers published since 2000 containing the keyword ‘organocatalysis’ (Data from Scifinder, searching CAPLUS and MEDLINE databases, Dec 2011)

2.2.1: Organocatalysis: General Activation Mechanisms & Selected Examples - Introduction

Within the remit of organocatalysis, many different reactions and catalyst systems have been developed. However, in depth analysis of the literature shows that the vast majority of organocatalytic reactions can be defined by five common modes of activation. These activation modes are summarised below (Figure 26), and each will be discussed in more detail below, including examples of the reactions which they are utilised within.

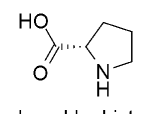
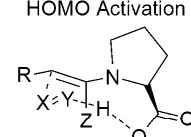
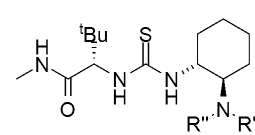
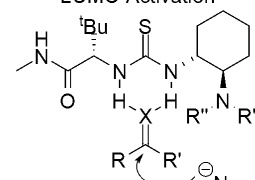
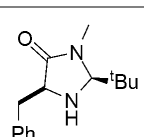
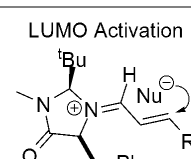
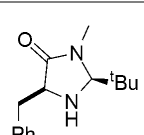
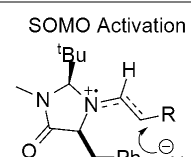
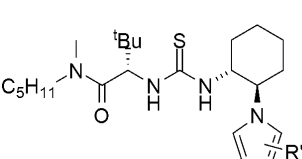
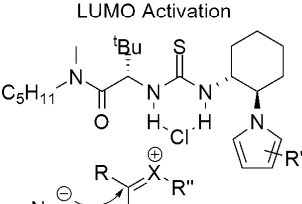
Type of Catalysis	Substrate	Example of Catalyst	Activation Mode
Enamine Catalysis	$\text{R}-\text{CH}_2-\overset{\text{O}}{\parallel}{\text{C}}-\text{Z} + \text{X}=\text{Y}$ <p>R = organic aliphatic, ring, or aromatic system X = C, N, O, S Y = organic atom Z = alkyl, H</p>	 <p>(Developed by List <i>et al</i>)</p>	<p>HOMO Activation</p> 
Hydrogen Bonding Catalysis	$\text{R}-\overset{\text{X}}{\parallel}{\text{C}}-\text{R}'$ <p>X = O, NR R, R', R'' = alkyl, aryl</p>	 <p>(Developed by Jacobsen <i>et al</i>)</p>	<p>LUMO Activation</p> 
Iminium Catalysis	$\text{R}-\text{CH}=\text{CH}-\overset{\text{O}}{\parallel}{\text{C}}-\text{H}$ <p>R = aryl, alkyl</p>	 <p>(Developed by MacMillan <i>et al</i>)</p>	<p>LUMO Activation</p> 
SOMO Catalysis	$\text{R}-\overset{\text{O}}{\parallel}{\text{C}}-\text{H}$ <p>R = aryl, alkyl</p>	 <p>(Developed by MacMillan <i>et al</i>)</p>	<p>SOMO Activation</p> 
Counterion Catalysis	$\text{R}'-\overset{\text{Cl}}{\text{C}}(\text{R})-\overset{\text{O}}{\parallel}{\text{C}}-\text{R}''$ <p>X = O, NR R, R', R'' = alkyl, aryl</p>	 <p>(Developed by Jacobsen <i>et al</i>)</p>	<p>LUMO Activation</p> 

Figure 28: Summary of the generic activation methods in organocatalysis

2.2.2: Organocatalysis: General Activation Mechanisms & Selected Examples – Enamine Catalysis

One of the first papers to be grouped into the category of organocatalysis was the development of an asymmetric aldol reaction, catalysed by (*S*)-proline, carried out by List *et al* (see Scheme 30). Although at the time this reaction was discovered, rather than designed; subsequent analysis has led to an understanding of this activation mode. By

examining a general carbonyl substrate for the aldol reaction with a molecular orbital (MO) approach, it can be demonstrated that the activation provided by enamine catalysis is most likely activation of the HOMO of the reactant (Figure 29).

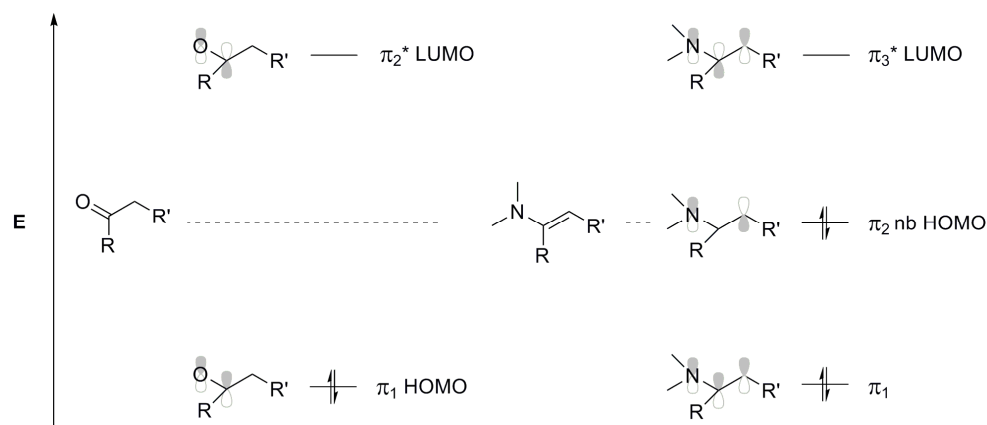
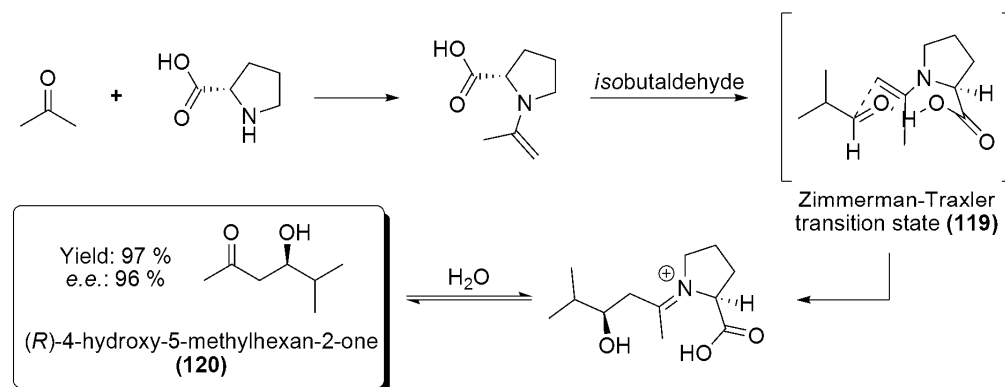


Figure 29: MO energy level diagram demonstrating activation of the substrate HOMO by enamine formation

As outlined in Figure 29 above, enamine formation populates a non-bonding orbital within the substrate. This orbital is higher in energy than that of the HOMO of the original carbonyl species, activating the substrate towards electrophilic attack, leading to the increased nucleophilic character observed.

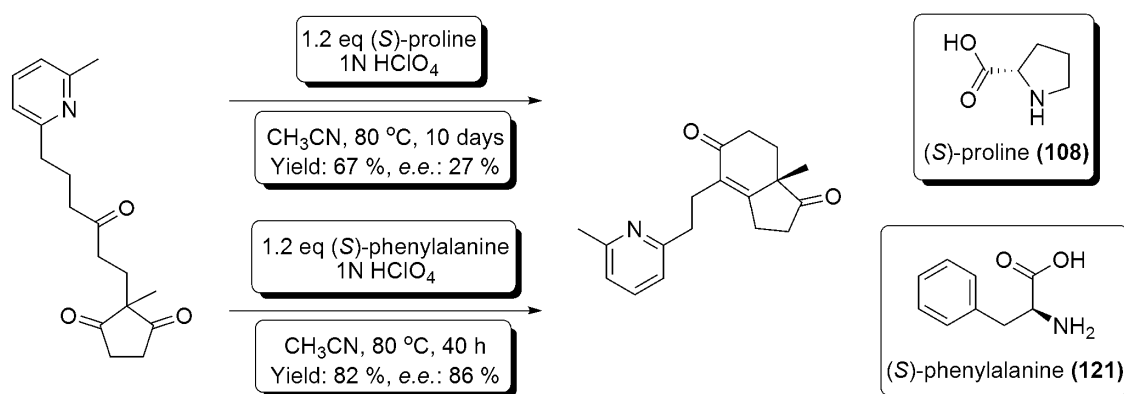
Although the MO treatment suggests that the formation of an enamine intermediate should activate the nucleophile, it does not account for the observed enantioselectivity during the initial aldol reactions carried out by List *et al.* Within the initial study, *e.e.*'s as high as 97 % were noted for the condensation of acetone with *isobutaldehyde* in the presence of 30 mol % of an (*S*)-proline catalyst (Scheme 32).¹²⁷ List *et al* hypothesised that the high enantioselectivity arose due to the acid functionality contained within the (*S*)-proline catalyst. In effect, proline was acting as a bifunctional catalyst; both activating the nucleophile, and engaging the electrophile through hydrogen bonding. This can be demonstrated if the Zimmerman-Traxler transition state (**119**) is considered (Scheme 32).



Scheme 32: (*S*)-proline catalysed aldol condensation of acetone and *isobutaldehyde* to produce (120**); demonstrated by List *et al***

As the Zimmerman-Traxler transition state demonstrates, the hydrogen bonding interaction between the electrophilic aldehyde and the catalyst can strongly favour formation of a chair-like transition state, from which the stability of the *pseudo*-equatorial isopropyl substituent ensures nucleophilic attack from only one face. This interpretation was further reinforced by computational calculations, carried out by List *et al*, showing the Zimmerman-Traxler transition state detailed above is indeed favoured energetically.¹²⁹

This (*S*)-proline mediated enantioselective activation mechanism has been employed in many differing aldol-type reactions, for example, both *enolendo* and *enolexo* intramolecular aldolisations have been shown to be catalysed *via* enamine formation. The work of Danishefsky *et al* and Agami *et al* are good examples of these 6-*enolendo* intramolecular aldolisation reactions (*i.e.* Hajos-Parrish-Eder-Sauer-Wiechert type reactions). Independently, Danishefsky *et al* and Agami *et al* showed that for certain substrates, utilising (*S*)-phenylalanine (**121**) as the catalyst species furnished higher *e.e.*'s than the traditional (*S*)-proline catalyst (**108**) within these reactions (Scheme 33).^{130,131}

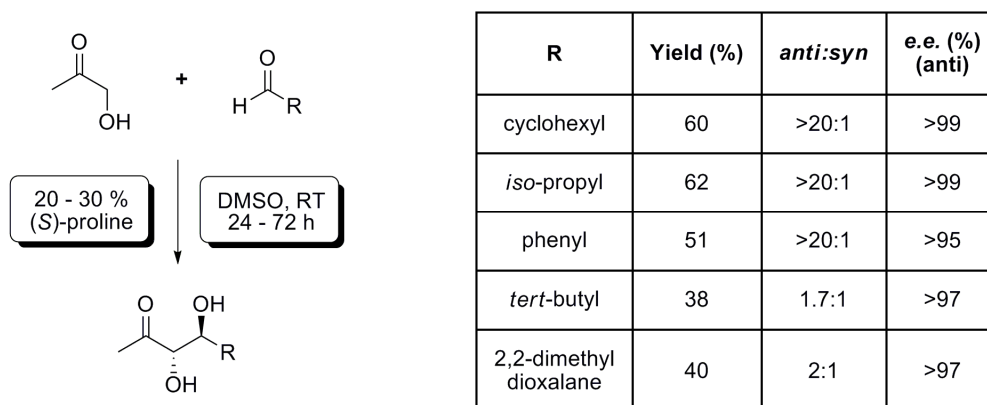


Scheme 33: 6-*enolendo* aldolisation reaction catalysed by (*S*)-proline (108**) or (*S*)-phenylalanine (**121**) by Danishefski *et al***

It is worthy of note that (*S*)-phenylalanine (**121**) retains the same structural motif as (*S*)-proline (**108**) in its retention of both amine and acid functionality, allowing for the formation of ordered Zimmerman-Traxler transition states. Initially, this transition state was at odds with the generally accepted mechanism of the Hajos-Parrish-Eder-Sauer-Wiechert reaction, however, subsequent ¹⁸O-labelling studies by List *et al*,¹³² and computational studies by Houk *et al*,^{133,134} have been published in support of the enamine mechanism suggested by List *et al*.

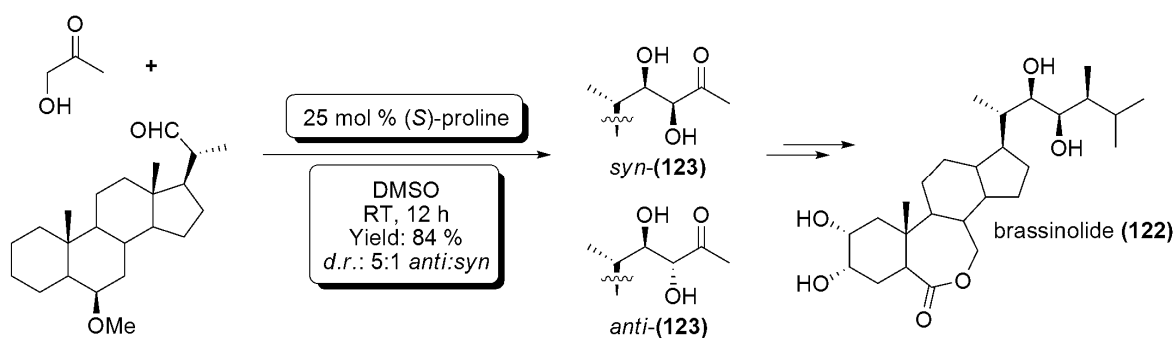
Cross aldolisation reactions can also be catalysed *via* enamine formation. Of particular interest is the development of cross aldol reactions involving α -hydroxycarbonyl substrates. These reactions are of particular use due to the traditional difficulty in synthesising *anti*-1,2-diols. Although *anti*-1,2-diols can be produced *via* Sharpless

asymmetric dihydroxylation,¹³⁵ the potential of using a simple hydroxycarbonyl starting material, along with a cheap, readily available catalyst, holds considerable attraction. To this end, the work of List *et al* shows that again utilising (*S*)-proline as a catalyst, *anti*-1,2-diols can be produced with good levels of *enantio*-, *regio*-, and *diastereoselectivity* and with moderate yields of *ca.* 60 % (Scheme 34).¹³⁶



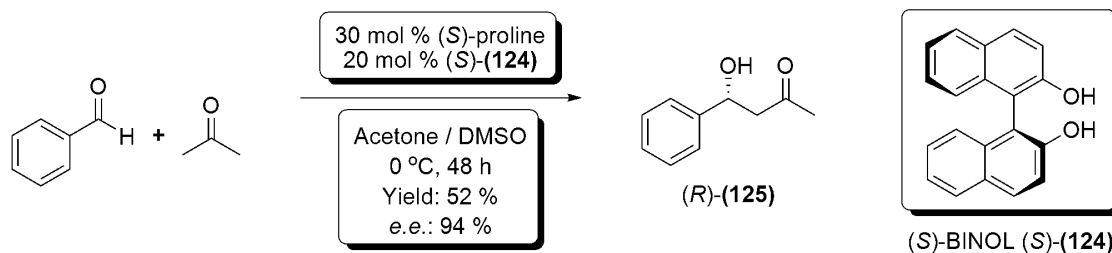
Scheme 34: *Anti*-1,2-diol formation *via* cross aldol reactions catalysed by (*S*)-proline; by List *et al*

The cross aldolisation reaction has found use in natural product synthesis as well as general synthetic chemistry.¹³⁷⁻¹³⁹ For example, Li *et al* utilized a cross aldolisation reaction within a novel synthesis of the side chain of brassinolide (**122**) (Scheme 35).¹⁴⁰



Scheme 35: Application of the organocatalytic asymmetric cross aldolisation reaction within the synthesis of the side chain (**123**) of brassinolide (**122**); by Li *et al*

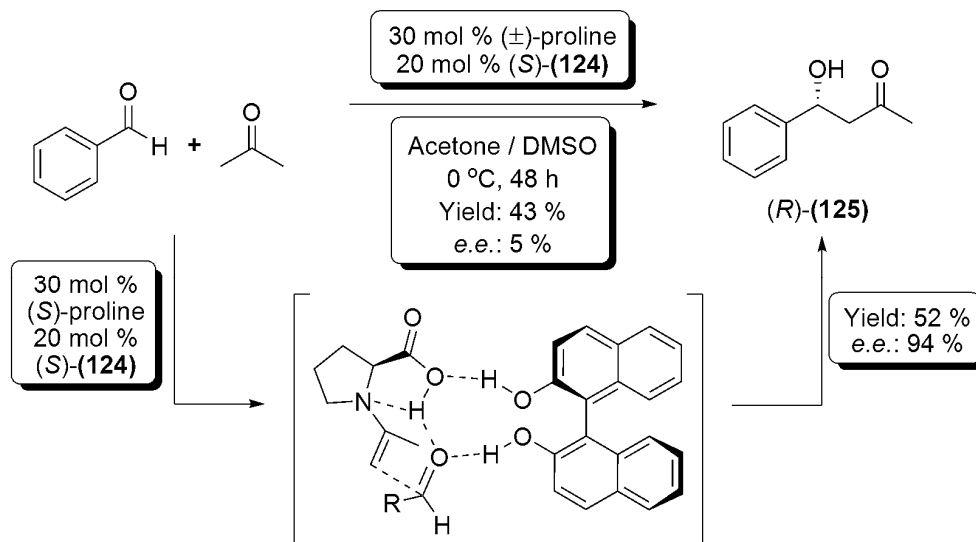
While optically active proline is effective, and still commonly used as an organocatalyst for cross aldol reactions, many other organocatalysts have been developed in attempts to offer improved reactivity, enantioselectivity, and ease of use. Although not strictly utilising a new catalyst, the work of Shan *et al* is an interesting example. Shan *et al* demonstrated that the enantioselectivity, and yields, of (*S*)-proline catalysed aldol reactions could be increased *via* the addition of chiral diols. For example, the addition of 20 mol % of (*S*)-BINOL (**124**, (*S*)-1,1'-binaphthyl-2,2'-diol) to the cross aldol reaction of benzaldehyde and acetone led to an increase in *e.e.* of the afforded product (*R*)-(**125**) of up to 22 % (72 % *e.e.* afforded with no (**124**)) (Scheme 36).



Scheme 36: Observed increase in *e.e.* of the cross aldol reaction product (125) between acetone and benzaldehyde upon addition of 20 mol % (S)-(124); by Shan *et al*

Interestingly, the enantiomer of (124) added had no effect upon the chirality of the product, with both enantiomers of (124) affording (R)-(125), with no noticeable loss of *e.e.*; suggesting that the chirality of the product was being determined by the catalyst, as opposed to the chiral diol.

This hypothesis was tested by utilising 20 mol % (S)-(124) as a chiral additive, while using 30 mol % (±)-proline as the catalyst; again in the cross aldol reaction of benzaldehyde and acetone. In line with the hypothesis, the *e.e.* of the afforded product (R)-(125) was seen to fall dramatically, from 94 % to 5 % (Scheme 37). Thus it was concluded that the addition of (124) leads to the formation of a ‘supramolecular complex’ between the substrate, chiral diol, and (S)-proline catalyst which favours attack from one face of the substrate during the reaction, leading to the observed increase in *e.e.* (Scheme 37).¹⁴¹



Scheme 37: Observed loss in enantioselectivity upon use of (±)-proline in the cross aldol reaction of benzaldehyde and acetone, and proposed ‘supramolecular complex’; by Shan *et al*

Examples of other catalysts for cross aldol reactions are also prevalent in the literature; these include: polymer bound (S)-proline species ((126), Benaglia & Cozzi *et al*),^{142,143} bisprolinamide species ((127), Zhao *et al*),¹⁴⁴ and bifunctional C₂-symmetric 1,1-binaphthyl derived species ((128), (129), Maruoka *et al*);^{145,146} these catalysts are shown in Figure 30.

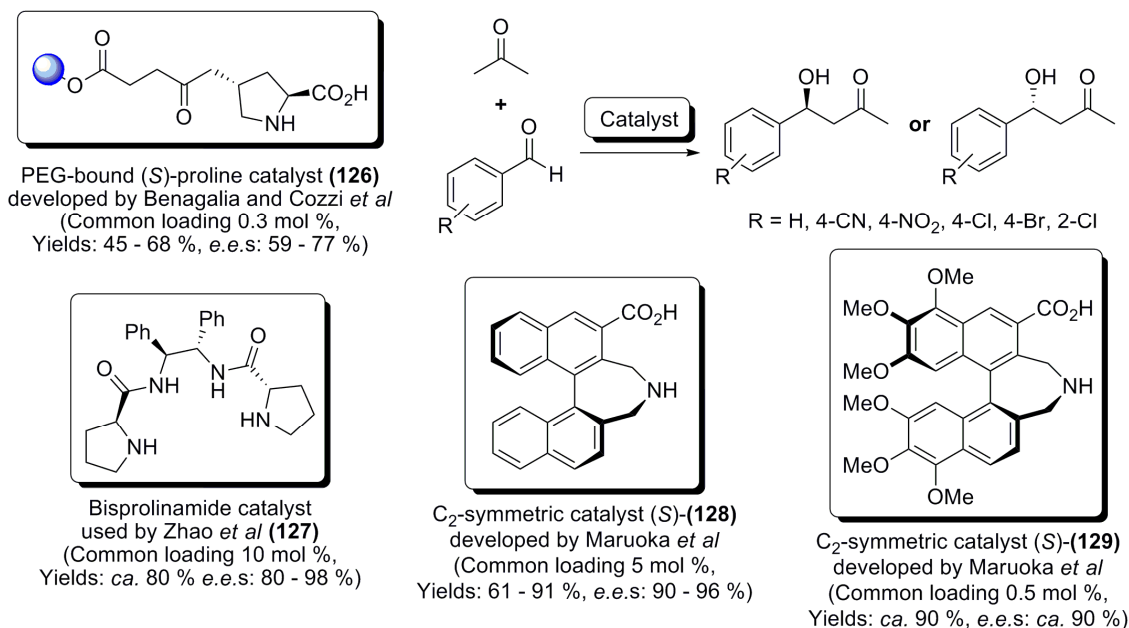
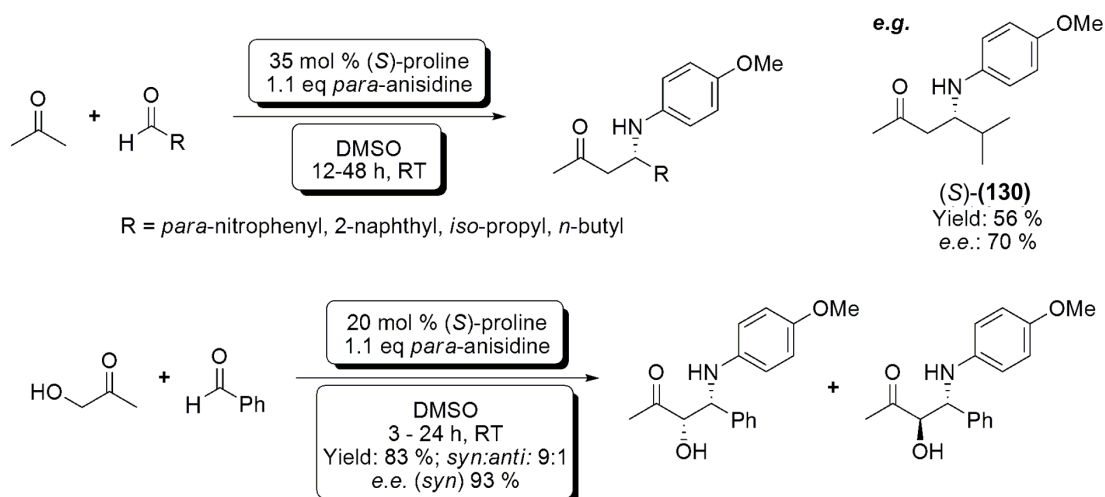


Figure 30: Organocatalyst species employed in cross aldol reactions by Benaglia *et al*, Zhao *et al*, and Maruoka *et al*

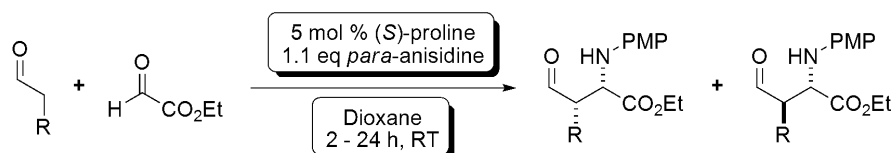
Enamine catalysis has also found use within the Mannich reaction. The Mannich reaction proceeds *via* the condensation of two carbonyl components and an amine, affording β -amino carbonyl compounds, and is widely used within organic synthesis.

The first example of an efficient three-component, asymmetric, organocatalysed, Mannich reaction was demonstrated by List *et al* in 2000.¹⁴⁷ Utilising an (S)-proline catalyst, List *et al* carried out reactions between acetone, *para*-anisidine, and various aliphatic or aromatic aldehydes utilising 35 mol % proline (Scheme 38); these reactions afforded enantioenriched β -aminoketones (*e.g.* (**130**)) in yields ranging from 35 – 90 %, and with *e.e.*'s ranging from 70 – 96 % (Scheme 38). This methodology has also been employed within the synthesis of optically active α -hydroxy- β -aminoketones, utilising α -hydroxyketones as starting materials, again by List *et al* (Scheme 38).¹⁴⁸



Scheme 38: 3-component, asymmetric, organocatalysed mannich reactions; by List *et al*

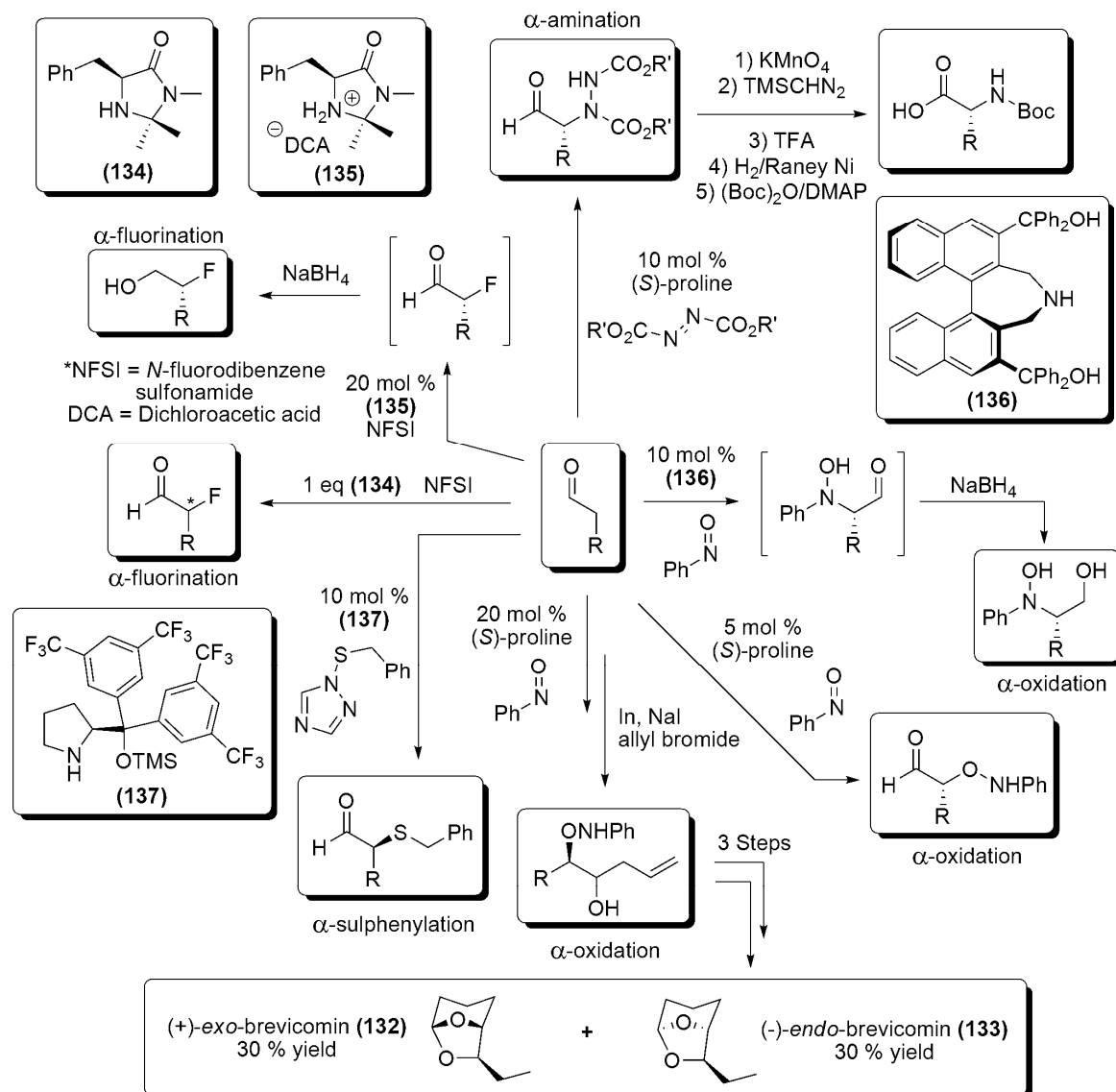
Further to the work by List *et al*, Barbas *et al* have carried out research concerned with the use of multiple aldehydic substrates within asymmetric three component Mannich reactions, catalysed by (*S*)-proline (Scheme 39). Interestingly, a catalyst screen within the report by Barbas *et al* suggested that proline itself was the most effective catalyst for these reactions. For example, within the synthesis of β -formyl- α -amino ester (**131**) (Scheme 39), no catalyst screened performed better than (*S*)-proline; the closest rival being *trans*-4-*tert*-butoxy (*S*)-proline, which gave a slightly improved yield of 91 %, but required a longer reaction time of 4 hours (compared to 3 hours required with (*S*)-proline).¹⁴⁹



Substrate	Product	Yield (%)	<i>d.r</i>	e.e. (%) (<i>syn</i>)	Substrate	Product	Yield (%)	<i>d.r</i>	e.e. (%) (<i>syn</i>)
Propanal		72	3:1	99	Heptanal		81	19:1	99
Butanal		57	7:1	99	hex-5-enal		71	19:1	99
3-methyl butanal		81	19:1	93	5-(OTBS) pentanal		81	1.5:1	91

Scheme 39: Asymmetric Mannich reactions catalysed by 5 mol % (*S*)-proline; by Barbas *et al*

The final area within organocatalytic enamine catalysis is that of α -functionalisation of carbonyl compounds. These reactions include α -amination (producing α -amino acids or amino alcohols, of interest in life sciences),¹⁵⁰ α -oxidation (potentially useful within natural product synthesis, *e.g.* total synthesis of brevicomin (**132**), (**133**)),¹⁵¹ α -halogenation (in particular, α -fluorination, potentially producing synthons for the synthesis of oxidation resistant drugs),^{152,153} and α -sulfenylation (producing materials potentially of interest within biological systems, *e.g.* for the inhibition of zinc containing enzymes).^{154,155} These reactions, and the examples referenced above are summarised in Scheme 40, however a complete review of α -functionalisation reactions is also available in the literature by Jørgensen *et al*.¹⁵⁶



Scheme 40: Summary of selected α -functionalisation reactions which proceed *via* enamine catalysis

2.2.3: Organocatalysis: General Activation Mechanisms & Selected Examples – Iminium Catalysis

As noted within the introduction to this section (See *Organocatalysis: A Brief Early History*), MacMillan *et al* were responsible for the development of iminium catalysis as a general activation mode in 2000 (selected work outlined in Scheme 31) as part of a directed effort to produce a catalyst system which would mimic Lewis acid catalysis.

Lewis acid catalysis relies upon lowering the LUMO of a system by coordination of a Lewis acid to a suitable lone pair containing functional group (for example, an aldehyde, or ketone). This coordination leads to increased polarisation of the carbon heteroatom bond within the Lewis basic functional group (for example, increased polarisation of the carbon oxygen bond within ketones); which in turn leads to the lowering of the LUMO of the substrate.

Within iminium catalysis, lowering of the LUMO energy comes about due to formation of the formally positively charged iminium species; leading to increased polarisation of the carbon nitrogen bond (analogous to the increased polarisation seen within Lewis acid coordination), decreasing the energy barrier to reaction, and thus activating the substrate (Figure 31).

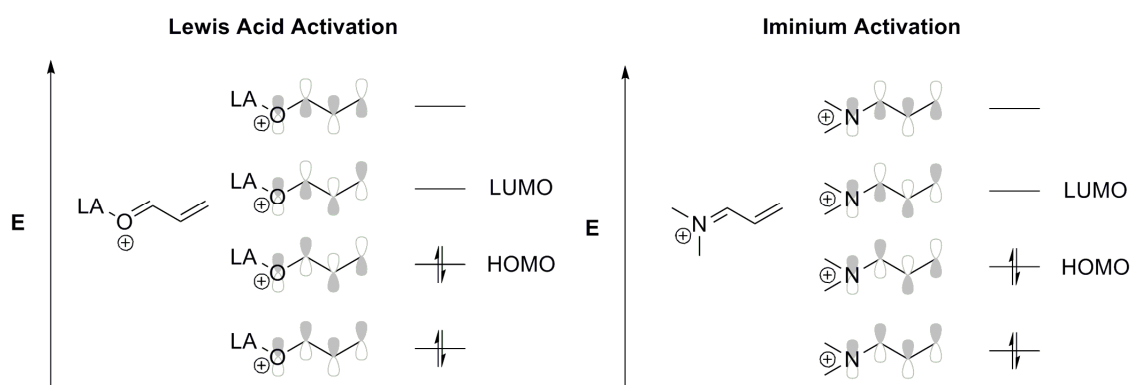
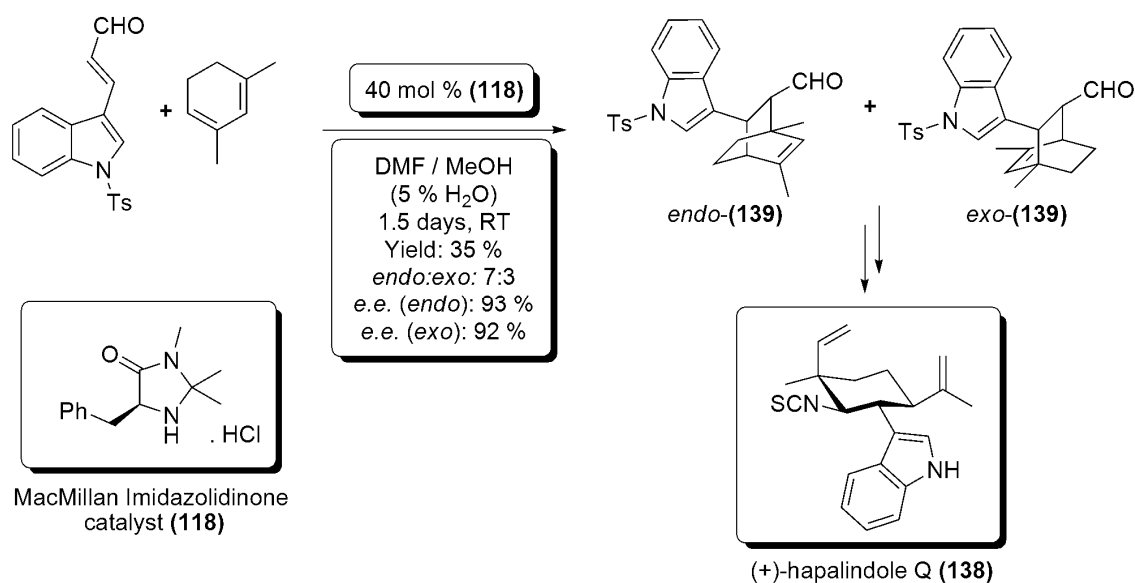


Figure 31: Comparison of the similarities between Lewis acid and iminium LUMO activation

When published in 2000 by MacMillan *et al*, the majority of their iminium catalysis work was focussed upon applications within Diels-Alder cycloaddition reactions; utilising the imidazolidinone catalyst (**118**) (see Scheme 31).

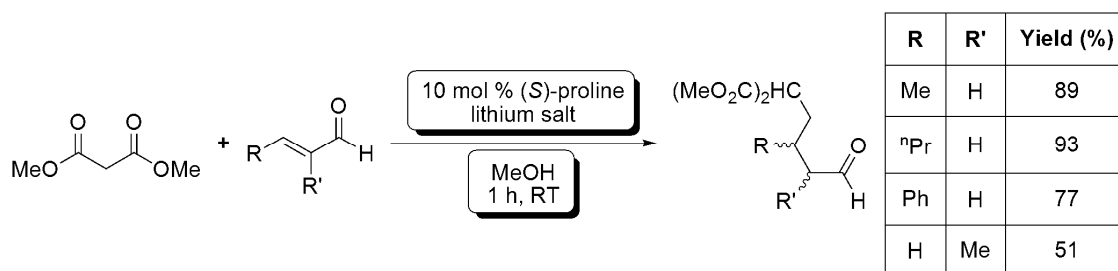
One example of the use of iminium catalysed Diels-Alder chemistry is contained within the total synthesis of (+)-hapalindole-Q (**138**) by Kinsman and Kerr, published in 2003, utilising the MacMillan imidazolidinone salt (**118**) (Scheme 41).¹⁵⁷ Despite the relatively low yield of this reaction, the complex intermediate produced by this Diels-Alder cycloaddition, from achiral starting materials, makes this reaction attractive.



Scheme 41: Synthesis of (+)-hapalindole-Q utilising an iminium catalysed Diels-Alder cycloaddition step to form intermediate (139); by Kinsman and Kerr

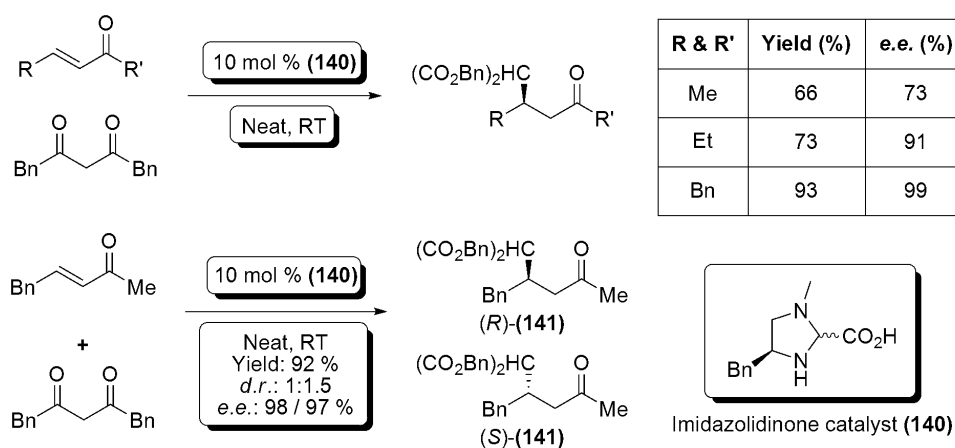
Various other catalysts been developed which take advantage of the polarisation effect of iminium catalysis in order to activate substrates within the context of the Diels-Alder reaction; including: polymer bound,¹⁵⁸ fluorous,¹⁵⁹ C₂-symmetric binaphthyl,¹⁶⁰ and (further to the MacMillan *et al* initial work) imidazolidinone¹²⁸ based catalysts.

The use of iminium catalysis within conjugate addition reactions has also seen significant development. For example, the Michael addition of carbon based nucleophiles has been a subject of much research; initially observed by Yamaguchi *et al* in 1991, it was demonstrated that the addition of dimethyl malonate to α,β -unsaturated aldehydes (including hexenal) could be catalysed by the lithium salt of (*S*)-proline, *via* intermediate iminium formation (Scheme 42).¹⁶¹



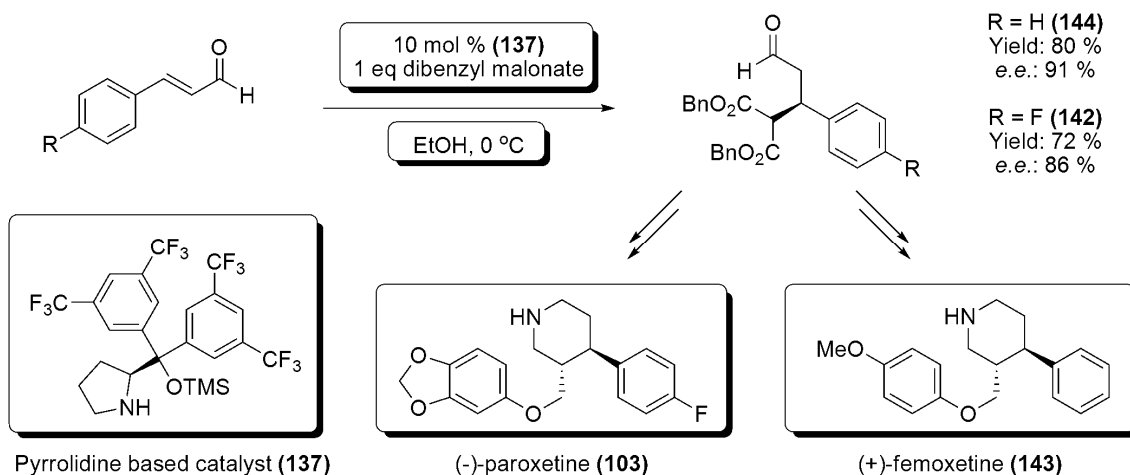
Scheme 42: Initial iminium ion catalysed Michael additions, utilising (*S*)-proline lithium salt; by Yamaguchi *et al*

The Yamaguchi *et al* publication was the first of several developing various methods and catalysts for Michael addition reactions; an interesting example among these being the methodology developed by Jørgensen *et al* which was published initially in 2003.¹⁶² Utilising 10 mol % of the imidazolidinone (**140**), prepared from (\pm)-phenylalanine, as the catalyst; the conjugate addition of various malonates upon enone substrates was carried out (Scheme 43). However, the use of the malonate as the reaction solvent was required; and furthermore, significant lowering of the diastereoselectivity was noted when unsymmetrical malonates were employed (see synthesis of (**141**), Scheme 43).



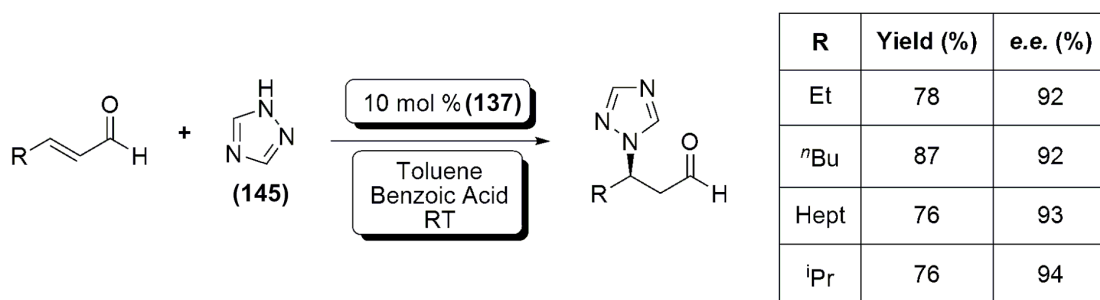
Scheme 43: Asymmetric, organocatalysed, Michael additions utilising symmetrical and unsymmetrical malonates; by Jørgensen *et al*

In 2006, Jørgensen *et al* published further examples of iminium catalysed conjugate addition to α,β -unsaturated aldehyde substrates, which were carried out with a view to synthesising compounds of pharmaceutical interest; included within these were the syntheses of the antidepressants (-)-paroxetine (**103**) (intermediate (**142**)) and (+)-femoxetine (**143**) (intermediate (**144**)) (Scheme 44).¹⁶³



Scheme 44: Iminium catalysed conjugate addition to α,β -unsaturated aldehydes, within syntheses of pharmaceutically interesting products (103**) and (**104**); by Jørgensen *et al***

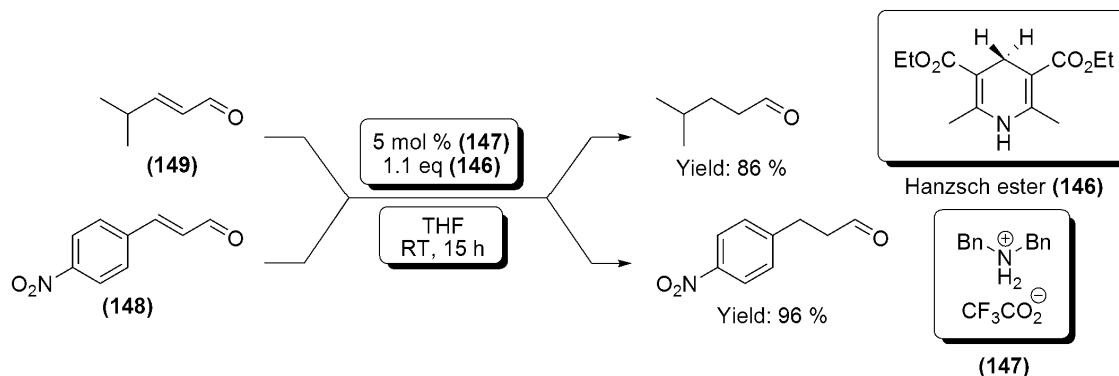
The use of iminium catalysis within conjugate addition reactions is not limited to carbon nucleophiles however. Nitrogen, oxygen, and sulfur containing nucleophiles within the Michael addition have all been reported, examples of which have again been published by (but are not limited to) Jørgensen *et al*.¹⁶⁴⁻¹⁶⁶ For example, it has been demonstrated by Jørgensen *et al* that the pyrrolidine catalyst (**137**) (see Scheme 44) can facilitate the asymmetric conjugate addition of nitrogen heterocycles, such as 1,2,4-triazole (**145**) to aliphatic aldehydes, in yields of *ca.* 80 %, and *e.e.s* of > 90 % (Scheme 45).



Scheme 45: Organocatalytic, asymmetric conjugate addition of 1,2,4-triazole (145**) to aliphatic aldehydes; by Jørgensen *et al***

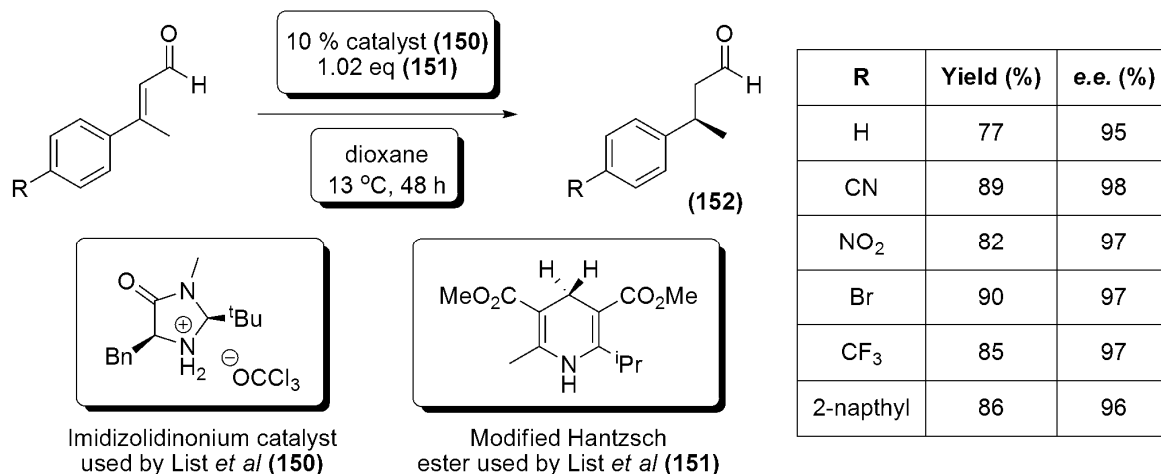
A further interesting example is the organocatalysed conjugate addition of hydrogen to unsaturated aldehydes within transfer hydrogenation reactions. The first example of this was developed by List *et al*. The initial method utilised the Hantzsch ester (**146**), and 5 mol % dibenzylammonium trifluoroacetate (**147**) as the catalyst. This

methodology allowed for the organocatalytic transfer hydrogenation of α,β -unsaturated aldehydes (such as 4-(nitrophenyl)acrylaldehyde (**148**) and 4-methylpentenal (**149**)), in yields of *ca.* 90 % (Scheme 46). However, the reaction generated racemic products.



Scheme 46: Racemic organocatalysed transfer hydrogenation reactions catalysed by 5 mol % (146**); by List *et al***

The above methodology was subsequently improved upon *via* the use of the chiral imidazolidinone salt (**150**), and the modified Hantzsch ester (**151**), which afforded the desired reaction products in similar yields of *ca.* 90 %, but also 90 – 96 % *e.e.* (Scheme 47). For example, treatment of 3-phenylbut-2-enal with 10 mol % (**150**), and 1.02 eq (**151**) afforded the desired product of the form of (**152**) in 77 % yield, and 95 % *e.e.*¹⁶⁷



Scheme 47: Organocatalytic hydrogen transfer reaction developed by List *et al*

The examples shown above are a selection of the reactions that have been developed utilising iminium catalysis. Further examples and discussion can be found within the literature in review format.¹⁶⁸

2.2.4: Organocatalysis: General Activation Mechanisms & Selected Examples – Hydrogen Bonding Catalysis

Electronically, the activation of substrates *via* hydrogen bonding comes about due to inductive polarisation of the π -system of the hydrogen bond acceptor substrate, caused

by formation of the hydrogen bond. This polarisation brings about a lowering of the LUMO energy within the hydrogen bonded substrate, thus promoting nucleophilic attack (Figure 32). This effect can be viewed as analogous to the polarisation noted upon coordination of a Lewis acid to a Lewis basic substituent (See 2.2.3: *Iminium Catalysis*).

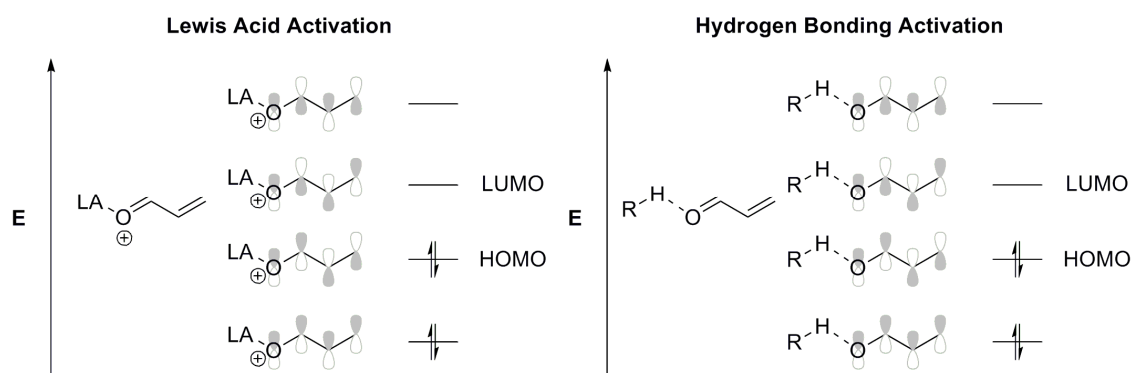


Figure 32: Comparison of the similarities between Lewis acid and hydrogen bonding LUMO activation

Originally, the use of hydrogen bonding as a form of organocatalysis stemmed from two realisations; these being that hydrogen bond donors could both enhance reactivity within a reaction (due to the polarisation effect detailed above), and also that they allowed for highly ordered assemblies and transition states (Figure 33). These initial reports by Hine *et al.*,¹⁶⁹ and Etter *et al.*,¹⁷⁰ paved the way for the development of a generalised approach to hydrogen bond catalysis, and further to this, asymmetric reactions based upon the highly ordered assemblies and transition states allowed by hydrogen bonded intermediates.

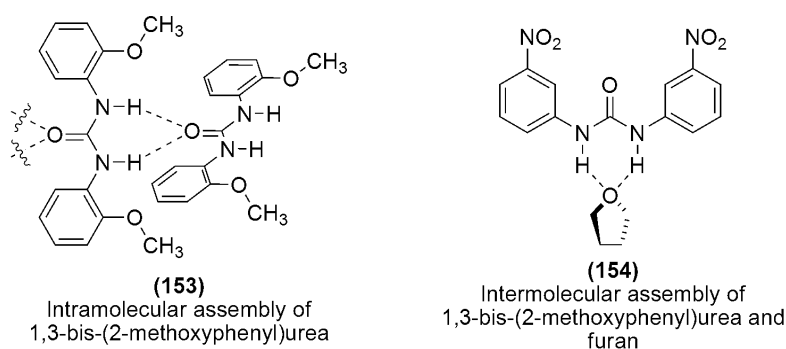
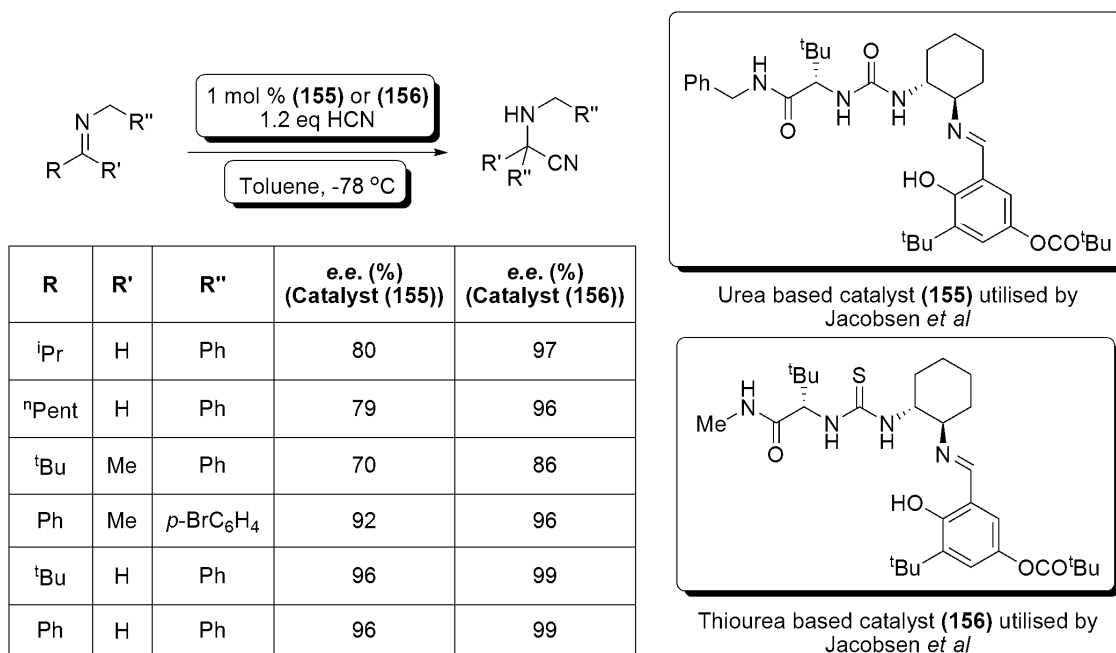


Figure 33: Highly organised molecular assemblies of 1,3-bis-(2-methoxyphenyl)urea with itself (153), and 1,3-bis-(3-nitrophenyl)urea with furan (154), promoted by hydrogen bonding; proposed and observed by Etter *et al*

Examples of both the polarisation and ordering effects of hydrogen bonding catalysis can be found within the work of Jacobsen *et al.*¹⁷¹ Jacobsen and Vachal have reported that urea and thiourea containing peptide compounds (**155**) and (**156**) catalyse the asymmetric Strecker hydrocyanation of aldimine and ketoimine substrates, affording the

desired products in *e.e.s* of between 86 and 99 %; although yields were not reported for these reactions (Scheme 48).



Scheme 48: Asymmetric Strecker hydrocyanation of aldimine and ketoimine substrates, catalysed by 1 mol % (**155**) or (**156**); carried out by Jacobsen *et al*

The exact mechanism of activation within the above reactions was initially unknown; however, subsequent structure activity studies showed that only the urea (or thiourea) functionality of (**155**) or (**156**) was required for reaction to be observed. It was also found that by increasing the steric demands of the environment around the urea functionality (within (**155**) or (**156**)), higher enantioselectivity could be induced within the reaction. These observations directly support the hypothesis that the substrate is both activated, and held within an organised conformation (allowing favoured attack from one face), *via* hydrogen bonding interactions with the catalyst (Figure 34).

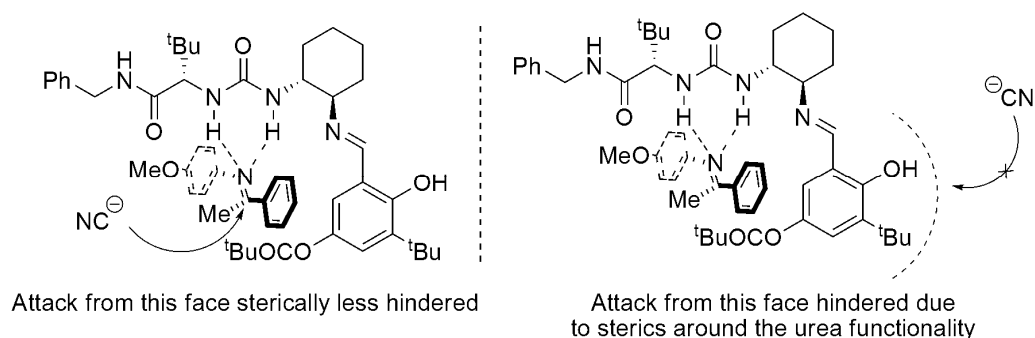
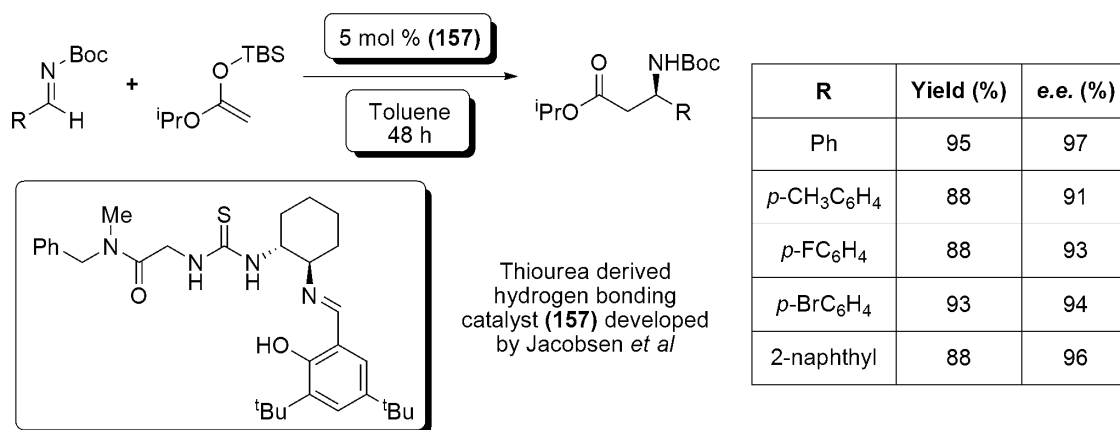


Figure 34: Representation of the structure provided by hydrogen bonding of (**155**) to an imine substrate, and steric hindrance to attack from one face of that substrate

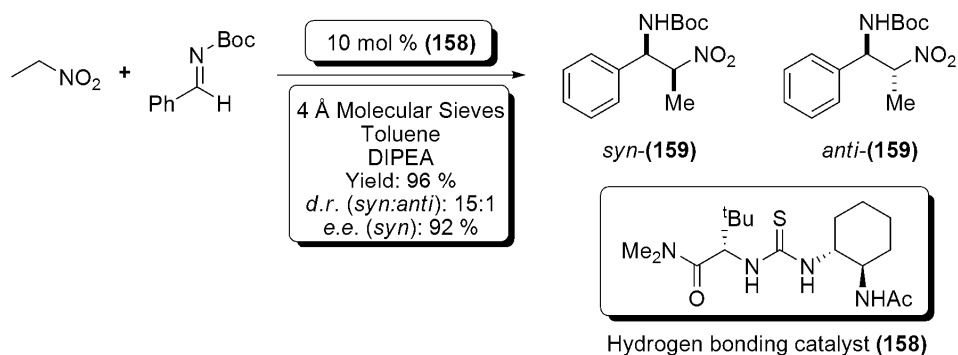
Following on from the development of the asymmetric Strecker hydrocyanation of ketoimines, and the subsequent elucidation of the hydrogen bonding mode of action of the

catalysts (**155**) and (**156**), Jacobsen *et al* developed an asymmetric organocatalytic Mannich reaction,¹⁷² with the new hydrogen bonding catalyst (**157**). Utilising functionalised *N-tert*-butoxycarbonyl aldimines and aliphatic silyl enol ethers as substrates, together with 5 mol % (**157**), Jacobsen *et al* achieved yields of the desired Mannich adducts ranging between 87 and 99 %, along with *e.e.*s of *ca.* 90 % (Scheme 49).¹⁷³



Scheme 49: Asymmetric Mannich reactions catalysed by 5 mol % (**157**); carried out by Jacobsen *et al*

Jacobsen *et al* have also applied hydrogen bonding organocatalysis to nitro-Mannich reactions.¹⁷⁴ Utilising a similar catalyst to the previous examples, functionalised with an amide side group (catalyst (**158**)), the reaction of nitroalkanes to *N-tert*-butoxycarbonyl imines in yields ranging from 85 – 99 %, *syn:anti* selectivity of *ca.* 15:1, and *e.e.*'s of the predominant *syn* diastereomer ranging from 92 – 95 % (Scheme 50).



Scheme 50: Enantioselective nitro-Mannich reaction catalysed by 10 mol % (**158**); carried out by Jacobsen *et al*

As demonstrated by the above examples, the Jacobsen type catalyst (represented by, but not limited to (**155**), (**156**), (**157**), and (**158**)) shows reactivity within many classes of reaction. This has led to Jacobsen stating that the subtype could be classified as a ‘privileged’ catalyst.¹⁷⁵ Usually applied in pharmacology, this classification implies that the structure is capable of catalysing many different processes, and is further supported by the reported use of these catalysts within acyl-Pictet-Spengler,¹⁷⁶ cyanosilylation,¹⁷⁷ and hydrophosphonylation¹⁷⁸ reactions; although these are not discussed in detail here.

2.2.5: Organocatalysis: General Activation Mechanisms & Selected Examples – SOMO Catalysis

A relatively new activation method within organocatalysis is the field of SOMO catalysis. Pioneered by MacMillan *et al* in 2006,¹⁷⁹ SOMO catalysis was inspired by consideration of the differing frontier molecular orbital systems which characterise enamine and iminium catalysts. In general, iminium catalysis is based upon lowering the LUMO energy of the system *via* polarisation of a carbon-nitrogen bond; and the system contains a minimum of two π -electrons (Figure 31). In enamine catalysis, the energy of the HOMO is increased, and the system tends to contain four π -electrons (Figure 29). SOMO catalysis is based upon oxidation of enamine type systems, thus producing a radical cationic species with a minimum of three π -electrons (Figure 35).

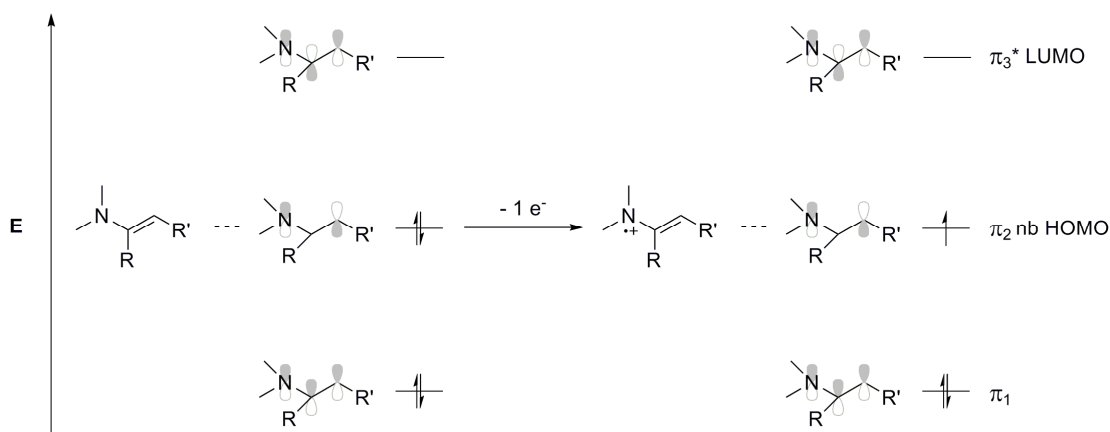


Figure 35: General SOMO catalysis frontier MO diagram

Direct evidence for the generation of the radical cation species involved within the transition state of a SOMO catalysed reaction has recently been provided by Engeser *et al* (Figure 36).¹⁸⁰ By treating a typical MacMillan imidazolidinone catalyst (**134**) with phenylacetaldehyde (**160**) within a reaction vessel equipped with an online ESI mass spectrometer, Engeser *et al* were able to monitor the formation of the intermediate enamine (**161**). When this intermediate was treated with a one electron oxidant, (tris(*p*-bromophenyl)aminiumhexachloroantimonate (**162**)), the online mass spectrum showed a new peak at m/z 348.2, *i.e.* the required m/z for the radical cation species (**163**). Further treatment of this species with styrene, and a subsequent oxidation, yielded the coupling product (**164**) (Figure 36).

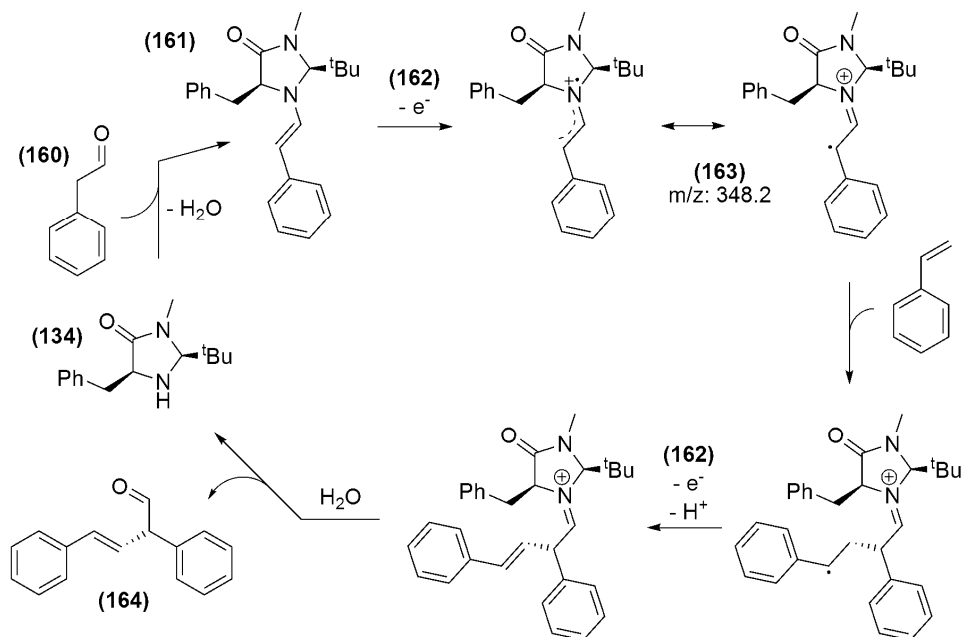
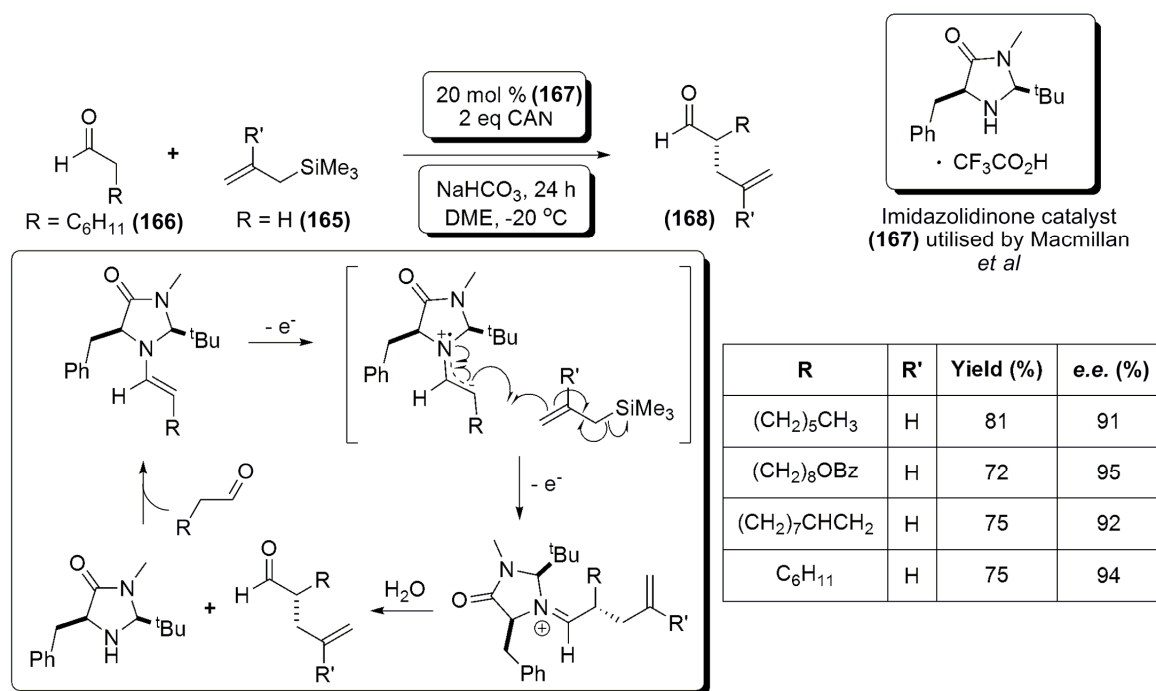


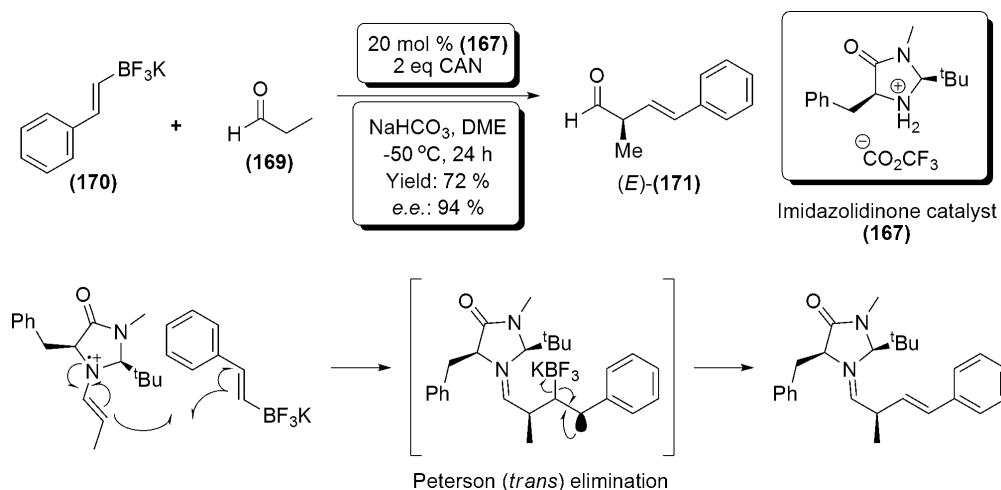
Figure 36: Catalytic cycle for the formation of (164), and MS evidence for the presence of the radical cationic species (163)

In general terms, SOMO reactants (*i.e.* cationic radical species generated from enamines) will react with substrates containing electron-rich π -systems, so-called SOMOphiles. One such example of this was demonstrated by MacMillan *et al* during the initial publication of SOMO catalysis. They demonstrated that allylsilane (**165**) will react with aldehydes such as cyclohexanecarbaldehyde (**166**) in the presence of 20 mol % of the imidazolidinone catalyst (**167**) and 2 equivalents of cerium ammonium nitrate (CAN) in order to form the formal allylation product (**168**) in 75 % yield, and 94 % *e.e.* (Scheme 51).



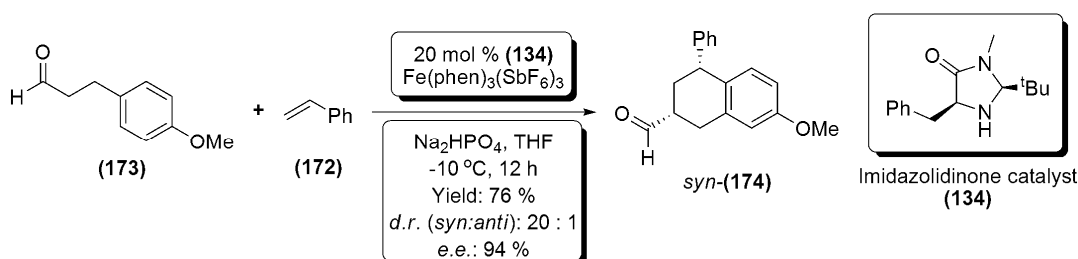
Scheme 51: Catalytic cycle, and selected results for the SOMO allylation reaction; by MacMillan *et al*

Further to allylation reactions, MacMillan *et al* have also demonstrated the use of SOMO catalysis for vinylation reactions, utilising potassium fluoroborate species as the SOMOphile reagents. This reaction type has the advantage that the final product is not only enantioenriched, but that the alkene functionality is selectively of *trans* orientation due to the Peterson (*trans*) elimination step involved within the mechanism (Scheme 52).¹⁸¹ For example, treatment of propanal (**169**) with potassium trifluoro(styryl)borate (**170**) in the presence of 20 mol % of the imidazolidinone catalyst (**167**) afforded the desired product (*E*)-(**171**) in 72 % yield, and 94 % *e.e.* (Scheme 52).



Scheme 52: SOMO vinylation reaction including a Peterson elimination step; carried out by MacMillan *et al*

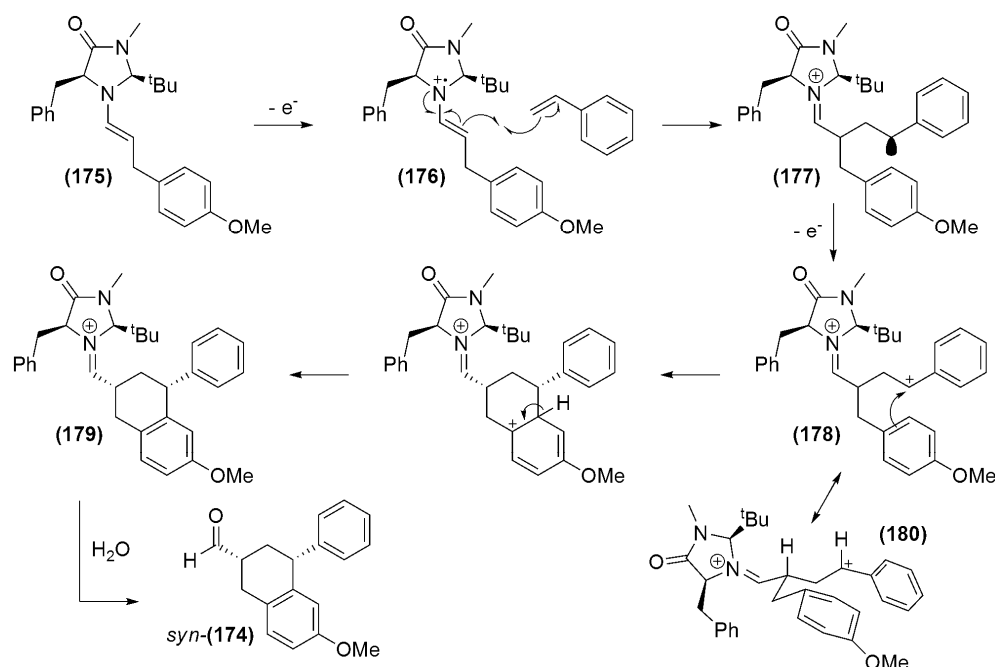
A number of ring forming and cascade reactions have also been developed by MacMillan *et al* with the aim of quickly incorporating, and establishing, complexity within organic molecules. Utilising both nucleophilic attack and a further [4+2] cycloaddition step, MacMillan *et al* synthesised a range of multicyclic compounds, utilising a one pot SOMO catalysed cascade reaction.¹⁸² For example, treatment of styrene (**172**) and 3-(4-methoxyphenyl)propanal (**173**) with 20 mol % (**134**) afforded the desired bicyclic product (**174**) in a yield of 76 %, with a diastereomeric ratio of 20:1 (with *syn* predominant), and an *e.e.* of 94 % for the major *syn* diastereomer (Scheme 53).



Scheme 53: Synthesis of *syn*-(174) via a SOMO cascade reaction; by MacMillan *et al*

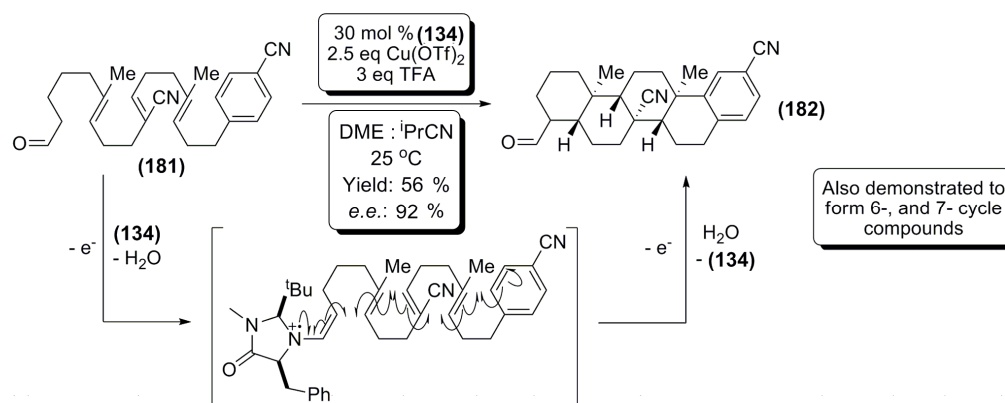
The mechanism of this reaction relies upon initial enamine formation to give **(175)**. This is then subjected to a one electron oxidation in order to form the SOMO reagent **(176)**. This then undergoes nucleophilic attack by a suitable SOMOphile (in this case, styrene) forming the intermediate **(177)**. **(177)** can then undergo a further one electron oxidation, generating the formal cationic species **(178)**; which is set up for stereoselective nucleophilic ring closing, followed by rearomatisation of the phenyl ring, generating **(179)**. Hydrolysis of the enamine then generates the desired product **(174)** (Scheme 53 & 54).

The stereoselectivity of the reaction comes about due to the potential formation of a ‘chair like’ transition state shown in Scheme 54 as **(180)**. This state allows both bulky phenyl groups to adopt pseudo-equatorial positions, and ensures that the nucleophilic attack by the phenyl ring will occur favourably from one face.



Scheme 54: Mechanism of formation of (174), showing the chair-like transition state (180)

A further recent example of a SOMO cascade reaction is that of the bio-mimetic synthesis of steroid like molecules. Similar to the biosynthesis of steroids from squalene oxide *via* a ‘chair-boat-chair’ conformation, these polycyclisation reactions were shown to be possible in yields of between 56 – 63 %, and *e.e.s* of up to 93 % (Scheme 55).^{183,184}



Scheme 55: Biomimetic synthesis of (182) via a SOMO polycyclisation reaction; by MacMillan *et al*

It is worthy of note that SOMO catalysis is still an emerging area within organocatalysis, with the possibility arising to combine the activation mode with other branches of chemistry in order to create unique reactions. For example, the combination of SOMO catalysis and photochemistry.¹⁸⁵

2.2.6: Organocatalysis: General Activation Mechanisms & Selected Examples – Counterion Catalysis

The final activation mode to be discussed here is that of counterion catalysis. Although only a recent discovery, several new reactions utilising this approach have been developed. Within counterion catalysis, there are two general fields of research. One of these is ACDC (asymmetric counterion directed catalysis) developed by List *et al*.¹⁸⁶

This methodology involves use of a chiral catalyst salt, TRIP (**183**). Activation of the carbonyl containing substrate (*i.e.* aldehyde or ketone) occurs *via* iminium formation with the morpholino component of the catalyst salt. The chiral anionic portion of the catalyst salt then facilitates a steric directing effect to subsequent reaction upon the iminium species, thus favouring attack from one face (Figure 37). List *et al* have also applied this concept to transition metal based chemistry.¹⁸⁷

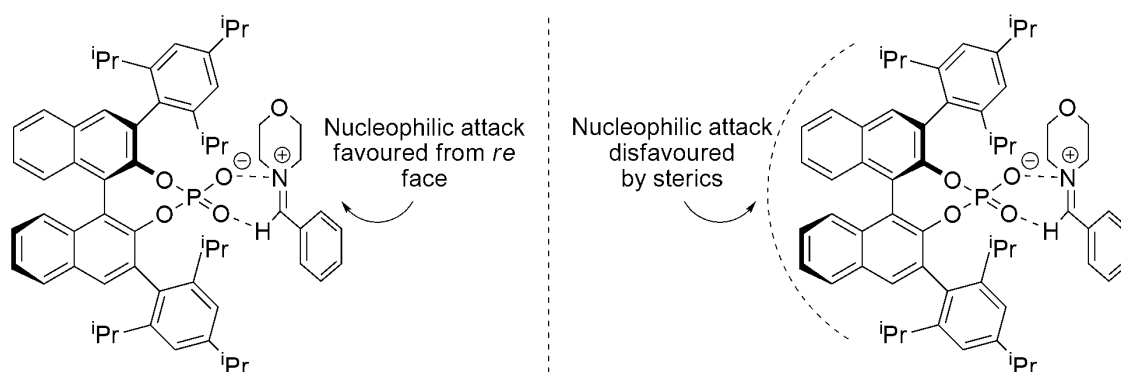
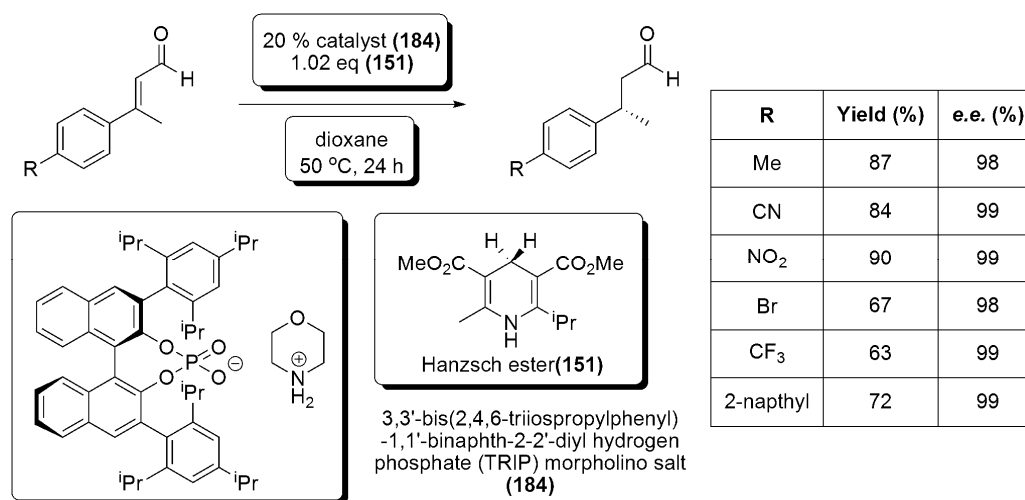


Figure 37: Representation of the formation of a 'chiral ion pair' between the iminium ion and phosphate anion formed by the treatment of benzaldehyde with TRIP (183)

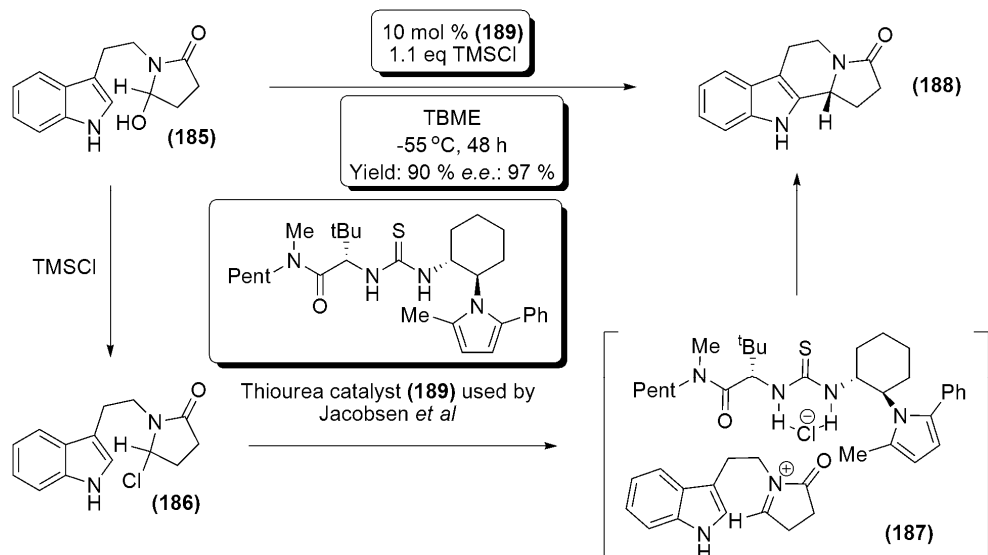
An example of the use of ACDC and TRIP is the transfer hydrogenation of α,β -unsaturated aldehydes performed by Meyer and List. The method allowed for the enantioselective reduction of these α,β -unsaturated aldehydes in good yields and excellent *e.e.s* (Scheme 56).¹⁸⁶ For example, 3-(4-toluy)butenal was treated with 20 mol % (**184**), and 1.02 equivalents (**151**), affording the desired reduced product in 87 % yield, and 98 % *e.e.*.



Scheme 56: TRIP anion directed asymmetric transfer hydrogenation by Meyer and List

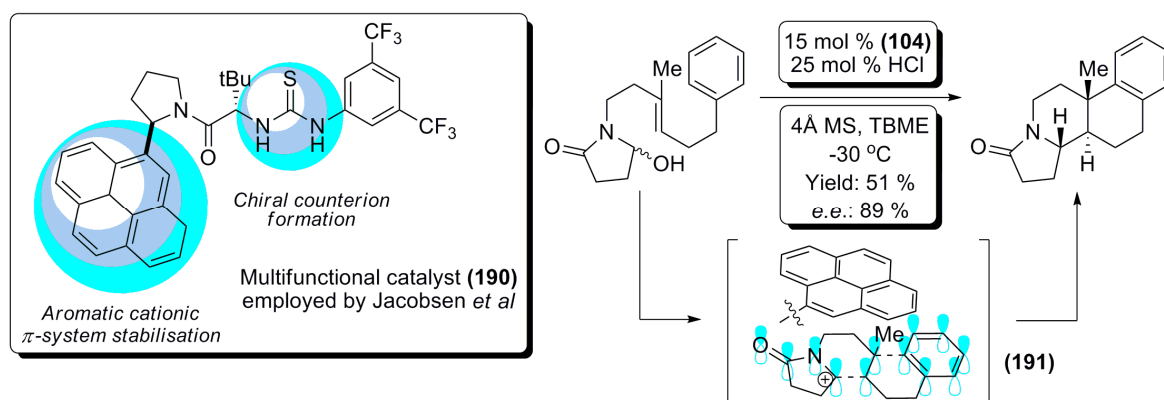
The second form of counterion catalysis can be described as a hydrogen bonding catalysis mode. However, as the name suggests, the difference from traditional hydrogen bonding catalysis comes about in the fact that the hydrogen bonding encourages dissociation of a suitable leaving group anion from the substrate; thus allowing a chiral ion pair to form between the now cationic substrate and the chiral anionic catalyst complex.

This methodology was first elucidated by Jacobsen *et al*, while investigating the reaction mechanism of their urea/thiourea containing hydrogen bonding catalysts (see 2.2.4: *Hydrogen Bonding Catalysis*) when employed upon the intramolecular cyclisation of hydroxylactam substrates (Scheme 57).¹⁸⁸ It was shown that treatment of the hydroxylactam species (**185**) with trimethylsilyl chloride led to displacement of the hydroxy group with chlorine. The activated substrate (**186**) then underwent interaction with the hydrogen bonding donor group of the catalyst (**189**) leading to weakening of the carbon halogen bond within the substrate (**186**). This weakening occurred to such a degree as to cause dissociation, forming the subsequent chiral ion pair (**187**) (Scheme 57).



Scheme 57: Jacobsen counterion catalysis in the synthesis of harmicine derivative (188)

Polycyclisation reactions of multiply unsaturated systems have also been shown to be catalysed *via* counterion catalysis, one example of such is shown in Scheme 58 below. Jacobsen *et al* have demonstrated that by including aromatic groups within the periphery of a thiourea based hydrogen bonding catalyst, an interaction can occur between the cationic π -system of the substrate intermediate, and the aromatic upon the catalyst. This interaction both stabilises the substrate, and holds it into a position amenable for enantioselective cyclisation to occur (which is catalysed by formation of a chiral ion pair (191) with catalyst (190)) (Scheme 58). Using this method, Jacobsen *et al* synthesised steroid-like compounds in yields ranging from 54 – 72 %, and *e.e.s* ranging from 89 – 94 % (Scheme 58).¹⁸⁹



Scheme 58: Polycyclisation reaction catalysed by (190); demonstrated by Jacobsen *et al*

2.3: Organocatalysis: Chiral Brønsted Acid Catalysts

As the body of this thesis is concerned with the use of chiral strong Brønsted acids as organocatalysts, this section will focus upon the forms of chiral Brønsted acids that have been developed for asymmetric synthesis. Examples related to the use of chiral Brønsted

acids in the synthesis of aziridines have been excluded from this section and are covered in *Chapter 3: Aziridines and Aziridination*.

The major class of chiral Brønsted acid catalysis are those based upon the optically active 1,1'-binaphthyl scaffold, which is often substituted at the 2,2'-positions with OH, to form BINOL (**124**). Further substitution can also be carried out at the 3,3'-positions. These axially chiral molecules are conformationally rigid due to steric interactions between the corresponding hydrogen atoms at the 8,8'-positions (Figure 38). Thus, these scaffolds are attractive starting points for the development of a chiral acid, due to potential of substitution, and lack of interconversion.

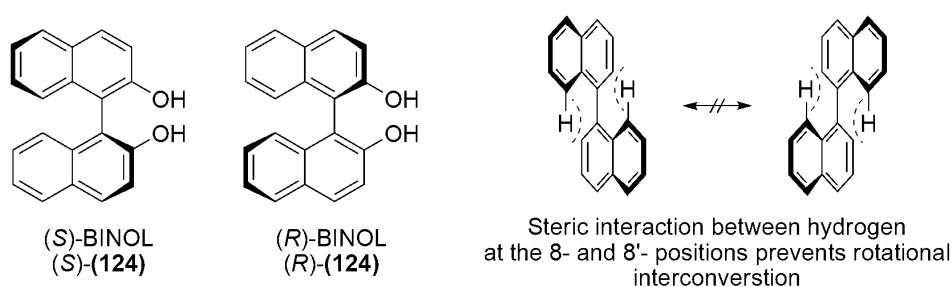
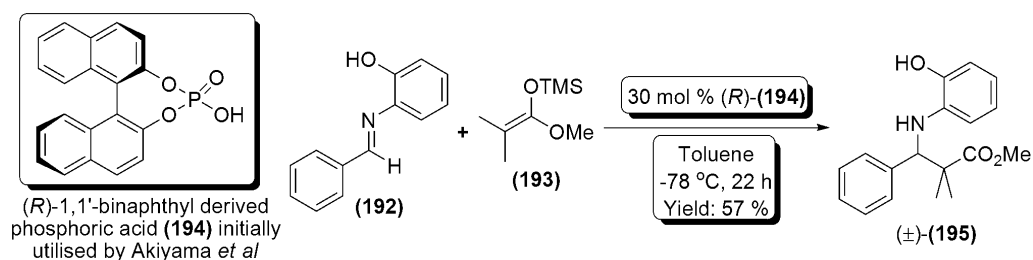


Figure 38: Representation of the axial chirality of 1,1'-binaphthyl-2,2'-diol, showing the steric interaction between the 8,8'-hydrogens

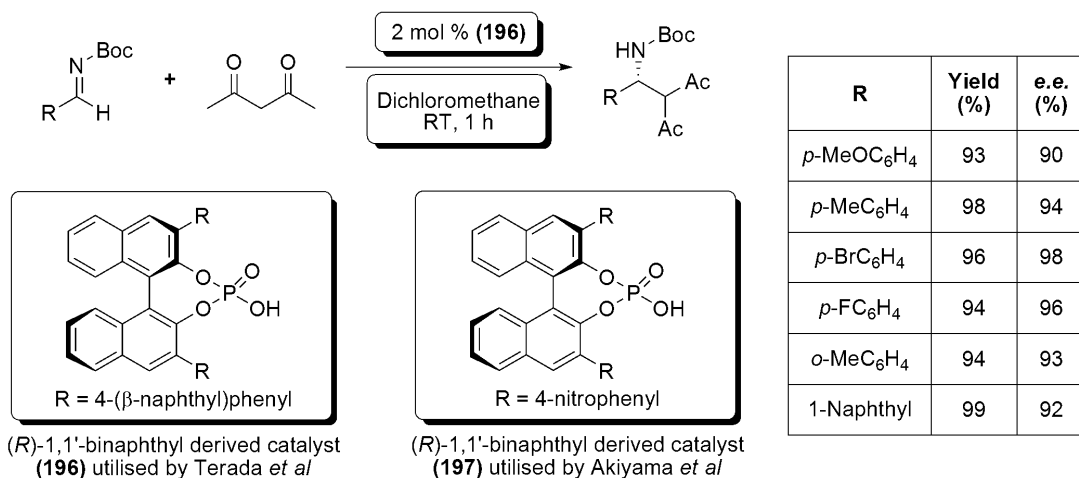
The first examples of chiral Brønsted acid catalysts of the type discussed above were simple phosphoric acids, (formed by treating (*S*)- or (*R*)-BINOL with phosphorus oxychloride and HCl) developed independently by the groups of Terada *et al* and Akiyama *et al*, and applied originally to asymmetric Mannich reactions. Initially, studies had been carried out upon the reaction of (**192**) with (**193**), utilising the phosphoric acid binaphthyl derivative (*R*)-(**194**), and were carried out by Akiyama *et al* (Scheme 59); however, no enantioselectivity was observed within the reaction product (**195**).¹⁹⁰



Scheme 59: Initial Brønsted acid catalysed Mannich reaction carried out by Akiyama *et al*

Further to this initial example, utilising (*R*)-(**196**) and (*R*)-(**197**) (formed by 3,3'-substitution of (**194**) with bulky aromatic groups), Akiyama *et al* and Terada *et al* independently demonstrated that chiral non-racemic Brønsted acids catalysed the asymmetric Mannich reactions of both aromatic, and *N*-Boc protected imines, affording the

Mannich products with yields and *e.e.s* as high as 100 % and 96 % respectively (Akiyama *et al*)¹⁹⁰, and 99 % and 98 % respectively (Terada *et al*)¹⁹¹ (Scheme 60).



Scheme 60: Brønsted acid catalysed asymmetric Mannich reactions; by Terada *et al*

Subsequent to this work, the mechanism of stereoselectivity within the Mannich reactions detailed above was elucidated further by Terada and Gridnev *et al*, who concluded that a hydrogen bonding interaction between substrate and catalyst could be responsible. Therefore, in order to induce high stereoselectivity, free rotation around the hydrogen bond had to be restricted (Figure 39). This hypothesis accounts for the lack of stereoselectivity in the initial Mannich reaction carried out by Akiyama *et al* utilising (*R*)-**(194)** (see Scheme 59); as no bulky substitution at the 3,3'-positions was present within (*R*)-**(194)** to prevent free rotation of the imine about the hydrogen bond.¹⁹²

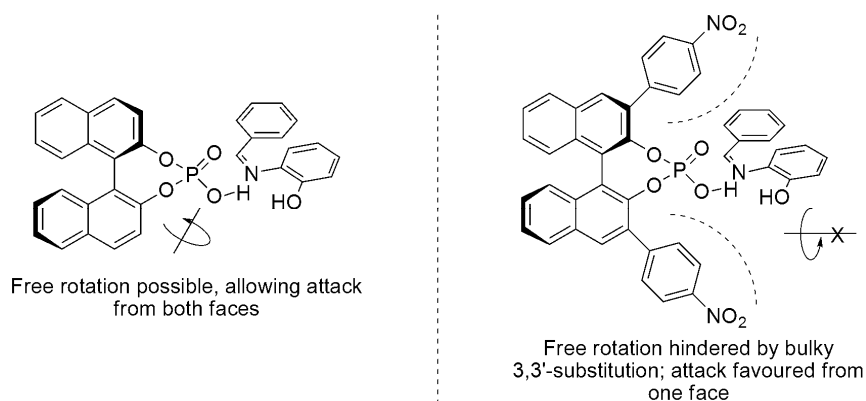
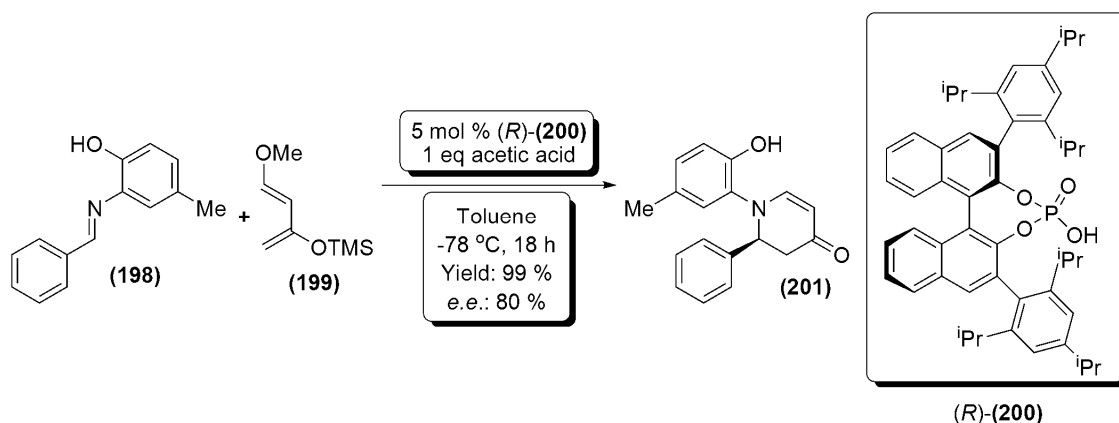


Figure 39: Representation of free rotation about a hydrogen bond, and its inhibition within the Mannich reactions of Akiyama *et al* and Terada *et al*

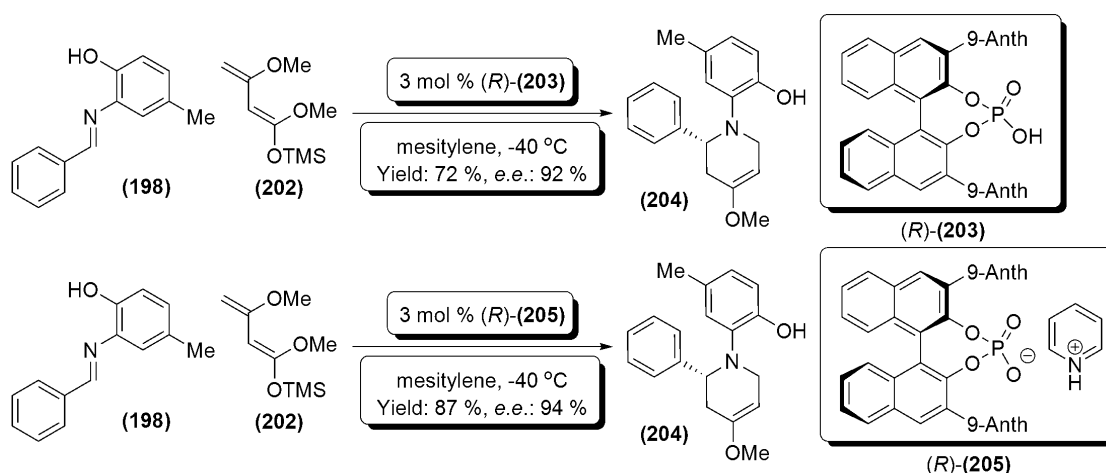
Chiral phosphoric acids have also been shown to catalyse aza-Diels-Alder reactions in an enantioselective manner. For example, Akiyama *et al* have shown that by treating the aldimine substrate **(198)** derived from benzaldehyde and 2-amino-4-methylphenol, and Danishefsky's diene **(199)**, with 10 mol % of the 3,3'-substituted BINOL phosphoric acid

(**200**) the desired cycloaddition product could be formed in a yield of 99 %, with a corresponding *e.e.* of 80 % (Scheme 61).¹⁹³



Scheme 61: Synthesis of Diels-Alder adduct (**201**) utilising 5 mol % (*R*)-(**200**); by Akiyama *et al*

Akiyama *et al* have also utilised chiral Brønsted acids in the aza-Diels-Alder reactions of Brassard's diene (**202**); in particular, with the aldimine (**198**). In general cycloaddition reactions with Brassard's diene are a synthetic challenge due to the reactivity and lability of the substrate, and therefore they are usually low yielding. Within their attempts to develop an enantioselective catalytic version of this cycloaddition, Akiyama *et al* attempted to use various catalysts, including a *bis*-9-anthryl BINOL derived phosphoric acid (**203**), which had shown to be the most effective catalyst during a catalyst screen for the aza-Diels-Alder reaction.¹⁹⁴ However, although yielding the desired product (**204**) in 72 % yield, and 92 % *e.e.*, it was found that alteration of the catalyst *via* formation of its pyridinium salt (**205**) increased the yield of (**204**) to 87 % while maintaining a comparable *e.e.* (Scheme 62). It was believed that this increase in yield was due to the reduction in acid strength between the free acid, and the salt, thus reducing decomposition of the substrate diene.¹⁹⁵

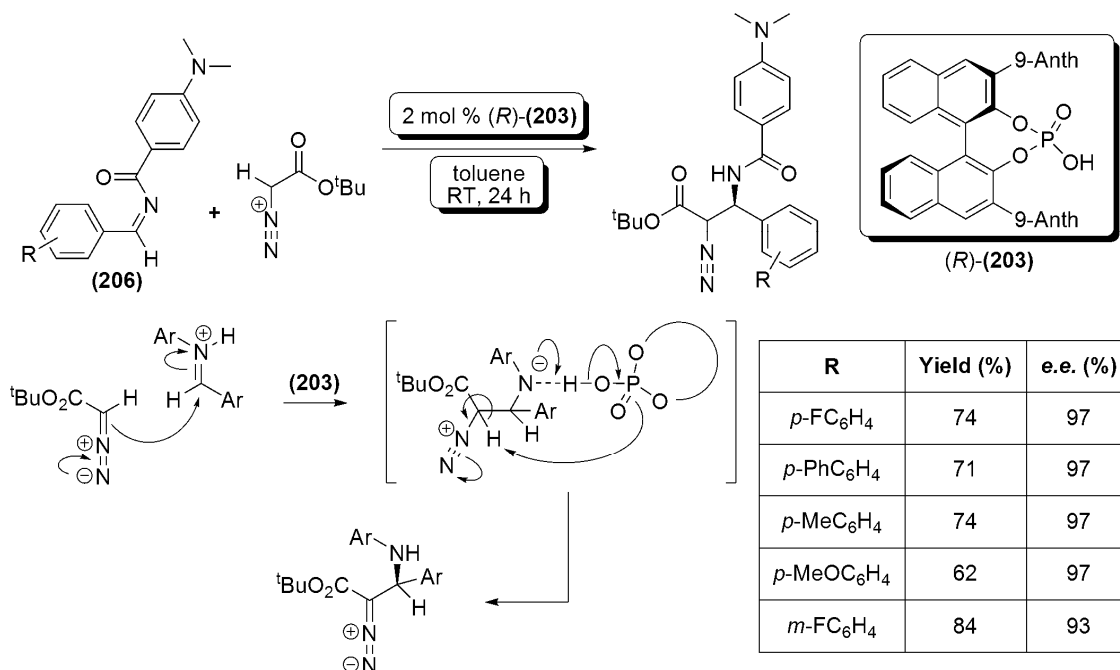


Scheme 62: Synthesis of Diels-Alder cycloadduct (**204**) utilising 3 mol % (*R*)-(**203**), or (*R*)-(**205**)

This reduction in decomposition was proven *via* an NMR experiment; monitoring the decomposition of Brassard's diene (**202**) in the presence of either (**203**) or (**205**) after one hour. In the presence of (**203**), only 12 % of the Brassard's diene was intact after this time, whereas, in the presence of (**205**), 75 % of the initial Brassard's diene remained.

A further interesting example of the use of chiral BINOL derived phosphoric acids is that of the 'Friedel-Crafts like' alkylation of an imine substrate developed by Terada *et al.* Utilising imines such as (**206**), and a diazoacetate (*i.e.* ethyl or *tert*-butyl diazoacetate) as the alkylating agent, in the presence of 2 mol % (*R*)-(**203**) the reaction afforded the desired alkylated products in yields of between 62 and 89 %, and *e.e.s* of between 91 and 97 % (Scheme 63).

This reaction is worthy of interest as treatment of an imine with a diazoacetate and a protic catalyst is a commonly used method of producing aziridines *i.e.* the aza-Darzens aziridination reaction (see *Chapter 3: Aziridines & Aziridination*). In this case however, Terada *et al* had demonstrated a formal alkylation of the imine, as opposed to aziridine formation. Terada *et al* hypothesised that the reaction proceeded *via* an addition elimination pathway, invoking an intracomplex deprotonation step in order to explain the suppression of the aza-Darzens reaction (Scheme 63).¹⁹⁴



Scheme 63: Examples of the 'Friedel-Crafts like' alkylation reaction developed by Terada *et al.*, and the hypothesised intracomplex deprotonation mechanism

As the area of chiral Brønsted acid catalysis has grown, it has become an attractive proposition to produce more highly acidic chiral Brønsted acids; in order to allow protonation of less basic substrates, such as carbonyl compounds. This area was first approached by Yamamoto *et al.*, who amended the traditional BINOL derived phosphoric

acid motif to contain a strong electron withdrawing functionality in the form of a trifluoromethane sulfonamide group (Figure 40),¹⁹⁶ thus decreasing the pK_a of the system to *ca.* -1 when compared with the less acidic pK_a of *ca.* 1 – 2 (*ca.* 13 – 14 in acetonitrile) typical of a standard BINOL derived phosphoric acid. It is worthy of note that *N*-triflylphosphoramidate based catalysts were designed to have pK_a values of *ca.* 7 in acetonitrile.¹⁹⁷

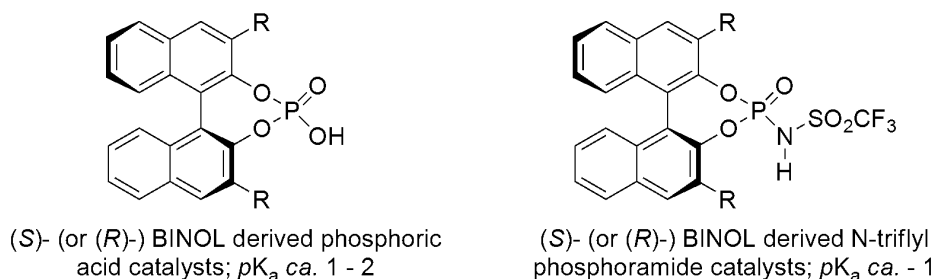
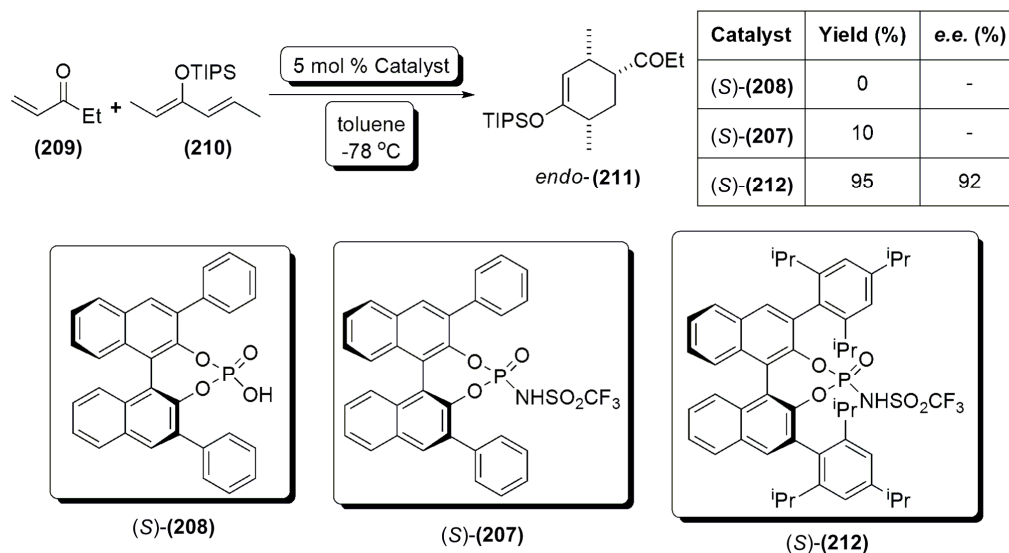


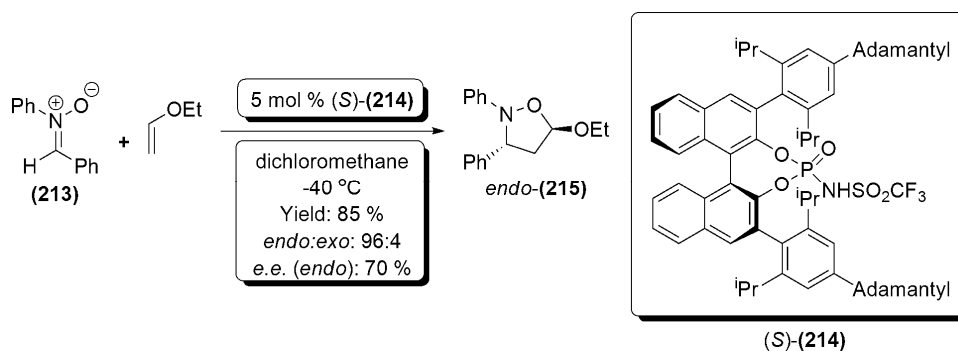
Figure 40: Representation of the general form of BINOL derived phosphoric acids and *N*-triflylphosphoramidates

The higher acidity of these *N*-triflylphosphoramidate containing BINOL derived catalysts was demonstrated by Yamamoto *et al* who carried out a direct comparison between the *N*-triflylphosphoramidate catalyst (**207**), and a traditional phosphoric acid catalyst (**208**) within the scope of the Diels-Alder reaction. Treating ethyl vinyl ketone (**209**) and diene (**210**) (Scheme 64) with the BINOL derived phosphoric acid catalyst (**208**), no reaction was observed. However, upon treatment under the same conditions utilising the BINOL derived *N*-triflylphosphoramidate catalyst (**207**), a yield of *ca.* 10 % of the racemic *endo* cycloaddition product (**211**) were obtained. However, upon optimisation of the 3,3'-substitution of the catalyst, a yield of 95 % and e.e. of 92 % of the *endo* addition product were achieved with catalyst (**212**).¹⁹⁶ The observed higher activity is believed to come about as a direct result of the increased ability of the *N*-triflylphosphoramidate catalyst to protonate the less basic ketone carbonyl.



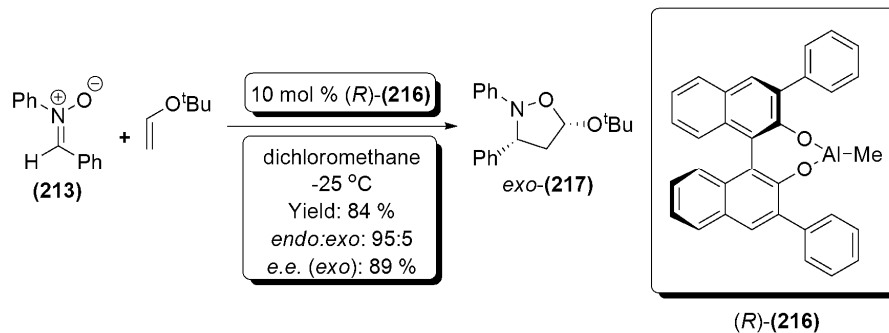
Scheme 64: Direct comparison of the phosphoric acid based catalyst (208) and the *N*-triflylphosphoramidate catalysts (207) and (212) within the Diels-Alder reaction of (209) with (210)

Further to the Diels-Alder cycloaddition, BINOL derived *N*-triflylphosphoramidates have also been employed by Yamamoto *et al* within 1,3-dipolar cycloaddition reactions.¹⁹⁸ Utilising nitron starting materials such as (213), Yamamoto *et al* were able to demonstrate organocatalysed cycloaddition with ethyl vinyl ether catalysed by 5 mol % of the chiral BINOL based *N*-triflylphosphoramidate catalyst (214) affording, in general, good to excellent yields of 66 – 99 %, and *e.e.s* ranging from 56 – 93 % (Scheme 65).



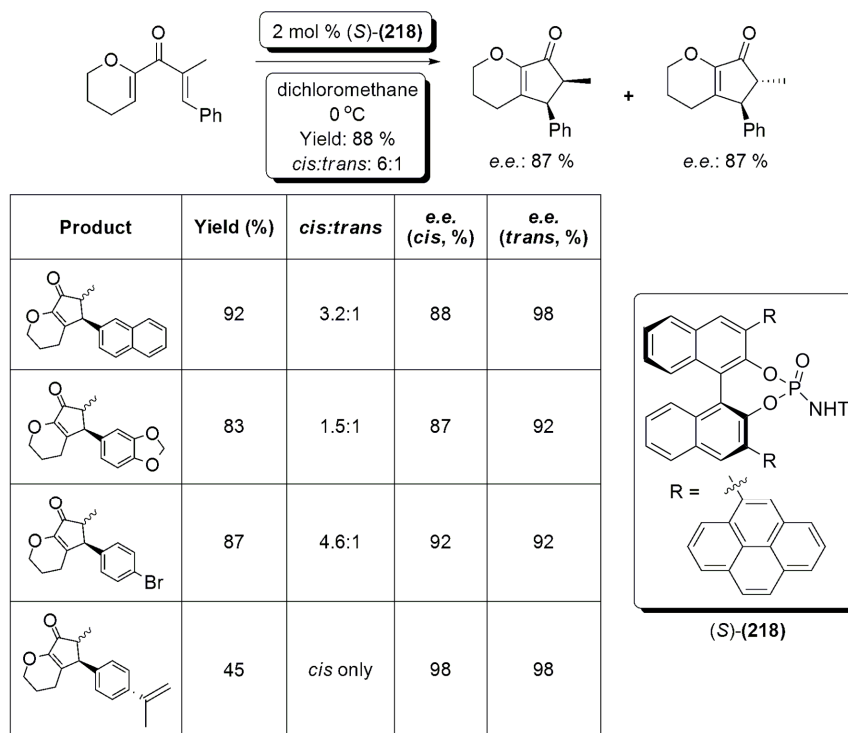
Scheme 65: 1,3-dipolar cycloaddition reaction, catalysed by 5 mol % (214); by Yamamoto *et al*

These results are worthy of note due to the ability of (214) to catalyse the reaction at lower temperatures than the methodology previously reported by Jørgensen *et al* (utilising BINOL derived aluminium Lewis acid catalysts, at temperatures of *ca.* -25 °C); and also, the reaction afforded *endo* products as the major diastereoisomer (as opposed to the *exo* materials afforded within the Jørgensen method, Scheme 66).¹⁹⁹



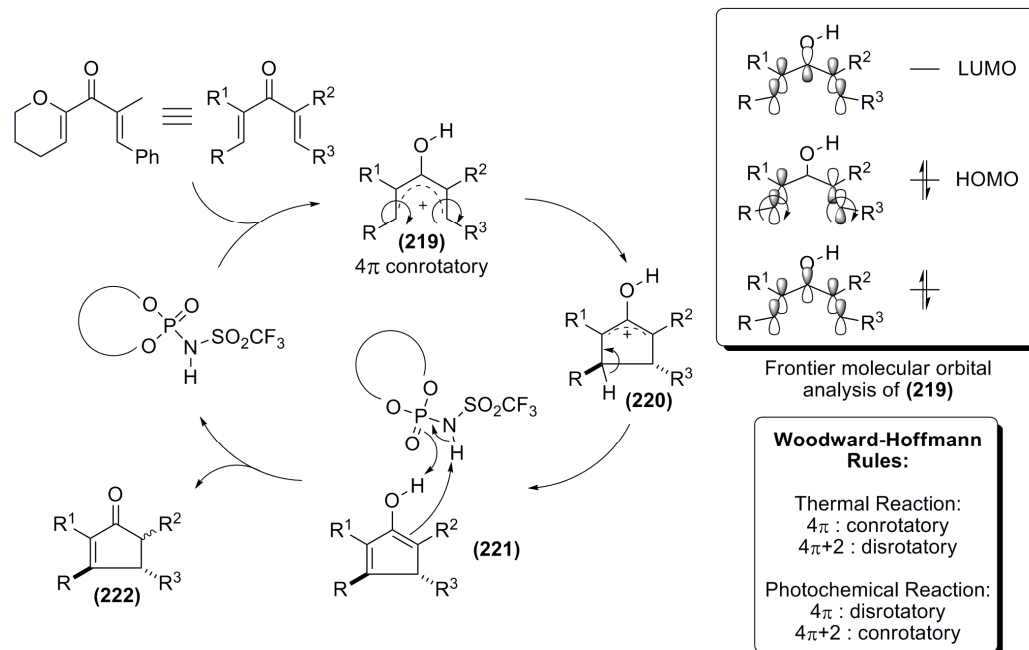
Scheme 66: 1,3-dipolar cycloaddition catalysed by 10 mol % (216); reported by Jørgensen *et al*

Further to the reactions detailed above, Rueping *et al* have also reported an enantioselective organocatalytic Nazarov reaction. Utilising 2 mol % of the BINOL derived *N*-triflylphosphoramidate (218) (Scheme 67), Rueping *et al* demonstrated that yields ranging from 45 – 88 %, and *e.e.s* of ~90 % were readily achievable; with various functionality tolerated, including aromatic, halogenated, and ether linkages (Scheme 67).²⁰⁰



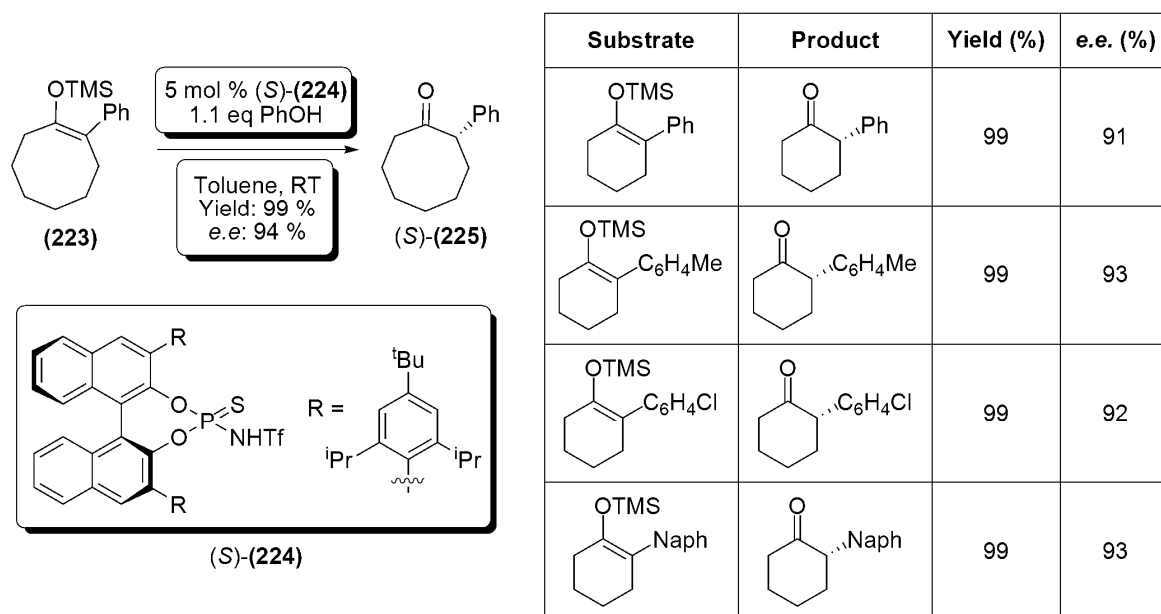
Scheme 67: Examples of the catalytic asymmetric Nazarov reaction developed by Rueping *et al*

The mechanism of these Nazarov reactions is an initial protonation of the carbonyl, leading to a 4π conrotatory electrocyclic ring closure (219) (as predicted by the Woodward-Hoffman rules), followed by proton elimination (220), and finally protonation of the intermediate (221) to produce the desired product (222) (Scheme 68).



Scheme 68: Mechanism of the asymmetric Nazarov reaction developed by Rueping *et al*

Moving away from cyclic reactions, Brønsted acid phosphoramidates have also been employed for enantioselective protonation reactions. Yamamoto *et al* have developed an asymmetric protonation of cyclic silyl enol ethers in order to produce the corresponding asymmetric carbonyl compounds.²⁰¹ For example, treatment of (223) with 10 mol % (S)-(224), and 1.1 equivalents of phenol led to the asymmetric protonation of (223), affording (S)-(225) in 99 % yield, and 91 % *e.e.* (Scheme 69).

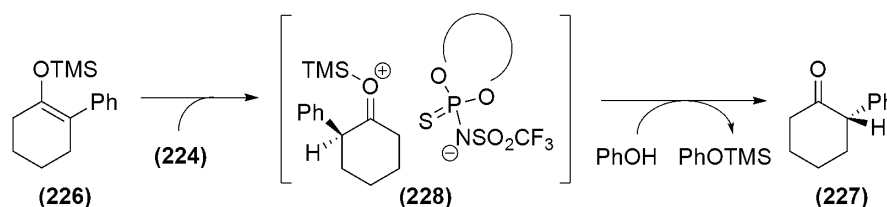


Scheme 69: Asymmetric protonation reactions utilizing 5 mol % (224); by Yamamoto *et al*

It was found that a stoichiometric achiral proton source was also required in order for the asymmetric protonation to be successful. This achiral proton source was believed by Yamamoto *et al* to serve two functions within the reaction. Firstly to act as a source of

proton to regenerate the asymmetric Brønsted acid species; and secondly to facilitate the removal of the silyl protecting group from the substrates. Within the work of Yamamoto *et al*, phenol was utilised in this role; as it has an affinity for silyl groups which is much higher than that of the conjugate base of the asymmetric Brønsted acid (**224**) (utilised as the chiral proton source).

The necessity of the achiral proton source was demonstrated by treating (**226**) with a stoichiometric amount of the asymmetric Brønsted acid, (**224**). After 2 days, no reaction had been observed. By addition of a stoichiometric amount of acetic acid, the reaction was then seen to be complete within 2 hours, yielding (**227**) in 99 % yield, and 88 % *e.e.*. This result suggests the reaction is proceeding by an initial formation of a chiral ion pair (**228**) (carried out by (**224**)), followed by removal of the silyl group by the achiral proton source, generating the chiral product (**227**) required (Scheme 70).



Scheme 70: Proposed mechanism of the asymmetric protonation reaction, showing generation of the chiral ion-pair (228**); proposed by Yamamoto *et al***

Further to the reactions outlined above, BINOL based phosphoric acids, and *N*-triflylphosphoramides (and their derivatives), have been utilised in many other reaction types and are the subject of several dedicated reviews.²⁰²⁻²⁰⁴

Worthy of note at the end of this section is the further development of novel chiral Brønsted acids (Figure 53); some of which are stronger even than the *N*-triflylphosphoramides described above. For example, the synthesis of bis(sulfuryl)imide based Brønsted acids (JINGLEs) by Berkessel *et al*. These catalysts were based upon initial work by List,²⁰⁵ and Giernoth *et al*,²⁰⁶ which led to the production of so-called BINBAM species; examples of the general structure of both JINGLEs (**229**) and BINBAMs (**230**) are shown in Figure 41.

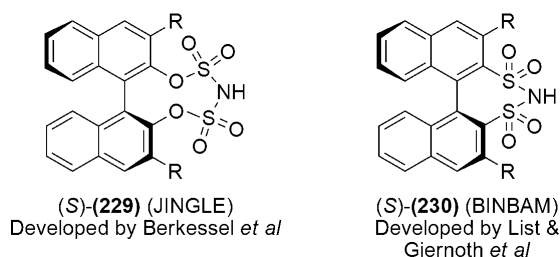


Figure 41: General structures of the JINGLE (229**), and BINBAM (**230**) type novel, chiral Brønsted acids**

Chapter 3: Aziridines & Aziridination

3.1: Aziridines: Introduction

Aziridines in general are classified as saturated three membered heterocycles, containing one nitrogen atom. The simplest example of which is aziridine itself, otherwise known as ethylene imine, or azacyclopropane.

Despite the apparent simplicity of the aziridine ring system, the bonding within the ring is unusual; this being due to the strain inherent within producing the required bond angles. If traditional sp^3 hybridisation is considered, the bond angles required within the ring system (60°) are impossible. Thus, in order to accommodate these tight bonding angles, the σ -bonds gain p -orbital character. This p -character leads to the observation of so called ‘banana bonds’, or bent bonding between the ring substituents. This mixing has the subsequent effect of leading to an increase in the s -orbital character of the C-R and N-R bonds, leading to shorter bond lengths. The increased s -character can also be implicated in the decreased basicity of the nitrogen lone pair in aziridines; the observed pK_a of the aziridinium ion being 7.98, compared to common values of acyclic secondary amines which are generally *ca.* 11.²⁰⁷

The reactions of aziridines tend to be focussed upon relieving the steric ring strain placed upon the system by the required bonding angles. The strain inherent within the aziridine ring system is similar to that found within cyclopropane systems *c.a.* 27 kcal/mol.²⁰⁷ Thus aziridines can be seen to undergo various ring opening reactions with nucleophiles.

From a synthetic chemistry view, aziridines are the nitrogen equivalent of epoxides; and like their oxygen counterparts, are highly useful synthetic intermediates within synthetic organic chemistry. Also, due to the inclusion of the aziridine ring in various natural, and biologically active, compounds, aziridines themselves are seen as a valuable target of synthetic chemistry. Despite their potential uses, aziridines tend to be utilised less within this remit, due, in part, to the lack of efficient or easy to use methods of synthesis that are available.

3.2: Aziridines: An Overview of General Synthesis Methods

In general, there are three traditional methods by which aziridines can be synthesised. These being: transfer of nitrogen to olefins, amine cyclisation reactions, and transfer of carbon to imines.

The transfer of nitrogen to olefins is an attractive method of synthesising aziridines, due to the direct nature of the transformation, and also the high availability of unsaturated starting materials. On an initial look, this method seems analogous to the oxygen atom transfers which are commonly used to produce epoxides. However, systems which are effective in these epoxidation reactions tend to not be effective within aziridination systems; for example porphyrin based epoxidation systems²⁰⁸⁻²¹⁰ are generally of limited use within aziridination reactions.

The principal method for undertaking nitrogen additions to olefins involves utilising nitrenes or nitrenoids as the nitrogen source. This in itself presents issues when considering the stereoselective production of aziridines. The issue comes about due to the nature of the nitrene starting material used. Nitrenes can exist in both singlet and triplet states, and both states will undergo aziridine formation with a different mechanism. Thus, singlet nitrenes will undergo aziridination with a concerted process, allowing for stereoselectivity within the reaction. However, triplet nitrenes will undergo a two step aziridination process, thus allowing time for free rotation about the carbon bond, and the potential loss of any stereoselectivity (Figure 42).²¹¹

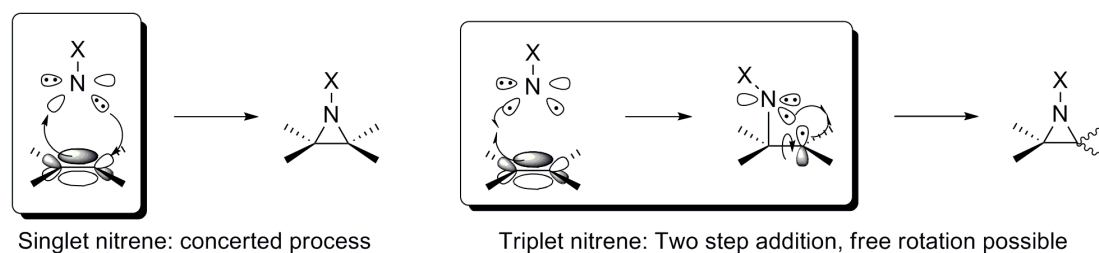
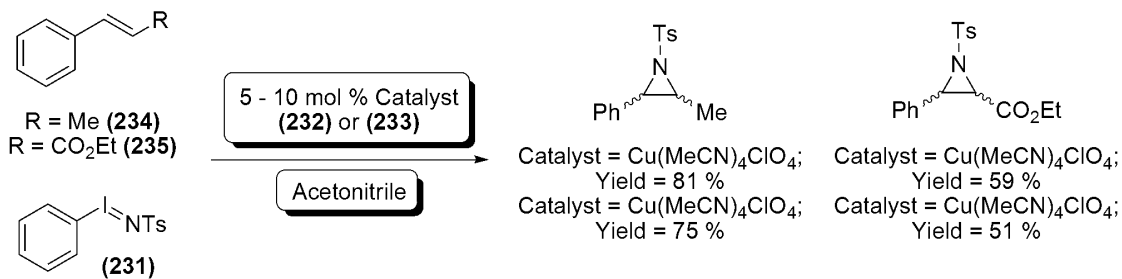


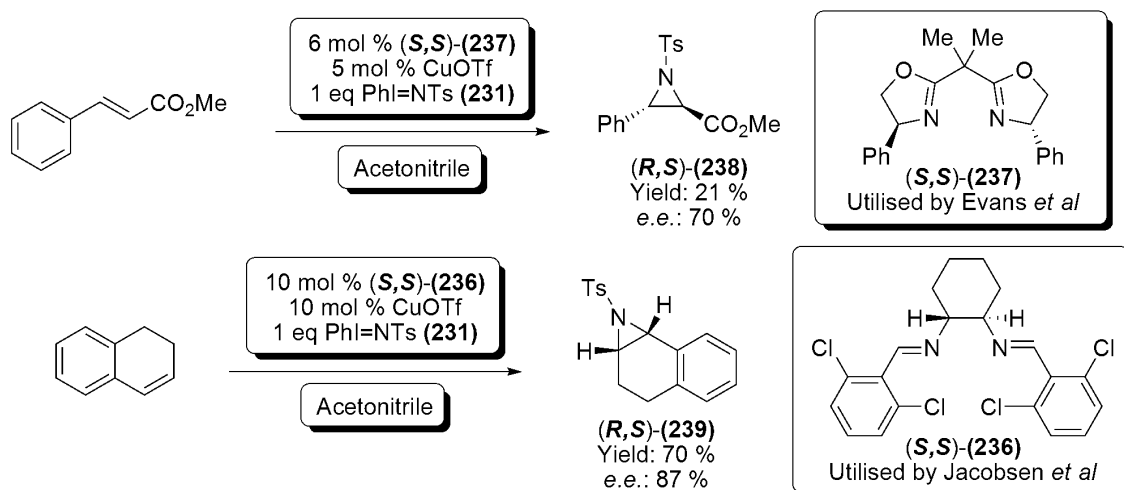
Figure 42: The two addition mechanisms of a nitrene to an olefin

In 1991, Evans *et al* disclosed the use of (*N*-(*p*-toluenesulfonyl)imino)phenyliodine (231), and copper (I) (*e.g.* (Cu(MeCN)₄ClO₄ (232)) or (II) (*e.g.* Cu(acac)₂ (233)) catalysts as an aziridination system for both electron rich (*e.g.* prop-1-enylbenzene (234)), and electron deficient (*e.g.* ethyl cinnamate (235)), olefins (Scheme 71).²¹²



Scheme 71: Initial publication of the use of (231) and Cu(I) (232) or Cu(II) (233) catalysts in order to synthesise aziridines from electron-rich (234) and electron-deficient (235) olefins; by Evans *et al*

This was followed with publications in 1993 by both Evans *et al* and Jacobsen *et al* concerned with the enantioselective synthesis of aziridines utilising (231) and Cu(I) catalysts functionalised with chiral ligands ((*S,S*)-(236) by Jacobsen *et al*, (*S,S*)-(237) by Evans *et al*, Scheme 72).^{213,214} These systems both allow stabilisation of the singlet nitrene, and thus facilitate enantioselective aziridination reactions.

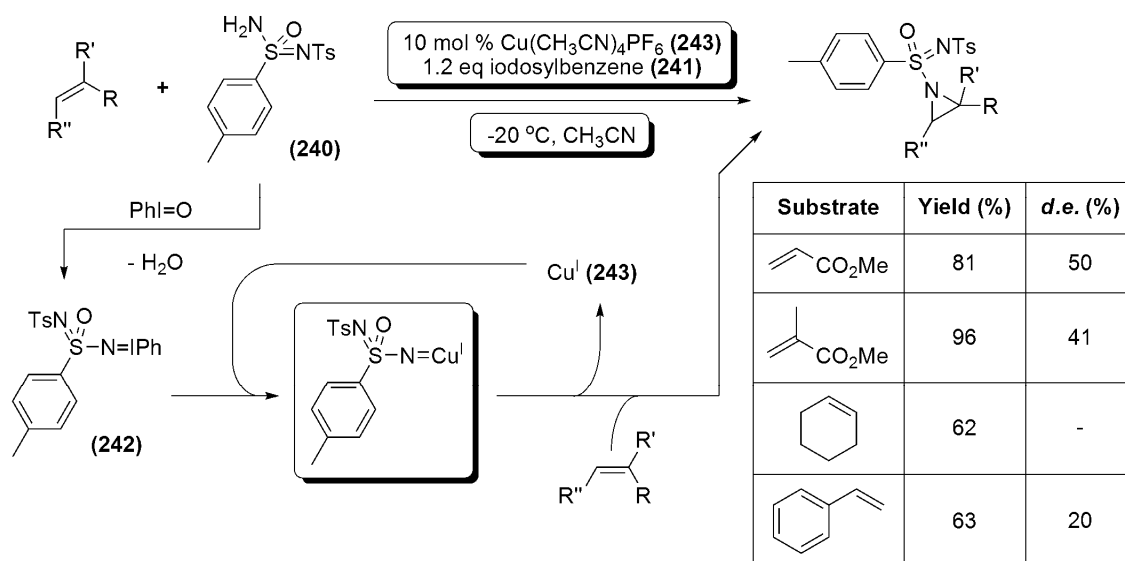


Scheme 72: Enantioselective syntheses of aziridines (238) and (239) utilising (231) as a stabilised singlet nitrene; carried out by Evans *et al*, and Jacobsen *et al*

While these reactions allow for the production of aziridines in generally good yields (16 – 89 % Evans *et al*, 50 – 79 % Jacobsen *et al*), and in some cases *e.e.*'s (19 – 97 % Evans *et al*, 30 – 98 % Jacobsen *et al*), the use of isolated hypervalent iodine species such as (231) can be difficult and in some cases dangerous (some of these materials have been reported as explosive).²¹⁵

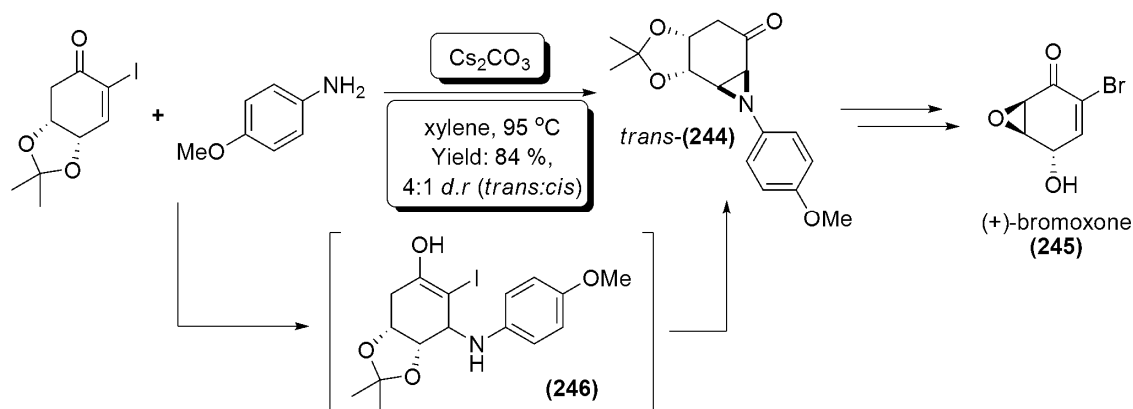
The use of hypervalent iodine species has been improved somewhat in recent times by the development of methods for generating nitrenes *in situ*, thus avoiding isolation. The work of Dauban *et al* is of note in this area. They have shown that *N*-(*p*-toluenesulfonyl)-*p*-toluenesulfonimidamide (240) when treated with iodobenzene (241) will generate the nitrene species (242) *in situ*,²¹⁶ which can be subsequently transferred to olefinic substrates (catalysed by the Cu(I) species Cu(CH₃CN)₄PF₆ (243)). This reaction allowed for the

production of aziridines in yields of between 35 – 96 % and *d.e.* as high as 50 % (Scheme 73).²¹⁷



Scheme 73: *In situ* generation of the nitrene species (242), and Cu(I) catalysed transfer of (242) to olefins to form aziridines; by Dauban *et al*

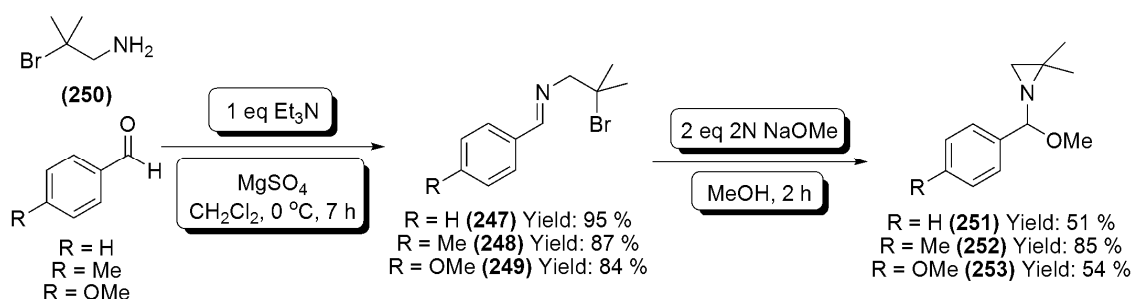
An interesting example of aziridine synthesis by addition of nitrogen to a double bond is that of the work of Maycock *et al.* Utilising the Gabriel-Cromwell reaction process,²¹⁸ that is, an addition-elimination route to aziridines (See synthesis of *trans*-(244), Scheme 74), the group were able to synthesise precursors in a short total synthesis of (+)-bromoxone (245) (Scheme 74).²¹⁹



Scheme 74: Synthesis of (+)-bromoxone; an example of cyclisation of amines to form aziridines

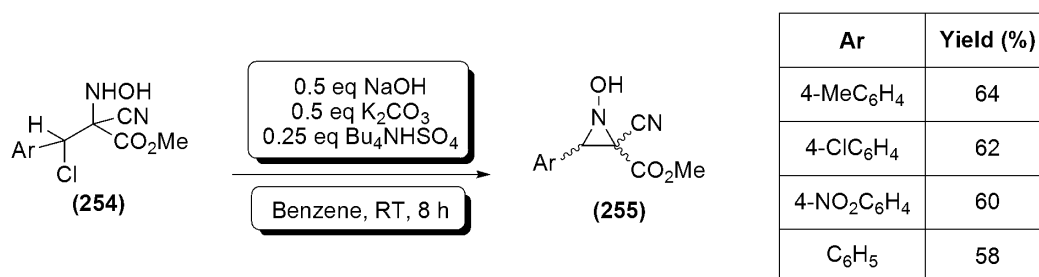
The aziridine synthesis demonstrated in Scheme 74 leads into the second and potentially more attractive area of aziridine synthesis; that concerned with the cyclisation of amines bearing a leaving group. These methods rely upon a 1,2-arrangement of the amine to the leaving group, allowing a 3-*exo*-tet cyclisation to take place (as can be seen within intermediate (246), Scheme 74). Typically, substrates for this type of aziridine synthesis include 1,2-amino halides, and 1,2-azido alcohols.

For example, De Kimpe *et al* have demonstrated that treatment of *N*-substituted imines (**247**) – (**249**) (derived from 2-bromo-2-methylpropylamine hydrobromide (**250**) and substituted benzaldehydes, Scheme 75) under basic conditions leads to the formation of racemic aziridines (*e.g.* (**251**) – (**253**), Scheme 75) *via* intramolecular displacement of bromide.²²⁰ Using this method, yields of 51 – 85 % have been obtained.



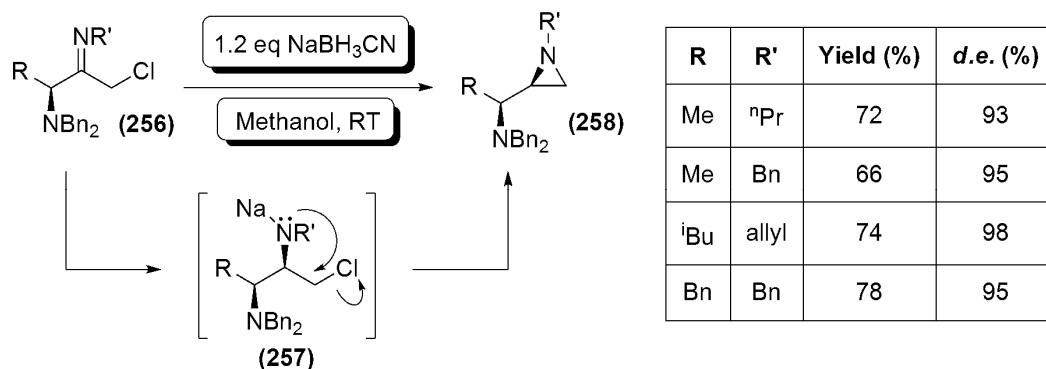
Scheme 75: Base catalysed synthesis of aziridines (251**) – (**253**) *via* intramolecular displacement of bromide**

Further to this example, various other halide displacement procedures for the synthesis of racemic aziridines have been reported, including the use of β -halo-amino esters (*e.g.* (**254**)) by Boukhris *et al.*²²¹ This methodology allowed for the synthesis of racemic *N*-hydroxy 2-cyano-aziridine-2-carboxylates (*e.g.* (**255**)) in moderate yields of between 58 and 65 % (Scheme 76).



Scheme 76: Cyclisation of β -halo-amino esters (254**) to form *N*-hydroxy 2-cyano-aziridine-2-carboxylates (**255**) by Boukhris *et al***

Related to the above examples, the work of Concellón *et al* utilising α -amino- α -chloro ketamines is a good example of utilising an amine cyclisation method in order to produce enantiopure aziridines (Scheme 77). The reaction proceeds *via* reduction of the starting material ketamine (for example, (**256**)) with sodium cyanoborohydride, generating an intermediate species (such as (**257**)), which undergoes spontaneous intramolecular cyclisation to afford the desired enantioenriched aziridine (based upon (**258**)). Although this method does allow for the production of enantiopure aziridines in *e.e.s* of up to 95 %, it requires the use of enantiopure ketamine species, which is far from ideal as they have been shown to decompose in *ca.* 24 hours at -10 °C.²²²



Scheme 77: Selected examples of the cyclisation of amino- α -chloro ketamines to produce enantioenriched aziridines; by Concellón *et al*

The final major methodology utilised in the synthesis of aziridines relies upon the transfer of carbon to an imine. The major reaction type within this area being those reactions termed as aza-Darzens reactions. The aza-Darzens mechanism is essentially a reversible nucleophilic attack upon the C=N bond of an imine, followed by a 3-*exo*-tet cyclisation step, which is generally favoured, and typically irreversible (Figure 43).²²³

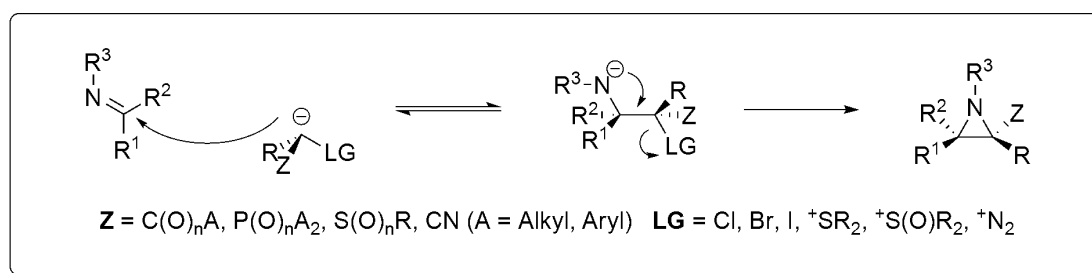
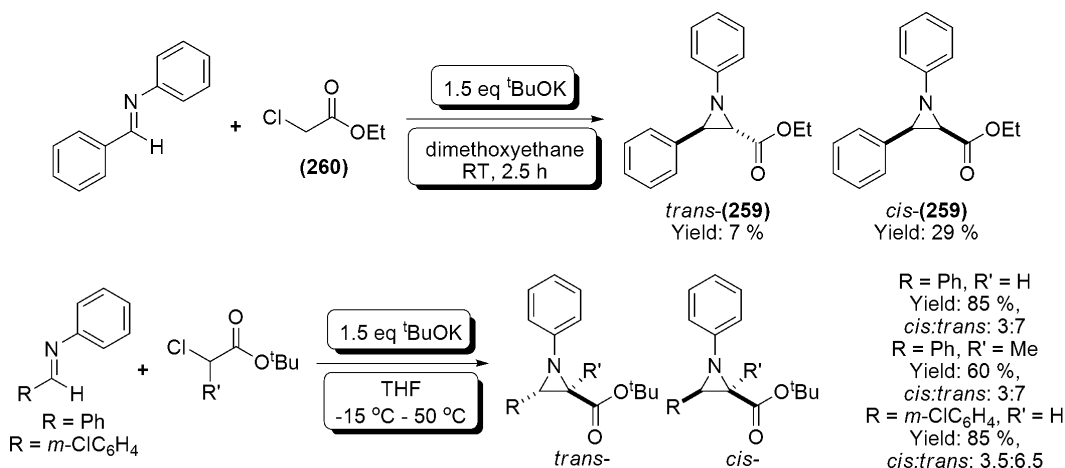


Figure 43: The aza-Darzens mechanism for aziridination

Commonly utilised substrates within aza-Darzens reactions include carbenes/carbenoids,²²⁴ ylides,²²⁵ and α -haloenolates.²²⁶ These reactions have been widely exploited within the synthesis of aziridines due to the broad range of compatible substrates available, and also, the possibility of producing chiral non-racemic aziridines *via* the use of either a chiral imine,²²⁷ chiral nucleophile,²²⁸ or chiral catalyst.²²³

The aza-Darzens reaction was first employed as early as 1969 in the synthesis of the phenyl substituted aziridine-2-carboxylate species (**259**).²²⁹ This single reaction by Deyrup involved the use of ethyl chloroacetate (**260**) as the nucleophile, producing the desired aziridine (**259**) with a *cis:trans* ratio of *ca.* 9:1, and in a yield of 36 % comprising both the *cis*- and *trans*- products (Scheme 78). This initial work led into the development of a general method by Wartski in a publication containing the aza-Darzens reaction of a range of imines and esters to give aziridine-2-carboxylates (Scheme 78).²³⁰



Scheme 78: Initial aza-Darzens type aziridinations carried out by Deyrup, and Wartski *et al*

As the main body of this thesis is concerned with the utilisation of alkyl diazoacetates as the nucleophilic substrate for the chiral non-racemic production of aziridines, this area will be discussed in more detail in the following paragraphs.

3.3.1: Aziridination: Aziridination with Alkyl Diazoacetates - Introduction

Although the ring closure step within the aza-Darzens reaction is generally favourable (and thus a driving force for the reaction), the initial nucleophilic attack of a diazoacetate onto an imine to form the intermediate species will not occur through simple mixing. This is due to the relatively weak nucleophilicity of alkyl diazoacetates (due to both resonance stabilisation, and inductive effects, Figure 44). Thus, in order to allow the formation of aziridines *via* this method, some form of catalysis is required. This catalysis usually takes the form of an acid; be it a Lewis, or Brønsted acid species.

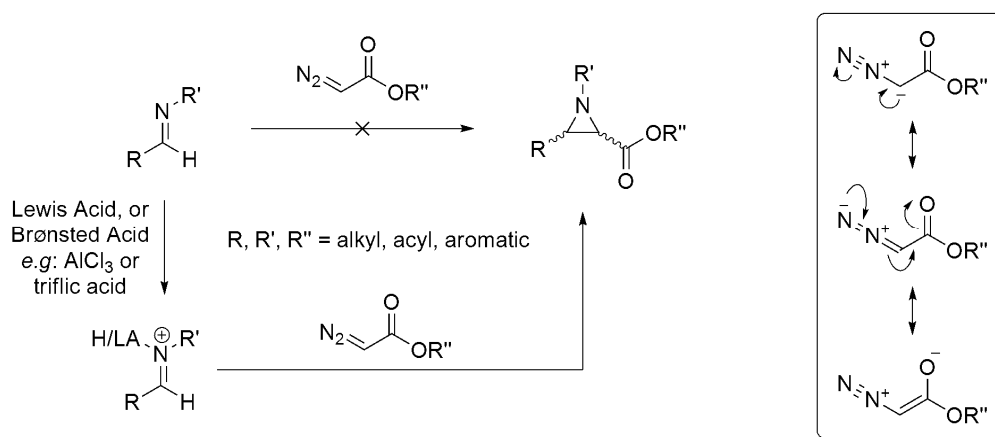


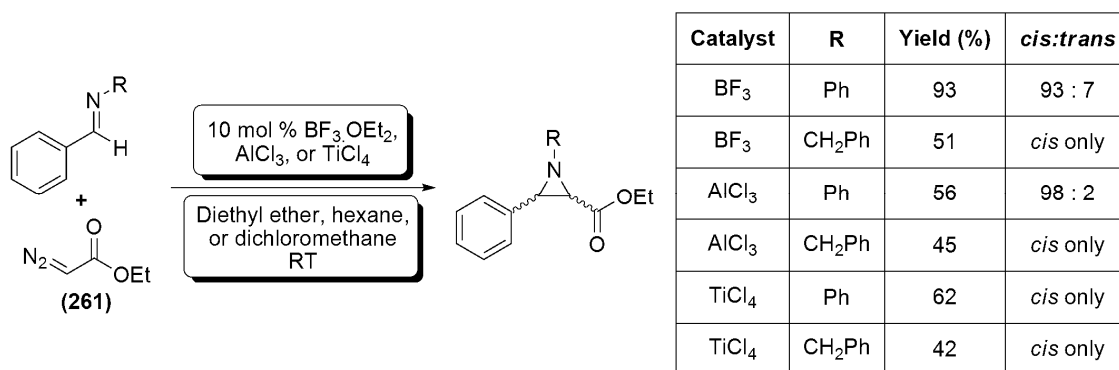
Figure 44: Resonance stabilisation of alkyl diazoacetates, and demonstration of Lewis acid and Brønsted acid activation of *N*-substituted imines

Both Brønsted and Lewis acid activation rely upon the lowering of the LUMO of the imine due to polarisation of the carbon nitrogen bond, thus increasing the electrophilicity of the imine carbon. This is analogous to the activation mode found within

the area of iminium catalysis (see Figure 31, and 2.2.3: *Organocatalysis: General Activation Mechanisms & Selected Examples – Iminium Catalysis*).

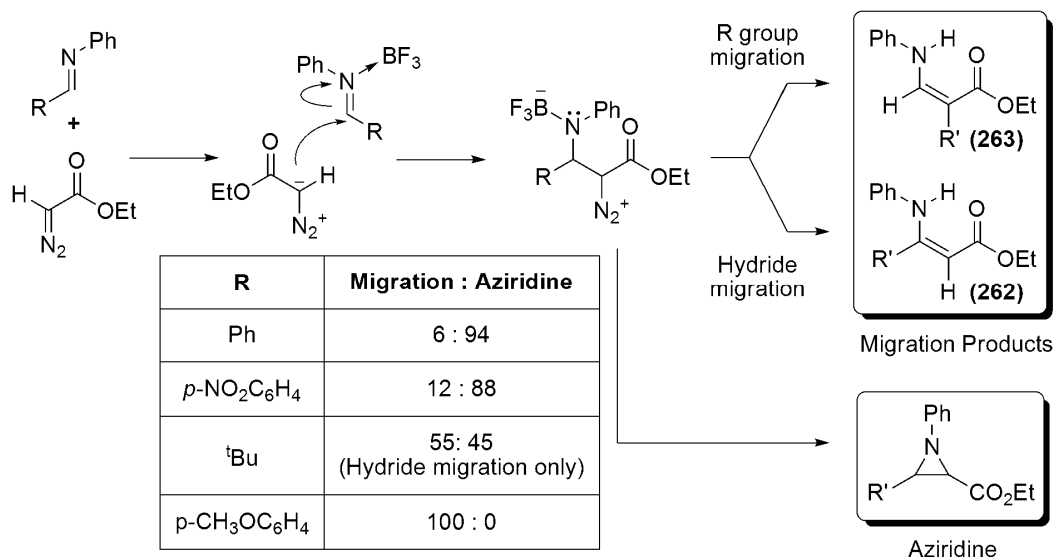
3.3.2: Aziridination: Aziridination with Diazoacetates - Lewis Acid Catalysis

The catalytic application of Lewis acids within the scope of the aza-Darzens reaction was initially reported in the mid 1990s, by Brookhart and Templeton *et al* (although the use of copper(II) triflate had been explored by Jorgensen *et al* at a similar time).²³¹ Carrying out a wide ranging study using common Lewis acids upon the formation of aziridines, Templeton and Brookhart were able to show that 10 mol % boron trifluoride, aluminium trichloride, and titanium tetrachloride catalysed the formation of racemic aziridines from various *N*-substituted imines (Scheme 79), and ethyl diazoacetate (EDA, (**261**)), in yields of between 42 and 93 %.²³²



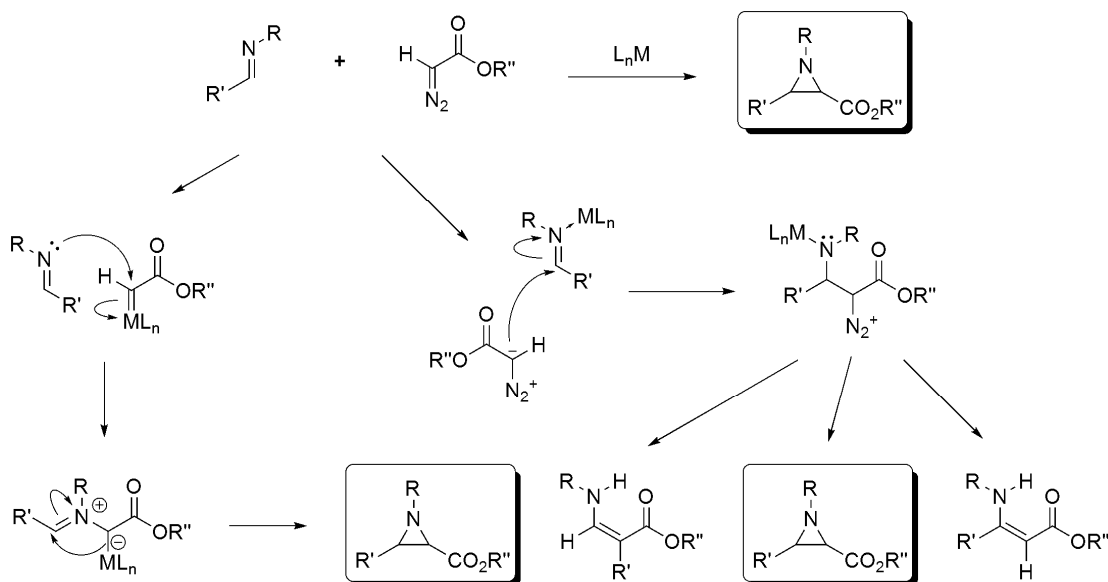
Scheme 79: Selected examples of the Lewis acid catalysed aziridination chemistry demonstrated by Templeton and Brookhart *et al*

In the majority of cases, the reaction shown in Scheme 79 yielded predominantly, or only, the *cis*-aziridine; however, it is worthy of note that two by-products (**262**) and (**263**) (Scheme 80) were also present within the reaction. Templeton and Brookhart hypothesised that the formation of these enamine by-products could be accounted for by migration of either hydride (forming (**262**)), or the R group from the imine (forming (**263**)). This hypothesis was supported by the observation that when differing aryl substituents were utilised, electron withdrawing groups favoured the aziridine formation; whereas, aziridine formation was suppressed when electron donating substituents were used (Scheme 80), in line with the migratory aptitude of each group.



Scheme 80: Proposed mechanism of formation of the observed enamine by-products (262) and (263) within the aziridination reactions of Templeton and Brookhart *et al*

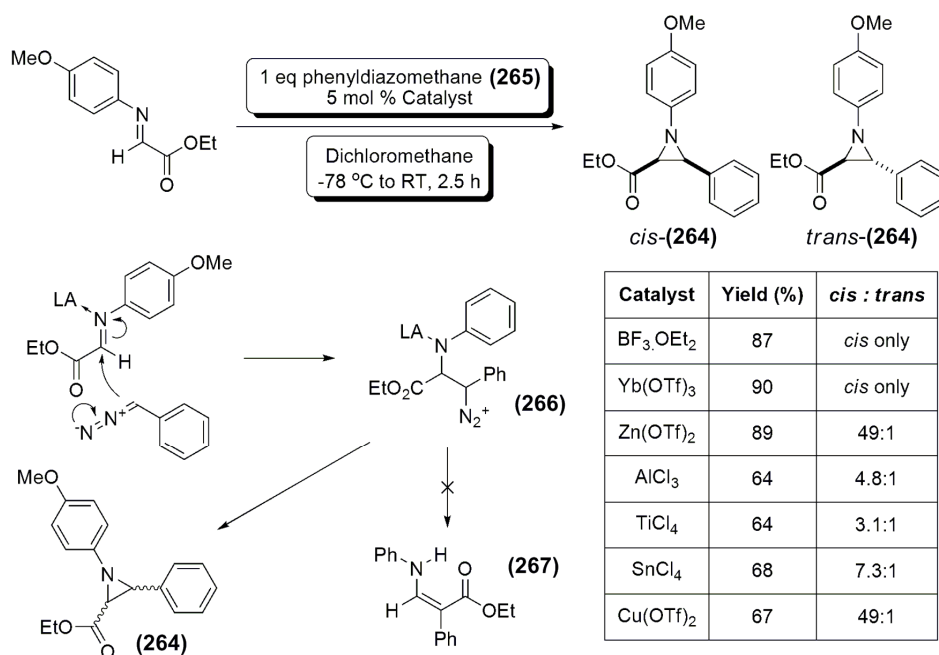
The understanding of the mechanism of aziridination and enamine formation by Templeton and Brookhart has been further added to by the studies of Jørgensen *et al*. Based upon reactivity, crystal studies, and trapping experiments utilising various metal catalysts, Jørgensen *et al* proposed that various mechanisms are in effect (Scheme 81); the predominant difference between these being either Lewis acid action of the metal centre, or, the formation of a formal metal-carbene complex between the catalyst and the diazoacetate reagent (Scheme 81).^{233,234}



Scheme 81: Mechanism of Lewis acid catalysed aziridine formation by Jorgensen *et al*, Templeton *et al*, and Brookhart *et al*

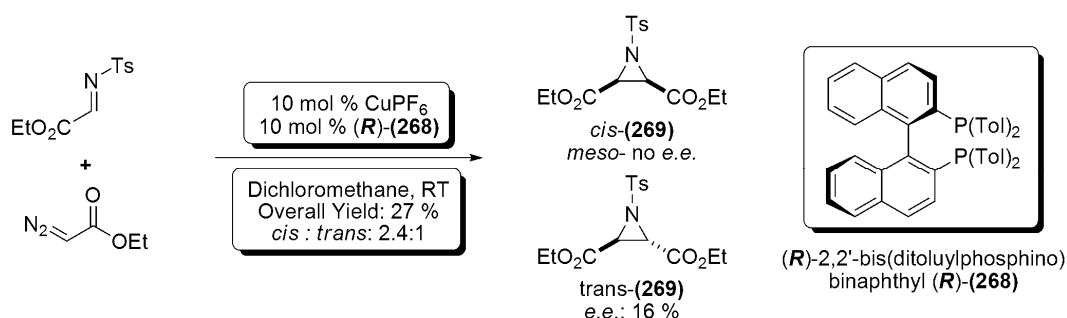
The main advantage and attractive feature of the initial work by Templeton and Brookhart was the relative simplicity and generality of the procedure. This attractive property led on to further developments within the area; for example, the work of Mayer *et*

al utilising boron trifluoride diethyl etherate as the catalyst for an aza-Darzens type synthesis of racemic aziridine-2-carboxylate esters (*i.e.* **(264)**, Scheme 82), utilising phenyldiazomethane **(265)** as the carbon source. This reaction allowed for virtual elimination of the migration enamine by-products (due to the low migratory aptitude of the ethyl carboxylate functionality present in intermediate **(266)**), and was applicable to various Lewis acids, including Yb(OTf)₃, Zn(OTf)₂, AlCl₃, TiCl₄, SnCl₄, and Cu(OTf)₂ based systems. Yields from aziridination utilising these Lewis acids were moderate to excellent, with reported isolated yields of 45 – 90% (Scheme 82).²³⁵



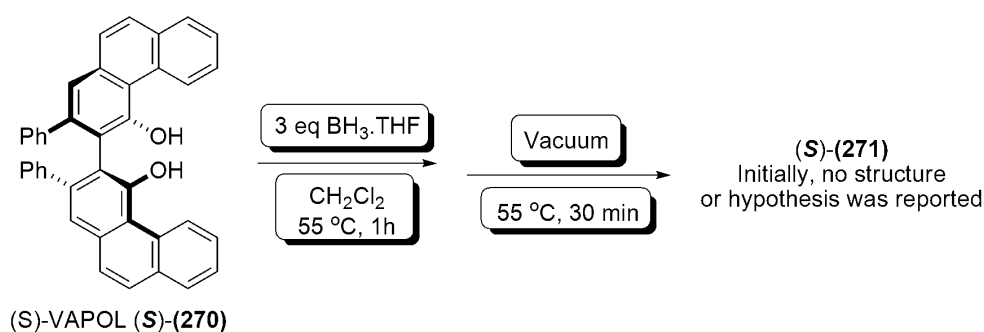
Scheme 82: aza-Darzens aziridination to form *N*-substituted aziridine-2-carboxylate ester ((264)**); and suppression of the migration product (**(267)**)**

Although the methods shown so far are, in general, effective, the enantioselective synthesis of aziridines *via* Lewis acid promoted mechanisms remained limited to the use of chiral starting materials. Indeed, initial attempts by Jørgensen *et al* into the use of chiral ligands (*i.e.* **(268)**) appended to a Lewis acid catalyst were disappointing, affording *e.e.s* of between 16 - 32 %, when utilising alkyl diazoacetates as the carbon source (Scheme 83).²³⁶



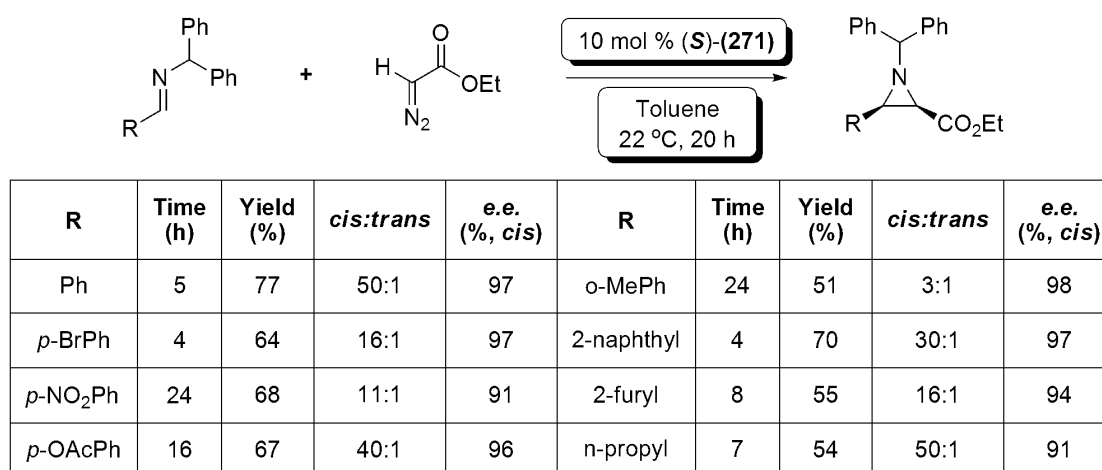
Scheme 83: Synthesis of chiral non-racemic aziridine ((269)**) utilising a copper centred Lewis acid catalyst appended with the chiral ligand (**(R)**-(**(268)**), carried out by Jørgensen *et al***

Leading on from these previous and disappointing results, Wulff *et al* published an asymmetric synthesis of aziridines that employed a polycyclic optically active ring system (VAPOL, (**270**)) appended with a boron Lewis acid.²³⁷ Formed by treating (*S*)-VAPOL (*S*)-(**270**) with borane tetrahydrofuran complex, initially the structure of the catalyst (*S*)-(**271**) was not entirely certain (Scheme 84).



Scheme 84: Reaction conditions reported for the synthesis of catalyst species (**271**)

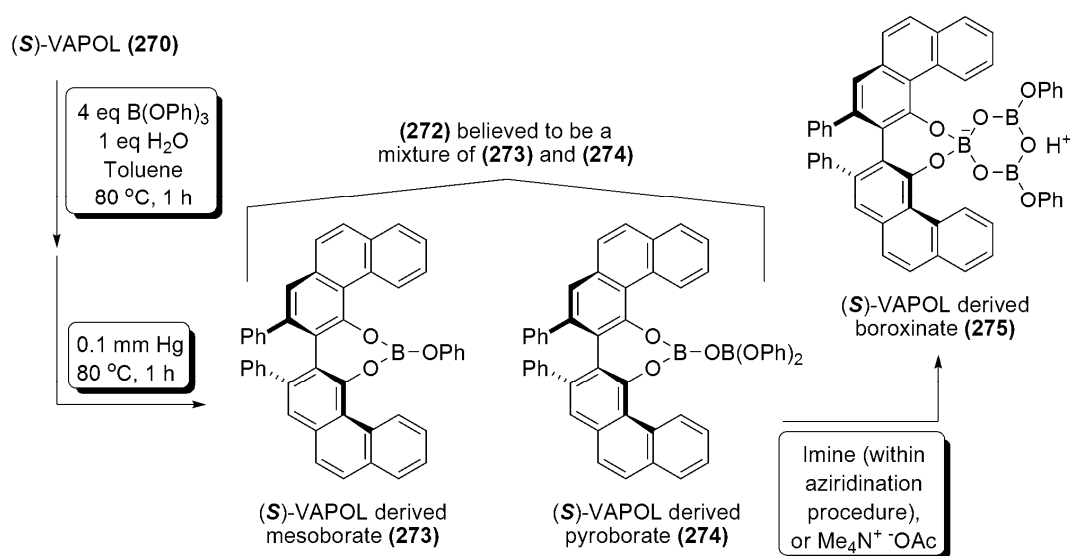
However, treatment of phenyl-*N*-benzohydril imine with ethyl diazoacetate (**261**) in the presence of 10 % of the catalyst species (**271**) led to the formation of the corresponding asymmetric aziridine, in a *cis:trans* ratio of >50:1, yield of 74 %, and *e.e.* of 98 %. This result was by far the best achieved for an asymmetric Lewis acid catalysed aziridination published up to that point. Within the publication, it was noted that catalyst loadings as low as 1 % could be employed; however, optimal reaction conditions involved the use of 2.5 mol % of the catalyst species (**271**). Subsequent to this initial result, this methodology was applied to various *N*-benzohydril imines, with good results achieved in general (Scheme 85).



Scheme 85: Asymmetric aziridination reactions carried out utilising 10 mol % (**271**) reported by Wulff *et al*

Further to this work, Wulff *et al* carried out a detailed study to attempt to identify the active catalyst species. It was found that the catalyst species (**271**) formed from

treatment of (*S*)-VAPOL with borane tetrahydrofuran complex was in fact a mixture of various borate species, formed due to decomposition of the borane tetrahydrofuran starting material.²³⁸ Thus, screening was carried out of various borate esters in order to find the most effective. This was found to be triphenyl borate, and subsequently, treatment of (*S*)-VAPOL (**270**) with 3 equivalents of triphenyl borate led to the formation of a new catalyst mixture (**272**), which was believed to consist of the mesoborate species (**273**), and the pyroborate species (**274**) (Scheme 86).²³⁹ However, further investigations concluded that, under aziridination conditions, these disparate species ((**273**) and (**274**)) were converted into a single boroxinate species (**275**) which is, to date, believed to be the active species (Scheme 86).



Scheme 86: Proposed composition of the catalyst mixture (272**), and structure of the boroxinate (**275**)**

This throws up an interesting debate as to whether the catalyst is in fact acting as a Lewis acid, or a Brønsted acid species. If the latter conclusion is correct in that (**275**) is the active catalytic species, then the catalyst is actually proceeding *via* a Brønsted acid activation mode (Figure 45).

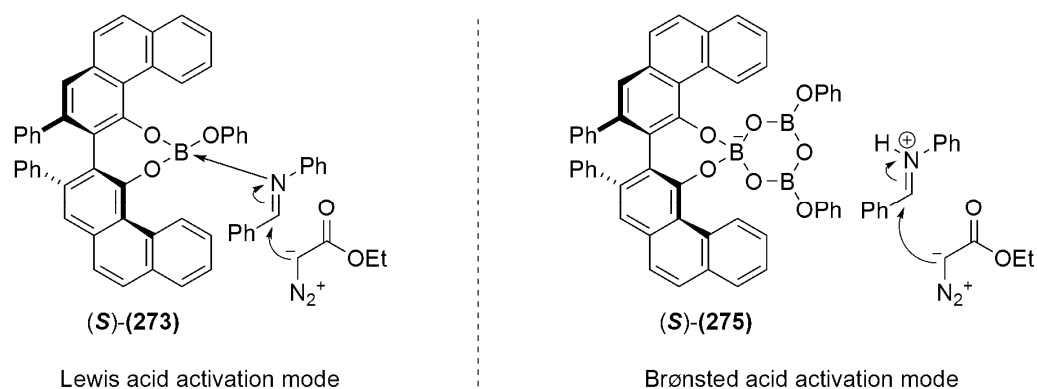
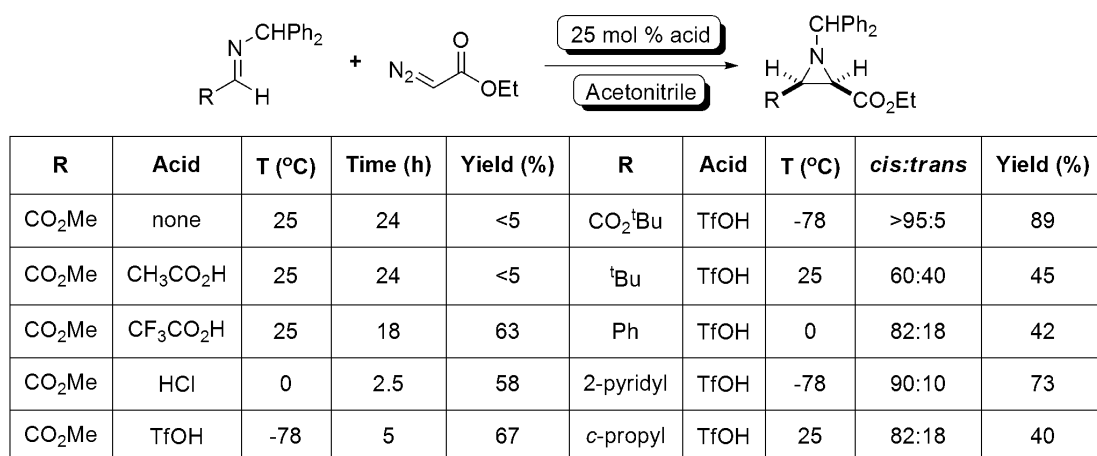


Figure 45: Potential Lewis acid activation of a simple *N*-substituted imine by (273**), or Brønsted acid activation by (**275**)**

3.3.3: Aziridination: Aziridination with Diazoacetates - Brønsted Acid Catalysis

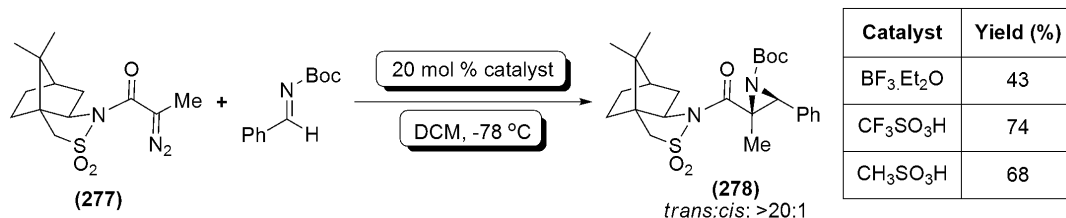
Within the area of catalysis, it can be argued that the proton is in fact the simplest and most readily available Lewis acid. Thus a logical extension of the previously discussed aziridination techniques is the use of Brønsted acid catalysts for the activation of aziridination substrates. The first method of aziridination to take advantage of the proton as a catalyst was that of Johnston *et al.* Initially, concern was raised within the research for the potential efficacy of a catalytic proton source, due to the generation of a stoichiometric basic product during the aziridination reaction, however, these were proven unfounded.

Efforts originally focussed upon the use of acetic acid; however, it was found that the addition of acetic acid had no discernable effect upon the reaction. Despite this, when trifluoroacetic acid was added to the reaction, the desired aziridine was formed in a yield of 63 % as a single diastereomer. Carrying on from this initial result, Johnston *et al* found that utilising acids with decreased pK_a led to an increase in the reaction rate; and thus trifluoromethane sulfonic acid (triflic acid, **(276)**) was found to be the most effective option (Scheme 87).²⁴⁰



Scheme 87: Initial Brønsted acid catalysed aziridinations reported by Johnston *et al*

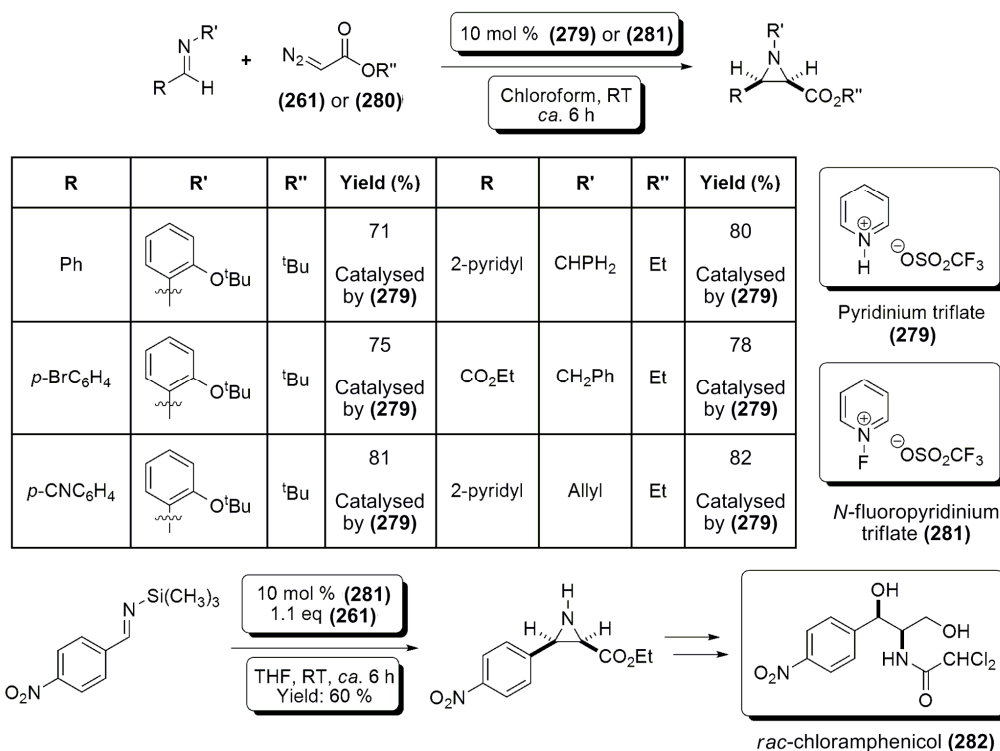
Testament to the effectiveness of the method developed by Johnston *et al*, the methodology is still in use in recent times. For example, recent work by Maruoka *et al* utilised triflic acid (**(276)**) as the catalyst for the synthesis of trisubstituted aziridines based upon the use of *N*- α -diazoacyl camphorsultam (**(277)**) as the carbene source. After testing various catalysts including BF₃.Et₂O, and acetic acid, Maruoka *et al* found that by utilising 20 mol % triflic acid (**(276)**), the desired aziridines could be formed in moderate to good yields of 50 – 74 % (74 % yield of (**(278)**)); also, the reaction showed a significant degree of diastereoselectivity, with *trans*:*cis* ratios as high as 20:1 (*trans*:*cis* >20:1 (**(278)**), Scheme 88).²⁴¹



Scheme 88: Aziridination reaction utilising *N*- α -diazoacyl camphorsultam by Maruoka *et al*

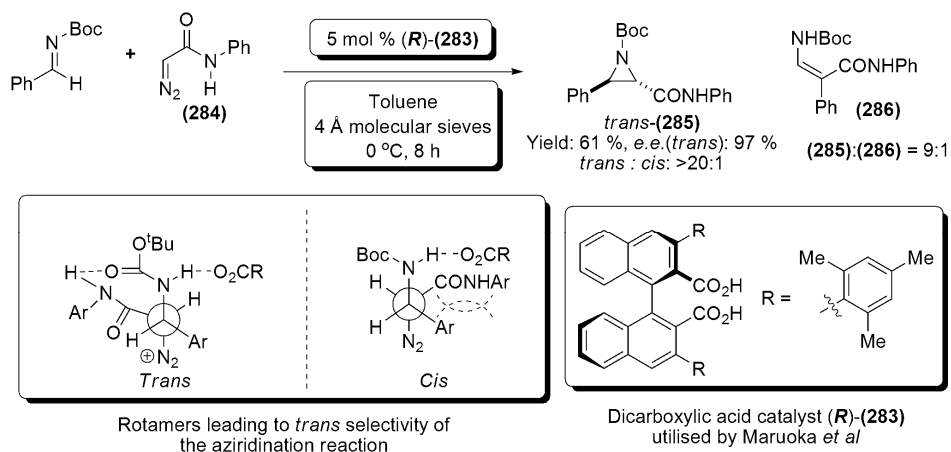
Related to these examples is the methodology developed by Bew *et al* utilising pyridinium triflate (279).²²⁴ The use of such a salt was shown to have several advantages over the use of triflic acid (276). The most prominent of these being ease of handling, and the lack of strict anhydrous reaction conditions required. It was shown that by utilising 10 mol % (279), structurally diverse *N*-substituted aziridine-2-carboxylates were able to be formed in good to excellent yields (71 – 90 %), from the corresponding imine and either *tert*-butyl (280), or ethyl (261), diazoacetates. The reaction was also found to produce, in most cases, exclusively *cis*-aziridines, with no trace of the *trans*- products seen.

Alongside this method, Bew *et al* also developed the use of the fluoronium cation as a catalyst for aziridination reactions. Utilising *N*-fluoropyridinium triflate (281) as the catalyst source, again along with suitable imines and alkyl diazoacetates (*tert*-butyl (280) or ethyl (261)), the desired *N*-substituted aziridine-2-carboxylate esters were formed in moderate yields of *ca.* 65 %. Also included was the synthesis of *rac*-chloramphenicol (282), with the key aziridination step affording a yield of 60 % (Scheme 89).²⁴²



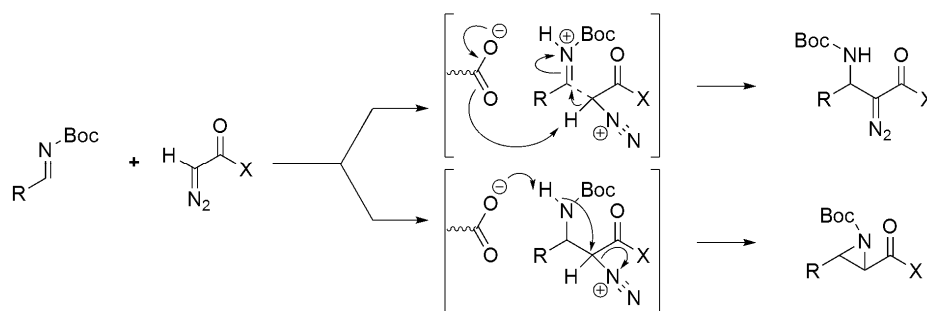
Scheme 89: Selected aziridination reactions utilising pyridinium triflate (279) and *N*-fluoropyridinium triflate (281) as catalysts, by Bew *et al*

Moving away from the production of racemic aziridines, Maruoka *et al* demonstrated the use of (*R*)-BINOL derived dicarboxylic acids (*e.g.* (**283**), Scheme 90) as catalysts for a highly *diastereo*- and *enantio*- selective aziridination procedure, utilising *N*-aryldiazoacetamides (*e.g.* (**284**)) and *N*-Boc imines, within which *e.e.s* of up to 97 % were reported (Scheme 90).²⁴³



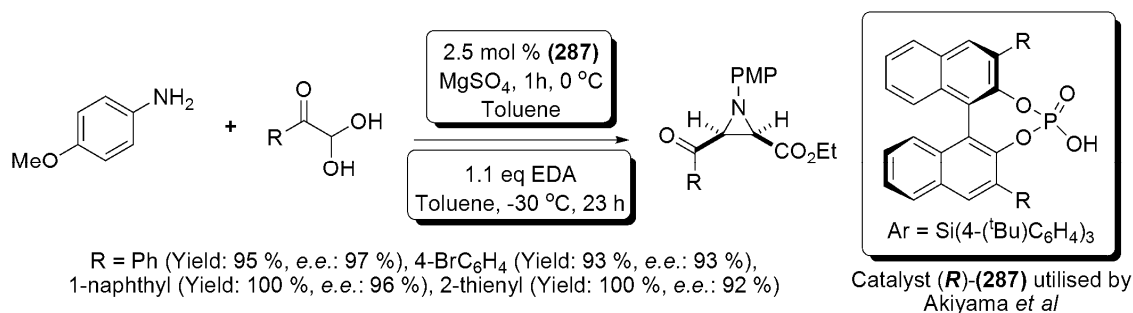
Scheme 90: Asymmetric synthesis of (285), utilising an (*S*)-BINOL dicarboxylic acid catalyst (283); developed by Maruoka *et al*

The strategy utilised by Maruoka *et al* was based upon the work of Terada *et al* (and further work by Maruoka *et al*),^{194,244} who had shown that chiral Brønsted acids could enable a Friedel-Crafts type reaction between *N*-acyl imines and alkyl diazoacetates (See 2.3: *Organocatalysis: Brønsted acid catalysis*, Scheme 63). However, within the Maruoka procedure shown in Scheme 90, modification of the diazo substrate to reduce the acidity of the α -proton (pK_a *N*-phenyldiazoacetamide = *ca.* 26.0,²⁶⁷ pK_a ethyl diazoacetate = 20.7)²⁴⁵ biased the reaction mechanism towards the production of aziridines (Scheme 91). More intriguing is the observed *trans*- selectivity of these reactions. The proposed cause of this unusual selectivity was the potential steric interaction between substituents within the transition state. This is believed to lead to preferential formation of a rotamer containing an antiperiplanar arrangement of the carboxamide and aryl groups, thus leading to the observed *trans*- selectivity within the product.



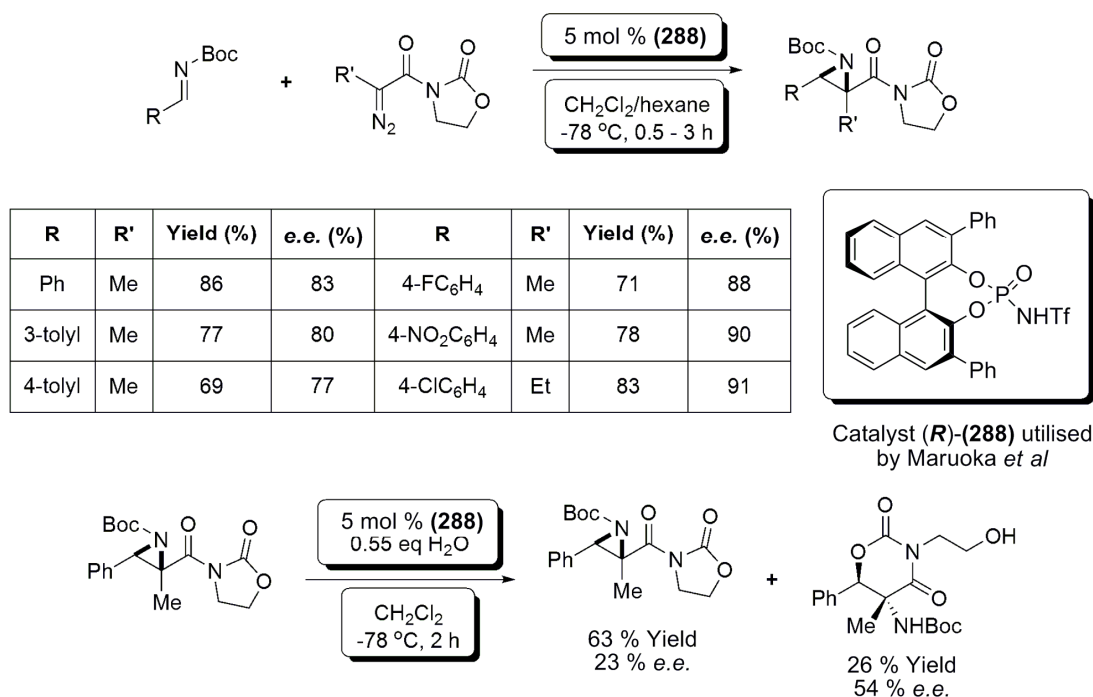
Scheme 91: Mechanisms leading to both the proton abstraction, and cyclisation products observed within the methodology detailed in Scheme 90

Moving on from this methodology, Akiyama *et al* developed the use of chiral (*R*)-BINOL phosphoric acids as catalysts for asymmetric aziridination reactions. It was found that substitution of the BINOL scaffold of the catalyst at the 3,3'- positions with bulky silyl groups produced the best suited catalyst (*R*)-(287) for these reactions.²⁴⁶ Utilising imines derived from phenyl glyoxal as the substrates, and ethyl diazoacetate as the carbon source, 2.5 mol % (*R*)-(287) allowed the synthesis of asymmetric aziridines (of the type shown in Scheme 92) in yields ranging from 84% to quantitative, with *e.e.s* ranging from 92 – 97 % (Scheme 92).²⁴⁶



Scheme 92: Asymmetric aziridination method developed by Akiyama *et al*

Further to this work, Maruoka *et al* have recently developed a methodology which yields hitherto difficult to synthesise trisubstituted aziridines, utilising an (*S*)-BINOL derived *N*-triflylphosphoramidate catalyst (288). Based upon the use of oxazolidinone functionalised diazoacetates, the procedure allowed for the production of trisubstituted aziridines in *cis:trans* ratios of up to 20:1, yields of up to 91 %, and *e.e.s* between 74 and 95 % (Scheme 93).²⁴⁷

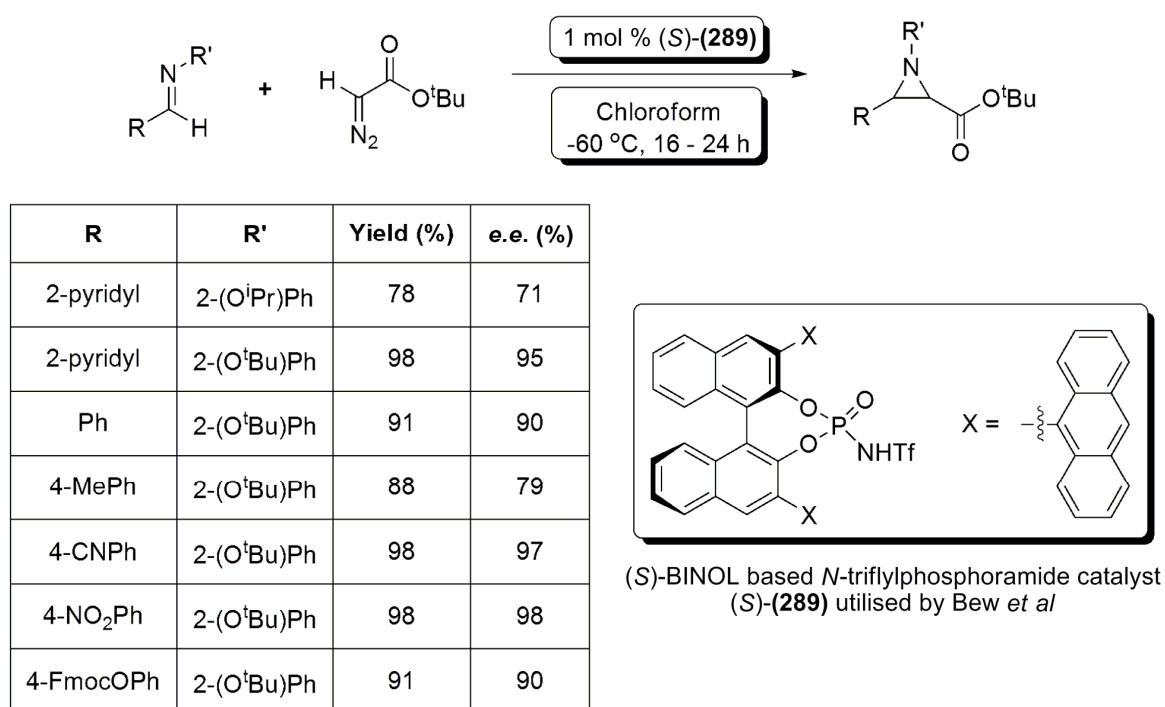


Scheme 93: Selected work by Maruoka *et al* showing asymmetric aziridination, and kinetic resolution procedures

Interestingly, when reaction times were extended, enantioselectivity was observed to increase, with a corresponding decrease in yields. Analysis of the reaction *via* mass spectrometry led to the realisation that a hydrolytic ring opening was taking place. This effect was exploited to a certain extent by the subsequent development of a kinetic resolution *in situ*, utilising adventitious water within the reaction (Scheme 93).

The above examples (along with the potential inclusion of the Wulff *et al* catalytic system) are the only published Brønsted acid catalytic enantioselective methods of producing aziridines. However, within the research group of Bew *et al*, work has been ongoing towards the development of an enantioselective Brønsted acid catalysed procedure.

Utilising the *N*-triflyl phosphoramidate catalyst (**289**), functionalised at the 9,9'-positions with 9-anthracenyl groups, the protocol involves the treatment of various readily available *N*-aryl imines with either ethyl (**261**), or *tert*-butyl (**280**), diazoacetates with as low as 0.1 mol % (**289**) in order to form the desired *N*-substituted aziridine-2-carboxylate esters in high yields (78 – 98 %) and *e.e.s* (71 – 98 %) (Scheme 94). It is worthy of note that the aziridine products were produced in exclusively the *cis*- form, and also, various functionality was tolerated with little loss of *e.e.* or yield (For example; aromatic, electron withdrawing, electron donating, halogenated, heteroaromatic, and bicyclic, substrates are tolerated). With regard to the catalyst, as it is a stable single species, which does not require activation; purification and characterisation are viable (unlike the catalyst species utilised by Wulff *et al*).



Scheme 94: Selected asymmetric aziridination reactions by Bew *et al*

Further development of this methodology is the subject of this thesis, and will be discussed in much greater detail in the following chapters.

3.4.1: Aziridines: Utilisation in Synthesis

The chemistry of aziridines and their utilisation within organic synthesis protocols is dominated by their ring opening reactions. These reactions are predominantly favoured due to the reduction in the steric ring strain inherent within the aziridine (*ca.* 27 kJ mol⁻¹).²⁰⁷ In general terms, nucleophilic ring opening of aziridines can take place with a variety of nucleophiles including those based upon carbon, oxygen, sulfur, nitrogen, hydrogen, or halogens. Several reviews have been focussed upon these reactions, significant examples of these being those by Hu,²⁴⁸ and Davis *et al.*²⁴⁹ The following paragraphs will show a small selection of the possible ring opening reactions, along with selected examples demonstrating the applied uses of these methods; also a brief discussion of the factors which influence the reactivity of aziridines towards these nucleophiles is included.

3.4.2: Aziridines: Utilisation in Synthesis – Reactivity and Activation

The reactivity of aziridines towards various nucleophiles is influenced by the classic determinants of reactivity. The electronegativity of the nitrogen component polarises the bonding within the cycle, thus activating the carbon substituents towards nucleophilic attack. Determination of which carbon (in an asymmetric aziridine) will undergo reaction can be carried out with consideration of the steric hindrance and electronic effects brought about by the inherent substitution of the reaction centre; thus attack will take place at the least hindered, most highly charged, centre. It is worthy of note that, in general, high regioselectivity can be achieved within nucleophilic ring openings.

Also requiring consideration is the effect of the *N*-substituent upon the reactivity of the aziridine. Considering the electronics of the system, a quandary arises. In general, in order to achieve aziridine formation (considering the generally applied aza-Darzens mechanism) a nucleophilic nitrogen is required; thus, an electron donating substituent will increase the rate of aziridine formation. However, considering nucleophilic ring opening, an electron donating substituent is disadvantageous, due to a reduction in the polarisation of the aziridine ring, and thus a lack of electrophilic character on the aziridine ring carbons C2 and C3 (Figure 46).

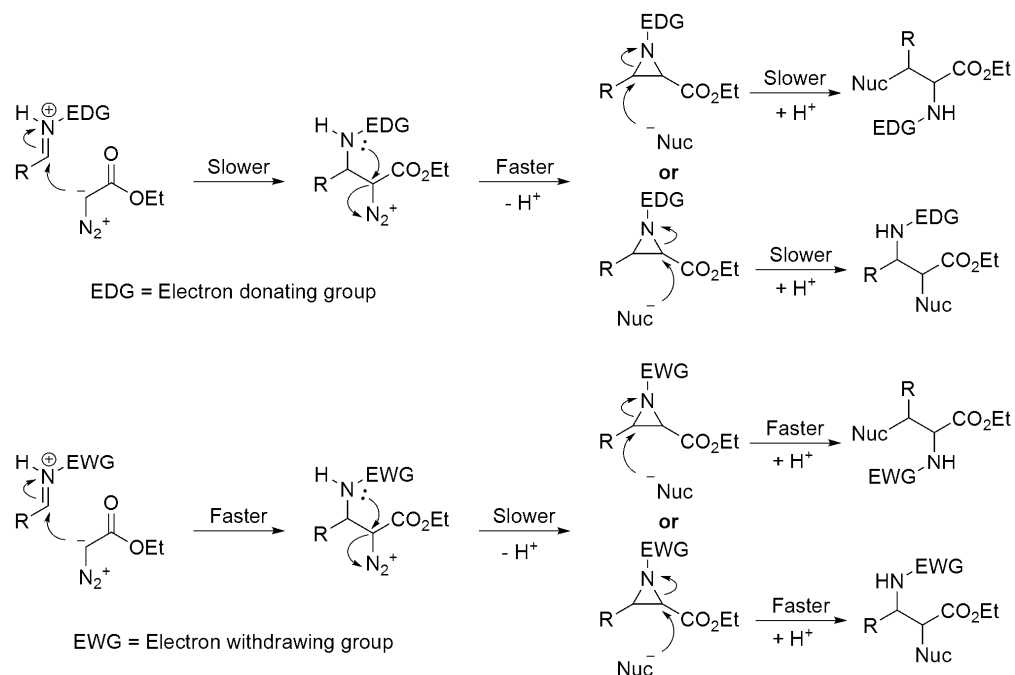


Figure 46: Demonstration of the effect of *N*-substitution with electron withdrawing, or electron donating groups upon aziridine formation (via an aza-Darzens mechanism), and nucleophilic ring opening reactions

Further consideration is also required regarding the transition state of the ring opening reaction. In general, electron withdrawing *N*-substituents are favourable, as they are capable of stabilising the resulting negative charge from ring opening under basic conditions, and also destabilising the positive charge relating from protonation of the ring nitrogen during ring opening under acidic conditions. Aziridines which are capable of these two functions tend to be of much greater reactivity towards nucleophilic attack, and thus have been termed as ‘activated’ aziridines.²⁵⁰ For those aziridines containing substituents or electronic properties which are not amenable to ring opening (NH being the simplest of these unactivated species), it is sometimes possible to induce reactivity *via* coordination, protonation, or indeed other methods of generating a partial, or formal, positive charge upon the ring nitrogen, such as quaternisation (Figure 47).

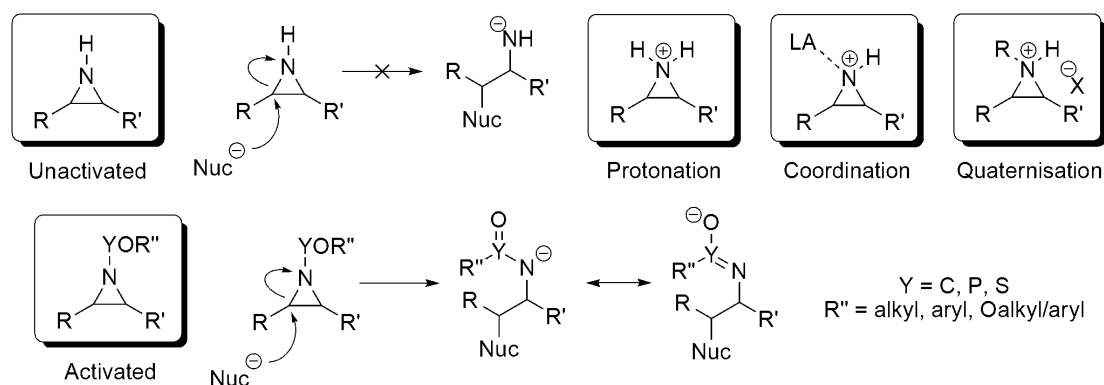
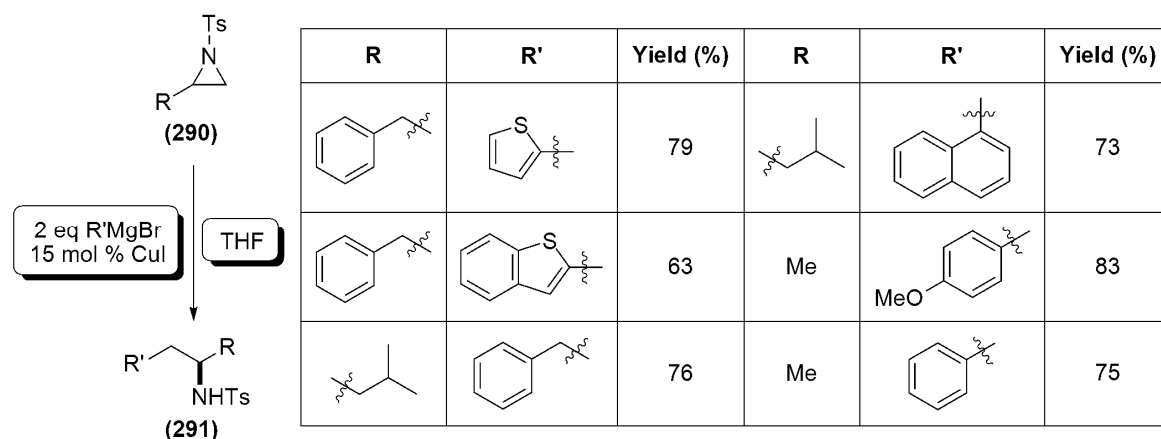


Figure 47: Unactivated and activated ring opening reactions; also potential activators of unactivated aziridines

3.4.3: Aziridines: Utilisation in Synthesis – Ring Opening Reactions

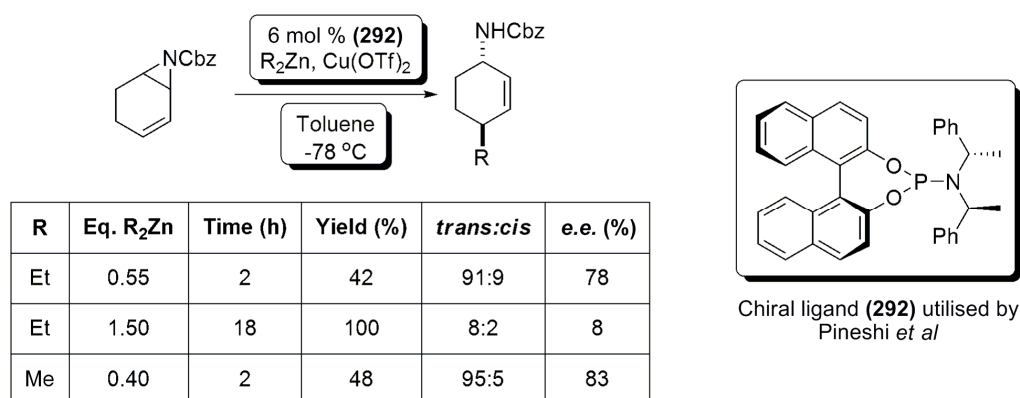
As mentioned within the introduction to this section, various nucleophiles have been applied to the ring opening reactions of aziridines.

Carbon nucleophiles which have found use within these reactions include alkyl and aryl carbanions, enamines, olefins and enolates, and cyano species. One such example is provided by Nenajdenko *et al*, who have shown that treatment of *N*-tosyl aziridines (such as **(290)**) with Grignard reagents leads to, in the majority of cases, regioselective ring opening to only give β -aryl amines, in 63 – 89 % yields (Scheme 95).²⁵¹



Scheme 95: Regioselective ring opening of *N*-tosyl aziridines via treatment with aryl magnesium bromides in order to form β -aryl amines; demonstrated by Nenajdenko *et al*

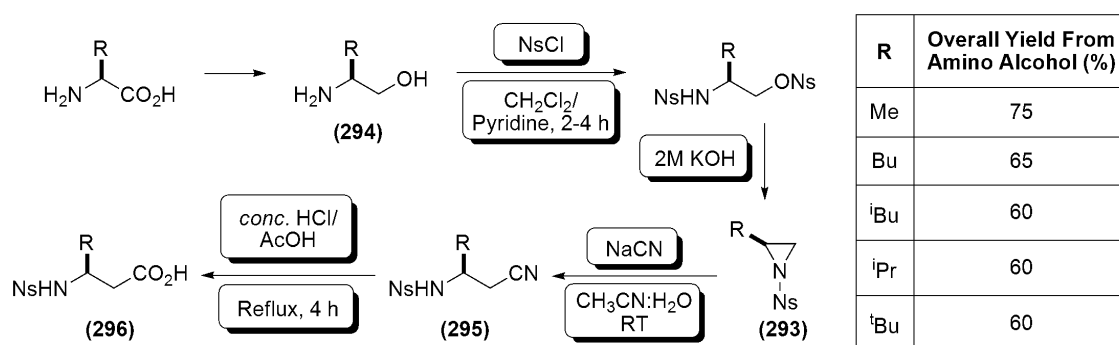
Further to this example, Pineshi *et al* have demonstrated that with the introduction of a chiral (*S*)-BINOL derived ligand (**(292)**) into copper catalysed ring opening reactions utilising alkylzinc species, addition products showing enantiomeric excesses of up to 83 % can be achieved (Scheme 96).²⁵²



Scheme 96: Enantioselective ring openings by Pineshi *et al*

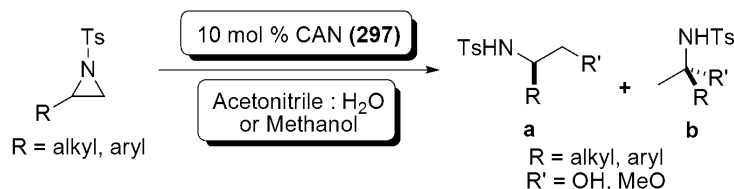
A final example of carbon nucleophile use is that of cyanide. Although due to relatively weak nucleophilicity, cyanide requires activation of most aziridine species, its use as a nucleophile is widely popular due to the potential α - or β - amino acid products,

depending upon the regioselectivity of the ring opening reaction. For example, the work of Farrás *et al* and Romea *et al* demonstrates that *via* an aziridine intermediate, it is possible to interconvert α -amino acid species into their equivalent β -form. Utilising *N*-nosyl aziridines (such as **(293)**, synthesised by treatment of the desired α -amino alcohol (*e.g.* **(294)**) with nosyl chloride, followed by base catalysed ring closure), the group were able to demonstrate a regioselective nucleophilic ring opening with sodium cyanide as the nucleophile, resulting in formation of the desired β -cyano species (*e.g.* **(295)**), which could then be hydrolysed *via* treatment with concentrated hydrochloric and acetic acids to form the desired β -amino acid species (*e.g.* **(296)**) (Scheme 97).²⁵³



Scheme 97: Conversion of α -amino acids to β -amino acids by Farrás *et al*

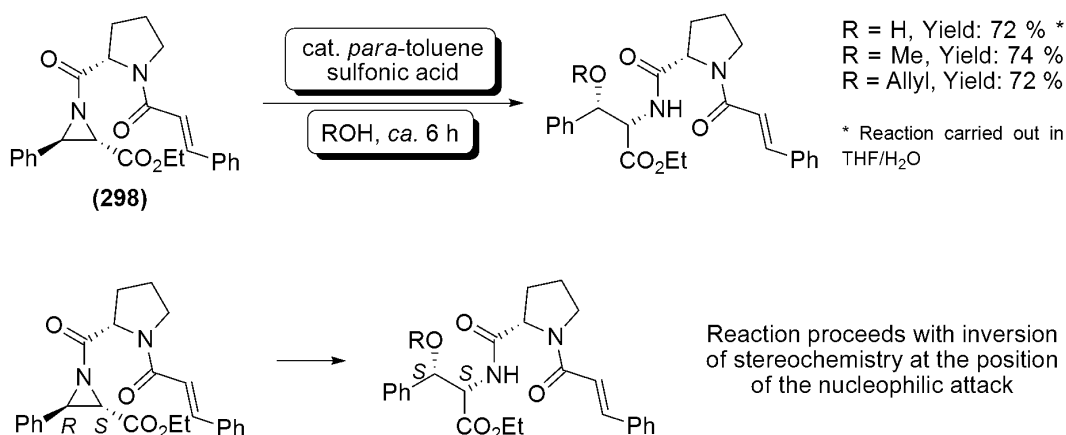
Moving away from carbon based nucleophiles, oxygen centred nucleophiles such as alcohols, hydroxyl compounds, and carboxylates have also been used to ring open aziridines. One of the most extensive publications in recent times related to these substrates has been the use of cerium ammonium nitrate (CAN, **(297)**) in order to catalyse the regioselective addition of alcohols, or water, to aziridines. First published by Chandrasekhar *et al* this mild procedure involved the treatment of various *N*-tosyl aziridines with 10 mol % CAN (**(297)**), and either water, or methanol in order to afford the ring opened products in yields of up to 95 %. As would be expected, ring opening was regioselective for the less hindered CH_2 of the aziridine ring, as opposed to the substituted carbon; however, this broke down to some extent when sterically undemanding substitution was present (Scheme 98).²⁵⁴



R	Nucleophile	Yield (%)	a : b	Nucleophile	Yield (%)	a : b
p-OMeC ₆ H ₄	H ₂ O	90	all a	MeOH	92	all a
p-BrC ₆ H ₄	H ₂ O	87	all a	MeOH	85	all a
ⁿ Bu	H ₂ O	90	7:3	MeOH	87	8:2

Scheme 98: Ring opening of aziridines utilising 10 mol % CAN (297) as the catalyst, and H₂O or methanol as the nucleophile; demonstrated by Chandrasekhar *et al*

One further interesting example of the use of oxygen based nucleophiles is that of the work of Iqbal *et al.*²⁵⁵ This work involved the ring opening of an aziridine intermediate (298) as the key step within the synthesis of analogues related to tripeptide based HIV protease inhibitors such as those shown in Scheme 99.

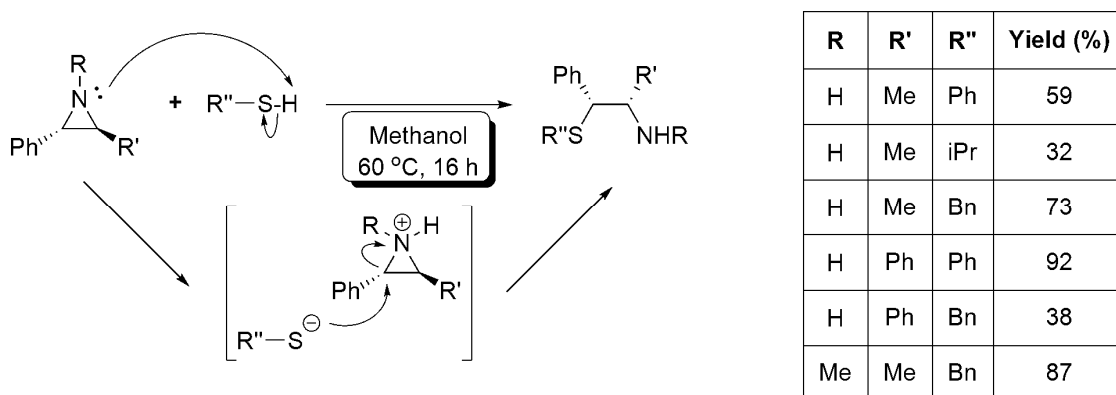


Scheme 99: Ring opening of aziridine intermediate (298), and observed selectivity; carried out by Iqbal *et al*

The key points from the procedure shown in Scheme 99 are the use of *para*-toluenesulfonic acid (299) as the catalyst for the addition of water or alcohols to the aziridine in order to facilitate the ring opening reaction, and also the stereoselectivity, as the reaction took place with the expected inversion of stereochemistry at the position of attack (Scheme 99).

The addition of sulfur based nucleophiles to aziridines follows a similar course to that of oxygen, however, some subtle differences are to be noted. For example, the work of Leeuwen *et al* concerned with the addition of thiophenols to C2-C3 substituted N-H aziridines shows interesting differences in reactivity to those expected. It was shown that the addition of various thiophenols to these unactivated aziridines took place under

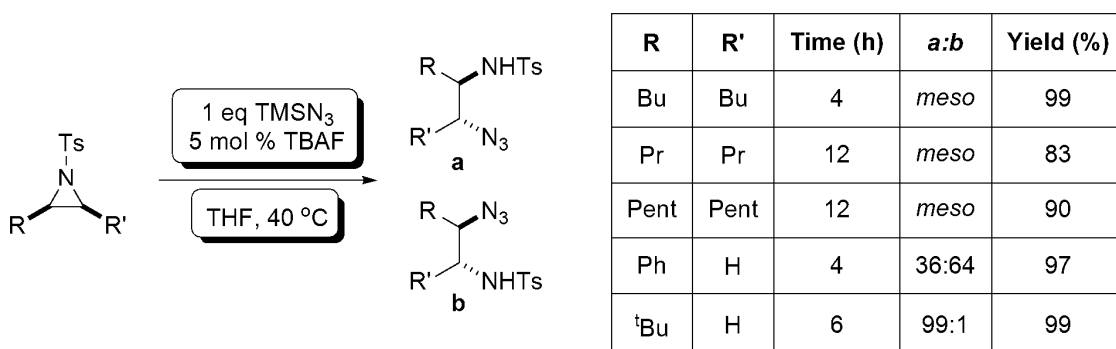
relatively mild conditions with no catalyst employed (Scheme 100). With consideration this reactivity is to be expected, due to the possibility of protonation of the aziridine nitrogen (pK_a generic aziridines *ca.* 7.98,²⁰⁷ pK_a thiophenol 6.62),²⁵⁶ thus activating the ring carbons, and allowing attack of the generated sulfur nucleophile.²⁵⁷



Scheme 100: Addition of sulfur nucleophiles to unactivated NH aziridines by Leeuwen *et al*

Azido compounds have many applications within organic synthesis, so a logical extension to the ring opening chemistry of aziridines is that of the addition of azides. One such example of this addition was developed by Hou *et al*, utilising trimethylsilyl azide, *N*-tosyl aziridines, and TBAF as an activator. This method generated the desired ring opened azido compounds (Scheme 101) in yields of between 83 – 99 %. The reaction was also shown to proceed regioselectively, with nucleophilic attack occurring predominantly at the least hindered ring carbon, as expected.²⁵⁸

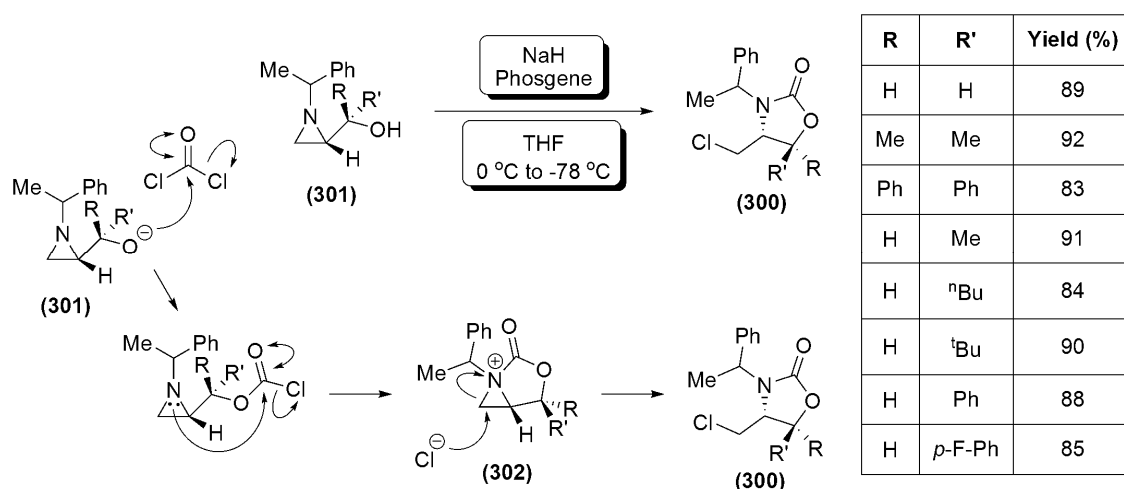
The role of TBAF within the reaction is believed to be that of an exchange catalyst, allowing for stabilisation of the negative charge upon nitrogen within the transition state of the reaction, resulting from ring opening.



Scheme 101: Ring opening of *N*-tosyl aziridines with trimethylsilyl azide; developed by Hou *et al*

Various other methods are available within the literature for the addition of azides to aziridines, including the utilisation of sodium azide and CAN (**297**) shown by Chandrasekhar *et al*, utilising similar reaction conditions to those shown in Scheme 98.²⁵⁴

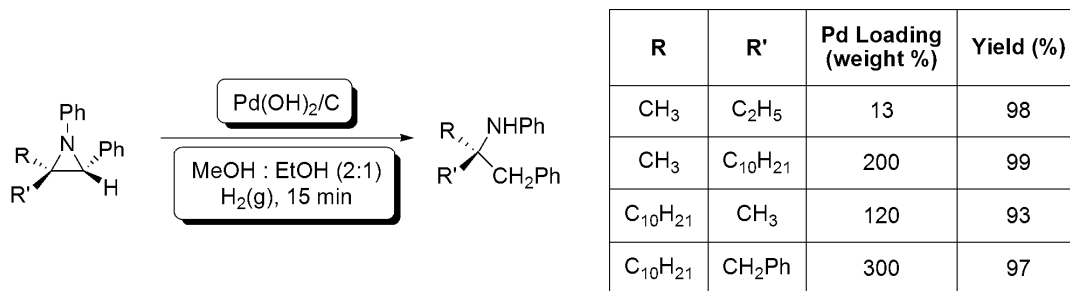
The addition of halides to aziridines can afford various useful substrates for further synthesis, as well as interesting products in their own right. One such example of this is the work of Lee *et al.* As part of a project to produce oxazolidinones (such as **(300)**) *via* ring opening of aziridines,²⁵⁹ Lee *et al* demonstrated the production of chloro functionalised oxazolidinones in yields ranging from 83 to 90 %, from *N*-substituted aziridines bearing alcohols (such as **(301)**) (Scheme 102).²⁶⁰ Treatment of the starting material aziridine **(301)** with sodium hydride and phosgene led to an intermediate bicyclic aziridine species **(302)**, which activated the unhindered C3 carbon to nucleophilic attack from chloride, in order to produce the desired oxazolidinone species **(300)** in a regiospecific manner.



Scheme 102: Synthesis of substituted oxazolidin-2-ones *via* ring opening of *N*-substituted aziridines

While not essentially a nucleophile, the reductive hydrogenation of aziridines is of significant interest due to the possibility of producing unnatural α -, or β - 'amino acid-like' products, *via* relatively simple procedures. The hydrogenolysis of the C-N bond within aziridines has been shown to be regioselective in many cases, with varying catalysts producing cleavage at specific centres within the molecule of interest.

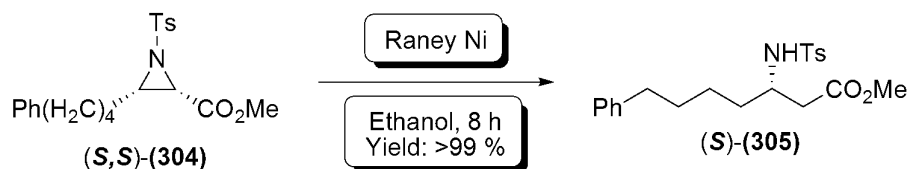
One such example of the application of regioselective hydrogenolysis of aziridines is the work of Satoh *et al.*²⁶¹ Utilising a previously developed procedure by Kim *et al.*,^{262,263} the treatment of various *N*-aryl trisubstituted aziridines (of the type shown in Scheme 103) with palladium hydroxide on carbon **(303)** under hydrogen gave the desired amine products (ring opened from the least hindered carbon) with retention of stereochemistry, in excellent yields of between 93 and 99 % (Scheme 103).



Scheme 103: Regioselective hydrogenolysis of *N*-aryl trisubstituted aziridines, promoted by Pd(OH)₂/C; demonstrated by Satoh *et al*

However, in order to achieve these results, stoichiometric amounts of (**303**) were required, with 100 – 300 % by weight (**303**) employed. Reduction of loading was said to led to significant reductions in yield (no values available), which was not corrected by increased reaction time. Presumably this is due to inhibition of the catalyst by the amine species produced within the reaction cycle.²⁶⁴

Further to this work is the synthesis of β -amino esters containing quaternary centres from aziridine-2-carboxylate esters (*i.e.* (**304**), as shown in Scheme 104), carried out by Davis *et al.*²⁶⁵ It was found that Raney nickel was the most efficient catalyst for the ring opening, and gave regioselective ring opening to the desired β -amino esters (such as (**305**)) in up to quantitative yield (Scheme 104).



Scheme 104: Hydrogenolysis of *N*-tosyl aziridine-2-carboxylate ester (304**) to form β -amino ester (**305**) with retention of stereochemistry; demonstrated by Davis *et al***

The examples shown above are a small selection of those which have been developed within the area of aziridine ring opening. Further examples will be examined in the due course of the research contained within this thesis, and are also available within the literature, as discussed previously.^{248,249}

Section 2: Results and Discussion

Chapter 4: Pyridinium Triflate Catalysed Aziridination Reactions, the One-pot Method, and Asymmetric Aziridinations

4.1.1: Pyridinium Triflate Catalysed Aziridination Methods - Introduction

Traditionally, the synthesis of aziridines has relied upon the utilisation of methods which require sensitive, and often toxic, metal based catalytic systems; be it with the inclusion of metal based Lewis acids (such as BF_3 , AlCl_3 , TiCl_4 ; the work of Templeton *et al*),²³² or homogeneous metal catalysts (*e.g.* $\text{Cu}(\text{OTf})_2$ systems; the work of Jørgensen *et al*).^{213,231} However, the recent push towards ‘green chemistry’ and organocatalysis has led to the development of various new methods, including the work of Johnston *et al* into the use of triflic acid.^{240,241} Despite the slightly greener profile of using non-metal based systems such as triflic acid, the potential experimental issues become focussed upon ease of use and applicability (*i.e.* the methods developed by Johnston *et al* still require the use of dry solvents and anhydrous conditions in order to produce the desired aziridine products). Thus the development of easy to use, ‘green chemistry’ methods for the production of aziridines is a potential area of development.

Recent work within our research group has been concerned with developing new aziridination methodologies along the lines mentioned previously. We have developed the use of pyridinium triflate (**279**)²²⁴ and *N*-fluoropyridinium triflate (**281**),²⁴² as stable, easy to use, organocatalysts for the production of racemic (predominantly) *cis*-aziridines in an efficient procedure from easily synthesised imine based starting materials, and alkyl diazoacetates (see Scheme 89). This reaction fits with the ethos of ‘green chemistry’ as it features high atom economy, and the only by-product is nitrogen gas.

As part of our continuing development of this methodology, various advances have been made towards improving the accessibility and ease of use of these procedures, and these are reported herein.

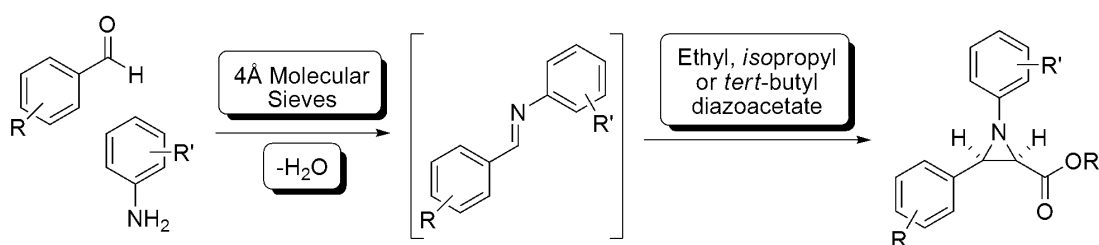
4.1.2: Pyridinium Triflate Catalysed Aziridination Methods – Development of the One-pot Procedure

Within the organic chemistry environment, hundreds of reactions and procedures are published every year. However, not all of these find use within the laboratory environment. This can be for a variety of reasons; predominant among these are cost, availability of materials, and ease of use.

Previously, the cost effective (and readily available) salt pyridinium triflate has proven an effective catalyst for the synthesis of racemic structurally diverse aziridines.

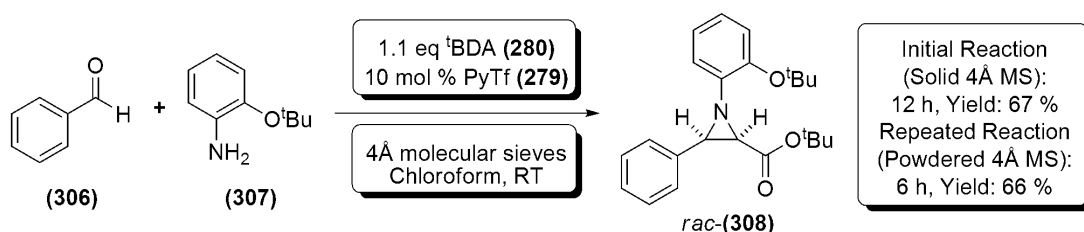
Thus, treatment of preformed *N*-substituted imines with 10 mol % pyridinium triflate (**279**) and 1.1 equivalents of ethyl diazoacetate (**261**) or *tert*-butyl diazoacetate (**280**), has been shown to afford the desired racemic *N*-substituted *cis*-aziridine-2-carboxylate esters in high yields.²²⁴ These reactions are believed to proceed *via* an aza-Darzens type mechanism (See 3.3: *Aziridination with Alkyl Diazoacetates*).^{229,230,232}

However, the potential for simplification of this method with the development of a one-pot procedure was a tempting target. Thus, it was hypothesised that a one-pot procedure could be developed using the requisite *N*-substituted imine starting materials (aldehyde and amine) under reaction conditions which would allow formation of the desired imine *in situ*; which could then undergo formation of the desired *cis-N*-substituted aziridine carboxylate ester (Scheme 105).



Scheme 105: Proposed one-pot synthesis of *cis-N*-substituted aziridine carboxylate esters, showing the intermediate imine formation

Initial attempts towards the one-pot aziridination were focussed upon the use of benzaldehyde (**306**) and 2-*tert*-butoxy aniline (**307**). Treatment of these with pyridinium triflate (**279**), and *tert*-butyl diazoacetate (^tBDA, (**280**)), over flame dried 4 Å molecular sieves, in anhydrous chloroform, led to the formation of the desired *cis*-aziridine *rac*-(**308**) in a yield of 67%. The identity of the product was confirmed by the presence of two doublets within the ¹H-NMR spectrum at 3.1 and 3.6 ppm, corresponding to the C2 and C3 protons (Scheme 106). Initially, the reaction times appeared longer than those of the previously developed method starting from imines (*ca.* 12 hours as opposed to 6 hours reported previously).²²⁴



Scheme 106: Synthesis of *rac*-(308**) *via* a one-pot aziridination reaction**

On repeat of the reaction, it was observed that stirring was inhibited by the molecular sieves; leading to the use of pre-powdered flame dried molecular sieves as the

desiccant. This allowed for much more efficient stirring of the reaction, and subsequently, a reduced reaction time (*ca.* 8 hours). It is also the author's observation that vigorous stirring of unpowdered molecular sieves can lead to breakdown of their integrity, potentially releasing captured water; which although potentially recaptured, could allow for decomposition of the intermediate imine within the reaction.

The generality of this one-pot method was confirmed upon the successful synthesis of several aziridine-2-carboxylate esters containing differing functionality upon the C3 phenyl substituent. First among these was the synthesis of an aziridine-2-carboxylate bearing 2-pyridyl functionality at the C3 position, *rac*-(**309**) (Figure 48). Indeed, application of the previously described conditions for the one-pot aziridination was successful, affording the desired *cis*-aziridine *rac*-(**309**) in a yield of 85%; with formation confirmed by both ¹H-NMR spectroscopy (two new doublets were seen at 3.1 and 3.6 ppm, corresponding to the C2, and C3 hydrogens (Figure 48)) and MS, with the required mass ion being detected at *m/z* 369.1.

Further to this, confirmation was required of the *cis*- nature of the product aziridine. Thus examination of the ¹H-NMR spectrum of *rac*-(**309**) revealed coupling constants of 6.8 Hz for both ring hydrogens at the C2 and C3 positions (As shown in Figure 48). This is within the expected range for *cis*-aziridines, which are commonly found to show vicinal coupling constants ($J_{2,3}$) of 5 – 9 Hz; whereas the values for the corresponding *trans*-aziridines are expected to be much lower (commonly between 2 and 6 Hz).²⁶⁶

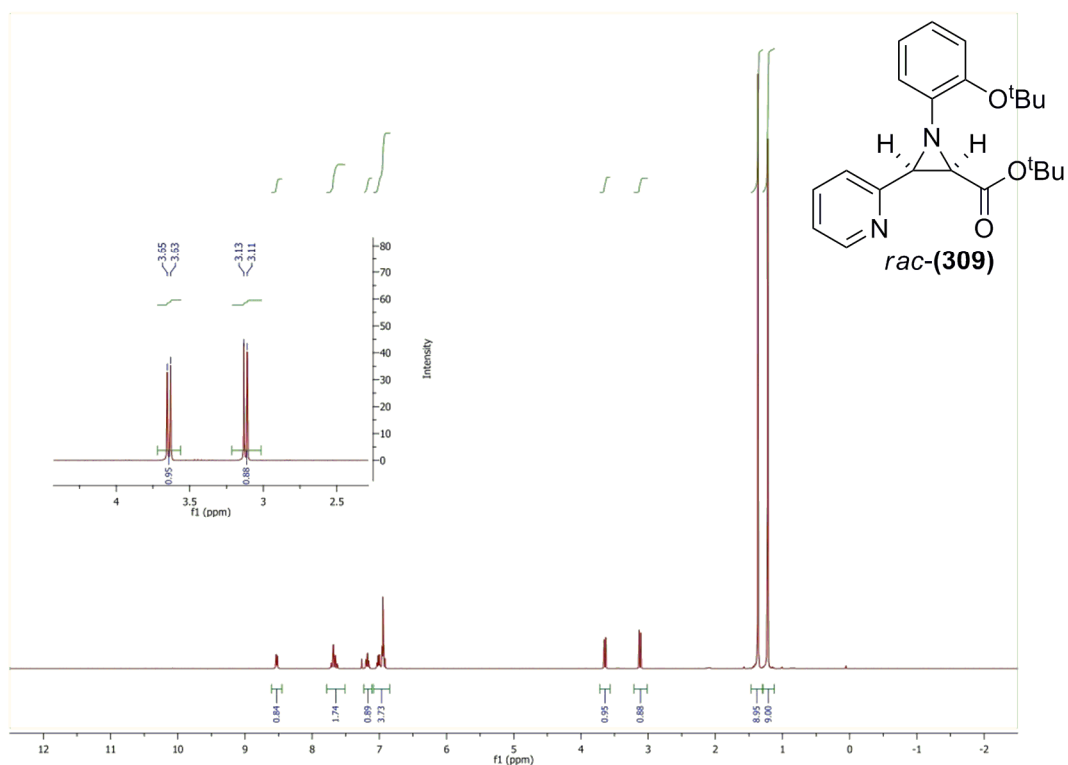
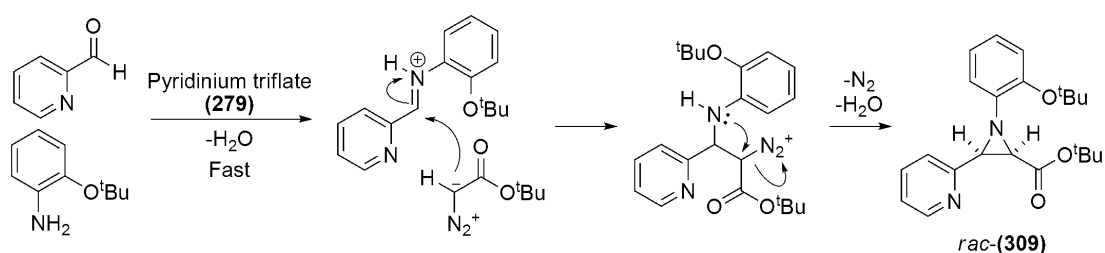


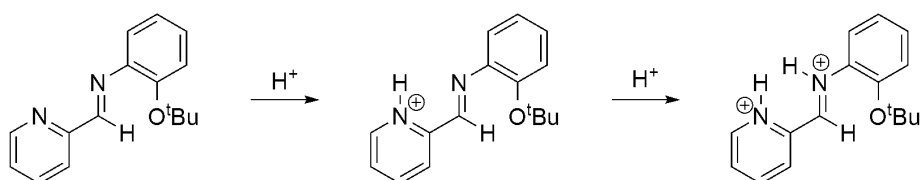
Figure 48: ¹H-NMR spectrum of *rac*-(**309**) showing the desired coupling constants for C2-*H* and C3-*H*

Considering the aforementioned increased reaction time of the one-pot aziridination system when compared to the previously developed method,²²⁴ it was decided to assess the rate of imine formation presuming the reaction proceeded *via* an aza-Darzens mechanism (Scheme 107). Thus, the addition of pyridine-2-carboxaldehyde to a prepared solution of 2-*tert*-butoxy aniline (**307**) and pyridinium triflate (**279**), over 4 Å molecular sieves, was carried out immediately before the addition of ^tBDA (**280**). However, the rate of imine formation was such that vigorous gas evolution (potentially N₂) was observed immediately upon the addition of the alkyl diazoacetate (**280**). Presumably, the evolution of N₂ is a result of the ring closure of the intermediate addition product, leading to the formation of *rac*-(**309**). It can therefore be concluded that imine formation is very rapid in this case (Scheme 107).



Scheme 107: Observed rapid rate of imine formation, demonstrated by the rapid evolution of N₂ during the formation of *rac*-(309**) *via* an aza-Darzens mechanism**

This observed rapid rate of imine and aziridine formation noted within the reaction above (Scheme 107) potentially could be due to the electronic withdrawing capabilities of the 2-pyridyl functionality; thus leading to increased electrophilic character at the carbonyl carbon of both pyridine-2-carboxaldehyde, and the intermediate imine. Also, potentially the pyridyl ring nitrogen could protonate under the reaction conditions (pK_a pyridyl nitrogen *ca.* 28; pK_a pyridinium 3.4);²⁶⁷ thus leading to the double cationic species shown in Scheme 108. This would lead to much greater nucleophilicity of the intermediate imine; affording the higher rate of reaction observed.



Scheme 108: Potential formation of a double cationic species leading to a rate acceleration in imine formation

Further to the synthesis of *rac*-(**309**), the one-pot aziridination procedure proved successful in synthesising several aziridine-2-carboxylate esters containing differing functionality upon the C3 position; including aromatic, halogenated, and bicyclic systems.

The results of these aziridinations are summarised in Figure 49 below. In general, these reactions were successful; with the desired aziridines obtained in all cases in good to very good yields of 64% to 85%. However, in the majority of cases, yields were roughly 5 to 10% lower than the corresponding aziridinations using isolated preformed imines; this is believed to be due to the fixed reaction time of 6 hours employed within this screen. It was also observed that no *trans*-aziridine product was produced within any of the examples shown in Figure 49 either within the crude material, or after purification by column chromatography.

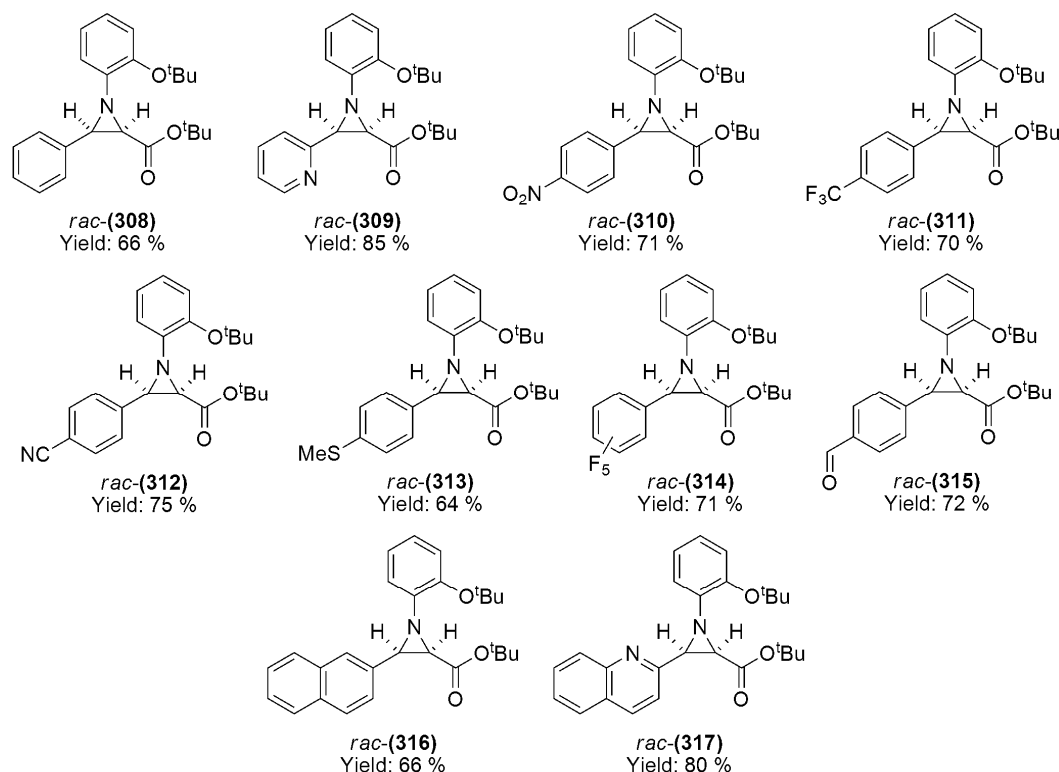
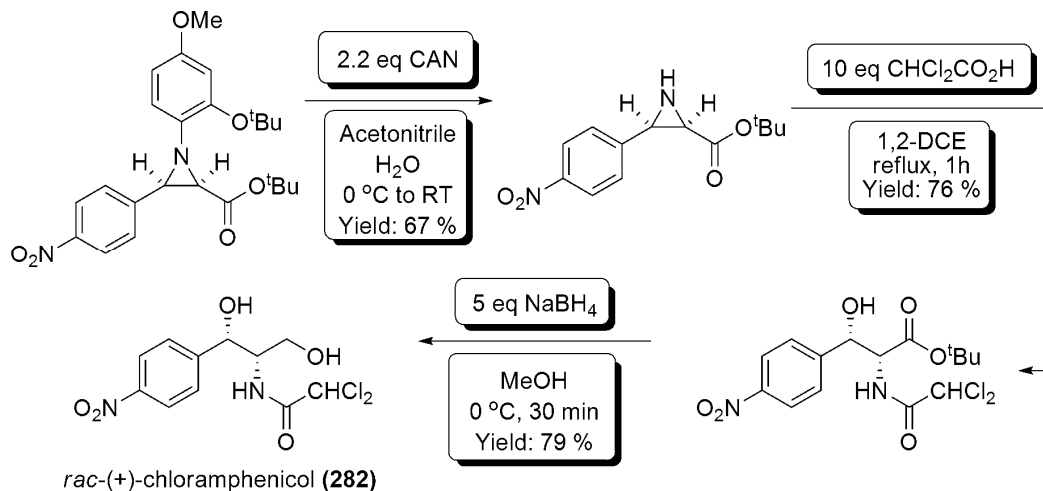


Figure 49: Aziridines rac -(308**) to rac -(**317**) produced by one-pot aziridination**

Characterisation of the above aziridines, and confirmation of the *cis*-stereochemistry, was predominantly carried out *via* $^1\text{H-NMR}$ spectroscopic analysis of the C2-*H* and C3-*H* doublets present within each product. The vicinal coupling constants of these being between the required range of 5 – 9 Hz for a *cis*-aziridine. MS and HRMS also confirmed the desired aziridine products, with peaks detected at the required m/z for all of the above aziridines (*e.g.* rac -(**312**), C2-*H* 3.11 ppm, $J_{2,3}$ 6.8 Hz; C3-*H* 3.49 ppm, $J_{3,2}$ 6.8 Hz; m/z , found 393.2174 $[\text{M}+\text{H}]^+$, theoretical 393.2173 $[\text{M}+\text{H}]^+$).

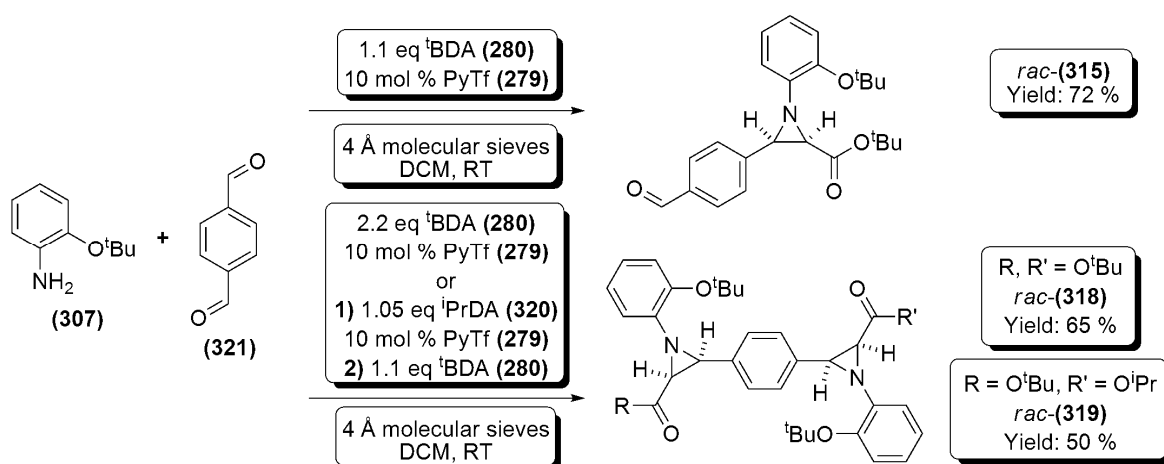
Several interesting results arose within the range of aziridines shown in Figure 49; including the synthesis of rac -(**310**), which is potential precursor to the antibiotic natural product chloramphenicol (**282**);²⁶⁸ and also, the synthesis of rac -(**313**), which *via* a similar route could become a viable precursor to another antibiotic compound, thiamphenicol (**322**).²⁶⁹ The synthesis of *rac*-(+)-chloramphenicol (**282**) has previously been

demonstrated utilising similar starting materials within the thesis work of Pesce,²⁶⁸ and within a publication by Bew *et al* (Scheme 109, and see 3.3.3: Aziridination: Aziridination with Diazoacetates - Brønsted Acid Catalysis: Scheme 89).²⁴² However, the use of *rac*-(**310**) within a synthesis of (**282**) has not been attempted, and will be the subject of future investigations.



Scheme 109: Synthesis of *rac*-(+)-chloramphenicol (**282**) by Bew *et al*, utilising an aziridine substrate similar to *rac*-(**310**)

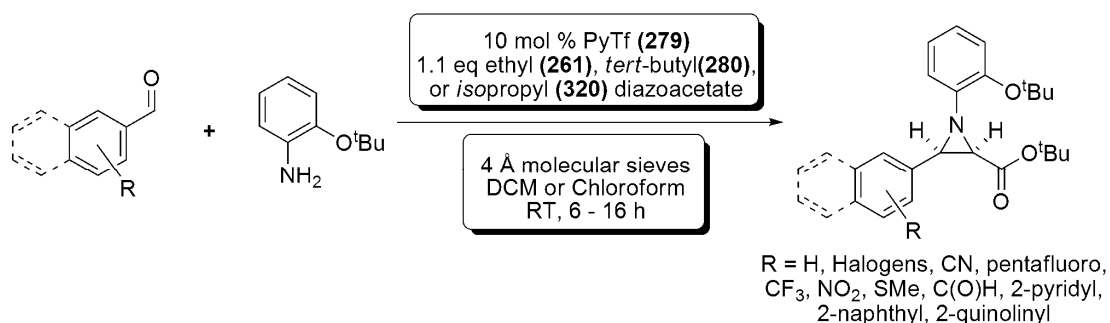
One other interesting result came out of the aziridinations shown in Figure 49, this being within the synthesis of *rac*-(**315**). During this synthesis, it was noted that a by-product was present; this was subsequently found to be the bis-aziridine *rac*-(**318**) (Scheme 110). Tailoring of the stoichiometry of the one-pot reaction (2.2 equivalents ^tBDA (**280**), and 2.2 equivalents 2-*tert*-butoxy aniline (**307**)) allowed for predominant formation of *rac*-(**318**), leading to the observed yield of 65% shown in Scheme 110.



Scheme 110: Synthesis of mono- and bis-aziridines *rac*-(**315**), (**318**), and (**319**), from terephthalaldehyde (**321**)

Having synthesised the symmetric bis-aziridine *rac*-(**318**), an intriguing target was the synthesis of a differentiated bis-aziridine, bearing differing ester functionality. Thus, *rac*-(**319**) was synthesised *via* a three step, one-pot procedure involving the addition of 1.05 equivalents *isopropyl* diazoacetate (¹PrDA (**320**)) to a solution of terephthalaldehyde (**321**), 2-*tert*-butoxy aniline (**307**), and 10 mol % pyridinium triflate (**279**), over powdered 4 Å molecular sieves, in dichloromethane. When the reaction was deemed complete (monitoring was carried out by ¹H-NMR spectroscopy, observing formation of the aziridine doublets at 3.03 and 3.46 ppm), *ca.* 16 hours, a further equivalent of 2-*tert*-butoxy aniline (**307**), and 1.1 equivalents of ¹BDA (**280**) were added, and the reaction was left to proceed to completion. Again monitoring of the reaction by ¹H-NMR spectroscopy showed consumption of the imine, and formation of C2-*H* and C3-*H* doublets at 3.03 and 3.46 ppm respectively. After purification, *rac*-(**319**) was obtained in a 50% yield.

Although the main body of this thesis is dedicated to the production of asymmetric, isotopically enriched aziridines and related products, the author feels that the background development of previously demonstrated aziridination reactions is worthy of note. This is due to the continued application of these methods for the synthesis of racemic aziridine standards (for use within HPLC, or NMR) throughout the project. Thus, reactions referred to as following standard one-pot aziridination conditions can be assumed to follow the general procedure outlined in Scheme 111, and detailed within the general procedures in the experimental section.



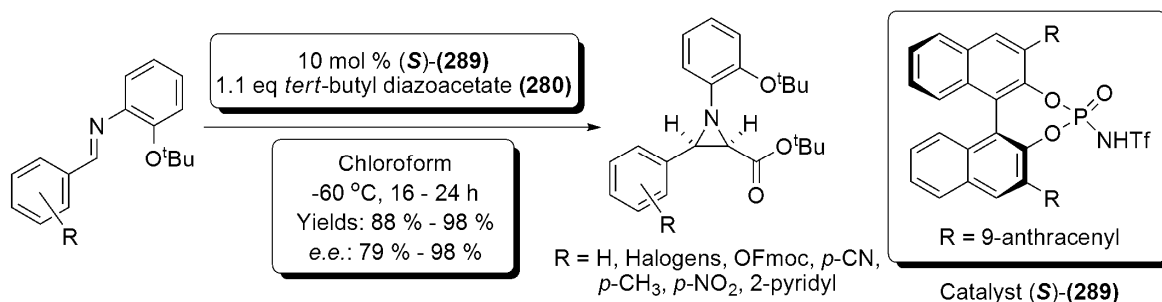
Scheme 111: General scheme of the racemic one-pot aziridination reaction

4.2.1: One-pot Asymmetric Aziridinations – Introduction

Having developed a methodology for the one-pot synthesis of racemic aziridines utilising pyridinium triflate as the catalyst, the next consideration was to extend the one-pot methodology to the production of non-racemic aziridines.

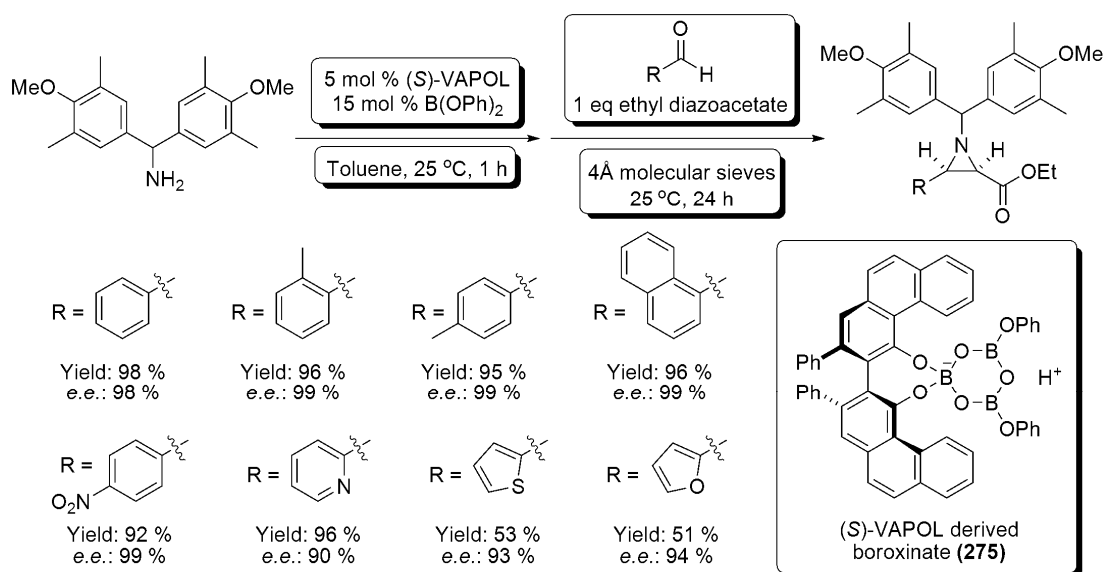
As has been previously demonstrated within the research group of Bew *et al*, (and in particular, within the work of Pesce),²⁶⁸ application of the *N*-triflyl phosphoramidate catalyst (**289**) based upon BINOL (as a strongly protic (pK_a *ca.* -1)¹⁹⁷ catalyst for

aziridinations), has led to a robust methodology for the production of a wide range of *cis*-*N*-substituted aziridine carboxylate esters in high yields (88 to 98%) and enantiopurities (79 to 98% *e.e.*'s) (see 3.3 Aziridination with diazoacetates, and Scheme 112). This method utilised predominantly *N*-phenyl imines as the starting materials. Thus the possibility of utilising a one-pot procedure from the composite aldehydes and amines would lead to an increase in the already wide applications of this robust procedure.



Scheme 112: Asymmetric synthesis of *cis*-*N*-substituted aziridine carboxylate esters utilising the *N*-triflyl phosphoramidate catalyst (289) by Pesce²⁶⁸

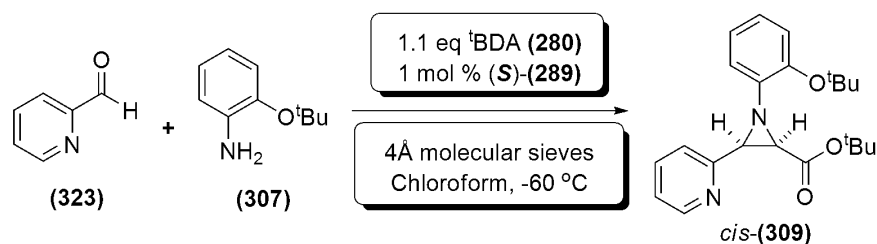
The development of a one-pot asymmetric aziridination method from aldehydes and amines was also seen as an important target in the development of the methodology, as at the time of the work, no example of such a reaction was available within the literature. Since the time of the work's completion, a recent publication by Wulff *et al* has elucidated a one-pot synthesis of aziridine-2-carboxylates utilising an (*S*)-VAPOL boroxinate catalyst (275) (see 3.3.2: Aziridination: Aziridination with Diazoacetates - Lewis Acid Catalysis, Scheme 86; and Scheme 113). However, the method developed within the following pages differs slightly from that of Wulff *et al* in the fact that a pure protic catalyst is used (as opposed to a boroxinate species).^{237-239,270}



Scheme 113: One-pot asymmetric aziridination reactions utilising the VAPOL catalyst (275) developed by Wulff *et al*²⁷⁰

4.2.2: One-pot Asymmetric Aziridinations – Synthesis of aziridines *cis*-(**309**) to *cis*-(**317**)

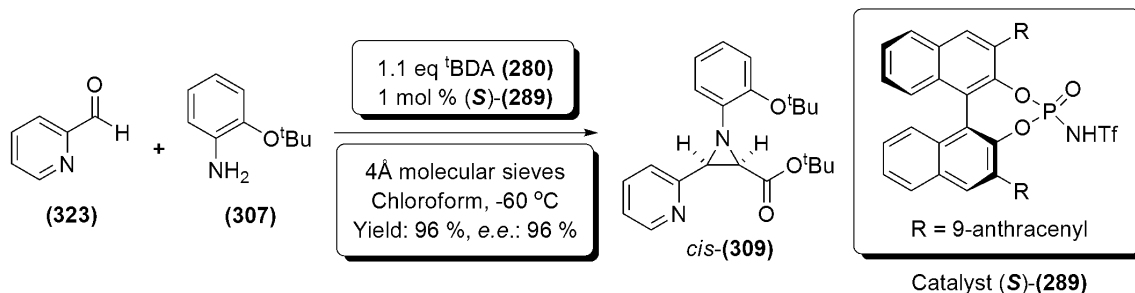
Initial efforts towards developing a one-pot asymmetric aziridination reaction were focussed upon the one-pot synthesis of *cis*-(**309**). Moving forward from the methodology developed previously (utilising pyridinium triflate as the catalyst), and combining this with the asymmetric aza-Darzens aziridination methodology developed by Pesce (Scheme 112);²⁶⁸ a one-pot reaction was attempted between pyridine-2-carboxaldehyde (**323**), 2-*tert*-butoxy aniline (**307**), and *tert*-butyl diazoacetate (^tBDA (**280**)); utilising the strongly protic catalyst (**289**) at -60 °C over powdered 4 Å molecular sieves (Scheme 114).



Scheme 114: Proposed one-pot synthesis of aziridine carboxylate ester *cis*-(309**) from pyridine-2-carboxaldehyde (**323**), 2-*tert*-butoxy aniline (**307**), and *tert*-butyl diazoacetate (**280**)**

Initially, catalyst loading was maintained at 1 mol % (*S*)-(**289**); which had previously been shown to be effective in the aziridination of 2-*tert*-butoxy-*N*-(pyridin-2-ylmethylene)aniline with *tert*-butyl diazoacetate (forming the desired aziridine carboxylate ester *cis*-(**309**) (Shown in Scheme 114) in 98% yield, and 95% *e.e.*).²⁶⁸

The synthesis of *cis*-(**309**) proceeded to completion in a time of 24 hours, as shown by monitoring of the appearance of aziridine C2-*H* and C3-*H* doublets at 3.12 and 3.64 ppm within the ¹H-NMR spectrum. The crude product was isolated by filtration straight from the reaction through a plug of silica gel; eluting with diethyl ether. This allowed for removal of the catalyst from the impure material. The resulting solution was evaporated to dryness, and submitted to flash column chromatography on silica. Subsequent ¹H-NMR spectroscopic analysis confirmed the *cis*-stereochemistry of *cis*-(**309**) *via* the vicinal coupling constants of the C2-*H*, and C3-*H* doublets present at 3.12 and 3.64 ppm respectively; these both being $J_{2,3}$: 6.8 Hz, which is consistent with the expected 5 – 9 Hz value for a *cis*- aziridine.²⁶⁶ ¹³C-NMR spectroscopy (appearance of the C2 and C3 carbon signals at 48.4 & 46.8 ppm), MS (m/z 369.1 [M+H]⁺), and HRMS ([M+H]⁺ theoretical m/z 369.2173, found m/z 369.2176) analysis also confirmed that the desired aziridine had been produced with an excellent yield of 96% (Scheme 115). The enantioselectivity of the reaction was quantified by submitting a sample of *cis*-(**309**) to chiral HPLC analysis, running against *rac*-(**309**) (produced *via* the one-pot pyridinium triflate catalysed aziridination reaction developed); the *e.e.* of *cis*-(**309**) was shown to be 96%.



Scheme 115: One-pot asymmetric synthesis of *tert*-butyl 1-(2-*tert*-butoxyphenyl)-3-(pyridin-2-yl)aziridine-2-carboxylate; *cis*-(309)

The asymmetric one-pot procedure was extended to further examples based upon the aziridines produced from the racemic one-pot aziridination protocol (*rac*-(310) – *rac*-(317); see 4.1.2: *Development of the one-pot procedure*). Syntheses of *cis*-(310) – *cis*-(317) were carried out under the same conditions utilised in the synthesis of *cis*-(309). This was successful for *cis*-(314) and *cis*-(317), however in the majority the reaction was deemed too slow at 1 mol % catalyst loading, as reaction times were prohibitive (~5 days). Therefore, in these cases, catalyst loading was increased to 5 mol % (S)-(289). At this loading, the reactions were seen to proceed smoothly within 36 – 48 hours, with good to very good yields (61% - 93%), and high *e.e.s* (74% – 99%) (Figure 50).

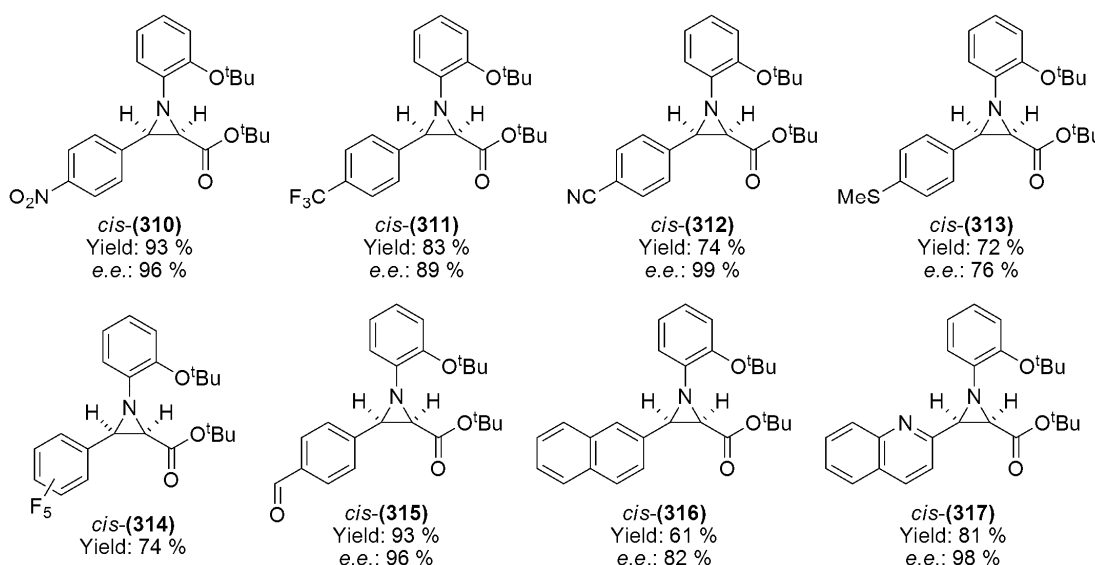


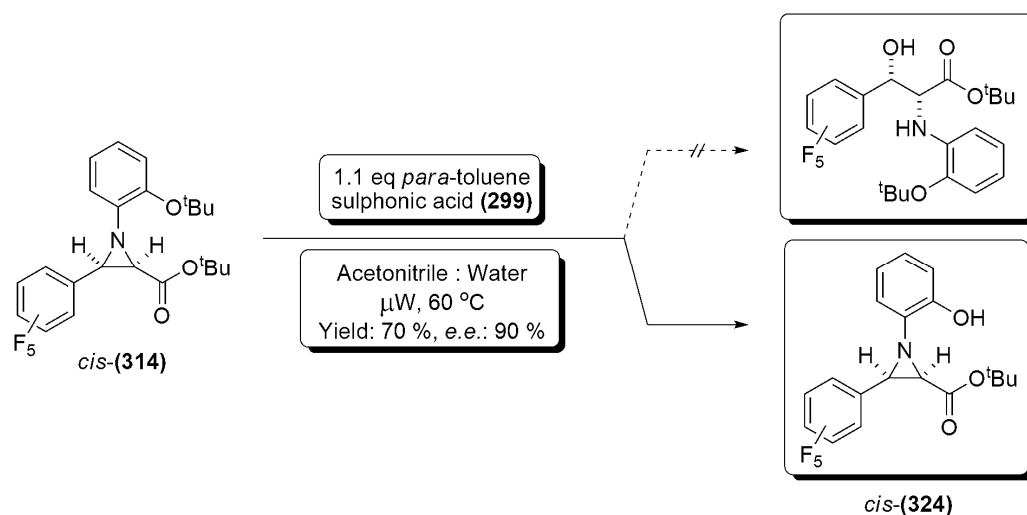
Figure 50: Aziridines *cis*-(310) to *cis*-(317) produced via an asymmetric three component one-pot aziridination protocol, catalysed by 5 mol % (S)-(289)

As had been the case with *rac*-(310) – *rac*-(317), aziridines *cis*-(310) – *cis*-(317) were characterised by ¹H-NMR spectroscopy via the C2-*H* and C3-*H* doublets (which also confirmed the *cis*- stereochemistry of the products, with coupling constants within the 5 – 9 Hz range expected for *cis*- aziridines). The enantiopurity of aziridines *cis*-(310) – *cis*-(317) was measured by chiral HPLC, running against the corresponding racemic aziridine.

However, although chiral HPLC allowed the enantiopurity of the product aziridines to be confirmed, at this stage no confirmation of the absolute stereochemistry of these aziridines was possible. Unfortunately, no examples similar enough to these existed within the literature in order to compare α_D , and no crystal structure was available. Thus the stereochemistry shown in Figure 50 (and throughout the thesis) should be considered as relative stereochemistry. Attempts have been made to elucidate the absolute stereochemistry of the aziridines produced through computational and spectroscopic methods, and these are discussed in Chapter 8: Spectroscopic and Computational Investigations.

Further to this, it proved difficult to gain good separation of the enantiomers of *cis*-(**314**) by chiral HPLC, or GC techniques. Therefore, it was decided to remove one *tert*-butyl group from the molecule as this, it was believed, would allow for a longer retention time upon the chiral HPLC column (due to the greater polarity of a free OH substituent), thus allowing for better separation of enantiomers. This insight came about as a result of consulting the online application guide for the Chiralpak AD-H column; which suggested that compounds with a free OH tended to give good separation.²⁷⁴

The method by which this cleavage was discovered was essentially serendipity; as the required product was isolated by column chromatography while attempting a ring-opening reaction of *cis*-(**314**) (see Chapter 7; and Scheme 116).



Although $^1\text{H-NMR}$ and $^{13}\text{C-NMR}$ spectroscopic analysis of *cis*-(**324**) made it clear that a *tert*-butyl group had been removed from the starting material aziridine, initially there was uncertainty as to which *tert*-butyl group had been removed. The structure of the product was elucidated by IR spectroscopy, as an absorption band was clearly shown at 3408 cm^{-1} , well within the expected range for phenolic stretching. Also, a broad peak was

visible in the $^1\text{H-NMR}$ spectrum, at 6.54 ppm (Figure 51). Although this is slightly low for a phenolic peak, it is much closer to the acceptable range than that of a carboxylic acid (typically 12 – 14 ppm). This was further confirmed by the C=O peak at 166.4 ppm within the $^{13}\text{C-NMR}$ spectrum, which was not significantly shifted from that of the starting material, found at 167.2 ppm. If the ester had been cleaved to give a free acid, this peak would be expected to shift towards a higher ppm due to the increased deshielding effect of the carboxyl functionality.

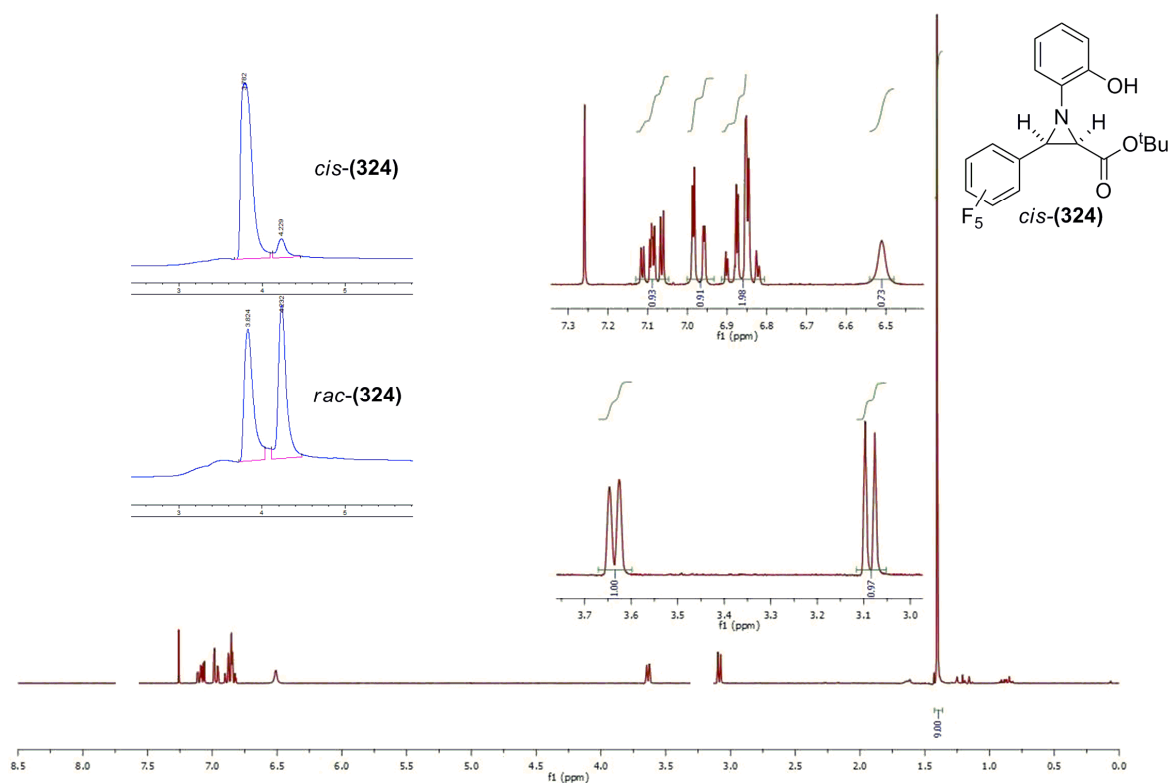


Figure 51: $^1\text{H-NMR}$, and chiral HPLC data for compound *cis*-(324) (NMR correlation data for compound *cis*-(324) can be found in Appendix 1)

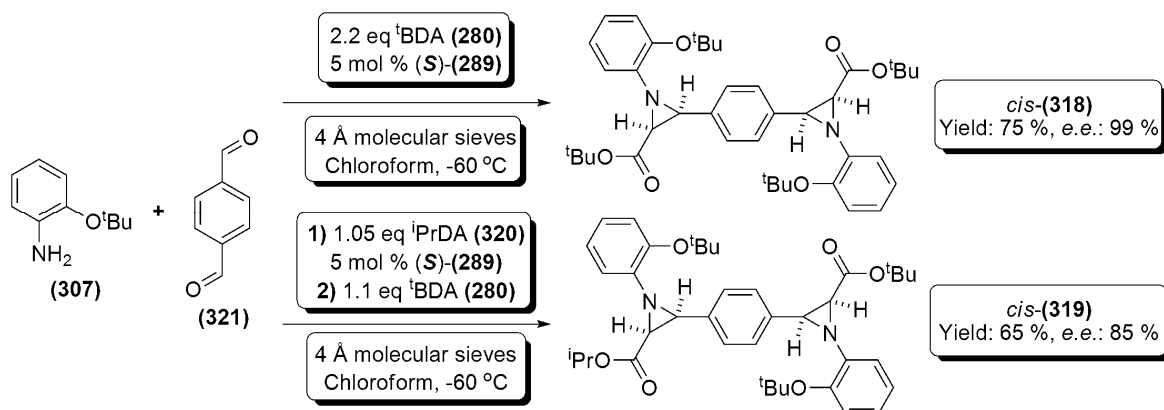
Further to this spectroscopic evidence, the cleavage of ethers to give phenolic functionality *via* the use of *para*-toluene sulphonic acid has precedence within the literature. For example, Wiemer *et al* have utilised similar conditions in order to cleave methoxymethyl ether protecting groups during the syntheses of schweinfurthin analogues.²⁷⁵

Cleavage of a *tert*-butyl group from aziridine *cis*-(314) yielded *cis*-(324), which was much more amenable to HPLC separation; allowing an *e.e.* of 90% to be recorded. As the *e.e.* is unlikely to have increased within the course of the cleavage reaction, it can be reasonably assumed that this *e.e.* can be transposed onto the starting material, *cis*-(314).

4.2.3: One-pot Asymmetric Aziridinations – Synthesis of bis-aziridines *cis*-(**318**) and *cis*-(**319**)

Having secured a synthesis of *cis*-(**317**) (Figure 50, 70% yield, 90% *e.e.*), a synthesis of the bis-aziridine *cis*-(**318**) was attempted, utilising one-pot aziridination conditions, but with corresponding adjustments in the stoichiometry of ^tBDA (**280**). This afforded the desired product *cis*-(**318**) in a very good 75% yield, and an excellent 99% *e.e.* (Scheme 117).

¹H-NMR spectroscopy confirmed the presence of *cis*-(**318**), with C2-*H* and C3-*H* peaks present at 3.03 and 3.46 ppm respectively, with integrations relating to 2 protons each. MS and HRMS also confirmed the presence of the desired aziridine, with mass ions being detected at 679.4 [M+Na]⁺, and 657.3895 (theoretical 657.3898). Interestingly, the C2-*H* signals for both aziridines overlap perfectly, with only one doublet seen, with a *J*_{2,3} of 6.7 Hz; suggesting a *cis*- conformation about the C2 – C3 positions of each aziridine.²⁶⁶ However, the C3-*H* signals at 3.46 ppm do not overlap perfectly, suggesting a different environment around the C3 position in each aziridine. ¹³C-NMR also suggests slight differences between each aziridine; with two signals being seen for the carbonyl functionalities at 167.1 and 167.0 ppm; and also, four peaks seen relating to the C2 and C3 carbons (47.6, 47.5, 47.4, 47.3 ppm). Potentially, these peaks could be caused by the presence of a meso form of the diaziridine; which would account for the doubling of the C2 and C3 peaks seen within NMR spectroscopy.



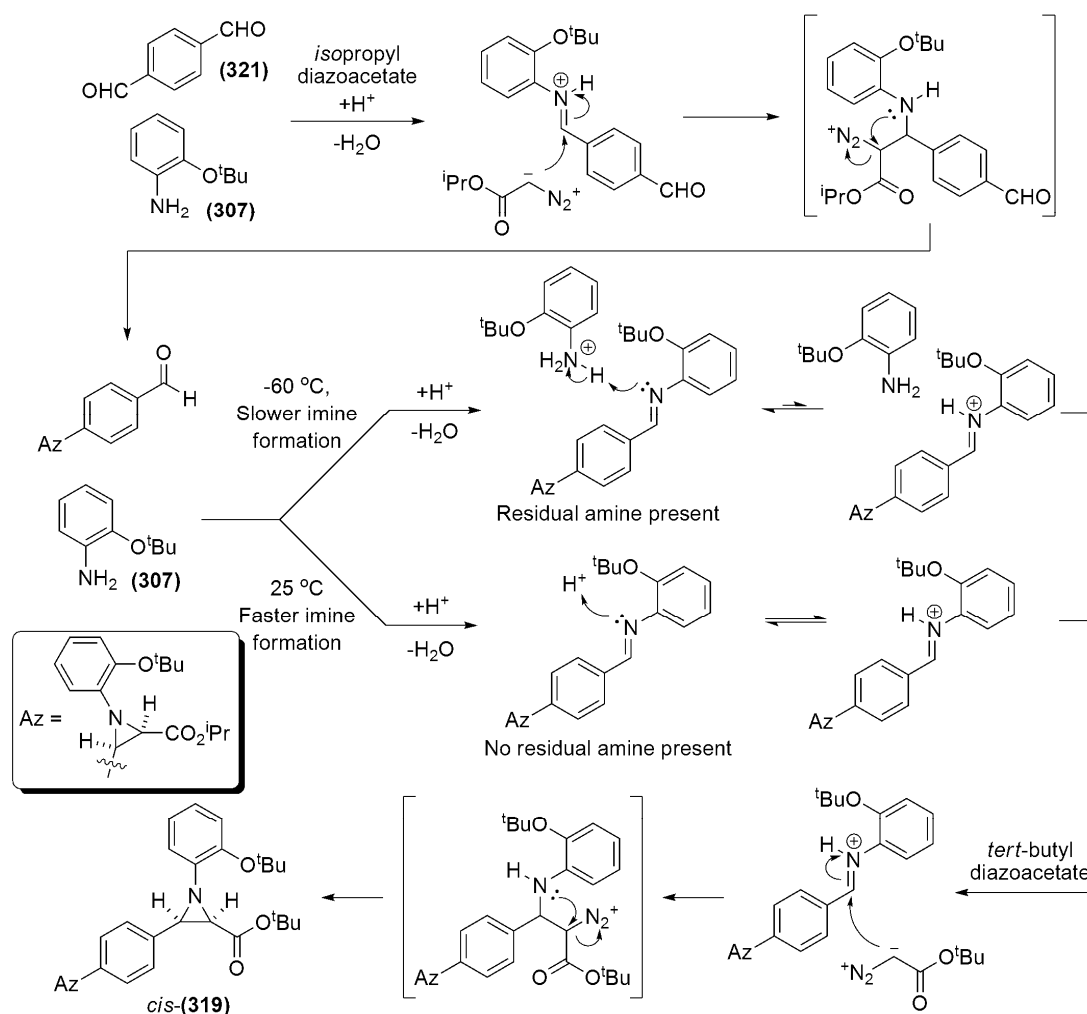
Scheme 117: Asymmetric syntheses of *cis*-(**318**), and *cis*-(**319**)

With *cis*-(**318**) in hand, a strategy was made for the synthesis of the differentiated *bis*-aziridine *cis*-(**319**). Within the synthesis of *rac*-(**319**) this had been achieved *via* a stepwise aziridination, limited by introduction of 1.05 equivalents of (**320**), followed by a further 1.1 equivalents of (**280**). In this case however, the method required the reaction to be kept at low temperature in order to increase the enantioselectivity of the reaction. Thus, 1 equivalent of 2-*tert*-butoxy aniline (**307**) was introduced to 1 equivalent

terephthalaldehyde (**321**) at room temperature, followed by cooling to $-60\text{ }^{\circ}\text{C}$, and addition of 1.05 equivalents of ${}^i\text{PrDA}$ (**320**). Upon completion of the first aziridination, (determined by ${}^1\text{H-NMR}$ spectroscopy) a further 1 equivalent of 2-*tert*-butoxy aniline (**307**) and 1.1 equivalents of ${}^t\text{BDA}$ (**280**) were added. However, upon addition of the second equivalent of 2-*tert*-butoxy aniline (**307**), aziridine formation was observed by ${}^1\text{H-NMR}$ spectroscopy to slow prohibitively.

This reduction in reaction rate could be due to capture of the catalytic proton by 2-*tert*-butoxy aniline (**307**). If the relative pK_a values of an *N*-substituted imine ($pK_a = 24.3$, in DMSO)²⁶⁷ and aniline ($pK_a = 30.5$, in DMSO)²⁶⁷ are compared it can be seen that the aniline has a higher pK_a , and thus is likely to protonate to a greater extent than the imine. At room temperature, the fall in the rate of reaction due to this effect is not observed. This can be explained by rapid imine formation consuming all present 2-*tert*-butoxy aniline.

However, at the low temperature conditions utilised within the above reaction, imine formation is likely to be slowed, thus allowing capture of the catalytic protons within the reaction by free 2-*tert*-butoxy aniline (**307**) to become significant (Scheme 118).



Scheme 118: Proposed mechanistic rationale for the rate reduction effect observed during the synthesis of *cis*-(319**), showing potential proton capture by residual 2-*tert*-butoxy aniline at $-60\text{ }^{\circ}\text{C}$**

In order to circumvent this effect, after the first aziridination was seen to reach completion (monitoring the appearance of C2-*H* and C3-*H* by ¹H-NMR) the reaction was warmed to 0 °C, followed by addition of 2-*tert*-butoxy aniline (**307**). After stirring at this temperature for 12 hours, the imine formation appeared to be well advanced, and the reaction was cooled to -60 °C once again, followed by addition of ¹BDA (**280**).

The aziridination proceeded successfully from this point, eventually yielding 35% of isolated product after a reaction time of 72 hours; however, this was increased to 65% considering recovered imine and starting materials. Upon submitting *cis*-(**319**) to chiral HPLC analysis, an *e.e.* of 85% was realised.

4.2.4: One-pot Asymmetric Aziridinations – Hypothesis upon the Enantioselectivity of the Asymmetric One-pot Aziridination Reaction

Throughout the syntheses detailed in the previous sections high enantioselectivities have been shown, with only *cis*-aziridines being observed. It is also the case that when utilising pyridinium triflate (**279**) to generate racemic aziridines, only *cis*-aziridines were produced. This is in agreement with the observed results during the use of (**289**) and (**279**) within the thesis work of Pesce.²⁶⁸

The high *cis*- selectivity of these aziridination reactions can be rationalised by considering Newman projections of the initial attack of *tert*-butyl diazoacetate upon a simple imine of the type employed within the previous reactions (For example (**325**), which is derived from benzaldehyde and 2-*tert*-butoxy aniline). In order for the desired aziridination reaction to occur (**325**) must be protonated, and therefore we must consider the protonated form of (**325**) within any Newman projections. This adds a further consideration to the analysis, as both the diazo group of the attacking diazoacetate and the protonated imine nitrogen, carry positive charge. Therefore, upon approach it is reasonable to assume these two groups will adopt a *trans*- orientation to one another in order to gain maximum separation between the like charges, leading to four possible orientations of approach (See Figure 52). However, steric interactions must also be considered. Interactions between the bulky *N*-2-*tert*-butoxy phenyl substitution of imine (**325**), and the *tert*-butyl group of *tert*-butyl diazoacetate are highly disfavoured; thus, only two possible approaches of the diazoacetate to the imine are observed (Figure 52). These lead to two possible *cis*- aziridines, which are enantiomers of one another (*i.e.* the racemic product observed upon use of pyridinium triflate (**279**) as the aziridination catalyst).

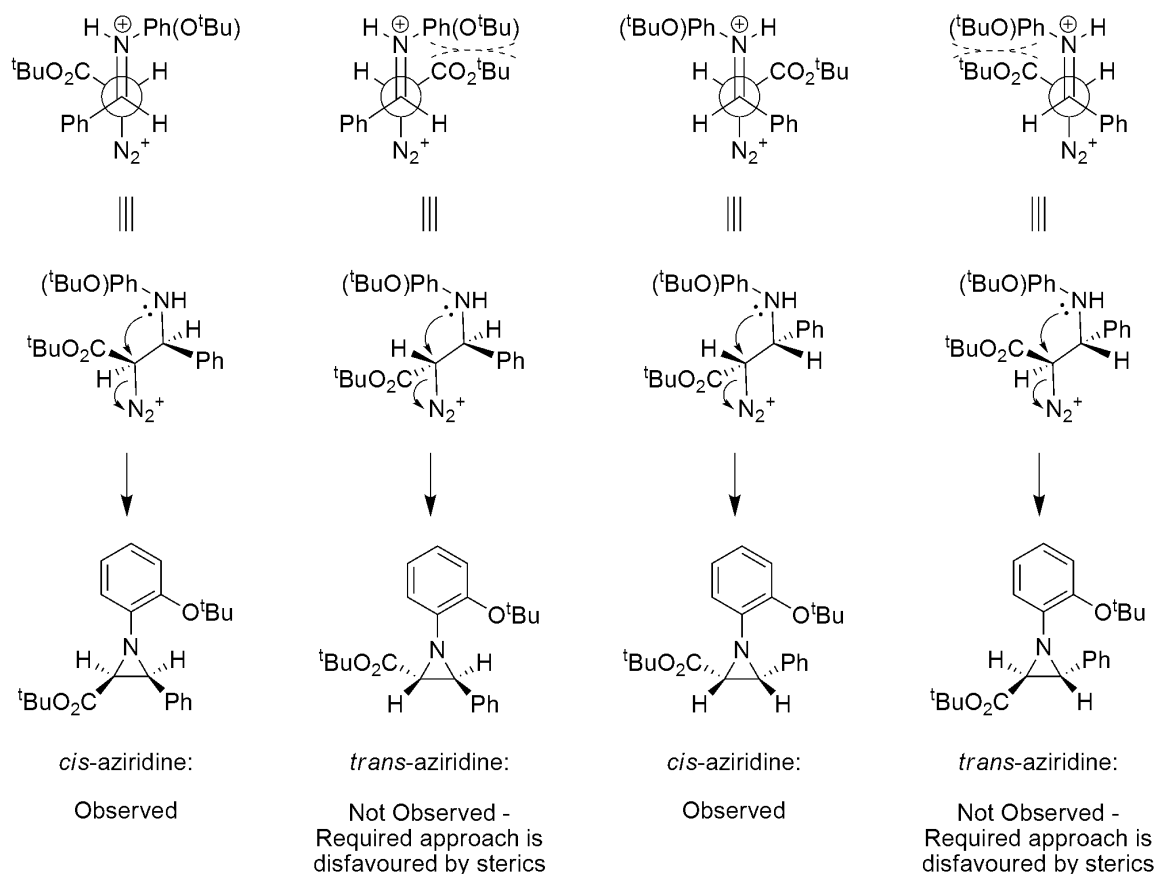
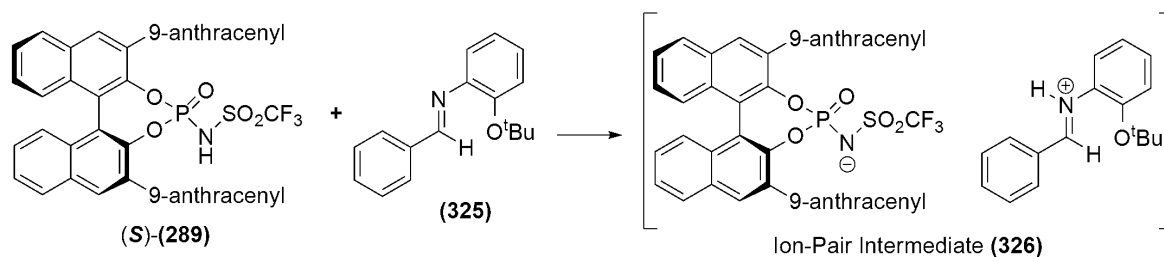


Figure 52: Newman projections of the attack of *tert*-butyl diazoacetate upon the protonated form of imine (325)

A high degree of enantioselectivity has also been observed in aziridination reactions utilising (*S*)-(289) as the catalyst. In an attempt to rationalise the mechanism by which this selectivity occurs, molecular modelling of the interaction between the protonated form of imine (325) within catalyst (*S*)-(289) during the transition state has been carried out at the MM2 theory level. Although a low level of theory, this model should allow a basic understanding of the shape of the intermediate species (326) believed to be formed between (*S*)-(289) and (325) upon proton transfer (Scheme 119, and Figure 53).



Scheme 119: Protonation of (325) by (*S*)-(289) to form the intermediate ion-pair (326)

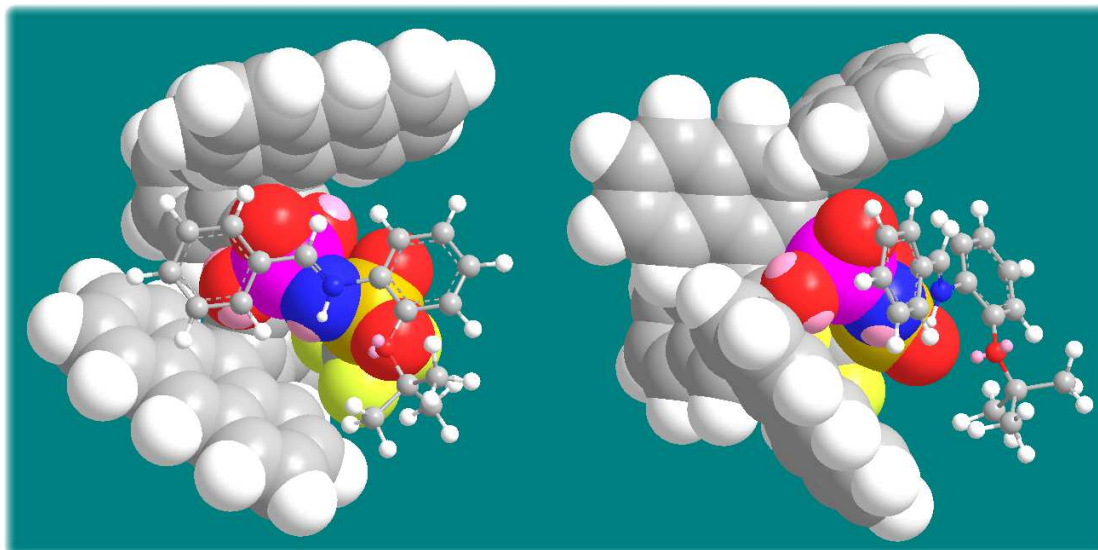


Figure 53: 'Front' and 'Side' views of the MM2 optimised structure for the intermediate (326) comprised of the anionic form of catalyst (S)-(289) and the protonated form of imine (325)

As shown in Figure 53, **(325)** is predicted to fit well within the cavity created by the 'shielding' 3,3'-(9-anthracenyl) groups upon the catalyst (S)-(289). The orientation of the imine within the cavity could potentially be explained by the formation of a hydrogen bond between the anionic nitrogen of the catalyst, and the NH of the imine intermediate; also, potentially hydrogen bonding could occur between the delta positive hydrogen of the imine CH, and the lone pairs upon the carbonyl oxygen of the catalyst, forming a double hydrogen bonded transition state (Figure 54). Transition states such as this have been invoked in various situations previously; including the work of List *et al* into the use of asymmetric counterion directed catalysis with TRIP (**183**) (see 2.2.6: *Counterion Catalysis*, Figure 37),^{186,187} and the work of Akayama *et al* and Terada *et al* into asymmetric Mannich reactions (See 2.3: *Organocatalysis: Chiral Brønsted Acid Catalysts*, Figure 39).¹⁹²

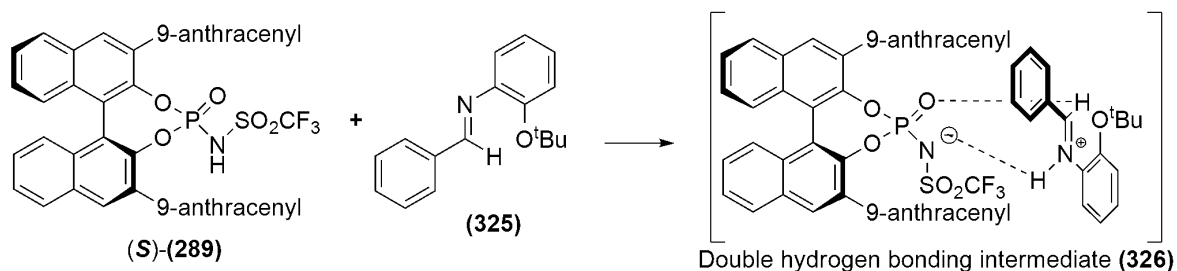


Figure 54: Representation of the potential double hydrogen bonded transition state within intermediate (326)

Further to this, evidence for the presence of a chiral intermediate similar to **(326)** arising from the interaction of catalyst (S)-(289) with an *N*-substituted imine substrate has been provided by CD spectroscopy, and is discussed in *Chapter 8: Spectroscopic and Computational Investigations*.

If a chiral intermediate species such as **(326)** is indeed formed between the chiral catalyst **(289)** and protonated imines, it becomes obvious that the nucleophilic attack of any diazoacetate will preferentially occur from the unshielded face of the imine, thus leading to the high enantioselectivity which is observed within the aziridination reactions utilising **(289)**. It is also reasonable to assume (as the aziridination reactions utilising **(298)** are still highly *cis*-selective) that the same Newman analysis of the approach of a diazoacetate to the intermediate discussed earlier in this section still holds true (Figure 55).

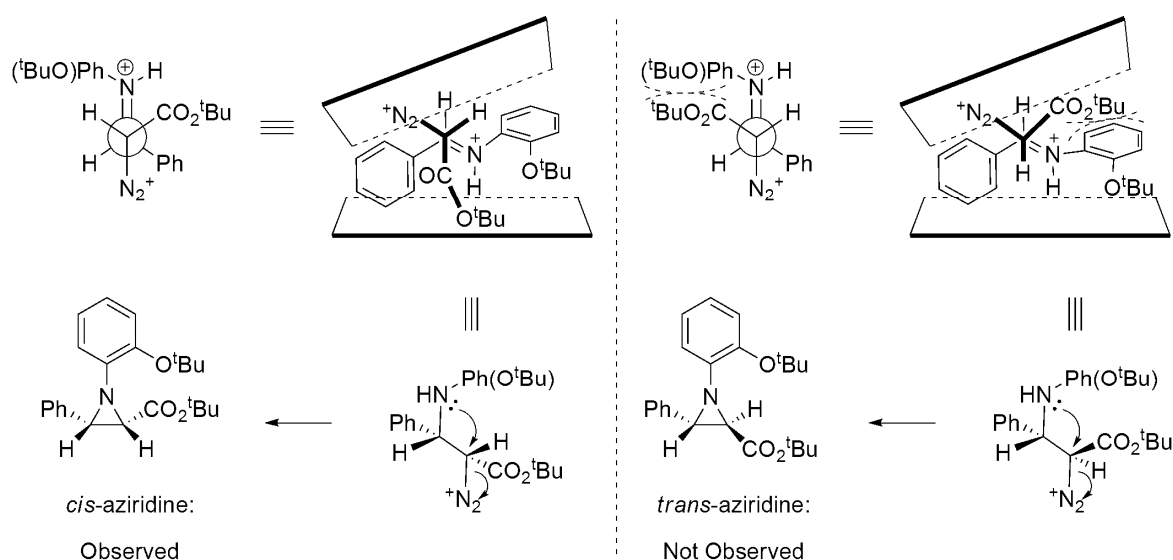


Figure 55: The two possible approaches of *tert*-butyl diazoacetate to the imine (325) whilst within the cavity of (S)-(289); showing the steric disfavoring of the approach which would produce *trans*-aziridine

Potentially, the analysis within this section could be extended to provide predictions upon the absolute stereochemistry of the aziridines produced utilising (S)-(289); however, no prediction has been made, as no experimental confirmation of the absolute stereochemistry of these aziridines has been possible thus far. Therefore, all graphical representation of chiral non-racemic aziridines throughout this thesis should be considered relative stereochemistry. Attempts have been made to elucidate the absolute stereochemistry of these aziridines utilising spectroscopic and computational techniques, and these are detailed within *Chapter 8: Spectroscopic and Computational Investigations*).

4.3.1: Development of a Flow Reactor Based Aziridination Procedure – Introduction and Advantages

When comparing flow chemistry to traditional batch type chemistry, the most striking difference is the way product is produced. Within batch type chemistry, each reaction is distinct; producing an amount of product after a set reaction time. Flow

chemistry differs in the fact that a product stream is produced; resulting in a smaller amount of product, but produced continuously.

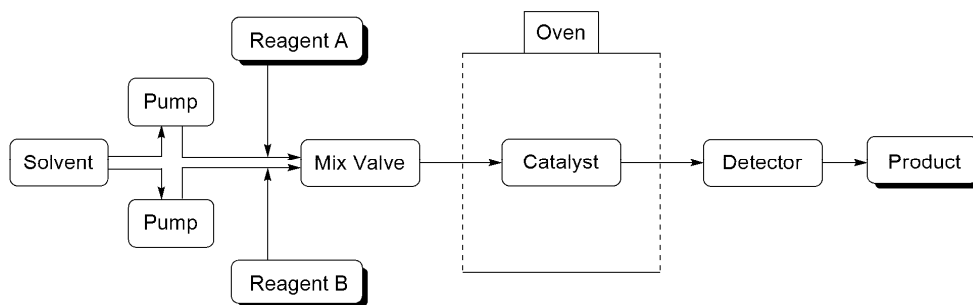


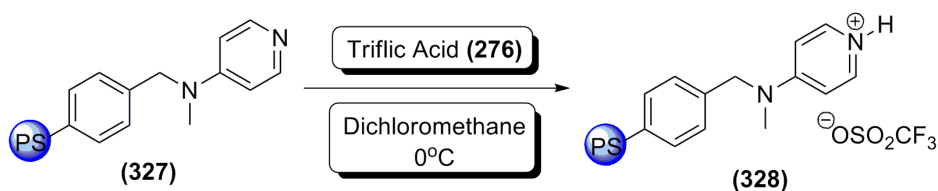
Figure 56: Schematic diagram of a basic flow chemistry reactor

The advantages of flow chemistry type procedures are pronounced; and include such factors as low catalyst contact time (reducing the potential for side reactions), reduced need for solvents and less waste (important factors in green chemistry), and less manual manipulation of hazardous materials and reagents. However, the disadvantages of flow chemistry are also reasonably strong; foremost among these being the sometimes prohibitive cost of setting up a flow reactor system (For example, the Sigma-Aldrich micro-reactor system, a commercial flow reactor retails at £18 800).²⁷³

As a proof of concept for the robustness of the aziridination procedures developed within this research, a flow reactor system was built (based upon HPLC equipment), capable of producing aziridines, with a view to ease of synthesis in the future.

4.3.2: Development of a Flow Reactor Based Aziridination Procedure – Chemical Basis for the Flow System

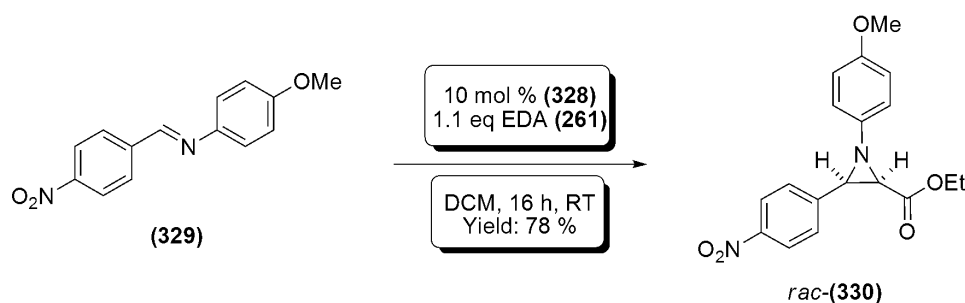
As has been demonstrated by Bew *et al*, the aziridination of phenyl substituted and derived imines with various alkyl diazoacetates in the presence of pyridinium triflate (**279**) is a facile and high yielding procedure.²²⁴ It is this basis upon which any potential flow reaction could be built. In order to utilise this methodology within a flow setting, an immobilised catalyst was required. A suitable immobilised pyridinium triflate based catalyst had previously been reported by Pesce,²⁶⁸ prepared by treatment of commercially available polystyrene bound DMAP (**327**), with triflic acid (**276**) (Scheme 120).



Scheme 120: Synthesis of polymer bound pyridinium triflate (328) by Pesce

The polystyrene immobilised catalyst (**328**) was washed with dichloromethane prior to use in order to remove any unreacted triflic acid, and was confirmed to be present by ATR-IR spectroscopy; with bands consistent with N-H stretching (3242 cm^{-1}), C=N stretching (1552 cm^{-1}), and sulfonyl asymmetric stretching ($1283 - 1163\text{ cm}^{-1}$).

In order to test the effectiveness of the polymer bound catalyst (**328**), a test aziridination in batch mode was carried out (Scheme 121). Treatment of imine (**329**) with *ca.* 10 mol % (**328**) (stoichiometry could not be accurately predicted due to approximation of the surface coating of the resin), and EDA (**261**) led to the production of the desired aziridine *rac*-(**330**) in a 78% yield at room temperature in 16 hours.



Scheme 121: Batch aziridination of (**329**) utilising polymer bound catalyst (**328**)

Confident that the catalyst (**328**) was effective under batch conditions, it was decided to attempt to utilise it under flow conditions; thus the next step was to develop the required hardware for the flow reactor.

4.3.3: Development of a Flow Reactor Based Aziridination Procedure – Sourcing and Set-up of the Reactor

As noted above, the main disadvantage of flow chemistry for an academic laboratory environment is the prohibitive cost of the flow reactor itself. Within this context, it was decided to utilise readily available HPLC equipment in order to produce a flow reactor capable of synthesising aziridines.

HPLC equipment already possesses many of the desirable features of a flow system: *i.e.* solvent resistant fittings and pumps, high pressure capability, finely controllable pump and valve equipment, detector capability, and an interface with software to facilitate control and method development.

The HPLC used within the flow system was a Beckman Gold System modular HPLC, equipped with a 128 series pump module, and 129 series diode array detector. In order to allow for introduction of the reactants, the system was fitted with a standard Rheodyne[®] valve, containing a 5 mL sample loop. The use of a Rheodyne[®] valve enabled the reagents to be introduced after the pumps, preventing potential corrosion of the pump

heads and seals. In order to determine when the reagents had passed through the system, the diode array detector was set up to monitor at the standard wavelengths for UV detection, 298 nm and 254 nm. The reaction chamber was provided by stripping and repacking a 10 x 0.7 cm analytical HPLC column with the polymer bound catalyst (**328**) (Figure 57). This column was kept under dichloromethane when not in use in order to remove the need for long column flushing times before use.

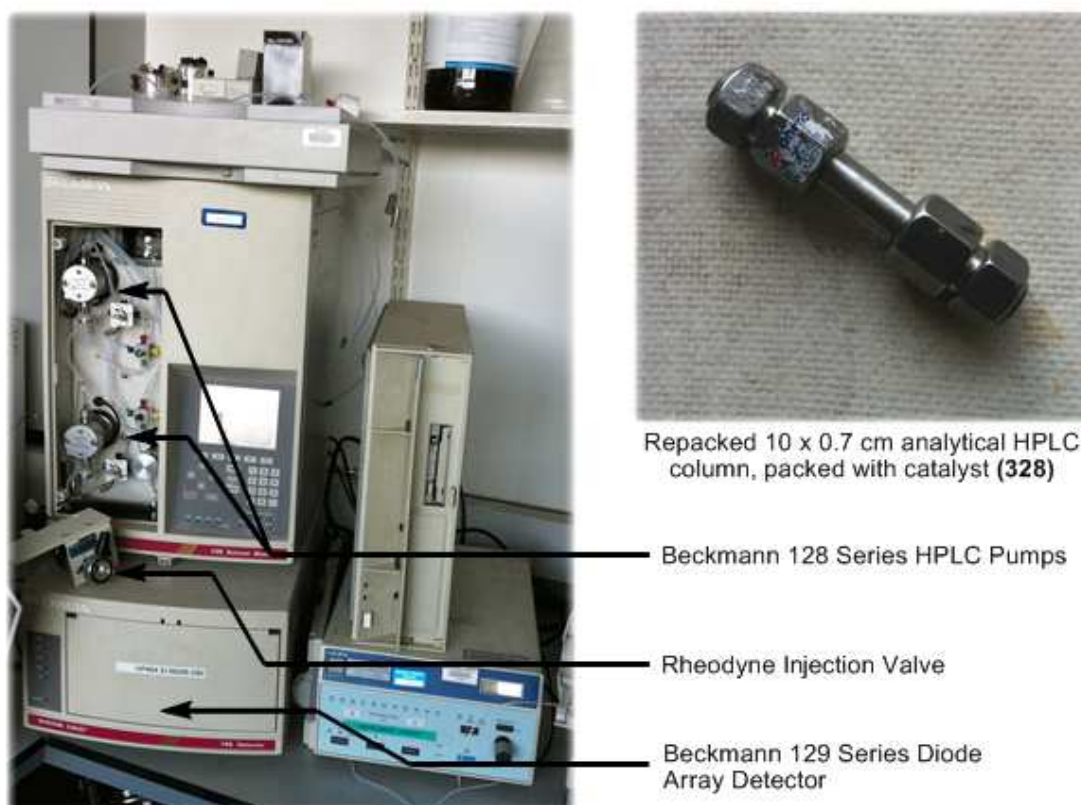


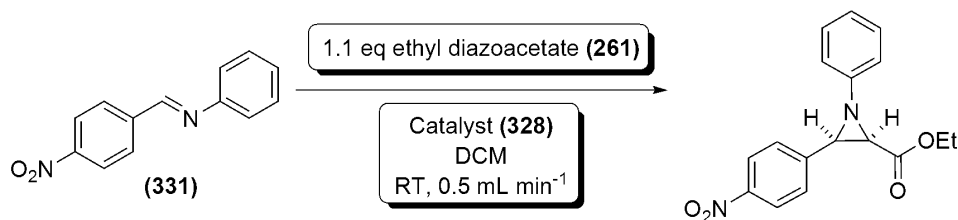
Figure 57: The basic flow system setup, based upon a Beckmann System Gold HPLC; and the repackaged 10 x 0.7 cm analytical HPLC column

As it has been shown, the pyridinium triflate catalysed aziridination protocol (utilising preformed imines) previously developed by Bew *et al* is tolerant to moisture and air;²²⁴ therefore, no attempt was made to dry, or vigorously degas the solvents used (although, solvents were sonicated before use). However, prior to use, the system was flushed with dichloromethane in order to remove any air bubbles present, as is standard practice within HPLC.

4.3.4: Development of a Flow Reactor Based Aziridination Procedure – Synthesis of a Racemic Aziridine via a Flow Chemistry Procedure

The initial test aziridination was similar to that demonstrated previously in Scheme 113, utilising imine (**331**) (derived from aniline, and 4-nitro benzaldehyde) and EDA (**261**). The system was set up at a flow rate of 0.5 mL min⁻¹, and the reagents premixed in

dichloromethane to a volume of 5 mL at a concentration of *ca.* 0.26 mmol/mL (Scheme 122).



Scheme 122: Initial flow aziridination attempted; utilising *N*-(4-nitrobenzylidene)aniline (331), ethyl diazoacetate (261), and polymer bound catalyst (328)

Pre-mixing of (331) and EDA does not bias the reaction; as a catalyst is required to sufficiently lower the activation energy and allow reaction between (331) and ethyl diazoacetate (261) (see 3.3.1: *Aziridination: Aziridination with Alkyl Diazoacetates – Introduction*, Figure 44). Ideally, in a second generation reactor, mixing would occur within the system, however, for the purpose of this proof of concept, pre-mixing was adequate. After injection, the system was run until the detector returned to a stable baseline; while the output of the system was collected and the solvent removed under reduced pressure.

The dried material from the flow reactor was analysed by ¹H-NMR spectroscopy, which revealed partial conversion of the starting materials to the desired aziridine. The characteristic doublets present within the spectrum at 3.18 and 2.66 ppm corresponding to the C2 and C3 protons were integrated to the imine proton signal, giving a ratio of roughly 1:2, suggesting around 33% conversion. Also, the coupling constants of the C2-*H* and C3-*H* peaks were 6.9 and 6.9 Hz respectively, suggesting the production of *cis*-aziridine.²⁶⁶ Also present within the ¹H-NMR spectrum were peaks relating to starting materials; *i.e.* the imine *CH* singlet present at 8.4 ppm (ethyl diazoacetate peaks were not present within the NMR spectrum, due to evaporation under high vacuum).

Although the conversion within this initial reaction was not high (*ca.* 33%), this test shows that passing the starting materials shown in Scheme 122 over catalyst (328) is a potential method of inducing an aza-Darzens aziridination reaction. To increase the conversion and yield of this process, the flow rate of the system was reduced to increase retention times. However, reduction of the flow rate below 0.5 mL min⁻¹ did not lead to any appreciable change in conversion. Manual calculation of the flow rate at this point suggested that at below 0.5 mL min⁻¹, the pump was not reliable to hold a steady rate, thus reduction of the flow rate was not effective in increasing contact time.

Despite the low conversion of this initial reaction, the demonstration of the principle is clear. With further development of the equipment used, it should be possible to

optimise all parameters of this flow reaction (*i.e.* retention time, concentration *etc*), leading to the possibility of continuous production of aziridines. However, further development or optimisation of the system was not carried forward due to developments concerned with the work discussed in the following chapters.

4.3.5: Development of a Flow Reactor Based Aziridination Procedure – Suggestions for Future Work

The main development which could be considered for the system is the introduction of more finely controlled pump apparatus. It is the author's belief that increasing the contact time of the reaction will lead to higher conversion of the starting materials. A further improvement could potentially be the use of in-line introduction of reagents; as opposed to injection *via* a Rheodyne[®] valve. This would allow concentrations of reagents to be kept low, thus preventing potential overloading of the reaction chamber, and allowing for more complete reaction (Figure 58).

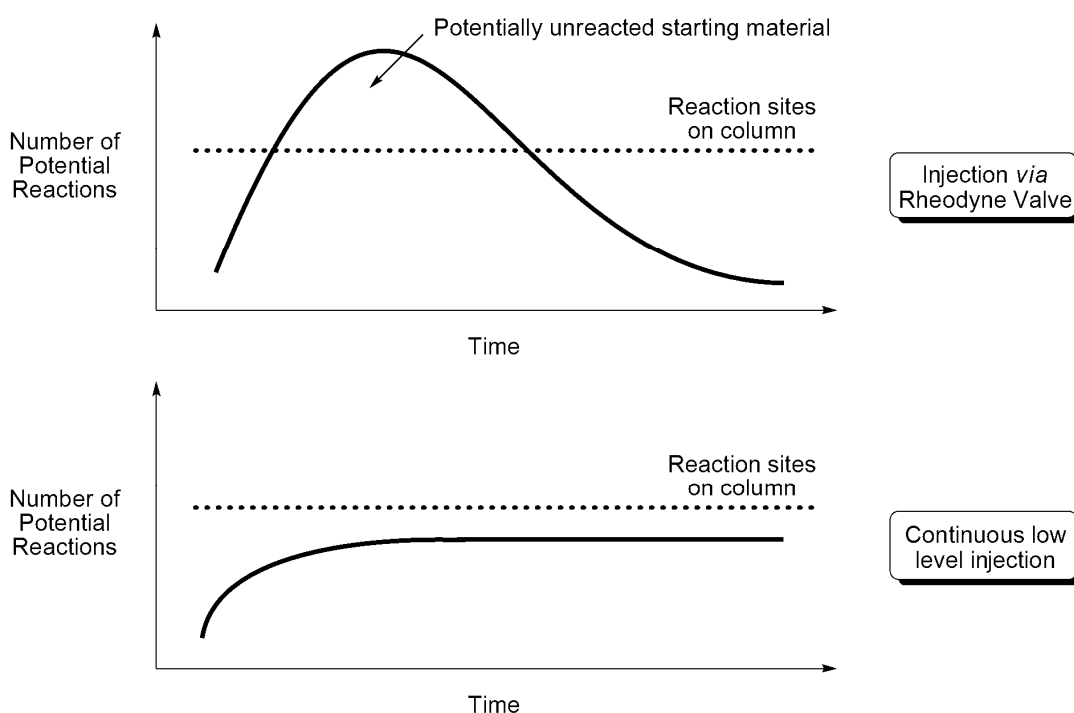
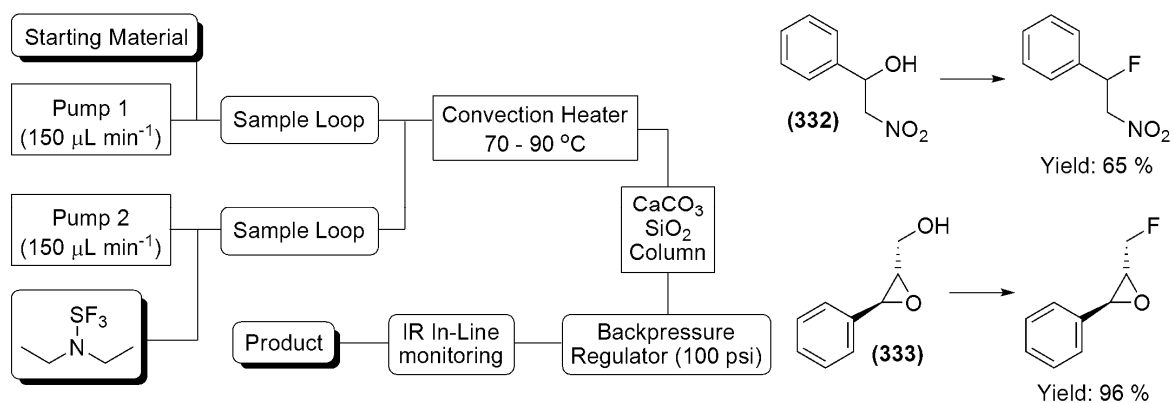


Figure 58: Demonstration of potential column overloading arising from starting material injection *via* a Rheodyne valve; and comparison with continuous low level starting material injection

One final suggestion could be the use of in-line monitoring such as the IR in-line monitoring and optimisation techniques developed by Ley *et al.*^{274,275} These techniques allow for continuous monitoring of the reaction output, enabling changes to be made to the system and their effects analysed immediately; also, through correlation of the IR output with the Beer-Lambert Law, concentrations of each component in the product stream can be calculated immediately. For example, Ley *et al* have utilised this technique to develop

and optimise conditions for the fluorination of various aliphatic and aromatic compounds including (332) and (333) shown in Scheme 123; utilising a continuous flow system.



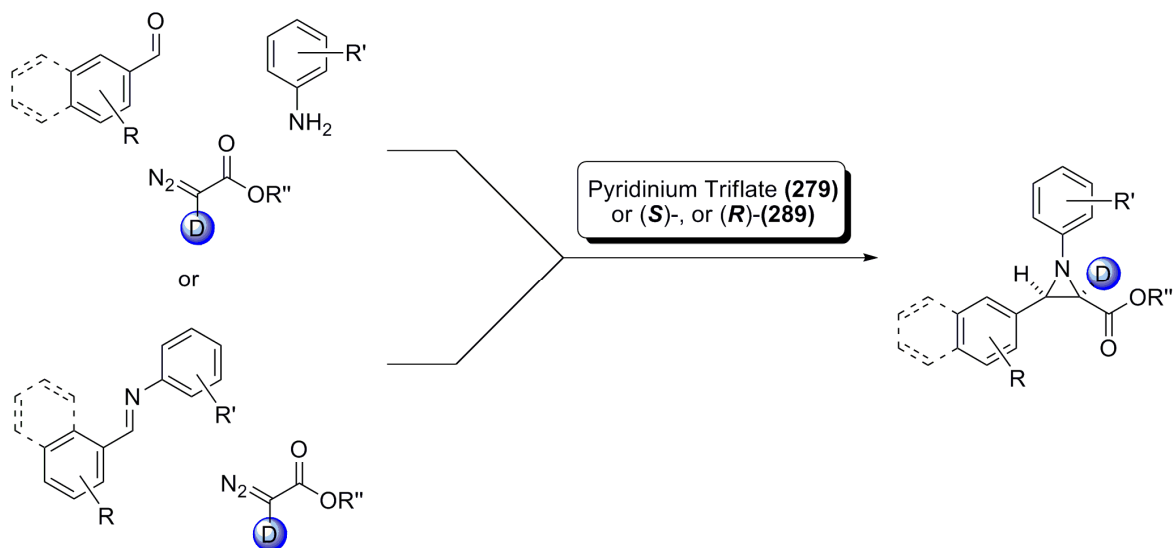
Scheme 123: Schematic representation of the flow system utilised by Ley *et al* within the synthesis and optimisation of the fluorination reactions of various starting materials including (332) and (333)

Chapter 5: Studies towards the Synthesis of C2-deuterated Aziridines

5.1.1: Development of Deuteration Techniques – Introduction

As shown within Chapter 1, there are many methods for introducing deuterium into an organic compound (See 1.5: *Synthesis of deuterated compounds*); although the majority of these focus upon introducing deuterium at a late stage of a synthesis, and tend to show poor selectivity for specific positions within a substrate. The exception to this rule is the H/D exchange chemistry of Ir(I) based catalysts.⁸⁹⁻⁹¹ These have been shown to selectively introduce deuterium 5 or 6 bonds away from a directing carbonyl group (See 1.5.3.4.2). However, for the purposes of aziridination chemistry, the most useful deuteration positions are the ring carbons, C2 and C3, which are 2 or 3 bonds away from the carbonyl functionality.

The main aim of this project was to develop a selective, accessible and easy to use deuteration technique. Initially, efforts were concentrated upon the production of deuterated alkyl diazoacetate starting materials, which would be suitable for application within our aziridination methodologies (Scheme 124). This would allow introduction of deuterium at the beginning of the synthesis; relying upon the stability of the ring carbons to exchange in order to maintain deuteration levels throughout ongoing reactions. For the purposes of our methodology, it was decided to attempt to use deuterium oxide as a deuterium source, due to the relative ease of handling, and reduced cost compared to pure deuterium gas, which has been used in H/D exchange reactions previously.^{86,92,95}

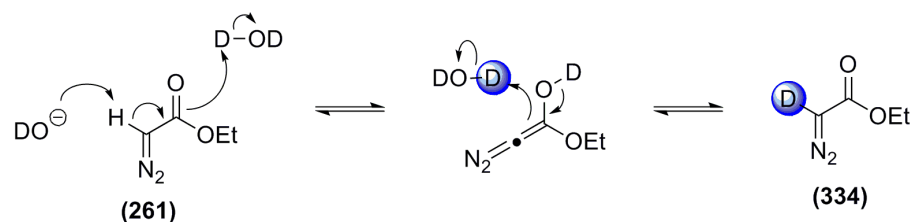


Scheme 124: Proposed synthesis of C2-deuterated aziridines from deuterated alkyl diazoacetates

5.1.2: Development of Deuteration Techniques – Deuteration of Ethyl diazoacetate

Initially, deuteration efforts were focussed upon ethyl diazoacetate (EDA, **(261)**). The main reason for this was the ready availability of commercial EDA; ensuring a ready supply of starting material for future work. As the α -position of EDA is vulnerable to

exchange, it was decided to attempt a simple base catalysed exchange reaction with deuterium oxide (Scheme 125).



Scheme 125: Proposed base catalysed H/D exchange mechanism for the α -position of ethyl diazoacetate (261)

Thus, a deuteration of EDA (**261**) was attempted; utilising a catalytic amount of potassium carbonate in a biphasic mixture of diethyl ether, and deuterium oxide. After stirring vigorously for 16 hours, the layers were separated, and the organic layer was carefully evaporated to remove the solvent, without evaporating the desired product. The ¹H-NMR spectrum of this crude material showed that to a certain extent, deuterium had been incorporated into the desired α -position (Figure 59). The deuterium incorporation level was determined by consideration of the relative integrations of the CH₃ (1.30 ppm), CH₂ (4.22 ppm) and residual CH (4.70 ppm) peaks to be 21% (Figure 59).

However, this level of deuterium incorporation was not deemed high enough to move on to the next step. It was also noticed that recovery of the EDA was lower than would be expected; potentially due to base catalysed hydrolysis of the ester due to the conditions and reaction time employed, leading to loss of the resulting diazocarboxylic acid species within the deuterium oxide during work up.

Therefore, a further reaction was attempted; treating EDA (**261**) again in the presence of potassium carbonate and excess deuterium oxide, however, in this case, two reaction cycles of 30 minutes were employed. This yielded α -deuterated EDA (**334**) in a 75% yield, and more importantly, with a deuterium incorporation of >90% determined by ¹H-NMR spectroscopy (Figure 59).

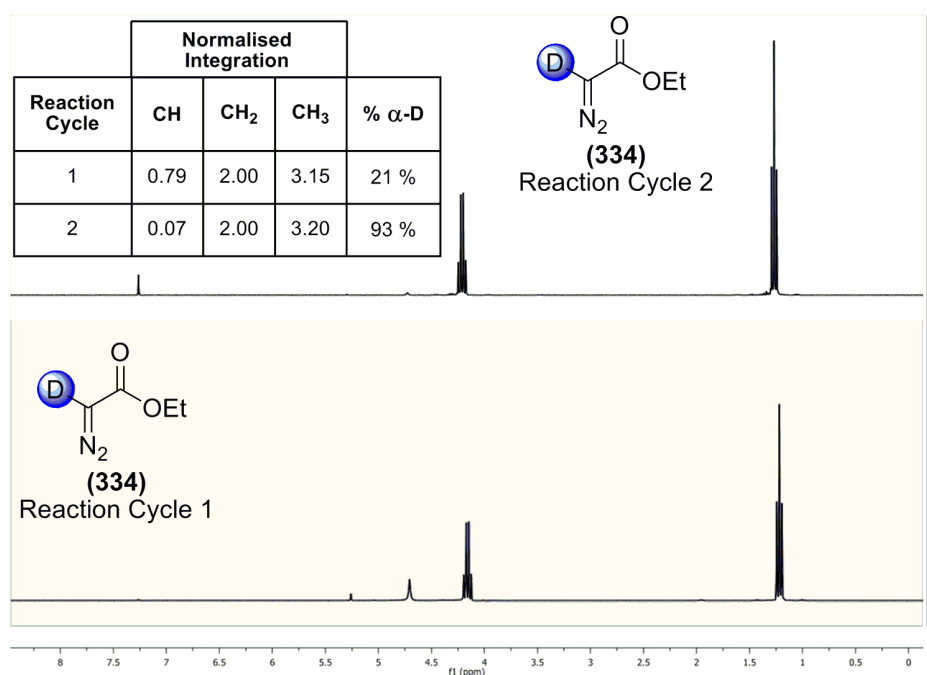


Figure 59: ^1H -NMR of EDA-*d* (334) after one, and two, reaction cycles

Interestingly, when the sample was submitted to ^{13}C -NMR spectroscopy, several signals appeared to be ‘missing’ from the spectrum. These being those related to the α -carbon (expected at 46 ppm), and also the carbonyl signal. The loss of the α -carbon signal can be attributed to signal splitting by deuterium (See 1.3: *Properties of Deuterium, Deuterium Oxide, and the Deuteron*), and also the effects of relaxation.

This splitting effect comes about due to the nuclear spin of a deuteron, which has a value of 1. This generates three distinct energy levels when the deuteron is placed within a magnetic field, meaning during spin-spin coupling, an adjacent nucleus (in this case, ^{13}C) can experience the effect of three distinct spins; generating a triplet signal (Figure 60).²⁷⁶

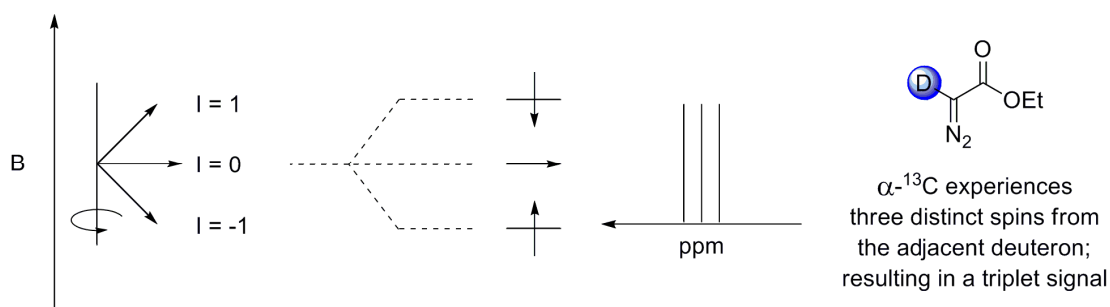


Figure 60: Representation of the spin energy levels of the deuteron, giving rise to a triplet signal in ^{13}C -NMR

Therefore, the α -C signal within EDA-*d* (334) should appear as a triplet. However, the effect of deuterium coupling also leads to a loss of signal intensity, as each peak of the triplet has 1/3 intensity; thus leading to the loss of the signal within the baseline of the spectrum (Figure 61).

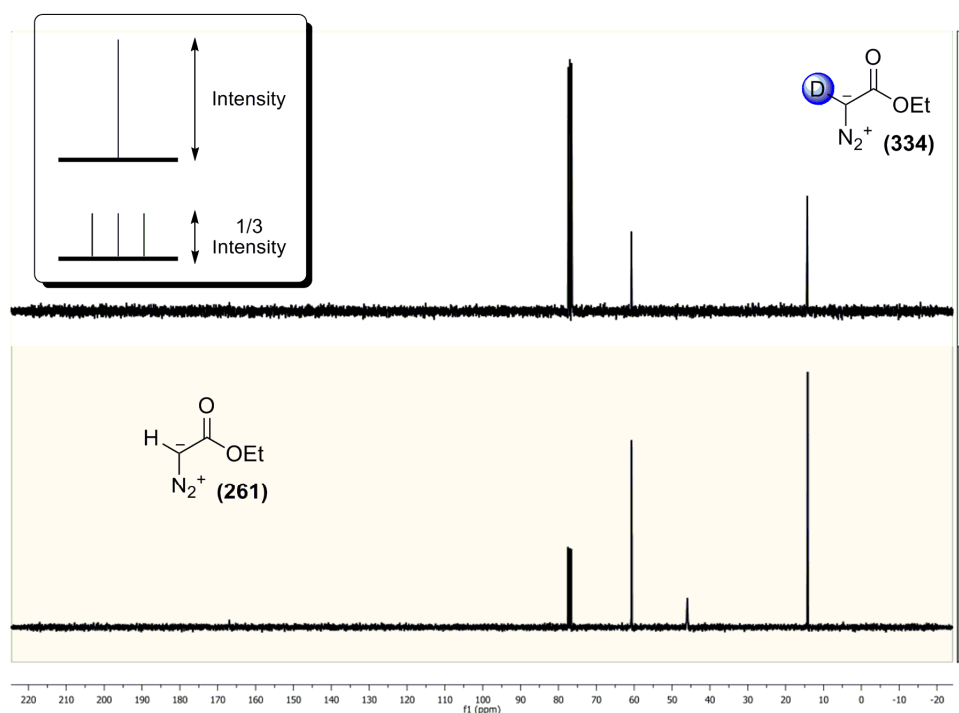
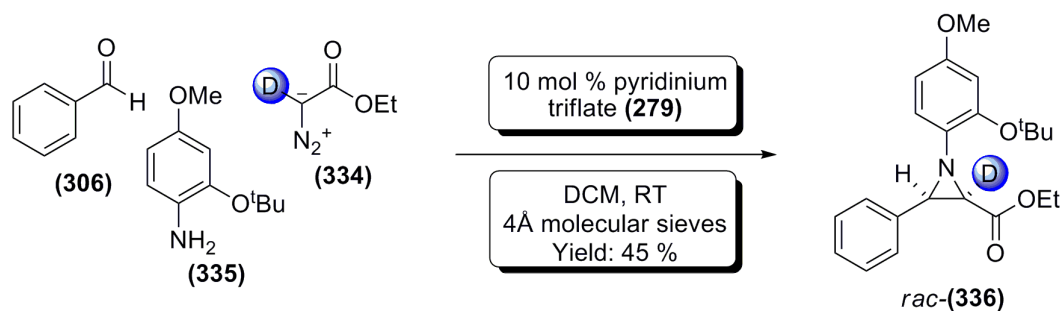


Figure 61: ^{13}C -NMR of EDA (261) and EDA-*d* (334)

Satisfied that the exchange procedure would function adequately to supply our research, the next step was to attempt the previously developed aziridination methodologies utilising α -deuterated EDA (**334**).

5.1.3: Development of Deuteration Techniques – Initial Aziridination Reactions

With α -deuterated EDA (EDA-*d* (**334**)) in hand, a test aziridination was required in order to establish any potential difficulties in utilising deuterated alkyl diazoacetates (compared to the conventional *proteo*- form) within the aziridination protocols. Therefore, a one-pot racemic aziridination of benzaldehyde (**306**), 2-*tert*-butoxy-4-methoxy aniline (**335**), and EDA-*d* (**334**) was attempted (Scheme 126). During this first reaction, best possible conditions were used; *i.e.* all glassware was flame dried and allowed to cool under nitrogen, dichloromethane was freshly distilled from calcium hydride, and the reaction was carried out in a sealed vial under nitrogen.



Scheme 126: Racemic aziridination reaction utilising EDA-*d* to produce aziridine *rac*-(336)

Gratifyingly, after 16 hours, $^1\text{H-NMR}$ spectroscopy revealed new peaks believed to correspond to the desired product, and the reaction was halted. After purification by flash column chromatography, further analysis revealed the production of the desired aziridine in a yield of 45%.

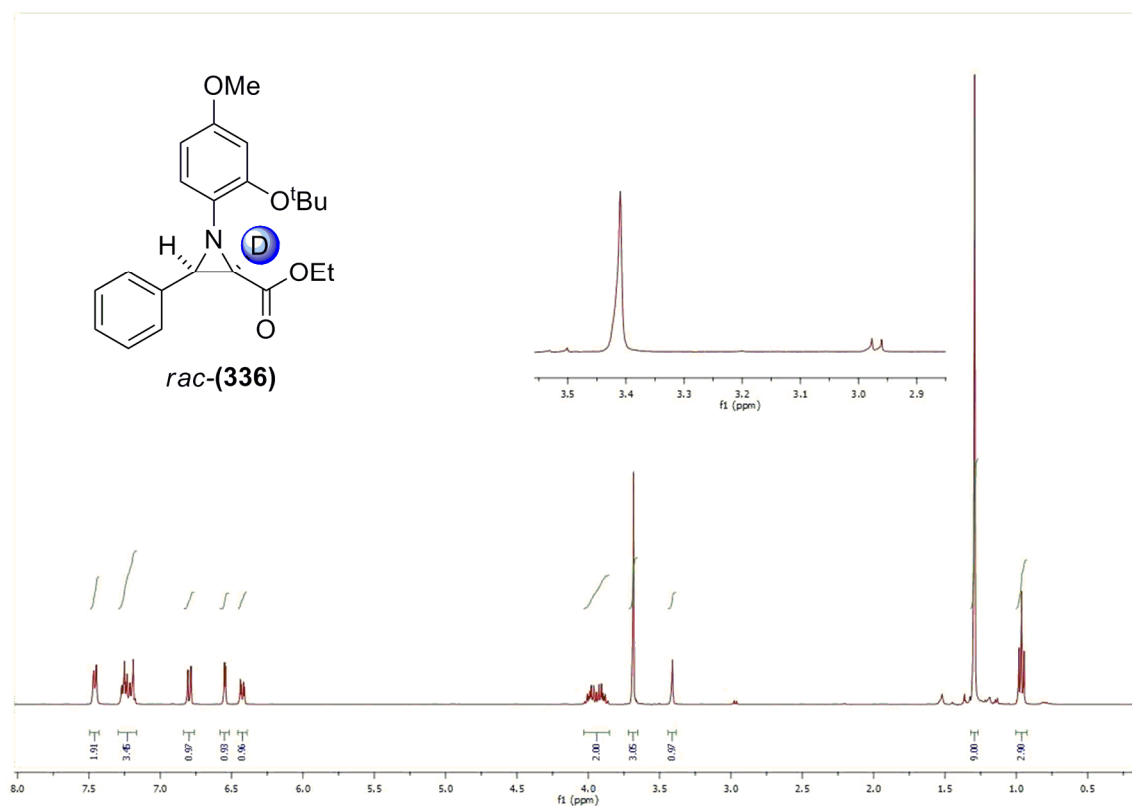


Figure 62: $^1\text{H-NMR}$ of *rac*-(336), indicating deuteration of the C2-position

As shown in Figure 62, the $^1\text{H-NMR}$ spectrum revealed residual proton to be present at the C2-position (characterised by the small residual doublet at 2.97 ppm), however, integration of the residual C2-H and C3-H (3.41 ppm) peaks revealed deuterium incorporation of 91%. Interestingly, theory suggests that the C3-H peak should appear as a triplet (due to spin coupling with the adjacent deuterium at the C2 position).²⁷⁶ However, experimentally this is not the case. This can be explained by the fact that although the coupling constants for H-D couplings are proportional to those of H-H coupling, they are reduced by a factor of *ca.* 7 (due to the differences in the H and D magnetogyric ratios (Figure 2)).²⁷⁶ Thus, the coupling constant for the C3-H to the C2-D can reasonably be expected to be *ca.* 0.9 Hz. Therefore, the triplet appears as a broad singlet within the $^1\text{H-NMR}$ spectrum.

Further evidence for the deuteration of *rac*-(336) was provided by MS, which, under ESI conditions provided the mass ions shown in Figure 63 for both $[\text{M}+\text{H}]^+$, and $[\text{M}+\text{Na}]^+$.

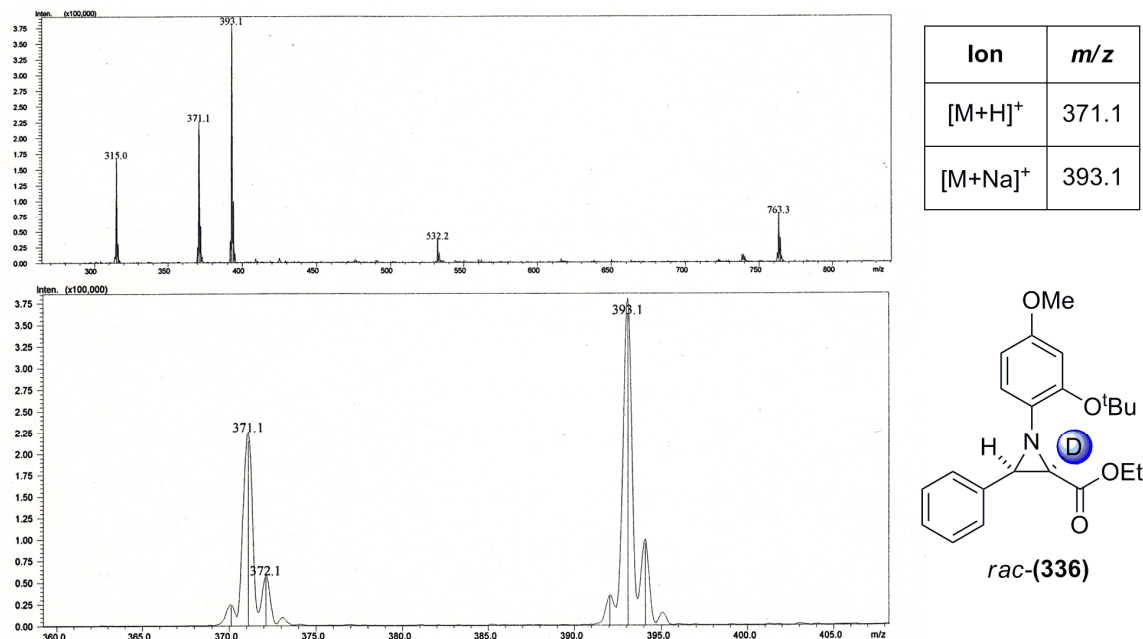


Figure 63: LC-MS data for *rac*-(336) showing [M+H]⁺ and [M+Na]⁺

Interestingly, although in most senses this reaction behaved as a standard aziridination reaction, the rate of reaction appeared to be slightly slower than that of the equivalent *proteo*-aziridination. Potentially, this could be due to a secondary kinetic isotope effect (See 1.4: *Deuterium and the Kinetic Isotope Effect*).

Secondary kinetic isotope effects come about when deuterium is not directly involved within the bond making/breaking step of a reaction, and have been shown to result primarily from changes in the vibrational frequencies (and thus the Zero Point Energies (ZPEs)) present within the transition state of a reaction (Figure 64).^{27,28} In this case, the changes in vibrational frequency (and thus ZPE) come about as a result of hybridisation changes within the C-D bond.²⁷⁷ These changes occur at only one point during the aziridination reaction (assuming an aza-Darzens mechanism is in effect); this being nucleophilic attack of EDA-*d* (334) upon the *N*-benzylidene-2-*tert*-butoxy-4-methoxyaniline (337) formed *in situ*, passing through TS1 (338). Although deuterium is α -to the ring closure of the intermediate (339), eliminating N₂, no rehybridisation occurs; thus TS2 (340) can be discounted as the source of a secondary KIE (Figure 64).

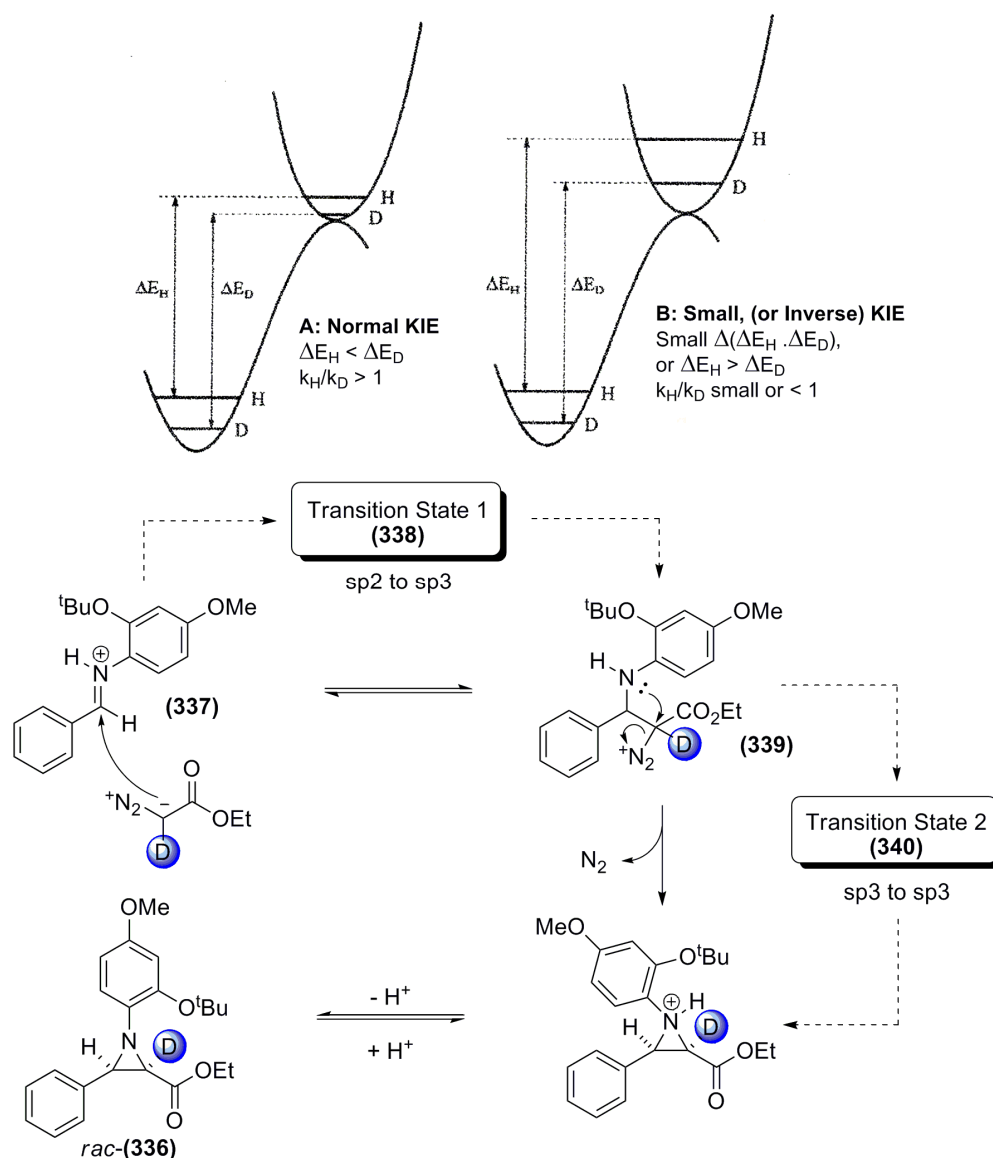


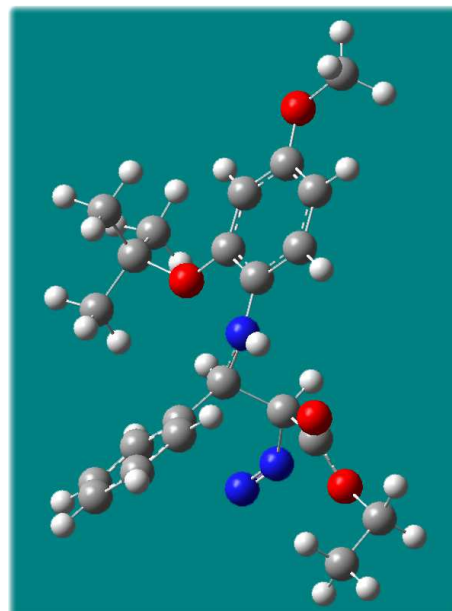
Figure 64: Energy surface diagrams representing the origins of secondary KIE's from changes in ZPE; and representations of the transition states during the formation of *rac*-(336) from which a secondary KIE could arise

Therefore, a very basic prediction as to if the observed loss of reaction rate is due to a secondary KIE can be made if the ZPEs of TS1 (338), and EDA-*d* (334) are calculated. If $\Delta ZPE_{(deutero)}$ is greater than $\Delta ZPE_{(proteo)}$ then the reaction will be slower in the *deutero*-form, due to the increased activation energy of the reaction (*i.e.* a normal KIE). If $\Delta ZPE_{(proteo)}$ is greater than $\Delta ZPE_{(deutero)}$ then an inverse KIE should be in effect. In order to calculate the ZPEs, a transition state minimisation was carried out at the B3LYP/6-31g level of theory within Gaussian '09 for TS1 (338), followed by frequency calculations for both the *proteo*- and *deutero*- forms. It should be noted that this calculation did not include a conformational search, or consider the effects of solvation, it was simply to provide a basic level of understanding. The results are shown in Figure 65.

Structure	ZPE _(proteo) (kJ/mol)	ZPE _(deutero) (kJ/mol)
EDA	275.533	267.209
TS1 (338)	1252.743	1243.567
Δ ZPE (kJ/mol)	977.21	976.358

$$\Delta\text{ZPE}_{(\text{proteo})} > \Delta\text{ZPE}_{(\text{deutero})}$$

Suggests small inverse KIE



3D representation of the Gaussian calculated transition state TS1 (**338**)

Figure 65: Calculated ZPEs for *proteo*- and *deutero*- TS1 (**338**); also *proteo*- and *deutero*- ethyl diazoacetate (**261**) & (**334**)

As shown in Figure 65, the changes in ZPE calculated with Gaussian suggest that a very small inverse secondary KIE may be in effect, which suggests that reaction should be very slightly faster with EDA-*d* (**334**) as opposed to EDA-*h* (**261**). Experimentally however, this was not seen to be the case; thus it can be concluded that either another factor is causing the longer reaction times observed (and potentially masking the inverse KIE), or higher level calculations are required in order to observe the potential normal secondary KIE. However, literature suggests that the presence of an inverse KIE is more likely upon rehybridisation from sp^2 to sp^3 .²⁷⁷

Having successfully synthesised the C2 deuterated aziridine *rac*-(**336**), the racemic one-pot C2-*deutero* aziridination methodology was expanded by the synthesis of aziridines bearing 4-fluorophenyl, 4-bromophenyl, 4-nitrophenyl, and 4-cyanophenyl functionalities upon the C3 position (*rac*-(**341**) – *rac*-(**344**)). These reactions proceeded well, with all complete within 16 hours. The results of these aziridinations are presented in Figure 66.

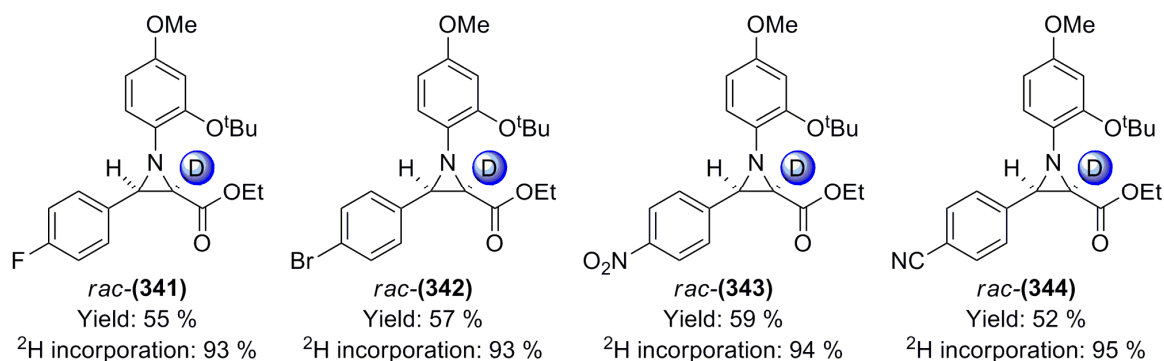


Figure 66: Results for the syntheses of aziridines *rac*-(**341**) to *rac*-(**344**)

As shown in Figure 66, the deuterium incorporation levels within *rac*-(**341**) to *rac*-(**344**) (determined by integration of the C3-*H* to the residual C2-*H* peak within the ¹H-NMR spectra) remained fairly constant throughout the range of aziridines; suggesting that the final level of deuterium incorporation within the product is a measure of the initial incorporation of deuterium within the starting material EDA-*d* (**334**) (*ca.* 93%, Figure 61). Also, experimental error within the determination of deuterium incorporations by ¹H-NMR spectroscopy should be considered. ¹H-NMR integration can be considered to be accurate to within *ca.* 5%, thus an error of ± 5% should be taken into account.²⁷⁸

At this point it was considered prudent to elucidate the *cis*-character of the deuterated aziridines (*rac*-(**340**) – *rac*-(**344**)) produced with the above method. During previous *proteo*-aziridinations utilising the same reaction conditions, only *cis*-aziridines had been formed (4.1.2: *Development of the one-pot procedure*, Scheme 106, Figure 49). This had been proven by the characteristic coupling constants of 5 – 9 Hz of the C2-*H* and C3-*H* peaks within ¹H-NMR spectra of the products.²⁶⁶ In this case however, ¹H-NMR confirmation of the *cis*-conformation of *rac*-(**340**) – *rac*-(**344**) was obtained *via* only the coupling constant of the residual C2-*H* doublet, present within each spectrum. These again were within the expected range of 5 – 9 Hz.²⁶⁶

Further confirmation of the *cis*-relationship about the C2 – C3 positions was sought *via* single-crystal structure analysis. Thus, crystallisation of *rac*-(**340**) – *rac*-(**344**) was attempted. Success was achieved in compound *rac*-(**342**) after crystallisation from 4:1 40 – 60 petroleum ether : diethyl ether, with the crystals obtained as colourless plates. The X-ray crystal structure confirmed the *cis*-relationship around the C2 – C3 positions.

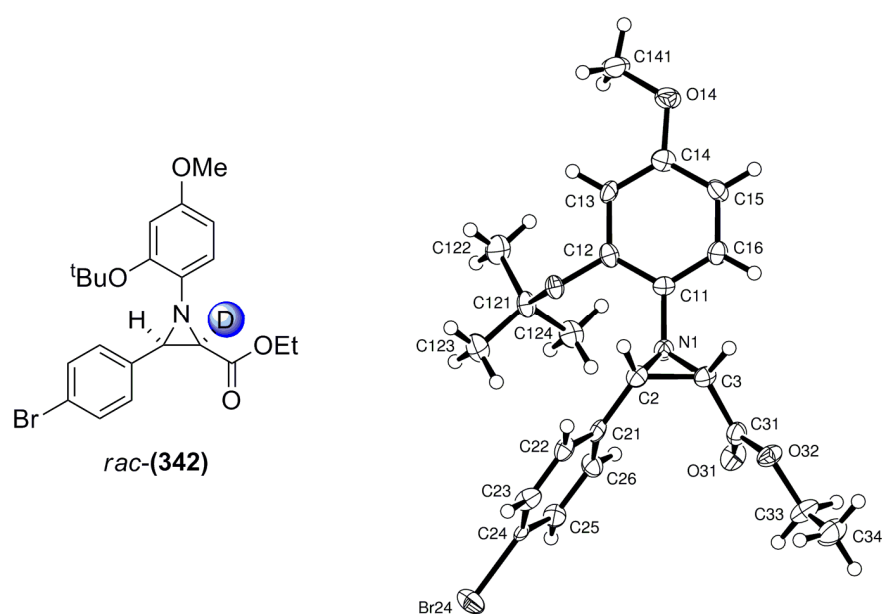


Figure 67: ORTEP representation of the X-ray crystal structure of *rac*-(342**) showing *cis*-stereochemistry around the C2 – C3 positions**

However, confirmation of the deuteration level within *rac*-(**342**) was not possible utilising the crystallographic equipment available at the time. This is due to the structure being acquired using X-ray diffraction, as opposed to neutron scattering. During X-ray diffraction to determine a crystal structure, the diffraction occurs between the X-rays and the electron clouds around individual atoms of a molecule; thus, information upon the isotopes contained within a molecule is not acquired. Neutron scattering occurs due to interactions with nuclei rather than electrons, thus each isotope generates a different interaction with the neutron source. This allows isotopic enrichment to be determined.²⁷⁹ These experiments are only able to be carried out at either nuclear facilities, or particle accelerators (such as the UK National Synchrotron; the Diamond Light Source located at the Harwell Science and Innovation Campus in Oxfordshire).²⁸⁰

5.1.4: Development of Deuteration Techniques – Attempted Deuteration of Pyridinium Triflate

Having demonstrated that the racemic one-pot aziridination protocol was tolerant to the use of EDA-*d* (**334**), it was considered prudent to test for a possible H/D exchange reaction between pyridinium triflate (**279**), and EDA-*d* (**334**); due to the potential decrease in deuterium incorporation within aziridine products if such an exchange reaction was occurring (Figure 68).

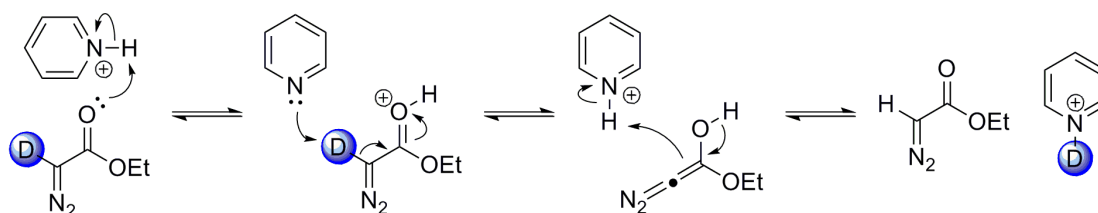


Figure 68: Proposed mechanism of H/D exchange between pyridinium triflate (279**), and EDA-*d* (**334**), leading to decreased deuterium incorporation within EDA-*d* (**334**)**

In order to test the potential for H/D exchange, an NMR experiment was carried out. One equivalent of pyridinium triflate (**279**) was mixed with one equivalent EDA-*d* (**334**) in anhydrous deuterated chloroform (dried over 4 Å molecular sieves); and an initial ¹H-NMR spectrum was recorded. The solution was then stirred within the NMR tube for 36 hours, with ¹H-NMR spectra being acquired at intervals. Integration of the residual CH peak at 4.70 ppm against the known peak for the CH₂ group (4.17 ppm) revealed a reduction in deuterium incorporation upon the EDA-*d* (**334**) from the initial value of *ca.* 99% (Figure 68, Spectra 1); this reduction was equivalent to loss of approximately 15% of the initial deuteration after 36 hours; suggesting gradual equilibration of deuterium between pyridinium triflate and EDA (Figure 69).

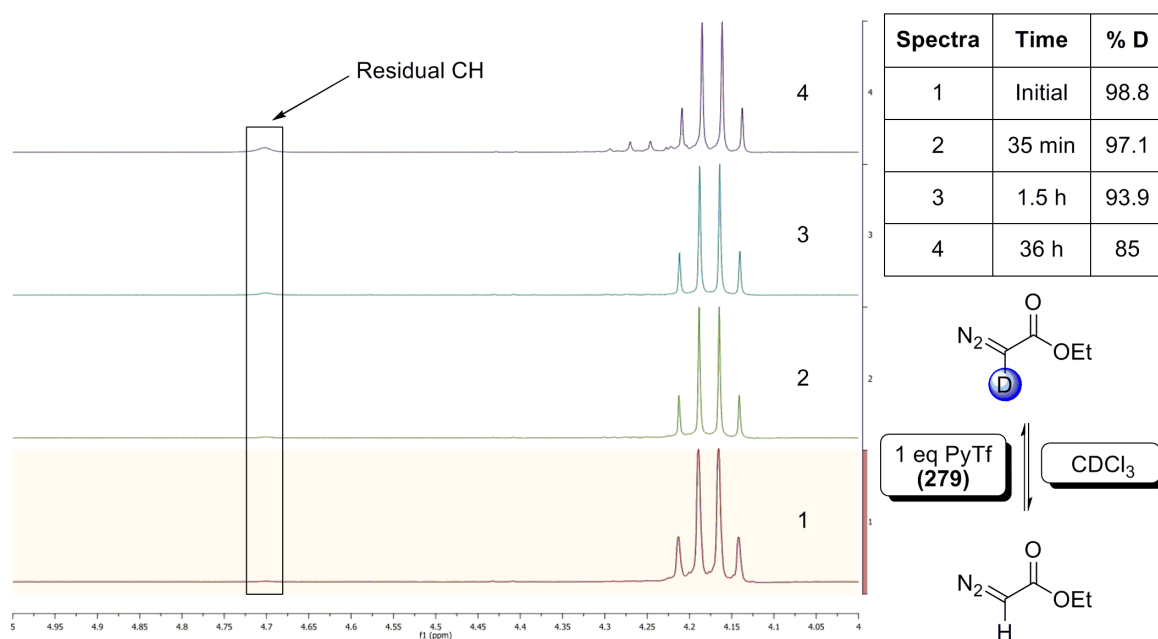
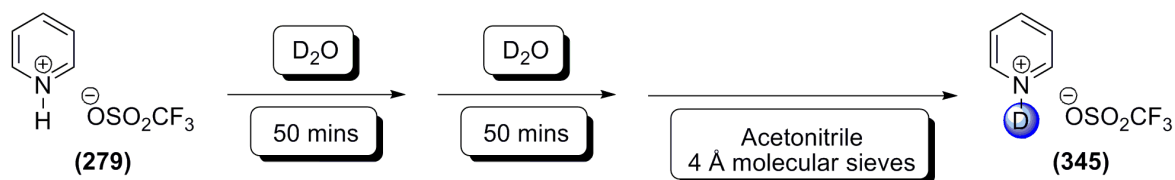


Figure 69: ^1H -NMR experiment to determine if H/D exchange occurs between pyridinium triflate (**279**) and EDA-*d* (**334**)

Although the H/D exchange reaction appears to be slow, this could potentially represent a route for an undesired decrease in deuterium incorporation within the C2-*deutero* aziridines produced using pyridinium triflate (**279**) as the catalyst. Therefore, it was decided to investigate the possibility of producing deuterated pyridinium triflate (PyTf-*d* (**345**)).

To achieve this, freshly prepared, recrystallised, and dried pyridinium triflate was treated under scrupulously dry conditions with deuterium oxide. After 50 minutes stirring, the deuterium oxide was removed under reduced pressure, utilising a nitrogen backfilled rotary evaporator. The resulting solid was treated with a further two cycles of deuterium oxide before redissolving the solid material in freshly distilled acetonitrile, drying over 4Å molecular sieves, filtration, and removal of the solvent. The resulting free flowing solid PyTf-*d* (**345**) was stored under nitrogen in a dry box until it was required (Scheme 127).



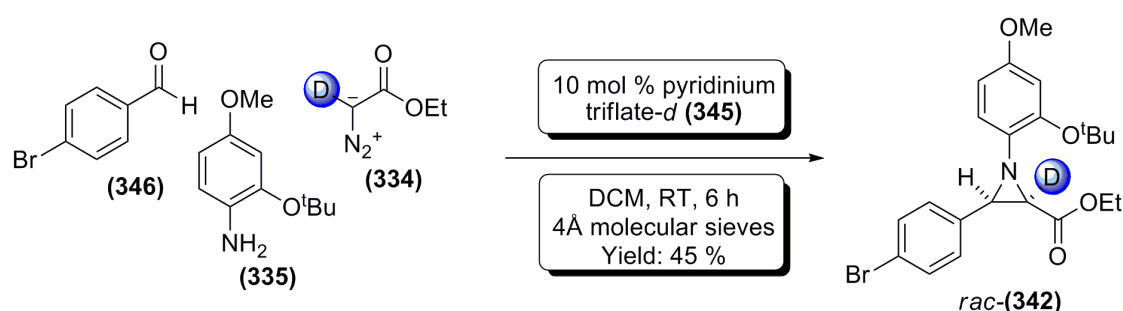
Scheme 127: Attempted deuteration of pyridinium triflate (**279**) to form pyridinium triflate-*d* (**345**)

Analysis of the PyTf-*d* (**345**) was attempted by both LC-MS, and HRMS; however, LC-MS (under ESI conditions) proved inconclusive, due to solvent contamination peaks at low mass present within the background of the spectrum (coming from contamination of the instrument itself). Also, treatment of PyTf-*d* (**345**) under nano electrospray HRMS

conditions was unable to provide conclusive evidence for the presence of deuterated pyridinium triflate; with the predominant ion found at m/z 80.2, consistent with a *proteo*-pyridinium ion. However, due to the acidity of the N-H or N-D bond (pK_a of pyridinium = 3.4 in DMSO)²⁶⁷ it is not unreasonable to envisage H/D exchange under ionising conditions, such as those present in HRMS and MS analysis.

5.1.5: Development of Deuteration Techniques – Test Aziridination to form *rac*-(**342**) Catalysed by Deuterated Pyridinium Triflate (**345**)

Despite the lack of conclusive evidence for the deuteration of pyridinium triflate; it was decided to carry out a simple one-pot *C2-deutero* aziridination in order to test the reactivity of the new catalyst; PyTf-*d* (**345**) (Scheme 128).



Scheme 128: Test aziridination to produce *rac*-(**342**) utilising pyridinium triflate-*d* (**345**)

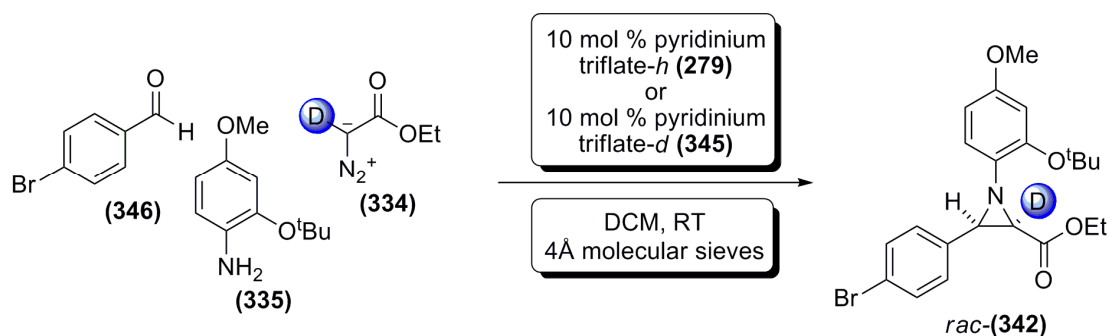
The reaction was seen to proceed by ¹H-NMR, and the resulting purification gave *rac*-(**342**) in a 45% yield after 6 hours. However, subsequent analysis of this product showed no significant change in deuteration level; with deuterium incorporation into *rac*-(**342**) roughly following that of the EDA-*d* (**334**) as noted previously (>90%).

In hindsight, this lack of change in deuteration level is expected, due to the relatively slow rate of H/D exchange noted within the NMR experiment shown in Figure 69 (15% H/D exchange over 36 hours); and also the fact that pyridinium triflate is only present in 10 mol %, rather than the one equivalent present within the NMR experiment. Thus the effects of any exchange reaction between pyridinium triflate and EDA under reaction conditions are likely to be negligible.

Despite this, the deuteration of pyridinium triflate did have one unexpected effect upon the reaction; a significant reduction in reaction rate was noted. After 6 hours, the equivalent formation of *rac*-(**342**) catalysed by PyTf-*h* (**279**) had reached *ca.* 60% yield (opposed to the 45% yield noted above, Scheme 128). Similar to the effect noted when changing from the use of EDA (**261**) to EDA-*d* (**334**), this slowing of the reaction was believed to result from primary kinetic isotope effects, and is examined in more detail below (See 5.1.6: *Determination of a potential primary kinetic isotope effect*).

5.1.6: Development of Deuteration Techniques – Determination of a Potential Primary Kinetic Isotope Effect

During the test aziridination to form *rac*-(**342**) utilising pyridinium triflate-*d* (**345**) as the catalyst, a marked decrease in the rate of reaction was noted. Initially it was thought this could be due to experimental error; however, it was decided to investigate this effect by carrying out two parallel aziridinations, differing only in the use of either pyridinium triflate-*h* (**279**), or pyridinium triflate-*d* (**345**), monitoring each by $^1\text{H-NMR}$ spectroscopy, and calculating a rate for the aziridination reaction.



Scheme 129: The two one-pot aziridination reactions studied within the rate experiment

Two parallel one-pot aziridinations were set up (Scheme 129), and allowed to equilibrate at 25 °C for 30 minutes in order to allow formation of the required imine intermediates. At this stage, EDA-*d* (**334**) was added, and an initial $^1\text{H-NMR}$ spectrum of each reaction was acquired. The reactions were staggered by 10 minutes in order to allow the NMR analysis at similar reaction times. From this point, $^1\text{H-NMR}$ spectra were acquired at hourly intervals.

When the reactions were deemed complete, analysis of the $^1\text{H-NMR}$ data allowed the percentage composition of each reagent at each stage to be calculated (Figure 70). This was achieved by relating the integrations of the aldehyde COH peak (9.92 ppm), the imine CH peak (8.40 ppm), and the aziridine C3 peak (3.35 ppm).

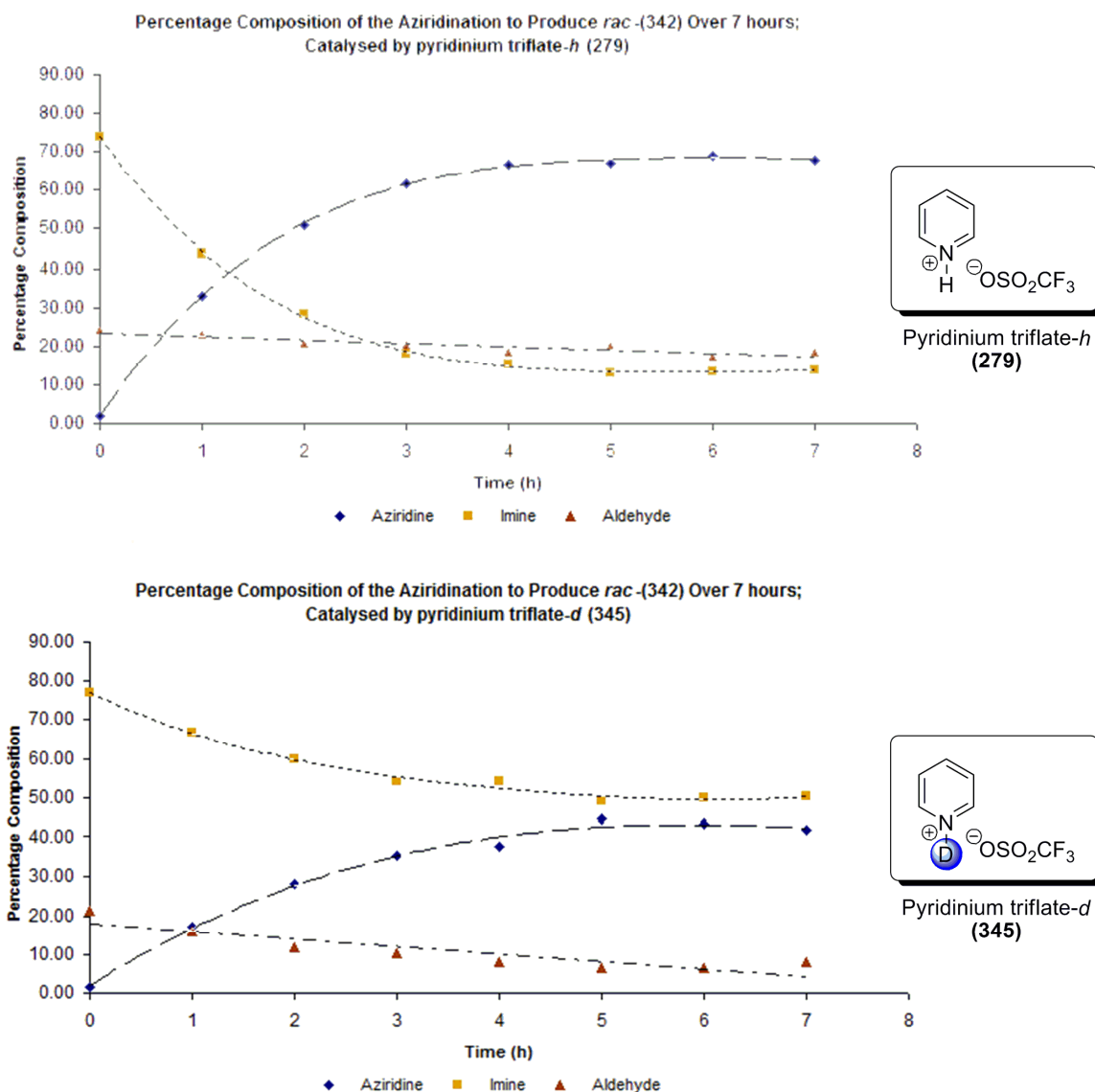
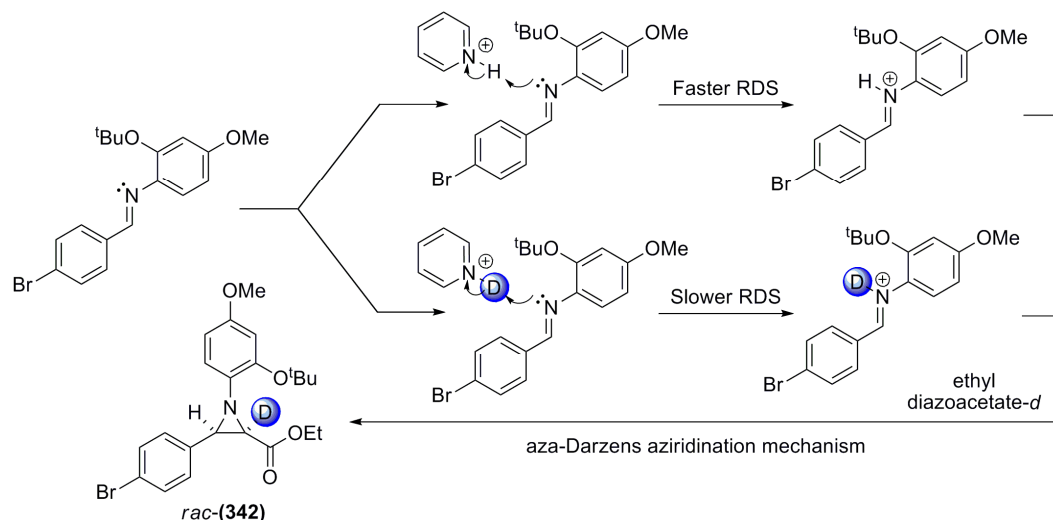


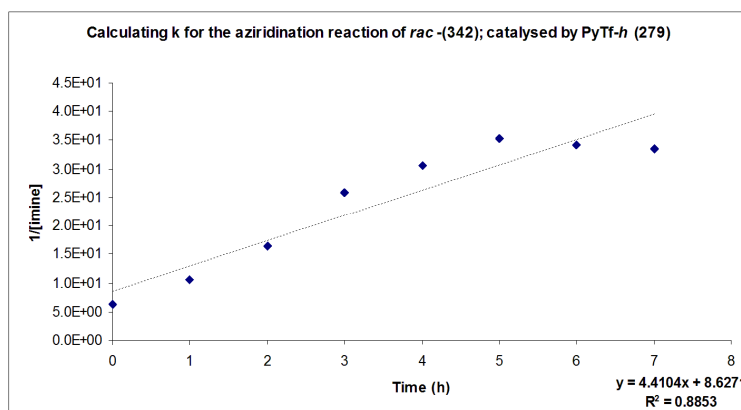
Figure 70: Comparison of the aziridination reactions forming *rac*-(342), catalysed by (279) and (345)

The reaction catalysed by (345) shows a much shallower decrease in the presence of imine, which corresponds to a much shallower increase in the presence of aziridine than that seen in the reaction catalysed by (279). This potentially indicates a slower reaction. In order to confirm this, an estimation of the rate of each reaction was calculated. For the purpose of the rate calculation, it was assumed that the rate of aziridine formation is dependent upon the rate of disappearance of imine (as the alkyl diazoacetate is in excess within the reaction, any potential effects from concentration of this reagent can be discounted), and that the rate determining step is the dissociation of H^+ (or D^+) from the pyridinium triflate, and subsequent protonation of the imine intermediate (Scheme 130).



Scheme 130: Proposed mechanistic rationale for the observed reduction in reaction rate upon use of pyridinium triflate-*d* (345) opposed to pyridinium triflate-*h* (279); an aza-Darzens mechanism for aziridine formation is presumed to be in effect

In order to calculate rate, the concentration of imine within the reaction mixture at each time was required. As the initial amount of aldehyde present within each reaction was known, the concentration of imine at each stage could be calculated from percentage composition (Data shown in Appendix 3). The reciprocal of these concentrations was then plotted against time, and the regression lines of the two data sets gave the rate constant of each reaction (Figure 71).



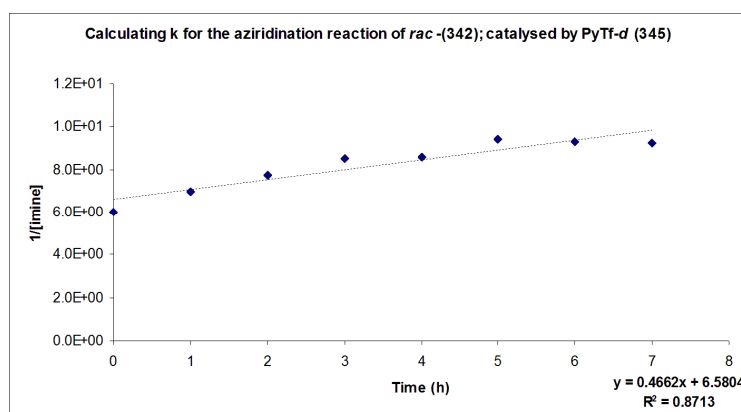
Equation of the regression line:

$$y = kx + c$$

Thus

$$k(h) = 4.41 \text{ mol L}^{-1} \text{ h}^{-1}$$

$$k(d) = 0.47 \text{ mol L}^{-1} \text{ h}^{-1}$$



$$\text{K.I.E.} = k(h)/k(d)$$

Therefore

$$\text{K.I.E.} = 4.41 / 0.47$$

$$\text{K.I.E.} = 9.38 \sim 9$$

Figure 71: Calculation of the rate constants for the PyTf-*h* (279), and PyTf-*d* (345), catalysed formation of *rac*-(342)

From the regression analysis data, an estimate of the kinetic isotope effect within the reaction was calculated. It was noted that the rate of reaction was approximately 9 times slower on changing from pyridinium triflate-*h* (**279**) to pyridinium triflate-*d* (**345**). Although this value is toward the higher end of primary kinetic isotope effects (See 1.4: *Deuterium and the Kinetic Isotope Effect*),²² taking into consideration the inherent potential for error in calculations from NMR data, this value could vary by *ca.* $\pm 5\%$.²⁷⁸ Also, this value is calculated from the overall reduction of reaction rate observed upon the use of pyridinium triflate-*d* (**345**) in the place of pyridinium triflate-*h* (**279**). Thus it is probable that this value includes several primary kinetic isotope effects throughout the reaction mechanism.

Despite these points, literature values for primary kinetic isotope effects relating to acid-base behaviour (*i.e.* the deprotonation of pyridinium triflate, and protonation of the intermediate imine) include the KIE value of 10 calculated for the acid base behaviour of nitroethane (as determined by Wynne-Jones *et al.*),²² and the KIE value of 8.7 for the protonation of (4-methoxy)methylstyrene (as determined by Richard *et al.*),²⁸¹ suggesting that the value of 9 calculated above is feasible.

This experiment clearly demonstrates a significant loss in reaction rate upon the use of deuterated pyridinium triflate as the catalyst for aziridination. This, coupled with the apparent lack of improvement in deuterium incorporation into the product aziridines, led to the conclusion that (**345**) was a less efficient aziridination catalyst than (**279**); thus, efforts were focussed upon improvement of the drying and storage conditions of both pyridinium triflate (**279**), and the deuterated alkyl diazoacetates employed within the *C2-deutero* aziridination chemistry. This is due to it being believed that loss of the deuteration level within the starting material alkyl diazoacetates (due to exchange with either residual water, or atmospheric water vapour) was the greatest issue in keeping deuterium incorporation high within the desired aziridines.

5.1.7: Development of Deuteration Techniques – Initial Development of Asymmetric Deuterated Aziridination Reactions and the Synthesis of *cis*-(**350**)

Having investigated the use of deuterated alkyl diazoacetates in order to form deuterated racemic aziridines; the next step of development was to adapt existing asymmetric, and one-pot asymmetric, aziridination procedures to utilise these substrates.

It was decided to begin development of these syntheses utilising the *N*-triflyl phosphoramidate catalyst (*S*)-(**347**), derivatised at the 3,3'-positions with pyrene; allowing for considerable steric bulk around the 1,1'-binaphthyl scaffold (Figure 72).

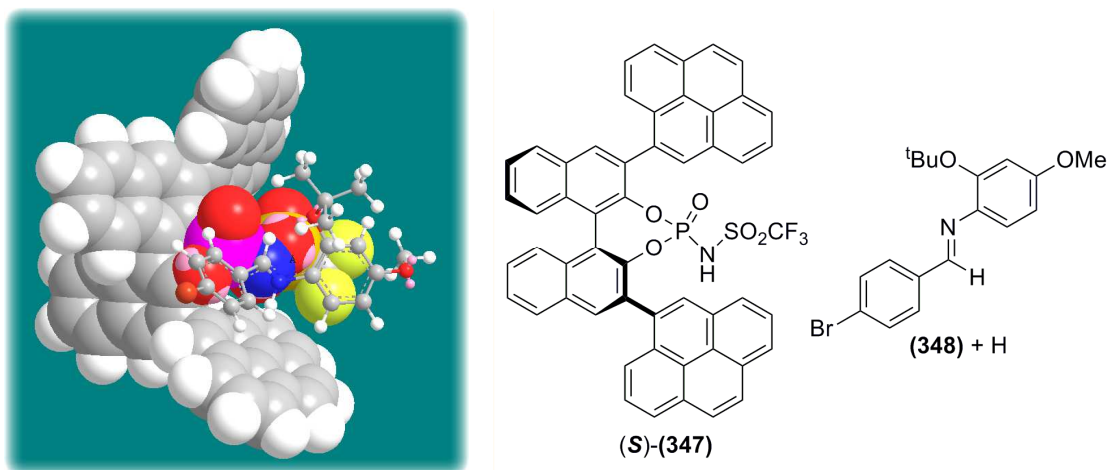
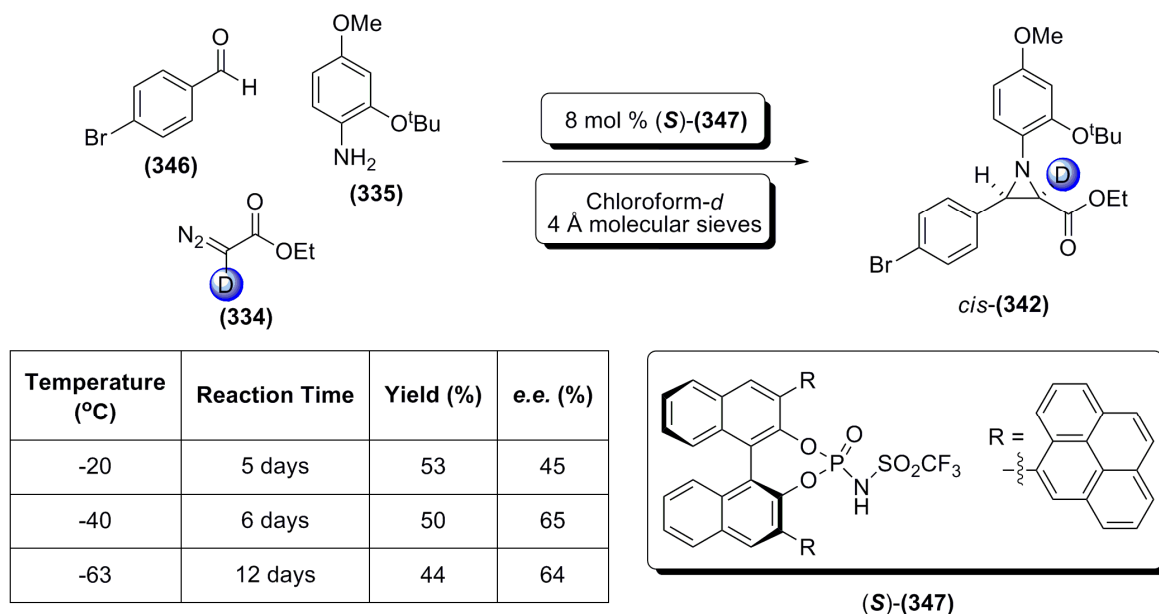


Figure 72: MM2 optimised structure of the protonated form of imine (348) within catalyst (S)-(347), demonstrating the ‘shielding’ effect of the 3,3’-pyrene substitution

As had been shown within the work of Pesce,²⁶⁸ it was hoped that the large, planar pyrene functionalities of (347) would act effectively as lateral ‘shields’ to the protonated imine substrate during the transition state, thus favouring nucleophilic attack from one face only. The MM2 optimised protonated structure of *N*-(4-bromobenzylidene)-2-*tert*-butoxy-4-methoxyaniline (348) within the catalyst (S)-(347) is shown in Figure 72, demonstrating the shielding effect of the pyrene substitution.

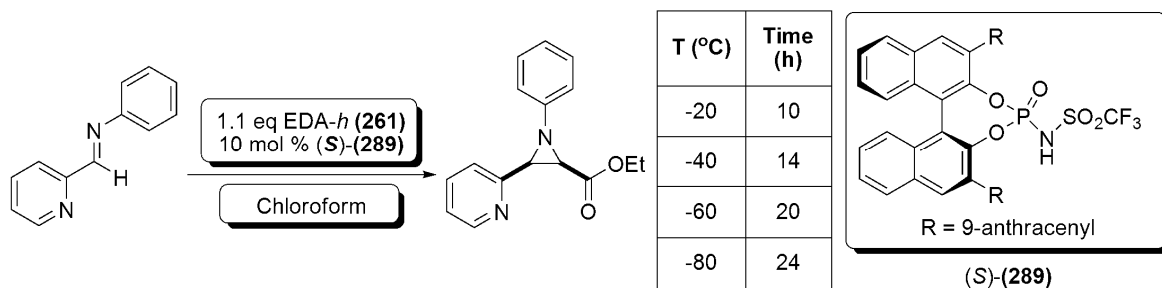
For continuity within these development reactions, it was decided to keep the substrate the same throughout. To this end, it was decided that the synthesis of ethyl 3-(4-bromophenyl)-1-(2-*tert*-butoxy-4-methoxyphenyl)-2-*deutero*aziridine-2-carboxylate (*cis*-(342), see Figure 66) would be employed as the model aziridination system. At this point a desired target for *e.e.* was set to 90%; as high enantioselectivity within the aziridination reaction was considered to be a major aim.

Thus, a temperature variation study was carried out using chloroform as the solvent in order to test the levels of enantioselectivity possible. Deuterated chloroform was chosen due to the effectiveness of chloroform as the solvent within previous asymmetric aziridinations (See 4.3: *One-pot asymmetric aziridinations*, and the work of Pesce),²⁶⁸ while deuterated chloroform allowed monitoring of the reaction by ¹H-NMR spectroscopy. The temperature screen ranged from -20 °C to -63 °C, and the results of this study are shown in Scheme 131.



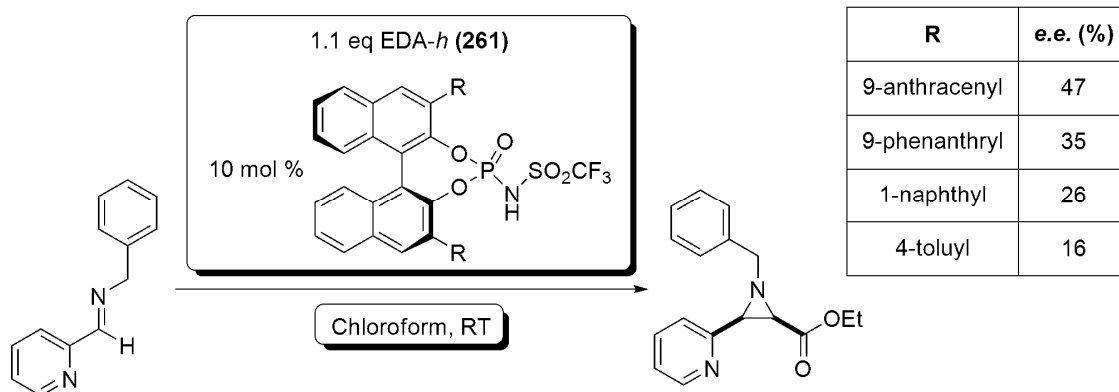
Scheme 131: Initial temperature study for the synthesis of *cis*-(342) utilising (S)-(347)

The study showed that *e.e.* of *cis*-(342) increased from a baseline level of 45% at -20 °C to a maximum of 65% at -40 °C and -63 °C. Unsurprisingly, reduction of the reaction temperature led to significant increases in reaction times, up to a maximum of 12 days at -64 °C. A similar effect had been observed within the thesis work of Pesce, who noted an increase of reaction time from 10 to 24 hours upon decrease of reaction temperature from -20 °C to -80 °C (within the aziridination reaction shown in Scheme 132, utilising the 3,3'-anthracenyl catalyst (S)-(134)).²⁶⁸



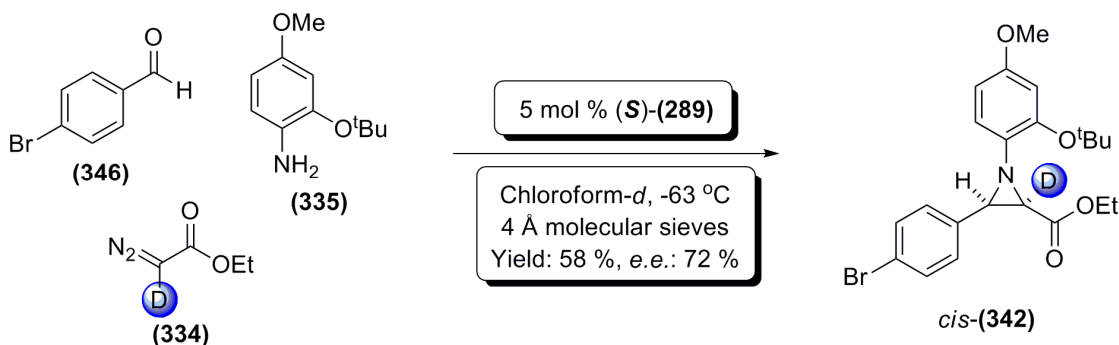
Scheme 132: Temperature study carried out by Pesce upon the aziridination of *N*-(pyridin-2-ylmethylene)aniline, catalysed by the 3,3'-anthracenyl substituted catalyst (S)-(289)

Having investigated various temperatures utilising the pyrene based catalyst (347), unfortunately the desired *e.e.* of 90% had not been achieved. Therefore it was decided to attempt the synthesis of *cis*-(342) utilising the 3,3'-anthracenyl substituted catalyst (289). This choice was based upon the trends seen within the work of Pesce,²⁶⁸ which had shown 9-anthracenyl substitution at the 3,3'-positions of the BINOL scaffold of the catalyst to be generally the most effective substitution for inducing high *e.e.* within the aziridination reactions attempted (Scheme 133).



Scheme 133: Catalyst study carried out by Pesce, demonstrating the effect of altering the 3,3'-substitution of the catalyst species²⁶⁸

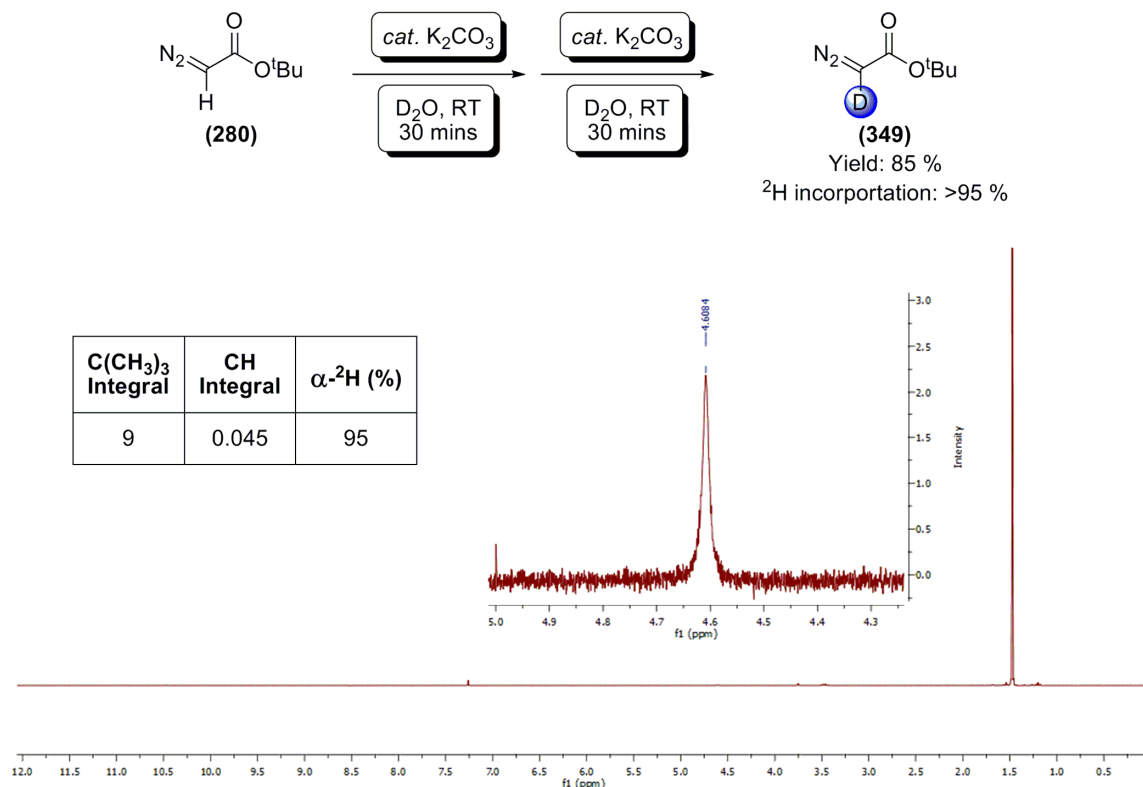
Therefore, a synthesis of *cis*-(**342**) was carried out utilising 5 mol % (*S*)-(**289**) at just below the freezing point of chloroform, -63 °C (as had been employed by Pesce, see Scheme 112).²⁶⁸ The results of this reaction are shown in Scheme 134.



Scheme 134: Test aziridination carried out near the freezing point of chloroform catalysed by (*S*)-(**289**), producing *cis*-(**342**)

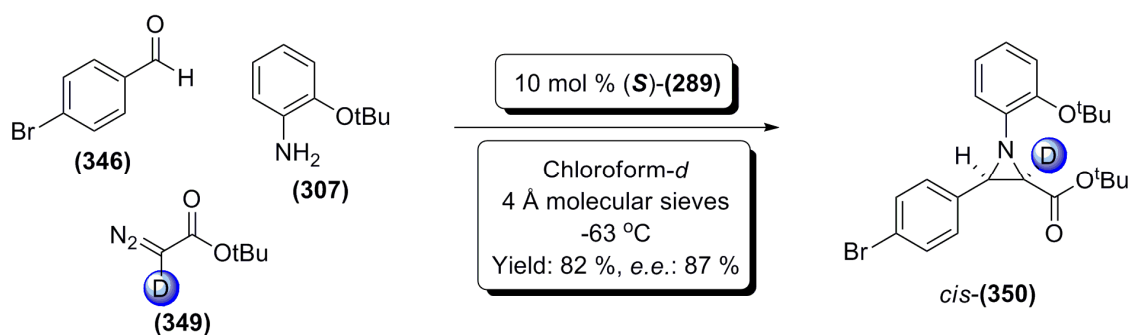
Unfortunately, although the enantioselectivity of this reaction was closer to the desired 90% *e.e.*, a further increase was desired. After re-examining the previous work; it was decided to bring the test aziridine structure more into line with those synthesised previously (See 4.2: *One-pot asymmetric aziridinations*) *i.e.* altering the amine used to 2-*tert*-butoxy aniline (**307**), and the alkyl substitution upon the alkyl diazoacetate to *tert*-butyl.

Therefore, α -deuteration of *tert*-butyl diazoacetate (**280**) was carried out utilising the previously developed procedure (see 5.1.2: *Deuteration of ethyl diazoacetate*, and Scheme 135 below). Gratifyingly, the desired deuterated *tert*-butyl diazoacetate (¹BDA-*d*, (**349**)) was afforded in 85% yield, and more importantly, >95% deuterium incorporation determined by ¹H-NMR spectroscopy (Scheme 134).



Scheme 135: Synthesis of, and ¹H-NMR data for, (349) confirming deuterium incorporation

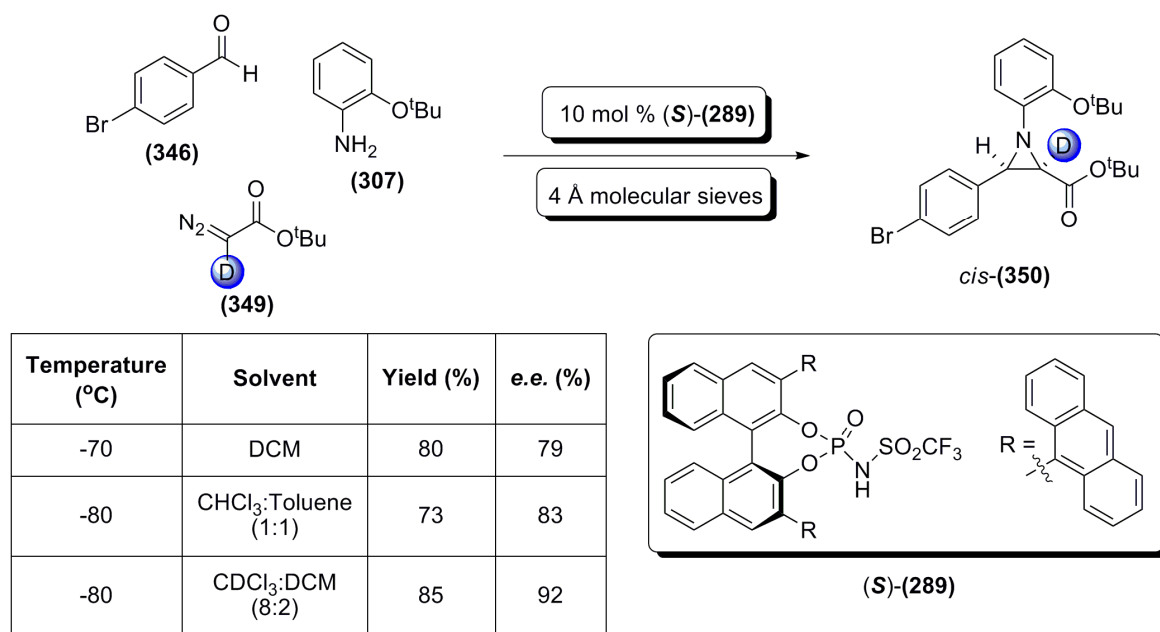
With (349) in hand, the one-pot aziridination reaction of 4-bromobenzaldehyde (346), 2-*tert*-butoxy aniline (307), and ¹BDA-*d* (349) was carried out, utilising 10 mol % (*S*)-(289) with chloroform-*d* as the solvent at -63 °C (Scheme 136). These conditions were chosen based upon the high yields (61 to 93%) and *e.e.s* (74 to 98%) obtained during the asymmetric syntheses of the *proteo*-aziridine-2-carboxylates discussed previously (see 4.2.2: *Asymmetric one-pot aziridinations*).



Scheme 136: One-pot C2-deutero aziridination reaction between 4-bromobenzaldehyde (346), 2-*tert*-butoxy aniline (307), and *tert*-butyl diazoacetate-*d* (349); catalysed by 10 mol % (*S*)-(289)

However, although these conditions afforded *cis*-(350) with a good *e.e.* of 87%, an increase was still desired. Thus, it was decided to alter the reaction solvents in an attempt to gain the required increase in *e.e.*. Solvents for this study were chosen in an attempt to lower the minimum temperature that could be achieved before the freezing point of the

solvent was reached (Scheme 137); while maintaining the presence of solvents which had proven effective within the work of Pesce. Therefore, the use of ethereal solvents was not considered, as these had shown poor compatibility with the aziridination protocols developed by Pesce.²⁶⁸



Scheme 137: Solvent and temperature study utilising catalyst (S)-(289)

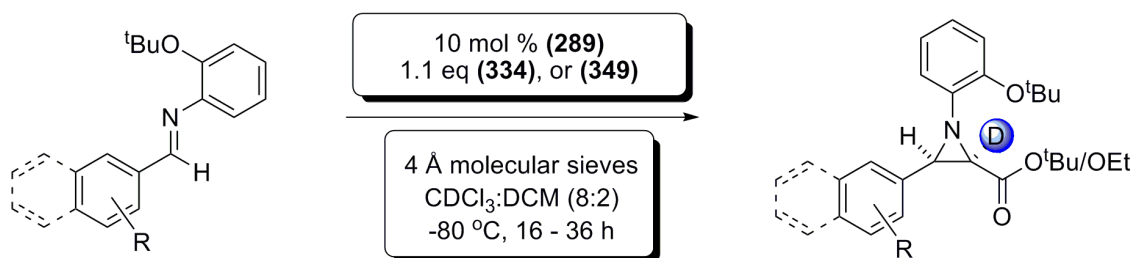
Utilising lower temperatures with differing solvents did not necessarily lead to higher enantioselectivities, as demonstrated in Scheme 137. An interesting case of this being the use of 1:1 chloroform : toluene; which although allowing for a significant decrease in reaction temperature, did not lead to a corresponding increase in enantiomeric excess.

More importantly to the development of the method, the use of an 8:2 mixture of chloroform:dichloromethane allowed for a reaction temperature of -80 °C, a reaction time of *ca.* 72 hours, and an *e.e.* of 92% within the *cis*-(**350**) product. This was not only above the desired target of 90%, but deuterium incorporation within the product was shown to be excellent, measured by ¹H-NMR spectroscopy as >95%. Further evidence for the presence of *cis*-(**350**) was provided by MS and HRMS, with mass ions detected at *m/z* 447.1 [M+H]⁺, and 447.1388 (theoretical 447.1388).

5.2.1: Asymmetric Synthesis of C2-deuterated Aziridines – Introduction

Having satisfied the initial major goal of developing a methodology capable of producing C2 deuterated aziridines in a highly enantioselective manner *via* a one-pot reaction; expansion of the applicability of the asymmetric C2-deutero aziridine synthesis was desired. Thus, substrate screening was carried out for the reaction using pre-formed

imines. Carrying out the reaction in this way allowed the imine formation to be checked for potential reactivity issues before adding in the complications of a one-pot procedure. Therefore, reactions within this section follow the general method shown in Scheme 138.



Scheme 138: General scheme for the synthesis of asymmetric C2 deuterated aziridines

5.2.2: Asymmetric Synthesis of C2-deuterated Aziridines – Synthesis of *cis*-(350) to *cis*-(359), *cis*-(363), and *cis*-(367) to *cis*-(370)

The first substrate screen focussed upon utilising phenyl, *para*-fluorophenyl, and *para*-chlorophenyl substitution at the C3 position. Thus, aziridines *cis*-(351) and *cis*-(352) (Figure 73) were synthesised utilising the asymmetric protocol; however, *cis*-(353) was synthesised utilising a one-pot asymmetric aziridination. It was also decided to repeat the synthesis of *cis*-(350) in order to test for any differences within the reaction outcome when starting from an imine instead of the one-pot procedure. The results of these reactions are shown in Figure 73.

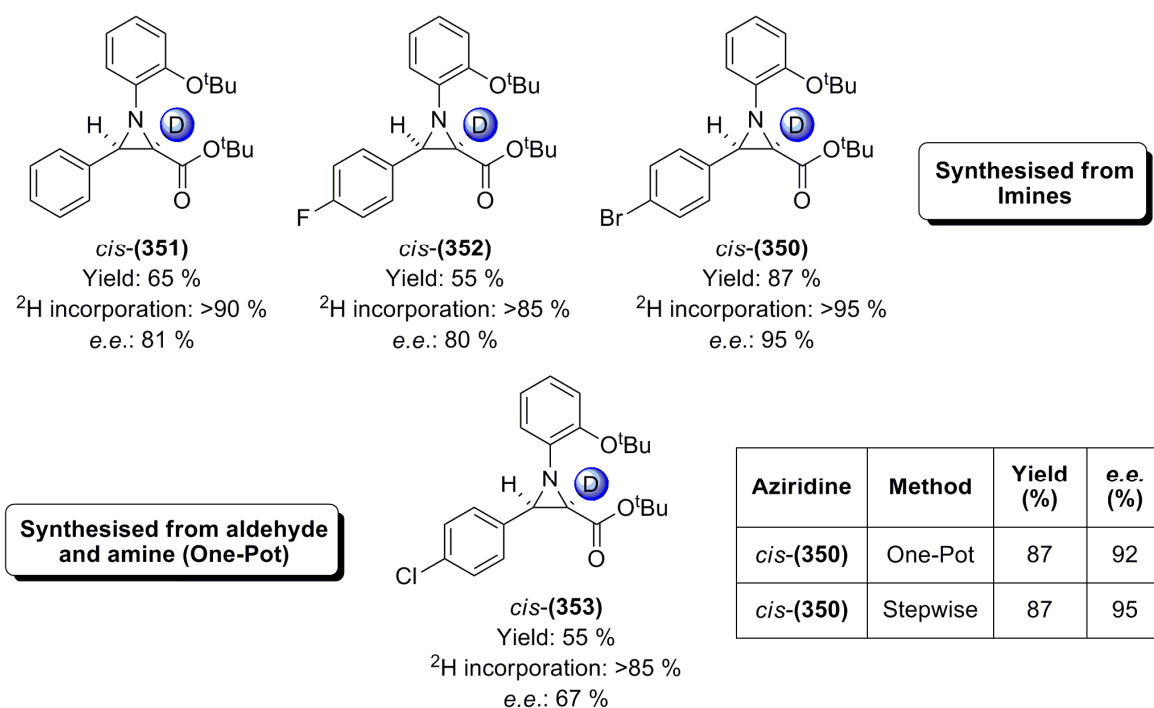


Figure 73: Asymmetric syntheses of C2 deuterated aziridines *cis*-(350) to *cis*-(353)

As shown in Figure 73, these aziridinations proceeded with reasonable yields of between 55% and 87%, and in general, good to excellent *e.e.s* (67 – 95%). A point of

interest is the loss of some deuterium incorporation within the syntheses of *cis*-(**352**) and *cis*-(**353**). It is believed that this came about during the reactions as a result of inadequate initial deuteration of the starting material alkyl diazoacetate.

Interestingly, the repeat synthesis of *cis*-(**350**) from the requisite imine (2-*tert*-butoxy-*N*-(4-bromophenylmethylene)phenylamine) as opposed to a one-pot process led to very similar results. Identical yields of 87% were achieved with the stepwise and one-pot methods, while *e.e.* was seen to slightly improve upon changing from one-pot to a stepwise synthesis. However, the difference in *e.e.* was essentially negligible (*c.a.* 3%).

In order to determine the enantiomeric excess of the above aziridines, chiral HPLC analysis was undertaken, utilising a Chiralpak AD-H chiral column. Determination of the peaks of interest was carried out by running each aziridine against the corresponding racemic aziridine as a standard. Initially, these aziridine standards were deuterated in order to be sure of peak identification. However, racemic aziridines were also synthesised in the *proteo*- form, and it was shown that the desired peaks overlapped well with the *deutero*-versions (Figure 74).

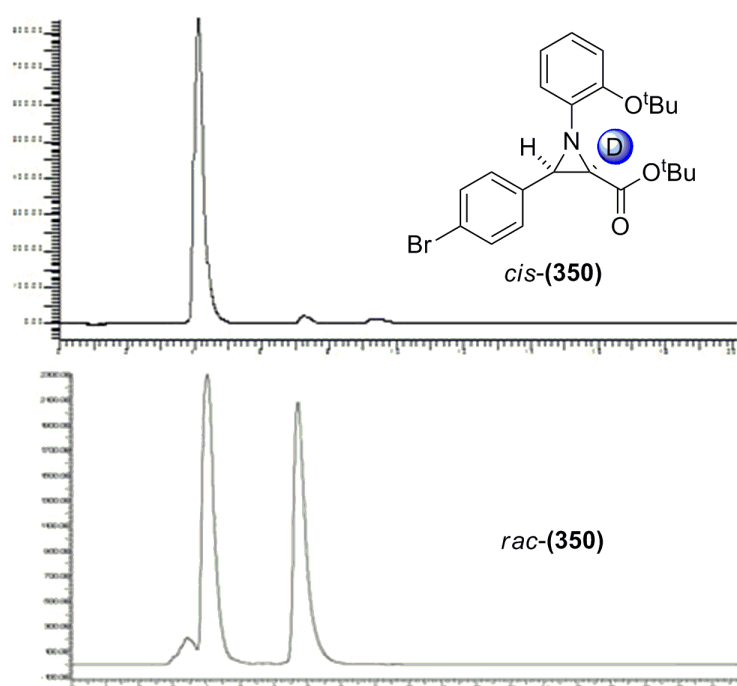


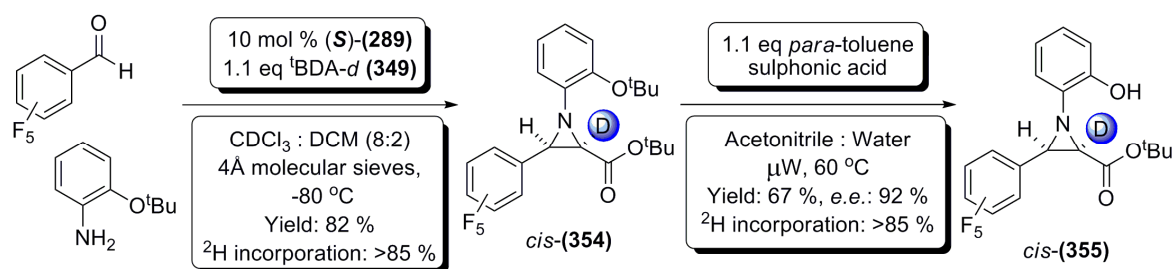
Figure 74: Demonstration of the overlap of peaks within chiral HPLC for *cis*- & *rac*-(350**)**

$^1\text{H-NMR}$, $^{13}\text{C-NMR}$, IR, MS, HRMS, and specific rotation data was collected for each of the above aziridines, with deuterium incorporations being confirmed by $^1\text{H-NMR}$ spectroscopy (*via* integration of the C3-*H* and residual C2-*H* peaks) as well as HRMS analysis. Selected data from the characterisation of *cis*-(**350**) (discussed below) is included in Appendix 4, demonstrating the effects of deuterium incorporation.

Within the $^1\text{H-NMR}$ spectra of *cis*-(**350**), the characteristic doublets for C2-*H* and C3-*H* (expected at 3.02 and 3.39 ppm)²⁶⁸ were no longer present; as would be expected with replacement of the C2-*H* with a deuterium. Instead, a singlet was present at 3.35 ppm, integrating to one proton, consistent with C3-*H*. The *cis*- stereochemistry of (**350**) was confirmed by the coupling constant of the residual C2-*H* doublet (6.9 Hz), which was well within the 5 - 9 Hz range expected with a *cis*- aziridine.²⁶⁶ Examination of the $^{13}\text{C-NMR}$ spectrum of *cis*-(**350**) shows the C2 carbon peak (expected at 47.5 ppm)²⁶⁸ has vanished into the baseline, as was seen with the deuteration of alkyl diazoacetates; due to deuterium coupling splitting the desired peak into three lines, each with one third intensity.²⁷⁶ HRMS data also demonstrates the incorporation of deuterium; with the major peak at 447.1388 corresponding to $[\text{M}+\text{H}]^+$ (theoretical 447.1388), whereas, the peak corresponding to the *proteo*- form of *cis*-(**350**) (m/z 446.1305 $[\text{M}+\text{H}]^+$) is not present within the data, suggesting high deuterium incorporation levels.

Similar effects to those detailed above were also noted in the data acquired for *cis*-(**351**) – *cis*-(**353**), with singlets observed for C3-*H* in the $^1\text{H-NMR}$ spectra. These peaks integrated to 1H, and were found at chemical shifts of 3.43, 3.42, and 3.44 ppm respectively. The residual C2-*H* peaks within the $^1\text{H-NMR}$ spectra of *cis*-(**351**) – *cis*-(**353**) confirmed the *cis*- stereochemistry about the C2 and C3 positions, with $J_{2,3}$ coupling constants of 6.8, 6.7, and 6.7 Hz respectively. HRMS also confirmed the presence of the deuterated products *cis*-(**351**) – *cis*-(**353**), with $[\text{M}+\text{H}]^+$ peaks found at m/z 369.2283 (*cis*-(**351**), theoretical 369.2289), m/z 387.2185 (*cis*-(**352**), theoretical 387.2189), and m/z 403.1889 (*cis*-(**353**), theoretical 403.1893).

Having successfully synthesised monohalogenated C2-deuterated *cis*-aziridines (**350**) – (**353**), it was decided to synthesise a deuterated pentafluorophenyl substituted aziridine *cis*-(**354**) (Scheme 139), similar to *cis*-(**314**) (see Figure 50). As previously it had proven difficult to separate *cis*-(**314**) under chiral HPLC conditions, the *tert*-butyl ester of the aziridine *cis*-(**354**) was cleaved utilising previously discussed methodology (Scheme 116) in order to give the phenolic species *cis*-(**355**) which was more amenable to chiral HPLC analysis.



Scheme 139: Synthesis of *cis*-(354**) and *cis*-(**355**) via a one-pot asymmetric aziridination procedure followed by *tert*-butyl ether cleavage**

Gratifyingly, the desired aziridine *cis*-(**354**), and deprotected aziridine *cis*-(**355**) were produced in yields of 82% and 67% respectively, while deuterium incorporation remained at the >95% level present within the starting material ¹BDA-*d* (**349**) throughout the synthesis. This stability of the isotopic enrichment level was seen to be a critical finding, as it suggests the stability of the C2, and potentially, the C3 positions to isotopic exchange; which was essential if the deuterated aziridines produced were to be employed in further syntheses.

Satisfied thus far with the syntheses attempted, the next set of substrates to be tested were the electron withdrawing substituents *para*-nitrophenyl, and *para*-cyanophenyl. Again starting from the requisite imines (2-*tert*-butoxy-*N*-(4-nitrophenylmethylene)phenylamine, and 2-*tert*-butoxy-*N*-(4-cyanophenylmethylene)phenylamine)), the syntheses of *cis*-(**356**) and *cis*-(**357**) (Figure 75) were attempted utilising 10 mol % (*S*)-(**289**), in 8:2 deuterated chloroform : dichloromethane, at -80 °C. The reactions proceeded well, yielding *cis*-(**356**) in 95%, and *cis*-(**357**) in 65% yields. Enantioselectivities were also high, as shown in Figure 75, with *cis*-(**357**) showing an excellent *e.e.* of 99% when run against a racemic standard by chiral HPLC.

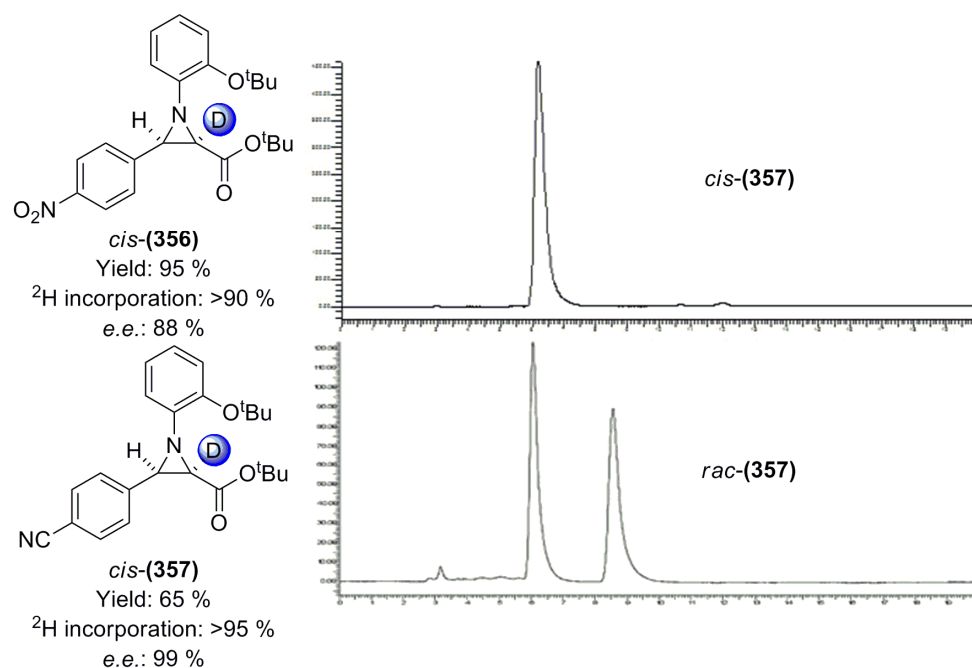


Figure 75: Synthesis results for *cis*-(**356**) and *cis*-(**357**); and chiral HPLC trace for *cis*-(**357**)

It was noted that during column chromatography, *cis*-(**356**) was seen to crystallise from a mixture of diethyl ether and petroleum ether. Therefore, purified *cis*-(**356**) was treated under similar conditions in order to recrystallise the material. The resulting crystals of *cis*-(**356**) were submitted for X-ray analysis, yielding in the crystal structure shown in Figure 76 (Full crystal data shown in Appendix 5). This structure clearly shows the *cis*-relationship of the C2 and C3 substituents of the aziridine. Confirmation of this *cis*-

relationship is important due to the potential difficulties of measuring coupling constants for the residual C2-H doublet within the $^1\text{H-NMR}$ spectra of these deuterated materials. Unfortunately, confirmation of the absolute stereochemistry of the aziridine produced was not provided, as the crystal was shown to be a racemate.

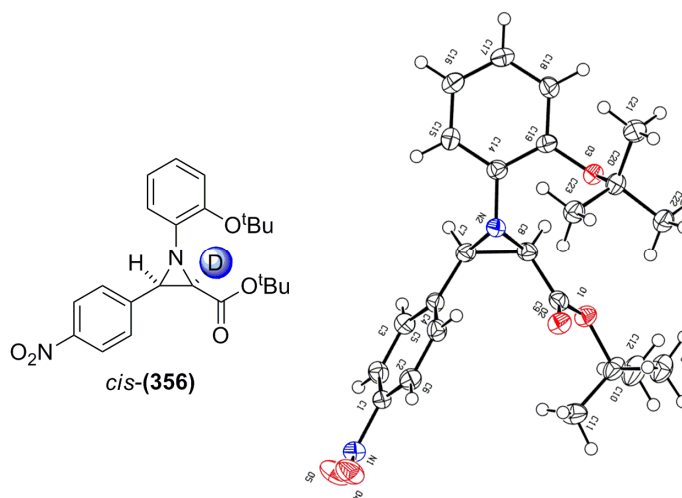
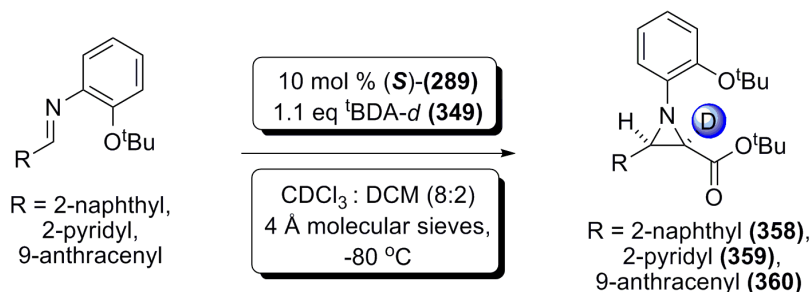


Figure 76: ORTEP representation of the X-ray crystal structure of *cis*-(356)

The next substrates to be tested were heteroaromatic, and polycyclic systems. These being the 2-naphthyl, 2-pyridyl, and 9-anthracenyl based *N*-aryl imines shown in Scheme 140).



Scheme 140: Attempted syntheses of 3-(2-naphthyl), 3-(9-anthracenyl), and 3-(2-pyridyl) functionalised aziridine-2-carboxylates *cis*-(358) to *cis*-(360)

From these three substrates two reactions were successful; with the 2-naphthyl (*cis*-(358)), and 2-pyridyl (*cis*-(359)) derived aziridines being obtained in 85%, and 82% yields respectively. Chiral HPLC analysis of these compounds revealed excellent enantiomeric excesses of 90% and 99% respectively; and excellent deuterium incorporation of >95% (Figure 77).

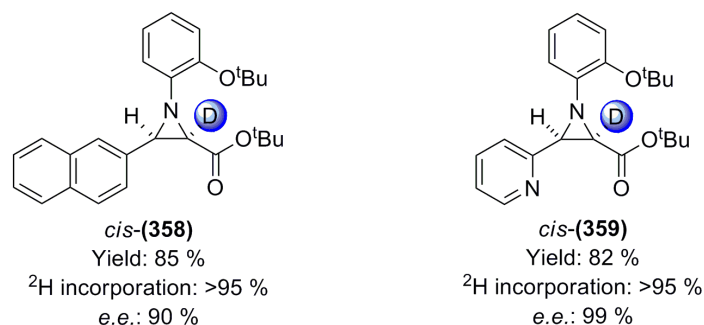
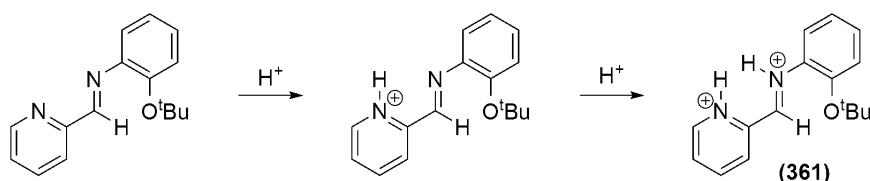


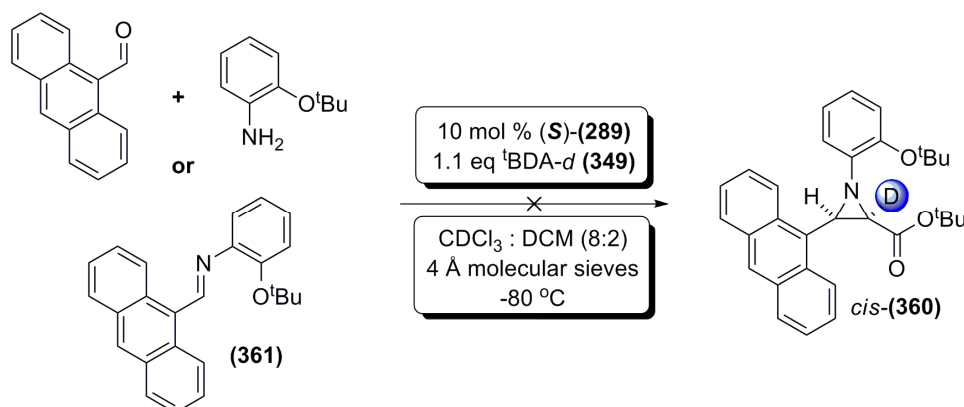
Figure 77: Results of the syntheses of $cis\text{-}(358)$ and $cis\text{-}(359)$ catalysed by 10 mol % (*S*)-(289)** at $-80\text{ }^\circ\text{C}$**

The synthesis of the 3-(2-pyridyl) aziridine-2-carboxylate $cis\text{-}(359)$ proceeded rapidly, with vigorous gas evolution being visible even at the low reaction temperature of $-80\text{ }^\circ\text{C}$. This rate acceleration could be due to protonation of the pyridyl ring leading to the highly reactive intermediate **(361)**, which has more electrophilic character at the imine carbon; thus increasing the rate of attack of the weakly nucleophilic alkyl diazoacetate (Scheme 141). The formation of **(361)** is supported by the relative pK_a values of the imine nitrogen ($pK_a \sim 24$, in DMSO)²⁶⁷, the pyridyl nitrogen ($pK_a \sim 28$, in DMSO)²⁶⁷, and the catalyst **(289)** ($pK_a \sim -1$)¹⁹⁷. These values show that the catalyst **(289)** is acidic enough to protonate both nitrogen positions, with the ring nitrogen protonating first, followed by the imine nitrogen.



Scheme 141: Formation of the dicationic species **(361), potentially leading to accelerated nucleophilic attack by *tert*-butyl diazoacetate-*d* (**349**)**

Unfortunately, the attempted synthesis of the 3-(9-anthryl)aziridine-2-carboxylate **(360)** was unsuccessful, with no aziridination being observed after 72 hours. A repeat of the reaction utilising the one-pot procedure gave the same results, with imine being formed successfully, but no further reaction to the aziridine being observed (Scheme 142).



Scheme 142: Attempted syntheses of the 3-(9-anthryl) substituted aziridine-2-carboxylate $cis\text{-}(360)$

There are two potential reasons for the lack of reaction seen during the attempted synthesis of *cis*-(**360**). The first of these being that free rotation of the anthracenyl group could lead to steric disfavouring of the required angles for nucleophilic attack upon the imine (**361**) (Figure 78), effectively preventing approach of the weakly nucleophilic alkyl diazoacetate (in this case ^tBDA-*d* (**349**)).

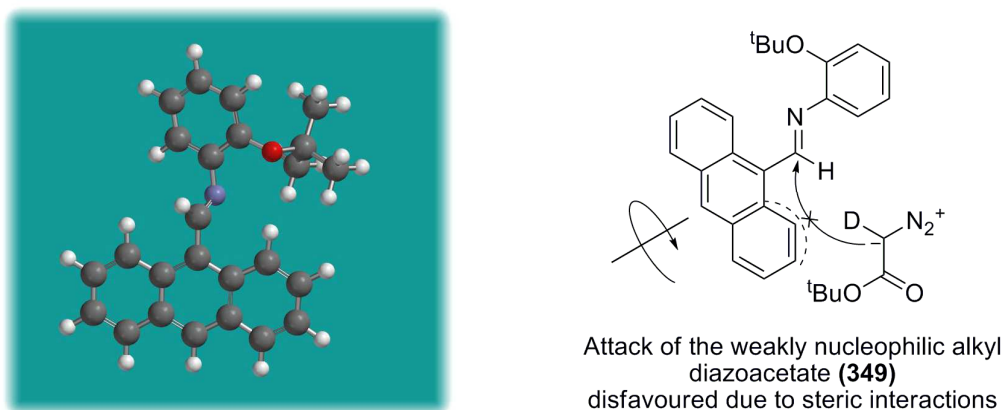


Figure 78: Hartree-Fock optimised structure of the anthracenyl functionalised imine (361**) and representation of the disfavoured nucleophilic attack, due to free rotation of the 9-anthracenyl group**

The second potential reason for the lack of reaction is that the 9-anthracenyl group of the imine (**361**) may be simply too large to be accommodated by the catalyst (*S*)-(**289**). As has been hypothesised previously (See 4.2.4: *Hypothesis upon the enantioselectivity of the asymmetric one-pot aziridination reaction*), substrate imines are believed to be accommodated within the steric ‘shielding’ of the 3,3’-(9-anthracenyl) functionalities of the catalyst (**289**). Thus potentially, if the 9-anthracenyl functionality of the imine (**361**) encounters significant steric interactions with the catalyst, preventing approach, protonation may not occur; resulting in the lack of reaction observed. This potential effect can be shown visually by considering the MM2 minimised structure of catalyst (*S*)-(**289**), showing the ‘shielding’ effect of the 3,3’-(9-anthracenyl) functionalities (Figure 79).

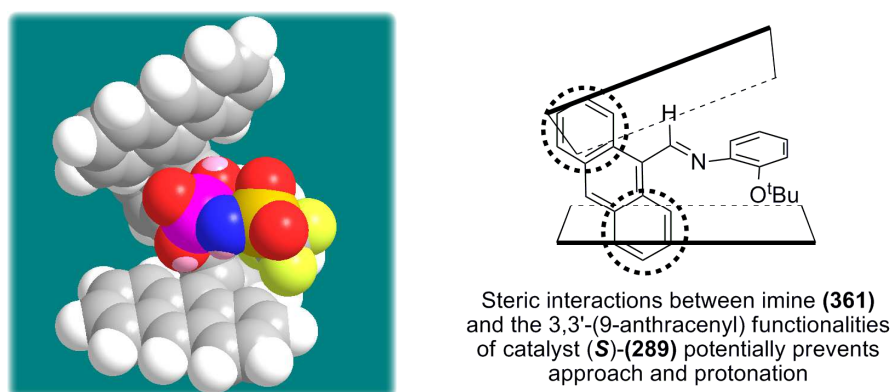
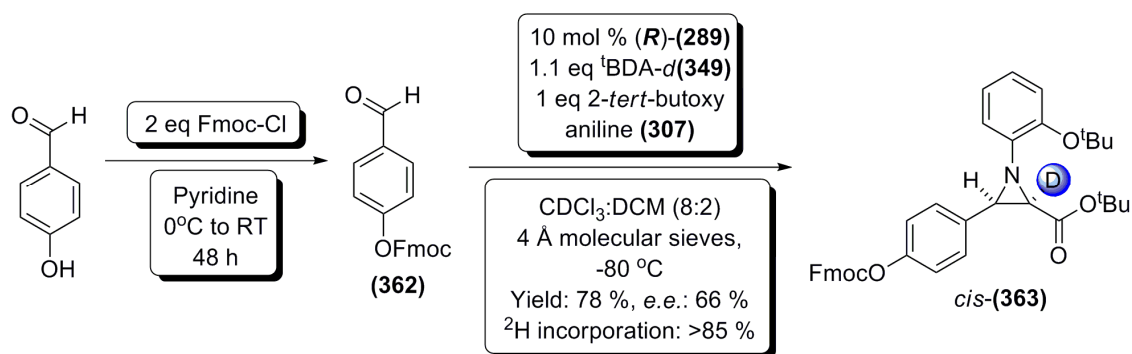


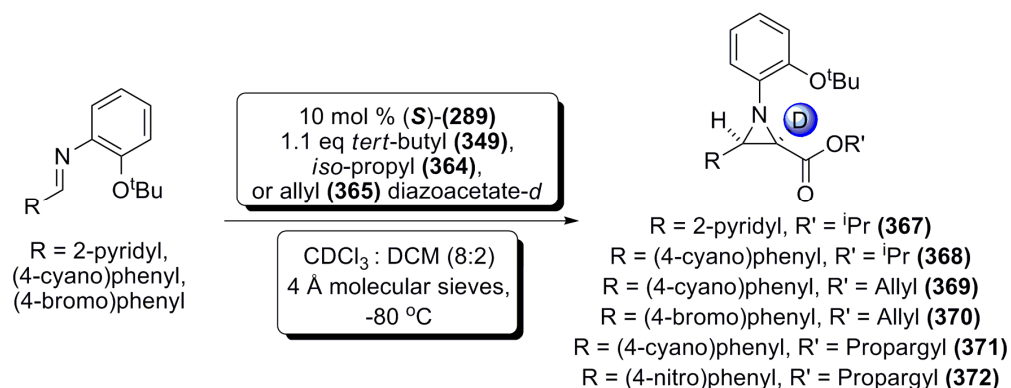
Figure 79: MM2 optimised structure of (*S*)-(289**), and representation of the potential steric interaction of the 9-anthracenyl group of imine (**361**) with the ‘shielding’ 3,3’-(9-anthracenyl) groups of (*S*)-(**289**), potentially preventing approach and protonation**

Having synthesised aromatic, heteroaromatic, *mono*- and *poly*- halogenated, bicyclic, nitro, and cyano functionalised enantioenriched C2 deuterated aziridines, the final C3 functionalisation to be tested was a masked phenolic group. To this end, 4-hydroxybenzaldehyde was reacted with Fmoc chloride in order to produce the masked hydroxy species ((**362**), Scheme 143) in accordance with literature procedures.²⁸² (**362**) was submitted to the asymmetric one-pot C2-*deutero* aziridination procedure, utilising 1 equivalent of 2-*tert*-butoxy aniline (**307**), 1.1 equivalents of ¹BDA-*d* (**349**), and 10 mol % (*R*)-(**289**) at -80 C. The desired aziridine *cis*-(**363**) was obtained in a yield of 78%, with a deuterium incorporation of >85%. Somewhat disappointingly however, the enantiomeric excess of *cis*-(**363**) was shown to be only 66%.



Scheme 143: Synthesis of (**362**) and C2-deuterated aziridine *cis*-(**363**)

As the aziridination reaction that had been developed seemed tolerant to changes upon the C3 substitution, the next logical step was to test the tolerance to C2 substitution; that is, the use of differing deuterated alkyl diazoacetates apart from ¹BDA-*d* (**349**). Therefore, a series of six aziridinations were attempted utilising various alkyl diazoacetates (Scheme 144); these being *iso*-propyl diazoacetate-*d* (¹PrDA-*d* (**364**)), allyl diazoacetate-*d* (**365**), and propargyl diazoacetate-*d* (**366**). ¹PrDA-*d* (**364**) was prepared utilising the same approach as that applied to the synthesis of EDA-*d* (**334**) and ¹BDA-*d* (**349**), that is treatment with excess deuterium oxide, and potassium carbonate (See 5.1.2: *Deuteration of ethyl diazoacetate*); whereas allyl diazoacetate-*d* (**365**) and propargyl diazoacetate-*d* (**366**) were prepared during the work of Bachera which is not included here.²⁸³



Scheme 144: Asymmetric aziridination reactions attempted utilising α -deuterated *iso*-propyl (364), allyl (365), and propargyl (366) diazoacetates

Disappointingly, the reactions attempted utilising (366) were seen not to proceed either at -80 °C, or room temperature. However, reactions with *i*PrDA-*d* (364) and allyl diazoacetate (365) were successful, and the products of these are shown in Figure 80.

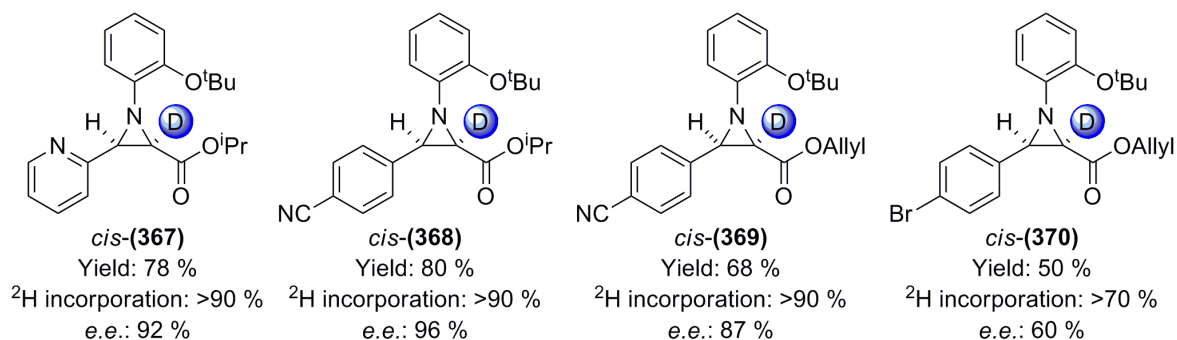


Figure 80: Deuterated aziridines *cis*-(367) to *cis*-(370) synthesised utilising α -deuterated *iso*-propyl (364), and allyl (365), diazoacetates

As shown within these examples, the reaction seems to be tolerant to the structurally diverse alkyl diazoacetates, with good yields (50 – 80%), and good enantiomeric excesses (60 - 96%) achieved. It should be noted that the loss of deuterium incorporation (expected at >90%, found to be >70%), and potentially *e.e.* within *cis*-(370) came about due to experimental error, wherein an *iso*-propanol leak occurred, contaminating the reaction.

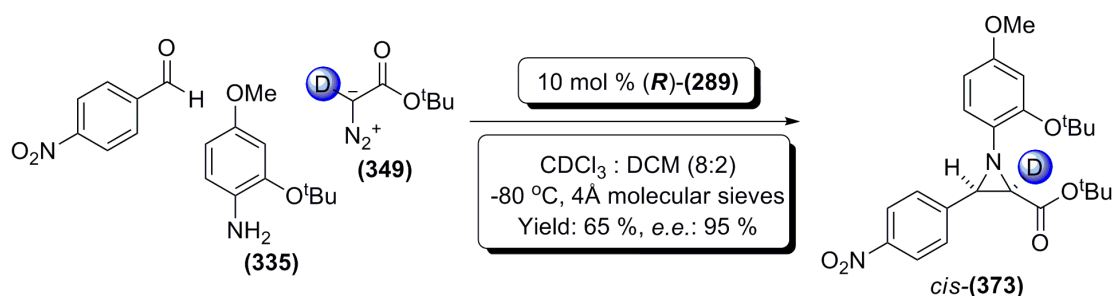
Characterisation of the aziridines shown in Figure 80 was carried out predominantly by ¹H-NMR spectroscopy, ¹³C-NMR spectroscopy, and HRMS analysis. Aziridine formation was confirmed by the presence of the C3-*H* singlet (3.62 ppm *cis*-(367); 3.52 ppm *cis*-(368); 3.49 ppm *cis*-(369); 3.42 ppm *cis*-(370)) within the ¹H-NMR spectra, while integration of these peaks against the residual C2-*H* peaks enabled calculation of the deuterium enrichment levels. The coupling constants of the residual C2-*H* peaks also confirmed the *cis*- stereochemistry of the aziridines, with the coupling

constants being well within the 5 – 9 Hz range expected for a *cis*-aziridine (6.8, 6.6, 6.4, and 6.5 Hz respectively).²⁶⁶

Incorporation of the differing alkyl diazoacetates was confirmed by the characteristic $CH(CH_3)_2$ septet of *iso*-propyl diazoacetate (4.81 ppm *cis*-(**367**); 4.87 ppm *cis*-(**368**)), or the signals for the allyl-*CH* and allyl-*CH*₂ of allyl diazoacetate (5.72-5.56, and 4.49-4.33 ppm respectively within *cis*-(**369**); 5.72-5.58, and 4.50-4.30 ppm respectively within *cis*-(**370**)).

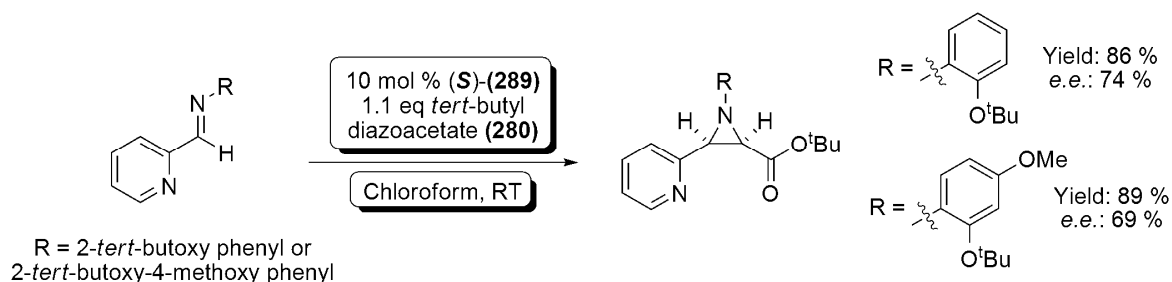
Final confirmation of the synthesis of aziridines *cis*-(**367**) – (**370**) was provided by HRMS, with mass ions being detected at the required *m/z* values (*cis*-(**367**) 356.2082 [M+H]⁺ (theoretical 356.2079); *cis*-(**368**) 380.2079 [M+H]⁺ (theoretical 380.2079); *cis*-(**369**) 378.1923 [M+H]⁺ (theoretical 378.1922); *cis*-(**370**) 431.1 [M+H]⁺ (sample was not sent for HRMS due to low deuterium incorporation, quoted value is for ESI-MS).

Finally, it was decided to attempt a one-pot deuterated asymmetric aziridination utilising 2-*tert*-butoxy-4-methoxy aniline (**335**), 4-nitrobenzaldehyde, and α -deuterated *tert*-butyl diazoacetate (**349**), producing the aziridine *cis*-(**373**). Gratifyingly, the reaction was successful, leading to a good yield of 65%, and an *e.e.* of 95%. (Scheme 145).



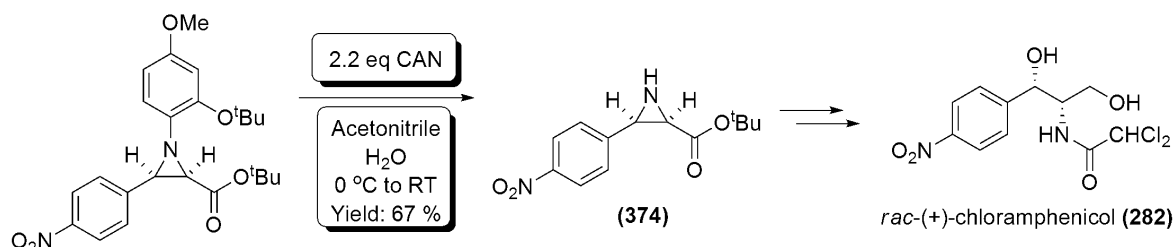
Scheme 145: Synthesis of *N*-substituted aziridine-2-carboxylate ester *cis*-(**373**)

This reaction was designed to test the differences in *e.e.* which occur upon changing the amine substituent within the one-pot reaction; as within the work of Pesce, the use of (**335**) had been shown to reduce the *e.e.* of aziridines it was included within by *ca.* 5% compared to 2-*tert*-butoxy aniline (Scheme 146).²⁶⁸ Thus, the *e.e.* of 95% achieved was unexpected.



Scheme 146: The effect of utilising 2-*tert*-butoxy-4-methoxy aniline in the place of 2-*tert*-butoxy aniline within the asymmetric aziridination work of Pesce

The synthesis of *cis*-(**373**) was also considered important as it had been shown by Bew *et al* that with the inclusion of the *N*-(4-methoxy-2-*tert*-butoxy)phenyl substituent, the subsequent aziridine was amenable to cleavage of the *N*-substitution; thus yielding the NH aziridine product (**374**) (as shown in Scheme 147). This potential cleavage of the *N*-substitution was a critical step in the synthesis of *rac*-(+)-chloramphenicol (**282**) from an aziridine similar to *cis*-(**373**) (Scheme 147).²²⁴

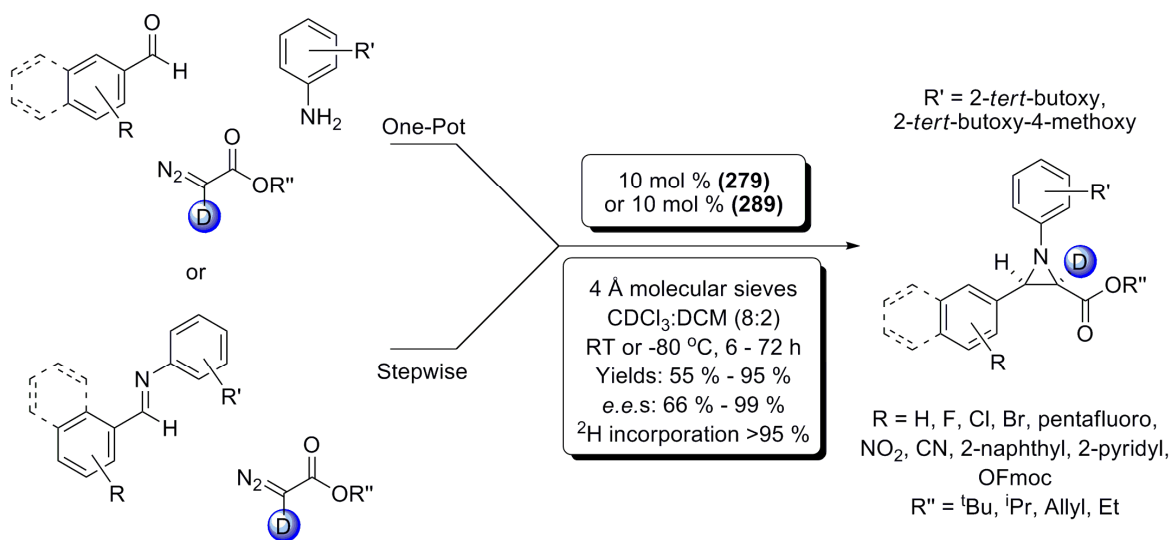


Scheme 147: Synthesis of NH aziridine (374**), and *rac*-(+)-chloramphenicol (**282**) from an aziridine similar to *cis*-(**373**); carried out by Pesce²⁶⁸**

5.2.3: Asymmetric Synthesis of C2-deuterated Aziridines – Summary and Conclusions

In summary, within this chapter the syntheses of various C2 deuterated enantioenriched aziridine-2-carboxylates have been demonstrated. Evidence (including HRMS and ¹H-NMR) has been presented to show high levels of deuteration (in the main >95%). As well as high deuterium incorporations, the enantioselectivity of the reaction is high, with enantiomeric excesses as high as 99% demonstrated (*i.e.* the synthesis of *tert*-butyl 1-(2-*tert*-butoxyphenyl)-3-(pyridin-2-yl)-2-deuteroaziridine-2-carboxylate; *cis*-(**359**)). Also, tolerance for varying substitution on all positions of the aziridine ring has been demonstrated; *i.e.* differing alkyl diazoacetates (ethyl, *tert*-butyl, *iso*-propyl, and allyl), differing amine constituents (*N*-(2-*tert*-butoxy-4-methoxy)phenyl; *N*-(2-*tert*-butoxy)phenyl), and differing starting aldehydes (incorporating aromatic, polycyclic, heteroaromatic, halogenated, and electron withdrawing functionalities).

Within the development of this method, various phenomena have been investigated including the possibility of both primary (5.1.6: *Determination of a potential primary kinetic isotope effect*) and secondary (5.1.3: *Development of deuteration techniques – Initial aziridination reactions*) kinetic isotope effects arising from the use of either deuterated pyridinium triflate, or deuterated alkyl diazoacetates.



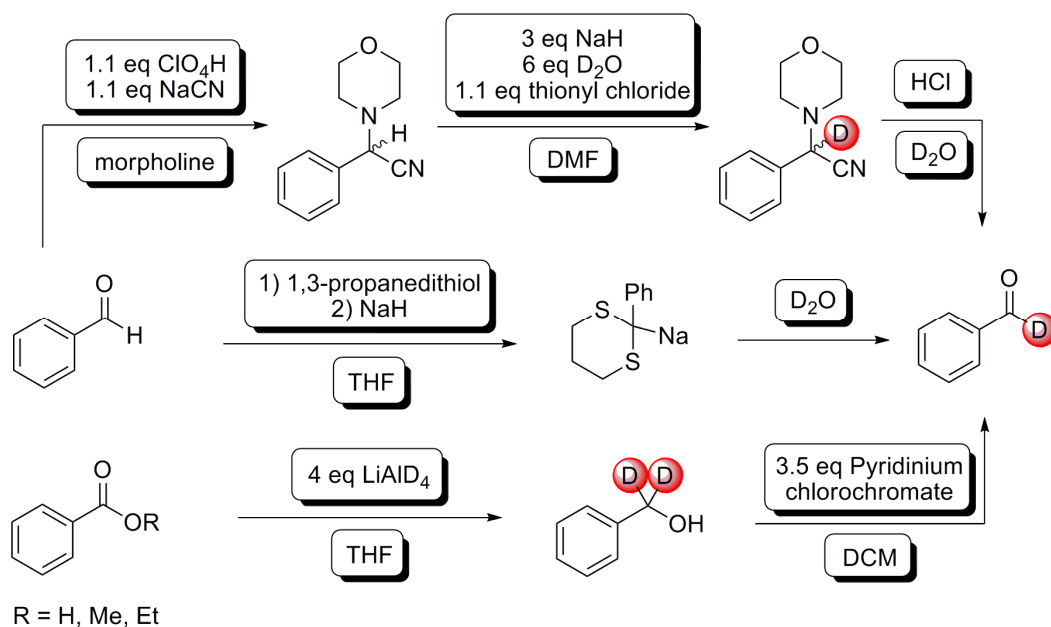
Scheme 148: General scheme for the deuterio aziridination chemistry developed thus far

Logically, the next step of development of the project would be the synthesis of C3 deuterated aziridines utilising the one-pot asymmetric aziridination protocol, and studies towards this goal are included within the following chapter.

Chapter 6: Studies towards the Synthesis of C3- and C2-, C3-deuterated Aziridines

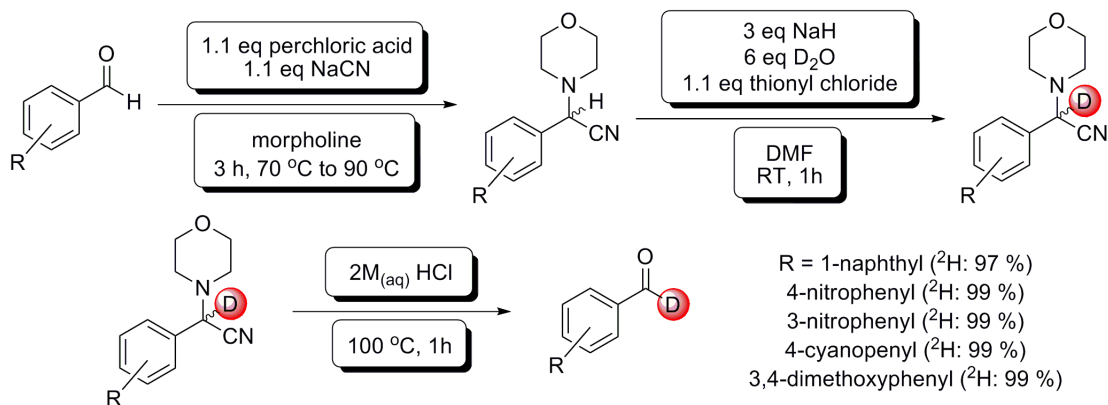
6.1.1: Synthesis of Deuterated Aldehydes – Introduction

In a similar manner to the synthesis of C2-deuterated aziridines, the approach taken to develop C3-deuterated aziridines involved the introduction of deuterium within the synthesis as opposed to the use of H/D exchange onto pre-synthesised aziridines. In order to facilitate this, formyl deuterated benzaldehydes were required. A search of the literature yielded several general methods, utilising readily available starting materials including: reduction of either carboxylic acids or esters, with deuterated lithium aluminium hydride followed by re-oxidation (Fitzpatrick *et al*),²⁸⁴ or formation of an intermediate morpholinoacetonitrile, or dithiane derived species which could be deprotonated and subsequently quenched with deuterium (Kirby *et al*, Chikashita *et al*).^{285,286} These methodologies are summarised in Scheme 149.



Scheme 149: Summary of the general methods within the literature for the production of formyl deuterated benzaldehyde derivatives

The method chosen was based upon the work of Kirby *et al*,²⁸⁵ involving the production of morpholinoacetonitrile species (Scheme 150). This procedure relies upon the ability of the intermediate morpholino species to stabilise a negative charge; allowing deprotonation and quenching with deuterium oxide in order to generate the subsequent deuterated morpholino species, which can then be hydrolysed to afford the desired formyl deuterated aldehyde.

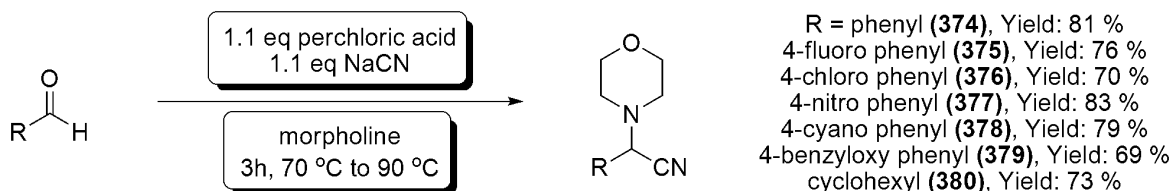


Scheme 150: Synthesis of formyl deuterated aldehydes by Kirby *et al*

This method was chosen as the intermediate morpholino species are crystalline solids allowing easy handling, and may also be stored for extended periods of time. This methodology had also been utilised in recent publications; including the synthesis of ^{15}N -labelled β -deuterated phenylalanine by Curley *et al*,²⁸⁶ which suggested it was a reliable method.

6.1.2: Synthesis of Deuterated Aldehydes – Morpholinoacetonitrile Methodology

As an initial test of the Kirby conditions,²⁸⁵ it was decided to synthesise a range of deuterated benzaldehyde derivatives that had been successfully employed as the *proteo*-form within the asymmetric one-pot aziridination methodology described in Chapter 5. Hence, benzaldehyde, 4-fluorobenzaldehyde, 4-chlorobenzaldehyde, 4-nitrobenzaldehyde, 4-cyanobenzaldehyde, 4-benzyloxybenzaldehyde, and cyclohexylcarbaldehyde were treated according to the methods shown in Scheme 151. During these initial reactions, extreme care was taken due to the procedure requiring the addition of perchloric acid to morpholine. However, it was found that the addition is only mildly exothermic, and no violent reactions were noted.

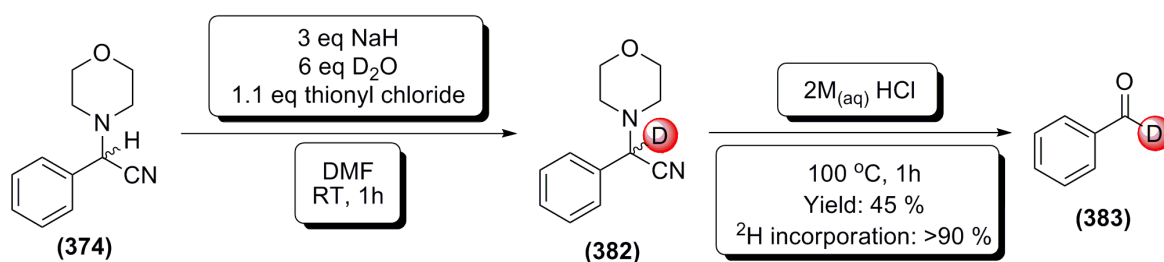


Scheme 151: Synthesis of morpholinoacetonitrile species (374) - (380)

The production of the desired morpholinoacetonitrile species was confirmed predominantly by ^1H -NMR and ^{13}C -NMR spectroscopy, with final confirmation by HRMS. Of particular interest within the ^1H -NMR spectra were the *CH* peaks relating to the central carbon (4.82 ppm (**374**), 4.78 ppm (**375**), 4.78 ppm (**376**), 4.89 ppm (**377**), 4.87 ppm (**378**), 4.75 ppm (**379**), 3.07 ppm (**380**)) as it was loss of this signal which would

indicate deuteration of the morpholino species. As would be expected, the *COH* peaks for each aldehyde starting material were no longer present.

Having synthesised the required precursors (**374**) – (**380**), the deuteration and hydrolysis reactions shown in Scheme 150 were carried out upon 2-morpholino-2-phenyl acetonitrile (**374**) (Scheme 152). The reaction appeared to proceed smoothly, with deuteration being observed by $^1\text{H-NMR}$ spectroscopy (*via* a reduction of intensity of the *CH* peak at 4.82 ppm). However, when hydrolysis of the intermediate (**382**) was attempted, the final yield of formyl deuterated benzaldehyde (**383**) was a disappointing 45%. Despite this, >90% deuterium incorporation by $^1\text{H-NMR}$ spectroscopy was achieved.



Scheme 152: Synthesis of formyl deuterated benzaldehyde (383**), utilising the Kirby *et al* methodology**

6.1.2: Synthesis of Deuterated Aldehydes – Further Comments

Although the above methodology was successful in synthesising deuterated benzaldehyde, results were difficult to obtain in a consistent manner. Yields of all steps of the procedure varied significantly ($\pm 15\%$) with each repeat; in some cases, hydrolysis of the deuterated morpholino species would lead to complete, or partial reversal of the deuteration; leading to recovery of a partially, or fully *proteo*- aldehyde.

At a similar time to this research, further work was ongoing under a similar project within the research group; leading to the availability of deuterated aldehydes in a more reliable manner. Thus, use of the Kirby procedure²⁸⁵ was discontinued, in favour of the deuterated aldehydes produced by the work of Bachera, involving treatment of the desired aldehyde with sodium cyanide, in D₂O, for 5 days.²⁸³

6.2.1: Asymmetric Synthesis of C3-deuterated Aziridines – Introduction

Having demonstrated the synthesis of deuterated benzaldehyde (**383**), and with various deuterated aldehydes available from the work of Bachera,²⁸³ the next step was to attempt the asymmetric synthesis of C3-deuterated aziridine-2-carboxylates utilising the methodology developed in Chapter 5.

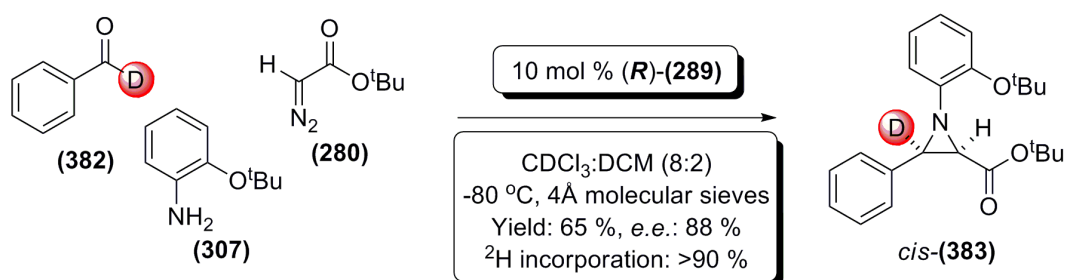
As confidence in the one-pot aziridination methodologies had grown with their further development, it was decided to utilise one-pot procedures in the synthesis of the

following aziridines. One-pot methodology also allowed for minimum exposure of the deuterated aldehyde substrates to air and moisture, in the hope that deuteration levels would remain high within the ongoing synthesis.

At this point, the aim of the project had been extended into development of the one-pot aziridination and deuteration techniques in order to enable a ‘dialled in’ approach to aziridine synthesis (Appendix 7). *i.e.* selective incorporation of deuterium at the C2 or C3 positions in high levels could be chosen (or ‘dialled in’) *via* use of either deuterated aldehydes or alkyl diazoacetates; along with selectivity of enantioenrichment, with enantiomers able to be selectable *via* the use of either the (*S*)- or (*R*)- enantiomers of the catalyst (**289**).

6.2.2: Asymmetric Synthesis of C3-deuterated Aziridines – Synthesis of aziridines *cis*-(**383**) to *cis*-(**388**), *cis*-(**392**) to *cis*-(**393**), and *cis*-(**398**) to *cis*-(**399**)

The first reaction attempted within this group was the one-pot asymmetric C3-*deutero* aziridination of benzaldehyde-*d* (**382**) with 2-*tert*-butoxy aniline (**307**), and ¹BDA (**280**). The results of this reaction are shown in Scheme 153.



Scheme 153: One-pot asymmetric synthesis of C3 deuterated aziridine *cis*-(383**)**

The reaction proceeded as expected, yielding the desired aziridine *cis*-(**383**) in a yield of 65% and *e.e.* of 88%. Further to this, subsequent ¹H-NMR spectroscopic analysis revealed the C3-deuterium incorporation to be >90%. The ¹H-NMR spectrum is shown in Figure 81, and it can clearly be seen that the doublet for C3-*H* (expected at 3.43 ppm) has been suppressed. A comparison with the ¹H-NMR spectrum of the C2-*deutero* aziridine *cis*-(**351**) shows that the singlet remaining for the aziridine ring hydrogen atom switches position between those expected for C3-*H* (3.43 ppm) and C2-*H* (2.97 ppm), depending upon which position is deuterated, as would be expected.

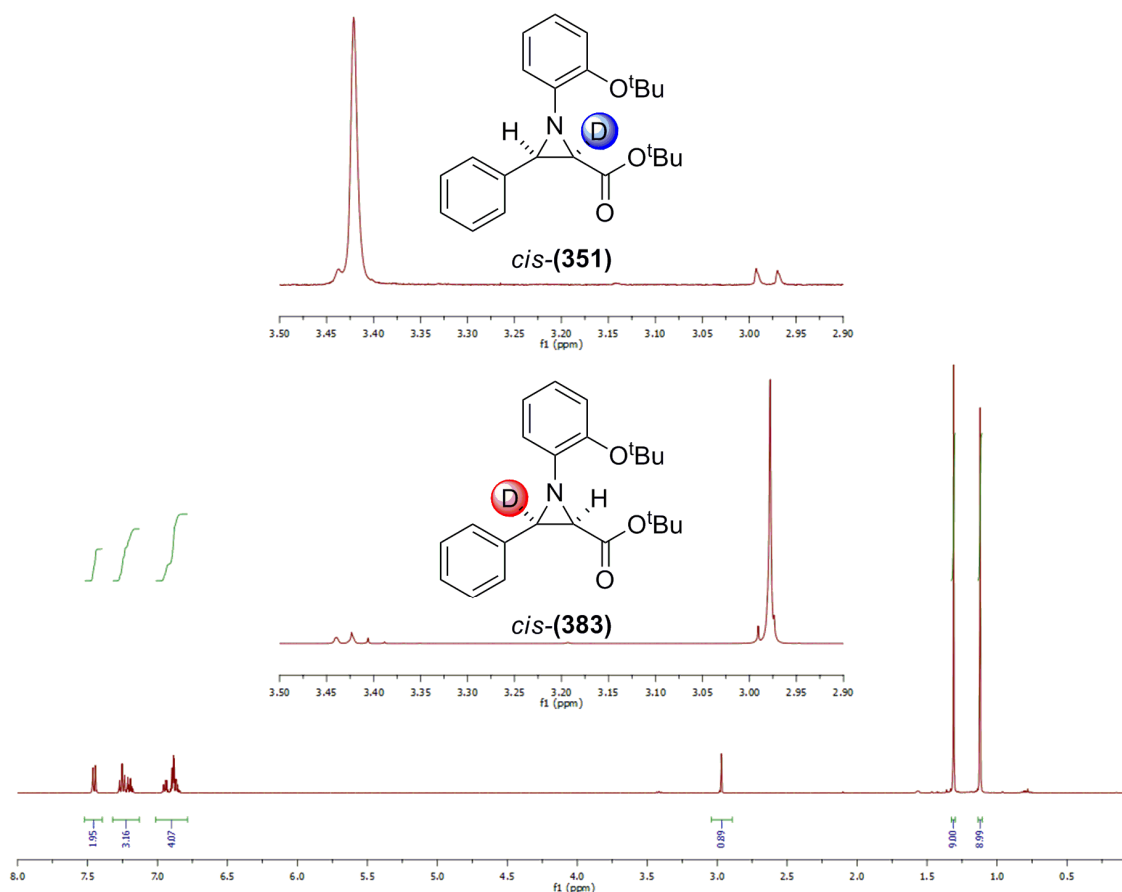


Figure 81: $^1\text{H-NMR}$ data for *cis*-(**383**), and comparison of the C2-*H*, and C3-*H* singlets present within the $^1\text{H-NMR}$ spectra of *cis*-(**351**) and *cis*-(**383**)

A further point of interest within the $^1\text{H-NMR}$ spectrum of *cis*-(**383**) was the coupling constant of the residual C3-*H* doublet, this being 6.6 Hz. This value is within the range of expected vicinal coupling constants for a *cis*-aziridine (5 – 9 Hz),²⁶⁶ and also offers good correlation with the *proteo*- version of *cis*-(**222**) synthesised by Pesce ($J_{2,3} = 6.7$ Hz),²⁶⁸ confirming the *cis*- stereoselectivity of the reaction.

Having demonstrated the one-pot asymmetric synthesis of a C3-deuterated aziridine, the next step was to test the tolerance of the procedure to differing C3 substitution. To this end, aziridines *cis*-(**384**) to *cis*-(**388**) were synthesised (under the conditions shown in Scheme 153) utilising halogenated deuterated aldehydes 4-fluorobenzaldehyde-*d*, 4-bromobenzaldehyde-*d*, 4-chlorobenzaldehyde-*d*, 3-chlorobenzaldehyde-*d*, and 2-chlorobenzaldehyde-*d*. The results of these are shown in Figure 82.

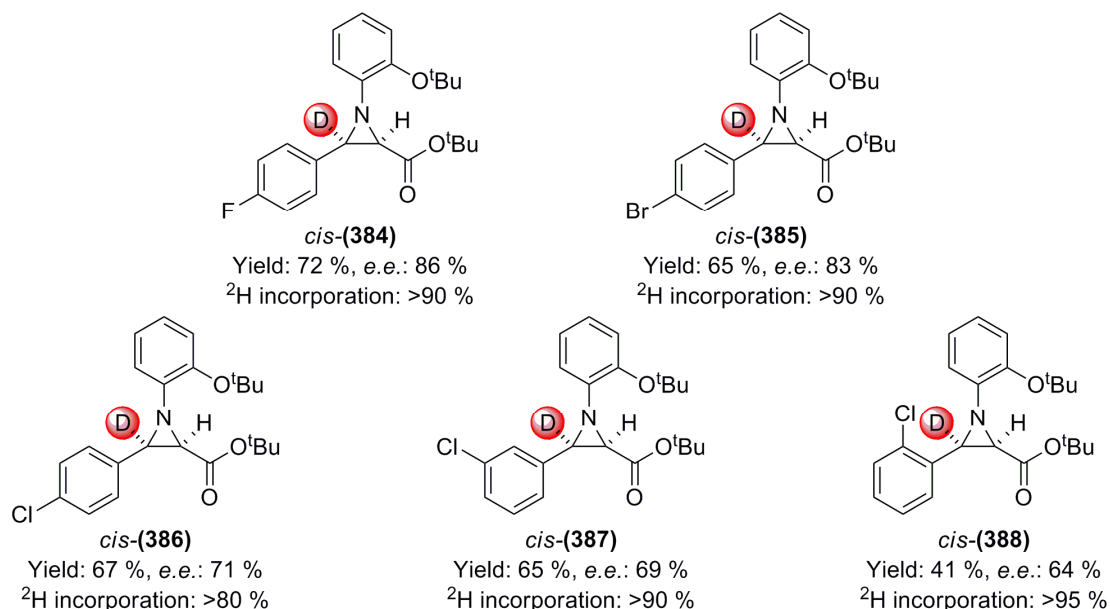


Figure 82: Halogenated C3-deuterated aziridines *cis*-(384) to *cis*-(388)

As can be seen from the yields and enantioselectivities shown in Figure 82, some substrates performed better than others, with *cis*-(384) and *cis*-(388) providing the best overall results, with yields of 72% and 65% respectively, and high *e.e.s* of 86% and 83%. Deuterium incorporation was universally high among the set, in the main being a conservative >90% obtained by integration of the C2-*H* singlet peak present within the ^1H -NMR spectra of *cis*-(384) – *cis*-(388) (found at 3.03, 3.04, 3.01, 3.05, and 3.08 ppm respectively) against the residual C3-*H* doublet. The coupling constants of the residual C3-*H* doublet also confirmed the *cis*-stereochemistry of the C2 and C3 substitution in *cis*-(384) – *cis*-(388), with coupling constants of 6.5, 6.8, 6.7, 6.8, and 6.7 Hz respectively.

The formation of the desired aziridines *cis*-(384) – *cis*-(388), and the presence of deuterium within the structures was also confirmed by HRMS; with $[\text{M}+\text{H}]^+$ ions being detected for each product at the required *m/z* (*cis*-(384) 387.2192; *cis*-(385) 447.1391; *cis*-(386) 403.1889; *cis*-(387) 403.1893; *cis*-(388) 403.1894).

Having synthesised halogenated C3-deuterated aziridines, the next set of substrates to be attempted were those bearing C3-electron withdrawing substituents. To this end, *cis*-(392) and *cis*-(393) were synthesised utilising 4-nitrobenzaldehyde-*d*, and 4-cyanobenzaldehyde-*d*.

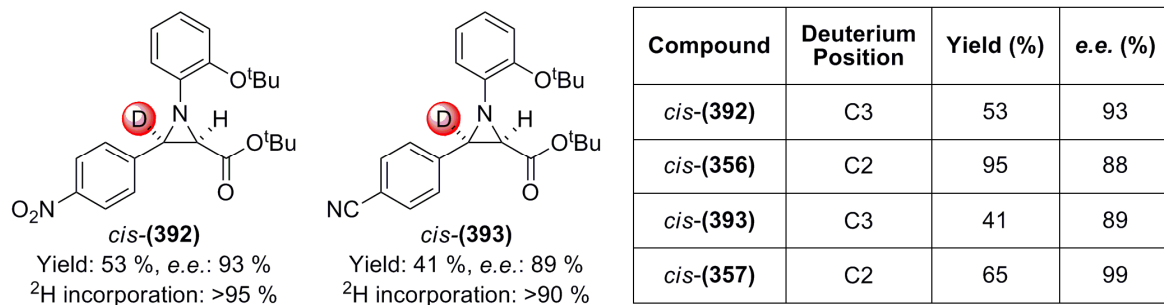


Figure 83: Syntheses of C3-deutero aziridines *cis*-(392**) and *cis*-(**393**) bearing C3 electron withdrawing substituents**

As shown in Figure 83, *cis*-(**392**) and *cis*-(**393**) were produced in moderate yields of 53% and 41% respectively, with very good enantioselectivity observed (93% and 89% *e.e.* respectively). More relevantly to the project, deuterium was incorporated at the C3 position in enrichment levels of >95% and >90% respectively, as determined by ¹H-NMR spectroscopy; which also confirmed the *cis*-stereochemistry of aziridines *cis*-(**392**) and *cis*-(**393**), with coupling constants for the residual C3-*H* doublets being 6.2 and 6.7 Hz respectively; well within the 5 – 9 Hz range expected for a *cis*-aziridine.²⁶⁶

It was noted at this stage that both yields and the achieved enantioselectivities of the aziridines produced appeared to be lower than the corresponding C2 deuterated aziridines produced *vide supra*. The decrease in yield could be brought about as a result of slower reactions due to a secondary kinetic isotope effect during imine formation.

Secondary KIE in this case would come about as a result of changes in the Zero Point Energy of the relevant transition state, arising from differences in the vibrational frequency of the formyl C-D or C-H bond. These differences become significant upon changing the hybridisation of the C-H or C-D bond. Thus, the relevant transition states within imine formation are the initial nucleophilic attack of the amine upon the aldehyde carbonyl, and the elimination of water to form the imine (Figure 84).

In order to provide evidence for this potential secondary KIE, Gaussian calculations of the relevant transition states resulting from the reaction of 4-cyanobenzaldehyde with 2-*tert*-butoxy aniline (**307**) were carried out (Figure 85). This allowed calculation of the vibrational frequencies of the formyl C-H and C-D bonds during the transition states TS1 (**394**) and TS2 (**395**), and thus calculation of the differences in Zero Point Energy between the *proteo*- and *deutero*- forms.

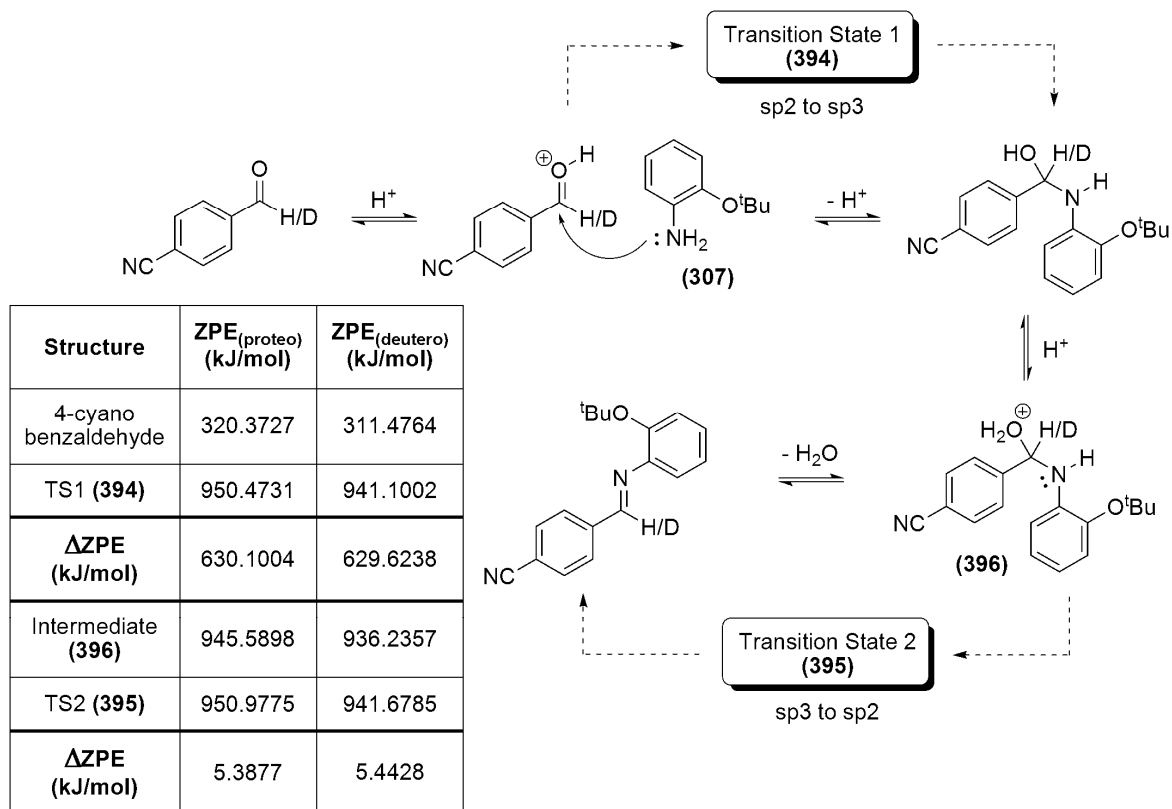
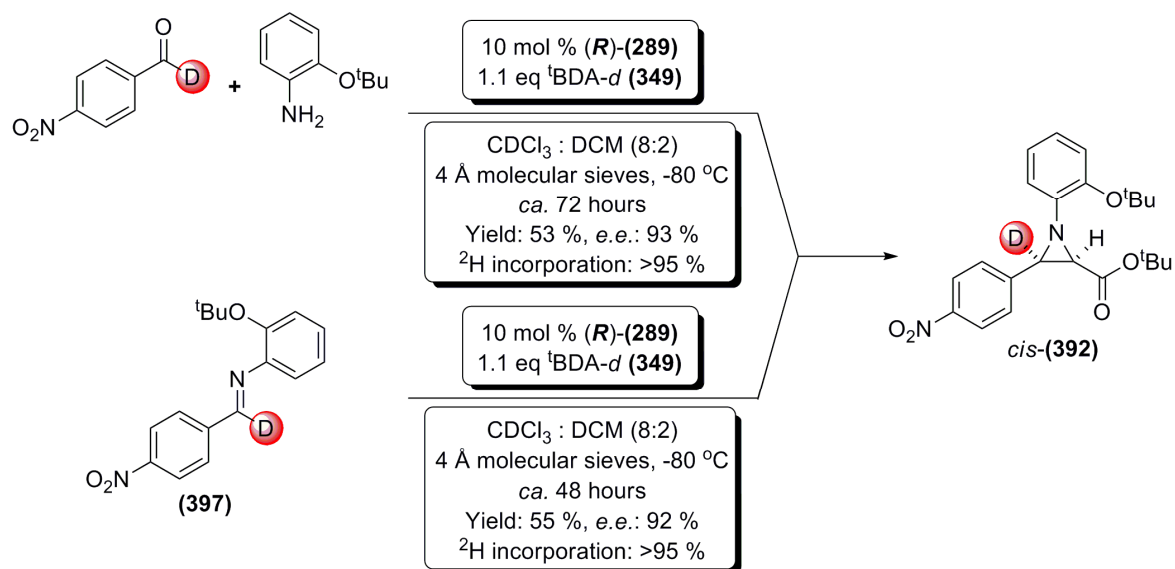


Figure 84: Gaussian calculations (carried out at B3LYP/6-11g theory level) and comparison of the ZPEs of TS1 and TS2 during imine formation in both *proteo*- and *deutero*- form

As shown in Figure 84, the Δ ZPE between the proteo and deutero forms of TS1 is very small (*ca.* 0.5 kJ/mol), suggesting little, or no KIE is present at this step. Δ ZPE for TS2 is also very small (*ca.* 0.06 kJ/mol), suggesting the presence of a small, normal secondary KIE. However, when taken together, these two effects essentially cancel out; suggesting that either a higher level of theory is required to account for the KIE, or another effect is present. It is worthy of note that the calculations used did not take into account conformers of the transition states, or the effects of solvation. Thus, the results of the calculation only allow for a very basic prediction.

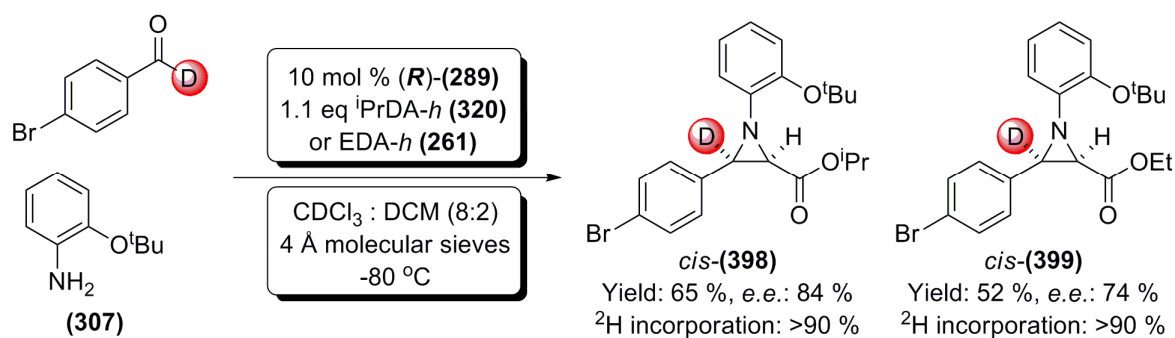
Despite the lack of evidence from computational work, evidence for the reduced rate of imine formation leading to increased reaction time was provided by the synthesis of *cis*-(392) via the preformed imine *N*-(2-*tert*-butoxyphenyl)-4-nitrobenzimidoyl deuteride (397). The use of (397) as the starting material led to a significantly reduced reaction time of *ca.* 48 hours; as opposed to *ca.* 72 hours for the one-pot approach (Scheme 154).



Scheme 154: Comparison of the required reaction times for the synthesis of *cis*-(392) utilising one pot, or stepwise synthesis routes; demonstrating the potential presence of a secondary KIE within the one-pot procedure

Thus (with the decrease in reaction time when (397) was utilised as starting material, as evidence), it can be concluded that the increased reaction times observed when utilising deuterated aldehydes come about as a result of slower initial imine formation; potentially due to a secondary KIE.

Following on from the above examples, it was decided to attempt aziridinations utilising a range of alkyl diazoacetates. To this end, one-pot aziridinations were attempted utilising 4-bromobenzaldehyde-*d*; and EDA (261), or ¹PrDA (320), as the carbon sources. Carrying out the standard one-pot asymmetric aziridination protocol, aziridines *cis*-(398) and *cis*-(399) were produced (Scheme 155).

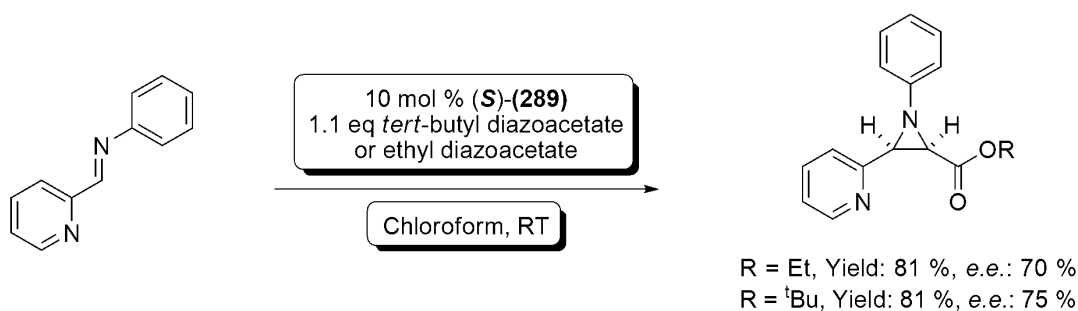


Scheme 155: Compounds *cis*-(398) and *cis*-(399)

Characterisation of *cis*-(398) and *cis*-(399) was predominantly carried out by ¹H-NMR spectroscopy, and HRMS; with the desired C2-*H* singlet present in the ¹H-NMR spectra of both *cis*-(398) and *cis*-(399) at 3.10 ppm. Incorporation of the desired alkyl diazoacetates was confirmed by the presence of the characteristic CH(CH₃)₂ septet of the *iso*-propyl residue (in the case of *cis*-(398)) at 4.89 ppm; or the CH₂ multiplet (4.21-3.87

ppm) and CH₃ triplet (1.09 ppm) of the ethyl residue in the case of *cis*-(**399**). ¹H-NMR spectroscopy also allowed confirmation of the *cis*-stereochemistry of (**398**) and (**399**), with both showing residual C3-*H* doublets with coupling constants of 6.6 and 6.5 Hz respectively. HRMS provided final confirmation of the synthesis of *cis*-(**398**) and *cis*-(**399**), with [M+H]⁺ ions found at the required *m/z* (*cis*-(**398**) found: 433.1233, required: 433.1232; *cis*-(**399**) found: 419.1082, required: 419.1075).

Interestingly, there was no noticeable drop in enantioselectivity in changing from the use of *tert*-butyl diazoacetate (*i.e.* *cis*-(**385**), Figure 82, 83% *e.e.*) to *iso*-propyl diazoacetate (*i.e.* *cis*-(**398**), Scheme 155, 84% *e.e.*); as expected, however, a roughly 10% loss in enantioselectivity was experienced upon changing to ethyl diazoacetate (*i.e.* *cis*-(**399**), Scheme 155, 74% *e.e.*). This loss in *e.e.* upon switching to ethyl diazoacetate was expected as a similar effect was noted by Pesce during the synthesis of chiral non-racemic *N*-substituted aziridine-2-carboxylate esters (Scheme 156).²⁶⁸



Scheme 156: Demonstration of the loss of enantioselectivity upon switching from *tert*-butyl diazoacetate to ethyl diazoacetate; carried out by Pesce

This effect can be rationalised by consideration of the MM2-minimised structure of the imine 4-bromo-*N*-(2-*tert*-butoxyphenyl)benzimidoyl deuteride (**400**) (formed from 4-bromobenzaldehyde-*d*, and 2-*tert*-butoxy aniline) within the cavity of catalyst (*S*)-(**289**) (Figure 85). This demonstrates the high steric demand around (**400**) during the transition state; thus, attack from the disfavoured face of (**400**) is more likely with an alkyl diazoacetate bearing a less bulky alkyl substituent *i.e.* ethyl *vs.* *tert*-butyl or *iso*-propyl, leading to the observed lower *e.e.s.*

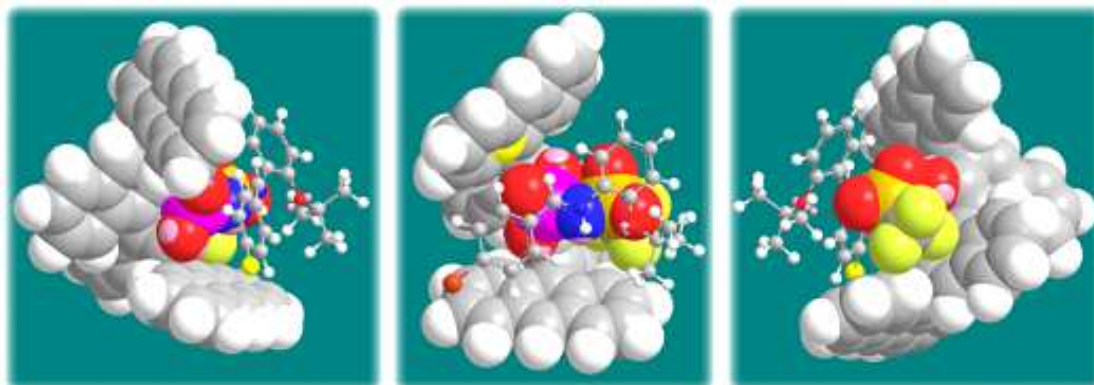


Figure 85: Front and side MM2 minimised structures of imine (400) within the cavity of (S)-(289), demonstrating the steric demand about the C=N bond

6.2.3: Asymmetric synthesis of C3-deuterated Aziridines – General Remarks

Having switched from the use of deuterated alkyl diazoacetates to deuterated aldehydes, it was found that generally the developed one-pot methodologies for aziridine formation were tolerant to this change, with yields of 41 - 72% and *e.e.s* of 64 - 93% achieved. However, several points of interest arose during this screen. It was found that, in general, yields were lower, and reaction times longer when deuterated aldehydes were used in the place of deuterated alkyl diazoacetates. This is presumed to be due to a secondary kinetic isotope effect when utilising deuterated aldehydes, although computational work has not provided conclusive evidence for this.

The secondary kinetic isotope effect is presumed to come about during imine formation, meaning that the imine formation is significantly slower with a deuterated aldehyde. This effect, when compounded by the low reaction temperatures required, led to increased reaction times (Figure 84). As during the project the aim was to develop a useful procedure, many reactions were cut short due to long reaction times, meaning that possibly, these yields would be increased if reaction times had been allowed to run beyond 72 hours. To a certain extent this was confirmed by carrying out the synthesis of *cis*-(**392**) from a preformed deuterated imine (Scheme 154). The subsequent asymmetric aziridination was then seen to proceed in a shorter reaction time of *ca.* 48 hours, along with a yield more consistent with those expected.

Throughout the syntheses shown during this chapter, deuterium incorporation was high, and the incorporation levels stable; again confirming the stability of the aziridine C2 and C3 carbons to H/D exchange. The aziridines synthesised were able to be stored on the bench at room temperature for several weeks with no appreciable deterioration, and when stored at reduced temperature under nitrogen, the products seem to be stable over an extended period (>12 months). This property becomes important when the potential uses of

aziridines as intermediates in synthesis are considered, and especially, the potential uses of deuterated aziridines.

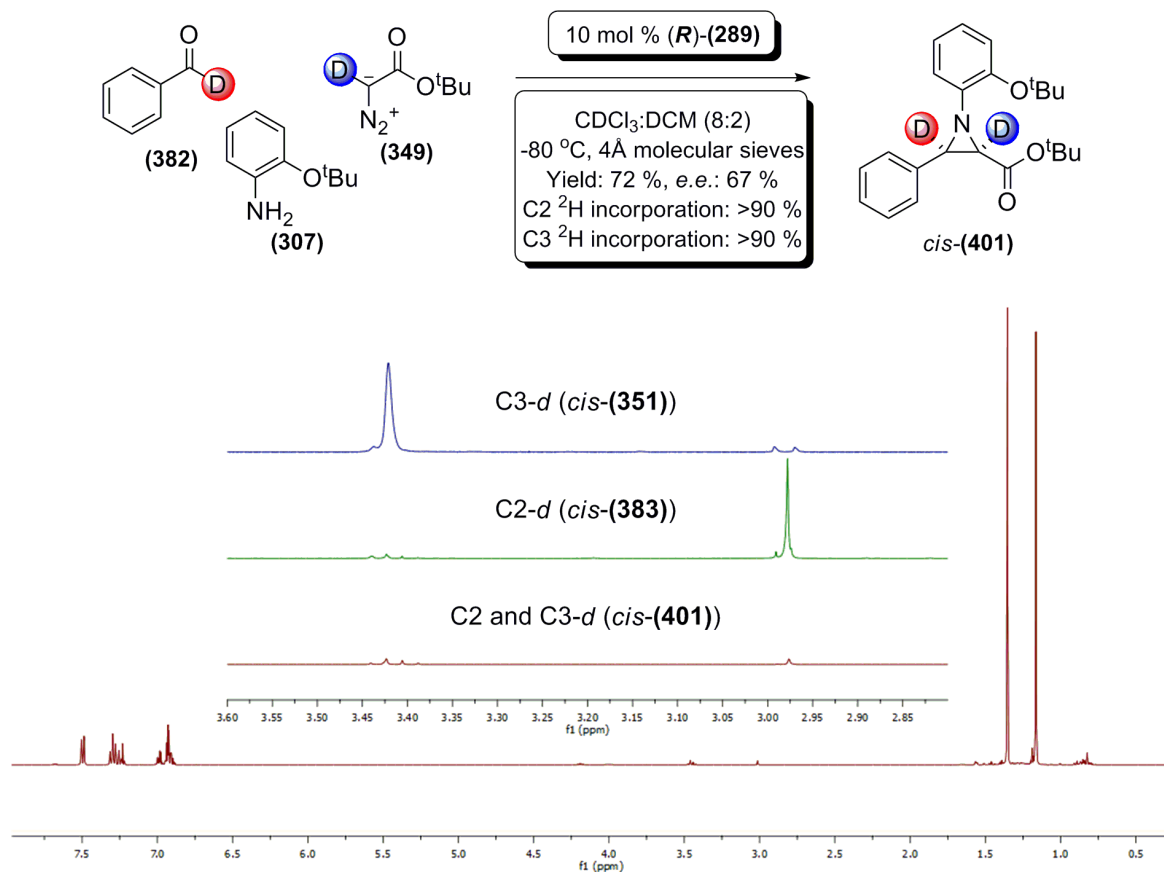
6.3.1: Asymmetric Synthesis of C2-, C3-deuterated Aziridines – Introduction

As both deuterated aldehydes and deuterated alkyl diazoacetates were now available, and having developed a pool of experience in synthesising and purifying deuterated aziridine products; at this point the aim of developing a ‘dialled in’ methodology for the synthesis of aziridines was becoming more feasible.

Having demonstrated the synthesis of both C2 and C3 deuterated aziridines, the next development was a combination of the two methods in order to produce C2-, C3-, *di*-deuterated aziridines. The following aziridinations were carried out in an attempt to demonstrate the potential to choose single or double deuteration within the asymmetric aziridine product, which was a key aim of the ‘dialled in’ methodology.

6.3.2: Asymmetric Synthesis of C2-, C3-deuterated Aziridines – Synthesis of aziridines *cis*-(401) to *cis*-(408)

The first *di*-deuterated aziridine to be synthesised utilising the one-pot asymmetric aziridination protocol was the simple phenyl derivative *cis*-(401). The reaction was carried out utilising standard one-pot methods, leading to the production of the desired aziridine in a yield of 72% and an enantiomeric excess of 67% (Scheme 157).



Scheme 157: Synthesis of *cis*-(401), and expansion of the 2.8 – 3.6 ppm region of the ¹H-NMR spectra of *cis*-(351), *cis*-(383), and *cis*-(401) showing the effect of deuteration at the C2, C3, and C2-C3 positions

As shown in Scheme 157, confirmation of the deuterium incorporation levels within *cis*-(401) was provided by ¹H-NMR spectroscopy. Clearly, both C2-*H* (expected at 2.9 ppm) and C3-*H* (expected at 3.4 ppm) doublets had been suppressed.²⁶⁸ Integration of the residual C2-*H* and C3-*H* peaks at 2.98 and 3.42 ppm showed deuterium incorporation of >90% at both C2 and C3 positions, although this value should be considered to contain an error of *ca.* 5% due to potential error within the integration of ¹H-NMR spectra.²⁷⁸ The presence of *cis*-(401) was further supported by HRMS, and LC-MS, both showing peaks at *m/z* 370(.2348) consistent with the doubly deuterated [M+H]⁺ ion.

One point of interest is the loss of enantioselectivity within *cis*-(401) (*e.e.* 67%) when compared to the equivalent C2 or C3 deuterated aziridines *cis*-(351) (*e.e.* 81%) and *cis*-(383) (*e.e.* 88%). Intrigued by this, and wishing to demonstrate the applicability of the aziridination methodology, further aziridinations were carried out, focused upon producing halogenated aziridines *cis*-(402) and *cis*-(403), along similar lines of inquiry as used in previous chapters (See 5.2.2 and 6.2.2).

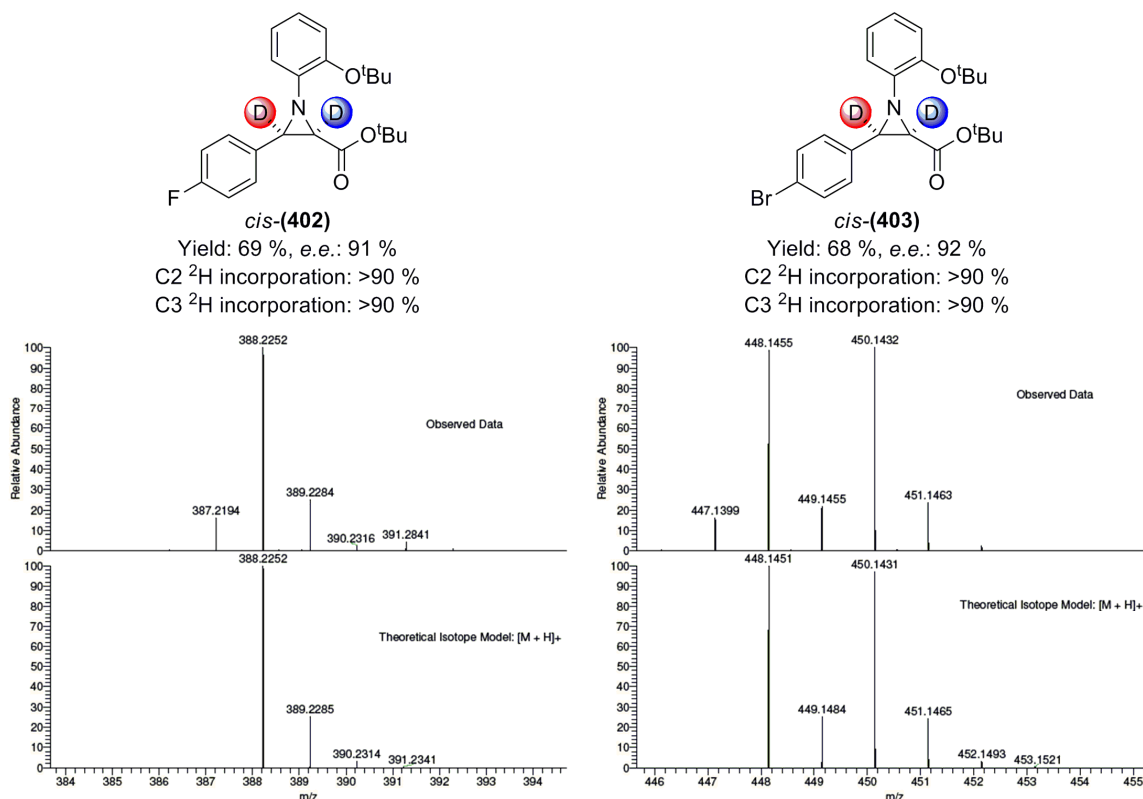


Figure 86: Synthesis and HRMS data for C2-C3 doubly deuterated aziridines *cis*-(402) and *cis*-(403)

As can be seen in Figure 86, both *cis*-(402) and *cis*-(403) were produced in reasonable yields of 69% and 68% respectively. These are in line with those expected, with little difference between these materials and the corresponding C3 deuterated aziridines *cis*-(384) (C3-*d* 4-fluorophenyl substituted, 72% yield), and *cis*-(385) (C3-*d* 4-bromophenyl substituted, 65% yield).

Confirmation of the synthesis of *cis*-(402) and *cis*-(403) was obtained primarily by ¹H-NMR spectroscopy and HRMS; with integration of the residual C2-*H* and C3-*H* peaks (3.03 and 3.45 ppm, *cis*-(402); 3.04 and 3.42 ppm, *cis*-(403)) confirming >90% deuterium incorporation in both products at the C2 and C3 positions; and HRMS showing [M+H]⁺ peaks at *m/z* values consistent with C2-C3 deuteration (*cis*-(402) found 388.2252, required 388.2252; *cis*-(403) found 448.1376, required 448.1378; see Figure 86).

Perhaps unexpectedly (considering the loss of *e.e.* seen within the synthesis of *cis*-(401)), the enantioenrichment of the C3-*para*-bromophenyl aziridine *cis*-(403) was higher than that seen within the corresponding C3 singly deuterated species *cis*-(385) (83% *e.e.*), bringing the results back into line with those of the C2-deuterated product *cis*-(350) (95% *e.e.*). This is an unusual result, as it suggests that within this example, single deuteration of the C3 position has a significantly adverse effect upon the enantioselectivity of the reaction, which is subsequently reversed upon deuteration of both the C2 and C3 positions (Figure 87).

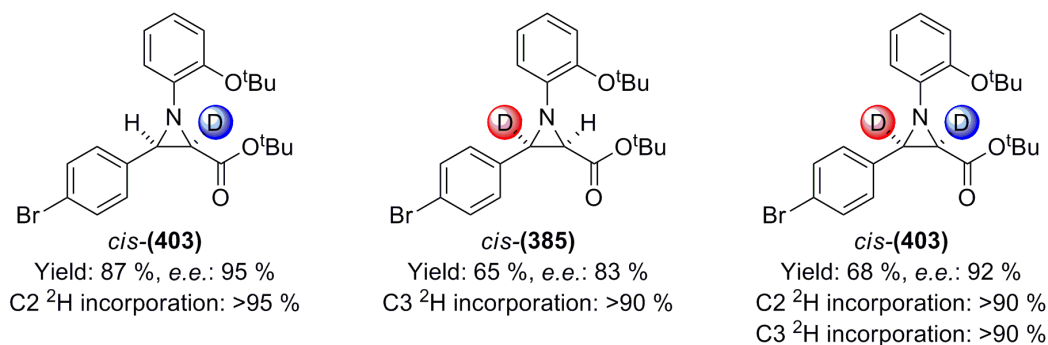
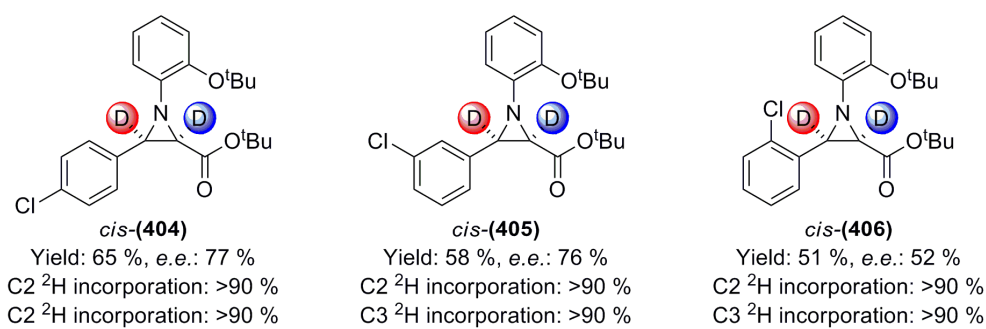


Figure 87: Comparison of the yields and *e.e.s* achieved with C2, C3, and C2-C3 deuteration of aziridines bearing C3-*para*-bromophenyl substitution

With a view to investigating the effects of varying substitution patterns upon the C3 position, a set of C3-chlorophenyl substituted C2-C3 deuterated aziridines were synthesised, *cis*-(404) to *cis*-(406). Figure 88 shows the results of these syntheses.



Compound	C3 Substitution	Deuterium Position	Yield (%)	<i>e.e.</i> (%)
<i>cis</i> -(386)	4-chloro phenyl	C3	67	71
<i>cis</i> -(404)	4-chloro phenyl	C2, C3	65	77
<i>cis</i> -(387)	3-chloro phenyl	C3	65	69
<i>cis</i> -(405)	3-chloro phenyl	C2, C3	58	76
<i>cis</i> -(388)	2-chloro phenyl	C3	41	64
<i>cis</i> -(406)	2-chloro phenyl	C2, C3	51	52

Ring Substitution Position	Average Yield (%)	Average <i>e.e.</i> (%)
4-	66	72
3-	62	72
2-	46	58

Figure 88: Effect of varying substitution position on yields and *e.e.* of chloro- substituted *mono*- and *di*-deuterated aziridines

As can be seen, the enantioselectivities of these reactions were of the same order as those of the corresponding C3-deuterated aziridines (64 – 71%, *cis*-(386) – *cis*-(388)), with a similar pattern emerging concerning the effect of substitution position. That being the enantioselectivity of the reaction drops as ring substitution position is changed from 4- to 2-, with *e.e.* decreasing in the order 4- > 3- > 2-.

The final C3 substitution to be tested was that of an electron-withdrawing functionality. Thus, *cis*-(**407**) was synthesised, furnished with an electron-withdrawing C3- (*para*-nitro)phenyl group, from 4-nitrobenzaldehyde-*d*, 2-*tert*-butoxy aniline (**307**), and ¹BDA-*d* (**349**). *cis*-(**407**) was afforded in a 57% yield from the one-pot aziridination procedure, while ¹H-NMR spectroscopy confirmed a deuterium incorporation of >90% at both the C2 and C3 positions (*via* integration of the residual C2-*H* and C3-*H* peaks at 3.13 and 3.50 ppm respectively). HRMS also confirmed the C2- C3- deuteration, with the [M+H]⁺ ion found at *m/z* 415.2196 (theoretical *m/z* 415.2197)

Gratifyingly, the enantioselectivity of the reaction was excellent, with an *e.e.* of 97% confirmed by chiral HPLC analysis (Figure 89). This *e.e.* was unexpected, as it was higher than those achieved previously with both the C2-*deutero* (*cis*-(**356**), 88% *e.e.*) and C3-*deutero* (*cis*-(**392**), 93% *e.e.*) derivatives of this aziridine.

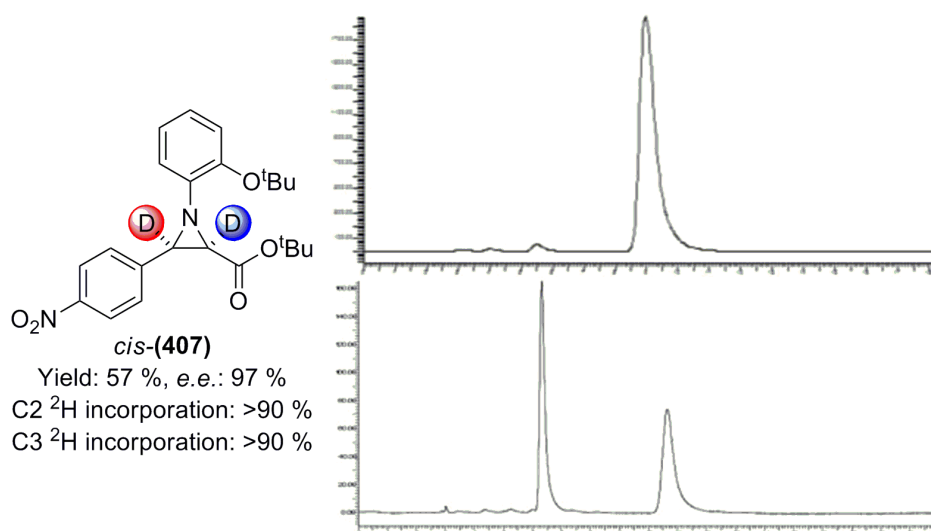
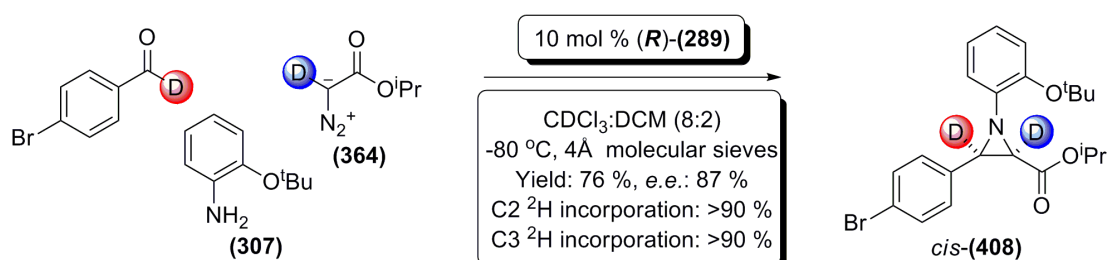


Figure 89: Yield, *e.e.*, and chiral HPLC trace for *cis*-(**407**)

The final test to be carried out upon the tolerances of the deuterated aziridination protocol was that of variation of the C2 substitution. Thus the synthesis of *cis*-(**408**) a C2- C3- *di*-deuterated C3-(*para*-bromo)phenyl-substituted aziridine bearing a C2-*iso*-propyl ester (synthesised from 4-bromobenzaldehyde-*d*, 2-*tert*-butoxy aniline (**307**), and ¹PrDA-*d* (**364**)) is shown in Scheme 158.



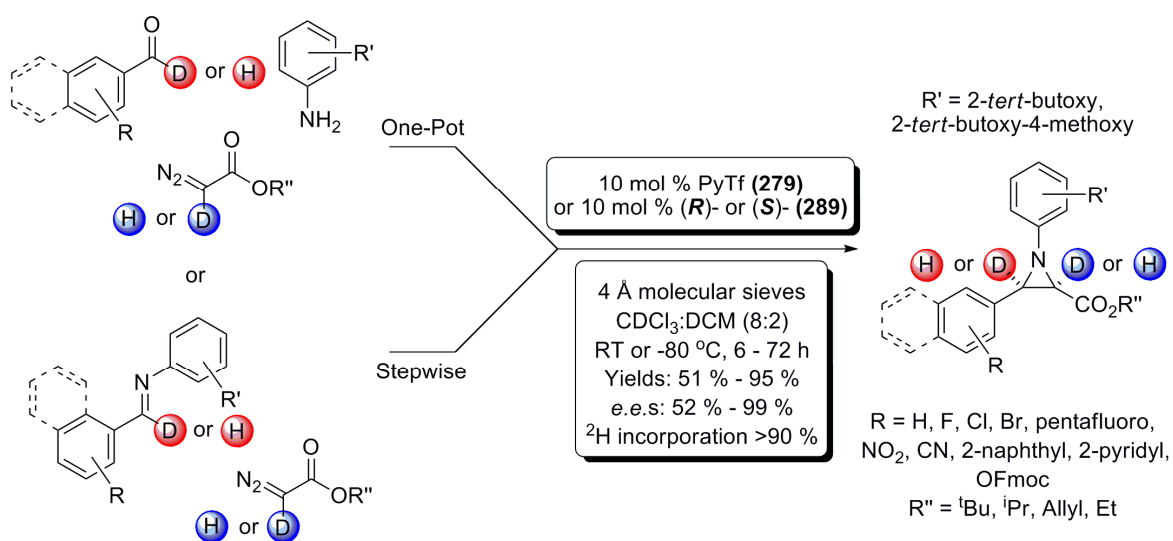
Scheme 158: One-pot asymmetric synthesis of *cis*-(**408**)

The reaction proceeded well, with a yield of 76%, and an *e.e.* of 87%. Deuterium incorporation within *cis*-(**408**) was determined by the integration of the residual C2-*H* (3.09 ppm) and C3-*H* (3.46 ppm) peaks within the ¹H-NMR spectrum as >90%. Incorporation of the desired C2 *iso*-propyl ester was confirmed by the presence of the characteristic CH(CH₃)₂ septet of the *iso*-propyl residue at 4.89 ppm within the ¹H-NMR spectrum. Finally, the presence of the *di*-deuterated species *cis*-(**408**) was confirmed by HRMS, with [M+H]⁺ ions detected at *m/z* 434.1296 (theoretical 434.1294).

6.4: Conclusions upon the synthesis of C2-, C3-di-deuterated Aziridines, and the overall 'Dialled in' Methodology

As is demonstrated in this chapter, various C2, C3 *di*-deuterated aziridines have been synthesised using a one-pot asymmetric aziridination procedure, generating deuterated products in moderate to good yields (51 – 76%), and good to excellent enantiomeric excesses (52 – 97%). The reaction has been shown to be tolerant to aromatic (Scheme 157), halogenated (Figures 86 – 88), and electron-withdrawing substituents (Figure 89), and also tolerant to the alteration of the alkyl diazoacetate used as the substrate carbon source (Scheme 158).

To this end, in this and the previous chapter, a 'dialled in' approach (Appendix 7) has been adopted for the integration of deuterium selectively into the C2, C3, or C2 and C3 positions of aziridines, in a highly enantioselective procedure. The development present in this, and the preceding chapter (See *Chapter 5: Studies towards the synthesis of C3-deuterated Aziridines*) led to the possibility of selecting the enantiomer, substitution, deuterium position, and alkyl diazoacetate substitution desired; and synthesising the corresponding aziridine in good yields, and in high enantioselectivity (Scheme 159).



Scheme 159: Summary of the 'dialled in' synthesis of deuterated aziridines

The next development of this procedure was to attempt ongoing syntheses of materials from these aziridines, in order to test the potential viability of the 'dialled in' approach to the syntheses of useful materials, or natural products. The attempted utilisation of these aziridines in ongoing syntheses is the subject of the following chapter.

Chapter 7: Studies towards the ‘Dialled in’ Synthesis of Deuterated α -amino acid Derivatives

7.1.1: Synthesis of Deuterated α -amino acids – Introduction

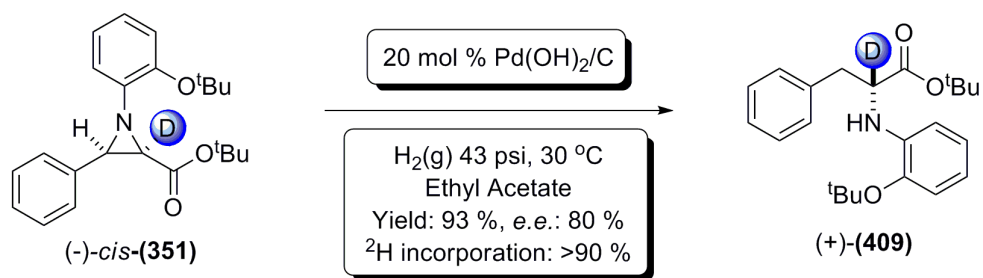
With the ongoing development of methods for the production of deuterated enantioenriched aziridines discussed within the previous chapters, it was decided to investigate the possibilities of utilising these as starting materials for the synthesis of potentially useful amino acids.

As described within the introduction of this text, the ring-opening chemistry of aziridines is a very large area of ongoing research, and as such it was decided to search for available chemistry which could be of use with the deuterated aziridines on hand. The chemistry which was settled on was that developed by Lee *et al* into the regioselective ring-opening of aziridines by molecular hydrogen catalysed by palladium. Kim *et al* found that treatment of aziridines with Pd(OH)₂/C and hydrogen gas led to selective ring-opening, breaking the nitrogen C2 bond, and forming an α -amino species.²⁵⁸⁻²⁶¹

It was hoped that application of this methodology to the aziridine products obtained *vide supra* would lead to regioselective ring-opening, and thus, selective production of deuterated α -amino acid species. It was also anticipated that the deuteration levels obtained from the aziridine synthesis would be translated effectively into high levels of selective deuterium incorporation within the subsequent α -amino acid species. It is worthy of note that up to this point it had proven impossible to assign the absolute stereochemistry of the aziridines produced *via* the developed aziridination methodology. Thus, within the following work, the products and aziridines are referred to depending on the sign of their optical rotation. It is also noted within the experimental section which enantiomer of the catalyst (**289**) the starting aziridines were synthesised from.

7.1.2: Synthesis of Deuterated α -amino acids – Synthesis of (**409**) to (**428**)

With the aim of producing α -amino acids, it was decided to attempt the ring-opening methodology of Kim *et al* upon *cis*-(**351**); a C2 deuterated aziridine with simple C3 phenyl substitution. Kim *et al* had utilised stoichiometric amounts of palladium hydroxide on carbon in order to facilitate their hydrogenolysis reaction; however, in our case, it was decided initially to treat the aziridine under milder conditions. Thus, 20 mol % palladium hydroxide on carbon was employed, and the reaction was carried out under 43 psi H₂ at 30 °C (Scheme 160). Ethyl acetate was used as the solvent, as this offered the best solubilisation of the starting material.



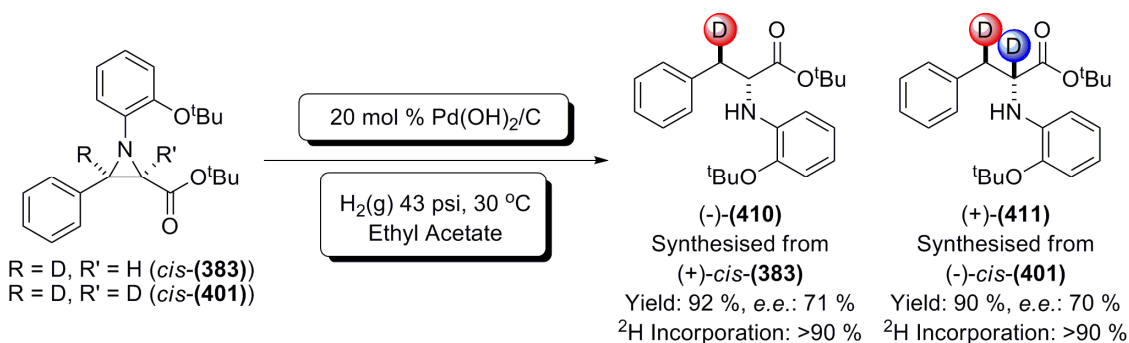
Scheme 160: Synthesis of (+)-(409)

After 12 hours the uptake of hydrogen gas was seen to cease; suggesting completion of the reaction. After the reaction mixture was filtered through Celite[®] (in order to remove the catalyst), and the solvent was removed under reduced pressure, ¹H-NMR spectroscopy revealed the reaction mixture to be remarkably clean; with only starting material and product present. Subsequent purification by column chromatography gave the desired product (**409**) in an excellent 93% yield.

Deuterium incorporation within (**409**) was established by the relative integrations of the β-CH₂ and residual α-CH peaks within the ¹H-NMR spectrum at 3.11 and 4.20 ppm respectively; and was determined to be >85% (initially, a low deuterium content aziridine sample (>85%) was used as we were unsure that the reaction would work), a result which suggests no loss of deuterium incorporation during the hydrogenolysis reaction. Further evidence for the synthesis of (**409**) (and the presence of deuterium) was provided by LC-MS and HRMS; with the required [M+H]⁺ ion being found at *m/z* 371(.2443) (theoretical [M+H]⁺ *m/z* 371.2439).

Initially, it proved difficult to obtain an enantiomeric excess measurement for (**409**), as the enantiomers were inseparable utilising the Chiralpak AD-H chiral HPLC column available at the time. However, upon use of a differing HPLC column (Chiralcel OD, with a gradient CO₂/*iso*-propanol system as the mobile phase), the *e.e.* was confirmed as 80%; this is within the experimental error of full retention of enantiopurity from the initial starting material (*cis*-(**351**), 81% *e.e.*).

Although the hydrogenolysis worked well, and only one major product was isolated, at the time uncertainty persisted as the nature of the regioselectivity of the hydrogenolysis reaction had not been confirmed. In order to confirm the regioselectivity of the ring-opening, and in order to move towards proving the generality of the method, it was decided to synthesise the β-deutero and α,β-deutero versions of (**409**), these being (**410**) and (**411**) respectively. The results of these reactions are summarised in Scheme 161.



Scheme 161: Synthesis of compounds (-)-(410) and (+)-(411)

As shown in Scheme 161, the yields of **(410)** and **(411)** were both excellent (92% and 90% respectively), along with good enantioselectivities of 71% *e.e.* and 70% *e.e.* respectively; demonstrating reasonable retention of stereochemistry from the starting materials *cis*-**(383)** (88% *e.e.*), and *cis*-**(401)** (67% *e.e.*).

Deuterium incorporation within **(410)** and **(411)** was confirmed both by ¹H-NMR integration (an error of *ca.* 5% should be considered due to the insensitivity of ¹H-NMR integration),²⁷⁸ and mass spectrometry (LC-MS and HRMS), with [M+H]⁺ peaks being detected for **(246)** and **(247)** at 371(.2442), and 372(.2431) respectively.

The primary concern at this point was confirmation of the regioselectivity of the reaction. Analysis of the structures of **(409)**, **(410)** and **(411)** allowed several predictions about which peaks would be expected within the ¹H-NMR spectra between 2.5 and 5 ppm, *i.e.* the expected range for the α - and β - protons, along with the NH (Figure 90).^{288,289}

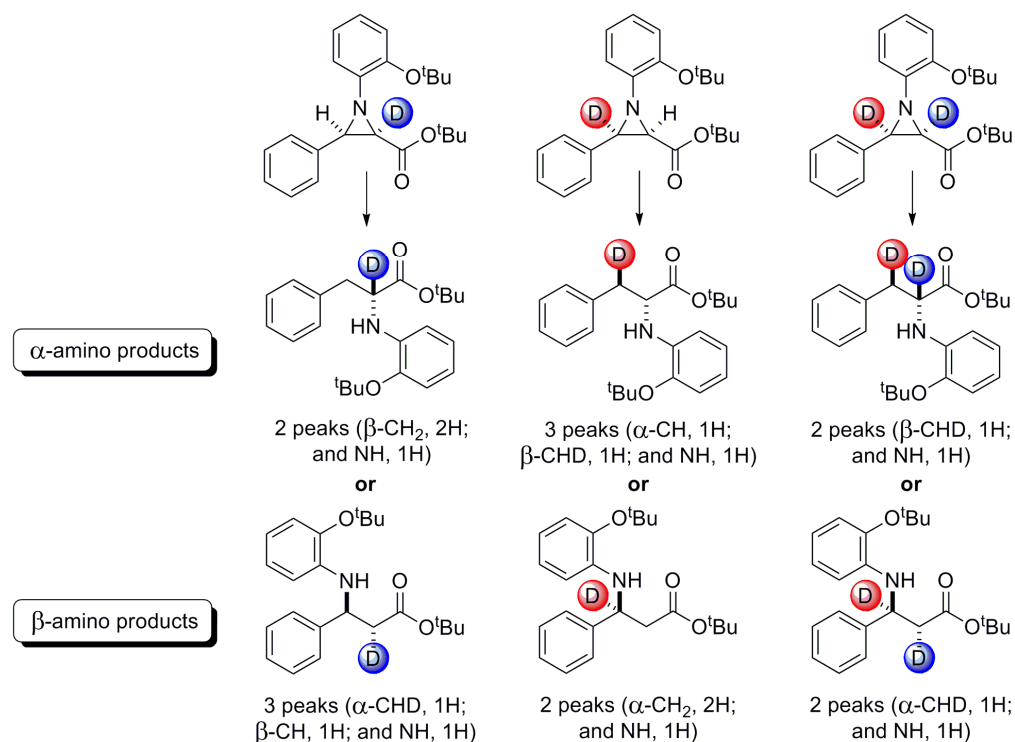


Figure 90: Predictions of the peaks within the 2.8 – 5 ppm range of the ¹H-NMR spectra of the α - and β - amino products from the ring-opening of **(351), **(383)**, and **(401)****

With the predictions in hand, the α -selectivity of the ring-opening reaction was confirmed by comparison of the $^1\text{H-NMR}$ spectra of **(409)**, **(410)**, and **(411)**. COSY and HSQC data was also collected for compound **(410)**, allowing the coupling within the molecule to be assessed. Thus, the 2.8 – 5 ppm region of the $^1\text{H-NMR}$ spectrum of **(409)** contained one peak. This pair of doublets corresponds to the diastereotopic β -hydrogen atoms (3.11 ppm, 2H), however, the NH (expected at 4.80 ppm, 1H), was not present (possibly due to exchange). Despite this, the spectrum was still consistent with the predictions shown in Figure 90 for the α -amino product. Whereas, within the $^1\text{H-NMR}$ spectrum of **(410)**, the 2.8 – 5 ppm region contains three peaks (with relative integrations of 1:1:1), consistent with the NH (4.80 ppm), the singly deuterated β -position (3.11 ppm), and the final peak corresponding to the α - CH (4.19 ppm). Again, these are consistent with the expected peaks for the α -amino product. COSY coupling also supported these assignments, and is included in Appendix 6 along with $^1\text{H-NMR}$, $^{13}\text{C-NMR}$, and HSQC spectra of **(410)**. Finally, as expected, the $^1\text{H-NMR}$ spectrum of **(411)** contains two peaks within the region of 2.8 – 5 ppm; corresponding to the NH (4.80 ppm), and singly deuterated β - CH_2 (3.11 ppm), consistent with the α -amino product.

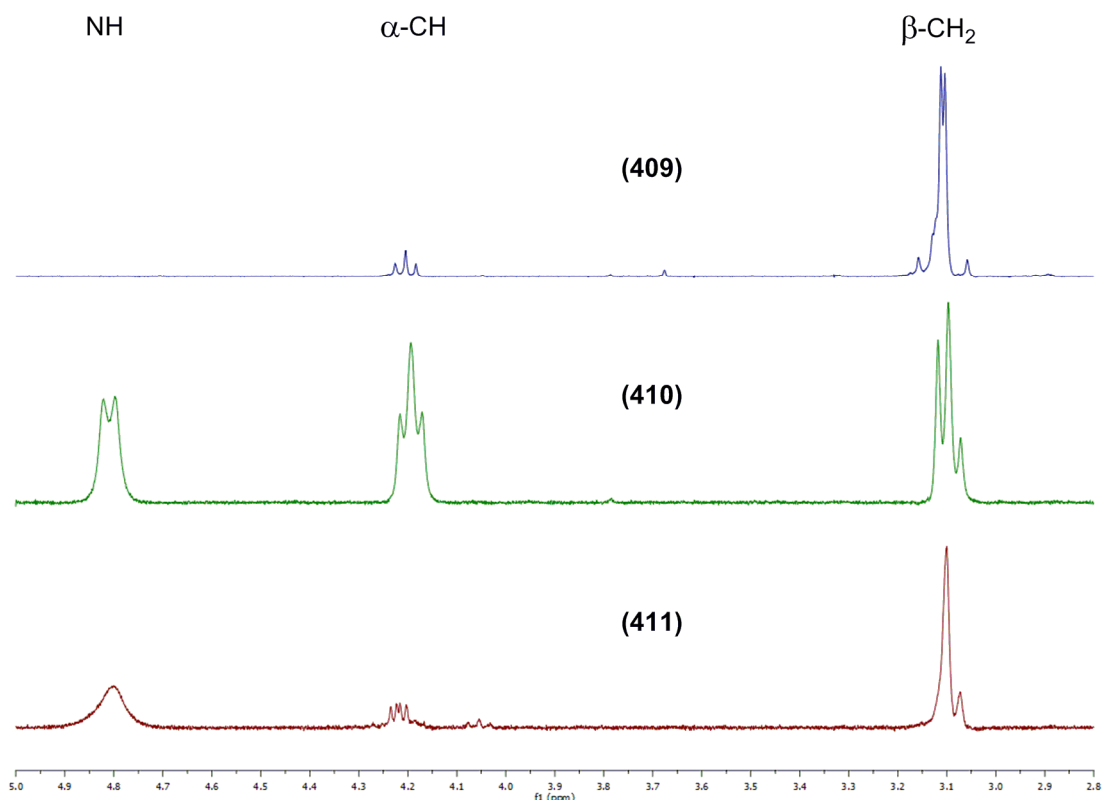
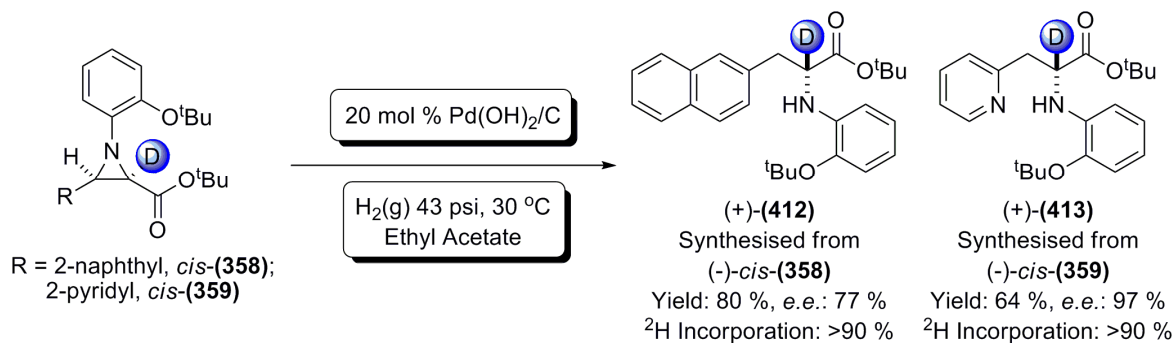


Figure 91: Comparison of the 2.8 – 5.0 ppm range of the $^1\text{H-NMR}$ spectra of **(409)**, **(410)**, and **(411)**

Having demonstrated that the ring-opening hydrogenolysis behaved in the desired manner; and that the deuterium incorporation and, on the whole, enantioenrichment of the products (inherited from the starting material aziridines) was conserved during

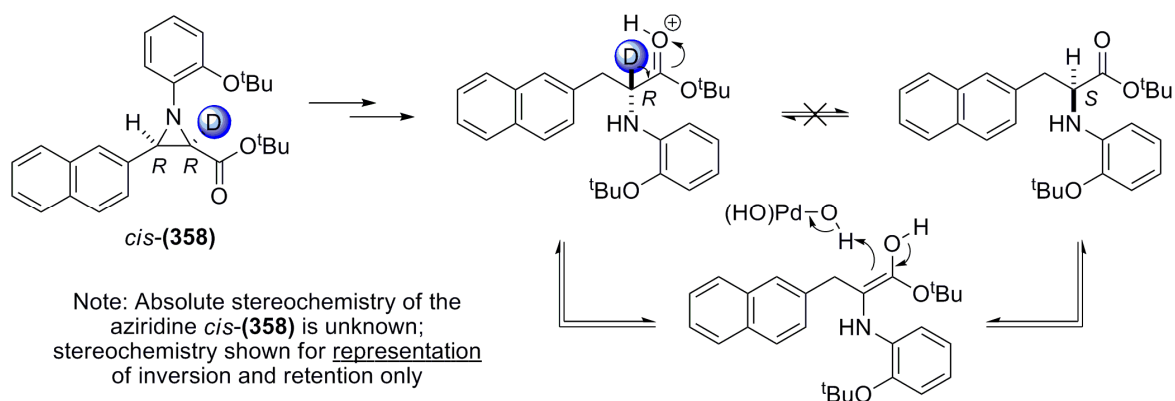
hydrogenolysis; the substrate range was expanded to include bicyclic and heteroaromatic aziridines produced with the one-pot aziridination methodology. Therefore, *cis*-(**201**) and *cis*-(**202**) were submitted under the same reaction conditions detailed above (Scheme 160), those being 43 psi H₂ at 30 °C for 12 hours. The results of these reactions are shown in Scheme 162.



Scheme 162: Synthesis results for (+)-(412), (+)-(413)

¹H-NMR spectra of (**412**) and (**413**) confirmed the regioselectivity of the ring-opening reaction to produce α -amino acids, with both compounds showing diastereotopic AB doublet peaks with integrations of 2H (at 3.29, and 3.40 ppm respectively) corresponding to the β -CH₂ group present within each compound. Integration of these peaks against the residual α -CH peak at 4.31 and 4.28 ppm respectively confirmed deuterium incorporations of >90% for both compounds, roughly equal to that of the starting materials *cis*-(**358**) and *cis*-(**359**).

The yields and enantioselectivities of the reactions were also good, although, a significant loss of enantiopurity was discovered upon chiral HPLC analysis of (+)-(412) (77% *e.e.* compared to 85% *e.e.* for the starting material, *cis*-(**358**)). This was unexpected, as the entering group at the C3 position is a hydrogen atom, therefore the stereochemical information at the C3 position is lost (as it is no longer chiral). Thus, any inversion or scrambling of stereochemistry must occur at the C2 position. However, it is unlikely that this is occurring through a simple acid catalysed racemisation, as the deuterium incorporation within (**412**) remains high; which would not be the case if acid catalysed racemisation were in effect, due to the relative abundances of protons vs. deuterons (Scheme 163).



Scheme 163: Mechanism of the acid catalysed racemisation of amino acids, demonstrating loss of deuterium

Further development of the ring-opening methodology was carried out by the reactions of the *para*-chlorophenyl substrates *cis*-(**195**), *cis*-(**225**), and *cis*-(**240**) under the ring-opening conditions shown in Scheme 160. These conditions afforded the desired *mono*- and *di*- deuterated, α -amino products (**414**), (**415**), and (**416**) (see Figure 92) in excellent yields of 95%, 92%, and 98% respectively.

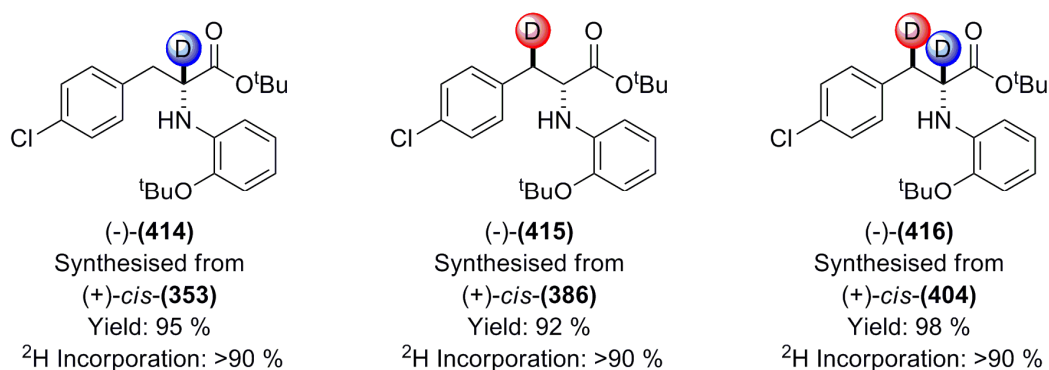
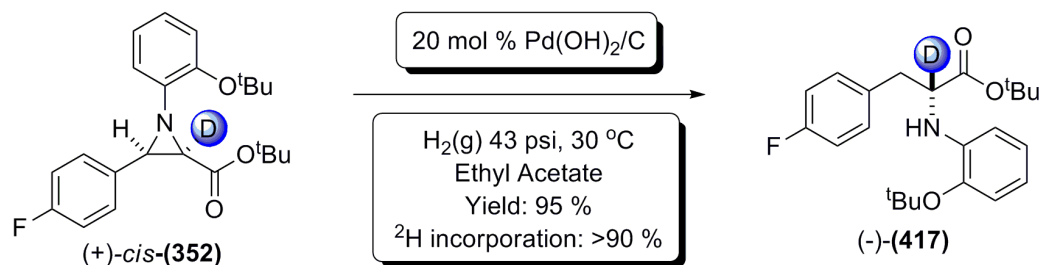


Figure 92: Results for the syntheses of (414), (415), and (416)

Deuterium incorporation within the examples shown in Figure 92 was again found to be high, with deuterium levels of >90% for (**414**) – (**416**) inclusively, as determined by ^1H -NMR spectroscopy (determined by the relative integrations of the β - CH_2 (3.06 ppm), and α - CH (4.19 ppm) peaks). Unfortunately measuring the enantiomeric excess of these compounds by chiral HPLC analysis proved difficult with the columns and utilities available at the time. Analysis was attempted with standard solvent-based HPLC, as well as supercritical CO_2 based systems, but none were capable of separating the two enantiomers to a sufficient degree to allow assignment of enantiomeric excess. Despite this, as the majority of syntheses within this chapter demonstrate, it is reasonable to consider that the enantiomeric excesses shown for the starting materials will have been, within reason, unaltered by the ring-opening reaction. Thus, it can be inferred that the *e.e.s* of (**414**) – (**416**) were *ca.* 67%, 71%, and 77% respectively.

Undeterred by the inability to separate the 4-chlorophenyl derived amino acid species, a further halogenated substrate was submitted to the ring-opening procedure; this being *cis*-(**352**). The reaction was successful, affording the desired *para*-fluorophenylalanine derivative (**417**) in 95% yield (Scheme 164).

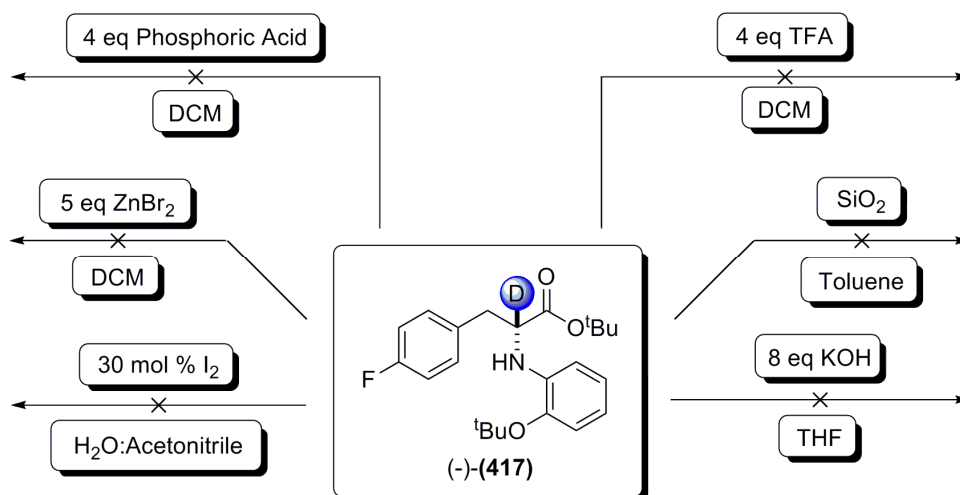


Scheme 164: Synthesis of (**417**) from *cis*-(**352**) utilising 20 mol % Pd(OH)₂/C

The regioselectivity of the ring-opening was confirmed by ¹H-NMR spectroscopy, with AB doublet peaks present within the ¹H-NMR spectrum at 3.09 ppm, integrating to 2H, corresponding to the desired diastereotopic β-CH₂ group of the α-amino product (**417**). Deuterium incorporation was also confirmed by ¹H-NMR spectroscopy, with the relative integrations of the β-CH₂ signal (3.09 ppm) and residual α-CH (4.19 ppm) showing deuterium incorporation of >90%.

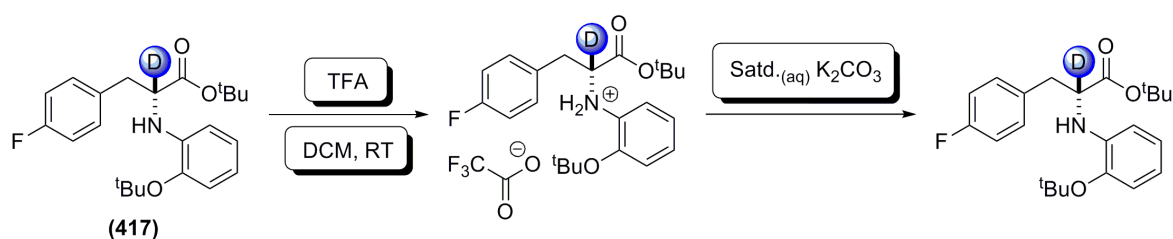
Unfortunately, separation of this compound proved difficult with the HPLC materials and methods available. Thus, it was decided to attempt a similar methodology as was applied in the case of the C3-pentafluorophenyl aziridine-2-carboxylate *cis*-(**355**) (Chapter 5, Scheme 139); this being removal of one *tert*-butyl group in order to deliver the required retention time for separation of enantiomers by chiral HPLC.

A literature search revealed a multitude of methods available for the cleavage of *tert*-butyl esters (it was decided to focus upon the ester functionality, as it was believed cleavage would be more facile, and therefore require milder conditions than those required for ether cleavage). A variety of these reactions were attempted, and the conditions employed are shown in Scheme 165.²⁹⁰⁻²⁹³



Scheme 165: Attempted hydrolysis of the *tert*-butyl ester of (417)

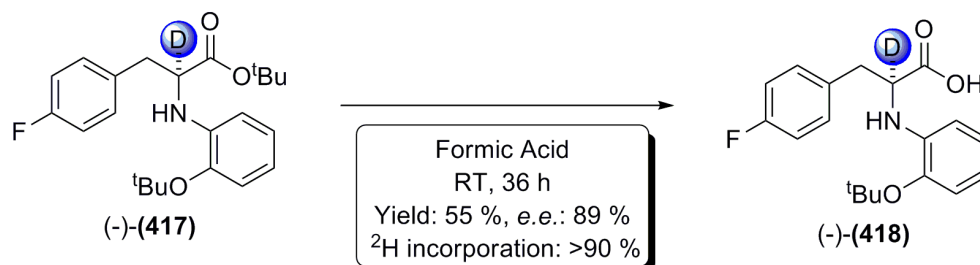
Generally, the methods shown in Scheme 165 were either entirely unsuccessful or produced product mixtures which were too complex to afford the desired material in a useful state, or yield. However, one interesting observation came about during the reaction with trifluoroacetic acid (TFA). Monitoring by TLC, it appeared that the starting material had been consumed within *ca.* 2 hours. $^1\text{H-NMR}$ spectroscopy of a sample supported this fact, but after a basic work up, analysis revealed complete recovery of the starting material. It was believed that this was due to salt formation, which was reversed during the basic work up, regenerating the starting material (Scheme 166).



Scheme 166: Formation of the TFA salt of (417), and subsequent regeneration of (417)

The method which was eventually settled upon was treatment of the starting material (417) with neat formic acid, stirring at room temperature for 36 hours. TLC analysis revealed that the starting material was consumed, and after purification by reversed phase chromatography, the desired product (418) was identified by $^1\text{H-}$ and $^{13}\text{C-}$ NMR spectroscopy, IR spectroscopy, and HRMS analysis. The $^1\text{H-NMR}$ spectrum clearly showed the loss of a *tert*-butyl group, with only one peak seen within the expected range of a *tert*-butyl group, at 1.35 ppm, integrating to 9H; while the required peaks for the diastereotopic $\beta\text{-CH}_2$ group (integrating to 2H) was present at 3.06 ppm. This was consistent with the $^{13}\text{C-NMR}$ spectrum, which contained only one peak corresponding to the tertiary carbon of the remaining *tert*-butyl group at 82.2 ppm. IR analysis showed the

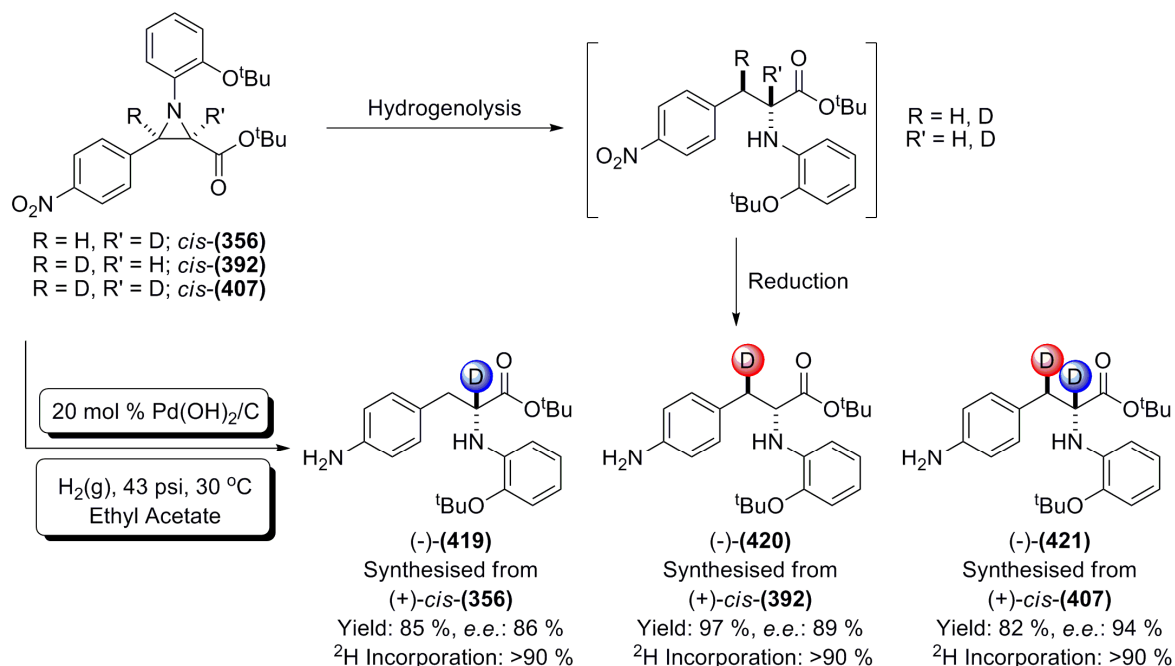
appearance of an absorbance band at a frequency of 2717 cm^{-1} , which is within the range of the O-H stretch within a free carboxylic acid (typically $2500 - 3300\text{ cm}^{-1}$); and finally, LCMS, and HRMS confirmed the presence of the $[M+H]^+$ ion of **(418)** at a mass of m/z 333(.1723), consistent with the desired deuterated product (Scheme 167).



Scheme 167: Synthesis of the α -amino free acid product (-)-(418)

Removal of the *tert*-butyl group increased the polarity of the molecule sufficiently to increase the retention time of **(418)** upon HPLC analysis to allow for separation of the enantiomeric peaks; thus, determination of the enantiomeric excess gave a value of 89%; this result is within the experimental error of full retention of enantiopurity from the aziridine starting material *cis*-**(352)**. Therefore, it can be reasonably inferred that the *e.e.* of the intermediate protected amino acid **(417)** was between 80% and 89%. The low yield of this reaction was believed to come about as a result of the potential decomposition of the product due to the harsh reaction conditions required to remove the *tert*-butyl group.

Having achieved HPLC separation of the enantiomers of **(418)**, the ring-opening procedure was expanded further by the use of the electron withdrawing group (C3-(4-nitro)phenyl) bearing aziridines *cis*-**(356)**, *cis*-**(392)**, and *cis*-**(407)** as substrates (Scheme 168). However, an additional complication was identified with these substrates. Due to the conditions used to perform the hydrogenolysis of the aziridine ring, reduction of the nitro group to give the corresponding amino species could also take place. Despite this, application of the previously utilised ring-opening procedure (see Scheme 160) proceeded smoothly; with the desired deuterated α -(*para*-amino)phenylalanine derivatives **(419)** – **(421)** afforded in excellent 85%, 97%, and 82% yields respectively (Scheme 168).



Scheme 168: Synthesis of compounds (419), (420), and (421)

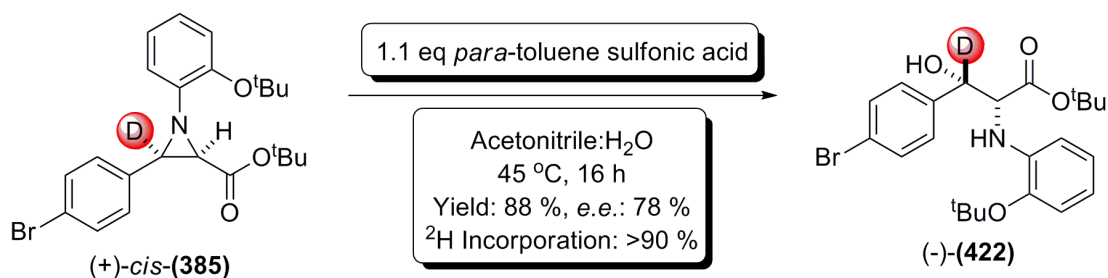
As had been seen previously during the syntheses of (**409**) – (**411**) (Figure 91), the presence of deuterium at the α - and/or β - positions of (**419**) – (**421**) led to differing integration and peak patterns within the 2.8 – 5.0 ppm range within their ¹H-NMR spectra; supporting the regiospecificity of the ring-opening to form α -amino products. Thus, the ¹H-NMR spectrum of (**419**) contained an AB doublet at 2.98 ppm, integrating to 2H, consistent with the diastereotopic β -CH₂; the ¹H-NMR spectrum of (**420**) contained two peaks, both integrating to 1H at 4.11 ppm and 3.00 ppm, consistent with the α -CH, and β -CHD; and finally, the ¹H-NMR spectrum of (**421**) contained a single peak at 2.99 ppm, integrating to 1H, consistent with the β -CHD. Within (**419**) – (**421**), deuterium incorporation (determined by ¹H-NMR spectroscopy) was found to be >90%. HRMS also confirmed the formation of the desired deuterated products, with mass ions being detected at the required *m/z* values ((**419**) *m/z* 386.2551, (**420**) *m/z* found 386.2552, (**421**) *m/z* found 387.2612).

Gratifyingly, (**419**) – (**421**) were amenable to separation by chiral HPLC analysis, recording *e.e.s* of 86%, 89%, and 94% respectively. These were within experimental error of full retention of stereochemistry from the starting material aziridines ((**356**) 88% *e.e.*; (**392**) 93% *e.e.*; (**407**) 97% *e.e.*).

Having demonstrated the applicability of regiospecific hydrogenolysis to the aziridine substrates developed *vide supra*, further ring-openings were carried out utilising water as the nucleophile. It was believed that this methodology would yield β -hydroxy- α -

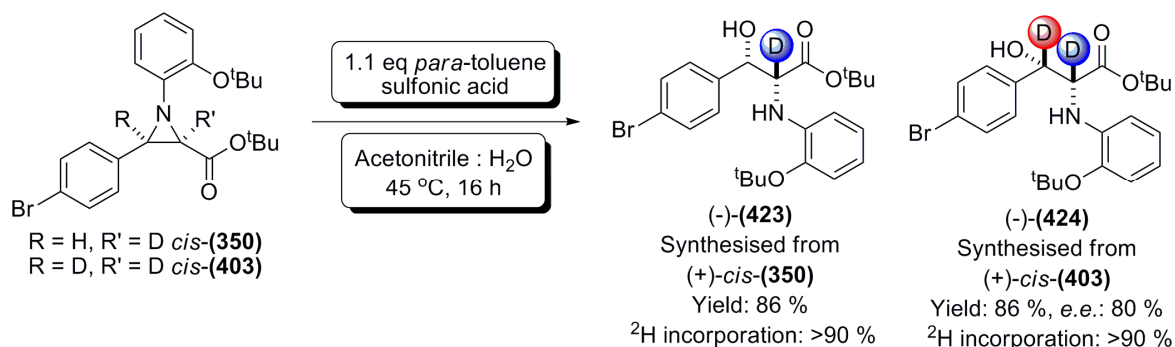
amino acids; applying the ‘dialled in’ approach could then yield the desired α -, β -, or α,β -deutero versions of these β -hydroxy- α -amino acid derivatives.

The water-based nucleophilic ring-opening procedure was initially tested upon substrates which were unsuitable for hydrogenolysis-based ring-opening. Foremost among these were compounds bearing bromine atoms, due to the potential cleavage of these during hydrogenolysis.²⁹⁴ Therefore, *cis*-(**385**) was treated according to the conditions shown in Scheme 169.²⁵⁵



Scheme 169: Synthesis of β -deutero- β -hydroxy- α -amino acid (-)-(422)

The reaction was monitored by TLC, and after 16 hours was deemed complete. Subsequent work up and purification by column chromatography gave the desired β -hydroxy- α -amino acid product. This was confirmed by $^1\text{H-NMR}$ spectroscopy, with the spectrum showing the presence of the β -OH with a singlet peak at 3.32 ppm integrating to 1H, α -CH at 4.07 ppm (singlet, 1H), and residual β -CH(OH) at 4.95 ppm (also present is the requisite peak for the α -NH, at 5.17 ppm). Deuterium incorporation assessed by $^1\text{H-NMR}$ spectroscopy was assigned as >90%. HRMS also confirmed the presence of the desired deuterated product, showing $[\text{M}+\text{H}]^+$ at the required m/z of 465.1495. An *e.e.* of 78% by chiral HPLC analysis was obtained for (**422**), which is within experimental error of the 83% *e.e.* of the starting material aziridine *cis*-(**385**). Further to the synthesis of (**422**), hydroxy ring-openings were carried out on the C2-deutero and C2-C3-deutero versions of *cis*-(**385**) (*cis*-(**350**), and *cis*-(**403**)), and the results of these are shown in Scheme 170.



Scheme 170: Synthesis of α - and α,β -deutero- β -hydroxy- α -amino acid derivatives (**423**) and (**424**)

These reactions proceeded well, producing both **(423)** and **(424)** in 86% yield. Formation of the desired products was confirmed by both $^1\text{H-NMR}$ and HRMS; with peaks present in the $^1\text{H-NMR}$ spectrum of **(423)** consistent with the $\alpha\text{-NH}$ (5.17 ppm, 1H), $\beta\text{-CH}_2$ (4.93 ppm, 1H) and $\beta\text{-OH}$ (3.33 ppm, 1H); while within the $^1\text{H-NMR}$ spectrum of **(424)** only residual peaks for the $\alpha\text{-}$ and $\beta\text{-CH}$ groups were found. Unusually, both $\alpha\text{-NH}$, and $\beta\text{-OH}$ peaks within the $^1\text{H-NMR}$ of **(424)** have been suppressed, possibly by H/D exchange; however, the source of this deuterium is unknown. A comparison of the peaks present within the 3.1 – 5.3 ppm regions of the $^1\text{H-NMR}$ spectra of **(422)** – **(424)** is shown in Figure 93 in order to demonstrate the suppression of the $\alpha\text{-CH}$, or $\beta\text{-CH}$ peaks by $\alpha\text{-}$, $\beta\text{-}$, or $\alpha\text{-}\beta\text{-}$ deuteration.

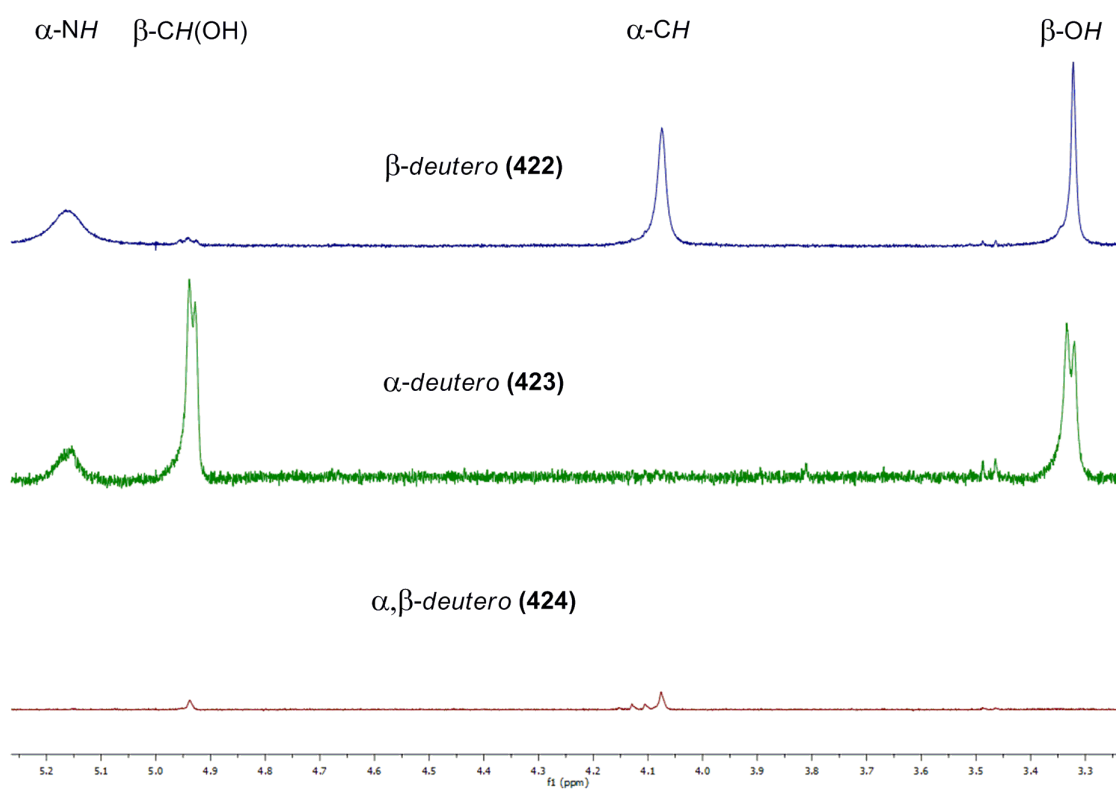
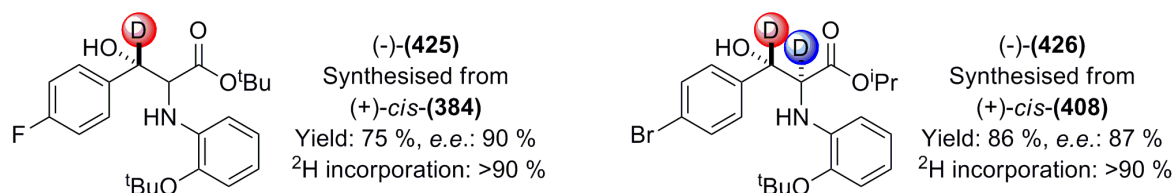


Figure 93: Comparison of the peaks present within the 3.1 – 5.3 ppm regions of the $^1\text{H-NMR}$ spectra of **(422)** – **(424)**

Further to confirmation of the formation of **(423)** and **(424)**, deuterium incorporation was also measured by $^1\text{H-NMR}$ integration; with levels of >90% recorded for both compounds. HRMS provided further confirmation of the deuterated products, with $[\text{M}+\text{H}]^+$ ions detected at the required m/z for both compounds (**(423)** m/z found 465.1495, required 465.1494; **(424)** m/z found 466.1556, required 466.1557). Unfortunately, decomposition of these products was found to be rapid; and thus no HPLC separation of **(423)** was possible. However, the *e.e.* of **(424)** was shown to be 80% by chiral HPLC.

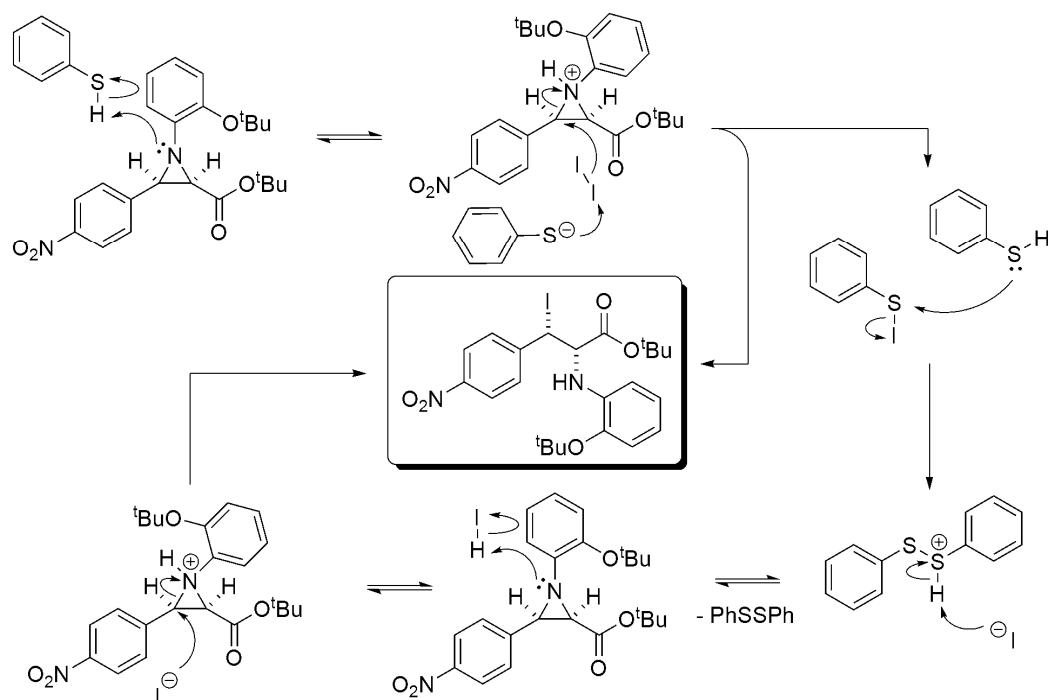
With the success of these reactions, it was decided to attempt the hydroxy ring-opening upon other substrates; these being the C3-*deutero*-C3-(*para*-fluoro)phenyl aziridine *cis*-(**384**), and the C2,C3-*deutero*-C2-*isopropoxy* ester functionalised aziridine *cis*-(**408**). These substrates were submitted to the ring-opening procedure as shown in Scheme 169, and the desired β -hydroxy- α -amino acid derivatives (**425**), and (**426**) were obtained (Scheme 171).



Scheme 171: Synthesis of β - and α - β -*deutero*- β -hydroxy- α -amino acid derivatives (425**) and (**426**)**

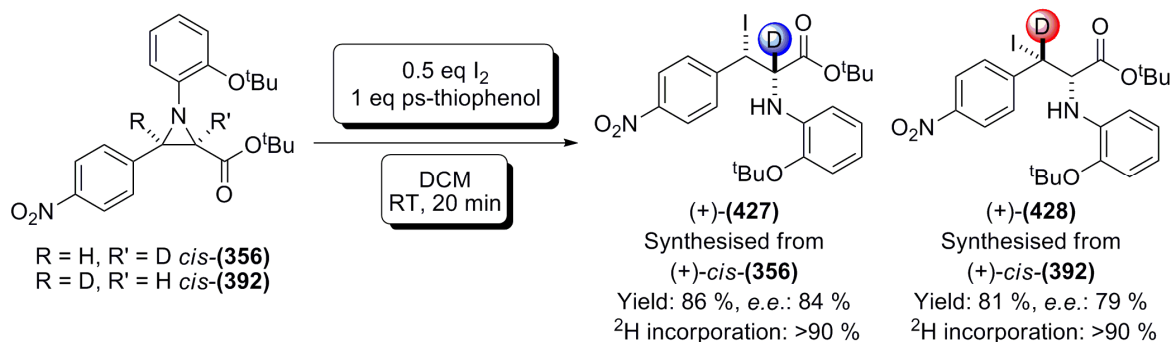
As demonstrated within the previous syntheses, yields were good, with (**425**) being afforded in a 75% yield after purification, while (**426**) was obtained in an 86% yield. The enantiomeric excesses of (**425**) and (**426**) were 90% and 87% respectively. Assignment of the peaks within the ^1H -NMR spectra of (**425**) and (**426**) was aided by the knowledge obtained during the deuteration study of compounds (**422**) – (**424**), as the peaks seen within these spectra followed similar patterns. Thus, the ^1H -NMR spectrum of (**425**) contained peaks relating to the α -NH (5.17 ppm, 1H), α -CH (4.09 ppm, 1H), and β -OH (3.30 ppm, 1H); whereas the spectrum of (**426**) contained peaks relating to the α -NH (5.17 ppm, 1H), the characteristic $\text{CH}(\text{CH}_3)_2$ (confirming retention of the *iso*-propoxy group, 4.94 ppm, 1H), and the β -OH (3.22 ppm, 1H).

Finally within the exploration of ring-opening methodologies, a set of ring-opening reactions were carried out based upon the use of a halide ion as the nucleophile. This methodology was provided by Wu *et al*, whereby the researchers had demonstrated the use of iodine and a catalytic amount of thiophenol to achieve the ring-opening of aziridines.²⁹⁵ The mechanism of the reaction allows this procedure to proceed cleanly, as the only by-product should be diphenyl disulphide (Scheme 172).



Scheme 172: Proposed mechanism for the ring-opening of aziridines by thiophenol and molecular iodine by Wu *et al*

Utilising a modification of the Wu procedure with polymer-bound thiophenol, ring-openings were carried out upon the C3-(*para*-nitro)phenyl aziridines *cis*-(**356**), and *cis*-(**392**). The reaction conditions and results are shown in Scheme 173.



Scheme 173: Syntheses of α -, and β -deutero- β -iodo- α -amino acid derivatives (427**) and (**428**)**

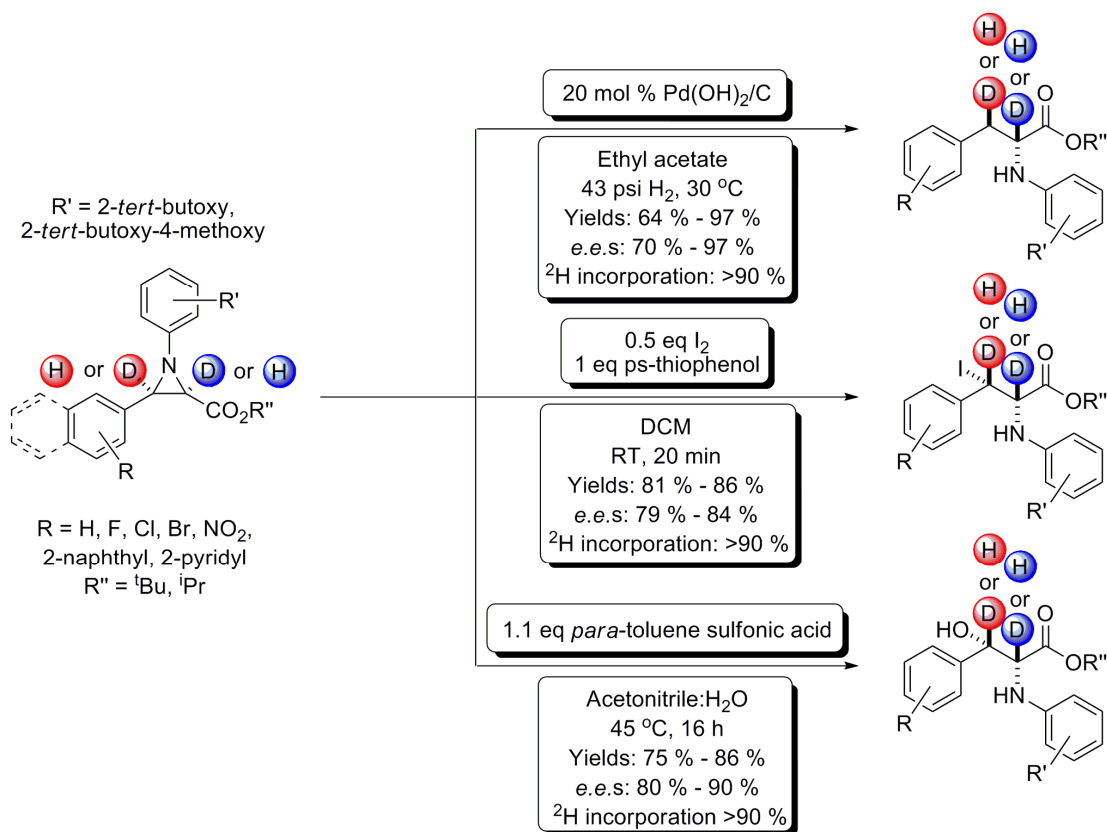
The relative simplicity of the procedure was unfortunately offset by the rapid decomposition of the products; and the first attempts to synthesise these compounds were met with failure. However, after careful consideration, the reaction was carried out in the dark, followed by filtration and column chromatography, again in the dark, and immediate characterisation. This approach led to the results shown in Scheme 173, with (**427**) and (**428**) afforded in good yields of 86% and 81%.

Confirmation of the regioselectivity of the ring-opening reaction to form the desired β -iodo- α -amino acid derivatives was provided by $^1\text{H-NMR}$ spectroscopy. Thus, the $^1\text{H-NMR}$ spectrum of (**427**) contained a singlet peak at 5.56 ppm, integrating to 1H,

consistent with the β -CH; and a further broad singlet at 5.28 ppm, integrating to 1H, consistent with the α -NH. A residual peak for the α -CH was also seen at 4.06 ppm, and integration of this against the β -CH peak provided the deuterium incorporation value of >90%. The ^1H -NMR spectrum of (**428**) contained two doublets, both integrating to 1H, at 5.28 and 4.06 ppm respectively. These were consistent with the α -NH, and α -CH. The coupling constants of these peaks were 9.7 and 9.7 Hz respectively; suggesting coupling between the two, consistent with a regioselective ring-opening to the desired β -iodo- α -amino species. Again, deuterium incorporation of >90% was quantified by integration of the α -CH peak against the residual β -CH at 5.58 ppm. Further evidence for the presence of both deuterium and iodine within (**427**) and (**428**) was obtained by HRMS, with the desired $[\text{M}+\text{H}]^+$ ions being detected at the required m/z of 542.1252 (**427**) and 542.1253 (**428**) (theoretical 542.1257).

The enantiomeric excesses achieved were also good, with *e.e.s* of 84% and 79% measured for (**427**) and (**428**) respectively. However, comparison of the *e.e.* of (**428**) with the starting material *cis*-(**392**) shows a significant loss of 14%. This was unexpected, as (**427**) shows only 4% loss from the 88% *e.e.* of *cis*-(**356**) which can be accounted for by experimental error.

7.1.3: Synthesis of Deuterated α -amino acids – Summary and Conclusions



Scheme 175: Summary of the ring-opening reactions developed *vide supra*

A summary of the ring-opening reactions developed above is shown in Scheme 175. In general, three differing ring-opening reactions have been attempted; all of which, in the main, allow for the retention of enantioenrichment, and deuterium incorporation, inherent within the aziridine starting materials.

Despite these successes, it is worthy of note that some of the amino acid products from these ring-opening reactions are prone to decomposition. Thus care should be taken upon synthesis of these compounds to ensure they are stored correctly under inert gas at low temperature.

The reactions above are a very small range of examples of the ring-opening chemistry of aziridines available within the literature (See 3.4: *Aziridines: Utilisation in Synthesis*). Therefore, it may be possible to apply many other ring-opening techniques to the aziridines produced by the methodologies developed (*vide supra*); however, within the timescale of this project, no other ring-opening methodologies were investigated.

7.2.1: 'Dialled in' Asymmetric Syntheses of α -amino acid Derivatives containing Multiple Isotopic Labels – Introduction

With the chemistry developed so far, the emphasis has been upon probing the possibilities and reactivity of the one pot aziridination methods, deuteration techniques, and ring-opening chemistries; and synthesising a broad range of materials. However, as the chemistry available increased, the 'dialled in' approach began to seem more viable (A summary of the 'dialled in' methodology can be found in Appendix 7). Thus, at this stage, several products were chosen as targets; and directed syntheses of these were undertaken *via* the 'dialled in' approach. In order to test the 'dialled in' methodologies appropriately, it was decided to incorporate multiple isotopic labels within the target molecules, and also, to generate these targets by a range of the ring-opening chemistry available. The molecules chosen are shown in Figure 94.

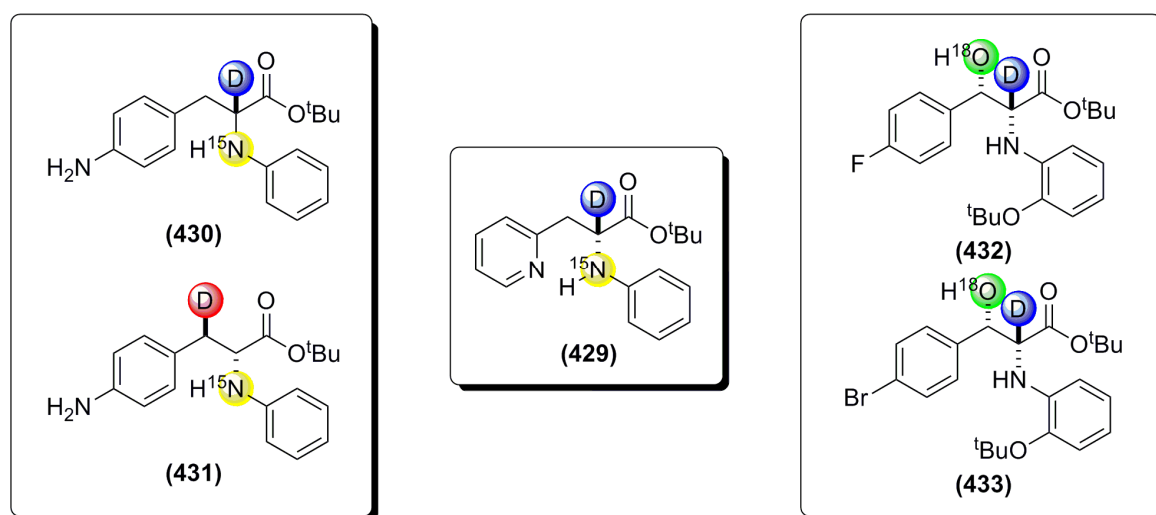
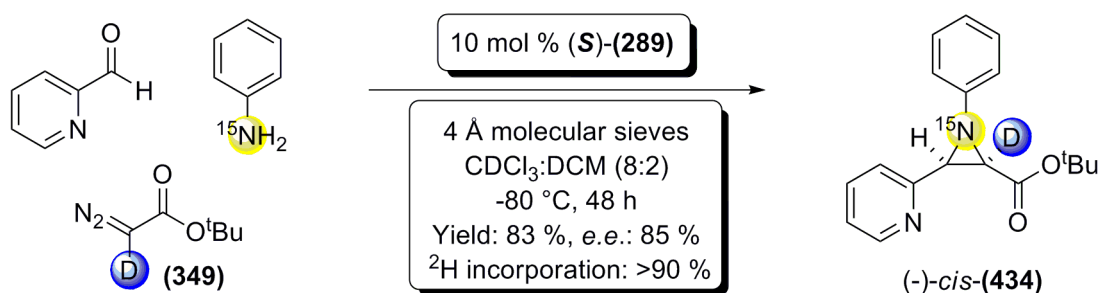


Figure 94: Targets set for testing of the 'dialled in' approach to the synthesis of α -amino acid derivatives bearing multiple isotopic labels

7.2.2: 'Dialled in' Asymmetric Syntheses of α -amino acid Derivatives containing Multiple Isotopic Labels – 'Dialled in' syntheses of (429) to (433)

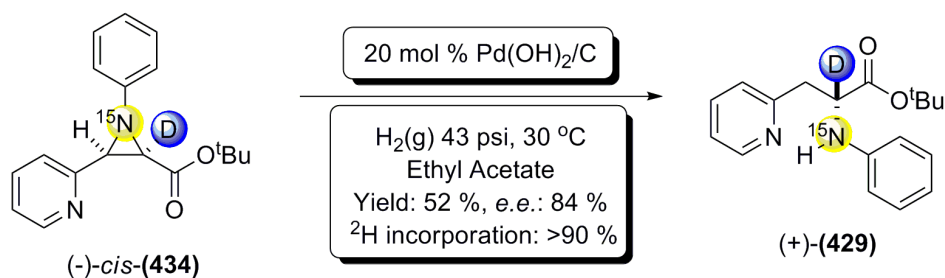
The first target to be attempted was the α -deutero- α - ^{15}N amino acid derivative (429). The 'dialled in' approach dictated that the intermediate required was the C2-deutero-C3-(2-pyridyl)- ^{15}N -aziridine-2-carboxylate ester, *cis*-(434), shown in Scheme 176. Thus, according to the 'dialled in' methodologies; pyridine-2-carboxaldehyde, ^{15}N -aniline, and deuterated *tert*-butyl diazoacetate ($^1\text{BDA-d}$ (349)) were submitted to the asymmetric one-pot aziridination methodology developed (*vide infra*), utilising 10 mol % (*S*)-(289) as the catalyst. The results of this reaction are shown below (Scheme 176).



Scheme 176: Synthesis of the C2-deutero- ^{15}N -aziridine *cis*-(434)

The reaction proceeded smoothly, and following the established work-up procedure and column chromatography, *cis*-(434) was obtained in an 83% yield. Subsequent analysis by ^1H - and ^{13}C -NMR spectroscopic techniques, and HRMS, confirmed the presence of both the ^{15}N and deuterium labels. ^{15}N is active within ^{13}C -NMR spectroscopy, and with a spin (*I*) of $1/2$, will split ^{13}C lines into two lines of equal intensity.²⁷⁶ This effect can be seen when considering the ^{13}C -peak associated with the C3 carbon of *cis*-(434), which has been split into two lines at 47.7, and 47.8 ppm. Confirmation of the C2 deuteration of *cis*-(434) was obtained by ^1H -NMR spectroscopy, as the C2-*H* doublet has been suppressed (residual peak present at 3.17 ppm), with the C3-*H* peak (3.67 ppm, 1H) now a singlet. Relative integrations of these peaks suggested deuterium incorporation of >90%, while the *cis*-stereochemistry of *cis*-(434) was confirmed by the coupling constant of the residual C2-*H* peak, which was found to be 6.9 Hz, well within the 5 – 9 Hz expected for a *cis*-aziridine.²⁶⁶ Further to the NMR spectroscopic data, HRMS confirmed the presence of both deuterium and ^{15}N , with the desired $[\text{M}+\text{H}]^+$ ion being found at the required m/z 299.1629 (theoretical m/z 299.1631). Finally, chiral HPLC of the sample revealed an *e.e.* of 85%.

With the intermediate aziridine *cis*-(434) in hand, the next step was hydrogenolysis of the aziridine ring to give the desired product (429) (Scheme 177). This was carried out using the standard method developed *vide infra*.



Scheme 177: Synthesis of the α -deutero- α -¹⁵N amino acid derivative (429**)**

Although the reaction proceeded smoothly, purification of the final product proved difficult, as purification by column chromatography gave some overlap between materials. However, the desired chiral non-racemic α -deutero- α -¹⁵N-amino acid derivative (**429**) was afforded in a 52% yield, with an *e.e.* of 84% by chiral HPLC. This value was within the range of complete retention of enantioenrichment from the starting aziridine *cis*-(**434**) (85% *e.e.*).

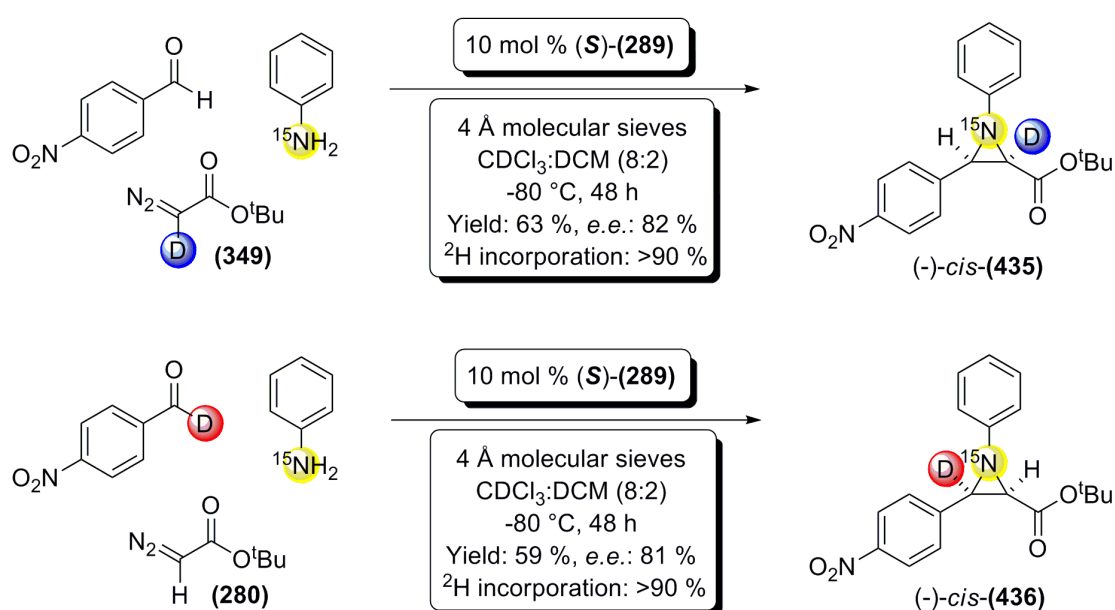
The regioselectivity of the ring-opening hydrogenolysis was confirmed by ¹H-NMR spectroscopy, with a singlet found for the β -CH₂ at 3.24 ppm, with an integration of 2H. ¹³C-NMR and HSQC experiments provided further confirmation of the α -amino product, with a signal indicating coupling between the AB doublet peak corresponding to the diastereotopic β -CH₂ (3.24 ppm), and the β -CH₂ signal at 40.5 ppm within the ¹³C-NMR spectrum. This coupling would not be present if the β -amino product had been formed, as the presence of the α -deuterium would split and suppress the ¹³C signal,²⁷⁶ therefore removing the coupling. Also, if the 40.5 ppm ¹³C peak were related to the β -product, coupling with the ¹⁵N nucleus would be expected, splitting the signal into two lines; which is not the case. Final confirmation of the α -amino product structure was provided by a ¹⁵N- ¹H-HMBC experiment (which provides correlations over two to four bonds),²⁷⁶ where a correlation was found between the ¹⁵N signal and the β -CH₂ group (¹H-NMR, 3.24 ppm), three bonds away. Full NMR spectroscopic data for compound (**429**) can be found in Appendix 8.

Deuterium incorporation was determined by integration of the ¹H-NMR spectrum, with the relative integrations of the β -CH₂ signal, and residual α -CH peak giving a value of >90% incorporation. Retention of the ¹⁵N enrichment, and deuterium incorporation were also confirmed by HRMS, with the desired peak for [M+H]⁺ being present at *m/z* 301.1791 (required *m/z* 301.1787).

Therefore, with this reaction, the first target molecule for the ‘dialled in’ synthesis was obtained in an overall 42% yield over the three-component one-pot asymmetric

aziridination and ring-opening steps, with an *e.e.* of 84%, and deuterium incorporation of >90%.

The next targets to be attempted were the compounds (**430**) and (**431**), consisting of a β -(*para*-amino)phenyl functionalised α -amino acid derivative, labelled with α - ^{15}N , and either α -deuterium (**430**) or β -deuterium (**431**). The ‘dialled in’ synthesis method employed dictated the required intermediates to be either a *C2-deutero*, or *C3-deutero* *C3*-(*para*-nitro)phenyl- ^{15}N -aziridine-2-carboxylate ester (*C2-deutero* (**435**), *C3-deutero* (**436**)). Therefore, ^{15}N -aniline, 4-nitrobenzaldehyde (or 4-nitrobenzaldehyde-*d*), and deuterated *tert*-butyl diazoacetate (**349**) (or *tert*-butyl diazoacetate (**280**)) were submitted to the one-pot asymmetric aziridination protocol utilising (*S*)-(**289**) as the catalyst (Scheme 178).



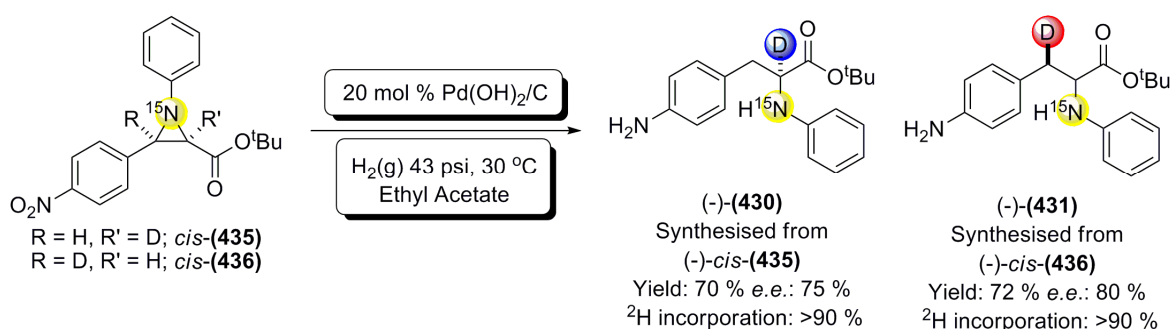
Scheme 178: Syntheses of the chiral non-racemic *C2*- or *C3-deutero* *C3*-(*para*-nitro)phenyl- ^{15}N -aziridine-2-carboxylate esters *cis*-(**435**) and *cis*-(**436**)

The results of these aziridinations were reasonable, with yields of 63% and 59% respectively. The enantiomeric excesses of the products were good, with a value of 82% achieved for *cis*-(**435**), and 81% achieved for *cis*-(**436**).

Confirmation of ^{15}N incorporation was obtained by both ^{15}N - ^1H -HMBC, and ^{13}C -NMR spectroscopy for *cis*-(**435**), and by ^{13}C -NMR spectroscopy for *cis*-(**436**). The ^{13}C -NMR spectra for both *cis*-(**435**) and *cis*-(**436**) contained signals relating to either the *C3* position (46.06, 45.99 ppm, *cis*-(**435**)), or *C2* position (46.67, 46.61 ppm, *cis*-(**436**)), split into two lines by coupling with the adjacent ^{15}N nucleus. The ^1H - ^{15}N -HMBC spectra acquired for *cis*-(**435**) contained a single ^{15}N peak, and correlations of this nucleus with the *C3-H* (3.52 ppm, ^1H -NMR), residual *C2-H* (3.13 ppm, ^1H -NMR), and aromatic protons of the *N*-phenyl group. Deuterium incorporation within *cis*-(**435**) and *cis*-(**436**) was measured

by $^1\text{H-NMR}$ spectroscopy, with the relative integrations of the C3-*H* and residual C2-*H* peaks (*cis*-(**435**), 3.52 ppm, and 3.13 ppm respectively), or C2-*H* and residual C3-*H* peaks (*cis*-(**436**), 3.13 ppm, and 3.52 ppm respectively) confirming deuterium incorporation of >90% for both compounds. The coupling constants of the residual C2-*H* (*cis*-(**435**), 6.8 Hz), and residual C3-*H* (*cis*-(**436**), 6.7 Hz) peaks also confirmed the *cis*- stereochemistry of the products, with the values within the range of 5 – 9 Hz expected of a *cis*-aziridine.²⁶⁶ Finally, HRMS revealed the desired $[\text{M}+\text{H}]^+$ ions at m/z 343.1527 (*cis*-(**435**)), and m/z 343.1533 (*cis*-(**436**)) (Theoretical m/z 343.1529).

With the required C2- or C3-*deutero* C3-(*para*-nitro)phenyl- ^{15}N -aziridine-2-carboxylate ester intermediates *cis*-(**435**) and *cis*-(**436**) in hand, the compounds were submitted to the developed hydrogenolysis methodology as dictated by the ‘dialled in’ synthesis; with reduction of the nitro group expected alongside the ring-opening reaction (Scheme 179).



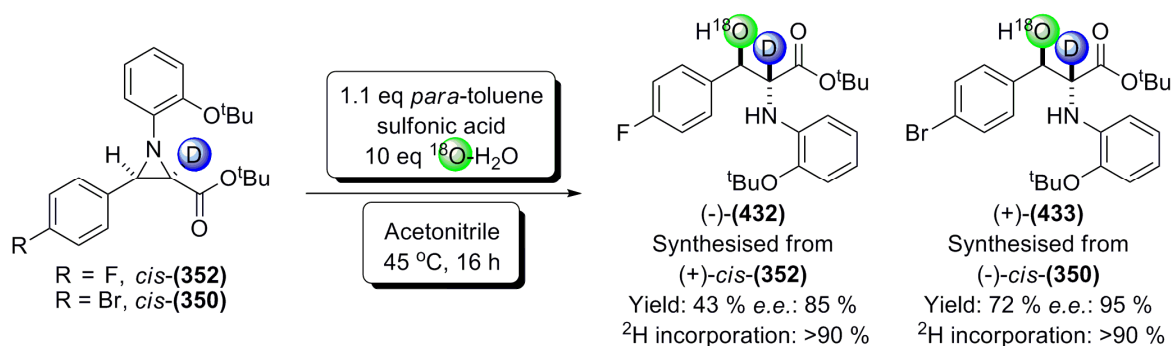
Scheme 179: Syntheses of the α - or β -*deutero* β -(*para*-amino)phenyl- α - ^{15}N amino acid derivatives (-)-(430) and (-)-(431)

As shown in Scheme 179, the ring-opening reactions proceeded well, in yields of 70% and 72% for (**430**) and (**431**) respectively. As expected, $^1\text{H-NMR}$ spectroscopy confirmed both the formation of the desired α -amino products and the reduction of the nitro functionality. Thus, peaks were present within the $^1\text{H-NMR}$ spectra of (**430**) and (**431**) for either the β - CH_2 ((**430**), 2.91 ppm, 2H), or the α - CH and β - CH ((**431**), 4.16 ppm, 1H; 2.96 ppm, 1H, respectively); while both contained a broad singlet peak at 3.60 ppm corresponding to the amine functionality. $^1\text{H-NMR}$ spectroscopy also revealed deuterium incorporation of >90%. $^{13}\text{C-NMR}$ spectroscopy confirmed the presence of ^{15}N in (**431**), with splitting of the peak related to the α -carbon into two signals of equal intensity (58.4 & 58.3 ppm), due to the presence of the neighbouring ^{15}N nucleus.²⁷⁶ Confirmation of the presence of ^{15}N within (**430**) could not be obtained by $^{13}\text{C-NMR}$ spectroscopy due to the presence of the α -deuterium splitting and reducing the α - ^{13}C peak into the baseline. Finally, HRMS confirmed the formation of both desired compounds, with the presence of

$[M+H]^+$ at the required m/z of 315.1939 (**430**), and 315.1939 (**431**) (Theoretical m/z 315.1944).

Therefore, with these reactions, two further target molecules had been synthesised, (**430**) and (**431**); overall yields from starting materials for these were 44% (75% *e.e.*, >90% deuterium incorporation), and 43% (80% *e.e.*, >90% deuterium incorporation) respectively over two steps.

The final two products to be synthesised using the ‘dialled in’ approach were to be the α -deutero- β - ^{18}O -hydroxy- α -amino acid derivatives (**432**) and (**433**); both were based upon existing aziridines synthesised within the work above, thus the syntheses of these intermediates (*cis*-(**352**) and *cis*-(**350**)) are not discussed here. However, the hydroxyl ring-openings with ^{18}O -enriched water that were required are shown in Scheme 180.



Scheme 180: Syntheses of the α -deutero- β - ^{18}O -hydroxy- α -amino acid derivatives (432**) and (**433**)**

As shown above, both ring-openings were successful, although the yield of (**432**) was lower than had been hoped due to a difficult purification. Despite the disappointing yield of (**432**), both products were afforded with good enantioselectivities of 85% and 95% *e.e.* for (**432**) and (**433**) respectively. Deuterium incorporation was also good, with >90% incorporation achieved in both cases as measured by ^1H -NMR spectroscopy. ^1H -NMR spectroscopy also confirmed the regioselectivity of the hydroxy ring-opening, with both (**432**) and (**433**) showing the requisite peak for the β -CH (4.94 ppm (**432**), 4.87 ppm (**433**)), and residual peak for the deuterated α -position 4.05 ppm (**432**), 4.03 ppm (**433**)). These peaks were also found to be consistent with the standard β -hydroxy amino acids (**422**) – (**425**) produced previously, as would be expected. The presence of ^{18}O could not be confirmed by NMR techniques, but HRMS confirmed the presence of ^{18}O in both compounds, with the required $[M+H]^+$ ions detected at m/z 407.2333 ((**432**) theoretical m/z 407.2337), and m/z 467.1536 ((**433**) theoretical m/z 467.1524).

Thus, the final two target molecules had been synthesised; with an overall yield (over aziridination and ring-opening) for (**432**) of 24% (*e.e.* of 85%, ^2H incorporation >90%), and for (**433**) of 63% (*e.e.* of 95%, ^2H incorporation >90%).

Chapter 8: Spectroscopic and Computational Investigations

8.1: Introduction

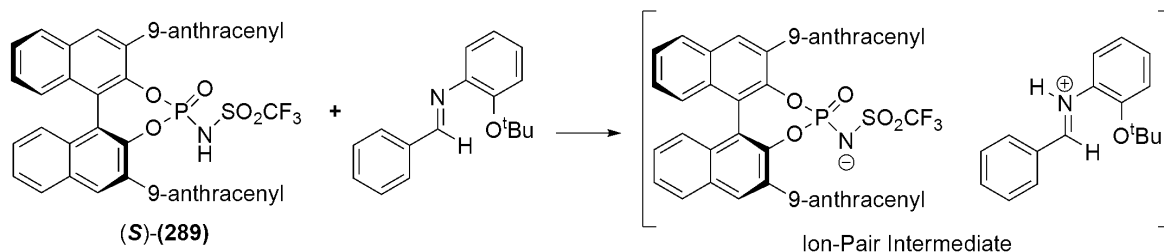
Throughout the work detailed above, several questions arose which required the use of spectroscopic and/or computational methods to answer: The first of these being the nature of the interaction leading to enantioselectivity within the aziridination reactions; and the second being the assignment of the absolute stereochemistry of the chiral aziridine products.

Investigations into the nature of the aziridination reaction intermediate were fuelled by a desire to prove the interaction between the chiral catalyst and the achiral imine. It was believed that due to the inherent pK_a difference between the highly acidic catalyst (**289**) (pK_a ca. -1),¹⁹⁷ and the starting material imines (pK_a ca. 24),²⁶⁷ protonation of the imine would be rapid. However, the nature, or indeed, the presence, of any subsequent interactions between the catalyst and iminium species had not been proven. Investigations into this phenomenon follow *vide infra*.

Despite obtaining a crystal structure of the enantioenriched aziridine *cis*-(**357**) produced utilising the methods detailed within this thesis; it had proven impossible to determine the absolute stereochemistry transferred to the product aziridines from the catalyst (**289**), beyond the *cis*- nature of the products. Therefore, it was decided to attempt to employ computational chemistry, combined with spectroscopic techniques, in order to provide insight into the stereochemistry of the aziridines (and subsequent products) produced *vide supra*. Details of this work are the subject of Section 8.3.

8.2: Determination of a Chiral Intermediate Utilising Circular Dichroism Techniques

As has been hypothesised previously (see 4.2.4: *Hypothesis upon the enantioselectivity of the asymmetric one-pot aziridination reaction*) it is believed that the enantioselectivity of the one-pot aziridination reactions developed within this work arises from the interaction of a starting material imine with the chiral catalyst (**289**). Due to the inherent pK_a differences between these species, it is reasonable to presume that protonation of the imine will be rapid, producing an intermediate ion-pair species of the type shown in Scheme 181.



Scheme 181: Representation of the ion-pair intermediate believed to be formed within aziridination

Due to the steric bulk and chiral nature of (**289**), it was believed that the ion-pair formed would itself be chiral, and thus, evidence for its existence could be provided by Circular Dichroism (CD) spectroscopy. CD spectroscopy measures the differences in the absorption of left or right polarised light within a sample; these differences being caused by the chirality of the sample.²⁹⁶ Thus, only chiral materials display a CD spectrum.²⁹⁶

This method seemed ideal for the purposes of determining the presence of a chiral intermediate within the aziridination methodology, as the starting catalyst is chiral, but the starting imine is achiral. Thus, a CD spectrum could be acquired of the catalyst (**289**), providing a background. Upon mixing of the catalyst and imine, a further CD spectrum could be acquired, from which this background could be subtracted, meaning any residual signal would be related to a new chiral intermediate formed from the catalyst and imine (potentially the chiral ion-pair intermediate). The simple imine *N*-benzylidene-2-*tert*-butoxyaniline (**437**) was chosen for this study.

To gain information upon the area of interest within the UV visible range, a standard UV-Vis spectrum was acquired of (*S*)-(**289**); and alongside the CD spectrum of (**289**), these are shown in Figure 95. As can be seen within Figure 98, (**289**) shows useful absorbencies within the range of 410-270 nm, and it was this range which was chosen to be investigated.

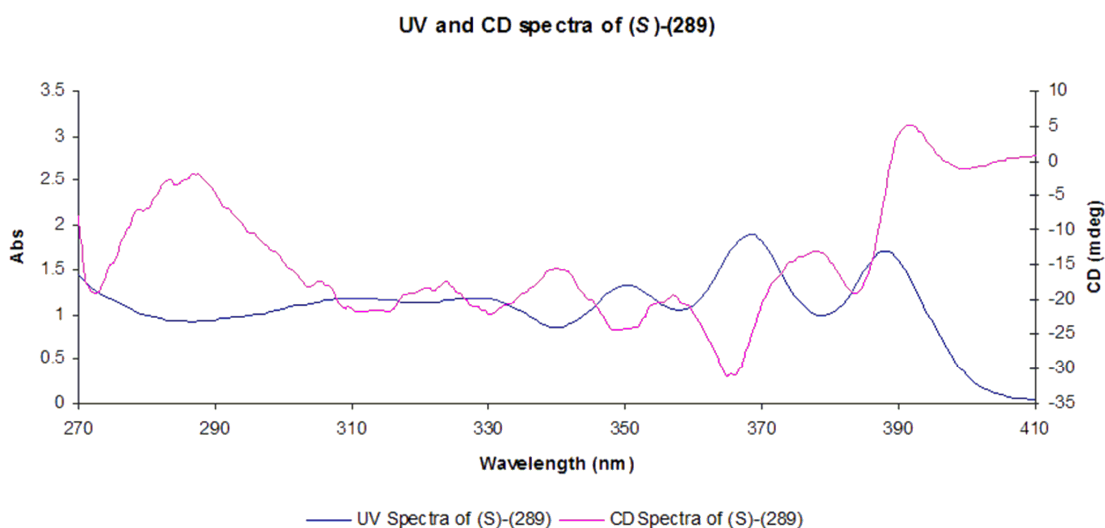


Figure 95: UV and CD spectra of (*S*)-(289**)**

Initially, as the reaction between (**289**) and (**437**) was believed to be rapid and facile, it was decided to simply mix equimolar solutions of the two samples and measure the UV and CD spectra related to the mixture. It is worthy of note that upon mixing of the two samples, a colour change from colourless to slight yellow was noted within 5 to 10 seconds, suggesting an interaction between the two compounds. This interaction was confirmed by acquiring a UV spectrum of the new mixture, and subtracting the baseline

spectra for (289). It is worthy of note that the concentrations of the backgrounds were calculated to be equal to the final concentration of the solutions upon mixing; thus concentration effects can be discounted from the following analysis. The new spectrum showed a general increase in absorbance; and also a shifting of the maximum absorbencies at *ca.* 390 nm, and 370 nm, with the suggestion of a second peak emerging as a shoulder from the peak at 370 nm (Figure 96).

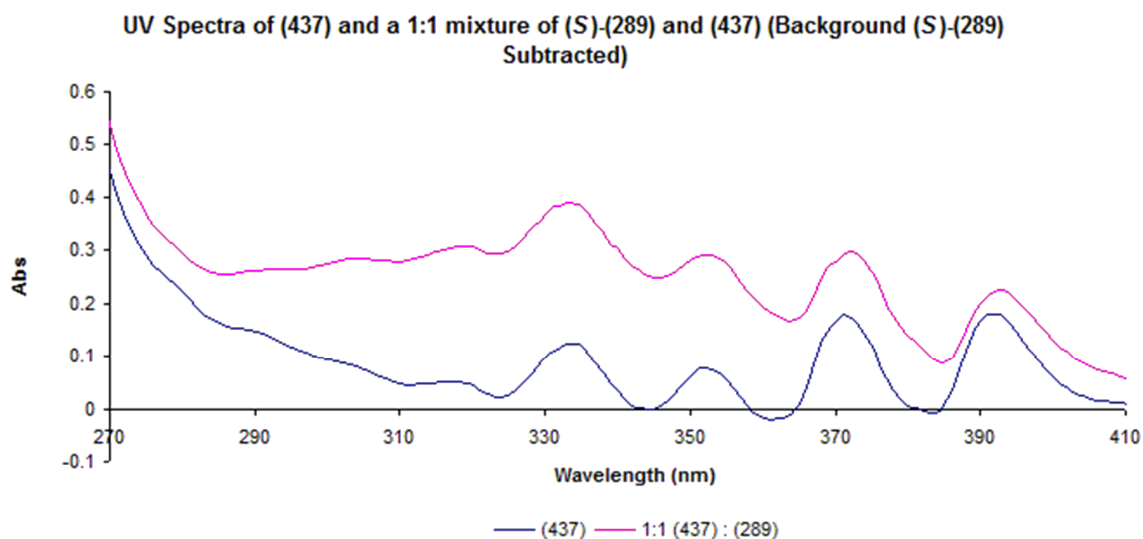


Figure 96: UV spectra of (437) and a 1:1 mixture of (289) and (437)

Interestingly, it was also noted that these changes in absorbance seemed to recede after a short time. Thus, in order to investigate this, a series of UV spectra were taken over a period of 8 minutes, with one complete scan being completed in one minute. The results are shown in Figure 97.

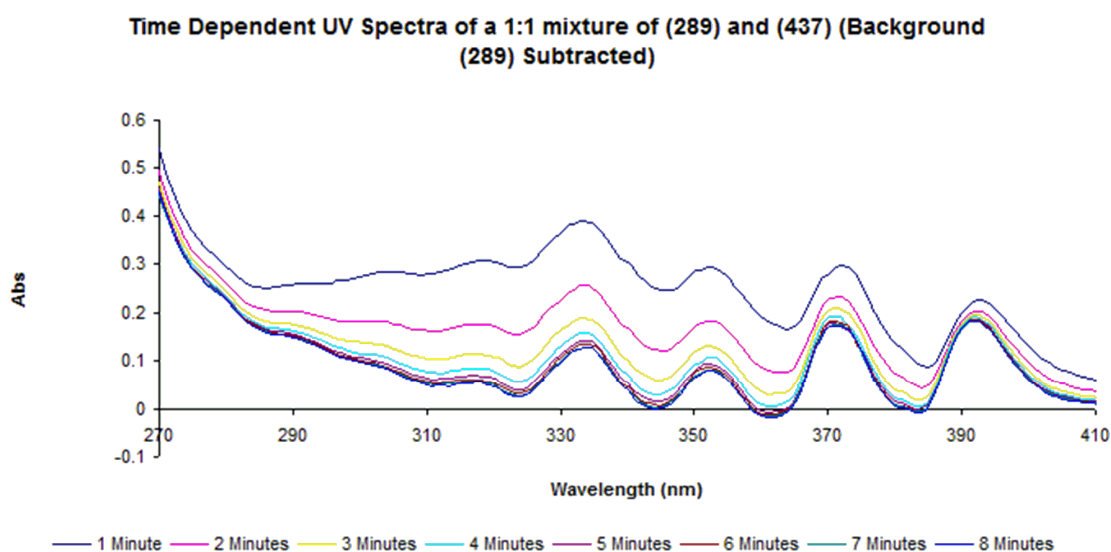
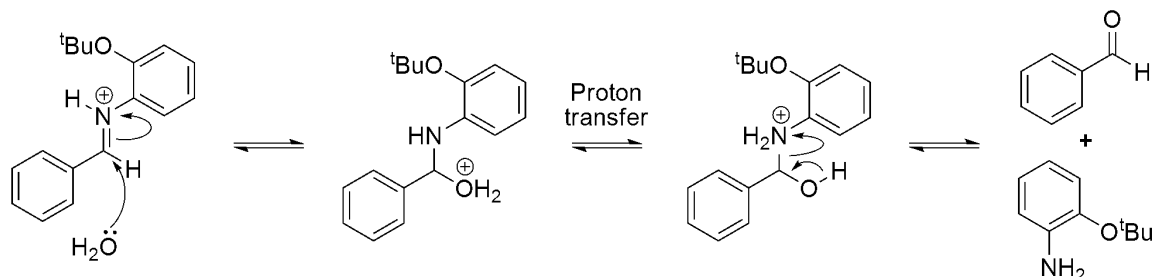


Figure 97: Time Dependent UV Spectrum of a 1:1 mixture of (289) and (437) acquired over 8 minutes

This study appears to suggest that the interaction causing the changes in absorbance is decaying over time; this could potentially be explained by decomposition of

the intermediate iminium species by hydrolysis. Although the solvent used for the study had been stored over molecular sieves, the experiment was not carried out under anhydrous conditions, and also, the concentrations involved within the UV experiment were very low, meaning little water would be required to cause decomposition (Scheme 182).



Scheme 182: Potential decomposition of the intermediate ion-pair *via* imine hydrolysis

Despite the apparent decomposition of the iminium intermediate, evidence of an interaction had been shown by UV; thus it was decided to go ahead with a similar set of experiments with CD spectroscopy. The use of CD spectroscopy would remove achiral species from the acquired spectrum, meaning that by subtracting the initial CD spectrum of (**289**) from the acquired data, any residual signal would have to come about due to the presence of the intermediate observed within UV spectroscopy; and also, that this intermediate would have to be chiral.

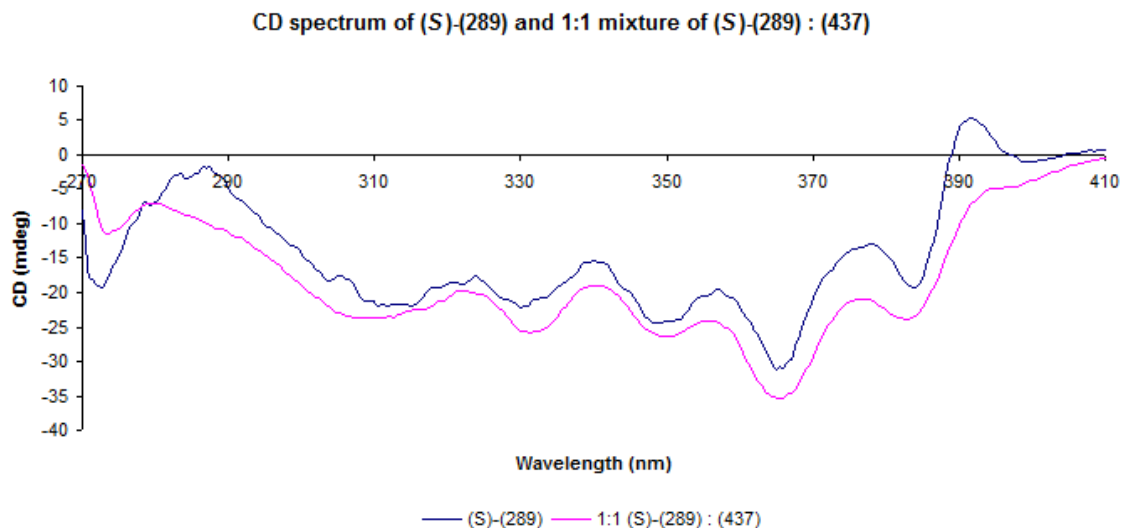


Figure 98: CD Spectra of (*S*)-(289) and a 1:1 mixture of (*S*)-(289) and (437)

Shown in Figure 98 is the initial background CD spectrum of (*S*)-(289) and also, the CD spectrum arising from the 1:1 mixture of (*S*)-(289) and (437). As is shown, a significant change in the CD spectrum is observed; related to this, the spectrum resulting from the subtraction of the background spectra for (*S*)-(289) is shown in Figure 102. The subtracted spectrum clearly shows the presence of a chiral intermediate species, with a significant peak being observed at 390 nm. Having noted a decomposition of the

intermediate species within UV spectrum, it was decided to also investigate this effect within the CD spectrum, using the signal at 390 nm as our probe. Thus, in a similar experiment to that carried out with UV spectroscopy, a time dependant CD spectrum was acquired over 8 minutes, with one spectra being acquired every minute. This spectrum is also shown in Figure 99.

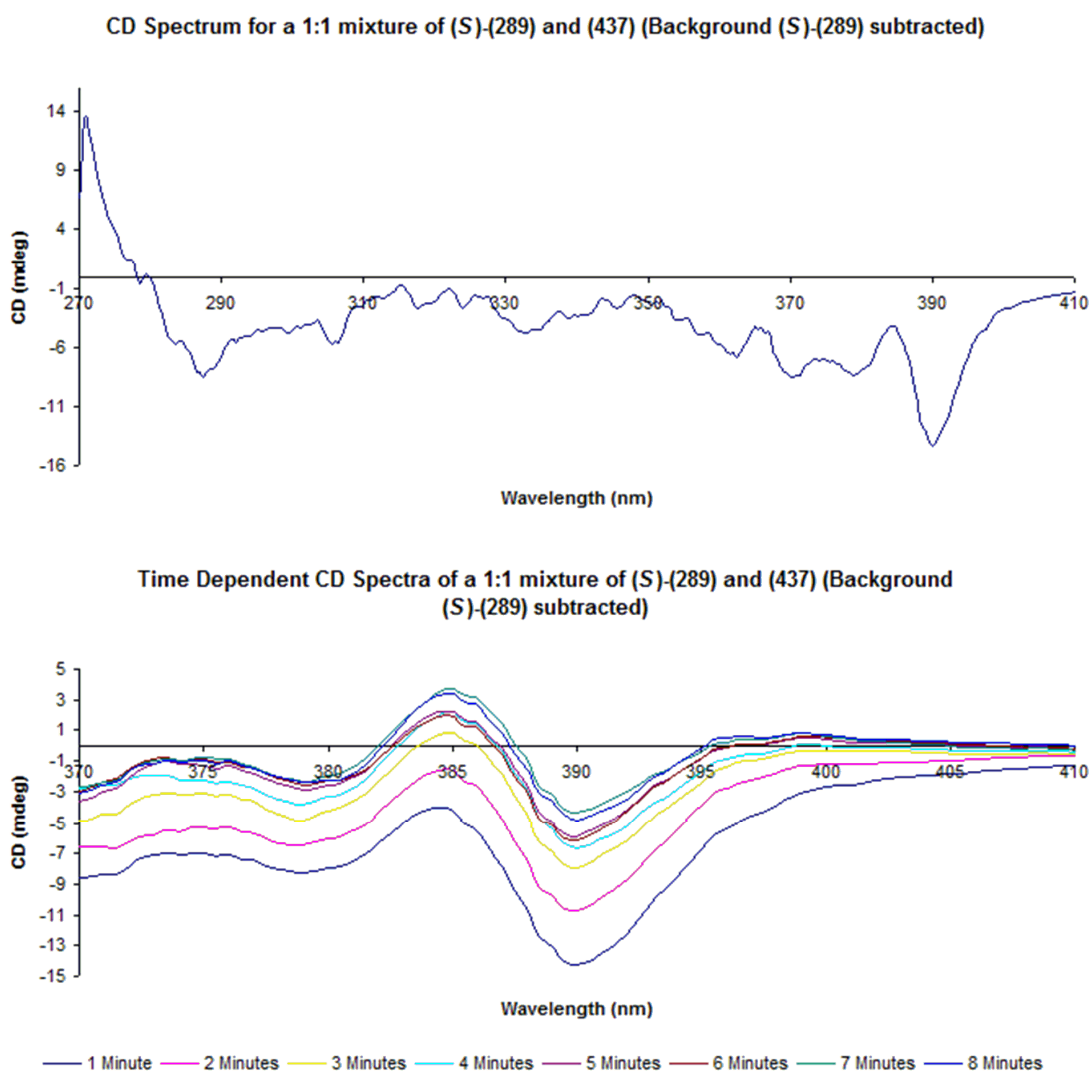


Figure 99: CD spectra for a 1:1 mixture of (S)-(289) and (437); and time dependent CD of the 410 – 370 nm wavelength range

Consistent with the UV traces, the CD signal also shows decay back to a baseline level over a period of around 8 minutes. This strengthens the theory that the observed differences within the UV spectrum arise due to a chiral intermediate, this in turn believed to arise due to continued interaction between the chiral catalyst (S)-(289), and the achiral iminium species.

Unfortunately, despite this evidence for the presence of a chiral intermediate ‘ion-pair’ between the catalyst and iminium species, CD and UV spectroscopies do not provide information into the nature of this interaction; thus no direct conclusions can be drawn

from about the structure, or type, of interaction, other than the presence of a chiral intermediate. Potentially, NMR studies have the possibility of elucidating this interaction, however, this is an area for future work, and has not been covered here.

8.3: Attempted Determination of the Absolute Stereochemistry of *cis*-(**351**) and *cis*-(**358**) via VCD and Computational Methods

As mentioned *vide supra*, during the project, despite the use of x-ray diffraction, determination of the absolute stereochemistry of the aziridines produced with the asymmetric aziridination chemistry developed proved impossible. Thus a differing approach was chosen, relying upon the use of VCD (vibrational circular dichroism) spectroscopy. VCD is essentially ‘chiral IR’ spectroscopy, utilising circularly polarised light and measuring the subsequent interactions with a molecule.²⁹⁷

As VCD is a CD technique, thus only chiral materials are VCD active, and opposite enantiomers will generate mirror image spectra.²⁹⁷ Therefore, if the VCD of each enantiomer of a compound is calculated (utilising computational methods) and a subsequent VCD of the enantioenriched material is acquired, the two can be matched in order to assign stereochemistry.

Although seemingly simple, the process for calculating a VCD spectrum requires consideration. VCD spectra inherently measure vibrational frequencies, and as such, are a composite of all accessible vibrational levels, of all conformers, accessible at the analysis temperature. Also, the presence of deuterium within the molecules of interest has to be considered, due to the difference in vibrational frequencies between deuterium and protium.^{27,28}

Taking the above factors into account, it was decided to begin with an energy minimised structure of both enantiomers of *cis*-(**351**) and *cis*-(**358**); these were calculated within Gaussian 09[®] (utilising the UEA Grace cluster) at the B3LYP/6-31g* level of theory.²⁹⁸ Care had to be taken at this stage to ensure the minimised structures were true minima, as opposed to saddle points within the energy surface; thus the keyword *freq=(readiso)* was included to ensure the absence of imaginary frequencies (present within a saddle point but not within a true minimum), and also that the presence of deuterium was taken into account during the analysis.

These minimised structures were checked to ensure correct convergence within the job, and subsequently were submitted to Spartan ‘10[®] for conformational searching. The conformational searches were carried out utilising a molecular mechanics approach, at the MMFF level, utilising a Monte-Carlo search method.²⁹⁹ As a large area of conformational

space was desired to increase the likely accuracy of the final composite VCD spectrum, the energy difference above the initial level was set to +160 kJ mol⁻¹. This generated 18 distinct conformers for each enantiomer of *cis*-(**351**), and 32 distinct conformers for each enantiomer of *cis*-(**358**). Further to this, searches of up to +1000 kJ mol⁻¹ were carried out, with no new conformers being generated. Several examples of the structures of these conformers are shown in Figure 100:

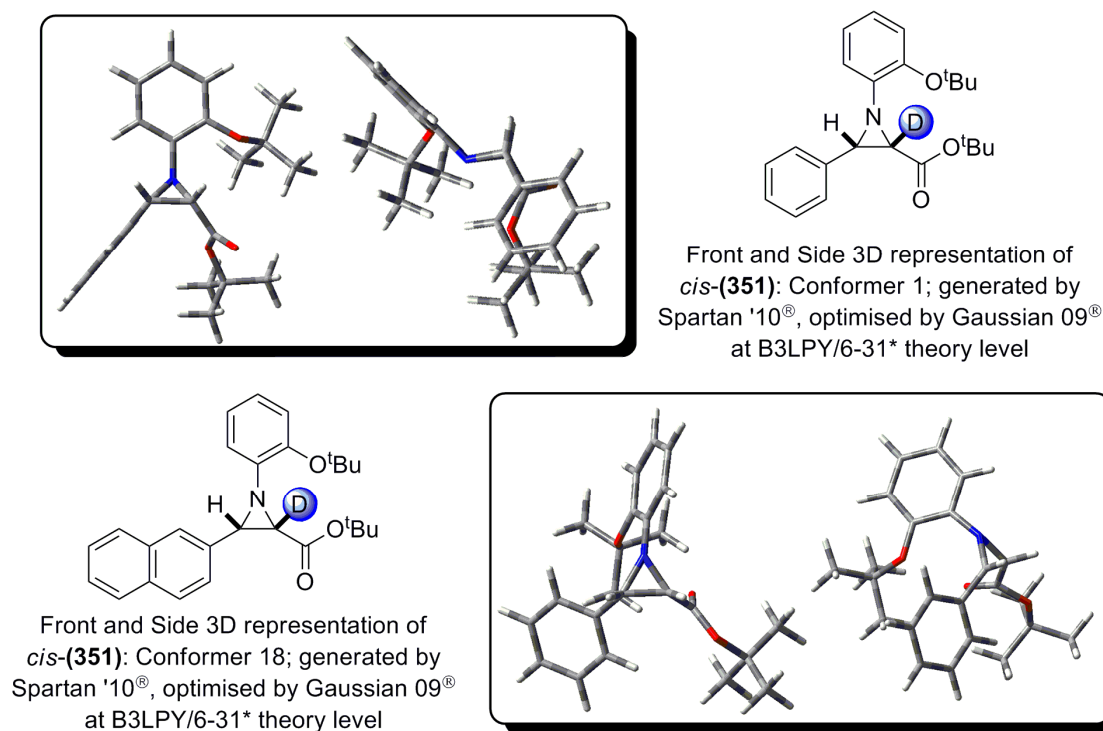


Figure 100: Selected conformers of *cis*-(**351**) generated by Spartan '10[®]

Having investigated an area of conformational space, the conformers generated were again submitted to Gaussian 09[®] for DFT energy minimisation, and frequency checking; also at this point, VCD calculation was carried out (*freq=(readiso,vcd)*; a typical input file can be found in Appendix 9). It is worthy of note that the average CPU time for each analysis related to *cis*-(**351**) was ~10 hours, and ~20 hours for *cis*-(**358**); leading to a total of *ca.* 1640 hours of CPU time; thankfully, the parallel processing available within the cluster reduced the actual processing time to between 1 and 9 hours per job.

Initially, the relevant data from these analyses was the energy of each conformer, and these are shown in Figures 101 and 102. The importance of these energies comes about due to the need for an understanding of the population of each conformer at the temperature of analysis. This is due to the fact that each conformer will produce a unique VCD, thus in order to predict the actual VCD, a weighted average was required. In order to understand the population of each conformer, a Boltzmann analysis of each enantiomer and the related conformers was carried out. The resulting data is also shown in Figures 101 & 102.

$$\frac{N_i}{N} = \frac{e^{-E_{relative} / RT}}{\sum e^{-E_{relative} / RT}}$$

Energy Level	Conformer	Energy (kJ mol ⁻¹)	N _i /N	Energy Level	Conformer	Energy (kJ mol ⁻¹)	N _i /N
0	4	-3085257.011	0.0564	0	4	-3085257.011	0.0563
0	8	-3085257.011	0.0564	0	8	-3085257.011	0.0563
1	1	-3085251.283	0.0563	1	1	-3085251.282	0.0562
2	3	-3085250.076	0.0562	2	3	-3085250.076	0.0562
2	7	-3085250.076	0.0562	2	7	-3085250.076	0.0562
3	2	-3085246.068	0.0561	3	2	-3085246.068	0.0561
4	5	-3085245.214	0.0561	4	5	-3085245.214	0.0561
5	6	-3085243.155	0.0561	5	6	-3085243.155	0.0560
6	9	-3085227.263	0.0557	6	9	-3085227.263	0.0557
6	14	-3085227.262	0.0557	6	14	-3085227.262	0.0557
7	13	-3085222.610	0.0556	7	13	-3085222.610	0.0556
8	15	-3085213.260	0.0554	8	11	-3085220.624	0.0555
9	12	-3085212.106	0.0554	9	15	-3085213.260	0.0554
10	10	-3085187.907	0.0548	10	12	-3085212.106	0.0553
10	11	-3085187.907	0.0548	11	10	-3085188.151	0.0548
11	18	-3085162.695	0.0543	12	18	-3085162.695	0.0543
12	16	-3085156.734	0.0542	13	17	-3085156.742	0.0541
12	17	-3085156.743	0.0542	14	16	-3085156.734	0.0541

Figure 101: Boltzmann distribution data for both enantiomers of *cis*-(351)

Energy Level	Conformer	Energy (kJ mol ⁻¹)	N _i /N	Energy Level	Conformer	Energy (kJ mol ⁻¹)	N _i /N
0	8	-3488919.805	0.0317	0	8	-3488919.805	0.0317
0	17	-3488919.805	0.0317	0	16	-3488919.805	0.0317
1	7	-3488919.702	0.0317	1	7	-3488919.702	0.0317
1	16	-3488919.702	0.0317	2	15	-3488919.702	0.0317
2	2	-3488914.280	0.0316	3	1	-3488914.280	0.0316
3	1	-3488913.643	0.0316	4	2	-3488913.643	0.0316
4	5	-3488912.930	0.0316	5	5	-3488912.930	0.0316
4	14	-3488912.930	0.0316	5	13	-3488912.930	0.0316
5	6	-3488912.646	0.0316	6	6	-3488912.646	0.0316
5	15	-3488912.646	0.0316	6	14	-3488912.646	0.0316
6	4	-3488908.829	0.0315	7	4	-3488908.829	0.0316
7	3	-3488908.532	0.0315	8	3	-3488908.532	0.0316
8	10	-3488908.481	0.0315	9	9	-3488908.481	0.0316
9	11	-3488907.943	0.0315	10	10	-3488907.943	0.0316
10	13	-3488906.257	0.0315	11	12	-3488906.257	0.0315
11	12	-3488906.180	0.0315	12	11	-3488906.180	0.0315
12	9	-3488895.988	0.0314	13	20	-3488890.159	0.0313
13	21	-3488890.159	0.0313	14	17	-3488889.601	0.0313
14	18	-3488889.601	0.0313	15	25	-3488885.430	0.0313
15	26	-3488885.430	0.0312	16	26	-3488884.441	0.0313
16	27	-3488884.441	0.0312	17	18	-3488883.626	0.0313
17	19	-3488883.625	0.0312	18	23	-3488875.587	0.0312
18	24	-3488875.587	0.0311	19	24	-3488874.135	0.0311
19	25	-3488874.134	0.0311	20	21	-3488850.908	0.0308
20	22	-3488850.908	0.0308	21	19	-3488847.566	0.0308
21	20	-3488847.566	0.0308	22	22	-3488838.258	0.0307
22	23	-3488838.258	0.0307	23	31	-3488826.878	0.0306
23	31	-3488826.878	0.0305	24	32	-3488823.992	0.0305
24	32	-3488823.992	0.0305	25	28	-3488819.733	0.0305
25	29	-3488819.733	0.0304	26	30	-3488819.676	0.0305
26	28	-3488819.194	0.0304	27	27	-3488819.194	0.0305
27	30	-3488819.194	0.0304	28	29	-3488819.194	0.0305

Figure 102: Boltzmann distribution data for both enantiomers of *cis*-(358)

Having calculated the relative population of each conformer within *cis*-(351) and *cis*-(358), the VCD data also calculated for each conformer could now be treated with a weighted average, based upon the calculated Boltzmann distribution, thus generating a

prediction of the composite VCD for each enantiomer. The generated VCD spectra are shown in Appendix 9.

As shown in the generated spectra, the calculated values for each enantiomer are mirror images of each other; this is to be expected, as each enantiomer will interact more strongly with circularly polarised light of a specific rotation.

Unfortunately, at this stage, despite the completion of the calculations required, no samples have been submitted to VCD for analysis. This is unfortunate, as the assignment of an aziridine produced with a specific enantiomer of the catalyst (**289**) would allow for assignment of both the aziridines produced within this project, and also, the products produced from them. However, the work above does demonstrate that such predictions are possible, although it remains to be seen to which degree of accuracy the predicted spectra would agree with the experimental data.

8.4: Conclusions and Future Work

Within the two sections contained within this chapter, evidence of a chiral intermediate formed from the interaction between (**289**) and an imine has been provided by CD and UV techniques, and also, computational work has led to the prediction of VCD spectra for both enantiomers of *cis*-(**351**) and *cis*-(**358**).

Future work within these areas could increase the value of this data. For example, NMR studies of the interaction between (**289**) and imines could provide useful insight into the exact nature of these interactions. Whereas, future stereochemical assignment work would be based upon the acquisition of experimental VCD data for compounds *cis*-(**351**) and *cis*-(**358**) in order to test both the accuracy of the computational predictions, and also in order to finally assign the absolute stereochemistry of the aziridines produced within the work previously discussed in this thesis.

Section 3: Experimental

9.1: General Information and Procedures

Drying of Solvents and Reagents

If noted as 'dry' or 'dried', solvents were treated as follows prior to use: acetonitrile was freshly distilled from calcium hydride; chloroform-*d* and chloroform-*h* were stored in darkened glass over flame dried 4Å molecular sieves; dichloromethane (DCM) was freshly distilled from calcium hydride; diethyl ether was freshly distilled from sodium wire and benzophenone; propionitrile was distilled from calcium hydride and stored over flame dried 4Å molecular sieves; tetrahydrofuran (THF) was freshly distilled from sodium wire and benzophenone. All other solvents were used as supplied.

Unless noted, reagents were used as supplied. However, the following reagents were treated as follows before use: phosphorus oxychloride was distilled under reduced pressure and stored under a nitrogen atmosphere; *tert*-butanol was distilled and stored over flame dried 4Å molecular sieves; triethylamine was freshly distilled from calcium hydride; trimethyl borate was freshly distilled from sodium wire.

Sourcing of the Isotopically Enriched Materials

¹⁵N-aniline, and ¹⁸O-water were purchased from Sigma-Aldrich, stored under nitrogen, and used as supplied. Deuterated alkyl diazoacetates (EDA-*d*, ¹BDA-*d*, and ¹PrDA-*d*) were prepared as per the procedures noted within the text, and within 9.9: *Syntheses of starting materials*, and stored under nitrogen in a dry-box.

Characterisation Methods and Instrumentation

¹H-NMR and ¹³C-NMR spectra were acquired at 400 MHz and 100 MHz or 300 MHz and 75 MHz respectively. FT-IR spectra were acquired neat *via* either thin film, or ATR techniques. Low resolution MS spectra were acquired using a Shimadzu 2010A LCMS utilised in either ESI or APCI modes. HRMS were acquired *via* the EPSRC mass spectrometry service centre, Swansea. X-ray crystal structures were acquired either *via* the UEA crystallography service, or *via* the EPSRC X-ray crystal service centre, Southampton.

Reactions carried out under microwave conditions were performed with a Biotage Creator microwave synthesiser. Hydrogenation reactions were carried out using a Biotage Endeavour catalyst screening system.

Preparation of the Cooling Bath for Asymmetric Aziridination Reactions

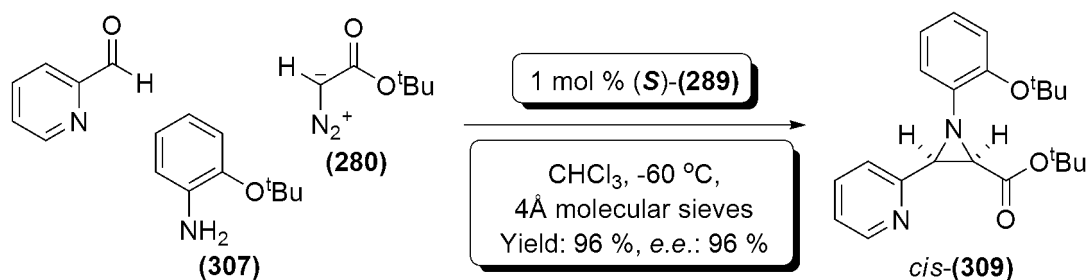
As the asymmetric aziridination reactions require sustained low temperature conditions in order to induce the desired level of enantiomeric excess, the use of an immersion chiller is recommended. The bath was prepared by the addition of *iso*-propanol to a dewar flask of the appropriate size, within which the chiller arm was submerged. Care was taken to ensure the arm was settled firmly into the bottom of the flask, leaving the central space free for a large magnetic stirrer. The arm was clamped securely above the bath to ensure no movement during the reaction, and the apparatus was placed upon a magnetic stirrer plate. Efficient stirring of the bath was essential in order to achieve uniform cooling, and also in preventing build up of ice. A thermometer was suspended within the bath in order to check the correlation between the temperature of the bath and the set temperature of the chiller. Any required offset could then be implemented. At -80 °C, the bath was reasonably expected to last around two weeks before requiring defrosting, and new *iso*-propanol. However, depending upon the strength of the chiller used, some heating of the bath may be observed before this point, and thus the bath may require more regular maintenance.

Synthesis of Racemic Aziridines

The one-pot methodology was frequently applied to the synthesis of racemic aziridines during the project. The method used for these reactions is essentially identical to those syntheses detailed in Section 9.8: Synthesis of C2-*deutero* aziridines *rac*-(**336**), and *rac*-(**341**) to *rac*-(**344**).

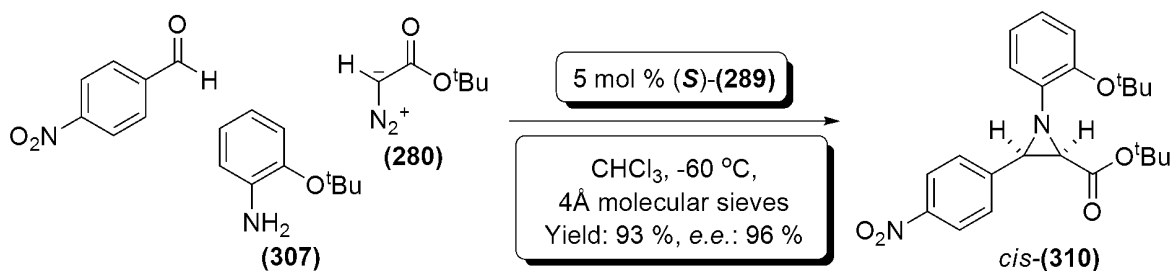
9.2: Synthesis of C2-, C3-proteo Aziridines

Three component One-Pot asymmetric synthesis of *tert*-butyl 1-(2-*tert*-butoxyphenyl)-3-(pyridin-2-yl)aziridine-2-carboxylate; *cis*-(**309**)



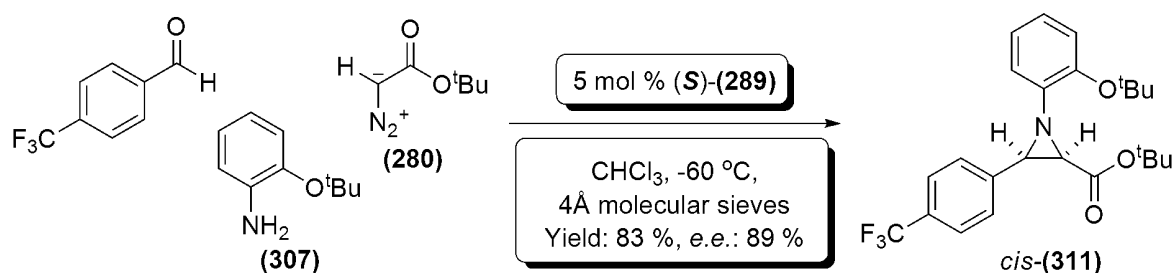
Pyridine-2-carboxaldehyde (27.8 mg, 25 μL , 0.26 mmol), 2-*tert*-butoxy aniline (**307**) (43 mg, 0.26 mmol), and catalyst (*S*)-(**289**) (2.2 mg, 0.0026 mmol, 1%) were added to a flame dried 2 mL vial under nitrogen. 1 mL of chloroform was added (pre-dried over 4Å molecular sieves), followed by ~40 mg of freshly powdered 4Å molecular sieves, and the vial was sealed with a PTFE crimp cap. After stirring at room temperature for 6 h, the reaction was cooled to $-60\text{ }^\circ\text{C}$. After 30 minutes, *tert*-butyl diazoacetate (**280**) (40.7 mg, 40 μL , 0.286 mmol) was added *via* syringe, and the reaction mixture was stirred at $-60\text{ }^\circ\text{C}$, monitoring by $^1\text{H-NMR}$ spectroscopy until the reaction was deemed complete (~24 h). At this point the reaction mixture was filtered through a short plug of silica, eluting with diethyl ether. The solvents were removed under reduced pressure, and the residue was purified *via* flash column chromatography (14 % diethyl ether in petroleum ether). A sample was submitted to chiral analytical HPLC analysis [Chiralpak AD, *iso*-hexane / *iso*-propanol : 8 / 2, 1 mL / min, 5.25 min (1st peak), 7.43 min (2nd peak), 96% *e.e.*]. The title product *cis*-(**309**) was a colourless oil afforded in a 96 % yield (92 mg, 0.25 mmol). $^1\text{H-NMR}$ (CDCl_3 , 400 MHz) δ 8.61-8.45 (m, 1H, ArH), 7.79-7.51 (m, 2H, ArH), 7.18 (ddd, 1H, *J* 1.8, 4.9, 6.9 Hz, ArH), 7.09-6.85 (m, 4H, ArH), 3.64 (d, 1H, *J* 6.8 Hz, C3-H), 3.12 (d, 1H, *J* 6.8 Hz, C2-H) 1.37 (s, 9H, $\text{C}(\text{CH}_3)_3$), 1.17 (s, 9H, $\text{C}(\text{CH}_3)_3$); $^{13}\text{C-NMR}$ (CDCl_3 , 100 MHz) 166.8, 155.6, 148.7, 148.2, 145.8, 135.9, 123.2, 123.1, 122.9, 122.7, 122.5, 120.9, 81.3, 80.1, 48.4, 46.8, 28.6, 27.6 ppm; $[\alpha]_{\text{D}}^{23}$ -41.8 (c 1.1 CHCl_3); FT-IR (thin film, cm^{-1}) 2976, 2908, 1741, 1717, 1589, 1569, 1489, 1450, 1435, 1391, 1365, 1223; MS (ES): m/z 369.1 $[\text{M}+\text{H}]^+$, 391.1 $[\text{M}+\text{Na}]^+$; HRMS (EI) Exact mass calculated for $[\text{C}_{22}\text{H}_{29}\text{N}_2\text{O}_3]$ requires m/z 369.2173 found m/z 369.2176

Three component One-Pot asymmetric synthesis of *tert*-butyl 1-(2-*tert*-butoxyphenyl)-3-(4-nitrophenyl)-aziridine-2-carboxylate; *cis*-(310**)**



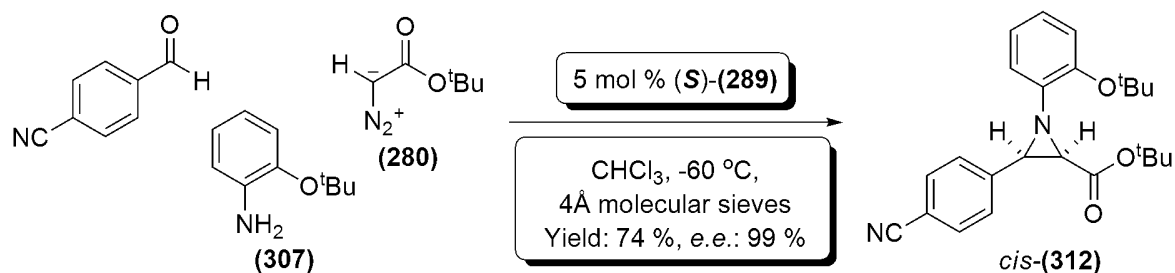
4-nitrobenzaldehyde (49 mg, 0.26 mmol), 2-*tert*-butoxy aniline (**307**) (43 mg, 0.26 mmol), and catalyst (*S*)-(**289**) (10.8 mg, 0.013 mmol, 5%) were added to a flame dried 2 mL vial under nitrogen. 1 mL of chloroform was added (pre-dried over 4Å molecular sieves), followed by ~40 mg of freshly powdered 4Å molecular sieves, and the vial was sealed with a PTFE crimp cap. After stirring at room temperature for 6 h, the reaction was cooled to $-60\text{ }^\circ\text{C}$. After 30 minutes, *tert*-butyl diazoacetate (**280**) (40.7 mg, 40 μL , 0.286 mmol) was added *via* syringe, and the reaction mixture was stirred at $-60\text{ }^\circ\text{C}$, monitoring by $^1\text{H-NMR}$ spectroscopy until the reaction was deemed complete (~48 h). At this point the reaction mixture was filtered through a short plug of silica, eluting with diethyl ether. The solvents were removed under reduced pressure, and the residue was purified *via* flash chromatography (12 % diethyl ether in petroleum ether). A sample was submitted to chiral analytical HPLC analysis [Chiralpak AD, *iso*-hexane / *iso*-propanol: 95 / 5, 1 mL / min, 5.62 min (1st peak), 9.32 min (2nd peak), 96% *e.e.*]. The title product *cis*-(**310**) was a colourless oil afforded in a 93 % yield (99 mg, 0.24 mmol). $^1\text{H-NMR}$ (CDCl_3 , 400 MHz) δ 8.20 (d, 2H, J 8.7 Hz, ArH), 7.72 (d, 2H, J 8.7 Hz, ArH), 7.11–6.88 (m, 4H, ArH), 3.53 (d, 1H, J 6.7 Hz, C3-H), 3.14 (d, 1H, J 6.7 Hz, C2-H), 1.35 (s, 9H, $\text{C}(\text{CH}_3)_3$), 1.22 (s, 9H, $\text{C}(\text{CH}_3)_3$); $^{13}\text{C-NMR}$ (CDCl_3 , 100 MHz) δ 166.9, 148.3, 147.6, 145.8, 135.8, 129.5, 128.9, 127.8, 126.3, 123.4, 123.1, 122.8, 121.2, 121.0, 81.6, 80.4, 49.2, 47.3, 28.9, 27.9 ppm; $[\alpha]_D^{23}$ -46.47 (c 2 CHCl_3); FT-IR (thin film, cm^{-1}) 2977, 2933, 1741, 1714, 1602, 1519, 1489, 1450, 1343, 1149, 1111; MS (ES) m/z 435.3 $[\text{M}+\text{Na}]^+$; HRMS (EI) Exact mass calculated for $[\text{C}_{23}\text{H}_{29}\text{N}_2\text{O}_5]$ requires 413.2134 found 413.2131.

Three component One-Pot asymmetric synthesis of *tert*-butyl 1-(2-*tert*-butoxyphenyl)-3-(4-(trifluoromethyl)phenyl)aziridine-2-carboxylate; *cis*-(311**)**



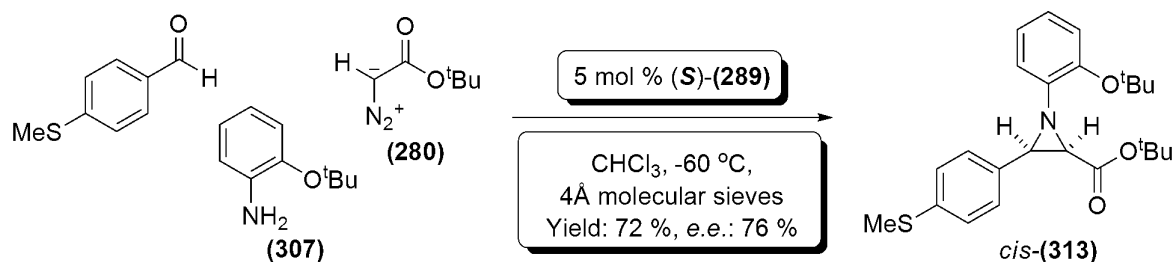
4-(trifluoromethyl)benzaldehyde (22.6 mg, 17 μ L, 0.13 mmol), 2-*tert*-butoxy aniline (**307**) (21 mg, 0.13 mmol), and catalyst (*S*)-(**289**) (5.4 mg, 0.0065 mmol, 5%) were added to a flame dried 2 mL vial under nitrogen. 1 mL of chloroform was added (pre-dried over 4 Å molecular sieves), followed by ~40 mg of freshly powdered 4 Å molecular sieves, and the vial was sealed with a PTFE crimp cap. After stirring at room temperature for 6 h, the reaction was cooled to -60 °C. After 30 minutes, *tert*-butyl diazoacetate (**280**) (20.4 mg, 20 μ L, 0.143 mmol) was added *via* syringe, and the reaction mixture was stirred at -60 °C, monitoring by ¹H-NMR spectroscopy until the reaction was deemed complete (~48 h). At this point the reaction mixture was filtered through a short plug of silica, eluting with diethyl ether. The solvents were removed under reduced pressure, and the residue was purified *via* flash chromatography (12 % diethyl ether in petroleum ether). A sample was submitted to chiral analytical HPLC analysis [Chiralpak AD, *iso*-hexane / *iso*-propanol : 95 / 5, 1 mL / min, 3.98 min (1st peak), 6.06 min (2nd peak), 89% *e.e.*]. The title product *cis*-(**311**) was a colourless oil afforded in a 83 % yield (47 mg, 0.11 mmol). ¹H-NMR (CDCl₃, 400 MHz) δ 7.64 (d, 2H, *J* 8.2 Hz, ArH), 7.57 (d, 2H, *J* 8.2 Hz, ArH), 7.06-6.90 (m, 4H, ArH), 3.49 (d, *J* 6.8 Hz, 1H, C3-H), 3.07 (d, 1H, *J* 6.8 Hz, C2-H) 1.37 (s, 9H, C(CH₃)₃), 1.19 (s, 9H, C(CH₃)₃); ¹³C-NMR (CDCl₃, 100 MHz) 166.8, 148.2, 146.1, 139.7, 130.1, 129.7, 129.4, 128.6, 125.8, 124.9, 124.8, 124.8, 124.8, 123.5, 123.3, 123.2, 123.1, 121.0, 81.8, 80.6, 47.6, 47.0, 28.9, 28.0 ppm; [α]_D²³ -41.0 (c 1 CHCl₃); FT-IR (thin film, cm⁻¹) 2978, 1844, 1715, 1620, 1593, 1489, 1450, 1392, 1323, 1280, 1159; MS (ES) *m/z* 458.1 [M+Na]⁺; HRMS (EI) Exact mass calculated for [C₂₄H₂₉F₃NO₃] requires *m/z* 436.2094 found *m/z* 436.2094.

Three component One-Pot asymmetric synthesis of *tert*-butyl 1-(2-*tert*-butoxyphenyl)-3-(4-cyanophenyl)aziridine-2-carboxylate; *cis*-(312**)**



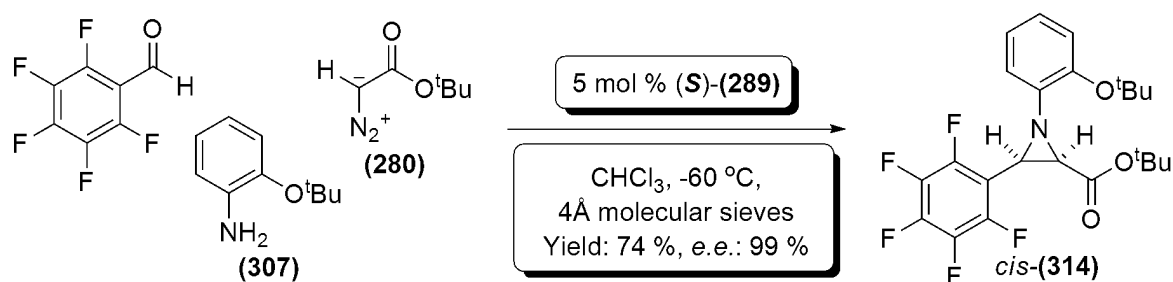
4-cyanobenzaldehyde (34 mg, 0.26 mmol), 2-*tert*-butoxy aniline (**307**) (43 mg, 0.26 mmol), and catalyst (*S*)-(289) (10.8 mg, 0.013 mmol, 5%) were added to a flame dried 2 mL vial under nitrogen. 1 mL of chloroform was added (pre-dried over 4 Å molecular sieves), followed by ~40 mg of freshly powdered 4 Å molecular sieves, and the vial was sealed with a PTFE crimp cap. After stirring at room temperature for 6 h, the reaction was cooled to -60 °C. After 30 minutes, *tert*-butyl diazoacetate (**280**) (40.7 mg, 40 μL, 0.286 mmol) was added *via* syringe, and the reaction mixture was stirred at -60 °C, monitoring by ¹H-NMR spectroscopy until the reaction was deemed complete (~48h). At this point the reaction mixture was filtered through a short plug of silica, eluting with diethyl ether. The solvents were removed under reduced pressure, and the residue was purified *via* flash column chromatography (14 % diethyl ether in petroleum ether). A sample was submitted to chiral analytical HPLC analysis [Chiralpak AD, *iso*-hexane / *iso*-propanol : 95 / 5, 1 mL / min, 7.04 min (1st peak), 13.69 min (2nd peak), 99% *e.e.*]. The title product *cis*-(**312**) was a colourless oil afforded in a 74 % yield (75 mg, 0.19 mmol). ¹H-NMR (CDCl₃, 400 MHz) δ 7.70-7.60 (m, 4H, ArH), 7.07-6.89 (m, 4H, ArH), 3.49 (d, *J* 6.8 Hz, 1H, C3-H), 3.11 (d, 1H, *J* 6.8 Hz, C2-H) 1.35 (s, 9H, C(CH₃)₃), 1.20 (s, 9H, C(CH₃)₃); ¹³C-NMR (CDCl₃, 100 MHz) 166.5, 148.0, 145.7, 141.0, 131.6, 128.9, 123.5, 123.1, 123.0, 120.8, 111.2, 81.8, 80.4, 47.5, 46.7, 28.6, 27.7 ppm; [α]_D²³ -61.6 (c 0.7 CHCl₃); FT-IR (thin film cm⁻¹) 2977, 2228, 1741, 1713, 1592, 1489, 1450, 1392, 1366, 1261, 1224, 1149; MS (ES) *m/z* 415.2 [M+Na]⁺; HRMS (EI) Exact mass calculated for [C₂₄H₂₉N₂O₃] requires *m/z* 393.2173 found *m/z* 393.2174.

Three component One-Pot asymmetric synthesis of *tert*-butyl 1-(2-*tert*-butoxyphenyl)-3-(4-(methylthio)phenyl)aziridine-2-carboxylate; *cis*-(313**)**



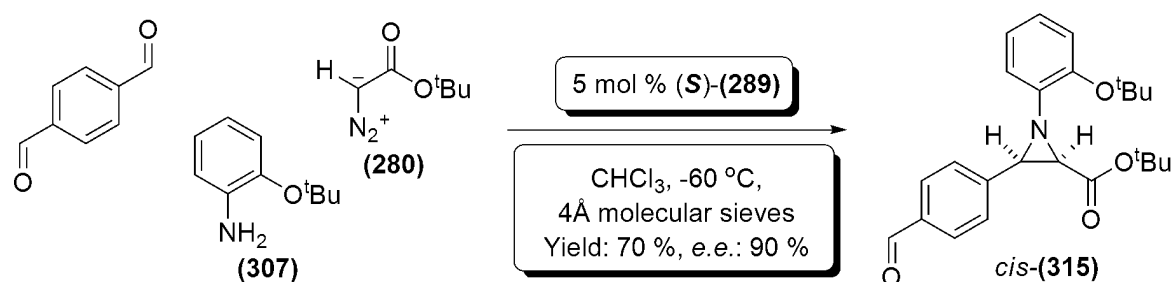
4-(methylthio)benzaldehyde (51 mg, 0.26 mmol), 2-*tert*-butoxy aniline (**307**) (43 mg, 0.26 mmol), and catalyst (*S*)-(289) (10.8 mg, 0.013 mmol, 5%) were added to a flame dried 2 mL vial under nitrogen. 1 mL of chloroform was added (pre-dried over 4 Å molecular sieves), followed by ~40 mg of freshly powdered 4 Å molecular sieves, and the vial was sealed with a PTFE crimp cap. After stirring at room temperature for 6 h, the reaction was cooled to -60 °C. After 30 minutes, *tert*-butyl diazoacetate (**280**) (40.7 mg, 20 µL, 0.286 mmol) was added *via* syringe, and the reaction mixture was stirred at -60 °C, monitoring by ¹H-NMR spectroscopy until the reaction was deemed complete (~72 h). At this point the reaction mixture was filtered through a short plug of silica, eluting with diethyl ether. The solvents were removed under reduced pressure, and the residue was purified *via* flash column chromatography (12 % diethyl ether in petroleum ether). A sample was submitted to chiral analytical HPLC analysis [Chiralpak AD, *iso*-hexane / *iso*-propanol : 95/ 5, 1 mL / min, 5.06 min (1st peak), 9.63 min (2nd peak), 76 % *e.e.*]. The title product *cis*-(**313**) was a slight yellow oil afforded in a 72 % yield (78 mg, 0.19 mmol). ¹H-NMR (CDCl₃, 400 MHz) δ 7.43 (d, 2H, *J* 8.4 Hz, ArH), 7.21 (d, 2H, *J* 8.4 Hz, ArH), 7.03-6.87 (m, 4H, ArH), 3.42 (d, *J* 6.7 Hz, 1H, C3-H), 3.01 (d, 1H, *J* 6.7 Hz, C2-H), 2.44 (s, 3H, SCH₃), 1.36 (s, 9H, C(CH₃)₃), 1.19 (s, 9H, C(CH₃)₃); ¹³C-NMR (CDCl₃, 100 MHz) 167.2, 148.1, 146.7, 137.6, 132.5, 128.7, 126.3, 123.4, 123.3, 123.2, 121.1, 81.5, 80.6, 47.6, 47.3, 28.9, 28.1, 16.3 ppm; [α]_D²³ -35.6 (c 1.4 CHCl₃); FT-IR (thin film, cm⁻¹) 2976, 2929, 1743, 1711, 1592, 1489, 1391, 1365, 1304, 1260; MS (ES) *m/z* 414.2 [M+H]⁺, 436.2 [M+Na]⁺; HRMS (EI) Exact mass calculated for [C₂₄H₃₂NO₃S] requires *m/z* 414.2097 found *m/z* 414.2099.

Three component One-Pot asymmetric synthesis of *tert*-butyl 1-(2-*tert*-butoxyphenyl)-3-(perfluorophenyl)aziridine-2-carboxylate; *cis*-(314**)**



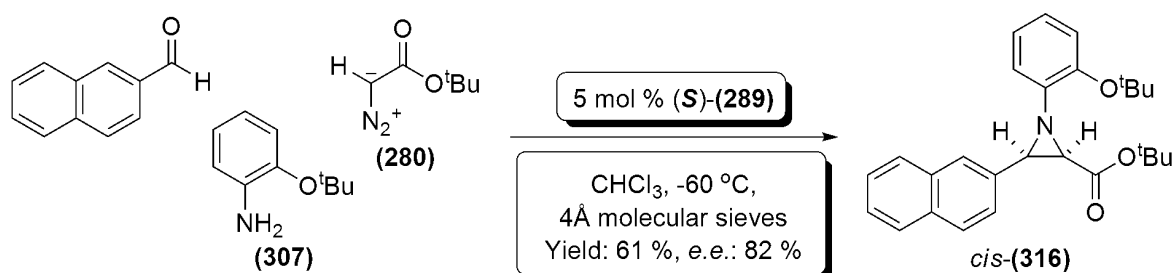
Pentafluorobenzaldehyde (51 mg, 0.26 mmol), 2-*tert*-butoxy aniline (**307**) (43 mg, 0.26 mmol), and catalyst (*S*)-(**289**) (10.8 mg, 0.013 mmol, 5%) were added to a flame dried 2 mL vial under nitrogen. 1 mL of chloroform was added (pre-dried over 4Å molecular sieves), followed by ~40 mg of freshly powdered 4Å molecular sieves, and the vial was sealed with a PTFE crimp cap. After stirring at room temperature for 6 h, the reaction was cooled to -60 °C. After 30 minutes, *tert*-butyl diazoacetate (**280**) (40.7 mg, 40 μL, 0.286 mmol) was added *via* syringe, and the reaction mixture was stirred at -60 °C, monitoring by ¹H-NMR spectroscopy until the reaction was deemed complete (~48 h). At this point the reaction mixture was filtered through a short plug of silica, eluting with diethyl ether. The solvents were removed under reduced pressure, and the residue was purified *via* flash column chromatography (12 % diethyl ether in petroleum ether). The title product *cis*-(**314**) was a colourless oil afforded in a 74 % yield (87 mg, 0.19 mmol); however, *cis*-(**314**) proved impossible to separate utilising available chiral HPLC techniques. ¹H-NMR (CDCl₃, 400 MHz) δ 7.14-6.88 (m, 4H, ArH), 3.33 (d, 1H, *J* 5.6 Hz, C3-H), 3.04 (d, 1H, *J* 5.6 Hz, C2-H), 1.40 (s, 9H, C(CH₃)₃), 1.38 (s, 9H, C(CH₃)₃); ¹³C-NMR (CDCl₃, 100 MHz) 167.2, 148.2, 147.7, 147.7, 147.5, 145.3, 144.5, 144.3, 139.3, 139.1, 139.0, 136.0, 135.8, 135.8, 123.7, 123.1, 122.8, 120.7, 110.5, 110.2, 110.2, 82.1, 80.5, 43.6, 36.8, 28.6, 27.6 ppm; [α]_D²³ -122.7 (c 0.8 CHCl₃); FT-IR (thin film, cm⁻¹) 2979, 2933, 1740, 1655, 1594, 1523, 1500, 1451, 1393, 1369, 1331; MS (ES) *m/z* 480.1 [M+Na]⁺; HRMS (EI) Exact mass calculated for [C₂₃H₂₅F₅NO₃] requires *m/z* 458.1749 found *m/z* 458.1748.

Three component One-Pot asymmetric synthesis of *tert*-butyl 1-(2-*tert*-butoxyphenyl)-3-(4-formylphenyl)aziridine-2-carboxylate; *cis*-(315**)**



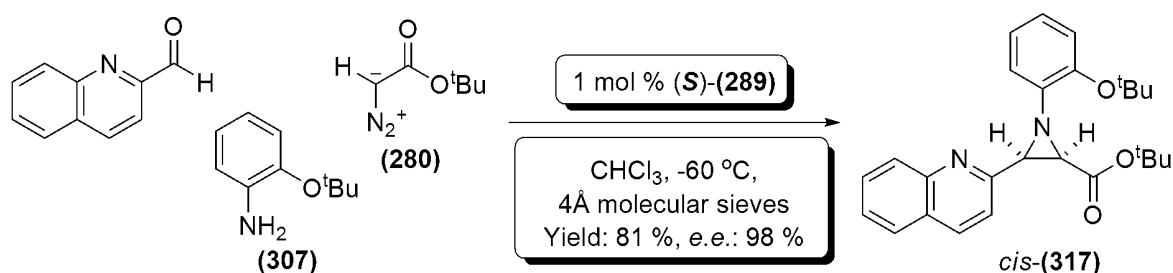
Terephthalaldehyde (34.8 mg, 0.26 mmol.), 2-*tert*-butoxy aniline (**307**) (43 mg, 0.26 mmol), and catalyst (*S*)-(**289**) (5.4 mg, 0.0065 mmol, 5%) were added to a flame dried 2 mL vial under nitrogen. 1 mL of chloroform was added (pre-dried over 4Å molecular sieves), followed by ~40 mg of freshly powdered 4Å molecular sieves, and the vial was sealed with a PTFE crimp cap. After stirring at room temperature for 6 h, the reaction was cooled to -60 °C. After 30 minutes, *tert*-butyl diazoacetate (**280**) (38 mg, 17.5 μL, 0.27 mmol) was added *via* syringe, and the reaction mixture was stirred at -60 °C, monitoring by ¹H-NMR spectroscopy until the reaction was deemed complete (~72 h). At this point the reaction mixture was filtered through a short plug of silica, eluting with diethyl ether. The solvents were removed under reduced pressure, and the residue was purified *via* flash column chromatography (12 % diethyl ether in petroleum ether). A sample was submitted to chiral analytical HPLC analysis [Chiralpak AD, *iso*-hexane / *iso*-propanol : 95/ 5, 1 mL / min, 6.94 min (1st peak), 14.85 min (2nd peak), 90 % *e.e.*]. The title product *cis*-(**315**) was a colourless oil afforded in a 70 % yield (72 mg, 0.18 mmol). ¹H-NMR (CDCl₃, 400 MHz) δ 10.01 (s, 1H, CHO), 7.86 (d, 2H, *J* 8.3 Hz, ArH), 7.71 (d, 2H, *J* 8.3 Hz, ArH), 7.11-6.85 (m, 4H, ArH), 3.52 (d, *J* 6.8 Hz, 1H, C3-H), 3.12 (d, 1H, *J* 6.8 Hz, C2-H), 1.35 (s, 9H, C(CH₃)₃), 1.19 (s, 9H, C(CH₃)₃); ¹³C-NMR (CDCl₃, 100 MHz) 192.2, 166.6, 148.1, 145.9, 142.6, 135.8, 129.3, 128.8, 123.4, 123.1, 123.0, 120.9, 81.6, 80.3, 47.5, 47.0, 28.6, 27.7 ppm; [α]_D²³ -67.4 (c 2.4 CHCl₃); FT-IR (thin film, cm⁻¹) 2976, 2932, 1742, 1701, 1608, 1592, 1577, 1489, 1450, 1391, 1303, 1279; MS (ES) *m/z* 418.3 [M+Na]⁺; HRMS (EI) Exact mass calculated for [C₂₄H₃₀N₁O₄] requires *m/z* 396.2169 found *m/z* 396.2170.

Three component One-Pot asymmetric synthesis of *tert*-butyl 1-(2-*tert*-butoxyphenyl)-3-(naphthalen-2-yl)aziridine-2-carboxylate; *cis*-(316**)**



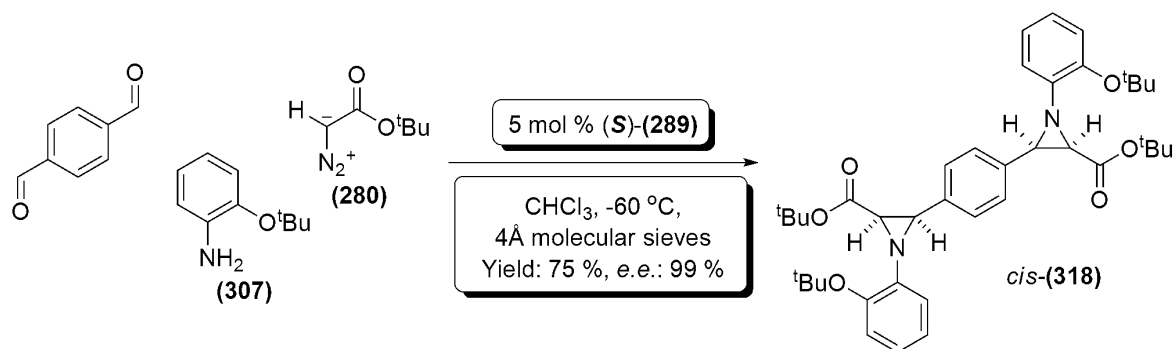
2-naphthaldehyde (40.6 mg, 0.26 mmol), 2-*tert*-butoxy aniline (**307**) (43 mg, 0.26 mmol), and catalyst (*S*)-(**289**) (10.8 mg, 0.013 mmol, 5%) were added to a flame dried 2 mL vial under nitrogen. 1 mL of chloroform was added (pre-dried over 4Å molecular sieves), followed by ~40 mg of freshly powdered 4Å molecular sieves, and the vial was sealed with a PTFE crimp cap. After stirring at room temperature for 6 h, the reaction was cooled to $-60\text{ }^\circ\text{C}$. After 30 minutes, *tert*-butyl diazoacetate (**280**) (40.7 mg, 40 μL , 0.286 mmol) was added *via* syringe, and the reaction mixture was stirred at $-60\text{ }^\circ\text{C}$, monitoring by $^1\text{H-NMR}$ spectroscopy until the reaction was deemed complete (~48 h). At this point the reaction mixture was filtered through a short plug of silica, eluting with diethyl ether. The solvents were removed under reduced pressure, and the residue was purified *via* flash column chromatography (14 % diethyl ether in petroleum ether). A sample was submitted to chiral analytical HPLC analysis [Chiralpak AD, *iso*-hexane / *iso*-propanol: 95 / 5, 1 mL / min, 5.11 min (1st peak), 11.66 min (2nd peak), 82% *e.e.*]. The title product *cis*-(**316**) was a colourless oil afforded in a 61 % yield (66 mg, 0.16 mmol). $^1\text{H-NMR}$ (CDCl_3 , 300 MHz) δ 8.02 (s, 1H, ArH), 7.93-7.72 (m, 3H, ArH), 7.64 (dd, 1H, J 1.6, 8.5 Hz, ArH), 7.58-7.35 (m, 2H, ArH) 7.18-6.85 (m, 4H, ArH), 3.64 (d, 1H, J 6.7 Hz, C3-H), 3.13 (d, 1H, J 6.7 Hz, C2-H), 1.39 (s, 9H, $\text{C}(\text{CH}_3)_3$), 1.15 (s, 9H, $\text{C}(\text{CH}_3)_3$); $^{13}\text{C-NMR}$ (CDCl_3 , 75 MHz) 166.2, 146.9, 145.4, 131.9, 131.8, 126.9, 126.6, 126.3, 126.0, 124.9, 124.6, 122.0, 121.9, 121.9, 120.0, 80.3, 79.3, 46.7, 46.5, 27.7, 26.7 ppm; $[\alpha]_{\text{D}}^{26}$ -25.6 (c 0.9 CHCl_3); FT-IR (thin film, cm^{-1}) 2977, 1740, 1708, 1591, 1449, 1413, 1392, 1367, 1261, 1160, 1111; MS (EI)⁺: m/z 440.2 $[\text{M}+\text{Na}]^+$, 857.5 $[2\text{M}+\text{Na}]^+$; HRMS (EI)⁺: exact mass calculated for $[\text{C}_{27}\text{H}_{32}\text{NO}_3]^+$ requires m/z 418.2377, found m/z 418.2377.

Three component One-Pot asymmetric synthesis of *tert*-butyl 1-(2-*tert*-butoxyphenyl)-3-(quinolin-2-yl)aziridine-2-carboxylate; *cis*-(317**)**



Quinoline-2-carboxaldehyde (40.8 mg, 0.26 mmol), 2-*tert*-butoxy aniline (**307**) (43 mg, 0.26 mmol), and catalyst (*S*)-(**289**) (2.2 mg, 0.0026 mmol, 1%) were added to a flame dried 2 mL vial under nitrogen. 1 mL of chloroform was added (pre-dried over 4 Å molecular sieves), followed by ~40 mg of freshly powdered 4 Å molecular sieves, and the vial was sealed with a PTFE crimp cap. After stirring at room temperature for 6 h, the reaction was cooled to $-60\text{ }^\circ\text{C}$. After 30 minutes, *tert*-butyl diazoacetate (**280**) (40.7 mg, 40 μL , 0.286 mmol) was added *via* syringe, and the reaction mixture was stirred at $-60\text{ }^\circ\text{C}$, monitoring by $^1\text{H-NMR}$ spectroscopy until the reaction was deemed complete (~24 h). At this point the reaction mixture was filtered through a short plug of silica, eluting with diethyl ether. The solvents were removed under reduced pressure, and the residue was purified *via* flash column chromatography (14 % diethyl ether in petroleum ether). A sample was submitted to chiral analytical HPLC analysis [Chiralpak AD, *iso*-hexane / *iso*-propanol : 8 / 2, 1 mL / min, 4.78 min (1st peak), 5.80 min (2nd peak), 98% *e.e.*]. The title product *cis*-(**317**) was a colourless oil afforded in a 81 % yield (88 mg, 0.21 mmol). $^1\text{H-NMR}$ (CDCl_3 , 400 MHz) δ 8.14 (d, 1H, *J* 8.5 Hz, ArH), 8.07 (d, 1H, *J* 8.5 Hz, ArH), 7.90 (d, 1H, *J* 8.5 Hz, ArH), 7.82 (d, 1H, *J* 8.1 Hz, ArH), 7.70 (t, 1H, *J* 7.7, 7.7 Hz, ArH), 7.52 (t, 1H, *J* 7.5, 7.5 Hz, ArH), 7.12-6.90 (m, 4H, ArH), 3.82 (d, 1H, *J* 6.8 Hz, C3-H), 3.21 (d, 1H, *J* 6.8 Hz, C2-H) 1.38 (s, 9H, $\text{C}(\text{CH}_3)_3$), 1.18 (s, 9H, $\text{C}(\text{CH}_3)_3$); $^{13}\text{C-NMR}$ (CDCl_3 , 100 MHz) 167.0, 156.7, 148.3, 147.7, 145.8, 135.9, 129.6, 128.9, 127.9, 127.8, 126.4, 123.5, 123.2, 122.9, 121.3, 121.1, 81.7, 80.5, 49.2, 47.4, 29.0, 28.0 ppm; $[\alpha]_{\text{D}}^{23}$ -78.2 (c 1.7 CHCl_3); FT-IR (thin film, cm^{-1}) 2976, 2931, 1740, 1718, 1618, 1597, 1562, 1489, 1449, 1426, 1330, 1311, 1227; MS (ES) m/z 419.2 $[\text{M}+\text{H}]^+$, 441.2 $[\text{M}+\text{Na}]^+$; HRMS (EI) Exact mass calculated for $[\text{C}_{26}\text{H}_{31}\text{N}_2\text{O}_3]$ requires m/z 419.2329 found m/z 419.2329.

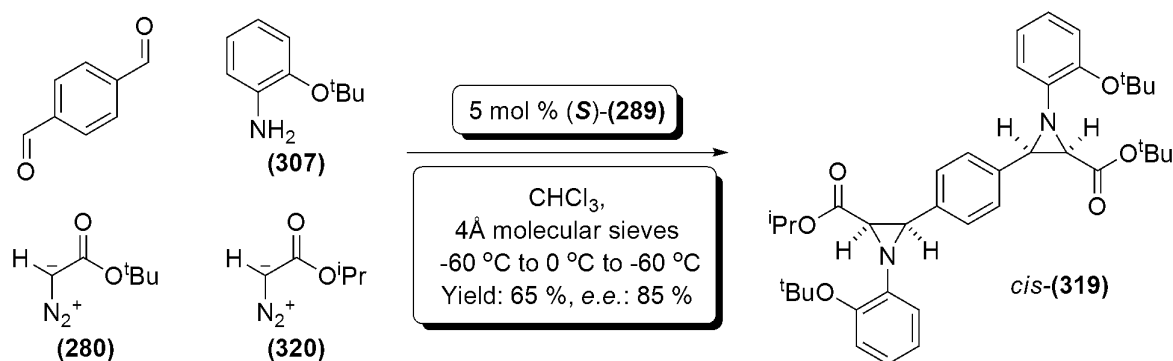
Three component One-Pot asymmetric synthesis of *tert*-butyl 3,3'-(1,4-phenylene)bis(1-(2-*tert*-butoxyphenyl)aziridine-2-carboxylate); *cis*-(318**)**



Terephthalaldehyde (8.8 mg, 0.065 mmol), 2-*tert*-butoxy aniline (**307**) (21 mg, 0.13 mmol), and catalyst (*S*)-(289) (5.4 mg, 0.0065 mmol, 5%) were added to a flame dried 2 mL vial under nitrogen. 1 mL of chloroform was added (pre-dried over 4 Å molecular sieves), followed by ~40 mg of freshly powdered 4 Å molecular sieves, and the vial was sealed with a PTFE crimp cap. After stirring at room temperature for 6 h, the reaction was cooled to -60 °C. After 30 minutes, *tert*-butyl diazoacetate (**280**) (20.4 mg, 20 μL, 0.142 mmol) was added *via* syringe, and the reaction mixture was stirred at -60 °C, monitoring by ¹H-NMR spectroscopy until the reaction was deemed complete (~72 h). At this point the reaction mixture was filtered through a short plug of silica, eluting with diethyl ether. The solvents were removed under reduced pressure, and the residue was purified *via* flash column chromatography (12 % diethyl ether in petroleum ether). A sample was submitted to chiral analytical HPLC analysis [Chiralpak AD, *iso*-hexane / *iso*-propanol : 95/ 5, 1 mL / min, 4.47 min (1st peak), 6.01 min (2nd peak), 99 % *e.e.*]. The title product *cis*-(**318**) was a colourless oil afforded in a 25 % isolated yield (11 mg, 0.016 mmol; 75 % based on recovered material). ¹H-NMR (CDCl₃, 400 MHz) δ 7.50 (d, 4H, *J* 3.2 Hz, ArH), 7.14-6.81 (m, 8H, ArH), 3.46 (dd*, *J* 3.6, 6.7 Hz, 2H, C3-H), 3.03 (d, 2H, *J* 6.7 Hz, C2-H), 1.37 (s, 18H, C(CH₃)₃), 1.27 (s, 18H, C(CH₃)₃); ¹³C-NMR (CDCl₃, 100 MHz) 167.1, 167.0, 148.0, 147.9, 146.9, 146.8, 134.6, 134.6, 127.6, 127.5, 123.3, 123.2, 123.1, 123.0, 121.1, 81.2, 80.3, 80.3, 47.6, 47.5, 47.4, 47.3, 28.6, 27.8 ppm; [α]_D²³ -43.7 (c 0.7 CHCl₃); FT-IR (thin film, cm⁻¹) 2977, 1745, 1716, 1450, 1367, 1262, 1163; MS (ES) *m/z* 679.4 [M+Na]⁺; HRMS (EI) Exact mass calculated for [C₄₀H₅₄N₂O₆] requires *m/z* 657.3898 found *m/z* 657.3895.

*Could potentially contain two doublets, one for the desired product, and one for the presence of a small amount of the *meso*- diaziridine within the product.

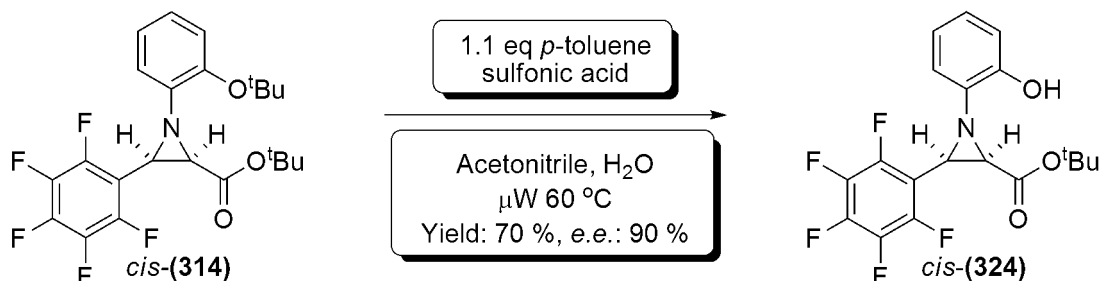
Four component One-Pot asymmetric synthesis of *tert*-butyl 1-(2-*tert*-butoxyphenyl)-3-(4-(1-(2-*tert*-butoxyphenyl)-3-(isopropoxycarbonyl)aziridin-2-yl)phenyl)aziridine-2-carboxylate; *cis*-(319**)**



Terephthalaldehyde (8.9 mg, 0.065 mmol), 2-*tert*-butoxy aniline (**307**) (11 mg, 6.5 mmol), and catalyst (*S*)-(**289**) (6 mg, 0.0065 mmol, 10%) were added to a flame dried 2 mL vial under nitrogen. 1 mL of chloroform was added (pre-dried over 4Å molecular sieves), followed by ~40 mg of freshly powdered 4Å molecular sieves, and the vial was sealed with a PTFE crimp cap. After stirring at room temperature for 16 h, the reaction was cooled to -60 °C. After 30 minutes, *iso*-propyl diazoacetate (**320**) (8.5 mg, 8.4 μL, 0.065 mmol) was added *via* syringe, and the reaction mixture was stirred at -60 °C, monitoring by ¹H-NMR spectroscopy until the reaction was deemed complete (~72 h). At this point 2-*tert*-butoxy aniline (**307**) (11 mg, 6.5 mmol) was added, and the reaction was stirred at 0 °C for 12 h; after which, the reaction was re-cooled to -60 °C. After 30 minutes, *tert*-butyl diazoacetate (**280**) (9.3 mg, 9.2 μL, 0.065 mmol) was added *via* syringe, and the reaction mixture was stirred at -60 °C, monitoring by ¹H-NMR spectroscopy until the reaction was deemed complete (~72 h). At this point the reaction mixture was filtered through a short plug of silica, eluting with diethyl ether. The solvents were removed under reduced pressure, and the residue was purified *via* flash column chromatography (12 % diethyl ether in petroleum ether). A sample was submitted to chiral analytical HPLC analysis [Chiralpak AD, *iso*-hexane / *iso*-propanol : 95/ 5, 1 mL / min, 4.70 min (1st peak), 6.64 min (2nd peak), 11.47 min (3rd peak), 15.28 min (4th peak) 85 % *e.e.*]. The title product *cis*-(**319**) was a colourless oil afforded in a 35 % overall isolated yield (15 mg, 0.023 mmol; 65 % based on recovered material). ¹H-NMR (CDCl₃, 400 MHz) δ 7.50 (2s, 4H, ArH), 7.00 (m, 8H, ArH), 4.87 (m, 1H, CH(CH₃)₂), 3.51 (dd, 1H, *J* 2.0, 6.7 Hz, C3-H), 3.46 (d, 1H, *J* 6.7 Hz, C3-H), 3.09 (d, *J* 6.7 Hz, 1H, C2-H), 3.03 (d, 1H, *J* 6.7 Hz, C2-H), 1.36 (2s, 18H, C(CH₃)₃), 1.25 (s, 9H, C(CH₃)₃), 1.08 (m, 6H, C(CH₃)₂); ¹³C-NMR (CDCl₃, 100 MHz) 167.4, 167.1, 148.0, 146.8, 146.7, 146.5, 146.4, 134.8, 134.7, 134.4, 127.6, 127.5, 123.2, 123.1, 123.0, 122.9, 122.9, 122.7, 121.1, 121.0, 81.2, 81.1, 80.3, 80.3, 80.2, 80.168.2, 68.1, 47.8, 47.4, 28.6, 27.8, 21.7, 21.6 ppm; [α]_D²³ -52.3 (c 2 CHCl₃); FT-IR (thin film, cm⁻¹) 2978, 2932, 1744,

1716, 1592, 1489, 1450, 1391, 1367, 1305, 1262, 1219, 1262; MS (ES) m/z 665.2 $[M+Na]^+$; HRMS (EI) Exact mass calculated for $[C_{39}H_{51}N_2O_6]$ requires m/z 643.3742 found m/z 643.3739.

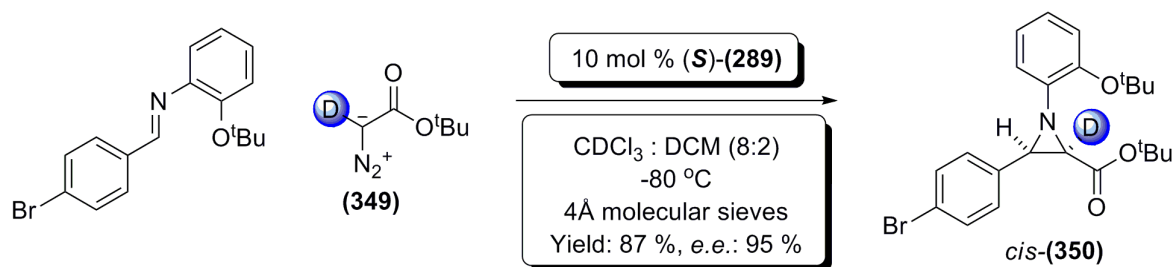
Synthesis of *tert*-butyl 1-(2-hydroxyphenyl)-3-(perfluorophenyl)aziridine-2-carboxylate; *cis*-(324)



To a stirred solution of *cis*-(314) (40 mg, 0.088 mmol) in 1 mL acetonitrile, in a 4 mL Biotage microwave vial, was added *para*-toluene sulfonic acid (19 mg, 0.096 mmol, 1.1 eq). 500 μ L distilled water was added, the reaction was capped with a PTFE seal, and heated to 60 °C for 5 h in a Biotage Creator[®] microwave synthesiser. After this time the reaction mixture was diluted with 10 mL ethyl acetate, washed with 15 mL saturated aqueous sodium hydrogen carbonate, and 10 mL brine. The organic layer was dried with magnesium sulphate, filtered, and the solvents removed under reduced pressure. The resulting material was purified *via* flash column chromatography (30 % diethyl ether in petroleum ether). A sample was submitted to chiral analytical HPLC analysis [Chiralpak AD, *iso*-hexane / *iso*-propanol : 95/ 5, 1 mL / min, 2.67 min (1st peak), 3.00 min (2nd peak), 90% *e.e.*]. The title product *cis*-(324) was a colourless oil afforded in a 70 % yield (25 mg, 0.061 mmol). ¹H-NMR (CDCl₃, 400 MHz) δ 7.13-7.05 (m, 1H, ArH), 6.97 (dd, 1H, *J* 8.0, 1.3 Hz, ArH), 6.91-6.81 (m, 2H, ArH), 6.51 (s, 1H, Ar-OH), 3.64 (d, 1H, *J* 6.2 Hz, C3-H), 3.09 (d, 1H, *J* 6.2 Hz, C2-H), 1.40 (s, 9H, C(CH₃)₃); ¹³C-NMR (CDCl₃, 100 MHz) 166.4, 151.5, 147.7, 147.6, 147.5, 144.3, 144.3, 144.2, 139.4, 139.3, 139.2, 139.2, 136.1, 126.4, 120.4, 117.6, 115.7, 83.0, 44.5, 37.1, 27.6 ppm; $[\alpha]_D^{23}$ 17.2 (c 1 CHCl₃); FT-IR (thin film cm⁻¹) 3408, 1721, 1597, 1523, 1501, 1458, 1370, 1281, 1156; MS (ES) m/z 424.1 $[M+Na]^+$; HRMS (EI) Exact mass calculated for $[C_{19}H_{17}F_5NO_3]$ requires m/z 402.1123 found m/z 402.1129.

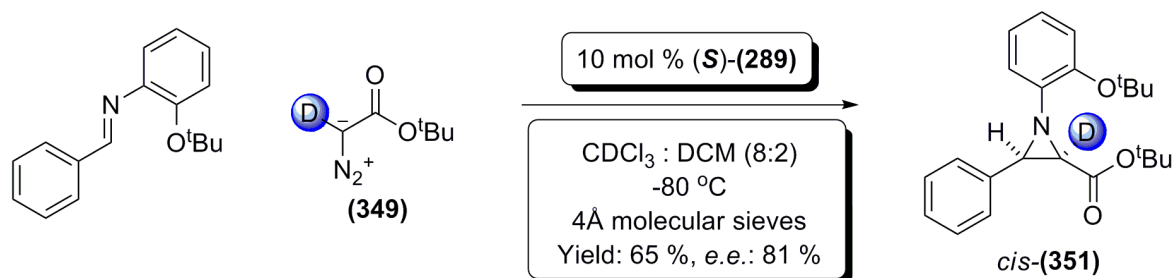
9.3: Synthesis of C2-deutero Aziridines

Asymmetric Synthesis of *tert*-butyl 3-(4-bromophenyl)-1-(2-*tert*-butoxyphenyl)-2-deuteroaziridine-2-carboxylate; *cis*-(350)



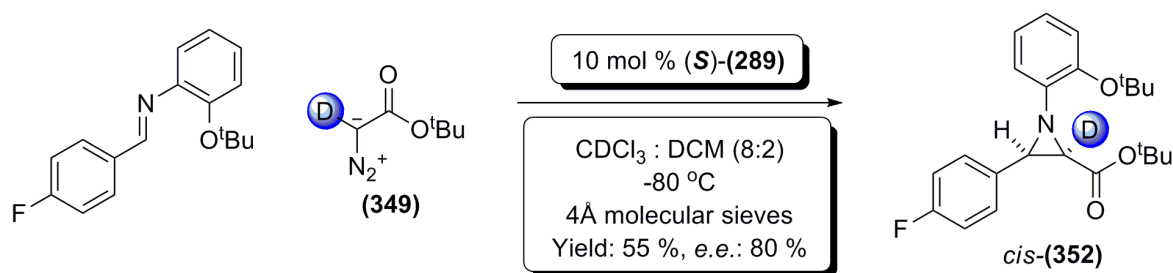
(*E*)-2-*tert*-Butoxy-*N*-(4-bromophenylmethylene)phenylamine (85 mg, 0.26 mmol), and catalyst (S)-(289) (21.6 mg, 0.026 mmol, 10%) were added to a flame dried 2 mL vial, containing ~ 40 mg of freshly powdered 4Å molecular sieves, under nitrogen. 800 µL of deuterated chloroform was added (pre-dried over 4Å molecular sieves), and the vial was sealed with a PTFE crimp cap. 200 µL of anhydrous DCM was added *via* syringe through the septum, and the reaction mixture was cooled to -80 °C. After 30 minutes, >95 % deuterated *tert*-butyl diazoacetate (349) (40.7 mg, 40 µL, 0.286 mmol) was added *via* syringe, and the reaction mixture was stirred at -80 °C, monitoring by ¹H-NMR spectroscopy until the reaction was deemed complete (~72 h). At this point the reaction mixture was filtered through a short plug of silica, eluting with diethyl ether. The solvents were removed under reduced pressure, and the residue was purified *via* flash column chromatography (14 % diethyl ether in petroleum ether). A sample was submitted to chiral analytical HPLC analysis [Chiralpak AD, *iso*-hexane / *iso*-propanol: 95 / 5, 1 mL / min, 4.12 min (1st peak), 7.27 min (2nd peak), 95 % *e.e.*]. The title product *cis*-(350) was a slight green oil afforded in 87 % yield (101 mg, 0.226 mmol). ¹H-NMR (CDCl₃, 400 MHz) δ 7.42-7.30 (m, 4H, ArH), 6.97-6.91 (m, 1H, ArH), 6.91-6.82 (m, 3H, ArH), 3.35 (s, 1H, C3-H), 1.29 (s, 9H, C(CH₃)₃), 1.16 (s, 9H, C(CH₃)₃); ¹³C-NMR (CDCl₃, 100 MHz) 167.0, 148.1, 146.3, 134.6, 131.0, 130.0, 123.3, 123.3, 123.3, 121.6, 121.1, 81.7, 80.6, 47.0, 28.9, 28.0 ppm; [α]_D²³ -23 (c 1.1 CHCl₃); FT-IR (thin film, cm⁻¹) 3010, 1770, 1750, 1495, 1395; MS (ES) *m/z* 447.1 [M+H]⁺, 469.1 [M+Na]⁺; HRMS (EI) Exact mass calculated for [C₂₃H₂₈DBrNO₃]⁺ requires *m/z* 447.1388 found *m/z* 447.1388

Asymmetric Synthesis of *tert*-butyl 1-(2-*tert*-butoxyphenyl)-3-phenyl-2-deuteroaziridine-2-carboxylate; *cis*-(351**)**



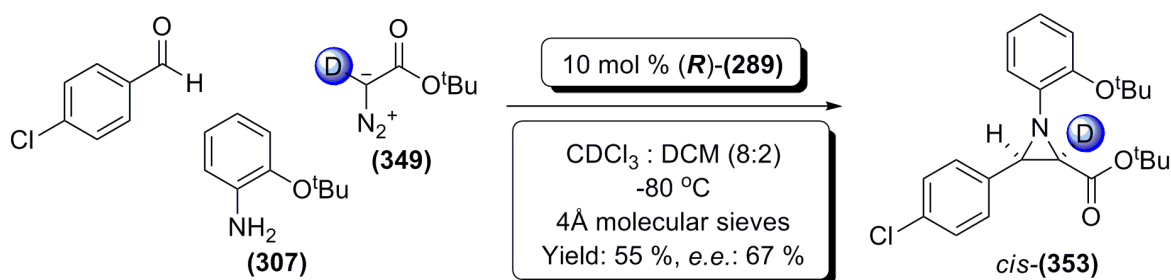
(*E*)-2-*tert*-Butoxy-*N*-(benzylidene)phenylamine (47 mg, 0.26 mmol), and catalyst (*S*)-(**289**) (21.6 mg, 0.026 mmol, 10%) were added to a flame dried 2 mL vial, containing ~40 mg of freshly powdered 4Å molecular sieves, under nitrogen. 800 μ L of deuterated chloroform was added (pre-dried over 4Å molecular sieves), and the vial was sealed with a PTFE crimp cap. 200 μ L of anhydrous DCM was added *via* syringe through the septum, and the reaction mixture was cooled to -80 °C. After 30 minutes, >95% deuterated *tert*-butyl diazoacetate (**349**) (40.7 mg, 40 μ L, 0.286 mmol) was added *via* syringe, and the reaction mixture was stirred at -80 °C, monitoring by $^1\text{H-NMR}$ spectroscopy until the reaction was deemed complete (~72 h). At this point the reaction mixture was filtered through a short plug of silica, eluting with diethyl ether. The solvents were removed under reduced pressure, and the residue was purified *via* flash column chromatography (14 % diethyl ether in petroleum ether). A sample was submitted to chiral analytical HPLC analysis [Chiralpak AD, *iso*-hexane / *iso*-propanol: 95 / 5, 1 mL / min, 3.81 (1st peak), 7.60 (2nd peak), 81 % *e.e.*]. The title product *cis*-(**351**) was afforded as a colourless oil in a 65 % yield (62 mg, 0.17 mmol). $^1\text{H-NMR}$ (CDCl_3 , 300 MHz) δ 7.56-7.48 (m, 2H, ArH), 7.38-7.27 (m, 3H, ArH), 7.06-6.90 (m, 4H, ArH), 3.43 (s, 1H, C3-H), 1.38 (s, 9H, $\text{C}(\text{CH}_3)_3$), 1.19 (s, 9H, $\text{C}(\text{CH}_3)_3$); $^{13}\text{C-NMR}$ (CDCl_3 , 75 MHz) 167.3, 148.0, 146.7, 135.3, 128.1, 127.8, 127.5, 123.2, 123.1, 123.0, 121.0, 81.2, 80.3, 47.3, 28.5, 27.6 ppm; $[\alpha]_{\text{D}}^{26}$ -30.6 (c 1 CHCl_3); FT-IR (thin film, cm^{-1}): 2977, 1746, 1716, 1593, 1490, 1449, 1392, 1367; MS (EI)⁺: m/z 369.2 $[\text{M}+\text{H}]^+$, 391.2 $[\text{M}+\text{Na}]^+$; HRMS (EI)⁺: exact mass calculated for $[\text{C}_{23}\text{H}_{29}\text{DNO}_3]^+$ requires m/z 369.2283, found m/z 369.2285

Asymmetric Synthesis of *tert*-butyl 3-(4-fluorophenyl)-1-(2-*tert*-butoxyphenyl)-2-deuteroaziridine-2-carboxylate; *cis*-(352)



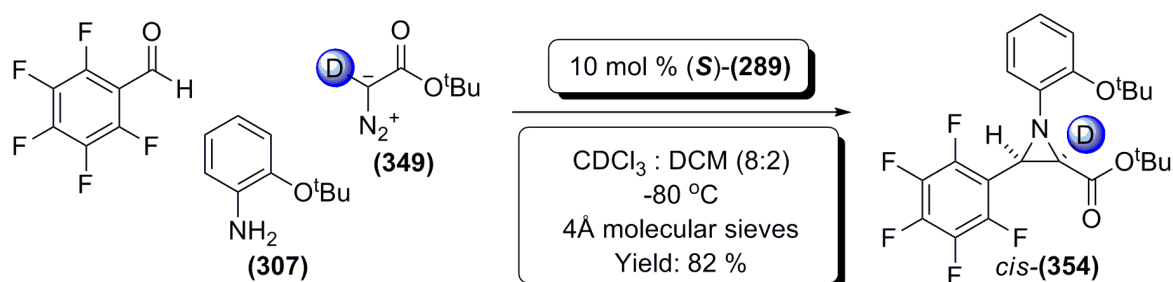
(E)-2-*tert*-Butoxy-*N*-(4-fluorophenylmethylene)phenylamine (71 mg, 0.26 mmol), and catalyst *(S)*-(**289**) (21.6 mg, 0.026 mmol, 10%) were added to a flame dried 2 mL vial, containing ~ 40 mg of freshly powdered 4Å molecular sieves, under nitrogen. 800 µL of deuterated chloroform was added (pre-dried over 4Å molecular sieves), and the vial was sealed with a PTFE crimp cap. 200 µL of anhydrous DCM was added *via* syringe through the septum, and the reaction mixture was cooled to -80 °C. After 30 minutes, >95 % deuterated *tert*-butyl diazoacetate (**349**) (40.7 mg, 40 µL, 0.286 mmol) was added *via* syringe, and the reaction mixture was stirred at -80 °C, monitoring by ¹H-NMR spectroscopy until the reaction was deemed complete (~72 h). At this point the reaction mixture was filtered through a short plug of silica, eluting with diethyl ether. The solvents were removed under reduced pressure, and the residue was purified *via* flash column chromatography (14 % diethyl ether in petroleum ether). A sample was submitted to chiral analytical HPLC analysis [Chiralpak AD, *iso*-hexane / *iso*-propanol: 95 / 5, 1 mL / min, 4.01 min (1st peak), 6.20 min (2nd peak), 80% *e.e.*]. The title product *cis*-(**352**) was a colourless oil afforded in a 55 % yield (55 mg, 0.143 mmol). ¹H-NMR (CDCl₃, 400 MHz) δ 7.50-7.44 (m, 2H, ArH), 7.04-6.96 (m, 3H, ArH), 6.95-6.87 (m, 3H, ArH), 3.42 (s, 1H, C3-H), 1.34 (s, 9H, C(CH₃)₃), 1.19 (s, 9H, C(CH₃)₃); ¹³C-NMR (CDCl₃, 100 MHz) 167.1, 163.7, 161.3, 148.1, 146.5, 131.2, 131.1, 129.9, 129.8, 123.3, 123.2, 121.1, 114.9, 114.7, 81.6, 80.6, 46.9, 28.9, 28.0, ppm; [α]_D²² -19.1 (c 1 CHCl₃); FT-IR (thin film, cm⁻¹) 2977, 2934, 1743, 1710, 1512, 1489, 1450, 1392, 1368; MS (ES) *m/z* 387.2 [M+H]⁺, 409.1 [M+Na]⁺; HRMS (EI) Exact mass calculated for [C₂₃H₂₈DFNO₃]⁺ requires *m/z* 387.2189 found *m/z* 387.2189.

Three Component One-Pot Asymmetric Synthesis of *tert*-butyl 1-(2-*tert*-butoxyphenyl)-3-(4-chlorophenyl)-2-deuteroaziridine-2-carboxylate; *cis*-(**353**)



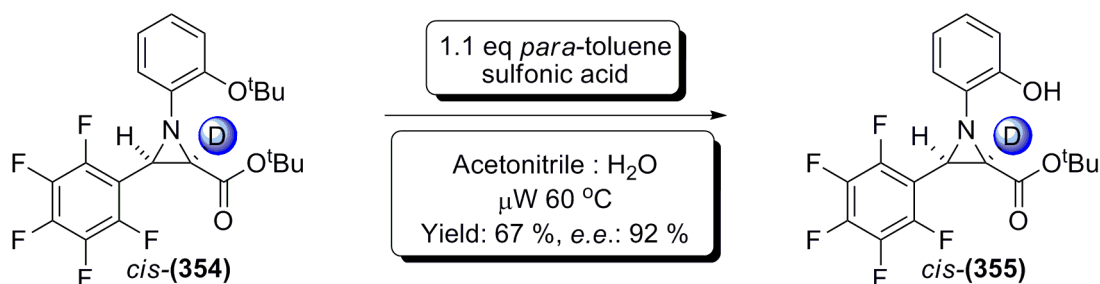
4-chlorobenzaldehyde (37 mg, 0.26 mmol), 2-*tert*-butoxy aniline (**307**) (43 mg, 0.26 mmol), and catalyst (*R*)-(289) (21.6 mg, 0.026 mmol, 10%) were added to a flame dried 2 mL vial under nitrogen. 800 μ L of deuterated chloroform was added (pre-dried over 4 Å molecular sieves), followed by ~40 mg of freshly powdered 4 Å molecular sieves, and the vial was sealed with a PTFE crimp cap. 200 μ L of anhydrous DCM was added *via* syringe through the septum, and the reaction mixture was cooled to -80 °C. After 30 minutes, >95 % deuterated *tert*-butyl diazoacetate (**349**) (40.7 mg, 40 μ L, 0.286 mmol) was added *via* syringe, and the reaction mixture was stirred at -80 °C, monitoring by ¹H-NMR spectroscopy until the reaction was deemed complete (~72 h). At this point the reaction mixture was filtered through a short plug of silica, eluting with diethyl ether. The solvents were removed under reduced pressure, and the residue was purified *via* flash column chromatography (12 % diethyl ether in petroleum ether). A sample was submitted to chiral analytical HPLC analysis [Chiralpak AD, *iso*-hexane / *iso*-propanol: 95 / 5, 1 mL / min, 4.45 min (1st peak), 7.34 min (2nd peak), 67 % *e.e.*]. The title product *cis*-(**353**) was a slight green oil afforded in a 55 % yield (58 mg, 0.143 mmol). ¹H-NMR (CDCl₃, 400 MHz) δ 7.47 (d, 2H, *J* 9.0 Hz, ArH), 7.30 (d, 2H, *J* 9.0 Hz, ArH), 7.06-6.91 (m, 4H, ArH), 3.44 (s, 1H, C3-H), 1.36 (s, 9H, C(CH₃)₃), 1.25 (s, 9H, C(CH₃)₃); ¹³C-NMR (CDCl₃, 100 MHz) 166.9, 148.0, 146.3, 133.9, 133.3, 129.5, 127.9, 123.2, 123.1, 120.9, 81.4, 80.3, 46.6, 28.6, 27.7 ppm; [α]_D²² 24.5 (c 0.05 CHCl₃); FT-IR (thin film, cm⁻¹) 2980, 2344, 1742, 1715, 1593, 1490, 1451, 1341, 1278, 1258; MS (ES) *m/z* 403.1 [M+H]⁺, 425.1 [M+Na]⁺; HRMS (EI) Exact mass calculated for [C₂₃H₂₇DCINO₃]⁺ requires *m/z* 403.1893 found *m/z* 403.1889.

Three Component One-Pot Asymmetric Synthesis of *tert*-butyl 1-(2-hydroxyphenyl)-3-(perfluorophenyl)-2-deuteroaziridine-2-carboxylate; *cis*-(354)



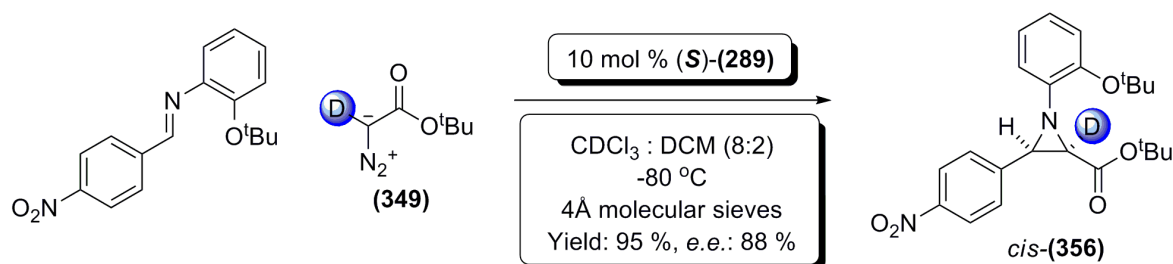
Pentafluorobenzaldehyde (40 mg, 0.26 mmol), 4-*tert*-butoxy aniline (**307**) (43 mg, 0.26 mmol), and catalyst (*S*)-(**289**) (21.6 mg, 0.026 mmol, 10%) were added to a flame dried 2 mL vial under nitrogen. 800 μ L of deuterated chloroform was added (pre-dried over 4Å molecular sieves), followed by ~40 mg of freshly powdered 4Å molecular sieves, and the vial was sealed with a PTFE crimp cap. 200 μ L of anhydrous DCM was added *via* syringe through the septum, and the reaction mixture was cooled to -80 °C. After 30 minutes, >95 % deuterated *tert*-butyl diazoacetate (**349**) (40.7 mg, 40 μ L, 0.286 mmol) was added *via* syringe, and the reaction mixture was stirred at -80 °C, monitoring by $^1\text{H-NMR}$ spectroscopy until the reaction was deemed complete (~72 h). At this point the reaction mixture was filtered through a short plug of silica, eluting with diethyl ether. The solvents were removed under reduced pressure, and the residue was purified *via* flash column chromatography (14 % diethyl ether in petroleum ether). The reaction product *cis*-(**354**) was a colourless oil afforded in an 82 % yield (98 mg, 0.21 mmol); however, *cis*-(**354**) could not be separated with the chiral HPLC techniques available at the time. $^1\text{H-NMR}$ (CDCl_3 , 400 MHz) δ 7.09-6.83 (m, 4H, ArH), 3.30 (s, 1H, C3-H), 1.40 (s, 9H, $\text{C}(\text{CH}_3)_3$), 1.38 (s, 9H, $\text{C}(\text{CH}_3)_3$); $^{13}\text{C-NMR}$ (CDCl_3 , 100 MHz) 167.2, 148.2, 147.7, 147.7, 147.5, 145.3, 144.5, 144.3, 139.3, 139.1, 139.0, 136.0, 135.8, 135.8, 123.7, 123.1, 122.8, 120.7, 110.5, 110.2, 110.2, 82.1, 80.5, 43.55, 36.82, 28.6, 27.6 ppm; $[\alpha]_{\text{D}}^{23}$ -121 (c 1.1 CHCl_3); FT-IR (thin film, cm^{-1}) 2979, 2933, 1743, 1738, 1594, 1524, 1502, 1451, 1393, 1369, 1331; MS (ES) m/z 459.2 $[\text{M}+\text{H}]^+$, 481.1 $[\text{M}+\text{Na}]^+$; HRMS (EI) Exact mass calculated for $[\text{C}_{23}\text{H}_{24}\text{F}_5\text{DNO}_3]$ requires m/z 459.1812 found m/z 459.1809.

Synthesis of *tert*-butyl 1-(2-hydroxyphenyl)-3-(perfluorophenyl)-2-deuteroaziridine-2-carboxylate; *cis*-(355**)**



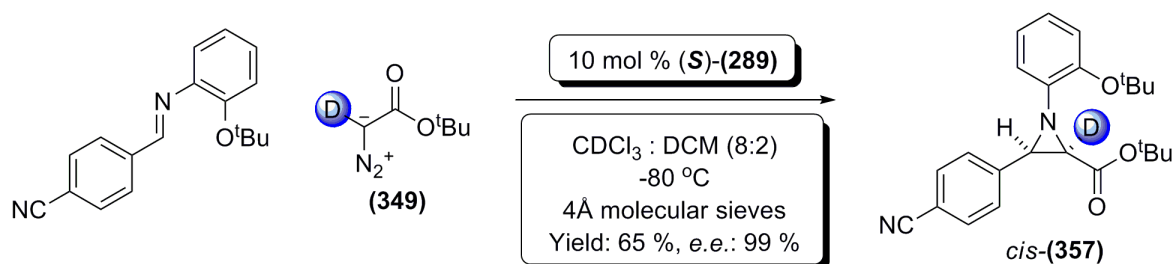
To a stirred solution of the optically active starting material *cis*-(**354**) (37 mg, 0.081 mmol) synthesised using (**R**)-(289), in 1 mL acetonitrile, in a 4 mL Biotage microwave vial, was added *para*-toluenesulfonic acid (17 mg, 0.087 mmol). 500 μL of water was added, the reaction was capped with a PTFE seal, and heated to 60 °C for 5 h in a Biotage Creator[®] microwave synthesiser. After this time, the reaction mixture was neutralised by addition of a saturated aqueous solution of sodium hydrogen carbonate. This was extracted with ethyl acetate, and the combined organic layers were washed with brine, dried with magnesium sulphate, filtered and the solvent removed under reduced pressure. The resulting material was purified *via* flash column chromatography (30 % diethyl ether in petroleum ether). A sample was submitted to chiral analytical HPLC analysis [Chiralpak IA, CO₂ / *iso*-propanol: 5% - 50% over 9 min, 0.7 mL / min, 3.78 min (1st peak), 4.23 min (2nd peak), 92 % *e.e.*] The reaction product *cis*-(**355**) was a pale brown oil afforded in a 67 % yield (22 mg, 0.054 mmol). ¹H-NMR (CDCl₃, 300 MHz) δ 7.12-7.04 (m, 1H, ArH), 7.00-6.93 (m, 1H, ArH), 6.91-6.80 (m, 2H, ArH), 6.54 (s br, 1H, Ar-OH), 3.62 (s, 1H, C3-H), 1.40 (s, 9H, C(CH₃)₃); ¹³C-NMR (CDCl₃, 75 MHz) 166.6, 151.6, 147.3, 147.2, 147.1, 144.8, 144.7, 144.6, 143.6, 143.6, 143.6, 138.9, 138.9, 138.9, 136.2, 126.5, 120.6, 117.9, 115.9, 83.2, 37.4, 27.9 ppm; [α]_D²² -18.2 (c 1 CHCl₃); FT-IR (thin film, cm⁻¹): 2982, 1720, 1597, 1502, 1458, 1395, 1370, 1277, 1094; MS (EI)⁺: *m/z* 425.3 [M+Na]⁺; HRMS (ASAP)⁺: exact mass calculated for [C₁₉H₁₆DF₅NO₃]⁺ requires *m/z* 403.1186, found *m/z* 403.1178.

Asymmetric Synthesis of *tert*-butyl 1-(2-*tert*-butoxyphenyl)-3-(4-nitrophenyl)-2-deuteroaziridine-2-carboxylate; *cis*-(356)



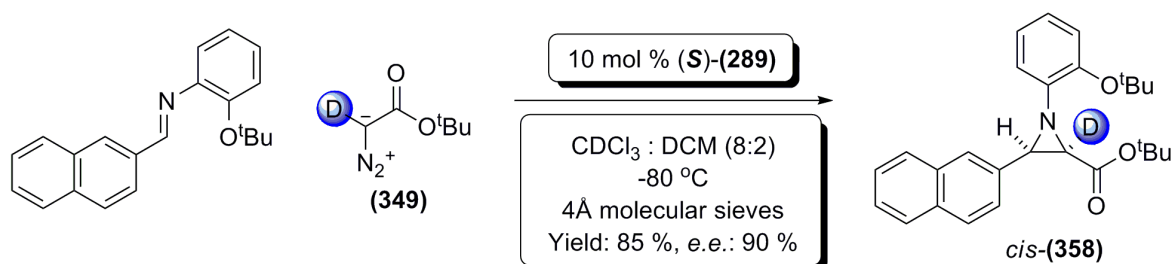
(E)-2-*tert*-Butoxy-*N*-(4-nitrophenylmethylene)phenylamine (77 mg, 0.26 mmol), and catalyst *(S)*-(**289**) (21.6 mg, 0.026 mmol, 10%) were added to a flame dried 2 mL vial, containing ~ 40 mg of freshly powdered 4Å molecular sieves, under nitrogen. 800 µL of deuterated chloroform was added (pre-dried over 4Å molecular sieves), and the vial was sealed with a PTFE crimp cap. 200 µL of anhydrous DCM was added *via* syringe through the septum, and the reaction mixture was cooled to -80 °C. After 30 minutes, >95 % deuterated *tert*-butyl diazoacetate (**349**) (40.7 mg, 40 µL, 0.286 mmol) was added *via* syringe, and the reaction mixture was stirred at -80 °C, monitoring by ¹H-NMR spectroscopy until the reaction was deemed complete (~72 h). At this point the reaction mixture was filtered through a short plug of silica, eluting with diethyl ether. The solvents were removed under reduced pressure, and the residue was purified *via* flash column chromatography (14 % diethyl ether in petroleum ether). A sample was submitted to chiral analytical HPLC analysis [Chiralpak AD, *iso*-hexane / *iso*-propanol: 95 / 5, 1 mL / min, 5.62 min (1st peak), 9.32 min (2nd peak), 88% *e.e.*]. The title product *cis*-(**356**) was a yellow oil, afforded in a 95 % yield (102 mg, 0.247 mmol); *cis*-(**356**) could be crystallised by treatment with 8:2 petroleum ether : diethyl ether. ¹H-NMR (CDCl₃, 400 MHz) δ 8.17 (d, 2H, *J* 6.9 Hz, ArH), 7.69 (d, 2H, *J* 6.9 Hz, ArH), 7.10-6.83 (m, 4H, ArH), 3.50 (s, 1H, C3-H), 1.33 (s, 9H, C(CH₃)₃), 1.20 (s, 9H, C(CH₃)₃); ¹³C-NMR (CDCl₃, 100 MHz) 166.5, 148.1, 147.5, 145.6, 143.2, 129.2, 123.7, 123.3, 123.2, 123.1, 121.0, 82.1, 80.6, 46.8, 28.9, 28.1 ppm; [α]_D²³ -5.33 (c 0.3 CHCl₃); FT-IR (thin film, cm⁻¹) 2978, 2933, 1743, 1715, 1520, 1345; MS (ES) *m/z* 414.2 [M+H]⁺; HRMS (EI) Exact mass calculated for [C₂₃H₂₈DN₂O₅] requires *m/z* 414.2134 found *m/z* 414.2131.

Asymmetric Synthesis of *tert*-butyl 1-(2-*tert*-butoxyphenyl)-3-(4-cyanophenyl)-2-deuteroaziridine-2-carboxylate; *cis*-(357**)**



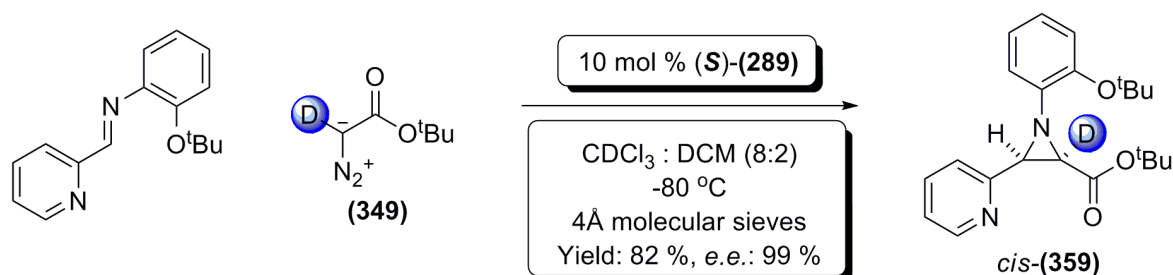
(E)-2-*tert*-Butoxy-*N*-(4-cyanophenylmethylene)phenylamine (72 mg, 0.26 mmol), and catalyst *(S)*-(**289**) (21.6 mg, 0.026 mmol, 10%) were added to a flame dried 2 mL vial, containing ~ 40 mg of freshly powdered 4Å molecular sieves, under nitrogen. 800 µL of deuterated chloroform was added (pre-dried over 4Å molecular sieves), and the vial was sealed with a PTFE crimp cap. 200 µL of anhydrous DCM was added *via* syringe through the septum, and the reaction mixture was cooled to -80 °C. After 30 minutes, >95 % deuterated *tert*-butyl diazoacetate (**349**) (40.7 mg, 40 µL, 0.286 mmol) was added *via* syringe, and the reaction mixture was stirred at -80 °C, monitoring by ¹H-NMR spectroscopy until the reaction was deemed complete (72 h). At this point the reaction mixture was filtered through a short plug of silica, eluting with diethyl ether. The solvents were removed under reduced pressure, and the residue was purified *via* flash chromatography (14 % diethyl ether in petroleum ether). A sample was submitted to chiral analytical HPLC analysis [Chiralpak AD, *iso*-hexane / *iso*-propanol: 95 / 5, 1 mL / min, 6.19 min (1st peak), 8.75 min (2nd peak), 99% *e.e.*]. The title product *cis*-(**357**) was a slight green oil afforded in a 65 % yield (66 mg, 0.17 mmol). ¹H-NMR (CDCl₃, 400 MHz) δ 7.72-7.58 (m, 4H, ArH), 7.09-6.88 (m, 4H, ArH), 3.48 (s, 1H, C3-H), 1.35 (s, 9H, C(CH₃)₃), 1.18 (s, 9H, C(CH₃)₃); ¹³C-NMR (CDCl₃, 100 MHz) 166.6, 148.1, 145.8, 141.1, 131.8, 129.1, 123.7, 123.3, 123.2, 121.0, 119.2, 82.0, 80.6, 47.0, 28.9, 28.0 ppm; [α]_D²³ -43.93 (c 1.4 CHCl₃); FT-IR (thin film, cm⁻¹) 2978, 1520, 1344; MS (ES) *m/z* 394.1 [M+H]⁺; HRMS (EI) Exact mass calculated for [C₂₄H₂₈DN₂O₃] requires *m/z* 394.2235 found *m/z* 394.2236.

Asymmetric Synthesis of *tert*-butyl 1-(2-*tert*-butoxyphenyl)-3-(naphthalen-2-yl)-2-deuteroaziridine-2-carboxylate; *cis*-(358)



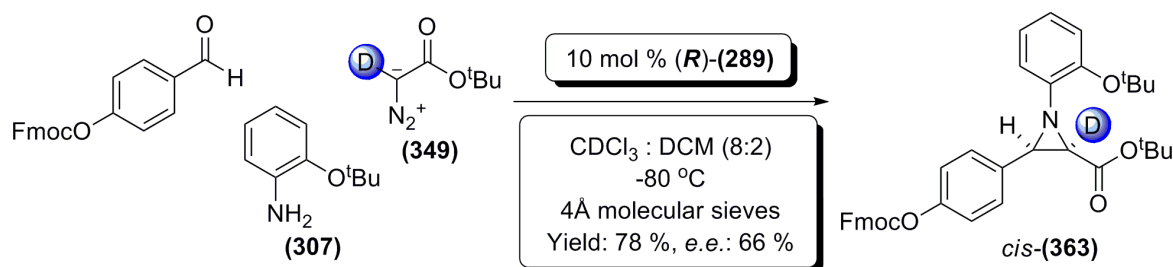
(*E*)-2-*tert*-Butoxy-*N*-(2-naphthylmethylene)phenylamine (79 mg, 0.26 mmol), and catalyst (*S*)-(289) (21.6 mg, 0.026 mmol, 10%) were added to a flame dried 2 mL vial, containing ~40 mg of freshly powdered 4Å molecular sieves, under nitrogen. 800 µL of deuterated chloroform was added (pre-dried over 4Å molecular sieves), and the vial was sealed with a PTFE crimp cap. 200 µL of anhydrous DCM was added *via* syringe through the septum, and the reaction mixture was cooled to -80 °C. After 30 minutes, >95 % deuterated *tert*-butyl diazoacetate (349) (40.7 mg, 40 µL, 0.286 mmol) was added *via* syringe, and the reaction mixture was stirred at -80 °C, monitoring by ¹H-NMR spectroscopy until the reaction was deemed complete (~72 h). At this point the reaction mixture was filtered through a short plug of silica, eluting with diethyl ether. The solvents were removed under reduced pressure, and the residue was purified *via* flash column chromatography (14 % diethyl ether in petroleum ether). A sample was submitted to chiral analytical HPLC analysis [Chiralpak AD, *iso*-hexane / *iso*-propanol: 95 / 5, 1 mL / min, 4.61 min (1st peak), 11.01 min (2nd peak), 90% *e.e.*]. The title product *cis*-(358) was afforded as a slight brown oil in an 85 % yield (92 mg, 0.22 mmol). ¹H-NMR (CDCl₃, 400 MHz) δ 7.94 (s, 1H, ArH), 7.81-7.68 (m, 3H, ArH) 7.57 (d, 1H, *J* 8.5 Hz, ArH), 7.46-7.34 (m, 2H, ArH), 7.01-6.83 (m, 4H, ArH), 3.57 (s, 1H, C3-H), 1.33 (s, 9H, C(CH₃)₃), 1.04 (s, 9H, C(CH₃)₃); ¹³C-NMR (CDCl₃, 100 MHz) 167.4, 148.2, 146.6, 133.1, 133.0, 128.1, 127.9, 127.5, 127.3, 126.2, 126.1, 125.9, 123.2, 123.2, 123.1, 121.2, 81.5, 80.5, 47.9, 28.9, 27.9 ppm; [α]_D²³ -13.93 (c 2.9 CHCl₃); FT-IR (thin film, cm⁻¹) 2977, 1742, 1713, 1592, 1489, 1449, 1392, 1367, 1332, 1261; MS (ES) *m/z* 419.2 [M+H]⁺, 441.1 [M+Na]⁺; HRMS (EI) Exact mass calculated for [C₂₇H₃₁DNO₃]⁺ required *m/z* 419.2439 found *m/z* 419.2441.

Asymmetric Synthesis of *tert*-butyl 1-(2-*tert*-butoxyphenyl)-3-(pyridin-2-yl)-2-deuteroaziridine-2-carboxylate; *cis*-(359**)**



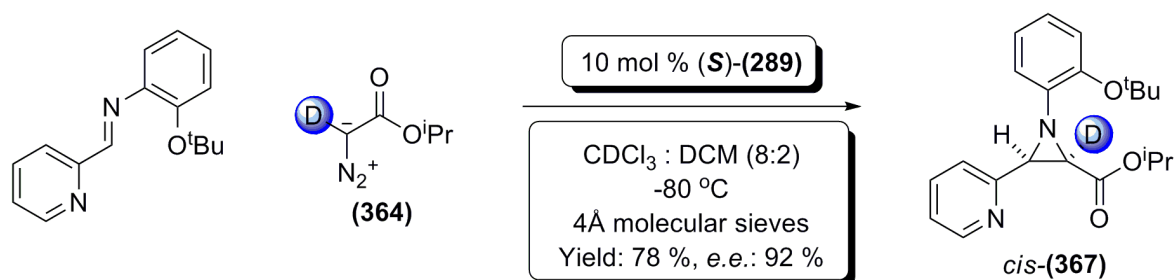
(E)-2-*tert*-Butoxy-*N*-(pyridin-2-ylmethylene)phenylamine (66 mg, 0.26 mmol), and catalyst *(S)*-(**289**) (21.6 mg, 0.026 mmol, 10%) were added to a flame dried 2 mL vial, containing ~ 40 mg of freshly powdered 4Å molecular sieves, under nitrogen. 800 µL of deuterated chloroform was added (pre-dried over 4Å molecular sieves), and the vial was sealed with a PTFE crimp cap. 200 µL of anhydrous DCM was added *via* syringe through the septum, and the reaction mixture was cooled to -80 °C. After 30 minutes, >95 % deuterated *tert*-butyl diazoacetate (**349**) (40.7 mg, 40 µL, 0.286 mmol) was added *via* syringe, and the reaction mixture was stirred at -80 °C, monitoring by ¹H-NMR spectroscopy until the reaction was deemed complete (72 h). At this point the reaction mixture was filtered through a short plug of silica, eluting with diethyl ether. The solvents were removed under reduced pressure, and the residue was purified *via* flash column chromatography (14 % diethyl ether in petroleum ether). A sample was submitted to chiral analytical HPLC analysis [Chiralpak AD, *iso*-hexane / *iso*-propanol: 8 / 2, 1 mL / min, 5.05 min (1st peak), 7.01 min (2nd peak), 99% *e.e.*]. The title product *cis*-(**359**) was a colourless oil afforded in a 82 % yield (79 mg, 0.21 mmol). ¹H-NMR (CDCl₃, 400 MHz) δ 8.61-8.48 (m, 1H, ArH), 7.78-7.60 (m, 2H, ArH), 7.24-7.13 (m, 1H, ArH), 7.08-6.88 (m, 4H, ArH), 3.65 (s, 1H, C3-H), 1.38 (s, 9H, C(CH₃)₃), 1.23 (s, 9H, C(CH₃)₃); ¹³C-NMR (CDCl₃, 100 MHz) 166.8, 155.6, 148.7, 148.2, 145.8, 135.9, 123.2, 123.1, 122.9, 122.7, 122.5, 120.9, 81.3, 80.2, 48.4, 28.6, 27.7 ppm; [α]_D²³ -43.30 (c 3.1 CHCl₃); FT-IR (thin film, cm⁻¹) 2977, 1738, 1715, 1589, 1570, 1489, 1450, 1435, 1392, 1367; MS (ES) *m/z* 370.1 [M+H]⁺, 392.1 [M+Na]⁺; HRMS (EI) Exact mass calculated for [C₂₂H₂₈DN₂O₃] requires *m/z* 370.2235 found *m/z* 370.2237.

Three Component One-Pot Asymmetric Synthesis of *tert*-butyl 3-(4-(((9H-fluoren-9-yl)methoxy)carbonyloxy)phenyl)-1-(2-*tert*-butoxyphenyl)-2-deuteroaziridine-2-carboxylate; *cis*-(363**)**



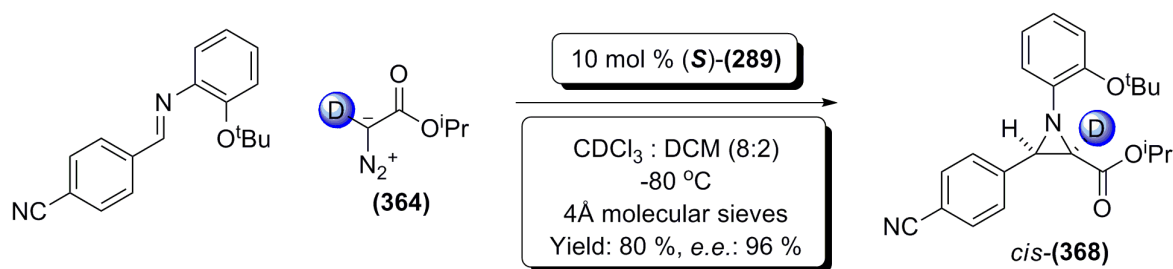
(9H-fluoren-9-yl)methyl 4-formylphenyl carbonate (44 mg, 0.13 mmol), 2-*tert*-butoxy aniline (**307**) (21.4 mg, 0.13 mmol), and catalyst (*R*)-(**289**) (11 mg, 0.013 mmol, 10%) were added to a flame dried 2 mL vial under nitrogen. 800 μ L of deuterated chloroform was added (pre-dried over 4 \AA molecular sieves), followed by \sim 40 mg of freshly powdered 4 \AA molecular sieves, and the vial was sealed with a PTFE crimp cap. 200 μ L of anhydrous DCM was added *via* syringe through the septum, and the reaction mixture was cooled to -80 $^{\circ}$ C. After 30 minutes, >95 % deuterated *tert*-butyl diazoacetate (**349**) (20.4 mg, 20 μ L, 0.143 mmol) was added *via* syringe, and the reaction mixture was stirred at -80 $^{\circ}$ C, monitoring by $^1\text{H-NMR}$ spectroscopy until the reaction was deemed complete (72 h). At this point the reaction mixture was filtered through a short plug of silica, eluting with diethyl ether. The solvents were removed under reduced pressure, and the residue was purified *via* flash column chromatography (18 % diethyl ether in petroleum ether). A sample was submitted to chiral analytical HPLC analysis [Chiralpak AD, *iso*-hexane / *iso*-propanol: 95 / 5, 1 mL / min, 8.9 min (1st peak), 34.48 min (2nd peak), 66 % *e.e.*]. The title product *cis*-(**363**) was a colourless oil afforded in a 78 % yield (61 mg, 0.10 mmol). $^1\text{H-NMR}$ (CDCl_3 , 300 MHz) δ 7.80 (d, 2H, *J* 7.4 Hz, ArH), 7.67 (d, 2H, *J* 7.4 Hz, ArH), 7.57 (d, 2H, *J* 8.7 Hz, ArH), 7.44 (t, 2H, *J* 7.4, 7.4 Hz, ArH), 7.35 (t, 2H, *J* 7.4, 7.4 Hz, ArH), 7.17 (d, 2H, *J* 8.4 Hz, ArH), 7.07-6.92 (m, 4H, ArH), 4.53 (d, 2H, *J* 7.4 Hz, CH_2), 4.34 (t, 1H, *J* 7.4, 7.4 Hz, ArH), 3.48 (s, 1H, C3-H), 1.39 (s, 9H, $\text{C}(\text{CH}_3)_3$), 1.22 (s, 9H, $\text{C}(\text{CH}_3)_3$); $^{13}\text{C-NMR}$ (CDCl_3 , 75 MHz) 167.2, 153.9, 150.7, 148.1, 146.5, 143.4, 141.5, 133.4, 129.4, 128.2, 127.4, 125.4, 123.3, 121.1, 120.6, 120.4, 110.0, 81.7, 80.6, 70.6, 46.9, 28.9, 28.0 ppm; $[\alpha]_D^{26}$ 80 (c 0.1 CHCl_3); FT-IR (thin film, cm^{-1}): 2976, 1760, 1712, 1591, 1489, 1449, 1366, 1253, 1229, 1205, 1159; MS (EI)⁺: *m/z* 629.3 [$\text{M}+\text{Na}$]⁺; HRMS (EI)⁺: exact mass calculated for $[\text{C}_{38}\text{H}_{39}\text{DNO}_6]^+$ requires *m/z* 607.2840, found *m/z* 607.2900.

Asymmetric Synthesis of isopropyl 1-(2-*tert*-butoxyphenyl)-3-(pyridin-2-yl)-2-deuteroaziridine-2-carboxylate; *cis*-(367**)**



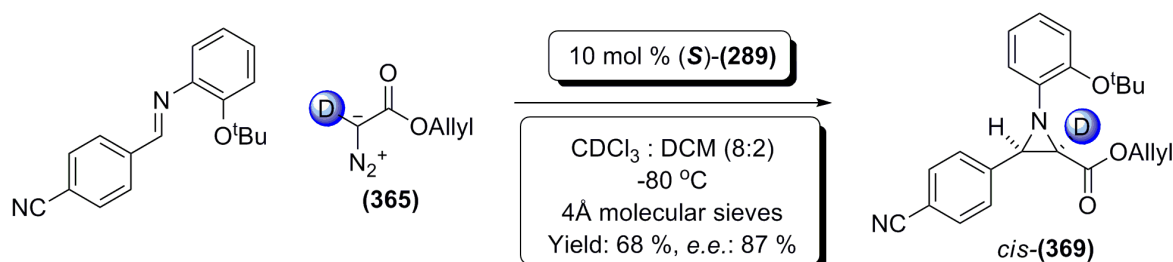
(*E*)-2-*tert*-Butoxy-*N*-(pyridin-2-ylmethylene)phenylamine (66 mg, 0.26 mmol), and catalyst (*S*)-(**289**) (21.6 mg, 0.026 mmol, 10%) were added to a flame dried 2 mL Biotage microwave vial, containing ~ 40 mg of freshly powdered 4Å molecular sieves, under nitrogen. 800 μ L of deuterated chloroform was added (pre-dried over 4Å molecular sieves), and the vial was sealed with a PTFE crimp cap. 200 μ L of anhydrous DCM was added *via* syringe through the septum, and the reaction mixture was cooled to -80 °C. After 30 minutes, >95 % deuterated *iso*-propyl diazoacetate (**364**) (36.6 mg, 36 μ L, 0.286 mmol) was added *via* syringe, and the reaction mixture was stirred at -80 °C, monitoring by $^1\text{H-NMR}$ spectroscopy until the reaction was deemed complete (~72 h). At this point the reaction mixture was filtered through a short plug of silica, eluting with diethyl ether. The solvents were removed under reduced pressure, and the residue was purified *via* flash column chromatography (14 % diethyl ether in petroleum ether). A sample was submitted to chiral analytical HPLC analysis [Chiralpak AD, *iso*-hexane / *iso*-propanol: 95 / 5, 1 mL / min, 6.60 min (1st peak), 11.90 min (2nd peak), 92% *e.e.*]. The title product *cis*-(**367**) was a colourless oil afforded in a 78 % yield (72 mg, 0.20 mmol). $^1\text{H-NMR}$ (CDCl_3 , 400 MHz) δ 7.72-7.54 (m, 2H, ArH), 7.17-7.08 (m, 1H, ArH), 7.01-6.93 (m, 1H, ArH), 6.93-6.83 (m, 4H, ArH), 4.81 (m, 1H, $\text{CH}(\text{CH}_3)_2$), 3.62 (s, 1H, C3-H), 1.29 (s, 9H, $\text{C}(\text{CH}_3)_3$), 1.01 (d, 3H, J 6.2 Hz, $\text{CH}(\text{CH}_3)_2$), 0.93 (d, 3H, J 6.7 Hz, $\text{CH}(\text{CH}_3)_2$); $^{13}\text{C-NMR}$ (CDCl_3 , 100 MHz) 167.5, 155.5, 148.9, 148.3, 145.5, 136.1, 123.5, 123.3, 122.9, 122.8, 122.4, 121.0, 80.3, 68.7, 48.9, 28.9, 21.8 ppm; $[\alpha]_{\text{D}}^{23}$ -8.5 (c 0.2 CHCl_3); FT-IR (thin film, cm^{-1}) 2977, 1738, 1715, 1589, 1570, 1493, 1451, 1440, 1393, 1365; MS (ES) m/z 356.1 $[\text{M}+\text{H}]^+$, 378.1 $[\text{M}+\text{Na}]^+$; HRMS (EI) Exact mass calculated for $[\text{C}_{21}\text{H}_{26}\text{DN}_2\text{O}_3]^+$ requires m/z 356.2079 found m/z 356.2082.

Asymmetric Synthesis of *isopropyl 1-(2-*tert*-butoxyphenyl)-3-(4-cyanophenyl)-2-deuteroaziridine-2-carboxylate; *cis*-(368)*



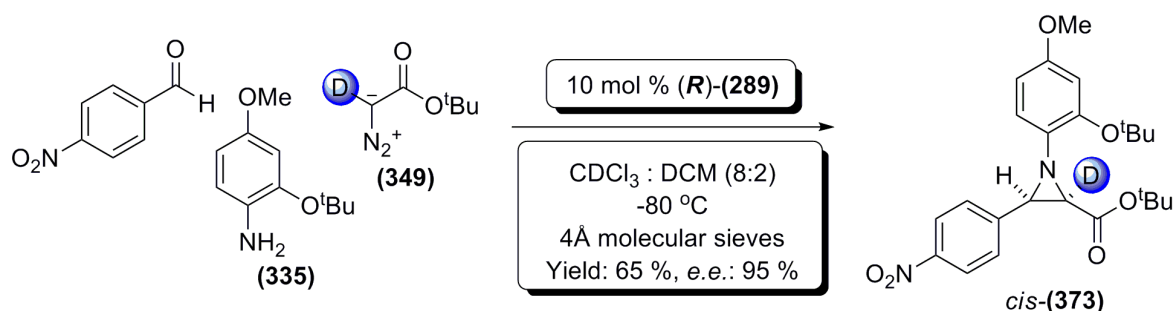
(*E*)-2-*tert*-Butoxy-*N*-(4-cyanophenylmethylene)phenylamine (74 mg, 0.26 mmol), and catalyst (*S*)-(289) (21.6 mg, 0.026 mmol, 10%) were added to a flame dried 2 mL vial, containing ~ 40 mg of freshly powdered 4Å molecular sieves, under nitrogen. 800 µL of deuterated chloroform was added (pre-dried over 4Å molecular sieves), and the vial was sealed with a PTFE crimp cap. 200 µL of anhydrous DCM was added *via* syringe through the septum, and the reaction mixture was cooled to -80 °C. After 30 minutes, >95 % deuterated *iso*-propyl diazoacetate (364) (36.6 mg, 36 µL, 0.286 mmol) was added *via* syringe, and the reaction mixture was stirred at -80 °C, monitoring by ¹H-NMR spectroscopy until the reaction was deemed complete (~72 h). At this point the reaction mixture was filtered through a short plug of silica, eluting with diethyl ether. The solvents were removed under reduced pressure, and the residue was purified *via* flash column chromatography (14 % diethyl ether in petroleum ether). A sample was submitted to chiral analytical HPLC analysis [Chiralpak AD, *iso*-hexane / *iso*-propanol: 95 / 5, 1 mL / min, 7.40 min (1st peak), 13.10 min (2nd peak), 96% *e.e.*]. The title product *cis*-(368) was a slight green oil afforded in a 80 % yield (79 mg, 0.21 mmol). ¹H-NMR (CDCl₃, 400 MHz) δ 7.71-7.59 (m, 4H, ArH), 7.07-6.89 (m, 4H, ArH), 4.87 (m, 1H, CH(CH₃)₂), 3.52 (s, 1H, C3-H), 1.33 (s, 9H, C(CH₃)₃), 1.02 (dd, 6H, *J* 6.3, 8.9 Hz, CH(CH₃)₂); ¹³C-NMR (CDCl₃, 100 MHz) 167.1, 148.2, 145.4, 140.9, 131.8, 129.1, 123.8, 123.1, 122.8, 120.9, 119.1, 111.5, 80.5, 69.0, 47.2, 28.9, 21.9, 21.7 ppm; [α]_D²³ -37.65 (c 1.7 CHCl₃); FT-IR (thin film, cm⁻¹) 2925, 2859, 1608, 1494, 1451, 1403, 1262, 1202; MS (ES) *m/z* 380.2 [M+H]⁺; HRMS (EI) Exact mass calculated for [C₂₃H₂₆DN₂O₃]⁺ requires *m/z* 380.2079 found *m/z* 380.2079.

Asymmetric Synthesis of allyl 1-(2-tert-butoxyphenyl)-3-(4-cyanophenyl)-2-deuteroaziridine-2-carboxylate *cis*-(369)



(*E*)-2-*tert*-Butoxy-*N*-(4-cyanophenylmethylene)phenylamine (74 mg, 0.26 mmol), and catalyst (*S*)-(289) (21.6 mg, 0.026 mmol, 10%) were added to a flame dried 2 mL vial, containing ~ 40 mg of freshly powdered 4Å molecular sieves, under nitrogen. 800 µL of deuterated chloroform was added (pre-dried over 4Å molecular sieves), and the vial was sealed with a PTFE crimp cap. 200 µL of anhydrous DCM was added *via* syringe through the septum, and the reaction mixture was cooled to -80 °C. After 30 minutes, >95 % deuterated allyl diazoacetate (365) (36 mg, 35 µL, 0.286 mmol) was added *via* syringe, and the reaction mixture was stirred at -80 °C, monitoring by ¹H-NMR spectroscopy until the reaction was deemed complete (~72 h). At this point the reaction mixture was filtered through a short plug of silica, eluting with diethyl ether. The solvents were removed under reduced pressure, and the residue was purified *via* flash column chromatography (14 % diethyl ether in petroleum ether). A sample was submitted to chiral analytical HPLC analysis [Chiralpak AD, *iso*-hexane / *iso*-propanol: 95 / 5, 1 mL / min, 12.20 min (1st peak), 20.40 min (2nd peak), 87% *e.e.*]. The title product *cis*-(369) was a slight green oil afforded in a 68 % yield (67 mg, 0.18 mmol). ¹H-NMR (CDCl₃, 400 MHz) δ 7.64-7.53 (m, 4H, ArH), 7.00-6.83 (m, 4H, ArH), 5.72-5.56 (m, 1H, allyl-CH), 5.15-5.03 (m, 2H, OCH₂), 4.49-4.33 (m, 2H, allyl-CH₂), 3.49 (s, 1H, C3-H), 1.25 (s, 9H, C(CH₃)₃); ¹³C-NMR (CDCl₃, 100 MHz) 167.2, 148.1, 145.2, 140.5, 131.8, 131.5, 128.9, 123.7, 123.0, 122.6, 120.7, 118.9, 111.5, 80.3, 65.7, 47.2, 28.6 ppm; [α]_D²³ -18.5 (c 1 CHCl₃); FT-IR (thin film, cm⁻¹) 2963, 2228, 1748, 1610, 1490, 1450, 1392, 1367, 1260; MS (ES) *m/z* 378.2 [M+H]⁺; HRMS (EI) Exact mass calculated for [C₂₃H₂₄DN₂O₃] requires *m/z* 378.1922 found *m/z* 378.1923.

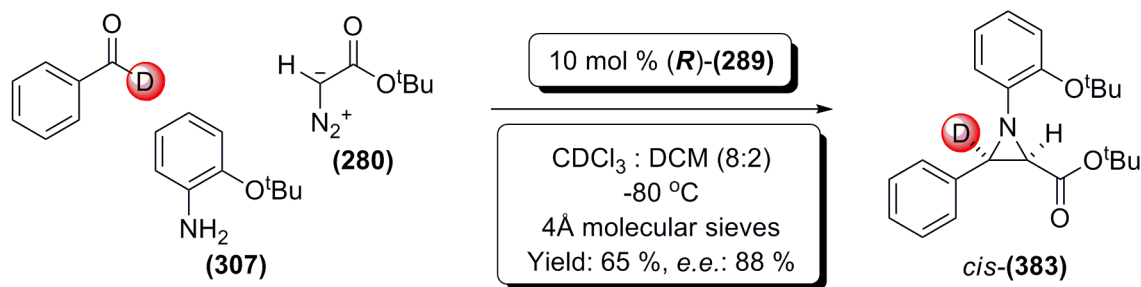
Three component One-Pot Asymmetric Synthesis of *tert*-butyl 1-(2-*tert*-butoxy-4-methoxyphenyl)-3-(4-nitrophenyl)-2-deuteroaziridine-2-carboxylate; *cis*-(373**)**



4-nitrobenzaldehyde (49 mg, 0.26 mmol), 4-methoxy-2-*tert*-butoxy aniline (**335**) (43 mg, 0.26 mmol), and catalyst (*R*)-(289) (21.6 mg, 0.026 mmol, 10%) were added to a flame dried 2 mL vial, under nitrogen. 800 μ L of deuterated chloroform was added (pre-dried over 4Å molecular sieves), followed by ~40 mg of freshly powdered 4Å molecular sieves, and the vial was sealed with a PTFE crimp cap. 200 μ L of anhydrous DCM was added *via* syringe through the septum, and the reaction mixture was cooled to -80 °C. After 30 minutes, >95 % deuterated *tert*-butyl diazoacetate (**349**) (40.7 mg, 40 μ L, 0.286 mmol) was added *via* syringe, and the reaction mixture was stirred at -80 °C, monitoring by ¹H-NMR spectroscopy until the reaction was deemed complete. At this point the reaction mixture was filtered through a short plug of silica, eluting with diethyl ether. The solvents were removed under reduced pressure, and the residue was purified *via* flash column chromatography (14 % diethyl ether in petroleum ether). A sample was submitted to chiral analytical HPLC analysis [Chiralpak AD, *iso*-hexane / *iso*-propanol : 95 / 5, 1 mL / min, 9.80 min (1st peak), 11.60 min (2nd peak), 95% *e.e.*]. The title product *cis*-(**373**) was a slight yellow oil afforded in a 65 % yield (75 mg, 0.17 mmol). ¹H-NMR (CDCl₃, 300 MHz) δ 8.20 (d, 2H, *J* 8.5 Hz, ArH), 7.71 (d, 2H, *J* 8.5 Hz, ArH), 6.84 (d, 1H, *J* 8.7 Hz, ArH), 6.62 (d, 1H, *J* 2.7 Hz, ArH), 6.51 (dd, 1H, *J* 8.7, 2.7 Hz, ArH), 3.75 (s, 3H, CH₃), 3.46 (s, 1H, C3-H), 1.35 (s, 9H, C(CH₃)₃), 1.21 (s, 9H, C(CH₃)₃); ¹³C-NMR (CDCl₃, 75 MHz) 165.4, 154.8, 147.7, 146.3, 142.1, 137.9, 128.0, 121.9, 119.7, 108.5, 106.1, 80.8, 79.6, 54.5, 45.8, 27.7, 26.8 ppm; [α]_D²⁶ 0.6 (c 1 CHCl₃); FT-IR (thin film, cm⁻¹): 2978, 1742, 1605, 1523, 1368, 1345; MS (EI)⁺: *m/z* 444.3 [M+H]⁺, 466.3 [M+Na]⁺; HRMS (EI)⁺: exact mass calculated for [C₂₄H₃₀DN₂O₆]⁺ requires *m/z* 444.2239, found *m/z* 444.2238.

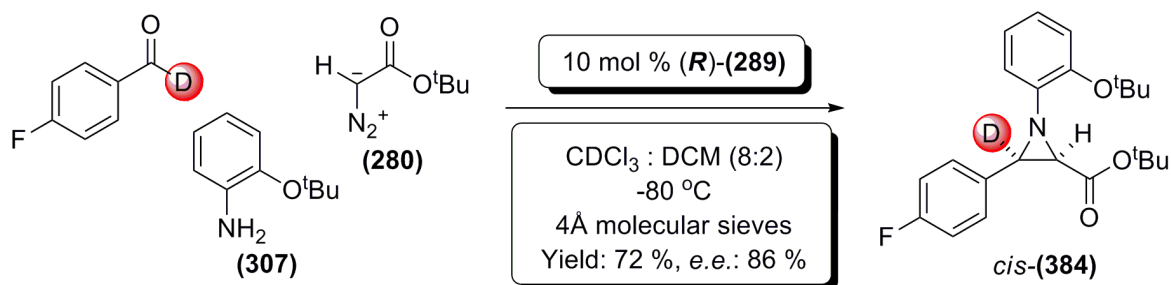
9.4: Synthesis of C3-deutero Aziridines

Three Component One-Pot Asymmetric Synthesis of *tert*-butyl 1-(2-*tert*-butoxyphenyl)-3-phenyl-3-deuteroaziridine-2-carboxylate; *cis*-(**383**)



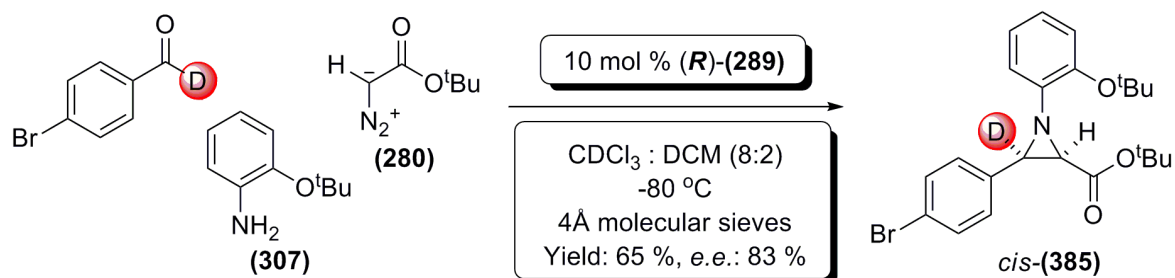
>95 % deuterated benzaldehyde (**221**) (27.8 mg, 28 μ L, 0.26 mmol), 2-*tert*-butoxy aniline (**307**) (43 mg, 0.26 mmol), and catalyst *(R)*-(**289**) (21.6 mg, 0.026 mmol, 10%) were added to a flame dried 2 mL vial under nitrogen. 800 μ L of deuterated chloroform was added (pre-dried over 4Å molecular sieves), followed by ~40 mg of freshly powdered 4Å molecular sieves, and the vial was sealed with a PTFE crimp cap. 200 μ L of anhydrous DCM was added *via* syringe through the septum, and the reaction mixture was cooled to -80 °C. After 30 minutes, *tert*-butyl diazoacetate (**280**) (40.7 mg, 40 μ L, 0.286 mmol) was added *via* syringe, and the reaction mixture was stirred at -80 °C, monitoring by ¹H-NMR spectroscopy until the reaction was deemed complete (~72 h). At this point the reaction mixture was filtered through a short plug of silica, eluting with diethyl ether. The solvents were removed under reduced pressure, and the residue was purified *via* flash column chromatography (14 % diethyl ether in petroleum ether). A sample was submitted to chiral analytical HPLC analysis [Chiralpak AD, *iso*-hexane / *iso*-propanol: 95 / 5, 1 mL / min, 3.77 min (1st peak), 7.10 min (2nd peak), 88% *e.e.*]. The title product *cis*-(**383**) was a colourless oil afforded in a 65 % yield (62 mg, 0.17 mmol). ¹H-NMR (CDCl₃, 300 MHz) δ 7.52-7.39 (m, 2H, ArH), 7.32-7.13 (m, 3H, ArH), 7.01-6.79 (m, 4H, ArH), 2.97 (s, 1H, C2-H), 1.31 (s, 9H, C(CH₃)₃), 1.12 (s, 9H, C(CH₃)₃); ¹³C-NMR (CDCl₃, 75 MHz) 166.1, 146.9, 145.6, 134.1, 127.0, 126.7, 126.4, 122.2, 122.1, 121.9, 119.9, 80.2, 79.3, 46.2, 27.6, 26.7 ppm; $[\alpha]_D^{26}$ 26.7 (c 1 CHCl₃); FT-IR (thin film, cm⁻¹): 2977, 1746, 1716, 1593, 1490, 1449, 1392, 1367; MS (EI)⁺: *m/z* 369.3 [M+H]⁺, 391.2 [M+Na]⁺; HRMS (EI)⁺: exact mass calculated for [C₂₃H₂₉DNO₃]⁺ requires *m/z* 369.2283, found *m/z* 369.2286.

Three Component One-Pot Asymmetric Synthesis of *tert*-butyl 3-(4-fluorophenyl)-1-(2-*tert*-butoxyphenyl)-3-deuteroaziridine-2-carboxylate; *cis*-(384**)**



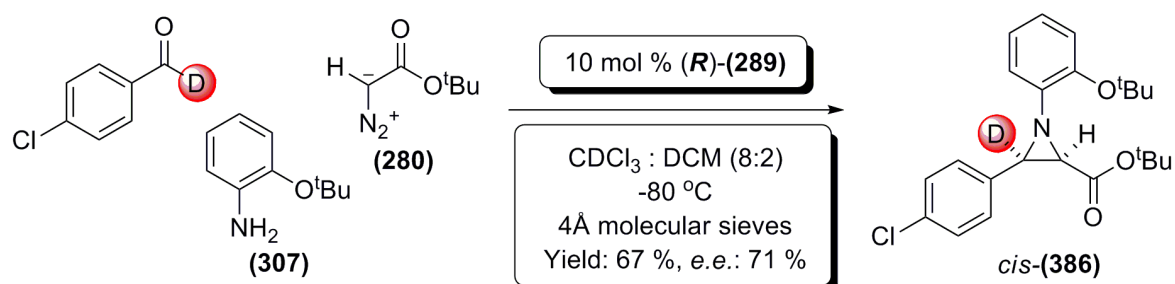
>95 % deuterated 4-fluorobenzaldehyde (40 mg, 0.26 mmol), 2-*tert*-butoxy aniline (**307**) (43 mg, 0.26 mmol), and catalyst (*R*)-(**289**) (21.6 mg, 0.026 mmol, 10%) were added to a flame dried 2 mL vial under nitrogen. 800 μ L of deuterated chloroform was added (pre-dried over 4Å molecular sieves), followed by ~40 mg of freshly powdered 4Å molecular sieves, and the vial was sealed with a PTFE crimp cap. 200 μ L of anhydrous DCM was added *via* syringe through the septum, and the reaction mixture was cooled to -80 °C. After 30 minutes, *tert*-butyl diazoacetate (**280**) (40.7 mg, 40 μ L, 0.286 mmol) was added *via* syringe, and the reaction mixture was stirred at -80 °C, monitoring by $^1\text{H-NMR}$ spectroscopy until the reaction was deemed complete (~72 h). At this point the reaction mixture was filtered through a short plug of silica, eluting with diethyl ether. The solvents were removed under reduced pressure, and the residue was purified *via* flash column chromatography (14 % diethyl ether in petroleum ether). A sample was submitted to chiral analytical HPLC analysis [Chiralpak AD, *iso*-hexane / *iso*-propanol: 95 / 5, 1 mL / min, 3.34 min (1st peak), 6.77 min (2nd peak), 86% *e.e.*]. The title product *cis*-(**384**) was a slight green oil afforded in a 72 % yield (72 mg, 0.19 mmol). $^1\text{H-NMR}$ (CDCl_3 , 300 MHz) δ 7.54-7.46 (m, 2H, ArH), 7.06-6.92 (m, 6H, ArH), 3.03 (s, 1H, C2-H), 1.36 (s, 9H, C(CH_3)₃), 1.22 (s, 9H, C(CH_3)₃); $^{13}\text{C-NMR}$ (CDCl_3 , 75 MHz) 167.1, 148.0, 146.4, 131.0, 129.7, 129.6, 123.1, 123.1, 120.9, 114.8, 114.5, 81.3, 80.3, 47.1, 28.5, 27.7 ppm; $[\alpha]_{\text{D}}^{26}$ 24 (c 1.4 CHCl_3); FT-IR (thin film, cm^{-1}): 3010, 1744, 1736, 1490, 1163; MS (EI)⁺: m/z 387.2 [M+H]⁺; HRMS (EI)⁺: exact mass calculated for $[\text{C}_{23}\text{H}_{28}\text{DFNO}_3]^+$ requires m/z 387.2189, found m/z 387.2192.

Three Component One-Pot Asymmetric Synthesis of *tert*-butyl 3-(4-bromophenyl)-1-(2-*tert*-butoxyphenyl)-3-deuteroaziridine-2-carboxylate; *cis*-(385**)**



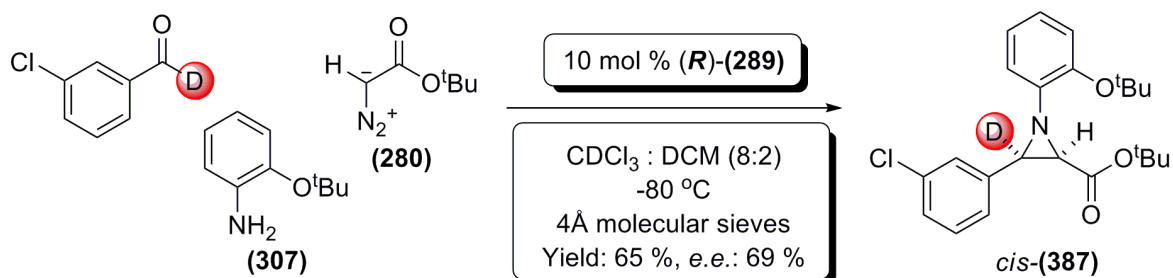
>95 % deuterated 4-bromobenzaldehyde (49 mg, 0.26 mmol), 2-*tert*-butoxy aniline (**307**) (43 mg, 0.26 mmol), and catalyst (*R*)-(**289**) (21.6 mg, 0.026 mmol, 10%) were added to a flame dried 2 mL vial under nitrogen. 800 μ L of deuterated chloroform was added (pre-dried over 4Å molecular sieves), followed by ~40 mg of freshly powdered 4Å molecular sieves, and the vial was sealed with a PTFE crimp cap. 200 μ L of anhydrous DCM was added *via* syringe through the septum, and the reaction mixture was cooled to -80 °C. After 30 minutes, *tert*-butyl diazoacetate (**280**) (40.7 mg, 40 μ L, 0.286 mmol) was added *via* syringe, and the reaction mixture was stirred at -80 °C, monitoring by ¹H-NMR spectroscopy until the reaction was deemed complete (~72 h). At this point the reaction mixture was filtered through a short plug of silica, eluting with diethyl ether. The solvents were removed under reduced pressure, and the residue was purified *via* flash column chromatography (14 % diethyl ether in petroleum ether). A sample was submitted to chiral analytical HPLC analysis [Chiralpak AD, *iso*-hexane / *iso*-propanol: 95 / 5, 1 mL / min, 4.01 min (1st peak), 6.68 min (2nd peak), 83% *e.e.*]. The title product *cis*-(**385**) was a slight green oil afforded in a 65 % yield (75 mg, 0.17 mmol). ¹H-NMR (CDCl₃, 300 MHz) δ 7.49-7.38 (m, 4H, ArH), 7.05-6.92 (m, 4H, ArH), 3.04 (s, 1H, C2-H), 1.36 (s, 9H, C(CH₃)₃), 1.24 (s, 9H, C(CH₃)₃); ¹³C-NMR (CDCl₃, 75 MHz) 166.9, 148.0, 146.3, 134.4, 130.9, 129.8, 123.2, 123.1, 121.4, 120.9, 81.5, 80.3, 47.2, 28.6, 27.7 ppm; [α]_D²⁶ 28.4 (c 1 CHCl₃); FT-IR (thin film, cm⁻¹): 2965, 1744, 1595, 1489, 1392, 1367, 1260; MS (EI)⁺: *m/z* 447.1 [M+H]⁺, 469.1 [M+Na]⁺; HRMS (EI)⁺: exact mass calculated for [C₂₃H₂₈DBrNO₃]⁺ requires *m/z* 447.1388, found *m/z* 447.1391.

Three Component One-Pot Asymmetric Synthesis of *tert*-butyl 1-(2-*tert*-butoxyphenyl)-3-(4-chlorophenyl)-3-deuteroaziridine-2-carboxylate; *cis*-(386**)**



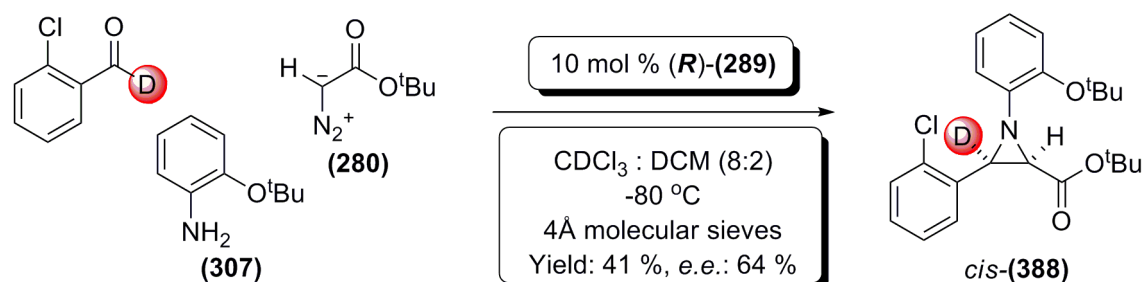
>95 % deuterated 4-chlorobenzaldehyde (19 mg, 0.13 mmol), 2-*tert*-butoxy aniline (**307**) (22 mg, 0.13 mmol), and catalyst (*R*)-(289) (10 mg, 0.013 mmol, 10%) were added to a flame dried 2 mL vial under nitrogen. 400 μ L of deuterated chloroform was added (pre-dried over 4Å molecular sieves), followed by ~40 mg of freshly powdered 4Å molecular sieves, and the vial was sealed with a PTFE crimp cap. 100 μ L of anhydrous DCM was added *via* syringe through the septum, and the reaction mixture was cooled to -80 °C. After 30 minutes, *tert*-butyl diazoacetate (**280**) (20.4 mg, 20 μ L, 0.142 mmol) was added *via* syringe, and the reaction mixture was stirred at -80 °C, monitoring by ¹H-NMR spectroscopy until the reaction was deemed complete (~72 h). At this point the reaction mixture was filtered through a short plug of silica, eluting with diethyl ether. The solvents were removed under reduced pressure, and the residue was purified *via* flash column chromatography (12 % diethyl ether in petroleum ether). A sample was submitted to chiral analytical HPLC analysis [Chiralpak AD, *iso*-hexane / *iso*-propanol: 95 / 5, 1 mL / min, 4.78 min (1st peak), 7.92 min (2nd peak), 71 % *e.e.*]. The title product *cis*-(**386**) was a slight yellow oil afforded in a 67 % yield (35 mg, 0.087 mmol). ¹H-NMR (CDCl₃, 400 MHz) δ 7.44 (d, 2H, *J* 9.0 Hz, ArH), 7.27 (d, 2H, *J* 9.0 Hz, ArH), 7.03-6.87 (m, 4H, ArH), 3.01 (s, 1H, C2-H), 1.34 (s, 9H, C(CH₃)₃), 1.20 (s, 9H, C(CH₃)₃); ¹³C-NMR (CDCl₃, 100 MHz) 167.0, 148.1, 146.4, 134.0, 133.4, 129.6, 128.1, 123.3, 123.3, 121.1, 81.7, 80.6, 47.5, 28.9, 28.0, ppm; [α]_D²¹ 21.8 (c 1 CHCl₃); FT-IR (thin film, cm⁻¹) 2977, 1743, 1491, 1367, 1258; MS (ES) *m/z* 403.0 [M+H]⁺, 425.1 [M+Na]⁺; HRMS (EI) Exact mass calculated for [C₂₃H₂₈DCINO₃]⁺ requires *m/z* 403.1893 found *m/z* 403.1889.

Three Component One-Pot Asymmetric Synthesis of *tert*-butyl 1-(2-*tert*-butoxyphenyl)-3-(3-chlorophenyl)-3-*deutero*aziridine-2-carboxylate; *cis*-(387**)**



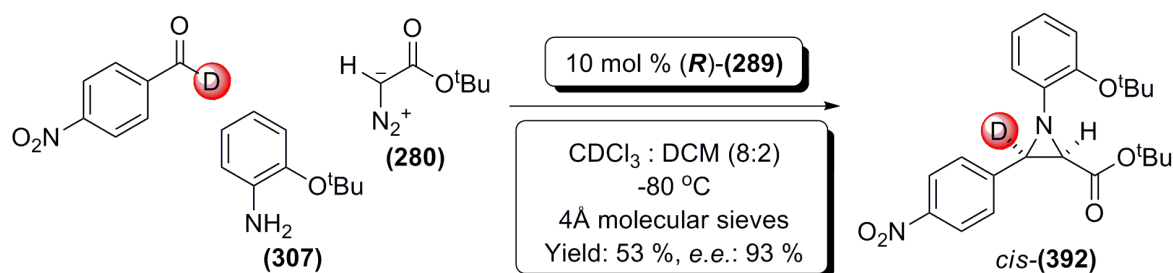
>95 % deuterated 3-chlorobenzaldehyde (37 mg, 0.26 mmol), 2-*tert*-butoxy aniline (**307**) (43 mg, 0.26 mmol), and catalyst (*R*)-(**289**) (21.6 mg, 0.026 mmol, 10%) were added to a flame dried 2 mL vial under nitrogen. 800 μ L of deuterated chloroform was added (pre-dried over 4Å molecular sieves), followed by ~40 mg of freshly powdered 4Å molecular sieves, and the vial was sealed with a PTFE crimp cap. 200 μ L of anhydrous DCM was added *via* syringe through the septum, and the reaction mixture was cooled to -80 °C. After 30 minutes, *tert*-butyl diazoacetate (**280**) (40.7 mg, 40 μ L, 0.286 mmol) was added *via* syringe, and the reaction mixture was stirred at -80 °C, monitoring by $^1\text{H-NMR}$ spectroscopy until the reaction was deemed complete (~72 h). At this point the reaction mixture was filtered through a short plug of silica, eluting with diethyl ether. The solvents were removed under reduced pressure, and the residue was purified *via* flash column chromatography (96 : 2 : 2 petroleum ether : dichloromethane : diethyl ether). A sample was submitted to chiral analytical HPLC analysis [Chiralpak AD, *iso*-hexane / *iso*-propanol: 95 / 5, 1 mL / min, 3.99 min (1st peak), 7.98 min (2nd peak), 69% *e.e.*]. The title product *cis*-(**387**) was a slight yellow oil afforded in a 65 % yield (68 mg, 0.17 mmol). $^1\text{H-NMR}$ (CDCl_3 , 300 MHz) δ 7.57-7.54 (m, 1H, ArH), 7.43-7.38 (m, 1H, ArH), 7.28-7.24 (m, 2H, ArH), 7.05-6.92 (m, 4H, ArH) 3.05 (s, 1H, C2-H), 1.38 (s, 9H, C(CH_3)₃), 1.23 (s, 9H, C(CH_3)₃); $^{13}\text{C-NMR}$ (CDCl_3 , 75 MHz) 167.2, 148.1, 146.2, 137.6, 133.9, 129.3, 128.4, 127.9, 126.5, 123.4, 123.2, 123.1, 121.1, 81.8, 80.5, 47.4, 28.9, 28.0 ppm; $[\alpha]_{\text{D}}^{26}$ 18.4 (c 1 CHCl_3); FT-IR (thin film, cm^{-1}): 2978; 1780, 1760, 1527, 1398; MS (EI)⁺: m/z 403.2 $[\text{M}+\text{H}]^+$, 425.1 $[\text{M}+\text{Na}]^+$; HRMS (EI)⁺: exact mass calculated for $[\text{C}_{23}\text{H}_{28}\text{DCINO}_3]^+$ requires m/z 403.1893, found m/z 403.1893.

Three Component One-Pot Asymmetric Synthesis of *tert*-butyl 1-(2-*tert*-butoxyphenyl)-3-(2-chlorophenyl)-3-deuteroaziridine-2-carboxylate; *cis*-(388**)**



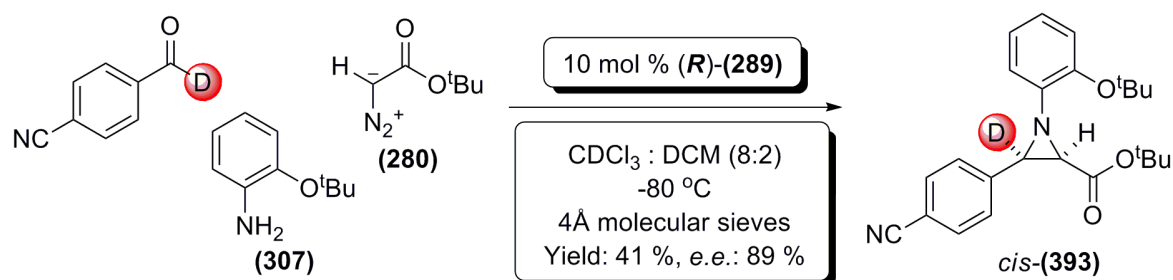
>95 % deuterated 2-chlorobenzaldehyde (30 μ L, 0.26 mmol), 2-*tert*-butoxy aniline (**307**) (43 mg, 0.26 mmol), and catalyst (*R*)-(**289**) (21.6 mg, 0.026 mmol, 10%) were added to a flame dried 2 mL vial under nitrogen. 800 μ L of deuterated chloroform was added (pre-dried over 4Å molecular sieves), followed by ~40 mg of freshly powdered 4Å molecular sieves, and the vial was sealed with a PTFE crimp cap. 200 μ L of anhydrous DCM was added *via* syringe through the septum, and the reaction mixture was cooled to -80 °C. After 30 minutes, *tert*-butyl diazoacetate (**280**) (40.7 mg, 40 μ L, 0.286 mmol) was added *via* syringe, and the reaction mixture was stirred at -80 °C, monitoring by ¹H-NMR spectroscopy until the reaction was deemed complete (~72 h). At this point the reaction mixture was filtered through a short plug of silica, eluting with diethyl ether. The solvents were removed under reduced pressure, and the residue was purified *via* flash column chromatography (96 : 2 : 2 petroleum ether : dichloromethane : diethyl ether). A sample was submitted to chiral analytical HPLC analysis [Chiralpak AD, *iso*-hexane / *iso*-propanol : 95 / 5, 1 mL / min, 3.52 min (1st peak), 7.01 min (2nd peak), 64% *e.e.*]. The title product *cis*-(**388**) was a slight yellow oil afforded in a 41 % yield (43 mg, 0.11 mmol). ¹H-NMR (CDCl₃, 300 MHz) δ 7.71-7.64 (dd, 1H, *J* 1.9, 7.5 Hz, ArH), 7.30-7.12 (m, 3H, ArH), 7.00-6.85 (m, 4H, ArH), 3.08 (s, 1H, C2-H), 1.34 (s, 9H, C(CH₃)₃), 1.13 (s, 9H, C(CH₃)₃); ¹³C-NMR (CDCl₃, 75 MHz) 167.0, 148.2, 146.1, 133.7, 130.8, 128.7, 128.5, 126.2, 123.2, 122.9, 122.7, 120.7, 81.1, 80.2, 46.5, 28.6, 27.5 ppm; [α]_D²⁶ 52.4 (c 0.86 CHCl₃); FT-IR (thin film, cm⁻¹): 2977, 2932, 1744, 1719, 1594, 1490, 1476, 1367, 1268, 1165; MS (ED)⁺: *m/z* 403.3 [M+H]⁺, 425.2 [M+Na]⁺; HRMS (ED)⁺: exact mass calculated for [C₂₃H₂₈DCINO₃]⁺ requires *m/z* 403.1893, found *m/z* 403.1894.

Three Component One-Pot Asymmetric Synthesis of *tert*-butyl 1-(2-*tert*-butoxyphenyl)-3-(4-nitrophenyl)-3-*deutero*aziridine-2-carboxylate; *cis*-(392**)**



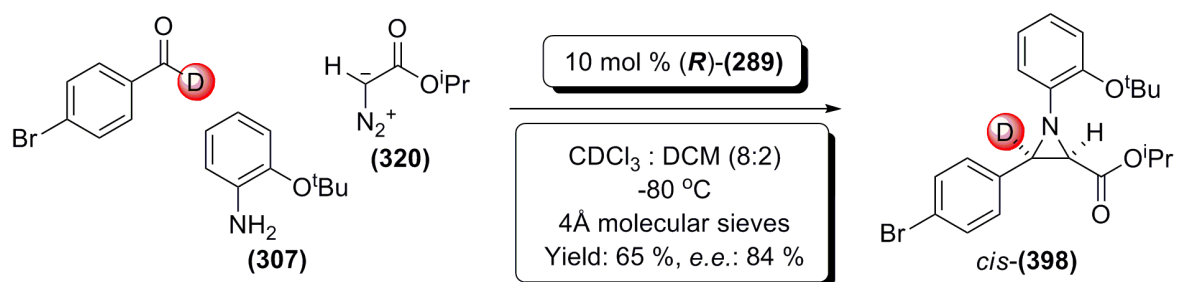
>95 % deuterated 4-nitrobenzaldehyde (40 mg, 0.26 mmol), 2-*tert*-butoxy aniline (**280**) (43 mg, 0.26 mmol), and catalyst (*R*)-(**289**) (21.6 mg, 0.026 mmol, 10%) were added to a flame dried 2 mL vial under nitrogen. 800 μ L of deuterated chloroform was added (pre-dried over 4Å molecular sieves), followed by ~40 mg of freshly powdered 4Å molecular sieves, and the vial was sealed with a PTFE crimp cap. 200 μ L of anhydrous DCM was added *via* syringe through the septum, and the reaction mixture was cooled to -80 °C. After 30 minutes, *tert*-butyl diazoacetate (**280**) (40.7 mg, 40 μ L, 0.286 mmol) was added *via* syringe, and the reaction mixture was stirred at -80 °C, monitoring by $^1\text{H-NMR}$ spectroscopy until the reaction was deemed complete (~72 h). At this point the reaction mixture was filtered through a short plug of silica, eluting with diethyl ether. The solvents were removed under reduced pressure, and the residue was purified *via* flash column chromatography (14 % diethyl ether in petroleum ether). A sample was submitted to chiral analytical HPLC analysis [Chiralpak AD, *iso*-hexane / *iso*-propanol : 95 / 5, 1 mL / min, 5.47 min (1st peak), 8.83 min (2nd peak), 93% *e.e.*]. The title product *cis*-(**392**) was a yellow oil afforded in a 53 % yield (57 mg, 0.14 mmol). $^1\text{H-NMR}$ (CDCl_3 , 300 MHz) δ 8.21 (d, 2H, *J* 6.9 Hz, ArH), 7.72 (d, 2H, *J* 6.9 Hz, ArH), 7.08-6.91 (m, 4H, ArH), 3.13 (s, 1H, C₂-H), 1.35 (s, 9H, C(CH₃)₃), 1.22 (s, 9H, C(CH₃)₃); $^{13}\text{C-NMR}$ (CDCl_3 , 75 MHz) 166.5, 148.1, 147.5, 145.6, 143.1, 129.2, 123.7, 123.3, 123.2, 123.1, 121.0, 82.1, 80.6, 47.8, 28.9, 28.1 ppm; $[\alpha]_{\text{D}}^{26}$ 55 (c 1.3 CHCl_3); FT-IR (thin film, cm^{-1}): 2978, 1742, 1603, 1520, 1891, 1520, 1491, 1367, 1345; MS (EI)⁺: *m/z* 414.3 [M+H]⁺, 436.2 [M+Na]⁺; HRMS (EI)⁺: exact mass calculated for [C₂₃H₂₈DN₂O₅]⁺ requires *m/z* 414.2134, found *m/z* 414.2134.

Three Component One-Pot Asymmetric Synthesis of *tert*-butyl 1-(2-*tert*-butoxyphenyl)-3-(4-cyanophenyl)-3-deuteroaziridine-2-carboxylate; *cis*-(393**)**



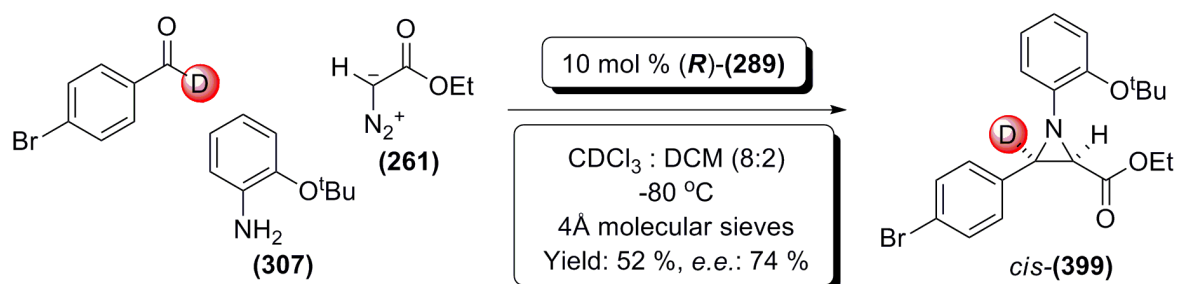
>95 % deuterated 4-cyanobenzaldehyde (10.6 mg, 0.08 mmol), 2-*tert*-butoxy aniline (**307**) (13 mg, 0.08 mmol), and catalyst (*R*)-(289) (7 mg, 0.008 mmol, 10%) were added to a flame dried 2 mL vial under nitrogen. 800 μ L of deuterated chloroform was added (pre-dried over 4Å molecular sieves), followed by ~40 mg of freshly powdered 4Å molecular sieves, and the vial was sealed with a PTFE crimp cap. 200 μ L of anhydrous DCM was added *via* syringe through the septum, and the reaction mixture was cooled to -80 °C. After 30 minutes, *tert*-butyl diazoacetate (**280**) (12.5 mg, 12 μ L, 0.088 mmol) was added *via* syringe, and the reaction mixture was stirred at -80 °C, monitoring by ¹H-NMR spectroscopy until the reaction was deemed complete (~72 h). At this point the reaction mixture was filtered through a short plug of silica, eluting with diethyl ether. The solvents were removed under reduced pressure, and the residue was purified *via* flash column chromatography (14 % diethyl ether in petroleum ether). A sample was submitted to chiral analytical HPLC analysis [Chiralpak AD, *iso*-hexane / *iso*-propanol : 92.5 / 7.5, 1.2 mL / min, 5.37 min (1st peak), 9.35 min (2nd peak), 89% *e.e.*]. The title product *cis*-(**393**) was a slight green oil afforded in a 41 % yield (13 mg, 0.033 mmol). ¹H-NMR (CDCl₃, 400 MHz) δ 7.72-7.58 (m, 4H, ArH), 7.09-6.88 (m, 4H, ArH), 3.10 (s, 1H, C2-H), 1.35 (s, 9H, C(CH₃)₃), 1.18 (s, 9H, C(CH₃)₃); ¹³C-NMR (CDCl₃, 100 MHz) 166.5, 148.1, 145.7, 141.0, 131.6, 128.9, 123.5, 123.1, 123.0, 120.8, 119.0, 111.2, 81.8, 80.4, 47.5, 28.6, 27.7 ppm; [α]_D²³ 35.1 (c 0.7 CHCl₃); FT-IR (thin film, cm⁻¹) 2978, 2310, 1721, 1523; MS (ES) *m/z* 394.2 [M+H]⁺; HRMS (EI) Exact mass calculated for [C₂₄H₂₈DN₂O₃] requires *m/z* 394.2235, found *m/z* 394.2237.

Three Component One-Pot Asymmetric Synthesis of *isopropyl 3-(4-bromophenyl)-1-(2-tert-butoxyphenyl)-3-deuteroaziridine-2-carboxylate; cis-(398)*



>95 % deuterated 4-bromobenzaldehyde (40 mg, 0.26 mmol.), 2-*tert*-butoxy aniline (**307**) (43 mg, 0.26 mmol), and catalyst (**R**)-(**289**) (21.6 mg, 0.026 mmol, 10%) were added to a flame dried 2 mL vial under nitrogen. 800 μ L of deuterated chloroform was added (pre-dried over 4Å molecular sieves), followed by ~40 mg of freshly powdered 4Å molecular sieves, and the vial was sealed with a PTFE crimp cap. 200 μ L of anhydrous DCM was added *via* syringe through the septum, and the reaction mixture was cooled to -80 °C. After 30 minutes, *iso*-propyl diazoacetate (**320**) (36.4 mg, 36 μ L, 0.286 mmol) was added *via* syringe, and the reaction mixture was stirred at -80 °C, monitoring by $^1\text{H-NMR}$ spectroscopy until the reaction was deemed complete (~72 h). At this point the reaction mixture was filtered through a short plug of silica, eluting with diethyl ether. The solvents were removed under reduced pressure, and the residue was purified *via* flash column chromatography (35 % DCM, 3 % diethyl ether in petroleum ether). A sample was submitted to chiral analytical HPLC analysis [Chiralpak AD, *iso*-hexane / *iso*-propanol : 95 / 5, 1 mL / min, 4.18 min (1st peak), 7.15 min (2nd peak), 84% *e.e.*]. The title product *cis*-(**398**) was a slight green oil afforded in a 65 % yield (73 mg, 0.17 mmol). $^1\text{H-NMR}$ (CDCl_3 , 300 MHz) δ 7.49-7.38 (m, 4H, ArH), 7.07-6.91 (m, 4H, ArH), 4.89 (m, 1H, $\text{CH}(\text{CH}_3)_2$), 3.10 (s, 1H, C2-H), 1.34 (s, 9H, $\text{C}(\text{CH}_3)_3$), 1.04 (dd, 6H, J 3.0, 6.3 Hz, $\text{C}(\text{CH}_3)_2$); $^{13}\text{C-NMR}$ (CDCl_3 , 75 MHz) 167.4, 148.1, 145.9, 134.2, 131.0, 129.8, 123.3, 123.0, 122.7, 121.6, 120.9, 80.2, 68.5, 46.7, 28.6, 21.6, 21.39 ppm; $[\alpha]_{\text{D}}^{26}$ 24.75 (c 0.4 CHCl_3); FT-IR (thin film, cm^{-1}): 2979, 1746, 1489, 1258, 1194, 1108; MS (EI)⁺: m/z 433.1 $[\text{M}+\text{H}]^+$, 455.1 $[\text{M}+\text{Na}]^+$; HRMS (EI)⁺: exact mass calculated for $[\text{C}_{22}\text{H}_{26}\text{DBrNO}_3]^+$ requires m/z 433.1232, found m/z 433.1233.

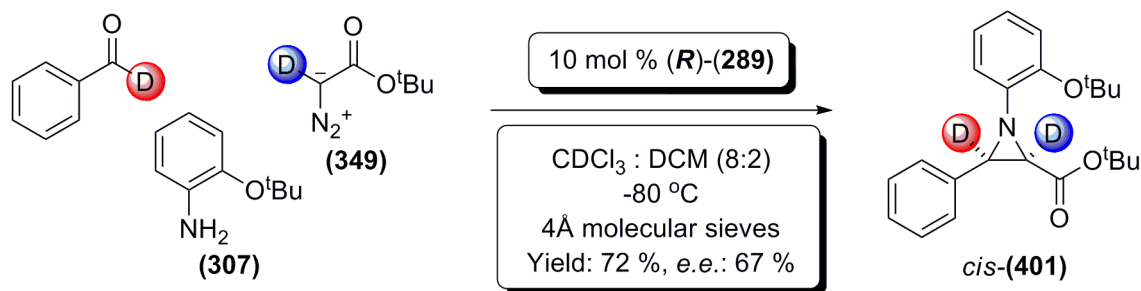
Three Component One-Pot Asymmetric Synthesis of ethyl 3-(4-bromophenyl)-1-(2-*tert*-butoxyphenyl)-3-*deutero*aziridine-2-carboxylate; *cis*-(399**)**



>95 % deuterated 4-bromobenzaldehyde (40 mg, 0.26 mmol), 2-*tert*-butoxy aniline (**307**) (43 mg, 0.26 mmol), and catalyst (*R*)-(**289**) (21.6 mg, 0.026 mmol, 10%) were added to a flame dried 2 mL vial under nitrogen. 800 μ L of deuterated chloroform was added (pre-dried over 4Å molecular sieves), followed by ~40 mg of freshly powdered 4Å molecular sieves, and the vial was sealed with a PTFE crimp cap. 200 μ L of anhydrous DCM was added *via* syringe through the septum, and the reaction mixture was cooled to -80 °C. After 30 minutes, ethyl diazoacetate (**261**) (32.6 mg, 32 μ L, 0.286 mmol) was added *via* syringe, and the reaction mixture was stirred at -80 °C, monitoring by ¹H-NMR spectroscopy until the reaction was deemed complete (~72 h). At this point the reaction mixture was filtered through a short plug of silica, eluting with diethyl ether. The solvents were removed under reduced pressure, and the residue was purified *via* flash column chromatography (35 % dichloromethane, in petroleum ether). A sample was submitted to chiral analytical HPLC analysis [Chiralpak AD, *iso*-hexane / *iso*-propanol : 95 / 5, 1 mL / min, 5.41 min (1st peak), 8.86 min (2nd peak), 74% *e.e.*]. The title product *cis*-(**399**) was a slight green oil afforded in a 52 % yield (56 mg, 0.135 mmol). ¹H-NMR (CDCl₃, 300 MHz) δ 7.51-7.35 (m, 4H, ArH), 7.11-6.88 (m, 4H, ArH), 4.21-3.87 (m, 2H, CH₂), 3.10 (s, 1H, C2-H), 1.33 (s, 9H, C(CH₃)₃), 1.09 (t, 3H, *J* 6.9, 6.9 Hz, CH₃); ¹³C-NMR (CDCl₃, 75 MHz) 167.9, 148.1, 145.7, 134.1, 131.0, 129.8, 123.4, 122.9, 122.6, 121.7, 120.8, 80.2, 60.8, 46.6, 28.5, 13.9 ppm; [a]_D²⁴ 14.9 (c 0.9 CHCl₃); FT-IR (thin film, cm⁻¹): 2978, 1747, 1595, 1489, 1449, 1366, 1258, 1217; MS (EI)⁺: *m/z* 419.3 [M+H]⁺, 441.3 [M+Na]⁺; HRMS (EI)⁺: exact mass calculated for [C₂₁H₂₄DBrNO₃]⁺ requires *m/z* 419.1075, found *m/z* 419.1082.

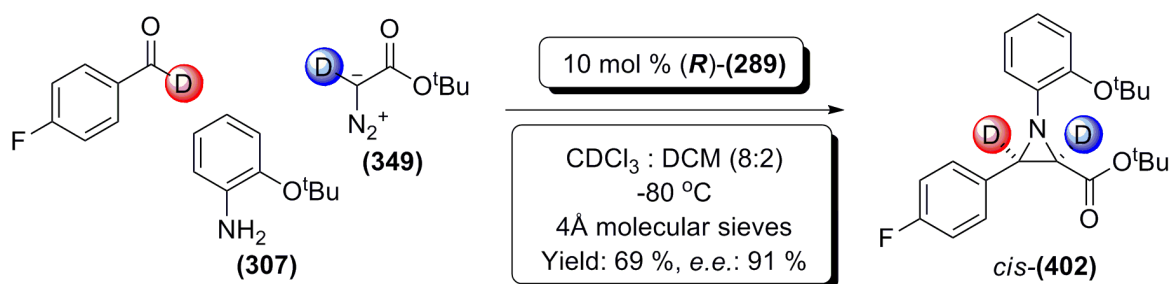
9.5: Synthesis of C2-, C3-di-deutero Aziridines

Three Component One-Pot Asymmetric Synthesis of *tert*-butyl 1-(2-*tert*-butoxyphenyl)-3-phenyl-2,3-dideuteroaziridine-2-carboxylate; *cis*-(**401**)



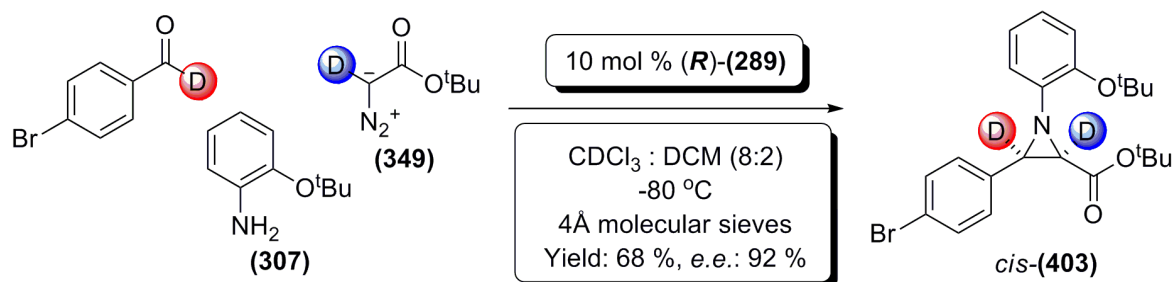
>95 % deuterated benzaldehyde (27.8 mg, 28 μ L, 0.26 mmol), 2-*tert*-butoxy aniline (**307**) (43 mg, 0.26 mmol), and catalyst (*R*)-(289) (21.6 mg, 0.026 mmol, 10%) were added to a flame dried 2 mL vial under nitrogen. 800 μ L of deuterated chloroform was added (pre-dried over 4 Å molecular sieves), followed by ~40 mg of freshly powdered 4 Å molecular sieves, and the vial was sealed with a PTFE crimp cap. 200 μ L of anhydrous DCM was added *via* syringe through the septum, and the reaction mixture was cooled to -80 °C. After 30 minutes, >95 % deuterated *tert*-butyl diazoacetate (**349**) (40.7 mg, 40 μ L, 0.286 mmol) was added *via* syringe, and the reaction mixture was stirred at -80 °C, monitoring by ¹H-NMR spectroscopy until the reaction was deemed complete (~72 h). At this point the reaction mixture was filtered through a short plug of silica, eluting with diethyl ether. The solvents were removed under reduced pressure, and the residue was purified *via* flash column chromatography (14 % diethyl ether in petroleum ether). A sample was submitted to chiral analytical HPLC analysis [Chiralpak AD, *iso*-hexane / *iso*-propanol : 95 / 5, 1 mL / min, 3.77 min (1st peak), 7.17 min (2nd peak), 67% *e.e.*]. The title product *cis*-(**401**) was a colourless oil afforded in a 72 % yield (69 mg, 0.19 mmol). ¹H-NMR (CDCl₃, 300 MHz) δ 7.53-7.46 (m, 2H, ArH), 7.34-7.21 (m, 3H, ArH), 7.02-6.86 (m, 4H, ArH), 1.35 (s, 9H, C(CH₃)₃), 1.17 (s, 9H, C(CH₃)₃); ¹³C-NMR (CDCl₃, 75 MHz) 167.3, 148.0, 146.7, 135.2, 128.1, 127.8, 127.5, 123.2, 123.2, 123.0, 121.0, 81.2, 80.3, 28.5, 27.6 ppm; [α]_D²⁶ 27 (c 0.9 CHCl₃); FT-IR (thin film, cm⁻¹): 2977, 1745, 1714, 1593, 1490, 1449, 1391, 1367; MS (EI)⁺: *m/z* 370.3 [M+H]⁺, 392.3 [M+Na]⁺; HRMS (EI)⁺: exact mass calculated for [C₂₃H₂₈D₂NO₃]⁺ requires *m/z* 370.2346, found *m/z* 370.2348.

Three Component One-Pot Asymmetric Synthesis of *tert*-butyl 1-(2-*tert*-butoxyphenyl)-3-(4-fluorophenyl)-2,3-dideuteroaziridine-2-carboxylate; *cis*-(402)



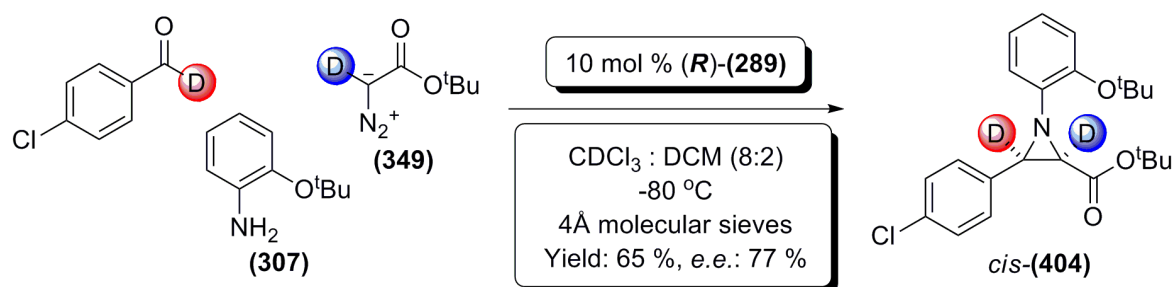
>95 % deuterated 4-fluorobenzaldehyde (40 mg, 0.26 mmol), 2-*tert*-butoxy aniline (**307**) (43 mg, 0.26 mmol), and catalyst (*R*)-(**289**) (21.6 mg, 0.026 mmol, 10%) were added to a flame dried 2 mL vial under nitrogen. 800 μ L of deuterated chloroform was added (pre-dried over 4Å molecular sieves), followed by ~40 mg of freshly powdered 4Å molecular sieves, and the vial was sealed with a PTFE crimp cap. 200 μ L of anhydrous DCM was added *via* syringe through the septum, and the reaction mixture was cooled to -80 °C. After 30 minutes, >95 % deuterated *tert*-butyl diazoacetate (**349**) (40.7 mg, 40 μ L, 0.286 mmol) was added *via* syringe, and the reaction mixture was stirred at -80 °C, monitoring by ¹H-NMR spectroscopy until the reaction was deemed complete (~72 h). At this point the reaction mixture was filtered through a short plug of silica, eluting with diethyl ether. The solvents were removed under reduced pressure, and the residue was purified *via* flash column chromatography (14 % diethyl ether in petroleum ether). A sample was submitted to chiral analytical HPLC analysis [Chiralpak AD, *iso*-hexane / *iso*-propanol : 95 / 5, 1 mL / min, 3.91 min (1st peak), 6.08 min (2nd peak), 91% *e.e.*]. The title product *cis*-(**402**) was a slight yellow oil afforded in a 69% yield (69 mg, 0.18 mmol). ¹H-NMR (CDCl₃, 300 MHz) δ 7.55-7.46 (m, 2H, ArH), 7.08-6.91 (m, 6H, ArH), 1.37 (s, 9H, C(CH₃)₃), 1.22 (s, 9H, C(CH₃)₃); ¹³C-NMR (CDCl₃, 75 MHz) 167.1, 164.1, 160.8, 148.0, 146.4, 130.9, 129.7, 129.6, 123.2, 123.1, 120.9, 114.8, 114.5, 81.4, 80.3, 28.5, 27.7 ppm; [α]_D²⁶ 21 (c 1 CHCl₃); FT-IR (thin film, cm⁻¹): 2978, 1744, 1512, 1490, 1367, 1257, 1160; MS (EI)⁺: *m/z* 388.2 [M+H]⁺, 410.3 [M+Na]⁺; HRMS (EI)⁺: exact mass calculated for [C₂₃H₂₇D₂FNO₃]⁺ requires *m/z* 388.2252, found *m/z* 388.2252.

Three Component One-Pot Asymmetric Synthesis of *tert*-butyl 3-(4-bromophenyl)-1-(2-*tert*-butoxyphenyl)-2,3-dideuteroaziridine-2-carboxylate; *cis*-(403**)**



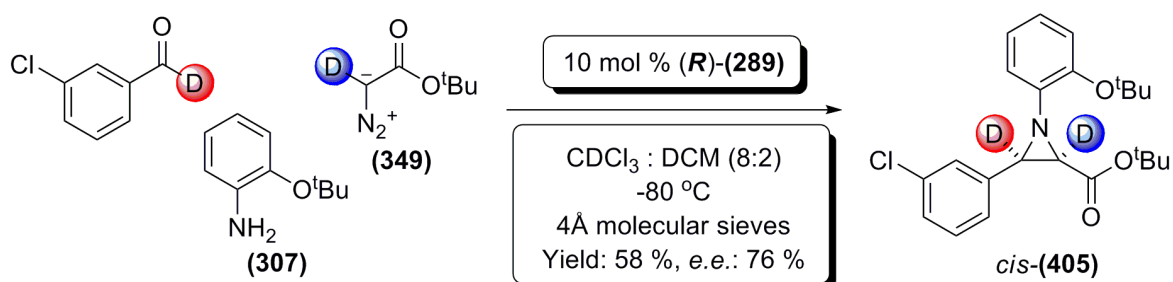
>95 % deuterated 4-bromobenzaldehyde (49 mg, 0.26 mmol), 2-*tert*-butoxy aniline (**307**) (43 mg, 0.26 mmol), and catalyst (*R*)-(**289**) (21.6 mg, 0.026 mmol, 10%) were added to a flame dried 2 mL vial under nitrogen. 800 μ L of deuterated chloroform was added (pre-dried over 4Å molecular sieves), followed by ~40 mg of freshly powdered 4Å molecular sieves, and the vial was sealed with a PTFE crimp cap. 200 μ L of anhydrous DCM was added *via* syringe through the septum, and the reaction mixture was cooled to -80 °C. After 30 minutes, >95 % deuterated *tert*-butyl diazoacetate (**349**) (40.7 mg, 40 μ L, 0.286 mmol) was added *via* syringe, and the reaction mixture was stirred at -80 °C, monitoring by ¹H-NMR spectroscopy until the reaction was deemed complete (~72 h). At this point the reaction mixture was filtered through a short plug of silica, eluting with diethyl ether. The solvents were removed under reduced pressure, and the residue was purified *via* flash column chromatography (14 % diethyl ether in petroleum ether). A sample was submitted to chiral analytical HPLC analysis [Chiralpak AD, *iso*-hexane / *iso*-propanol : 95 / 5, 1 mL / min, 4.01 min (1st peak), 6.77 min (2nd peak), 92% *e.e.*]. The title product *cis*-(**403**) was a slight green oil afforded in a 68 % yield (79 mg, 0.18 mmol). ¹H-NMR (CDCl₃, 300 MHz) δ 7.45-7.36 (m, 4H, ArH), 7.02-6.88 (m, 4H, ArH), 1.33 (s, 9H, C(CH₃)₃), 1.20 (s, 9H, C(CH₃)₃); ¹³C-NMR (CDCl₃, 75 MHz) 166.9, 148.0, 146.2, 134.4, 130.9, 129.8, 123.2, 123.1, 121.4, 120.9, 81.5, 80.3, 28.6, 27.7 ppm; [α]_D²⁶ 24 (c 1 CHCl₃); FT-IR (thin film, cm⁻¹): 2978, 1744, 1715, 1595, 1489, 1392, 1367, 1257; MS (EI)⁺: *m/z* 448.1 [M+H]⁺, 470.1 [M+Na]⁺; HRMS (EI)⁺: exact mass calculated for [C₂₃H₂₉D₂BrNO₃]⁺ requires *m/z* 448.1378, found *m/z* 448.1376.

Three Component One-Pot Asymmetric Synthesis of *tert*-butyl 1-(2-*tert*-butoxyphenyl)-3-(4-chlorophenyl)-2,3-dideuteroaziridine-2-carboxylate; *cis*-(404**)**



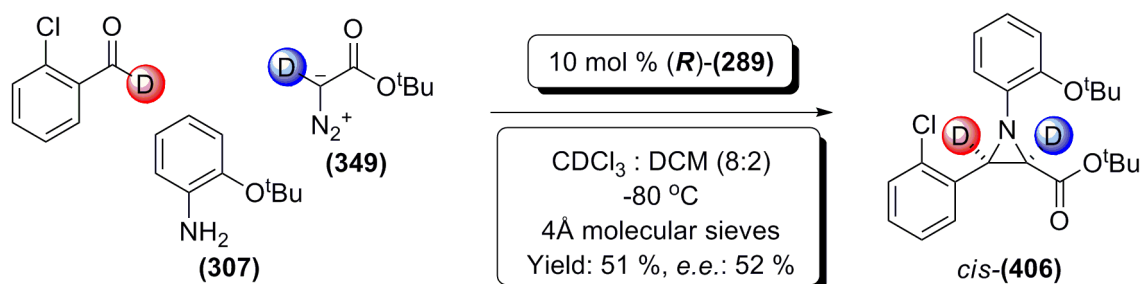
>95 % deuterated 4-chlorobenzaldehyde (19 mg, 0.13 mmol), 2-*tert*-butoxy aniline (**307**) (22 mg, 0.13 mmol), and catalyst (**R**)-(**289**) (10 mg, 0.013 mmol, 10%) were added to a flame dried 2 mL vial under nitrogen. 400 μ L of deuterated chloroform was added (pre-dried over 4 \AA molecular sieves) followed by ~40 mg of freshly powdered 4 \AA molecular sieves, and the vial was sealed with a PTFE crimp cap. 100 μ L of anhydrous DCM was added *via* syringe through the septum, and the reaction mixture was cooled to -80 $^{\circ}$ C. After 30 minutes, >95 % deuterated *tert*-butyl diazoacetate (**349**) (20.4 mg, 20 μ L, 0.142 mmol) was added *via* syringe, and the reaction mixture was stirred at -80 $^{\circ}$ C, monitoring by ^1H -NMR spectroscopy until the reaction was deemed complete (~72 h). At this point the reaction mixture was filtered through a short plug of silica, eluting with diethyl ether. The solvents were removed under reduced pressure, and the residue was purified *via* flash column chromatography (12 % diethyl ether in petroleum ether). A sample was submitted to chiral analytical HPLC analysis [Chiralpak AD, *iso*-hexane / *iso*-propanol : 95 / 5, 1 mL / min, 5.2 min (1st peak), 7.9 min (2nd peak), 77 % *e.e.*]. The title product *cis*-(**404**) was a yellow oil afforded in a 65 % yield (34 mg, 0.085 mmol). ^1H -NMR (CDCl_3 , 400 MHz) δ 7.47 (d, 2H, *J* 9.0 Hz, ArH), 7.30 (d, 2H, *J* 9.0 Hz, ArH), 7.06-6.91 (m, 4H, ArH), 1.36 (s, 9H, C(CH₃)₃), 1.23 (s, 9H, C(CH₃)₃); ^{13}C -NMR (CDCl_3 , 100 MHz) 166.9, 148.0, 146.3, 133.9, 133.3, 129.5, 127.9, 123.1, 123.1, 120.9, 81.4, 80.3, 28.5, 27.7 ppm; $[\alpha]_{\text{D}}^{21}$ 27.3 (c 1 CHCl_3); FT-IR (thin film, cm^{-1}) 2977, 2932, 1743, 1744, 1593, 1489, 1449, 1391; MS (ES) *m/z* 404.2 $[\text{M}+\text{H}]^+$, 426.1 $[\text{M}+\text{Na}]^+$; HRMS (EI): exact mass calculated for $[\text{C}_{23}\text{H}_{27}\text{D}_2\text{ClNO}_3]^+$ requires *m/z* 404.1956 found *m/z* 404.1952.

Three Component One-Pot Asymmetric Synthesis of *tert*-butyl 1-(2-*tert*-butoxyphenyl)-3-(3-chlorophenyl)-2,3-dideuteroaziridine-2-carboxylate; *cis*-(405**)**



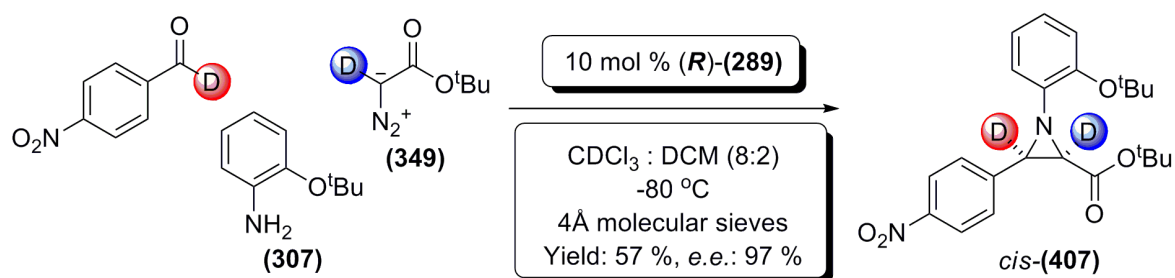
>95 % deuterated 3-chlorobenzaldehyde (37 mg, 0.26 mmol), 2-*tert*-butoxy aniline (**307**) (43 mg, 0.26 mmol), and catalyst (*R*)-(**289**) (21.6 mg, 0.026 mmol, 10%) were added to a flame dried 2 mL vial under nitrogen. 800 μ L of deuterated chloroform was added (pre-dried over 4Å molecular sieves), followed by ~40 mg of freshly powdered 4Å molecular sieves, and the vial was sealed with a PTFE crimp cap. 200 μ L of anhydrous DCM was added *via* syringe through the septum, and the reaction mixture was cooled to -80 °C. After 30 minutes, >95 % deuterated *tert*-butyl diazoacetate (**349**) (40.7 mg, 40 μ L, 0.286 mmol) was added *via* syringe, and the reaction mixture was stirred at -80 °C, monitoring by ¹H-NMR spectroscopy until the reaction was deemed complete (~72 h). At this point the reaction mixture was filtered through a short plug of silica, eluting with diethyl ether. The solvents were removed under reduced pressure, and the residue was purified *via* flash column chromatography (96 : 2 : 2 petroleum ether : dichloromethane : diethyl ether). A sample was submitted to chiral analytical HPLC analysis [Chiralpak AD, *iso*-hexane / *iso*-propanol : 95 / 5, 1 mL / min, 4.19 min (1st peak), 8.01 min (2nd peak), 76% *e.e.*]. The title product *cis*-(**405**) was a yellow oil afforded in a 58 % yield (61 mg, 0.15 mmol). ¹H-NMR (CDCl₃, 300 MHz) δ 7.52-7.47 (m, 1H, ArH), 7.38-7.31 (m, 1H, ArH), 7.24-7.16 (m, 2H, ArH), 7.00-6.85 (m, 4H, ArH), 1.31 (s, 9H, C(CH₃)₃), 1.17 (s, 9H, C(CH₃)₃); ¹³C-NMR (CDCl₃, 75 MHz) 167.1, 148.0, 146.0, 137.5, 133.8, 129.1, 128.3, 127.7, 126.3, 123.2, 123.0, 122.9, 120.9, 81.6, 28.6, 27.6 ppm; [α]_D²⁶ 24 (c 0.9 CHCl₃); FT-IR (thin film, cm⁻¹): 2978, 1744, 1715, 1595, 1490, 1367, 1263, 1160; MS (EI)⁺: *m/z* 404.2 [M+H]⁺, 426.2 [M+Na]⁺; HRMS (EI)⁺: exact mass calculated for [C₂₃H₂₇D₂ClNO₃]⁺ requires *m/z* 404.1956, found *m/z* 404.1957.

Three Component One-Pot Asymmetric Synthesis of *tert*-butyl 1-(2-*tert*-butoxyphenyl)-3-(2-chlorophenyl)-2,3-dideuteroaziridine-2-carboxylate; *cis*-(406**)**



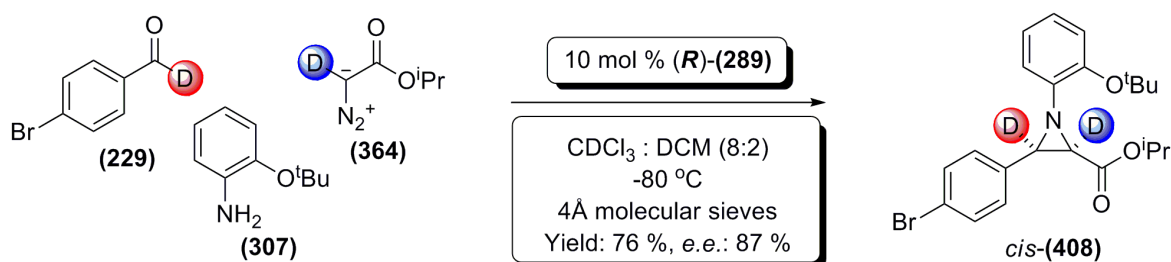
>95 % deuterated 2-chlorobenzaldehyde (30 μ L, 0.26 mmol), 2-*tert*-butoxy aniline (**307**) (43 mg, 0.26 mmol), and catalyst (**R**)-(**289**) (21.6 mg, 0.026 mmol, 10%) were added to a flame dried 2 mL vial under nitrogen. 800 μ L of deuterated chloroform was added (pre-dried over 4Å molecular sieves), followed by ~40 mg of freshly powdered 4Å molecular sieves, and the vial was sealed with a PTFE crimp cap. 200 μ L of anhydrous DCM was added *via* syringe through the septum, and the reaction mixture was cooled to -80 °C. After 30 minutes, >95 % deuterated *tert*-butyl diazoacetate (**349**) (40.7 mg, 40 μ L, 0.286 mmol) was added *via* syringe, and the reaction mixture was stirred at -80 °C, monitoring by ¹H-NMR spectroscopy until the reaction was deemed complete (~72 h). At this point the reaction mixture was filtered through a short plug of silica, eluting with diethyl ether. The solvents were removed under reduced pressure, and the residue was purified *via* flash column chromatography (96 : 2 : 2 petroleum ether : dichloromethane : diethyl ether). A sample was submitted to chiral analytical HPLC analysis [Chiralpak AD, *iso*-hexane / *iso*-propanol : 95 / 5, 1 mL / min, 4.19 min (1st peak), 8.01 min (2nd peak), 52 % *e.e.*]. The title product *cis*-(**406**) was a yellow oil afforded in a 51 % yield (53 mg, 0.13 mmol). ¹H-NMR (CDCl₃, 300 MHz) δ 7.71-7.63 (m, 1H, ArH), 7.31-7.12 (m, 1H, ArH), 6.99-6.85 (m, 4H, ArH), 1.35 (s, 9H, C(CH₃)₃), 1.13 (s, 9H, C(CH₃)₃); ¹³C-NMR (CDCl₃, 75 MHz) 167.0, 148.2, 146.1, 133.7, 133.4, 130.9, 128.7, 128.5, 126.2, 123.2, 122.9, 122.7, 120.7, 81.1, 80.2, 28.6, 27.5 ppm; [α]_D²⁶ 35 (c 0.9 CHCl₃); FT-IR (thin film, cm⁻¹): 2978, 1745, 1734, 1491, 1368, 1262, 1163; MS (EI)⁺: *m/z* 404.2 [M+H]⁺, 426.2 [M+Na]⁺; HRMS (EI)⁺: exact mass calculated for [C₂₃H₂₇D₂ClNO₃]⁺ requires *m/z* 404.1956, found *m/z* 404.1956.

Three Component One-Pot Asymmetric Synthesis of *tert*-butyl 1-(2-*tert*-butoxyphenyl)-3-(4-nitrophenyl)-2,3-dideuteroaziridine-2-carboxylate; *cis*-(**407**)



>95 % deuterated 4-nitrobenzaldehyde (40 mg, 0.26 mmol), 2-*tert*-butoxy aniline (**307**) (43 mg, 0.26 mmol), and catalyst (*R*)-(289) (21.6 mg, 0.026 mmol, 10%) were added to a flame dried 2 mL vial under nitrogen. 800 μ L of deuterated chloroform was added (pre-dried over 4Å molecular sieves), followed by ~40 mg of freshly powdered 4Å molecular sieves, and the vial was sealed with a PTFE crimp cap. 200 μ L of anhydrous DCM was added *via* syringe through the septum, and the reaction mixture was cooled to -80 °C. After 30 minutes, >95 % deuterated *tert*-butyl diazoacetate (**349**) (40.7 mg, 40 μ L, 0.286 mmol) was added *via* syringe, and the reaction mixture was stirred at -80 °C, monitoring by ¹H-NMR spectroscopy until the reaction was deemed complete (~72 h). At this point the reaction mixture was filtered through a short plug of silica, eluting with diethyl ether. The solvents were removed under reduced pressure, and the residue was purified *via* flash column chromatography (14 % diethyl ether in petroleum ether). A sample was submitted to chiral analytical HPLC analysis [Chiralpak AD, *iso*-hexane / *iso*-propanol : 95 / 5, 1 mL / min, 5.42 min (1st peak), 8.89 min (2nd peak), 97% *e.e.*]. The title product *cis*-(**407**) was a yellow oil afforded in a 57% yield (61 mg, 0.15 mmol). ¹H-NMR (CDCl₃, 300 MHz) δ 8.20 (d, 2H, *J* 6.9 Hz, ArH), 7.72 (d, 2H, *J* 6.9 Hz, ArH), 7.07-6.91 (m, 4H, ArH), 1.35 (s, 9H, C(CH₃)₃), 1.22 (s, 9H, C(CH₃)₃); ¹³C-NMR (CDCl₃, 75 MHz) 166.5, 148.1, 147.5, 145.6, 143.1, 129.2, 123.7, 123.3, 123.2, 123.1, 121.0, 82.1, 80.6, 28.9, 28.1 ppm; [α]_D²⁶ 65 (c 1 CHCl₃); FT-IR (thin film, cm⁻¹): 2978, 1743, 1602, 1520, 1891, 1367, 1345, 1258, 1159; MS (EI)⁺: *m/z* 415.3 [M+H]⁺, 437.2 [M+Na]⁺; HRMS (EI)⁺: exact mass calculated for [C₂₃H₂₇D₂N₂O₅]⁺ requires *m/z* 415.2197, found *m/z* 415.2196.

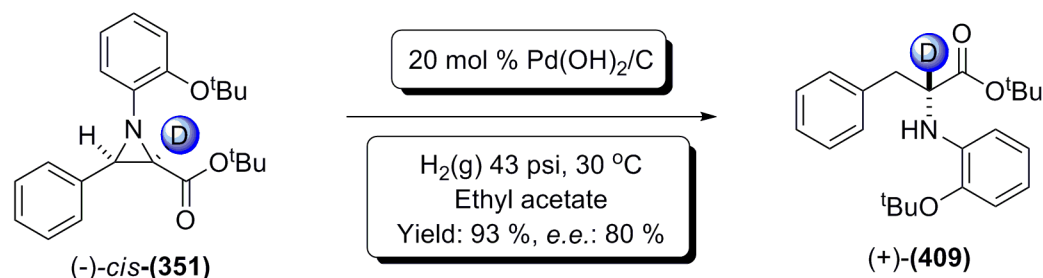
Three Component One-Pot Asymmetric Synthesis of *isopropyl 3-(4-bromophenyl)-1-(2-*tert*-butoxyphenyl)-2,3-dideuteroaziridine-2-carboxylate; *cis*-(408)*



>95 % deuterated 4-bromobenzaldehyde (40 mg, 0.26 mmol), 2-*tert*-butoxy aniline (**307**) (43 mg, 0.26 mmol), and catalyst (**R**)-(289) (21.6 mg, 0.026 mmol, 10%) were added to a flame dried 2 mL vial under nitrogen. 800 μ L of deuterated chloroform was added (pre-dried over 4Å molecular sieves), followed by ~40 mg of freshly powdered 4Å molecular sieves, and the vial was sealed with a PTFE crimp cap. 200 μ L of anhydrous DCM was added *via* syringe through the septum, and the reaction mixture was cooled to -80 °C. After 30 minutes, >95 % deuterated *iso*-propyl diazoacetate (**364**) (36.4 mg, 36 μ L, 0.286 mmol) was added *via* syringe, and the reaction mixture was stirred at -80 °C, monitoring by ¹H-NMR spectroscopy until the reaction was deemed complete (~72 h). At this point the reaction mixture was filtered through a short plug of silica, eluting with diethyl ether. The solvents were removed under reduced pressure, and the residue was purified *via* flash column chromatography (35 % dichloromethane, 3 % diethyl ether in petroleum ether). A sample was submitted for chiral analytical HPLC analysis [Chiralpak AD, *iso*-hexane / *iso*-propanol : 95 / 5, 1 mL / min, 4.18 min (1st peak), 7.15 min (2nd peak), 87% *e.e.*]. The title product *cis*-(408) was a slight green oil afforded in a 76 % yield (85 mg, 0.197 mmol). ¹H-NMR (CDCl₃, 300 MHz) δ 7.51-7.38 (m, 4H, ArH), 7.07-6.91 (m, 4H, ArH), 4.95-4.83 (m, 1H, CH(CH₃)₂), 1.34 (s, 9H, C(CH₃)₃), 1.04 (dd, 6H, *J* 3.0, 6.3 Hz, C(CH₃)₃); ¹³C-NMR (CDCl₃, 75 MHz) 167.4, 148.1, 145.9, 134.2, 131.0, 129.8, 123.3, 123.0, 122.7, 121.6, 120.9, 80.2, 68.5, 28.6, 21.6, 21.4 ppm; [α]_D²⁶ 25 (c 1 CHCl₃); FT-IR (thin film, cm⁻¹): 2979, 1746, 1489, 1258, 1194, 1108; MS (EI)⁺: *m/z* 434.2 [M+H]⁺, 456.1 [M+Na]⁺; HRMS (EI)⁺: exact mass calculated for [C₂₂H₂₅D₂BrNO₃]⁺ requires *m/z* 434.1294, found *m/z* 434.1296.

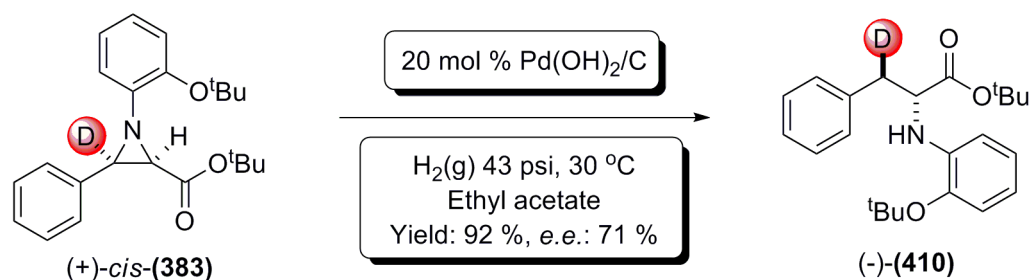
9.6: Synthesis of C2-, or C3-deutero, and C2-, C3-di-deutero Amino Acids

Synthesis of *tert*-butyl 2-(2-*tert*-butoxyphenylamino)-2-deutero-3-phenylpropanoate; (+)-(409)



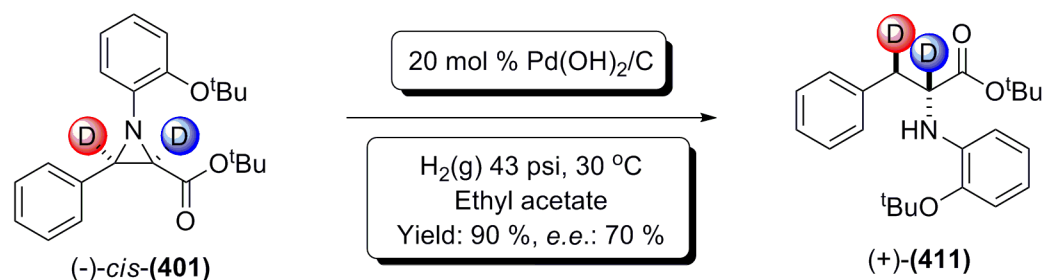
To a solution of the optically active starting material (-)-*cis*-(**351**) (15 mg, 0.041 mmol), synthesised using (*S*)-(**289**), in 4 mL ethyl acetate was added palladium hydroxide on carbon (20 % Pd by weight [6 mg, 0.0081 mmol, 20 %]). The reaction mixture was stirred at 30 °C, under 43 psi H₂ for ~12 h in a Biotage Endeavour catalyst screening system. The reaction was monitored by the uptake of hydrogen gas. When deemed complete, the reaction mixture was filtered through Celite[®], and the Celite[®] eluted with ethyl acetate. The resulting washings were combined, and the solvent removed under reduced pressure. The crude material was purified *via* flash column chromatography (15 % diethyl ether in petroleum ether). A sample was submitted to chiral analytical HPLC analysis [Chiralcel OD, CO₂ / *iso*-propanol : 5% – 50% over 9 min, 0.7 mL / min, 2.87 min (1st peak), 3.25 min (2nd peak), 80 % *e.e.*]. The title compound (+)-(**409**) was afforded as a slight brown oil in a 93 % yield (14 mg, 0.038 mmol). ¹H-NMR (CDCl₃, 300 MHz) δ 7.31-7.18 (m, 5H, ArH), 6.98-6.86 (m, 2H, ArH), 6.64-6.51 (m, 2H, ArH), 3.11 (2d, 2H, *J* 2.4 Hz, diastereotopic β-CH₂), 1.34 (s, 9H, C(CH₃)₃), 1.32 (s, 9H, C(CH₃)₃); ¹³C-NMR (CDCl₃, 75 MHz) 172.3, 143.0, 141.3, 136.8, 129.6, 128.4, 126.8, 123.6, 122.0, 116.6, 110.8, 81.4, 79.5, 38.6, 28.8, 27.8 ppm; FT-IR (thin film, cm⁻¹): 2977, 2931, 1729, 1599, 1509, 1368, 1254; [α]_D¹⁹ 6.5 (c 1 CHCl₃) MS (EI)⁺: *m/z* 371.2 [M+H]; HRMS (EI)⁺: exact mass calculated for [C₂₃H₃₁DNO₃]⁺ requires *m/z* 371.2439, found *m/z* 371.2443.

Synthesis of *tert*-butyl 2-(2-*tert*-butoxyphenylamino)-3-deutero-3-phenylbutanoate; (-)-(410)



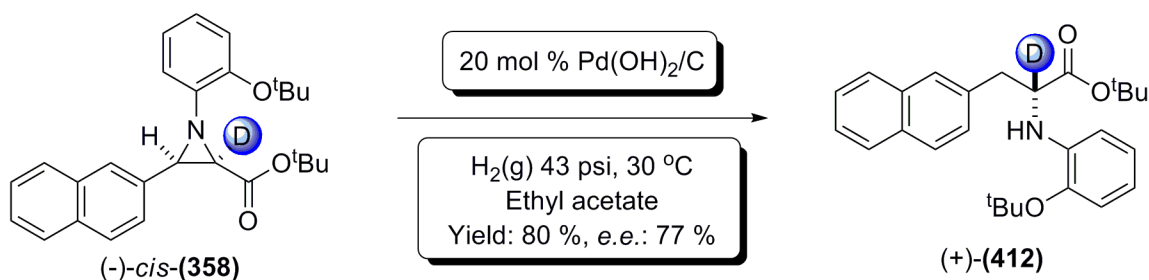
To a solution of the optically active starting material (+)-*cis*-(**383**) (15 mg, 0.041 mmol) synthesised using (*R*)-(289), in 4 mL ethyl acetate was added palladium hydroxide on carbon (20 % Pd by weight [6 mg, 0.0081 mmol, 20 %]). The reaction mixture was stirred at 30 °C, under 43 psi H₂ for ~12 h in a Biotage Endeavour catalyst screening system. The reaction was monitored by the uptake of hydrogen gas. When deemed complete, the reaction mixture was filtered through Celite[®], and the Celite[®] eluted with ethyl acetate. The resulting washings were combined, and the solvent removed under reduced pressure. The crude material was purified *via* flash column chromatography (15 % diethyl ether in petroleum ether). A sample was submitted to chiral analytical HPLC analysis [Chiralcel OD-3, CO₂ / *iso*-propanol : 5% - 50% over 9 min, 0.7 mL / min, 2.87 min (1st peak), 3.24 min (2nd peak), 71 % *e.e.*]. The title compound (-)-(410) was afforded as a slight brown oil in a 92 % yield (14 mg, 0.038 mmol). ¹H-NMR (CDCl₃, 300 MHz) δ 7.41-7.12 (m, 5H, ArH), 7.05-6.84 (m, 2H, ArH), 6.66-6.45 (m, 2H, ArH), 4.20 (d, 1H, *J* 6.2 Hz, α-CH) 3.11 (d, 1H, *J* 6.2 Hz, β-CHD), 1.34 (s, 9H, C(CH₃)₃), 1.32 (s, 9H, C(CH₃)₃); ¹³C-NMR (CDCl₃, 75 MHz) 172.3, 143.0, 136.8, 129.6, 128.4, 126.8, 123.6, 122.0, 116.6, 110.8, 81.4, 79.5, 57.7, 28.8, 27.8 ppm; FT-IR (thin film, cm⁻¹): 2977, 2927, 2362, 1729, 1599, 1507, 1368, 1254; [α]_D²² - 17.5 (c 0.2 CHCl₃); MS (EI)⁺: *m/z* 371.2 [M+H]; HRMS (EI)⁺: exact mass calculated for [C₂₃H₃₁DNO₃]⁺ requires *m/z* 371.2439, found *m/z* 371.2442.

**Synthesis of *tert*-butyl 2-(2-*tert*-butoxyphenylamino)-2,3-dideutero-3-phenylbutanoate;
(+)-(411)**



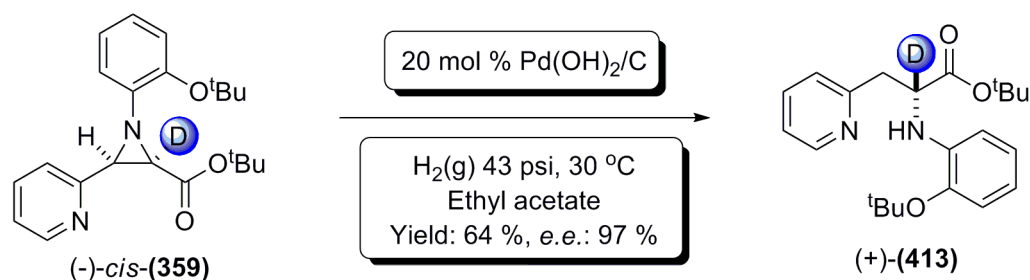
To a solution of the optically active starting material (-)-*cis*-(401) (15 mg, 0.041 mmol) synthesised using (*S*)-(289), in 4 mL ethyl acetate was added palladium hydroxide on carbon (20 % Pd by weight [6 mg, 0.0081 mmol, 20 %]). The reaction mixture was stirred at 30 °C, under 43 psi H₂ for ~12 h in a Biotage Endeavour catalyst screening system. The reaction was monitored by the uptake of hydrogen gas. When deemed complete, the reaction mixture was filtered through Celite[®], and the Celite[®] eluted with ethyl acetate. The resulting washings were combined, and the solvent removed under reduced pressure. The crude material was purified *via* flash column chromatography (15 % diethyl ether in petroleum ether). A sample was submitted to chiral analytical HPLC analysis [Chiralcel OD-3, CO₂ / *iso*-propanol : 5% - 50% over 9 min, 0.7 mL / min, 2.61 min (1st peak), 3.03 min (2nd peak), 70 % *e.e.*]. The title compound (+)-(411) was afforded as a slight brown oil in a 90 % yield (14 mg, 0.037 mmol). ¹H-NMR (CDCl₃, 300 MHz) δ 7.33-7.18 (m, 5H, ArH), 6.99-6.86 (m, 2H, ArH), 6.65-6.50 (m, 2H, ArH), 3.10 (s, 1H, β-CHD), 1.34 (s, 9H, C(CH₃)₃), 1.32 (s, 9H, C(CH₃)₃); ¹³C-NMR (CDCl₃, 75 MHz) 172.3, 143.0, 141.3, 136.8, 129.6, 128.4, 126.8, 123.6, 122.0, 116.6, 110.8, 81.4, 79.5, 28.8, 27.8 ppm; FT-IR (thin film, cm⁻¹) 2977, 2927, 2854, 2362, 1729, 1599, 1507, 1368, 1254; [α]_D²² 15 (c 1 CHCl₃) MS (EI)⁺: *m/z* 372.2 [M+H]; HRMS (EI)⁺: exact mass calculated for [C₂₃H₃₀D₂NO₃]⁺ requires *m/z* 372.2429, found *m/z* 372.2431.

Synthesis of *tert*-butyl 2-(2-*tert*-butoxyphenylamino)-2-*deutero*-3-(naphthalen-2-yl)propanoate; (+)-(412)



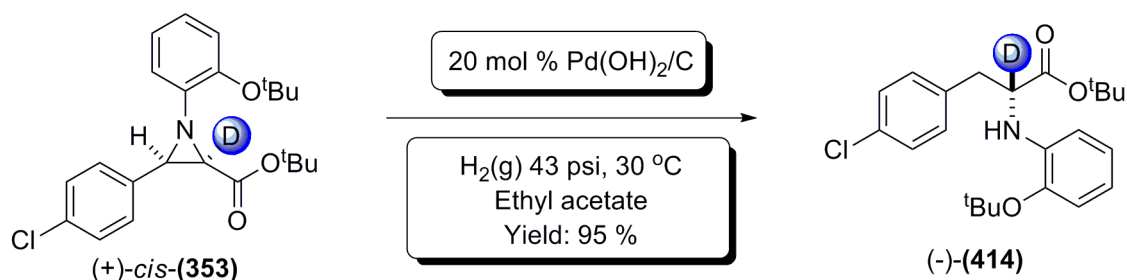
To a solution of the optically active starting material (-)-*cis*-(358) (20 mg, 0.048 mmol) synthesised using (*S*)-(289), in 4 mL ethyl acetate was added palladium hydroxide on carbon (20 % Pd by weight [6.7 mg, 0.0096 mmol, 20 %]). The reaction mixture was stirred at 30 °C, under 43 psi H₂ for ~8 h, in a Biotage Endeavour catalyst screening system. The reaction was monitored by the uptake of hydrogen gas. When deemed complete, the reaction mixture was filtered through Celite[®] and the Celite[®] eluted with ethyl acetate. The resulting washings were combined and the solvent removed under reduced pressure. The crude material was purified *via* flash column chromatography (15 % diethyl ether in petroleum ether). A sample was submitted to chiral analytical HPLC analysis [Chiralcel OD-3, CO₂ / *iso*-propanol : 5% - 50% over 9 min, 0.7 mL / min, 3.91 min (1st peak), 4.10 min (2nd peak), 77 % *e.e.*]. The title compound (+)-(412) was afforded as a colourless oil in an 80 % yield (16 mg, 0.038 mmol). ¹H-NMR (CDCl₃, 300 MHz) δ 7.84-7.72 (m, 3H, ArH), 7.68 (s, 1H, ArH), 7.51-7.32 (m, 3H, ArH), 6.99-6.87 (m, 2H, ArH), 6.68-6.57 (m, 2H, ArH), 3.29 (2d, 2H, *J* 6.0 Hz, diastereotopic β-CH₂), 1.30 (s, 9H, C(CH₃)₃), 1.28 (s, 9H, C(CH₃)₃); ¹³C-NMR (CDCl₃, 75 MHz) 172.3, 143.1, 141.5, 134.5, 133.6, 132.6, 128.4, 128.1, 127.9, 127.8, 127.7, 126.2, 125.7, 123.8, 122.3, 116.8, 111.0, 81.7, 79.7, 39.0, 29.1, 28.1 ppm; [α]_D²² 3.6 (c 1 CHCl₃); FT-IR (thin film, cm⁻¹): 2977, 2927, 2853, 1729, 1599, 1509, 1435, 1391, 1367, 1322, 1255; MS (EI)⁺: *m/z* 421.3 [M+H]⁺; HRMS (EI)⁺: exact mass calculated for [C₂₇H₃₃DNO₃]⁺ requires *m/z* 421.2596, found *m/z* 421.2596.

Synthesis of *tert*-butyl 2-(2-*tert*-butoxyphenylamino)-2-deutero-3-(pyridin-2-yl)propanoate; (+)-(413)



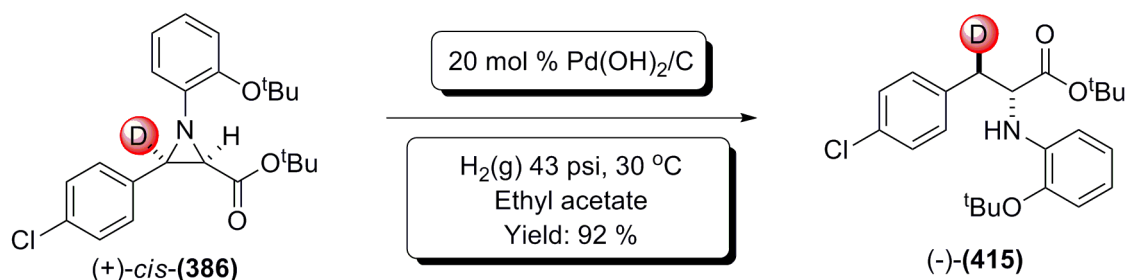
To a solution of the optically active starting material (-)-*cis*-(359) (25 mg, 0.06 mmol) synthesised using (*S*)-(289), in 4 mL ethyl acetate was added palladium hydroxide on carbon (20 % Pd by weight [9.6 mg, 0.014 mmol, 20 %]). The reaction mixture was stirred at 30 °C, under 43 psi H₂ for ~8 h, in a Biotage Endeavour catalyst screening system. The reaction was monitored by the uptake of hydrogen gas. When deemed complete, the reaction mixture was filtered through Celite[®], and the Celite[®] eluted with ethyl acetate. The resulting washings were combined, and the solvent removed under reduced pressure. The crude material was purified *via* flash column chromatography (15 % diethyl ether in petroleum ether). A sample was submitted to chiral analytical HPLC analysis [Chiralcel OD-3, CO₂ / *iso*-propanol : 5% - 50% over 9 min, 0.7 mL / min, 3.39 min (1st peak), 3.84 min (2nd peak), 97 % *e.e.*]. The title compound (+)-(413) was afforded as a slight brown oil in a 64 % yield (14 mg, 0.038 mmol). ¹H-NMR (CDCl₃, 300 MHz) δ 8.73 (d, 1H, *J* 4.7 Hz, ArH), 8.02-7.60 (m, 1H, ArH), 7.57-7.32 (m, 2H, ArH), 6.77-6.49 (m, 2H, ArH), 3.40 (2d, broad, 2H, diastereotopic β-CH₂), 1.37 (s, 9H, C(CH₃)₃), 1.34 (s, 9H, C(CH₃)₃); ¹³C-NMR (CDCl₃, 75 MHz) 171.6, 143.1, 141.1, 139.6, 125.7, 123.9, 123.0, 122.3, 117.2, 111.2, 82.3, 80.0, 39.1, 29.1, 28.0 ppm; [α]_D²¹ 22 (c 0.5 CHCl₃); FT-IR (thin film, cm⁻¹): 2978, 2931, 1735, 1598, 1511, 1507, 1368, 1253, 1157; MS (EI)⁺: *m/z* 372.3 [M+H]⁺, 394.2 [M+Na]⁺; HRMS (EI)⁺: exact mass calculated for [C₂₂H₃₀DN₂O₃]⁺ requires *m/z* 372.2392, found *m/z* 372.2396.

Synthesis of *tert*-butyl 2-(2-*tert*-butoxyphenylamino)-3-(4-chlorophenyl)-2-deuteropropanoate; (-)-(414)



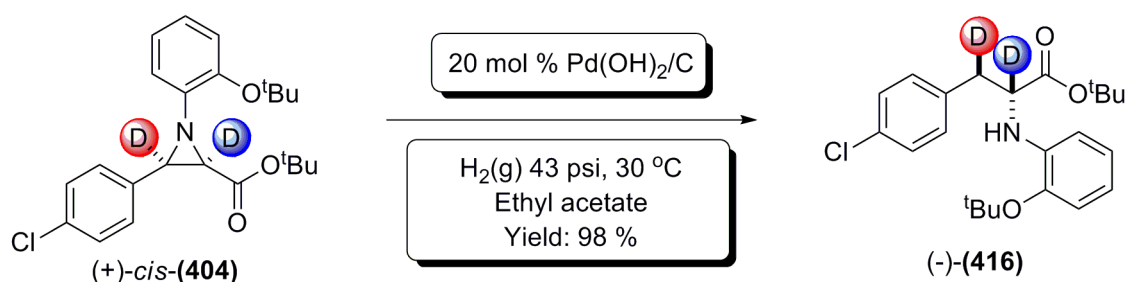
To a solution of the optically active starting material (+)-*cis*-(353) (25 mg, 0.062 mmol) synthesised using (*R*)-(289), in 2 mL ethyl acetate was added palladium hydroxide on carbon (20 % Pd by weight [8.7 mg, 0.012 mmol, 20 %]). The reaction mixture was stirred at 30 °C, under 45 psi H₂ for ~12 h, in a Biotage Endeavour catalyst screening system. The reaction was monitored by the uptake of hydrogen gas. When deemed complete, the reaction mixture was filtered through Celite[®], and the Celite[®] eluted with ethyl acetate. The resulting washings were combined, and the solvent removed under reduced pressure. The crude material was purified *via* flash column chromatography (15 % diethyl ether in petroleum ether). A sample was unable to be separated by chiral HPLC by any method that was available. The title compound (-)-(414) was a slight green oil afforded in a 95 % yield (24 mg, 0.059 mmol). ¹H-NMR (CDCl₃, 300 MHz) δ 7.32-7.18 (m, 4H, ArH), 6.97-6.85 (m, 2H, ArH), 6.64-6.51 (m, 2H, ArH), 3.11 (2d, 2H, *J* 2.1 Hz, diastereotopic β-CH₂), 1.31 (s, 18H, 2 C(CH₃)₃); ¹³C-NMR (CDCl₃, 75 MHz) 171.9, 143.0, 141.1, 135.4, 132.7, 131.0, 128.5, 123.7, 122.1, 116.8, 110.9, 81.7, 79.6, 37.7, 28.8, 27.8 ppm; [α]_D²² -1.87 (c 0.6 CHCl₃); FT-IR (thin film, cm⁻¹): 2977, 1730, 1599, 1507, 1367, 1255, 1159; MS (EI)⁺: *m/z* 405.2 [M+H]⁺; HRMS (EI)⁺: exact mass calculated for [C₂₃H₃₀DCINO₃]⁺ requires *m/z* 405.2050, found *m/z* 405.2046.

Synthesis of *tert*-butyl 2-(2-*tert*-butoxyphenylamino)-3-(4-chlorophenyl)-3-deuteropropanoate; (-)-(415)



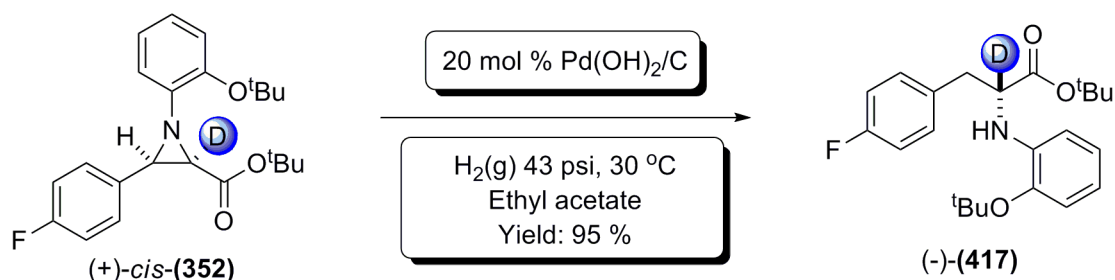
To a solution of the optically active starting material (+)-*cis*-(**386**) (12 mg, 0.03 mmol) synthesised using (*R*)-(**289**) in 1 mL ethyl acetate was added palladium hydroxide on carbon (20 % Pd by weight (4 mg, 0.006 mmol, 20 %)). The reaction mixture was stirred at 30 °C, under 45 psi H₂ for ~12 h, in a Biotage Endeavour catalyst screening system. The reaction was monitored by the uptake of hydrogen gas. When deemed complete, the reaction mixture was filtered through Celite[®], and the Celite[®] eluted with ethyl acetate. The resulting washings were combined, and the solvent removed under reduced pressure. The crude material was purified *via* flash column chromatography (15 % diethyl ether in petroleum ether). A sample was unable to be separated by chiral HPLC by any method that was available. The title compound (-)-(**415**) was afforded as a slight green oil in a 92 % yield (11 mg, 0.028 mmol). ¹H-NMR (CDCl₃, 300 MHz) δ 7.25 - 7.15 (m, 4H, ArH), 7.15, 6.99-6.87 (m, 2H, ArH), 6.65-6.52 (m, 2H, ArH), 4.19 (d, *J* 6.0 Hz, 1H, α-CH), 3.07 (d, 1H, *J* 6.0 Hz, β-CHD), 1.34 (s, 18H, 2 C(CH₃)₃); ¹³C-NMR (CDCl₃, 75 MHz) 171.9, 143.1, 141.2, 135.4, 132.8, 131.1, 128.6, 123.8, 122.2, 116.9, 111.0, 81.9, 79.8, 57.8, 29.1, 28.1 ppm; [α]_D²¹ -1.38 (c 0.8 CHCl₃); FT-IR (thin film, cm⁻¹): 2976, 2927, 1730, 1598, 1510, 1444, 1391, 1253, 1154; MS (EI)⁺: *m/z* 405.1 [M+H]⁺; HRMS (EI)⁺: exact mass calculated for [C₂₃H₃₀DCINO₃]⁺ requires *m/z* 405.2050, found *m/z* 405.2048.

Synthesis of *tert*-butyl 2-(2-*tert*-butoxyphenylamino)-3-(4-chlorophenyl)-2,3-dideuteropropanoate; (-)-(416)



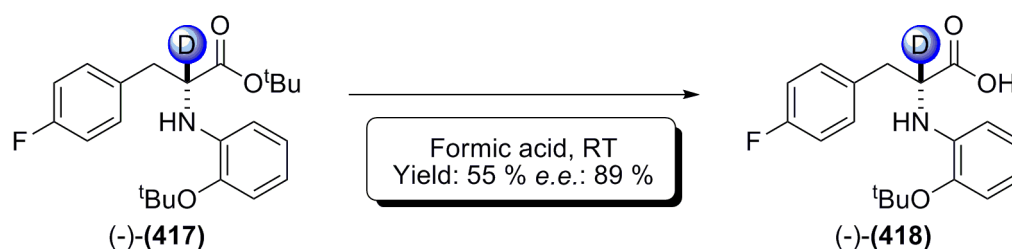
To a solution of the optically active starting material (+)-*cis*-(404) (15 mg, 0.037 mmol) synthesised using (*R*)-(289) in 1 mL ethyl acetate was added palladium hydroxide on carbon (20 % Pd by weight [6 mg, 0.007 mmol, 20 %]). The reaction mixture was stirred at 30 °C, under 45 psi H₂ for 12 h, in a Biotage Endeavour catalyst screening system. The reaction was monitored by the uptake of hydrogen gas. When deemed complete, the reaction mixture was filtered through Celite[®], and the Celite[®] eluted with ethyl acetate. The resulting washings were combined, and the solvent removed under reduced pressure. The crude material was purified *via* flash column chromatography (15 % diethyl ether in petroleum ether). A sample was unable to be separated by chiral HPLC by any method that was available. The title compound (-)-(416) was afforded as a slight green oil in a 98 % yield (15 mg, 0.036 mmol). ¹H-NMR (CDCl₃, 300 MHz) δ 7.25 - 7.14 (m, 4H, ArH), 6.97-6.86 (m, 2H, ArH), 6.64-6.51 (m, 2H, ArH), 3.06 (s, 1H, β-CHD), 1.34 (s, 18H, 2 C(CH₃)₃); ¹³C-NMR (CDCl₃, 75 MHz) 171.3, 143.0, 141.1, 135.3, 132.7, 131.0, 128.4, 123.7, 122.1, 116.8, 110.8, 81.7, 79.6, 28.8, 27.8 ppm; [α]_D²¹ -19.0 (c 1 CHCl₃); FT-IR (thin film, cm⁻¹): 2976, 2927, 1730, 1598, 1510, 1444, 1391, 1253, 1154; MS (EI)⁺: *m/z* 406.1 [M+H]⁺; HRMS (EI)⁺: exact mass calculated for [C₂₃H₂₉D₂ClNO₃]⁺ requires *m/z* 406.2113, found *m/z* 406.2103.

Synthesis of *tert*-butyl 2-(2-*tert*-butoxyphenylamino)-3-(4-fluorophenyl)-2-deuteropropanoate; (-)-(417)



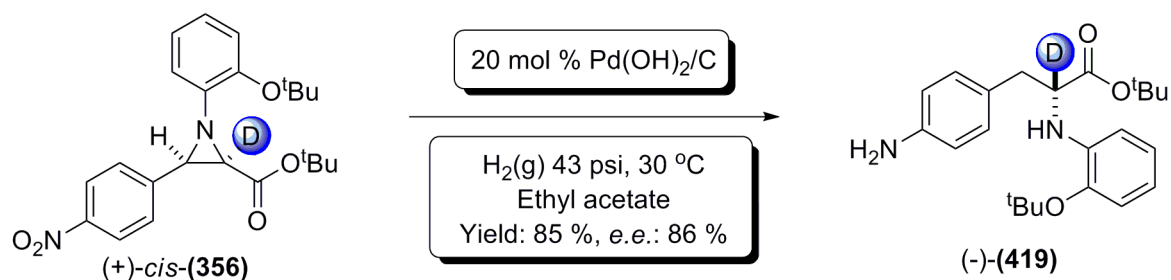
To a solution of the optically active starting material (+)-*cis*-(352) (45 mg, 0.116 mmol) synthesised using (*R*)-(289), in 4 mL ethyl acetate was added palladium hydroxide on carbon (20 % Pd by weight [16 mg, 0.0233 mmol, 20 %]). The reaction mixture was stirred at 30 °C, under 43 psi H₂ for ~12 h, in a Biotage Endeavour catalyst screening system. The reaction was monitored by the uptake of hydrogen gas. When deemed complete, the reaction mixture was filtered through Celite[®], and the Celite[®] eluted with ethyl acetate. The resulting washings were combined, and the solvent removed under reduced pressure. The crude material was purified *via* flash column chromatography (15 % diethyl ether in petroleum ether). The title compound (-)-(417) was afforded as a slight brown oil in a 95 % yield (43 mg, 0.11 mmol). ¹H-NMR (CDCl₃, 300 MHz) δ 7.21-7.12 (m, 2H, ArH), 7.01-6.86 (m, 4H, ArH), 6.65-6.50 (m, 2H, ArH), 3.09 (2d, 2H, *J* 5.4 Hz, diastereotopic β-CH₂), 1.34 (s, 18H, 2 C(CH₃)₃); ¹³C-NMR (CDCl₃, 75 MHz) 172.0, 163.6, 160.3, 143.0, 141.2, 132.5, 132.4, 131.2, 131.0, 123.7, 122.1, 116.8, 115.3, 115.0, 110.8, 81.6, 79.6, 37.6, 28.8, 27.8 ppm; [α]_D²² -6.14 (c 1 CHCl₃); FT-IR (thin film, cm⁻¹): 2976, 1728, 1599, 1508, 1430, 1367, 1325, 1253, 1222, 1156; MS (EI)⁺: *m/z* 389.3 [M+H]⁺; HRMS (EI)⁺: exact mass calculated for [C₂₃H₃DFNO₃]⁺ requires *m/z* 389.2345, found *m/z* 389.2347.

Synthesis of 2-(2-*tert*-butoxyphenylamino)-3-(4-fluorophenyl)-2-deuteropropanoic acid; (-)-(418)



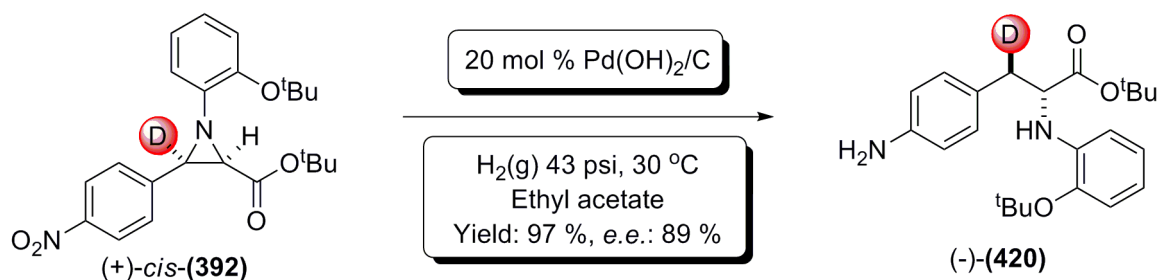
The optically active starting material (-)-(417) (59 mg, 0.152 mmol) was stirred in neat formic acid (500 μ L) for 36 h. After this time, TLC analysis (20 % diethyl ether in petroleum ether) revealed consumption of the starting material. At this point the solution was evaporated to dryness, and the residue was purified by reversed phase column chromatography (100% water \rightarrow 100% acetonitrile). A sample was submitted to chiral analytical HPLC analysis [Chiralpak AD, *iso*-hexane / *iso*-propanol (containing 1% TFA) : 90 / 10, 1 mL / min, 9.89 min (1st peak), 12.35 min (2nd peak), 89 % *e.e.*]. The title compound (-)-(418) was afforded as a colourless oil in a 55% yield (28 mg, 0.084 mmol). ¹H-NMR (CDCl₃, 300 MHz) δ 7.25-7.16 (m, 2H, ArH), 7.05-6.93 (t, 2H, *J* 8.6, 8.6 Hz, ArH), 6.84-6.61 (m, 4H, ArH), 3.06 (2d, 2H, *J* 5.4 Hz, diastereotopic β -CH₂), 1.35 (s, 9H, C(CH₃)₃); ¹³C-NMR (CDCl₃, 75 MHz) 173.2, 163.7, 160.4, 145.8, 134.6, 132.6, 131.1, 131.0, 121.1, 120.5, 115.6, 115.4, 115.1, 82.2, 38.0, 27.8 ppm; [α]_D²² -53.9 (c 0.1 CHCl₃); FT-IR (thin film, cm⁻¹): 2977, 2717, 2334, 1728, 1606, 1510, 1369, 1228; MS (EI)⁺: *m/z* 333.1 [M+H]⁺ 355.1 [M+Na]⁺; HRMS (EI)⁺: exact mass calculated for [C₁₉H₂₂DFNO₃]⁺ requires *m/z* 333.1719, found *m/z* 333.1723.

Synthesis of *tert*-butyl 3-(4-aminophenyl)-2-(2-*tert*-butoxyphenylamino)-2-deuteropropanoate; (-)-(419)



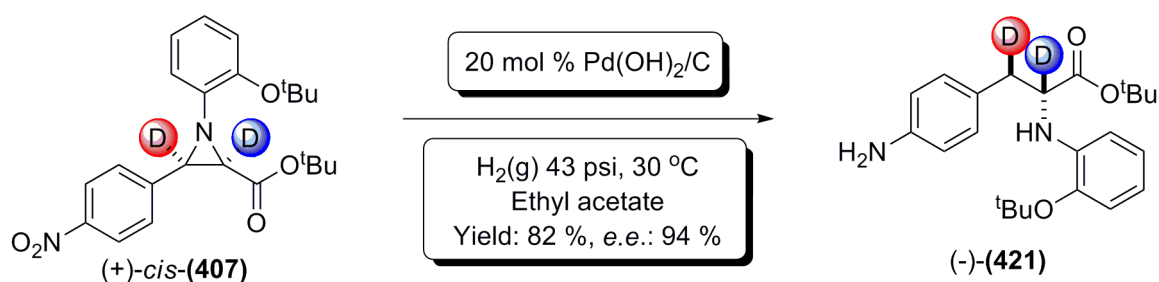
To a solution of the chiral starting material (+)-*cis*-(356) (30 mg, 0.073 mmol) synthesised using (*R*)-(289), in 4 mL ethyl acetate was added palladium hydroxide on carbon (20 % Pd by weight [10 mg, 0.0145 mmol, 20 %]). The reaction mixture was stirred at 30 °C, under 43 psi H₂ for ~12 h, in a Biotage Endeavour catalyst screening system. The reaction was monitored by the uptake of hydrogen gas. When deemed complete, the reaction mixture was filtered through Celite[®], and the Celite[®] eluted with ethyl acetate. The resulting washings were combined, and the solvent removed under reduced pressure. The crude material was purified *via* flash column chromatography (15 % diethyl ether in petroleum ether). A sample was submitted to chiral analytical HPLC analysis [Chiralcel OJ-3, CO₂ / *iso*-propanol : 5% - 50% over 9 min, 0.7 mL / min, 3.70 min (1st peak), 4.71 min (2nd peak), 86 % *e.e.*]. The title compound (-)-(419) was afforded as a dark brown/black oil in an 85 % yield (24 mg, 0.062 mmol). ¹H-NMR (CDCl₃, 300 MHz) δ 6.97-6.90 (m, 2H, ArH), 6.89-6.78 (m, 2H, ArH), 6.58-6.42 (m, 4H, ArH), 2.98 (2d, 2H, *J* 4.8 Hz, diastereotopic β-CH₂), 1.33 (s, 9H, C(CH₃)₃), 1.32 (s, 9H, C(CH₃)₃); ¹³C-NMR (CDCl₃, 75 MHz) 172.5, 145.1, 142.9, 141.5, 130.4, 126.7, 123.7, 122.1, 116.4, 115.2, 110.8, 81.2, 79.5, 37.7, 28.8, 27.8 ppm; FT-IR (thin film, cm⁻¹) 3374, 2976, 1725, 1599, 1514, 1429, 1367, 1280, 1253, 1156; [α]_D²² -9.90 (c 1 CHCl₃); MS (EI)⁺: *m/z* 387.3 [M+H]⁺; HRMS (EI)⁺: exact mass calculated for [C₂₃H₃₂DN₂O₃]⁺ requires *m/z* 386.2548, found *m/z* 386.2551.

Synthesis of *tert*-butyl 3-(4-aminophenyl)-2-(2-*tert*-butoxyphenylamino)-3-deuteropropanoate (-)-(420)



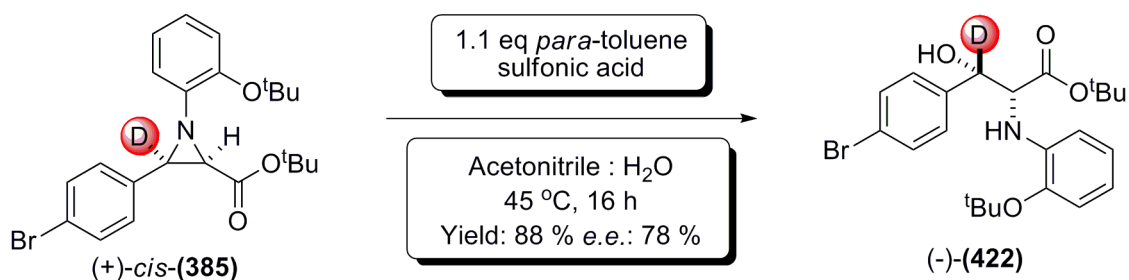
To a solution of the chiral starting material (+)-*cis*-(**392**) (30 mg, 0.073 mmol) synthesised using (*R*)-(**289**), in 4 mL ethyl acetate was added palladium hydroxide on carbon (20 % Pd by weight [10 mg, 0.0145 mmol, 20 %]). The reaction mixture was stirred at 30 °C, under 43 psi H₂ for ~12 h, in a Biotage Endeavour catalyst screening system. The reaction was monitored by the uptake of hydrogen gas. When deemed complete, the reaction mixture was filtered through Celite[®], and the Celite[®] eluted with ethyl acetate. The resulting washings were combined, and the solvent removed under reduced pressure. The crude material was purified *via* flash column chromatography (15 % diethyl ether in petroleum ether). A sample was submitted to chiral analytical HPLC analysis [Chiralcel OJ-3, CO₂ / *iso*-propanol : 5% - 50% over 9 min, 0.7 mL / min, 3.75 min (1st peak), 4.75 min (2nd peak), 89 % *e.e.*]. The title compound (-)-(420) was afforded as a dark brown/black oil in a 97 % yield (27 mg, 0.071 mmol). ¹H-NMR (CDCl₃, 300 MHz) δ 7.12-6.83 (m, 4H, ArH), 6.74-6.43 (m, 4H, ArH), 4.11 (s, 1H, α-CH), 3.00 (s, 1H, β-CHD), 1.33 (s, 9H, C(CH₃)₃), 1.32 (s, 9H, C(CH₃)₃); ¹³C-NMR (CDCl₃, 75 MHz) 172.5, 145.1, 142.9, 141.5, 130.4, 126.7, 123.7, 122.1, 116.4, 115.2, 110.8, 81.2, 79.5, 57.9, 28.8, 27.8 ppm; FT-IR (thin film, cm⁻¹) 2979, 1725, 1624, 1598, 1512, 1437, 1392, 1328, 1257, 1151; [α]_D²¹ -15.52 (c 1 CHCl₃); MS (EI)⁺: *m/z* 387.3 [M+H]⁺; HRMS (EI)⁺: exact mass calculated for [C₂₃H₃₂DN₂O₃]⁺ requires *m/z* 386.2548, found *m/z* 386.2552.

Synthesis of *tert*-butyl 3-(4-aminophenyl)-2-(2-*tert*-butoxyphenylamino)-2,3-dideuteropropanoate; (-)-(421)



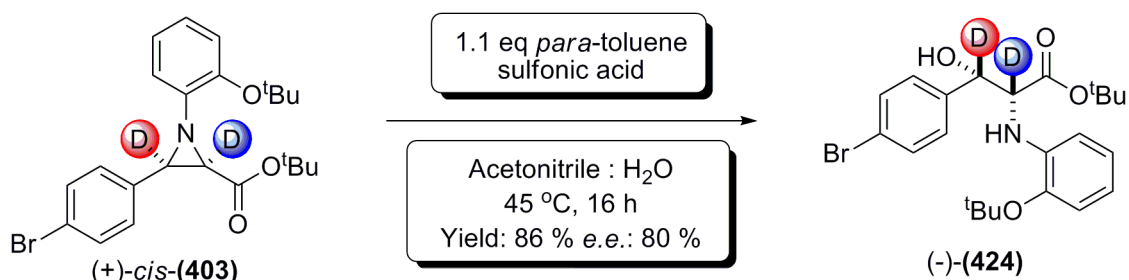
To a solution of the chiral starting material (+)-*cis*-(**407**) (26 mg, 0.063 mmol) synthesised using (*R*)-(**289**), in 4 mL ethyl acetate was added palladium hydroxide on carbon (20 % Pd by weight [9 mg, 0.0126 mmol, 20 %]). The reaction mixture was stirred at 30 °C, under 43 psi H₂ for ~12 h, in a Biotage Endeavour catalyst screening system. The reaction was monitored by the uptake of hydrogen gas. When deemed complete, the reaction mixture was filtered through Celite[®], and the Celite[®] eluted with ethyl acetate. The resulting washings were combined, and the solvent removed under reduced pressure. The crude material was purified *via* flash column chromatography (15 % diethyl ether in petroleum ether). A sample was submitted to chiral analytical HPLC analysis [Chiralcel OJ-3, CO₂ / *iso*-propanol : 5% - 50% over 9 min, 0.7 mL / min, 3.69 min (1st peak), 4.72 min (2nd peak), 94 % *e.e.*]. The title compound (-)-(**421**) was afforded as a dark brown/black oil in an 82 % yield (20 mg, 0.052 mmol). ¹H-NMR (CDCl₃, 300 MHz) δ 7.05-6.85 (m, 4H, ArH), 6.65-6.49 (m, 4H, ArH), 2.99 (s, 1H, β-CHD), 1.33 (s, 9H, C(CH₃)₃), 1.32 (s, 9H, C(CH₃)₃); ¹³C-NMR (CDCl₃, 75 MHz) 172.5, 145.1, 142.9, 141.5, 130.4, 126.7, 123.7, 122.1, 116.4, 115.2, 110.8, 81.2, 79.5, 28.8, 27.8 ppm; FT-IR (thin film, cm⁻¹) 3377, 2977, 2931, 1727, 1624, 1599, 1515, 1367, 1156; [α]_D²² -16.6 (c 1 CHCl₃); MS (EI)⁺: *m/z* 387.3 [M+H]⁺; HRMS (EI)⁺: exact mass calculated for [C₂₃H₃₁D₂N₂O₃]⁺ requires *m/z* 387.2611, found *m/z* 387.2612.

Synthesis of *tert*-butyl 3-(4-bromophenyl)-2-(2-*tert*-butoxyphenylamino)-3-hydroxy-3-deuteropropanoate; (-)-(422)



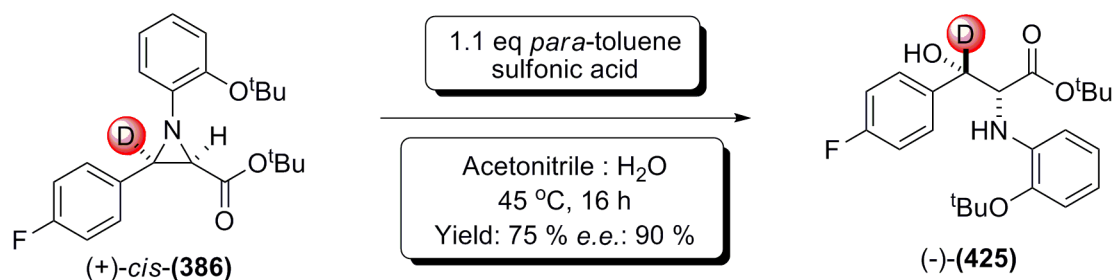
To a stirred solution of the optically active starting material (+)-*cis*-(**385**) (25 mg, 0.056 mmol) synthesised using (*R*)-(289), in 1 mL 1:1 acetonitrile : water was added *para*-toluene sulphonic acid (11.7 mg, 0.062 mmol), and the resulting mixture was heated to 45 °C with stirring for 16 h. After this time, the reaction mixture was neutralised by addition of a saturated aqueous solution of sodium hydrogen carbonate. This was extracted with ethyl acetate, and the combined organic layers were washed with brine, dried with magnesium sulphate, filtered, and the solvent removed under reduced pressure. The crude material was purified *via* flash column chromatography (30 % diethyl ether in petroleum ether). A sample was submitted to chiral analytical HPLC analysis [Chiralcel OD-3, CO₂ / methanol : 5% - 60% over 9 min, 0.7 mL / min, 4.01 min (1st peak), 4.44 min (2nd peak), 78 % *e.e.*]. The title product (-)-(422) was a slight brown oil afforded in an 88 % yield (23 mg, 0.049 mmol). ¹H-NMR (CDCl₃, 300 MHz) δ 7.47 (d, 2H, *J* 8.3 Hz, ArH), 7.30 (d, 2H, *J* 8.3 Hz, ArH), 6.96 (d, 1H, *J* 7.9 Hz, ArH), 6.85 (t, 1H, *J* 7.6, 7.6 Hz, ArH), 6.64 (t, 1H, *J* 7.6, 7.6 Hz, ArH), 6.49 (d, 1H, *J* 8.1 Hz, ArH), 4.07 (s, 1H, α-CH), 3.32 (s, 1H, OH), 1.40 (s, 9H, C(CH₃)₃), 1.31 (s, 9H, C(CH₃)₃); ¹³C-NMR (CDCl₃, 75 MHz) 171.0, 143.5, 141.1, 139.0, 131.4, 128.4, 123.6, 121.9, 117.9, 111.9, 82.7, 79.8, 63.4, 28.9, 27.7 ppm; [α]_D²² -43 (c 0.7 CHCl₃); FT-IR (thin film, cm⁻¹): 2978, 2931, 1728, 1599, 1509, 1488, 1253, 1156; MS (EI)⁺: *m/z* 487.2 [M+Na]⁺; HRMS (EI)⁺: exact mass calculated for [C₂₃H₃₀DBrNO₄]⁺ requires *m/z* 465.1494, found *m/z* 465.1495.

Synthesis of *tert*-butyl 3-(4-bromophenyl)-2-(2-*tert*-butoxyphenylamino)-3-hydroxy-2,3-dideuteropropanoate; (-)-(424)



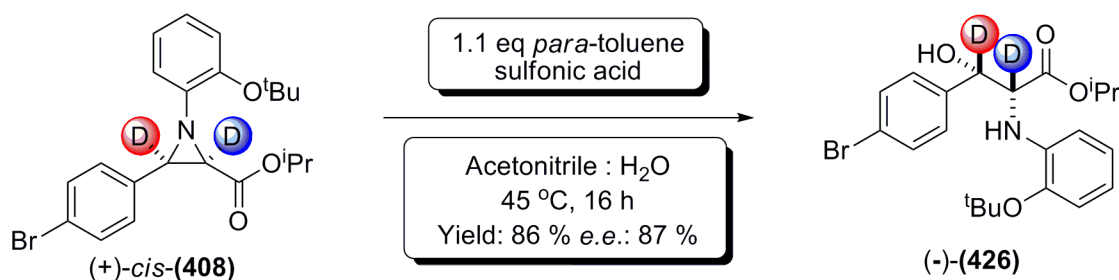
To a stirred solution of the optically active starting material (+)-*cis*-(403) (20 mg, 0.045 mmol) synthesised using (*R*)-(289) in 1 mL 1:1 acetonitrile : water was added *para*-toluene sulphonic acid (9.4 mg, 0.049 mmol), and the resulting mixture was heated to 45 °C with stirring for 16 h. After this time, the reaction mixture was neutralised by addition of a saturated aqueous solution of sodium hydrogen carbonate. This was extracted with ethyl acetate, and the combined organic layers were washed with brine, dried with magnesium sulphate, filtered, and the solvent removed under reduced pressure. The crude material was purified *via* flash column chromatography (30 % diethyl ether in petroleum ether). A sample was submitted to chiral analytical HPLC analysis [Chiralpak Chiralcel OD-3, CO₂ / methanol : 5% - 60% over 9 min, 0.7 mL / min., 4.03 min (1st peak), 4.45 min (2nd peak), 80 % *e.e.*]. The title product (-)-(424) was a slight brown oil afforded in an 86 % yield (18 mg, 0.039 mmol). ¹H-NMR (CDCl₃, 300 MHz) δ 7.47 (d, 2H, *J* 8.5 Hz, ArH), 7.30 (d, 2H, *J* 8.5 Hz, ArH), 6.96 (d, 1H, *J* 7.9 Hz, ArH), 6.86 (t, 1H, *J* 7.7, 7.7 Hz, ArH), 6.64 (t, 1H, *J* 7.7, 7.7 Hz, ArH). 6.50 (d, 1H, *J* 7.9 Hz, ArH), 1.40 (s, 9H, C(CH₃)₃), 1.31 (s, 9H, C(CH₃)₃); ¹³C-NMR (CDCl₃, 75 MHz) 171.0, 143.5, 141.0, 139.0, 132.5, 131.4, 128.4, 123.6, 121.9, 117.9, 111.9, 82.7, 79.8, 28.9, 27.7 ppm; [α]_D²² -46.05 (c 0.4 CHCl₃); FT-IR (thin film, cm⁻¹): 2978, 2931, 1726, 1599, 1508, 1488, 1431, 1392, 1254, 1156; MS (EI)⁺: *m/z* 488.2 [M+Na]⁺; HRMS (EI)⁺: exact mass calculated for [C₂₃H₂₉D₂BrNO₄]⁺ requires *m/z* 466.1557, found *m/z* 466.1556.

Synthesis of *tert*-butyl 2-(2-*tert*-butoxyphenylamino)-3-(4-fluorophenyl)-3-hydroxy-3-deuteropropanoate; (-)-(425)



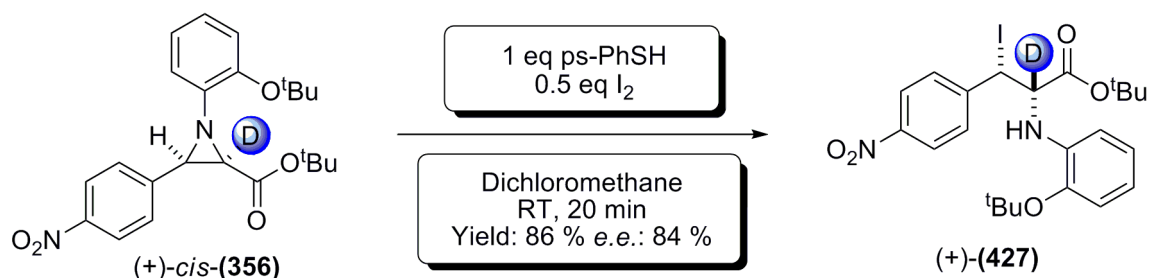
To a stirred solution of the optically active starting material (+)-*cis*-(**386**) (10 mg, 0.028 mmol) synthesised using (*R*)-(**289**) in 1 mL 1:1 acetonitrile : water was added *para*-toluene sulphonic acid (6 mg, 0.031 mmol), and the resulting mixture was heated to 45 °C with stirring for 16 h. After this time, the reaction mixture was neutralised by addition of a saturated aqueous solution of sodium hydrogen carbonate. This was extracted with ethyl acetate, and the combined organic layers were washed with brine, dried with magnesium sulphate, filtered, and the solvent removed under reduced pressure. The crude material was purified *via* flash column chromatography (30 % diethyl ether in petroleum ether). A sample was submitted to chiral analytical HPLC analysis [Chiralcel OD-3, CO₂ / methanol : 5% - 60% over 9 min, 0.7 mL / min, 3.28 min (1st peak), 3.77 min (2nd peak), 90 % *e.e.*]. The title product (-)-(425) was a slight brown oil afforded in a 75 % yield (8.5 mg, 0.021 mmol). ¹H-NMR (CDCl₃, 300 MHz) δ 7.44-7.36 (m, 2H, ArH), 7.08-6.93 (m, 3H, ArH), 6.87 (m, 1H, ArH), 6.64 (m, 1H, ArH), 6.52 (d, 1H, *J* 8.0 Hz, ArH). 4.09 (s, 1H, α-CH), 3.30 (s, 1H, OH), 1.40 (s, 9H, C(CH₃)₃), 1.29 (s, 9H, C(CH₃)₃); ¹³C-NMR (CDCl₃, 75 MHz) 171.1, 143.6, 141.2, 128.5, 128.4, 123.6, 121.9, 117.9, 115.3, 115.0, 111.9, 82.5, 79.8, 63.8, 28.9, 27.7 ppm [α]_D²² -20.0 (c 0.7 CHCl₃); FT-IR (thin film, cm⁻¹): 2977, 2922, 2852, 2344, 1727, 1600, 1510, 1477, 1392, 1368, 1253, 1158; MS (EI)⁺: *m/z* 405.1 [M+H]⁺; HRMS (ASAP)⁺: exact mass calculated for [C₂₃H₃₀DFNO₄]⁺ requires *m/z* 405.2294, found *m/z* 405.2287.

Synthesis of isopropyl 3-(4-bromophenyl)-2-(2-*tert*-butoxyphenylamino)-3-hydroxy-2,3-dideuteropropanoate; (-)-(426)



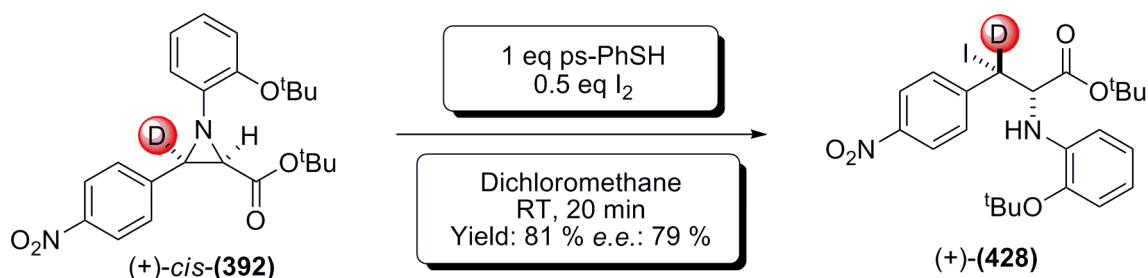
To a stirred solution of the optically active starting material (+)-*cis*-(**408**) (20 mg, 0.045 mmol) synthesised using (*R*)-(**289**), in 1 mL 1:1 acetonitrile : water was added *para*-toluene sulphonic acid (9.4 mg, 0.049 mmol), and the resulting mixture was heated to 45 °C with stirring for 16 h. After this time, the reaction mixture was neutralised by addition of a saturated aqueous solution of sodium hydrogen carbonate. This was extracted with ethyl acetate, and the combined organic layers were washed with brine, dried with magnesium sulphate, filtered, and the solvent removed under reduced pressure. The crude material was purified *via* flash column chromatography (30 % diethyl ether in petroleum ether). A sample was submitted to chiral analytical HPLC analysis [Chiralcel OD-3, CO₂ / methanol : 5% - 60% over 9 min, 0.7 mL / min, 4.12 min (1st peak), 4.50 min (2nd peak), 87 % *e.e.*]. The title product (-)-(**426**) was a slight brown oil afforded in an 86 % yield (17 mg, 0.039 mmol). ¹H-NMR (CDCl₃, 300 MHz) δ 7.47 (d, 2H, *J* 6.0 Hz, ArH), 7.30 (d, 2H, *J* 6.0 Hz, ArH), 6.96 (d, 1H, *J* 9.0 Hz, ArH), 6.85 (t, 1H, *J* 6.0, 15.0 Hz, ArH), 6.64 (t, 1H, *J* 6.0, 15.0 Hz, ArH), 6.45 (d, 1H, *J* 6.0 Hz, ArH), 4.94 (dt, 1H, *J* 6.2, 6.2, 12.5 Hz, CH(CH₃)₂), 1.40 (s, 9H, C(CH₃)₃), 1.31 (s, 9H, C(CH₃)₃); ¹³C-NMR (CDCl₃, 75 MHz) 171.5, 143.6, 140.9, 138.9, 131.5, 128.3, 123.6, 122.1, 121.9, 118.0, 111.8, 79.8, 77.2, 69.4, 28.9, 21.6, 21.4 ppm; [α]_D²² -61.1 (c 0.1 CHCl₃); FT-IR (thin film, cm⁻¹) 2977, 1599, 1508, 1488, 1463, 1431, 1367, 1254, 1161; MS (EI)⁺: *m/z* 452.1 [M+H]⁺ 474.1 [M+Na]⁺; HRMS (EI)⁺: exact mass calculated for [C₂₂H₂₇D₂BrNO₄]⁺ requires *m/z* 452.1400, found *m/z* 452.1401.

Synthesis of *tert*-butyl 2-(2-*tert*-butoxyphenylamino)-3-iodo-2-deutero-3-(4-nitrophenyl)propanoate; (+)-(427)



To a stirred solution of the optically active starting material (+)-*cis*-(356) (40 mg, 0.097 mmol, synthesised using (*R*)-(289)) solubilised in 1 mL dichloromethane, was added I₂ (11.9 mg, 0.049 mmol), and polystyrene bound benzenethiol (97 mg, ~1.0 mmol g⁻¹, 0.097 mmol). The resulting mixture was stirred in the dark for 20 minutes. After this time, the reaction mixture was filtered, and the solvent removed under reduced pressure. The crude material was purified *via* flash column chromatography (20 % dichloromethane, 10 % diethyl ether, in petroleum ether), in the dark. A sample was submitted to chiral HPLC analysis [Chiralpak IA, CO₂ / *iso*-propanol 5% - 50% over 9 min, 0.7 mL / min, 4.32 min (1st peak), 5.30 min (2nd peak), 84 % *e.e.*]. The title product (+)-(427) was a yellow oil afforded in a 86 % yield (45 mg, 0.083 mmol). ¹H-NMR (CDCl₃, 300 MHz) δ 8.12 (d, 2H, *J* 9.0 Hz, ArH), 7.71 (d, 2H, *J* 9.0 Hz, ArH), 7.00 (d, 1H, *J* 7.9, ArH), 6.83 (t, 1H, *J* 7.7, 7.7 Hz, ArH), 6.64 (t, 1H, *J* 7.7, 7.7 Hz, ArH). 6.34 (d, 1H, *J* 7.9 Hz, ArH), 5.56 (s, 1H, β-CHI), 5.28 (s, 1H, NH), 1.48 (s, 9H, C(CH₃)₃), 1.33 (s, 9H, C(CH₃)₃); ¹³C-NMR (CDCl₃, 75 MHz) 168.8, 147.8, 147.5, 143.4, 140.7, 129.7, 123.7, 123.6, 122.2, 117.9, 111.3, 83.1, 80.0, 31.5, 29.0, 27.7 ppm; [α]_D²² 87.1 (c 0.7 CHCl₃); FT-IR (thin film, cm⁻¹): 2976, 1726, 1597, 1509, 1507, 1483, 1345, 1251, 1154; MS (EI)⁺: *m/z* 542.4 [M+H]⁺; HRMS (EI)⁺: exact mass calculated for [C₂₃H₂₉DIN₂O₅]⁺ requires *m/z* 542.1257, found *m/z* 542.1249.

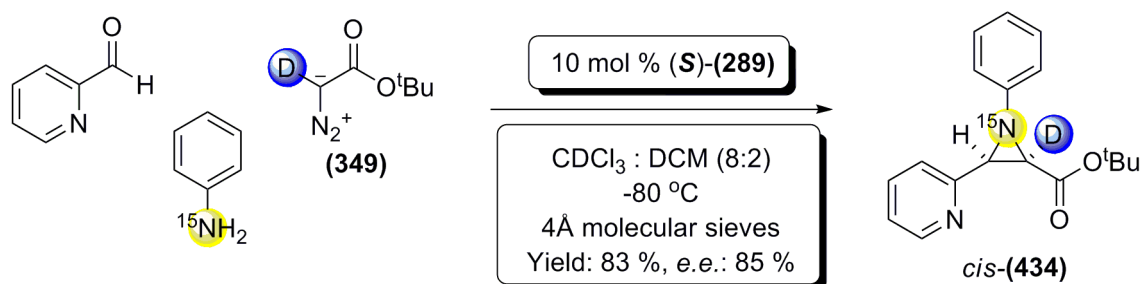
Synthesis of *tert*-butyl 2-(2-*tert*-butoxyphenylamino)-3-iodo-3-*deutero*-3-(4-nitrophenyl)propanoate; (+)-(428)



To a stirred solution of the optically active starting material (+)-*cis*-(**392**) (34 mg, 0.082 mmol, synthesised using (*R*)-(**289**)) solubilised in 1 mL dichloromethane, was added I₂ (10.4 mg, 0.041 mmol), and polystyrene bound benzenethiol (82 mg, ~1.0 mmol g⁻¹, 0.082 mmol). The resulting mixture was stirred in the dark for 20 minutes. After this time, the reaction mixture was filtered, and the solvent removed under reduced pressure. The crude material was purified *via* flash column chromatography (20 % dichloromethane, 10 % diethyl ether, in petroleum ether), in the dark. A sample was submitted to chiral HPLC analysis [Chiralpak IA, CO₂ / *iso*-propanol 5% - 50% over 9 min, 0.7 mL / min, 4.29 min (1st peak), 5.29 min (2nd peak), 79 % *e.e.*]. The title product (+)-(**428**) was a yellow oil afforded in a 81 % yield (36 mg, 0.066 mmol). ¹H-NMR (CDCl₃, 300 MHz) δ 8.12 (d, 2H, *J* 8.6 Hz, ArH), 7.71 (d, 2H, *J* 8.6 Hz, ArH), 7.00 (d, 1H, *J* 7.9, ArH), 6.82 (t, 1H, *J* 6.9, 7.0 Hz, ArH), 6.64 (t, 1H, *J* 7.0, 7.0 Hz, ArH). 6.33 (d, 1H, *J* 6.9 Hz, ArH), 5.28 (d, 1H, *J* 9.7 Hz, NH), 4.06 (d, 1H, *J* 9.7, α-CH), 1.48 (s, 9H, C(CH₃)₃), 1.34 (s, 9H, C(CH₃)₃); ¹³C-NMR (CDCl₃, 75 MHz) 168.8, 147.8, 147.5, 143.4, 140.7, 129.7, 123.7, 123.6, 122.2, 117.9, 111.3, 83.1, 80.0, 31.5, 29.0, 27.7 ppm; [α]_D²² 48.6 (c 0.5 CHCl₃); FT-IR (thin film, cm⁻¹): 2976, 1726, 1597, 1508, 1456, 1367, 1343, 1252, 1146; MS (EI)⁺: *m/z* 542.4 [M+H]⁺; HRMS (EI)⁺: exact mass calculated for [C₂₃H₂₉DIN₂O₅]⁺ requires *m/z* 542.1257, found *m/z* 542.1253.

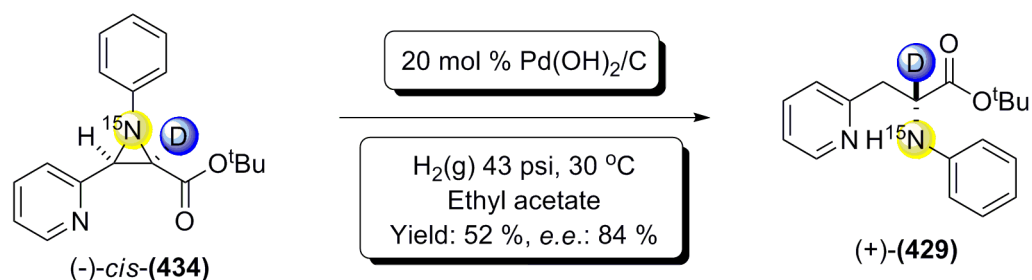
9.7: Synthesis of Deuterated ^{15}N and ^{18}O containing Aziridines, and Amino Acids/Alcohols

Three Component One-Pot Asymmetric Synthesis of *tert*-butyl 1- ^{15}N -1-phenyl-3-(pyridin-2-yl)-2-deuteroaziridine-2-carboxylate; *cis*-(**434**)



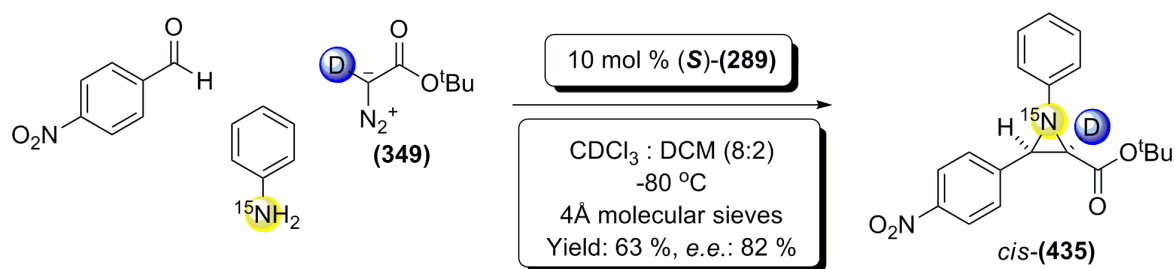
Pyridine-2-carboxaldehyde (27.8 mg, 25 μL , 0.26 mmol), ^{15}N -aniline (23 mg, 0.26 mmol), and catalyst (*S*)-(**289**) (21.6 mg, 0.026 mmol, 10%) were added to a flame dried 2 mL vial under nitrogen. 800 μL of deuterated chloroform was added (pre-dried over 4Å molecular sieves), followed by ~40 mg of freshly powdered 4Å molecular sieves, and the vial was sealed with a PTFE crimp cap. 200 μL of anhydrous dichloromethane was added *via* syringe through the septum, and the reaction mixture was cooled to $-80\text{ }^\circ\text{C}$. After 30 minutes, >95 % deuterated *tert*-butyl diazoacetate (**349**) (40.7 mg, 40 μL , 0.286 mmol) was added *via* syringe, and the reaction mixture was stirred at $-80\text{ }^\circ\text{C}$, monitoring by ^1H -NMR spectroscopy until the reaction was deemed complete. At this point the reaction mixture was filtered through a short plug of silica, eluting with diethyl ether. The solvents were removed under reduced pressure, and the residue was purified *via* flash column chromatography (20 % diethyl ether in petroleum ether). A sample was submitted to chiral analytical HPLC analysis [Chiralpak AD, *iso*-hexane / *iso*-propanol : 8 / 2, 1 mL / min, 6.38 min (1st peak), 8.20 min (2nd peak), 85% *e.e.*]. The title product *cis*-(**434**) was afforded as a slight brown oil in an 83 % yield (64 mg, 0.216 mmol). ^1H -NMR (CDCl_3 , 300 MHz) δ 8.56 – 8.51 (m, 1H, ArH), 7.70 – 7.64 (m, 2H, ArH), 7.30 – 7.15 (m, 3H, ArH), 7.09 – 6.98 (m, 3H, ArH), 3.67 (s, 1H, C3-H), 1.22 (s, 9H, $\text{C}(\text{CH}_3)_3$); ^{13}C -NMR (CDCl_3 , 75 MHz) 166.5, 166.4, 155.2, 155.1, 152.1, 152.1, 148.9, 136.2, 129.2, 123.5, 122.8, 122.7, 122.6, 120.0, 119.9, 81.7, 47.8, 47.7, 27.8 ppm; $[\alpha]_{\text{D}}^{26}$ -22.2 (c 1.1 CHCl_3); FT-IR (thin film, cm^{-1}): 2978, 1739, 1717, 1591, 1570, 1489, 1477, 1454, 1435, 1392, 1367; MS (EI)⁺: m/z 299.1 $[\text{M}+\text{H}]^+$, 321.1 $[\text{M}+\text{Na}]^+$; HRMS (EI)⁺: exact mass calculated for $[\text{C}_{18}\text{H}_{20}\text{DN}^{15}\text{NO}_2]^+$ requires m/z 299.1631, found m/z 299.1629.

Synthesis of *tert*-butyl 2-deutero-2-(phenyl-¹⁵N-amino)-3-(pyridin-2-yl)propanoate; (+)-(429)



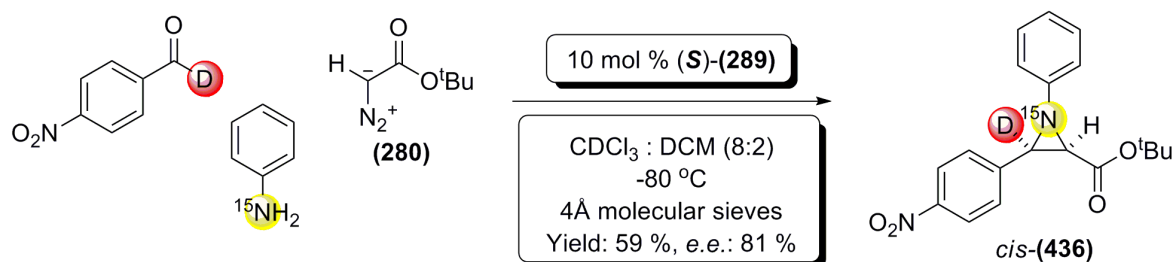
To a solution of the optically active starting material (-)-*cis*-(**434**) (36 mg, 0.12 mmol) synthesised using (*S*)-(**289**), in 4 mL ethyl acetate was added palladium hydroxide on carbon (20 % Pd by weight [17 mg, 0.024 mmol, 20 %]). The reaction mixture was stirred at 30 °C, under 43 psi H₂ for 12 h, in a Biotage Endeavour catalyst screening system. The reaction was monitored by the uptake of hydrogen gas. When deemed complete, the reaction mixture was filtered through Celite[®], and the Celite[®] eluted with ethyl acetate. The resulting washings were combined, and the solvent removed under reduced pressure. The crude material was purified *via* flash column chromatography (30 % diethyl ether in petroleum ether). A sample was submitted to chiral analytical HPLC analysis [Chiralpak ID, CO₂ / *iso*-propanol 5% - 50% over 9 min, 0.7 mL / min, 4.40 min (1st peak), 5.28 min (2nd peak), 84 % *e.e.*]. The title product (+)-(**429**) was afforded as a colourless oil in a 52 % yield (19 mg, 0.0624 mmol). ¹H-NMR (CDCl₃, 300 MHz) δ 8.57 (d, 1H, *J* 4.8 Hz, ArH), 7.60 (td, 1H, *J* 7.7, 7.7, 1.8 Hz, ArH), 7.22-7.08 (m, 4H, ArH), 6.69 (t, 1H, *J* 7.3, 7.3 Hz, ArH), 6.62 (d, 2H, *J* 7.3 Hz, ArH), 3.24 (2d, 2H, diastereotopic β-CH₂), 1.32 (s, 9H, C(CH₃)₃); ¹³C-NMR (CDCl₃, 75 MHz) 172.5, 157.7, 149.2, 147.1, 146.9, 136.5, 129.2, 124.0, 121.8, 118.0, 113.6, 113.5, 81.5, 40.5, 27.7 ppm; [α]_D²¹ 4.7 (c 0.6 CHCl₃); FT-IR (thin film, cm⁻¹): 2978, 1725, 1603, 1502, 1474, 1436, 1368, 1310, 1283, 1160; MS (EI)⁺: *m/z* 301.1 [M+H]⁺; HRMS (EI)⁺: exact mass calculated for [C₁₈H₂₂DN¹⁵NO₂]⁺ requires *m/z* 301.1787, found *m/z* 301.1791.

Three Component One-Pot Asymmetric Synthesis of *tert*-butyl 3-(4-nitrophenyl)-1-¹⁵N-1-phenyl-3-deuteroaziridine-2-carboxylate; *cis*-(**435**)



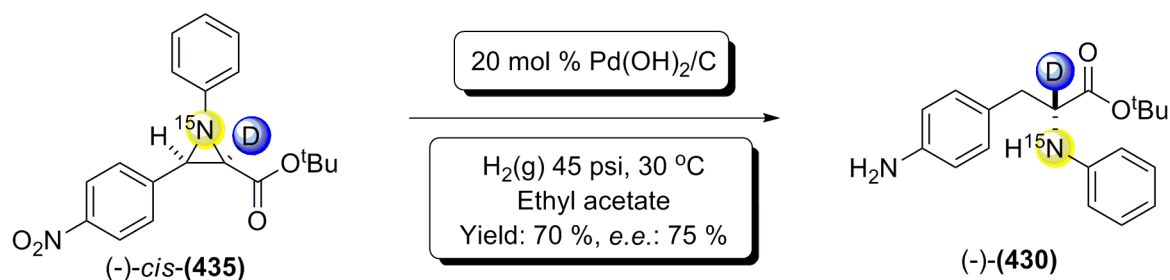
4-nitrobenzaldehyde (39.2 mg, 0.26 mmol), ¹⁵N-aniline (23 mg, 0.26 mmol), and catalyst (*S*)-(289) (21.6 mg, 0.026 mmol, 10%) were added to a flame dried 2 mL vial under nitrogen. 800 μL of deuterated chloroform was added (pre-dried over 4Å molecular sieves), followed by ~40 mg of freshly powdered 4Å molecular sieves, and the vial was sealed with a PTFE crimp cap. 200 μL of anhydrous dichloromethane was added *via* syringe through the septum, and the reaction mixture was cooled to -80 °C. After 30 minutes, >95 % deuterated *tert*-butyl diazoacetate (**349**) (40.7 mg, 40 μL, 0.286 mmol) was added *via* syringe, and the reaction mixture was stirred at -80 °C, monitoring by ¹H-NMR spectroscopy until the reaction was deemed complete. At this point the reaction mixture was filtered through a short plug of silica, eluting with diethyl ether. The solvents were removed under reduced pressure, and the residue was purified *via* flash column chromatography (17 % diethyl ether in petroleum ether). A sample was submitted to chiral analytical HPLC analysis [Chiralpak AD, heptane / *iso*-propanol : 97.5 / 2.5, 1 mL / min, 21.19 min (1st peak), 24.27 min (2nd peak), 82% *e.e.*]. The reaction product *cis*-(**435**) was afforded as a yellow oil in a 63 % yield (56 mg, 0.164 mmol). ¹H-NMR (CDCl₃, 300 MHz) δ 8.15 (d, 2H, *J* 8.9 Hz, ArH), 7.63 (d, 2H, *J* 8.9 Hz, ArH), 7.31-7.67 (m, 2H, ArH), 7.07 – 6.93 (m, 3H, ArH), 3.52 (s, 1H, C3-H), 1.15 (s, 9H, C(CH₃)₃); ¹³C-NMR (CDCl₃, 75 MHz) δ 166.2, 151.9, 147.7, 142.7, 129.5, 129.0, 128.9, 124.0, 123.4, 120.1, 120.1, 82.5, 46.1, 46.1, 28.0 ppm; [α]_D²⁶ -76.3 (c 0.9 CHCl₃); FT-IR (thin film, cm⁻¹): 2979, 1741, 1716, 1599, 1520, 1490, 1426, 1344, 1253; MS (EI)⁺: *m/z* 343.1 [M+H]⁺; HRMS (ED)⁺: exact mass calculated for [C₁₉H₂₀DN¹⁵NO₄]⁺ requires *m/z* 343.1529, found *m/z* 343.1527.

Three Component One-Pot Asymmetric Synthesis of *tert*-butyl 3-(4-nitrophenyl)-1-¹⁵N-1-phenyl-3-deuteroaziridine-2-carboxylate; *cis*-(436)



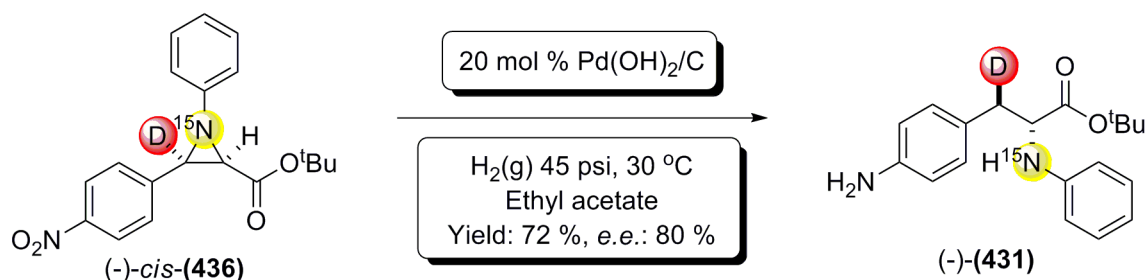
95 % Deuterated 4-nitrobenzaldehyde (24 mg, 0.155 mmol), ¹⁵N-aniline (14 μL, 0.155 mmol), and catalyst (*S*)-(289) (12 mg, 0.015 mmol, 10%) were added to a flame dried 2 mL vial under nitrogen. 800 μL of deuterated chloroform was added (pre-dried over 4Å molecular sieves), followed by ~40 mg of freshly powdered 4Å molecular sieves, and the vial was sealed with a PTFE crimp cap. 200 μL of anhydrous dichloromethane was added *via* syringe through the septum, and the reaction mixture was cooled to -80 °C. After 30 minutes, *tert*-butyl diazoacetate (280) (25.3 mg, 25 μL, 0.17 mmol) was added *via* syringe, and the reaction mixture was stirred at -80 °C, monitoring by ¹H-NMR spectroscopy until the reaction was deemed complete. At this point the reaction mixture was filtered through a short plug of silica, eluting with diethyl ether. The solvents were removed under reduced pressure, and the residue was purified *via* flash column chromatography (17 % diethyl ether in petroleum ether). A sample was submitted to chiral analytical HPLC analysis [Chiralpak AD, heptane / *iso*-propanol : 97.5 / 2.5, 1 mL / min, 21.14 min (1st peak), 24.74 min (2nd peak), 81% *e.e.*]. The reaction product *cis*-(436) was afforded as a yellow oil in a 59 % yield (31 mg, 0.0915 mmol). ¹H-NMR (CDCl₃, 400 MHz) δ 8.16 (d, 2H, *J* 8.9 Hz, ArH), 7.64 (d, 2H, *J* 8.9 Hz ArH), 7.27-7.19 (m, 2H, ArH), 7.04 – 6.95 (m, 3H, ArH), 3.13 (s, 1H, C2-H), 1.15 (s, 9H, C(CH₃)₃); ¹³C-NMR (CDCl₃, 75 MHz) δ 166.2, 151.9, 147.7, 142.6, 129.5, 129.0, 128.9, 124.0, 123.4, 120.1, 120.1, 82.5, 46.7, 46.6, 28.0 ppm; [α]_D²⁶ -76.7 (c 1 CHCl₃); FT-IR (thin film, cm⁻¹): 2979, 1740, 1720, 1599, 1519, 1490, 1426, 1344, 1253, 1154; MS (EI)⁺: *m/z* 343.1 [M+H]⁺; HRMS (EI)⁺: exact mass calculated for [C₁₉H₂₀DN¹⁵NO₄]⁺ requires *m/z* 343.1529, found *m/z* 343.1533.

Synthesis of *tert*-butyl 3-(4-aminophenyl)-2-deutero-2-(phenyl-¹⁵N-amino)propanoate; (-)-(430)



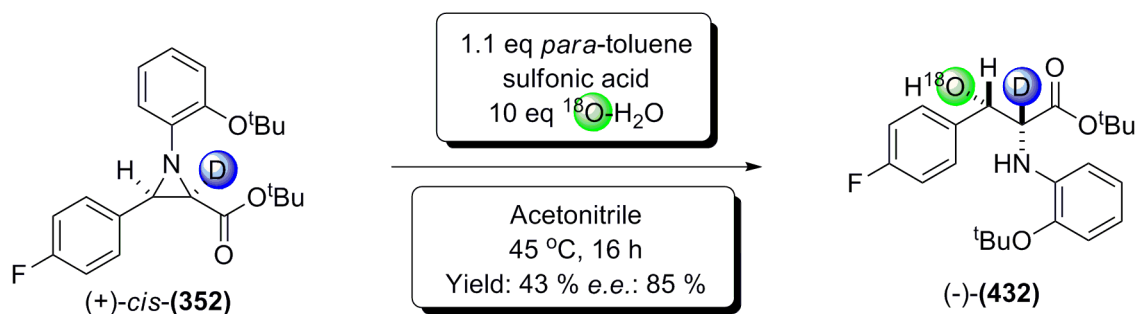
To a solution of the chiral starting material (-)-*cis*-(435) (20 mg, 0.076 mmol) synthesised using (*S*)-(289), in 4 mL ethyl acetate was added palladium hydroxide on carbon (20 % Pd by weight [10.7 mg, 0.015 mmol, 20 %]). The reaction mixture was stirred at 30 °C, under 45 psi H₂ for ~16 h, in a Biotage Endeavour catalyst screening system. The reaction was monitored by the uptake of hydrogen gas. When deemed complete, the reaction mixture was filtered through Celite[®], and the Celite[®] eluted with ethyl acetate. The resulting washings were combined, and the solvent removed under reduced pressure. The crude material was purified *via* flash column chromatography (20 % ethyl acetate in petroleum ether). A sample was submitted to chiral analytical HPLC analysis [Chiralpak AD, *iso*-hexane / *iso*-propanol with 0.1 % DEA : 80 / 20, 1.2 mL / min, 11.56 min (1st peak), 13.34 min (2nd peak), 75 % *e.e.*]. The desired product (-)-(430) was afforded as a dark brown/black oil in 70 % yield (17 mg, 0.053 mmol). ¹H-NMR (CDCl₃, 400 MHz) δ 7.09 (t, 2H, *J* 7.8 Hz ArH), 6.92 (d, 2H, *J* 8.4 Hz, ArH), 6.64 (t, 1H, *J* 7.3, 7.3 Hz, ArH), 6.57-6.50 (m, 4H, ArH), 2.91 (2d, 2H, diastereotopic β-CH₂), 1.29 (s, 9H, C(CH₃)₃); ¹³C-NMR (CDCl₃, 75 MHz) 172.6, 146.7, 145.2, 130.4, 129.3, 126.5, 118.0, 115.7, 113.6, 113.5, 81.5, 37.6, 37.5, 27.8 ppm; FT-IR (thin film, cm⁻¹) 2976, 2928, 1724, 1603, 1518, 1501, 1368, 1310, 1282, 1255, 1157; [α]_D²² -21.1 (c 0.5 CHCl₃); MS (EI)⁺: *m/z* 315.2 [M+H]⁺; HRMS (EI)⁺: exact mass calculated for [C₁₉H₂₄DN¹⁵NO₂]⁺ requires *m/z* 315.1944, found *m/z* 315.1939.

Synthesis of *tert*-butyl 3-(4-aminophenyl)-3-deutero-2-(phenyl-¹⁵N-amino)propanoate; (-)-(431)



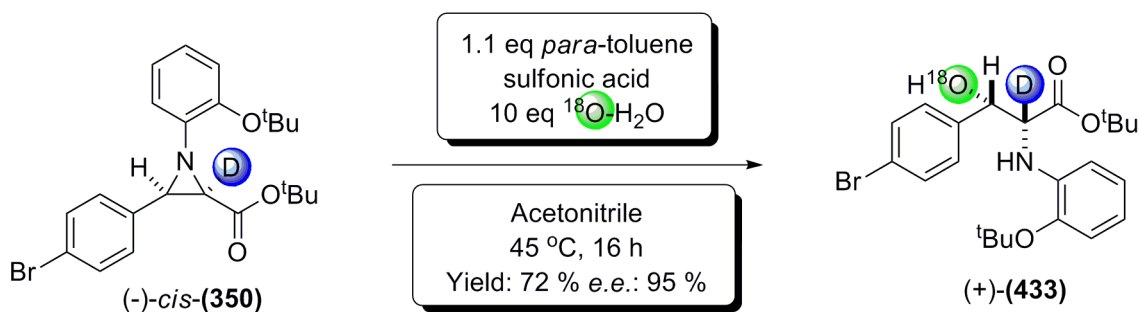
To a solution of the chiral starting material (-)-*cis*-(436) (19 mg, 0.055 mmol) synthesised using (*S*)-(289), in 4 mL ethyl acetate was added palladium hydroxide on carbon (20 % Pd by weight [8 mg, 0.011 mmol, 20 %]). The reaction mixture was stirred at 30 °C, under 45 psi H₂ for ~16 h, in a Biotage Endeavour catalyst screening system. The reaction was monitored by the uptake of hydrogen gas. When deemed complete, the reaction mixture was filtered through Celite[®], and the Celite[®] eluted with ethyl acetate. The resulting washings were combined, and the solvent removed under reduced pressure. The crude material was purified *via* flash column chromatography (20 % ethyl acetate in petroleum ether). A sample was submitted to chiral analytical HPLC analysis [Chiralpak AD, *iso*-hexane / *iso*-propanol with 0.1 % DEA : 80 / 20, 1.2 mL / min, 11.60 min (1st peak), 13.33 min (2nd peak), 80 % *e.e.*]. The desired product (-)-(431) was afforded as a dark brown/black oil in 72 % yield (12.4 mg, 0.0396 mmol). ¹H-NMR (CDCl₃, 400 MHz) δ 7.16 (t, 2H, *J* 7.9, 7.9 Hz ArH), 6.99 (d, 2H, *J* 8.5 Hz, ArH), 6.71 (t, 1H, *J* 7.3, 7.3 Hz, ArH), 6.65-6.57 (m, 4H, ArH), 4.16 (d, 1H, *J* 5.6 Hz, α-CH), 2.96 (d, 2H, *J* 5.6 Hz, β-CHD), 1.36 (s, 9H, C(CH₃)₃); ¹³C-NMR (CDCl₃, 75 MHz) 172.7, 146.9, 146.9, 145.3, 130.5, 129.4, 126.5, 118.2, 115.3, 113.7, 113.7, 81.8, 58.4, 58.3, 28.2 ppm; FT-IR (thin film, cm⁻¹) 2977, 1724, 1628, 1603, 1502, 1368, 1313, 1281, 1258, 1153; [α]_D²² -28.9 (c 0.7 CHCl₃); MS (EI)⁺: *m/z* 315.1 [M+H]⁺; HRMS (EI)⁺: exact mass calculated for [C₁₉H₂₄DN¹⁵NO₂]⁺ requires *m/z* 315.1944, found *m/z* 315.1939.

Synthesis of *tert*-butyl 2-(2-*tert*-butoxyphenylamino)-3-(4-fluorophenyl)-3-¹⁸O-hydroxy-2-deuteropropanoate; (-)-(432)



To a stirred solution of the optically active starting material (+)-*cis*-(**352**) (27 mg, 0.071 mmol, synthesised using (*R*)-(289)) in 1 mL dry acetonitrile was added *para*-toluene sulphonic acid (13 mg, 0.078 mmol), and ¹⁸O-H₂O (14.2 mg, 15 μL, 0.71 mmol). The resulting mixture was heated to 45 °C with stirring for 16 h. After this time, the reaction mixture was neutralised by addition of a saturated aqueous solution of sodium hydrogen carbonate. This was extracted with ethyl acetate, and the combined organic layers were washed with brine, dried with magnesium sulphate, filtered, and the solvent removed under reduced pressure. The crude material was purified *via* flash column chromatography (25 % diethyl ether in petroleum ether). A sample was submitted to chiral analytical HPLC analysis [Chiralpak OD, CO₂ / methanol 5% - 50% over 9 min, 1 mL / min, 3.42 min (1st peak), 3.73 min (2nd peak), 85 % *e.e.*]. The title product (-)-(432) was a slight brown oil afforded in a 43 % yield (12.4 mg, 0.031 mmol). ¹H-NMR (CDCl₃, 300 MHz) δ 7.49-7.31 (m, 2H, ArH), 7.09-6.99 (m, 2H, ArH), 6.96 (dd, 1H, *J* 7.9, 1.4 Hz, ArH), 6.87 (td, 1H, *J* 7.9, 7.7, 1.4 Hz, ArH), 6.64 (td, 1H, *J* 7.9, 7.7, 1.5 Hz, ArH), 6.52 (dd, 1H, *J* 7.9, 1.5 Hz, ArH). 4.94 (s, 1H, β-CH), 1.40 (s, 9H, C(CH₃)₃), 1.29 (s, 9H, C(CH₃)₃); ¹³C-NMR (CDCl₃, 75 MHz) 171.1, 143.5, 141.2, 135.7, 128.5, 128.4, 123.6, 121.9, 117.9, 115.3, 115.0, 111.9, 82.5, 79.8, 73.8, 28.9, 27.7 ppm [α]_D²² -23.3 (c 0.5 CHCl₃); FT-IR (thin film, cm⁻¹): 2977, 2934, 1726, 1601, 1509, 1368, 1392, 1255, 1157; MS (EI)⁺: *m/z* 407.1 [M+H]⁺, 429.2 [M+Na]⁺; HRMS: exact mass calculated for [C₂₃H₃₀DFNO₃¹⁸O]⁺ requires *m/z* 407.2337, found *m/z* 407.2333.

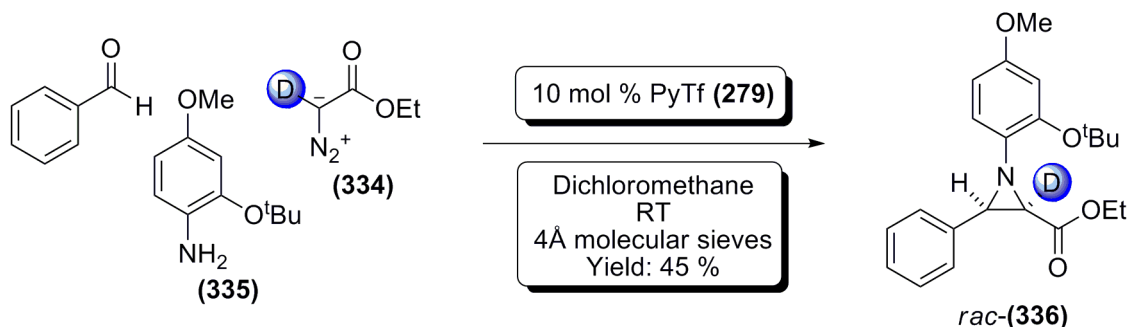
Synthesis of *tert*-butyl 2-(2-*tert*-butoxyphenylamino)-3-(4-bromophenyl)-3-¹⁸O-hydroxy-2-deuteropropanoate; (+)-(433)



To a stirred solution of the optically active starting material (-)-*cis*-(**350**) (37 mg, 0.083 mmol, synthesised using (*S*)-(**289**)) in 1 mL dry acetonitrile was added *para*-toluene sulphonic acid (20 mg, 0.083 mmol), and ¹⁸O-H₂O (16.6 mg, 17 μL, 0.83 mmol). The resulting mixture was heated to 45 °C with stirring for 16 h. After this time, the reaction mixture was neutralised by addition of a saturated aqueous solution of sodium hydrogen carbonate. This was extracted with ethyl acetate, and the combined organic layers were washed with brine, dried with magnesium sulphate, filtered, and the solvent removed under reduced pressure. The crude material was purified *via* flash column chromatography (25 % diethyl ether in petroleum ether). A sample was submitted to chiral analytical HPLC analysis [Chiralpak AD, CO₂ / methanol 5% - 50% over 9 min, 1 mL / min, 4.12 min (1st peak), 4.43 min (2nd peak), 95 % *e.e.*]. The title product (+)-(**433**) was a slight brown oil afforded in a 72 % yield (28 mg, 0.060 mmol). ¹H-NMR (CDCl₃, 300 MHz) δ 7.41 (d, 2H, *J* 8.5 Hz, ArH), 7.23 (d, 2H, *J* 8.5 Hz, ArH), 6.89 (d, 1H, *J* 7.9 Hz, ArH), 6.79 (t, 1H, *J* 7.7, 7.7 Hz, ArH), 6.58 (t, 1H, *J* 7.7, 7.7 Hz, ArH), 6.43 (d, 1H, *J* 7.9 Hz, ArH), 4.87 (s, 1H, β-CH), 1.33 (s, 9H, C(CH₃)₃), 1.24 (s, 9H, C(CH₃)₃); ¹³C-NMR (CDCl₃, 75 MHz) 171.1, 153.2, 143.6, 141.2, 139.1, 131.5, 128.6, 123.7, 122.1, 118.1, 112.1, 82.9, 80.0, 73.9, 29.2, 28.1 ppm; [α]_D²² 24.8 (c 0.8 CHCl₃); FT-IR (thin film, cm⁻¹): 2978, 1726, 1599, 1508, 1488, 1431, 1392, 1254, 1157; MS (EI)⁺: *m/z* 467.1 [M+H]⁺, 489.2 [M+Na]⁺; HRMS (EI)⁺: exact mass calculated for [C₂₃H₃₀DBrNO₃¹⁸O]⁺ requires *m/z* 467.1524, found *m/z* 467.1536.

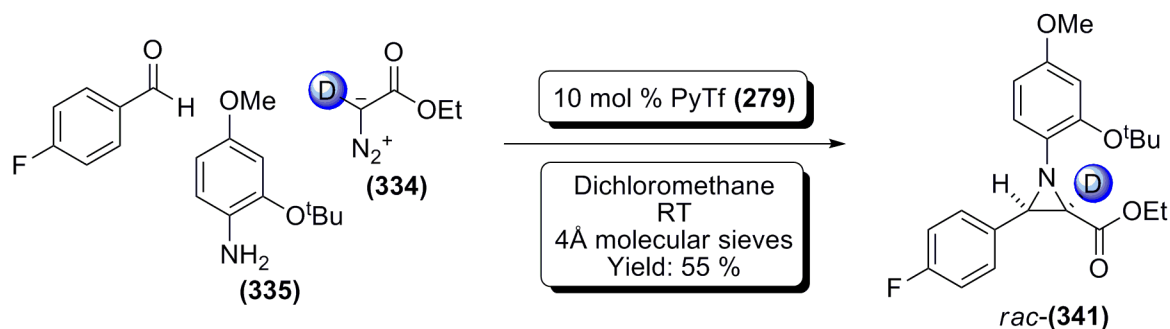
9.8: Synthesis of C2-deutero aziridines *rac*-(336), and *rac*-(341) to *rac*-(344)

Racemic synthesis of ethyl 1-(2-*tert*-butoxy-4-methoxyphenyl)-3-phenyl-2-deuteroaziridine-2-carboxylate; *rac*-(336)



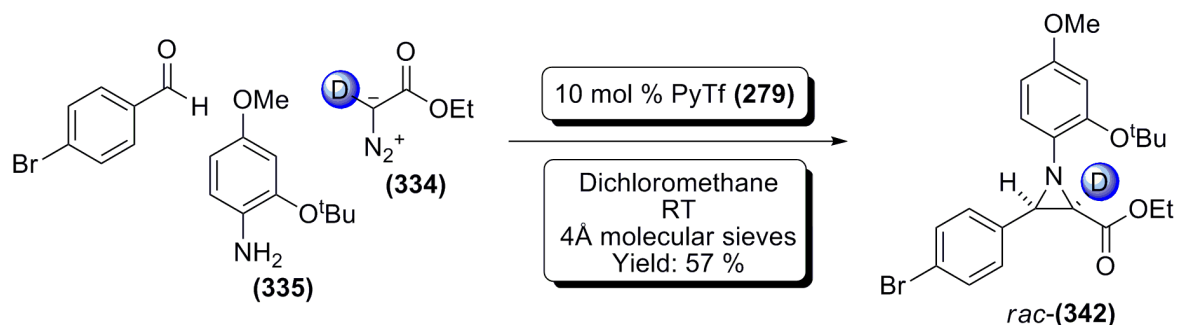
Benzaldehyde (27 μ L, 0.26 mmol), 2-*tert*-butoxy-4-methoxy aniline (335) (51 mg, 0.26 mmol), and pyridinium triflate (279) (6 mg, 0.026 mmol, 10%) were added to a flame dried 2 mL vial under nitrogen. 1 mL dichloromethane was added, followed by ~40 mg of freshly powdered 4 Å molecular sieves, and the vial was sealed with a PTFE crimp cap. After 30 minutes, >95 % deuterated ethyl diazoacetate (334) (32.6 mg, 30 μ L, 0.286 mmol) was added *via* syringe, and the reaction mixture was stirred at RT for 16 h. The reaction mixture was filtered through a short plug of silica, eluting with diethyl ether. The solvents were removed under reduced pressure, and the residue was purified *via* flash column chromatography (20 % diethyl ether in petroleum ether). The desired product *rac*-(336) was afforded as a colourless oil in a 45 % yield (43 mg, 0.117 mmol). $^1\text{H-NMR}$ (CDCl_3 , 400 MHz) δ 7.49 - 7.43 (m, 2H, ArH), 7.30 - 7.17 (m, 3H, ArH), 6.80 (d, 1H, J 8.7 Hz, ArH), 6.55 (d, 1H J 2.7 Hz, ArH), 6.42 (dd, 1H, J 8.7, 2.7 Hz), 4.03 - 3.85 (m, 2H, OCH_2), 3.68 (s, 3H, OCH_3), 3.41 (s, 1H, C3-H), 1.29 (s, 9H, $\text{C}(\text{CH}_3)_3$), 0.96 (t, 3H, J 7.1, 7.1 Hz, CH_3); $^{13}\text{C-NMR}$ (CDCl_3 , 75 MHz) 168.4, 155.8, 149.0, 139.8, 135.3, 128.2, 128.0, 127.8, 120.9, 109.4, 107.0, 80.6, 60.9, 55.7, 48.2, 28.8. 14.2 ppm; FT-IR (thin film, cm^{-1}): 2977, 2360, 1747, 1721, 1608, 1582, 1498, 1391, 1367, 1267, 1220; MS (EI) $^+$: m/z 371.1 $[\text{M}+\text{H}]^+$, 393.1 $[\text{M}+\text{Na}]^+$.

Racemic synthesis of ethyl 1-(2-*tert*-butoxy-4-methoxyphenyl)-3-(4-fluorophenyl)-2-deuteroaziridine-2-carboxylate; *rac*-(341**)**



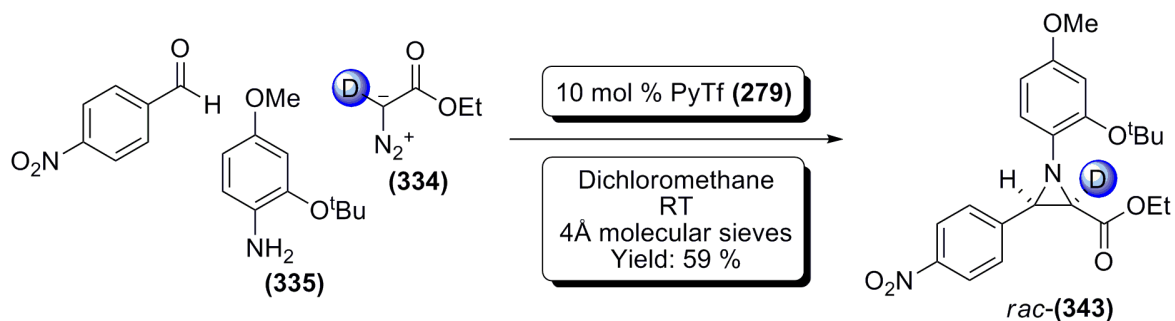
4-fluorobenzaldehyde (28 μL , 0.26 mmol), 2-*tert*-butoxy-4-methoxy aniline (**335**) (51 mg, 0.26 mmol), and pyridinium triflate (**279**) (6 mg, 0.026 mmol, 10%) were added to a flame dried 2 mL vial under nitrogen. 1 mL DCM was added, followed by ~40 mg of freshly powdered 4Å molecular sieves, and the vial was sealed with a PTFE crimp cap. After 30 minutes, >95 % deuterated ethyl diazoacetate (**334**) (32.6 mg, 30 μL , 0.286 mmol) was added *via* syringe, and the reaction mixture was stirred at RT for 16 h. The reaction mixture was then filtered through a short plug of silica, eluting with diethyl ether. The solvents were removed under reduced pressure, and the residue was purified *via* flash column chromatography (20 % diethyl ether in petroleum ether). The desired product *rac*-(**341**) was afforded as a colourless oil in a 55 % yield (56 mg, 0.143 mmol). $^1\text{H-NMR}$ (CDCl_3 , 300 MHz) δ 7.55 – 7.47 (m, 2H, ArH), 7.01 (t, 2H J 8.7, 8.7 Hz, ArH), 6.84 (d, 1H, J 8.7 Hz, ArH), 6.61 (d, 1H, J 2.7 Hz, ArH), 6.49 (dd, 1H, J 8.7, 2.7 Hz, ArH), 4.11 – 3.95 (m, 2H, OCH_2), 3.75 (s, 3H, OCH_3), 3.44 (s, 1H, C3-H), 1.35 (s, 9H, $\text{C}(\text{CH}_3)_3$), 1.06 (t, 3H, J 7.1, 7.1 Hz, CH_3); $^{13}\text{C-NMR}$ (CDCl_3 , 75 MHz) 168.2, 155.8, 148.9, 139.4, 129.7, 129.6, 120.7, 114.9, 114.6, 109.2, 106.9, 80.3, 60.7, 55.4, 47.2, 28.5, 13.9 ppm; FT-IR (thin film, cm^{-1}): 2978, 2918, 2851, 1746, 1721, 1606, 1585, 1498, 1391, 1367; MS (EI) $^+$: m/z 389.1 $[\text{M}+\text{H}]^+$, 411.1 $[\text{M}+\text{Na}]^+$.

Racemic synthesis of ethyl 3-(4-bromophenyl)-1-(2-tert-butoxy-4-methoxyphenyl)-2-deuteroaziridine-2-carboxylate; *rac*-(342)



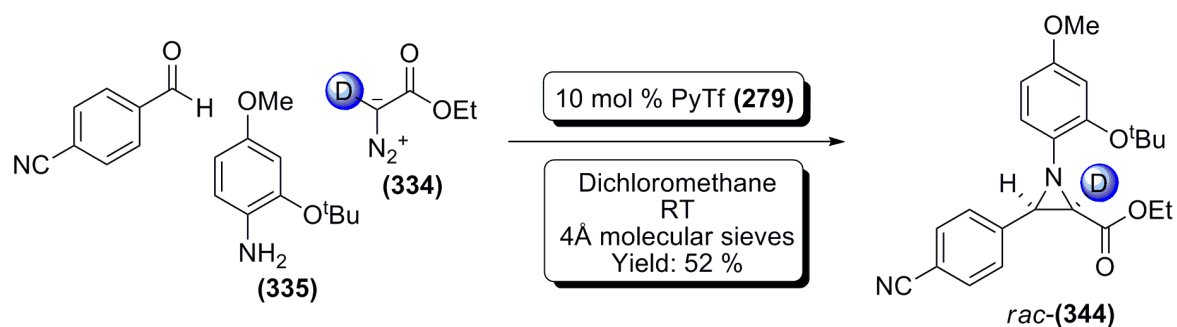
4-bromobenzaldehyde (48 mg, 0.26 mmol), 2-*tert*-butoxy-4-methoxy aniline (335) (51 mg, 0.26 mmol), and pyridinium triflate (279) (6 mg, 0.026 mmol, 10%) were added to a flame dried 2 mL vial under nitrogen. 1 mL DCM was added, followed by ~40 mg of freshly powdered 4Å molecular sieves, and the vial was sealed with a PTFE crimp cap. After 30 minutes, >95 % deuterated ethyl diazoacetate (334) (32.6 mg, 30 μ L, 0.286 mmol) was added *via* syringe, and the reaction mixture was stirred at RT for 16 h. The reaction mixture was then filtered through a short plug of silica, eluting with diethyl ether. The solvents were removed under reduced pressure, and the residue was purified *via* flash column chromatography (20 % diethyl ether in petroleum ether). The desired product *rac*-(342) was afforded as a slight yellow oil in a 57 % yield (66 mg, 0.148 mmol). The oil could be subsequently crystallised by treatment with 20 % diethyl ether in petroleum ether, yielding colourless plates. $^1\text{H-NMR}$ (CDCl_3 , 400 MHz) δ 7.42 – 7.31 (m, 4H, ArH), 6.76 (d, 1H, J 8.7 Hz, ArH), 6.54 (d, 1H, J 2.7 Hz, ArH), 6.42 (dd, 1H, J 8.7, 2.7 Hz, ArH), 4.06 – 3.88 (m, 2H, OCH_2), 3.68 (s, 3H, OCH_3), 3.34 (s, 1H, C3-H), 1.28 (s, 9H, $\text{C}(\text{CH}_3)_3$), 1.01 (t, 3H, J 7.1, 7.1 Hz, CH_3); $^{13}\text{C-NMR}$ (CDCl_3 , 75 MHz) 168.1, 155.9, 149.0, 139.4, 134.4, 131.1, 130.0, 121.8, 120.8, 109.4, 107.1, 80.6, 61.1, 55.7, 47.6, 28.9, 14.3 ppm; FT-IR (thin film, cm^{-1}): 2977, 2920, 2849, 1747, 1721, 1608, 1583, 1498, 1391, 1367; MS (EI) $^+$: m/z 449.1 $[\text{M}+\text{H}]^+$, 471.1 $[\text{M}+\text{Na}]^+$.

Racemic synthesis of ethyl 1-(2-*tert*-butoxy-4-methoxyphenyl)-3-(4-nitrophenyl)-2-deuteroaziridine-2-carboxylate; *rac*-(343**)**



4-nitrobenzaldehyde (39 mg, 0.26 mmol), 2-*tert*-butoxy-4-methoxy aniline (**335**) (51 mg, 0.26 mmol), and pyridinium triflate (**279**) (6 mg, 0.026 mmol, 10%) were added to a flame dried 2 mL vial under nitrogen. 1 mL DCM was added, followed by ~40 mg of freshly powdered 4Å molecular sieves, and the vial was sealed with a PTFE crimp cap. After 30 minutes, >95 % deuterated ethyl diazoacetate (**334**) (32.6 mg, 30 μ L, 0.286 mmol) was added *via* syringe, and the reaction mixture was stirred at RT for 16 h. The reaction mixture was then filtered through a short plug of silica, eluting with diethyl ether. The solvents were removed under reduced pressure, and the residue was purified *via* flash column chromatography (20 % diethyl ether in petroleum ether). The desired product *rac*-(**343**) was afforded as a yellow oil in a 59 % yield (64 mg, 0.153 mmol). $^1\text{H-NMR}$ (CDCl_3 , 300 MHz) δ 8.19 (d, 2H, J 8.8 Hz, ArH), 7.72 (d, 2H, J 8.6 Hz, ArH), 6.83 (d, 1H, J 8.6 Hz, ArH), 6.62 (d, 1H, J 2.7 Hz, ArH), 6.50 (dd, 1H, J 8.8, 2.7 Hz, ArH), 4.10 – 3.95 (m, 2H, OCH_2), 3.75 (s, 3H, OCH_3), 3.52 (s, 1H, C3-H), 1.33 (s, 9H, $\text{C}(\text{CH}_3)_3$), 1.07 (t, 3H, J 7.1, 7.1 Hz, CH_3); $^{13}\text{C-NMR}$ (CDCl_3 , 75 MHz) 166.4, 155.0, 147.8, 146.4, 141.7, 137.5, 128.0, 122.0, 119.5, 108.1, 105.8, 79.5, 60.1, 54.5, 46.2, 27.7, 13.1 ppm; FT-IR (thin film, cm^{-1}): 2978, 1742, 1605, 1523, 1368, 1345; MS (EI) $^+$: m/z 416.1 [$\text{M}+\text{H}$] $^+$, 438.1 [$\text{M}+\text{Na}$] $^+$.

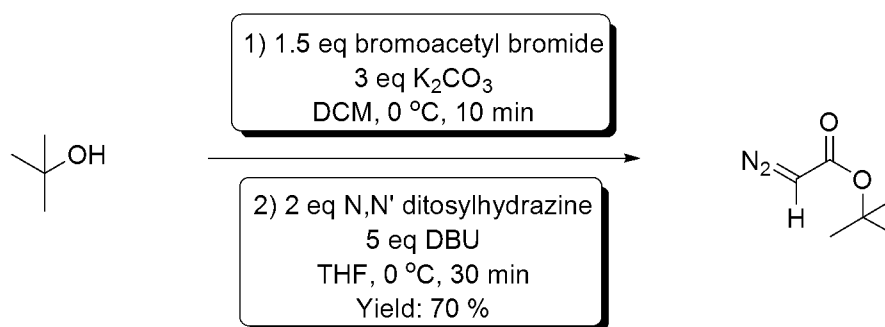
Racemic synthesis of ethyl 1-(2-*tert*-butoxy-4-methoxyphenyl)-3-(4-cyanophenyl)-2-deuteroaziridine-2-carboxylate; *rac*-(344**)**



4-cyanobenzaldehyde (34 mg, 0.26 mmol), 2-*tert*-butoxy-4-methoxy aniline (**335**) (51 mg, 0.26 mmol), and pyridinium triflate (**279**) (6 mg, 0.026 mmol, 10%) were added to a flame dried 2 mL vial under nitrogen. 1 mL DCM was added, followed by ~40 mg of freshly powdered 4Å molecular sieves, and the vial was sealed with a PTFE crimp cap. After 30 minutes, >95 % deuterated ethyl diazoacetate (**334**) (32.6 mg, 30 μ L, 0.286 mmol) was added *via* syringe, and the reaction mixture was stirred at RT for 16 h. The reaction mixture was then filtered through a short plug of silica, eluting with diethyl ether. The solvents were removed under reduced pressure, and the residue was purified *via* flash column chromatography (20 % diethyl ether in petroleum ether). The desired product *rac*-(**344**) was afforded as a slight green oil in a 52 % yield (53 mg, 0.135 mmol). $^1\text{H-NMR}$ (CDCl_3 , 300 MHz) δ 7.65 – 7.53 (m, 4H, ArH), 6.78 (d, 1H, J 8.7 Hz, ArH), 6.58 (d, 1H, J 2.7 Hz, ArH), 6.45 (dd, 1H, J 8.7, 2.7 Hz, ArH), 4.06 – 3.88 (m, 2H, OCH_2), 3.70 (s, 3H, OCH_3), 3.43 (s, 1H, C3-H), 1.29 (s, 9H, $\text{C}(\text{CH}_3)_3$), 1.02 (t, 3H, J 7.1, 7.1 Hz, CH_3); $^{13}\text{C-NMR}$ (CDCl_3 , 75 MHz) 167.7, 156.1, 148.9, 140.9, 138.8, 131.8, 129.0, 120.7, 119.1, 111.5, 109.3, 107.0, 80.6, 61.2, 55.7, 47.5, 28.8, 14.2 ppm; FT-IR (thin film, cm^{-1}): 2978, 2227, 1746, 1609, 1584, 1500, 1391, 1367, 1268, 1222, 1156, 1124; MS (EI) $^+$: m/z 418.1 $[\text{M}+\text{Na}]^+$.

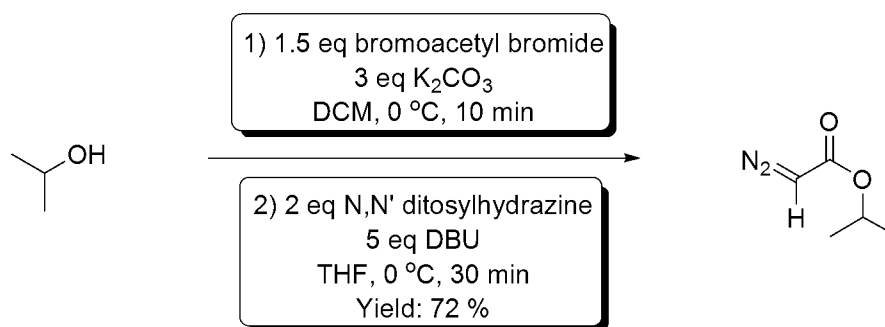
9.9: Synthesis of Starting Materials

Synthesis of *tert*-butyl diazoacetate (**280**)³⁰⁰



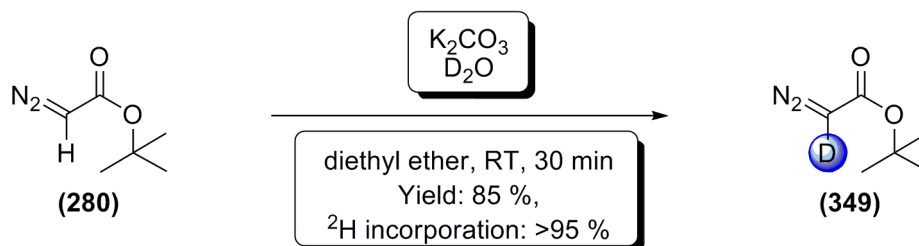
To a 250 mL flame dried round bottom flask, equipped with a magnetic stirrer bar, under N₂ was added potassium carbonate (14.4 g, 105 mmol). *tert*-butanol (2 mL, 35 mmol), and DCM (120 mL), were added *via* syringe, and the reaction was cooled to 0 °C with stirring. After 5 minutes, bromoacetyl bromide (4.5 mL, 52 mmol) was added dropwise over 5 minutes *via* syringe, and the reaction was stirred at 0 °C for a further 10 minutes. After this time, the reaction was quenched by the addition of 40 mL water, and extracted with dichloromethane (80 mL). The combined organic layers were washed with brine, dried with magnesium sulphate, filtered, and the solvent removed carefully under reduced pressure. The resulting crude material was redissolved in 120 mL dry THF, and *N,N'*-ditosylhydrazine (23.8 g, 70 mmol) was added. The reaction was cooled to 0 °C, and allowed to stir for 5 minutes before the dropwise addition of DBU (26.1 mL, 175 mmol) *via* syringe. After stirring for a further 30 minutes, the reaction was quenched by the addition of 60 mL saturated aqueous sodium hydrogen carbonate and extracted with 180 mL diethyl ether. The combined organic layers were washed with brine, dried with magnesium sulphate, filtered and the solvent carefully removed under reduced pressure. The resulting dark yellow liquid was purified *via* flash column chromatography (20 % diethyl ether in petroleum ether). The production of the desired product (**280**) was afforded as a yellow liquid in 70 % yield (3.45 g, 24.5 mmol). ¹H-NMR (CDCl₃, 300 MHz) δ 4.61 (s, 1H, CH), 1.47 (s, 9H, C(CH₃)₃); ¹³C-NMR (CDCl₃, 75 MHz) 81.6, 46.1, 21.5 ppm; FT-IR (thin film, cm⁻¹): 2924, 2853, 2106, 1658, 1458, 1370, 1258; HRMS (HEIP)⁺: exact mass calculated for [C₆H₁₀N₂O₂]⁺ requires *m/z* 142.0737, found *m/z* 142.0736.

Synthesis of *iso*-propyl diazoacetate (**320**)³⁰¹



To a 100 mL flame dried round bottom flask, equipped with a magnetic stirrer bar, under nitrogen was added potassium carbonate (5.35 g, 39 mmol). *iso*-propanol (1 mL, 13 mmol), and DCM (60 mL), were added *via* syringe, and the reaction was cooled to 0 °C with stirring. After 5 minutes, bromoacetyl bromide (1.7 mL, 19.5 mmol) was added dropwise over 5 minutes *via* syringe, and the reaction was stirred at 0 °C for a further 10 minutes. After this time, the reaction was quenched by the addition of 20 mL water, and extracted with DCM (40 mL). The combined organic layers were washed with brine, dried with magnesium sulphate, filtered, and the solvent removed carefully under reduced pressure. The resulting crude material was redissolved in 60 mL dry THF, and *N,N'*-ditosylhydrazine (8.8 g, 26 mmol) was added. The reaction was cooled to 0 °C, and allowed to stir for 5 minutes before the dropwise addition of DBU (9.7 mL, 65 mmol) *via* syringe. After stirring for a further 30 minutes, the reaction was quenched by the addition of 30 mL saturated aqueous sodium hydrogen carbonate and extracted with 90 mL diethyl ether. The combined organic layers were washed with brine, dried with magnesium sulphate, filtered and the solvent carefully removed under reduced pressure. The resulting dark yellow liquid was purified *via* flash column chromatography (20 % diethyl ether in petroleum ether). The desired product (**320**) was afforded as a yellow liquid in 72 % yield (1.19 g, 9.36 mmol). ¹H-NMR (CDCl₃, 300 MHz) δ 5.04 (septet, 1H, *J* 6.3 Hz, CH(CH₃)₂), 4.66 (s, 1H, CH), 1.20 (d, 6H, *J* 6.3 Hz, CH(CH₃)₂); ¹³C-NMR (CDCl₃, 75 MHz) 68.3, 46.1, 21.8 ppm; FT-IR (thin film, cm⁻¹): 2983, 2939, 2104, 1685, 1467, 1375, 1341, 1249, 1193, 1103, 991, 744; HRMS (HEIP)⁺: exact mass calculated for [C₅H₈N₂O₂]⁺ requires *m/z* 128.0580, found *m/z* 128.0580.

Synthesis of deuterated *tert*-butyl diazoacetate (**349**)



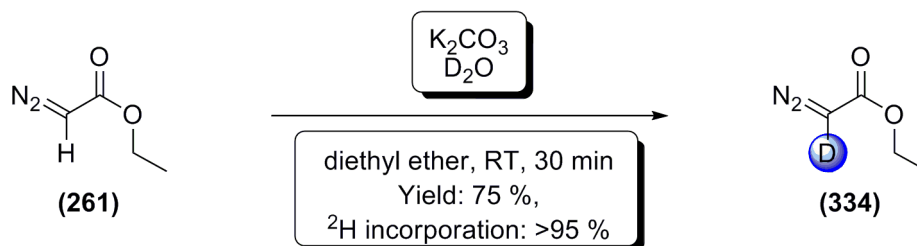
A 50 mL flame dried round bottom flask under nitrogen was charged with a stirred solution of *tert*-butyl diazoacetate (**280**) (5 mL, 36.3 mmol) in 5 mL dry diethyl ether, with stirring. Potassium carbonate (750 mg, 5.4 mmol) was added, followed by 10 mL deuterium oxide *via* syringe. The resulting biphasic mixture was stirred vigorously under nitrogen for 30 minutes at room temperature. After this time, the mixture was transferred to a flame dried separating funnel under nitrogen, and the aqueous layer was separated. The organic layer was returned to a flame dried round bottom flask under nitrogen, and further potassium carbonate (600 mg, 4.3 mmol), and deuterium oxide (7 mL), were added. The mixture was stirred vigorously for 30 minutes. At this point the organic layer was separated, and the aqueous layer extracted with 20 mL diethyl ether. The combined organic layers were washed with brine, dried with magnesium sulphate, filtered, and the solvent removed with care under reduced pressure. The desired product (**349**) was afforded as a yellow liquid in 85 % yield (4.38 g, 30.86 mmol). 1H -NMR ($CDCl_3$, 300 MHz) δ 1.47 (s, 9H, $C(CH_3)_3$); ^{13}C -NMR ($CDCl_3$, 75 MHz) 81.6, 21.5 ppm; FT-IR (thin film, cm^{-1}): 2924, 2853, 2106, 1658, 1458, 1370, 1258; MS (EI) $^+$: m/z 143.1 [M+H] $^+$.

Synthesis of deuterated *iso*-propyl diazoacetate (**364**)



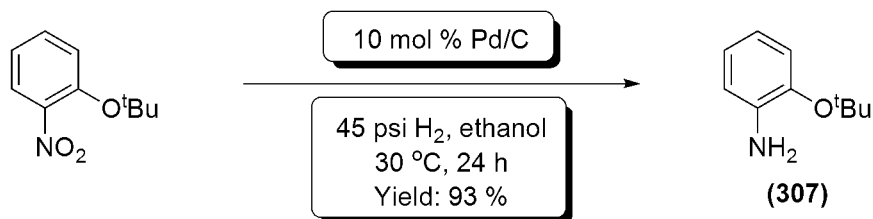
A 25 mL flame dried round bottom flask under N₂ was charged with a stirred solution of *iso*-propyl diazoacetate (**320**) (1 mL, 8.01 mmol) in 5 mL dry diethyl ether, with stirring. Potassium carbonate (300 mg, 2.17 mmol) was added, followed by deuterium oxide (3 mL) *via* syringe. The resulting biphasic mixture was stirred vigorously under N₂ for 30 minutes at room temperature. After this time, the mixture was transferred to a flame dried separating funnel under N₂, and the aqueous layer was separated. The organic layer was returned to a flame dried round bottom flask under N₂, and further potassium carbonate (300 mg, 2.17 mmol), and deuterium oxide (3 mL), were added. The mixture was stirred vigorously for 30 minutes. At this point the organic layer was separated, and the aqueous layer extracted with 10 mL diethyl ether. The combined organic layers were washed with brine, dried with magnesium sulphate, filtered, and the solvent removed with care under reduced pressure. The desired product (**364**) was afforded as a yellow liquid in 83 % yield (0.858 g, 6.64 mmol). ¹H-NMR (CDCl₃, 300 MHz) δ 5.04 (septet, 1H, *J* 6.3 Hz, CH(CH₃)₂), 1.20 (d, 6H, *J* 6.3 Hz, CH(CH₃)₂); ¹³C-NMR (CDCl₃, 75 MHz) 68.3, 22.0 ppm; FT-IR (thin film, cm⁻¹): 2983, 2939, 2879, 2109, 1732, 1658, 1458, 1455, 1374, 1350, 1306; MS (EI)⁺: *m/z* 130.1 [M+H]⁺.

Synthesis of deuterated ethyl diazoacetate (**334**)³⁰²



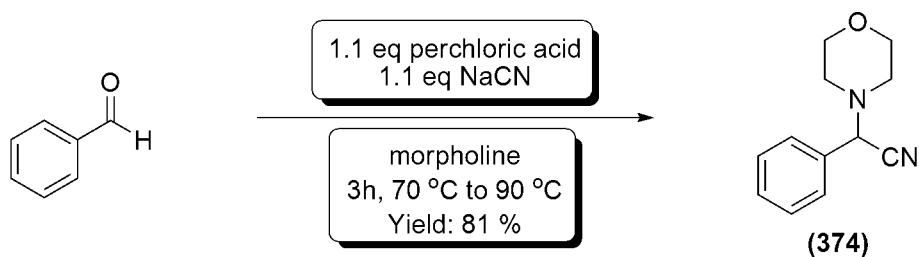
A 25 mL flame dried round bottom flask under N_2 was charged with a stirred solution of ethyl diazoacetate (**261**) (3 mL, 27 mmol) in 5 mL dry diethyl ether, with stirring. Potassium carbonate (400 mg, 2.9 mmol) was added, followed by 6 mL deuterium oxide *via* syringe. The resulting biphasic mixture was stirred vigorously under N_2 for 30 minutes at room temperature. After this time, the mixture was transferred to a flame dried separating funnel under N_2 , and the aqueous layer was separated. The organic layer was returned to a flame dried round bottom flask under N_2 , and further potassium carbonate (400 mg, 2.9 mmol), and deuterium oxide (6 mL), were added. The mixture was stirred vigorously for 30 minutes. At this point the organic layer was separated, and the aqueous layer extracted with 20 mL diethyl ether. The combined organic layers were washed with brine, dried with magnesium sulphate, filtered, and the solvent removed with care under reduced pressure. The desired product (**334**) was afforded as a yellow liquid in 75 % yield (2.33 g, 20.25 mmol). 1H -NMR ($CDCl_3$, 300 MHz) δ 4.22 (q, 2H, J 7.1, 7.1, 7.1 Hz, OCH_2), 1.30 (t, 3H, J 7.1, 7.1 Hz, CH_3); ^{13}C -NMR ($CDCl_3$, 75 MHz) 60.7, 14.2 ppm; FT-IR (thin film, cm^{-1}): 2112, 1735, 1700, 1370, 1259, 1180, 1096, 1026, 749; MS (EI)⁺ m/z : 114.9 $[M]^+$.

Synthesis of 2-*tert*-butoxy aniline (**307**)²⁶⁸



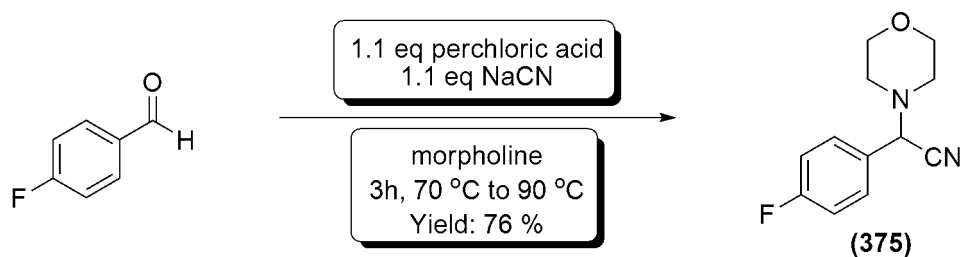
2-*tert*-butoxy nitrobenzene (5 g, 25.6 mmol) was dissolved in 20 mL ethanol and split between five 5 mL Biotage Endeavour catalyst screening vials. Palladium on carbon (10 %, 0.54 g) was added, and the reaction vials were heated to 30 °C, under 45 psi H₂, for 24 h in a Biotage Endeavour[®] catalyst screening system. After this time, the reaction was deemed complete by monitoring the uptake of H₂. The resulting suspensions were filtered through Celite[®], eluting with diethyl ether. Removal of the solvent under reduced pressure afforded the desired product (**307**) as a dark red oil, which quickly darkened to black, in 93 % yield (3.91 g, 23.8 mmol). ¹H-NMR (CDCl₃, 300 MHz) δ 6.96 (dd, 1H, *J* 7.9, 1.4 Hz, ArH), 6.89 (dt, 1H, *J* 7.8, 7.8, 1.4 Hz, ArH), 6.74 (dd, 1H, *J* 7.8, 1.7 Hz, ArH), 6.66 (dt, 1H, *J* 7.9, 7.9, 1.7 Hz, ArH), 3.72 (br s, 2H, NH₂), 1.42 (s, 9H, C(CH₃)₃); ¹³C-NMR (CDCl₃, 75 MHz) 143.0, 141.2, 123.7, 122.9, 118.1, 115.8, 79.5, 28.9 ppm; FT-IR (thin film, cm⁻¹): 2976, 1610, 1499, 1456, 1390, 1366, 1219, 1162, 1034, 898, 765; MS (ED)⁺: *m/z* ; HRMS (ASAP)⁺: exact mass calculated for [C₁₀H₁₅NO]⁺ requires *m/z* 165.1148, found *m/z* 165.1148.

Synthesis of 2-morpholino-2-phenyl acetonitrile (**374**)²⁸⁵



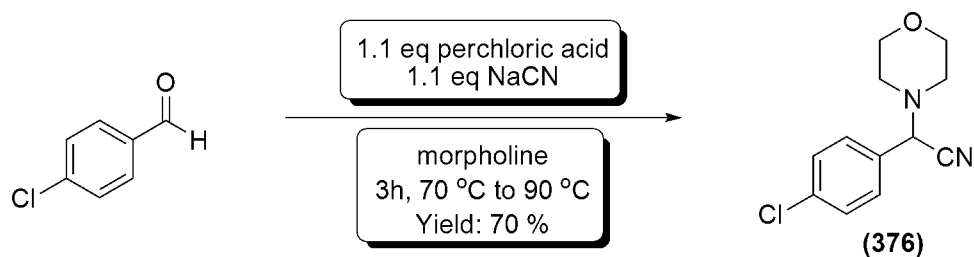
To a 250 mL round bottom flask equipped with a magnetic stirrer bar, containing 40 mL morpholine, was added perchloric acid (5.20 g, 4.5 mL, 51.8 mmol) dropwise over 5 minutes. After 5 minutes stirring, the resulting solution was heated to 70 °C. At this point, benzaldehyde (5.0 g, 4.8 mL, 47.1 mmol) dissolved in 40 mL morpholine was added dropwise with care, and the resulting solution was stirred for 2 h at 70 °C. Sodium cyanide (2.54 g, 51.8 mmol), dissolved in 15 mL water, was added slowly, and the reaction was heated to 90 °C for 1h. After this time, the reaction was allowed to cool slightly before pouring onto crushed ice. The resulting precipitate was collected by vacuum filtration, and recrystallised from hot ethanol. The desired product (**374**) was afforded as colourless crystals in 81 % yield (7.71 g, 38.15 mmol). ¹H-NMR (CDCl₃, 300 MHz) δ 7.61 – 7.47 (m, 2H, ArH), 7.47 – 7.32 (m, 3H, ArH), 4.82 (s, 1H, CH), 3.84 – 3.60 (m, 4H, CH₂OCH₂), 2.58 (t, 4H, *J* 4.6, 4.6 Hz, CH₂NCH₂); ¹³C-NMR (CDCl₃, 75 MHz) 132.5, 129.1, 128.9, 128.0, 115.2, 66.6, 62.3, 49.8 ppm; FT-IR (thin film, cm⁻¹): 1452, 1114, 906, 784; MS (EI)⁺: *m/z* ; HRMS (ASAP)⁺: exact mass calculated for [C₁₂H₁₅N₂O]⁺ requires *m/z* 203.1179, found *m/z* 203.1178.

Synthesis of 2-morpholino-2-(4-fluorophenyl) acetonitrile (**375**)³⁰³



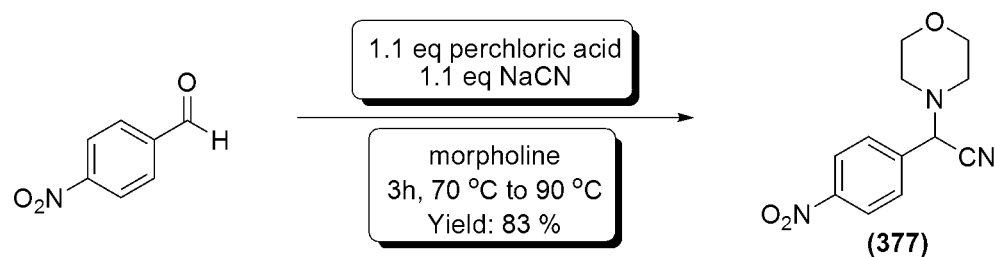
To a 250 mL round bottom flask equipped with a magnetic stirrer bar, containing 40 mL morpholine, was added perchloric acid (5.20 g, 4.5 mL, 51.8 mmol) dropwise over 5 minutes. After 5 minutes stirring, the resulting solution was heated to 70 °C. At this point, 4-fluorobenzaldehyde (5.84 g, 5.0 mL, 47.1 mmol) dissolved in 40 mL morpholine was added dropwise with care, and the resulting solution was stirred for 2 h at 70 °C. Sodium cyanide (2.54 g, 51.8 mmol), dissolved in 15 mL water, was added slowly, and the reaction was heated to 90 °C for 1h. After this time, the reaction was allowed to cool slightly before pouring onto crushed ice. The resulting precipitate was collected by vacuum filtration, and recrystallised from hot ethanol. The desired product (**375**) was afforded as colourless crystals in 76 % yield (7.88 g, 35.80 mmol). ¹H-NMR (CDCl₃, 300 MHz) δ 7.50 (dd, 2H, *J* 5.2, 8.3 Hz, ArH), 7.08 (t, 2H, *J* 8.5, 8.7 Hz, ArH), 4.78 (s, 1H, CH), 3.82 – 3.56 (m, 4H, CH₂OCH₂), 2.67 – 2.43 (m, 4H, CH₂NCH₂); ¹³C-NMR (CDCl₃, 75 MHz) 164.7, 161.4, 129.9, 129.8, 128.4, 128.4, 116.0, 115.7, 115.0, 66.5, 61.6, 49.8 ppm; FT-IR (thin film, cm⁻¹): 1607, 1508, 1453, 1294, 1114, 1005, 918, 728; MS (EI)⁺: *m/z* ; HRMS (HNESP)⁺: exact mass calculated for [C₁₂H₁₄FN₂O]⁺ requires *m/z* 221.1085, found *m/z* 221.1086.

Synthesis of 2-morpholino-2-(4-chlorophenyl) acetonitrile (**376**)³⁰³



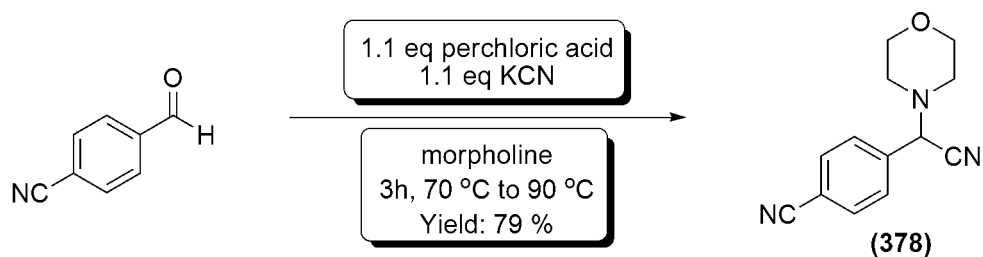
To a 250 mL round bottom flask equipped with a magnetic stirrer bar, containing 20 mL morpholine, was added perchloric acid (5.20 g, 4.5 mL, 51.8 mmol) dropwise over 5 minutes. After 5 minutes stirring, the resulting solution was heated to 70 °C. At this point, 4-chlorobenzaldehyde (6.6 g, 47.1 mmol) dissolved in 20 mL morpholine was added dropwise with care, and the resulting solution was stirred for 2 h at 70 °C. Sodium cyanide (2.54 g, 51.8 mmol), dissolved in 15 mL water, was added slowly, and the reaction was heated to 90 °C for 1h. After this time, the reaction was allowed to cool slightly before pouring onto crushed ice. The resulting precipitate was collected by vacuum filtration, and recrystallised from hot ethanol. The desired product (**376**) was afforded as slight green crystals in 70 % yield (7.78 g, 32.97 mmol). ¹H-NMR (CDCl₃, 300 MHz) δ 7.48 (d, 2H, *J* 8.3 Hz, ArH), 7.38 (d, 2H, *J* 8.3, ArH), 4.78 (s, 1H, CH), 3.80 – 3.60 (m, 4H, CH₂OCH₂), 2.64 – 2.46 (m, 4H, CH₂NCH₂); ¹³C-NMR (CDCl₃, 75 MHz) 135.2, 131.1, 129.4, 129.1, 114.8, 66.5, 61.7, 49.8 ppm; FT-IR (thin film, cm⁻¹): 1491, 1454, 1292, 1114, 1092, 1072, 1005, 908, 724; MS (EI)⁺: *m/z* ; HRMS (ASAP)⁺: exact mass calculated for [C₁₂H₁₃ClN₂O]⁺ requires *m/z* 237.0789, found *m/z* 237.0790.

Synthesis of 2-morpholino-2-(4-nitrophenyl) acetonitrile (**377**)²⁸⁵



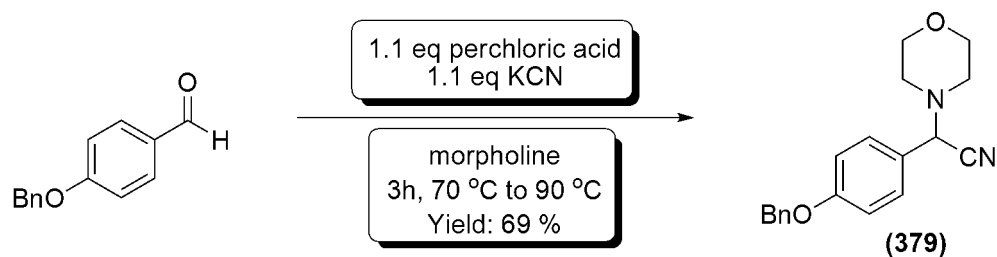
To a 250 mL round bottom flask equipped with a magnetic stirrer bar, containing 5 mL morpholine, was added perchloric acid (2.19 g, 1.9 mL, 21.78 mmol) dropwise over 5 minutes. After 5 minutes stirring, the resulting solution was heated to 70 °C. At this point, 4-nitrobenzaldehyde (3 g, 19.8 mmol) dissolved in 25 mL morpholine was added dropwise with care, and the resulting solution was stirred for 2 h at 70 °C. Sodium cyanide (1.06 g, 21.78 mmol), dissolved in 10 mL water, was added slowly, and the reaction was heated to 90 °C for 1h. After this time, the reaction was allowed to cool slightly before pouring onto crushed ice. The resulting precipitate was collected by vacuum filtration, and recrystallised from hot ethanol. The desired product (**377**) was afforded as orange crystals in 83 % yield (4.06 g, 16.43 mmol). ¹H-NMR (CDCl₃, 300 MHz) δ 8.23 (d, 2H, *J* 8.8 Hz, ArH), 7.74 (d, 2H, *J* 8.8 Hz, ArH), 4.89 (s, 1H, CH), 3.81 – 3.59 (m, 4H, CH₂OCH₂), 2.68 – 2.42 (m, 4H, CH₂NCH₂); ¹³C-NMR (CDCl₃, 75 MHz) 148.5, 139.7, 129.0, 124.1, 114.2, 66.4, 61.7, 49.9 ppm; FT-IR (thin film, cm⁻¹): 1607, 1520, 1454, 1345, 1322, 1294, 1112, 1006, 865, 854, 738, 707; MS (EI)⁺: *m/z* ; HRMS (ASAP)⁺: exact mass calculated for [C₁₂H₁₄N₃O₃]⁺ requires *m/z* 248.1030, found *m/z* 248.1030.

Synthesis of 2-morpholino-2-(4-cyanophenyl) acetonitrile (**378**)³⁰³



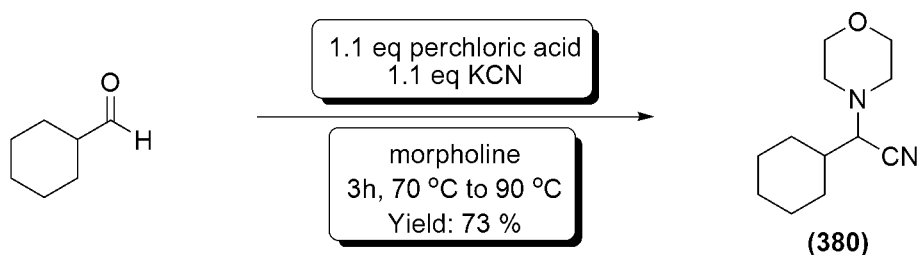
To a 250 mL round bottom flask equipped with a magnetic stirrer bar, containing 5 mL morpholine, was added perchloric acid (1.27 g, 1.1 mL, 12.6 mmol) dropwise over 5 minutes. After 5 minutes stirring, the resulting solution was heated to 70 °C. At this point, 4-cyanobenzaldehyde (1.5 g, 11.4 mmol) dissolved in 25 mL morpholine was added dropwise with care, and the resulting solution was stirred for 2 h at 70 °C. Potassium cyanide (820 mg, 12.6 mmol), dissolved in 5 mL water, was added slowly, and the reaction was heated to 90 °C for 1h. After this time, the reaction was allowed to cool slightly before pouring onto crushed ice. The resulting precipitate was collected by vacuum filtration, and recrystallised from hot ethanol. The desired product (**378**) was afforded as colourless crystals in 79 % yield (2.04 g, 9.01 mmol). ¹H-NMR (CDCl₃, 300 MHz) δ 7.80 – 7.70 (m, 4H, ArH), 4.87 (s, 1H, CH), 3.80 – 3.62 (m, 4H, CH₂OCH₂), 2.65 – 2.48 (m, 4H, CH₂NCH₂); ¹³C-NMR (CDCl₃, 75 MHz) 137.8, 132.7, 128.7, 118.1, 114.2, 113.3, 66.5, 62.0, 49.9 ppm; FT-IR (thin film, cm⁻¹): 2230, 1610, 1504, 1412, 1294, 1113, 1006; MS (EI)⁺: *m/z* ; HRMS (HNESP)⁺: exact mass calculated for [C₁₃H₁₃N₃ONa]⁺ requires *m/z* 250.0951, found *m/z* 250.0955.

Synthesis of 2-morpholino-2-(4-benzyloxyphenyl) acetonitrile (**379**)



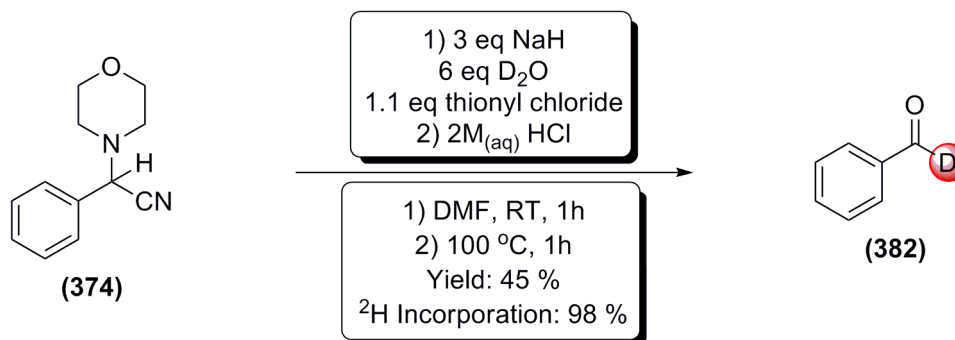
To a 250 mL round bottom flask equipped with a magnetic stirrer bar, containing 5 mL morpholine, was added perchloric acid (1.03 g, 0.9 mL, 10.3 mmol) dropwise over 5 minutes. After 5 minutes stirring, the resulting solution was heated to 70 °C. At this point, 4-benzyloxybenzaldehyde (2 g, 9.42 mmol) dissolved in 15 mL morpholine was added dropwise with care, and the resulting solution was stirred for 2 h at 70 °C. Potassium cyanide (675 mg, 10.37 mmol), dissolved in 5 mL water, was added slowly, and the reaction was heated to 90 °C for 1h. After this time, the reaction was allowed to cool slightly before pouring onto crushed ice. The resulting precipitate was collected by vacuum filtration, and recrystallised from hot ethanol. The desired product (**379**) was afforded as colourless crystals in 69 % yield (2.01 g, 6.50 mmol). $^1\text{H-NMR}$ (CDCl_3 , 300 MHz) δ 7.56 – 7.28 (m, 7H, ArH), 7.00 (d, 2H, J 9.2 Hz, ArH), 5.08 (s, 2H, CH_2), 4.75 (s, 1H, CH), 3.91 – 3.49 (m, 4H, CH_2OCH_2), 2.77 – 2.38 (m, 4H, CH_2NCH_2); $^{13}\text{C-NMR}$ (CDCl_3 , 75 MHz) 159.4, 136.6, 129.4, 128.7, 128.2, 127.5, 124.8, 115.4, 115.1, 70.1, 66.6, 61.8, 49.8 ppm; FT-IR (thin film, cm^{-1}): 1610, 1584, 1509, 1454, 1244, 1176, 1115, 1004, 865, 738; MS (EI) $^+$: m/z ; HRMS (ASAP) $^+$: exact mass calculated for $[\text{C}_{19}\text{H}_{21}\text{N}_2\text{O}_2]^+$ requires m/z 309.1525, found m/z 309.1602.

Synthesis of 2-morpholino-2-cyclohexyl acetonitrile (**380**)³⁰⁴



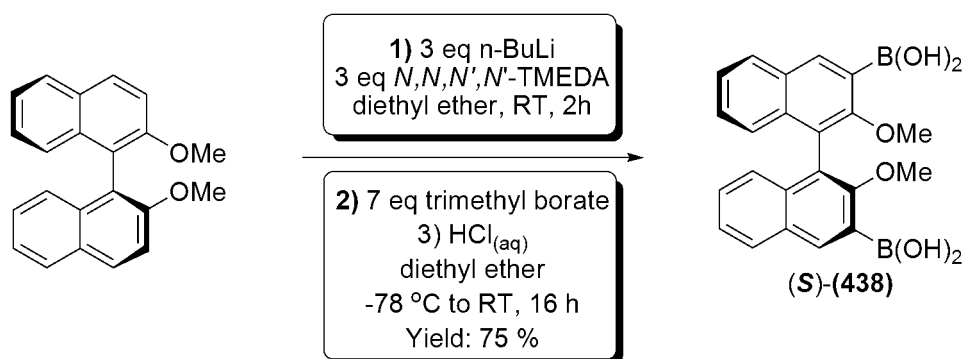
To a 250 mL round bottom flask equipped with a magnetic stirrer bar, containing 5 mL morpholine, was added perchloric acid (1.48 g, 1.3 mL, 14.7 mmol) dropwise over 5 minutes. After 5 minutes stirring, the resulting solution was heated to 70 °C. At this point, cyclohexanecarbaldehyde (1.49 g, 1.6 mL, 13.3 mmol) dissolved in 10 mL morpholine was added dropwise with care, and the resulting solution was stirred for 2 h at 70 °C. Potassium cyanide (957 mg, 14.7 mmol), dissolved in 5 mL water, was added slowly, and the reaction was heated to 90 °C for 1h. After this time, the reaction was allowed to cool slightly before pouring onto crushed ice. The resulting precipitate was collected by vacuum filtration, and recrystallised from hot ethanol. The desired product (**380**) was afforded as colourless crystals in 73 % yield (2.02 g, 9.71 mmol). ¹H-NMR (CDCl₃, 300 MHz) δ 3.80 – 3.58 (m, 4H, CH₂OCH₂), 3.07 (d, 1H, *J* 10.7 Hz, CH), 2.68 – 2.69 (m, 4H, CH₂NCH₂), 1.96 (d br, 2H, *J* 13.2 Hz, CH₂), 1.83 – 1.54 (m, 4H, 2 CH₂), 1.37 – 0.73 (m, 5H, 2 CH₂, CH); ¹³C-NMR (CDCl₃, 75 MHz) 116.3, 66.6, 64.3, 50.0, 37.0, 30.5, 29.6, 26.1, 25.4, 25.3 ppm; FT-IR (thin film, cm⁻¹): 1457, 1332, 1294, 1259, 1111, 1009, 927, 862; MS (EI)⁺: *m/z* ; HRMS (HNESP)⁺: exact mass calculated for [C₁₂H₂₁N₂O]⁺ requires *m/z* 209.1648, found *m/z* 209.1648.

Synthesis of deuterated benzaldehyde (**382**)³⁰⁵



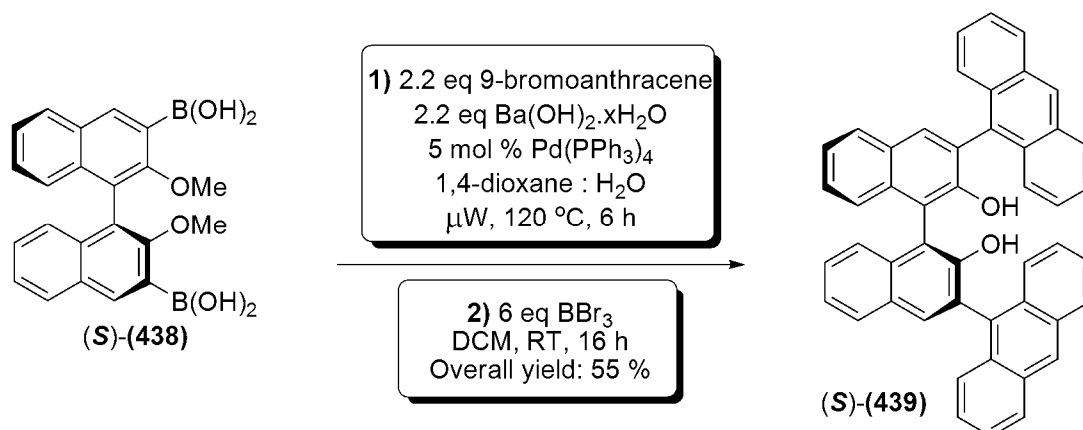
2-morpholino-2-phenyl acetonitrile (**374**) (2.5 g, 12.4 mmol) was dissolved in 10 mL dry DMF in a 50 mL flame dried round bottom flask under N₂. Sodium hydride (60 % in mineral oil, washed with hexane before use [1.48 g, 337 mmol]) was added to the reaction, suspended in 5 mL dry DMF. The resulting slurry was stirred vigorously under N₂ for 1 h. At this point, deuterium oxide (1.48 g, 1.4 mL, 74.4 mmol) was added *via* syringe, and the solution was stirred for 10 minutes. The reaction was cooled to 0 °C with an ice bath, before thionyl chloride (1.62 g, 0.9 mL, 13.6 mmol) was added slowly *via* syringe. After 10 minutes stirring, the reaction was allowed to warm to RT, at which point it was extracted with 90 mL diethyl ether. The combined organic layers were washed with 120 mL water, dried with magnesium sulphate, filtered and the solvent removed under reduced pressure. The resulting material was heated to reflux in 2 molar aqueous HCl (25 mL) for 1 h. After extraction with dichloromethane, drying with magnesium sulphate, filtration and removal of solvent, the crude material was purified by column chromatography (20 % diethyl ether in petroleum ether). The desired product (**382**) was afforded as a colourless liquid in 45 % yield (0.597 g, 5.58 mmol), and >90 % ²H incorporation (by ¹H-NMR). ¹H-NMR (CDCl₃, 300 MHz) δ 10.0 (s, residual, CHO), 7.87 (d, *J* 8.4 Hz, 2H, ArH), 7.62 (t, *J* 7.5 Hz, 1H, ArH), 7.51 (t, *J* 7.5 Hz, 2H, ArH); FT-IR (thin film, cm⁻¹): 1685; MS (EI)⁺: *m/z* 108.0 [M+H]⁺.

Synthesis of (*S*)-3,3'-bis(dihydroxyborane)-2,2'-dimethoxy-1,1'-dinaphthyl (**438**)^{268, 306}



To a flame dried 500 mL round bottom flask, charged with 200 mL anhydrous diethyl ether, was added *N,N,N',N'*-tetramethylethylenediamine (4.43 g, 5.8 mL, 38.2 mmol). *n*-butyl lithium (2.5M in hexanes [15.3 mL, 38.2 mmol]) was added with care *via* syringe, and the resulting mixture was stirred at RT for 30 minutes. At this point, (*S*)-2,2'-dimethoxy-1,1'-dinaphthyl (4 g, 12.7 mmol) was added quickly in one portion, taking care to minimise the exposure of the reaction to air. The reaction was then stirred for 3 h at RT. During this time the reaction darkened to a light brown colouration. The flask was then cooled to -78 °C using an acetone/CO₂ bath, and after 10 minutes at this temperature, trimethylborate (9.2 g, 10 mL, 89 mmol) was added at a constant rate *via* syringe over a period of 10 minutes. The reaction mixture was then allowed to warm to RT with stirring overnight, taking care not to disturb the bath or flask (as any perturbation of the reaction can lead to the formation of a colloid which prevents the reaction from stirring). After cooling the reaction to 0 °C with an ice bath, 150 mL 1 molar aqueous HCl was added, and the resulting solution was stirred for 1 h. During this time, any solid within the flask dissolved, allowing fairly rapid stirring of the reaction. After this time, the organic layer was separated, and the aqueous layer was extracted with diethyl ether. The combined organic layers were then washed with 1 molar aqueous HCl, brine, dried with magnesium sulphate, filtered, and the solvent removed under reduced pressure. The resulting white powder was recrystallised from hot toluene (note that the solid precipitated from hot toluene to give a very fine powder, rather than a crystalline form). The desired product (**438**) was afforded in 75 % yield (3.83 g, 9.53 mmol) as a very fine white powder. ¹H-NMR (*d*₆-acetone, 300 MHz) δ 8.59 (s, 2H), 8.02 (d, 2H, 8.1 Hz), 7.45-7.40 (m, 2H), 7.39 (s, 4H), 7.31-7.05 (m, 4H), 3.40 (s, 6H); ¹³C-NMR (*d*₆-acetone, 75 MHz) 160.6, 138.5, 138.3, 135.9, 130.7, 129.0, 127.6, 127.4, 125.8, 125.5, 125.1, 124.9, 123.5, 61.1, 60.9 ppm; FT-IR (thin film, cm⁻¹): 3428, 2934, 1619, 1587, 1493, 1444, 1410, 1337, 1262, 1219, 1148, 1017.

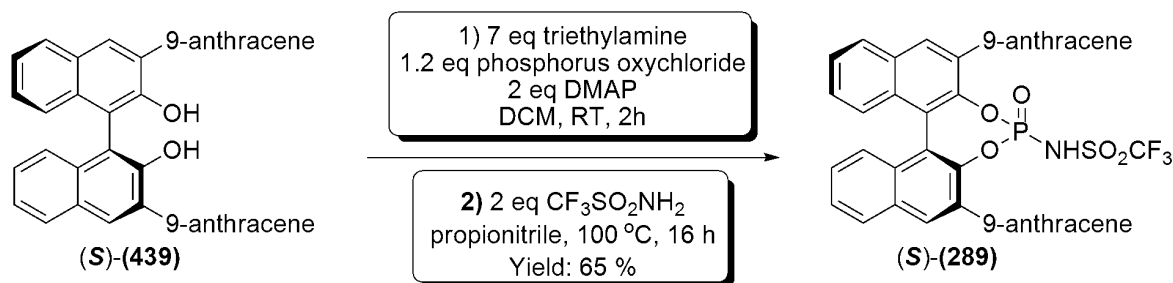
Synthesis of (S)-3,3'-bis(anthracene-9-yl)-2,2'-dihydroxy-1,1'-dinaphthyl (**439**)²⁶⁸



To a 5 mL Biotage microwave *vial* equipped with a magnetic stirrer bar was added 9-bromoanthracene (283 mg, 1.07 mmol), (S)-3,3'-bis(dihydroxyborane)-2,2'-dimethoxy-1,1'-dinaphthyl (**438**) (200 mg, 0.498 mmol), and barium hydroxide (345 mg, 1.09 mmol). The vial was sealed with a rubber septum, and the vial was placed under nitrogen on a schlenk line. 4 mL 3:1 dioxane:H₂O was added, and the mixture was degassed with N₂ for 5 minutes before the addition of tetrakis(triphenyl)phosphine palladium (29 mg, 0.025 mmol). The vial was sealed with a PTFE crimp cap, and heated at 120 °C in a Biotage creator microwave synthesiser for 6 h. After this time, the resulting mixture was evaporated to dryness, and redissolved in dichloromethane, washing with 1M_(aq) HCl, followed by water, and brine. The organic layer was then dried with magnesium sulphate, filtered, and the solvent removed under reduced pressure. The resulting crude material was filtered through a short column of silica, eluting with 10 % ethyl acetate in petroleum ether in order to separate unreacted 9-bromoanthracene. The resulting material was redissolved in dichloromethane, and cooled to 0 °C. Boron tribromide (751 mg, 282 μ L, 3 mmol) was added slowly *via* syringe, and the reaction was allowed to warm to RT with stirring for 16 h. After cooling again to 0 °C, the reaction was quenched by the addition of water, and extracted with dichloromethane. After washing the organic layer with water and brine, and drying with magnesium sulphate; filtering and removal of the solvent under reduced pressure gave the crude material. This was purified by column chromatography (25 % - 35 % DCM in petroleum ether) to give the desired product (**439**) as a very light brown powder in 55 % yield (175 mg, 0.274 mmol) over two steps. ¹H-NMR (CDCl₃, 300 MHz) δ 8.57 (s, 2H), 8.21-8.00 (m, 6H), 7.93 (d, 2H, *J* 7.6 Hz), 7.87 (d, 2H, *J* 8.3 Hz), 7.68 (d, 2H, *J* 8.8 Hz), 7.59 (d, 2H, *J* 6.0 Hz), 7.57-7.36 (m, 10H), 7.36-7.25 (m, 2H), 5.08 (s, 2H); ¹³C-NMR (CDCl₃, 75 MHz) 151.2, 134.1, 133.3, 132.5, 131.7, 131.7, 131.1, 131.0, 129.5, 128.9, 128.8, 128.7, 128.0, 127.6, 127.4, 126.4, 125.6, 125.1, 124.5, 113.7 ppm; FT-IR (thin film,

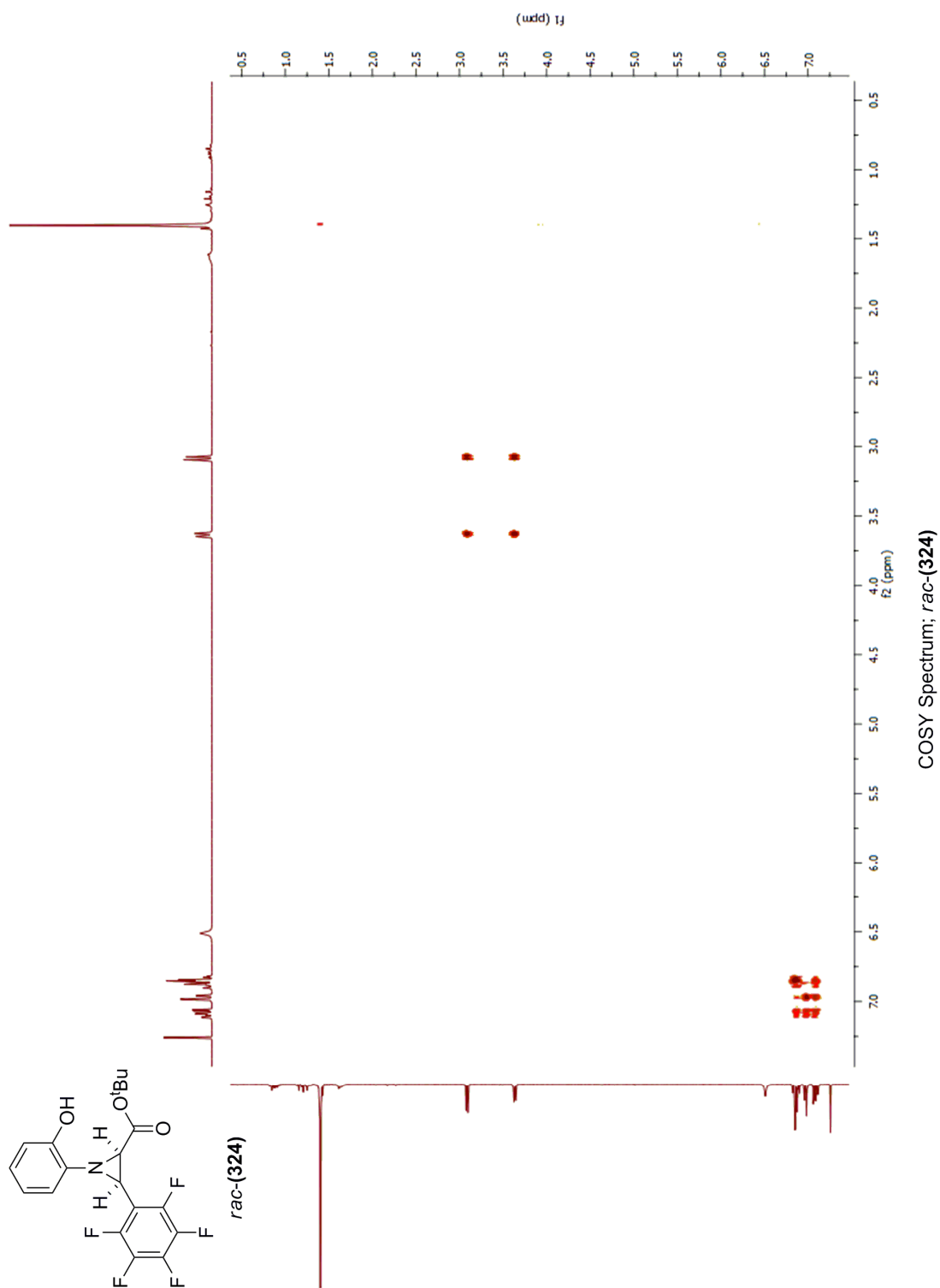
cm⁻¹): 3527, 3052, 1706, 1624, 1600, 1519, 1497, 1441, 1403, 1382, 1353, 1321; MS (EI)⁻: *m/z* 637.4 [M-H]⁻

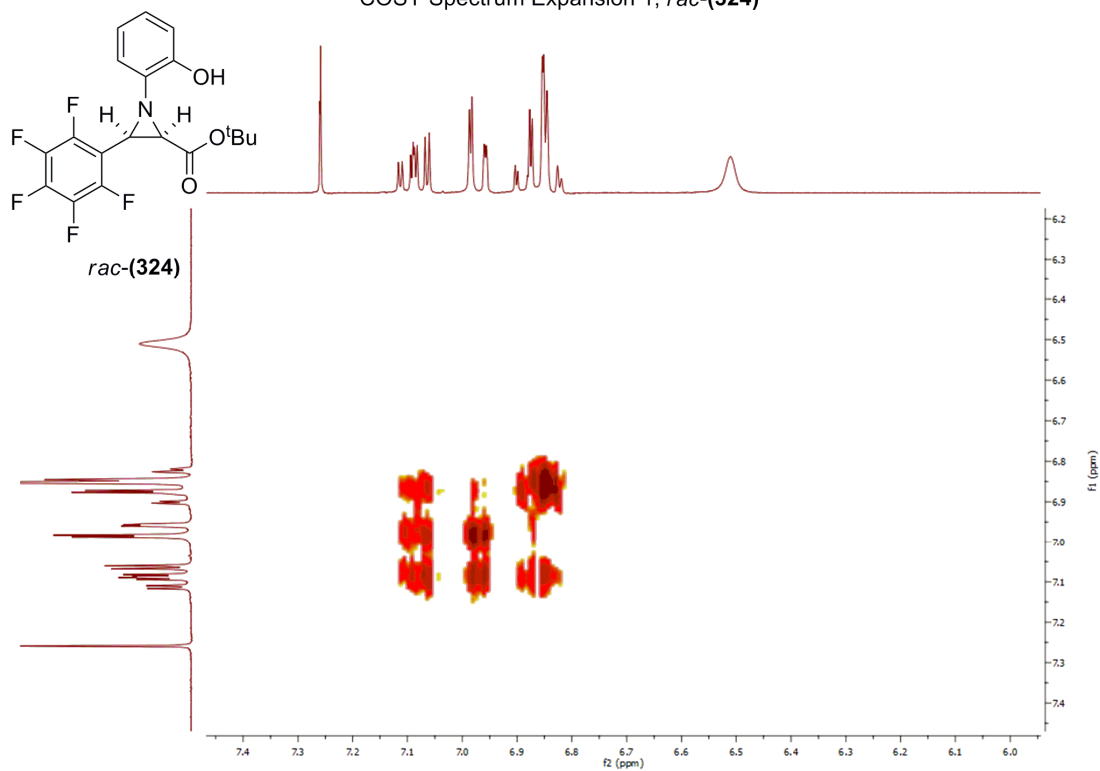
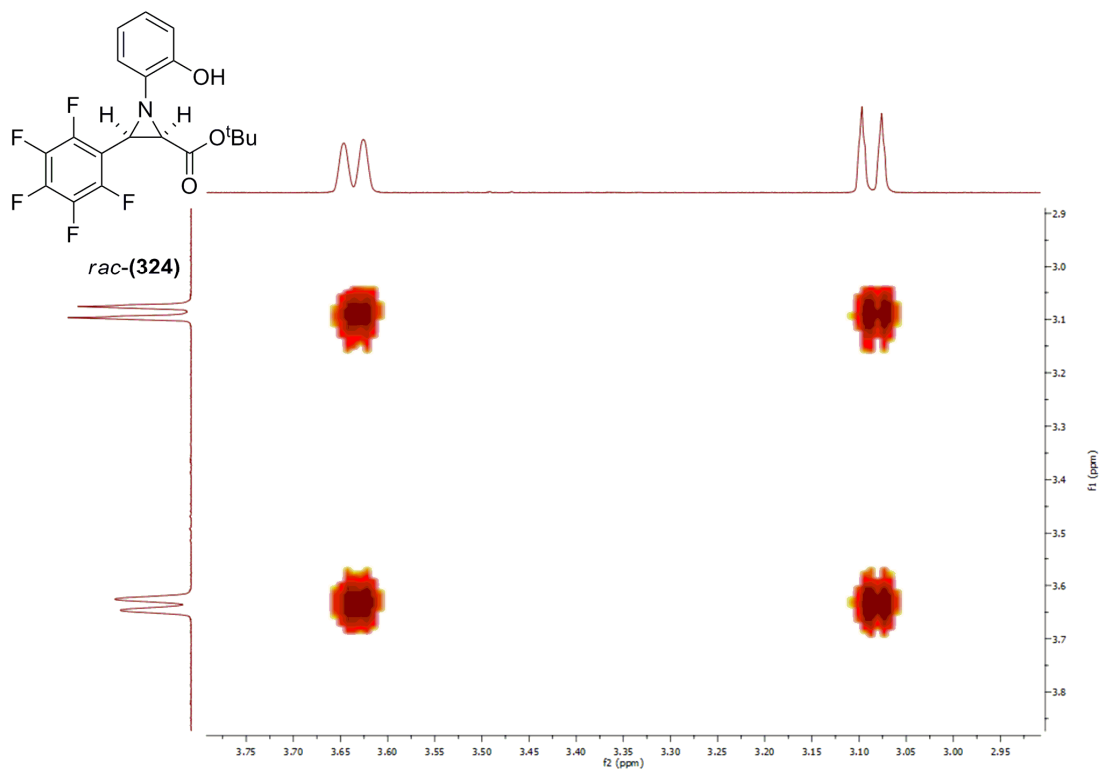
Synthesis of (*S*)-3,3'-bis(anthracene-9-yl)-[1,1']-binaphthalen-2,2'-yl N-triflyl phosphoramidate (**289**)²⁶⁸

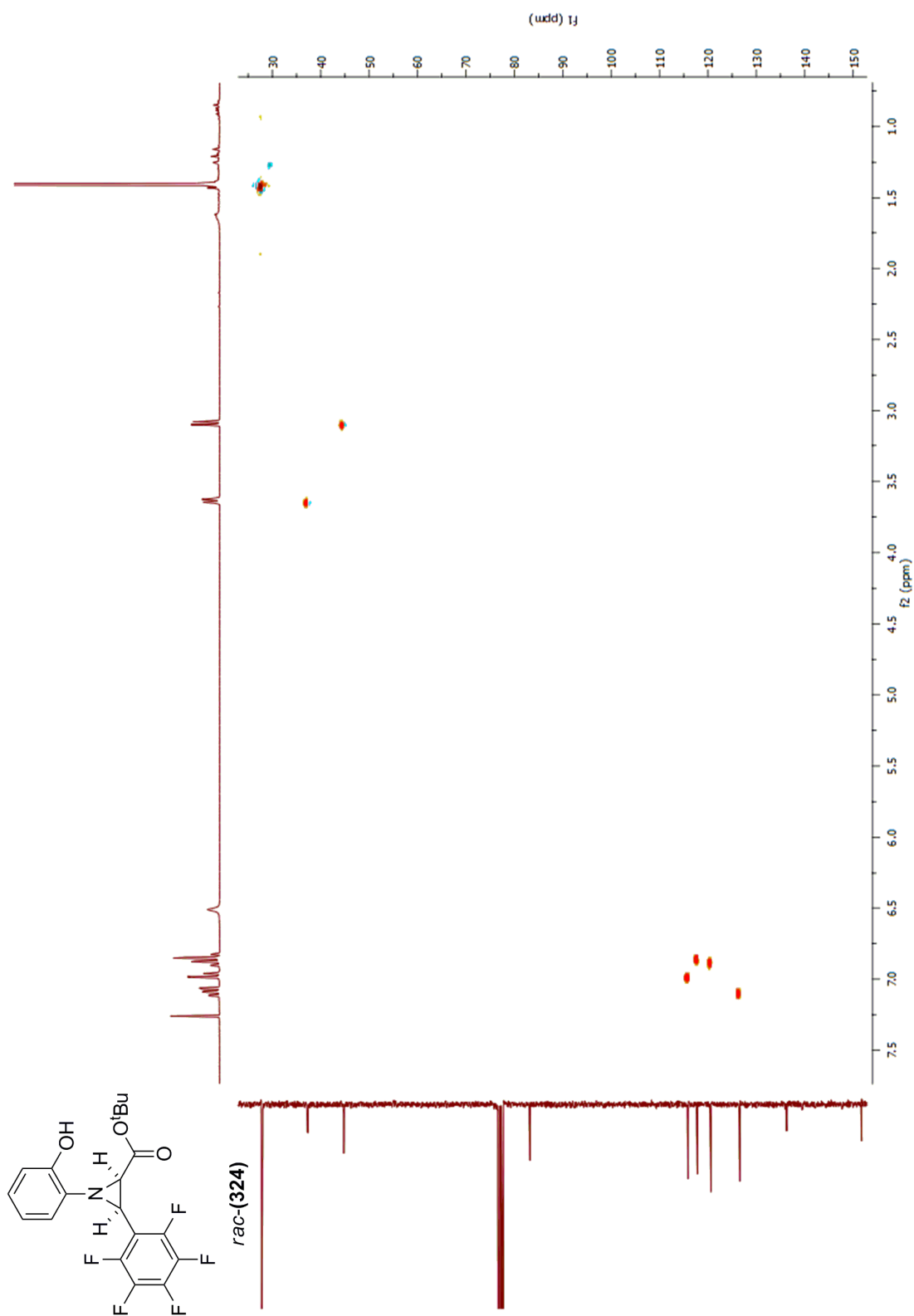


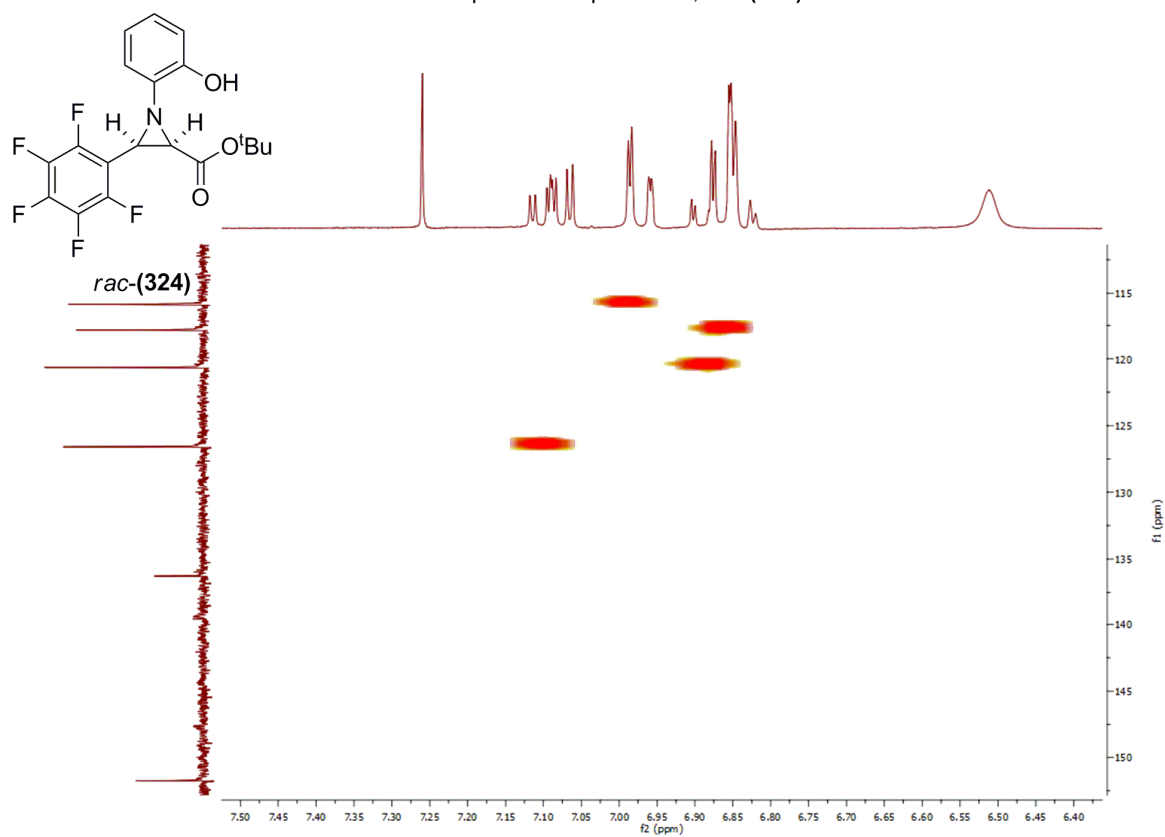
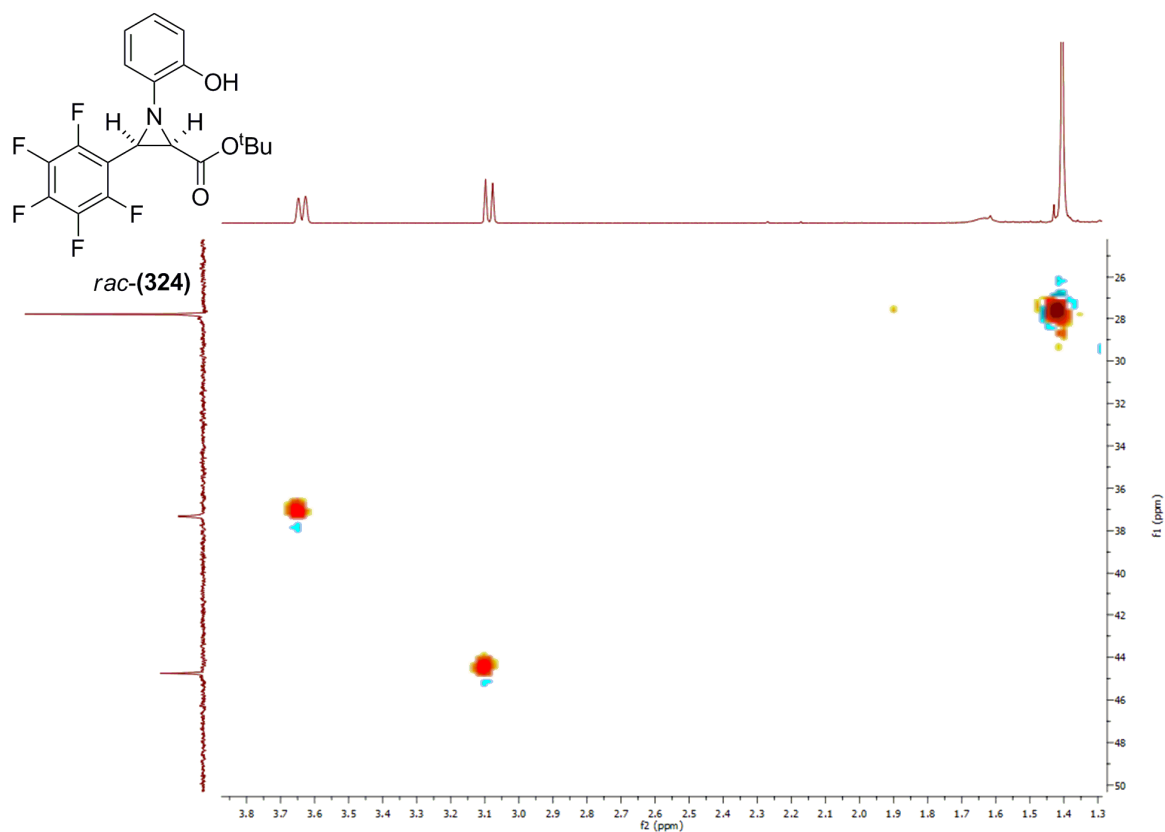
To a flame dried 50 mL two necked round bottom flask, equipped with a reflux condenser and stirrer bar, under N₂ was added (*S*)-**(439)** (900 mg, 1.41 mmol). This was dissolved in 5 mL dichloromethane, and cooled to 0 °C with stirring. To this solution was added respectively triethylamine (1 g, 1.39 mL, 9.87 mmol), freshly distilled phosphorus oxychloride (158 μL, 1.69 mmol), and *N,N*-4-dimethylaminopyridine (343 mg, 2.81 mmol). The resulting solution was allowed to warm to RT, with stirring for 2 h. At this point, trifluoromethanesulfonyl amide (419 mg, 2.81 mmol) was added, and the reaction was diluted by the addition of 10 mL propionitrile. The reaction was then heated to 100 °C for 16 h. After this time, the reaction was allowed to cool to RT, and was diluted by addition of 40 mL water. The resulting mixture was extracted with 150 mL diethyl ether, and the combined organic layers were washed with saturated aqueous sodium hydrogen carbonate, 6 molar aqueous HCl, and brine. After drying with magnesium sulphate, filtration, and removal of the solvent under reduced pressure, the crude material was purified by column chromatography (40 % ethyl acetate in petroleum ether). Subsequently, the pure material was redissolved in diethyl ether, and washed with 6 molar aqueous HCl to ensure protonation of the product. This gave the desired material (*S*)-**(289)** as a very light brown solid in 65 % yield (761 mg, 0.917 mmol). ¹H-NMR (CDCl₃, 400 MHz) δ 8.39 (s, 1H), 8.33 (s, 1H), 8.06 (d, 2H, *J* 9.3 Hz), 8.00 (d, 2H, *J* 8.3 Hz), 7.97-7.85 (m, 3H), 7.78 (d, 1H, *J* 8.76 Hz), 7.74-7.46 (m, 10H), 7.46-7.26 (m, 6H), 6.73-6.53 (m, 2H); ¹³C-NMR (CDCl₃, 75 MHz) 134.4, 134.1, 132.7, 131.8, 131.7, 131.6, 131.1, 131.0, 130.8, 130.7, 130.5, 130.4, 130.2, 128.7, 128.3, 128.0, 127.8, 127.7, 127.6, 127.4, 127.2, 127.0, 126.6, 126.4, 126.2, 125.6, 125.3, 124.9, 122.6, 122.1 ppm; FT-IR (thin film, cm⁻¹): 3052, 1444, 1402, 1303, 1198, 1199, 1088, 955; MS (EI)⁻: *m/z* 830.1 [M-H]⁻.

9.10.1: Appendix 1: COSY and HSQC Correlation Spectra for compound rac-(324)









9.10.2: Appendix 2: Crystal Structure Data for compound rac-(342)

Identification code	seant2b
Elemental formula	C ₂₂ H ₂₆ Br N O ₄
Formula weight	448.4
Crystal system	Monoclinic
Space group	P2 ₁ /c (no. 14)
Unit cell dimensions	a = 11.3776(5) Å α = 90 ° b = 22.6095(11) Å β = 108.569(5) ° c = 8.8388(4) Å γ = 90 °
Volume	2155.34(17) Å ³
No. of formula units, Z	4
Calculated density	1.382 Mg/m ³
F(000)	928
Absorption coefficient	1.934 mm ⁻¹
Temperature	140(1) K
Wavelength	0.71073 Å
Crystal colour, shape	colourless plate
Crystal size	0.29 x 0.23 x 0.07 mm
Crystal mounting	on a glass fibre, in oil, fixed in cold N ₂ stream
On the diffractometer:	
Theta range for data collection	3.6 to 25.0 °
Limiting indices	-13<=h<=13, -26<=k<=26, -10<=l<=10
Completeness to theta = 25.0	99.6 %
Absorption correction	Semi-empirical from equivalents
Max. and min. transmission	1.125 and 0.862
Reflections collected (not including absences)	27295
No. of unique reflections = 3789 [R(int) for equivalents = 0.053]	
No. of 'observed' reflections (I > 2σ _I)	2607
Structure determined by:	direct methods, in SHELXS
Refinement:	Full-matrix least-squares on F ² , in SHELXL
Data / restraints / parameters	3789 / 0 / 253
Goodness-of-fit on F ₂	1.054

Final R indices ('observed' data) $R_1 = 0.056$, $wR_2 = 0.144$
 Final R indices (all data) $R_1 = 0.082$, $wR_2 = 0.150$
 Reflections weighted:
 $w = [\sigma^2(F_o^2) + (0.0787P)^2 + 2.09P]^{-1}$ where $P = (F_o^2 + 2F_c^2) / 3$
 Largest diff. peak and hole 1.63 and $-0.39 \text{ e.}\text{\AA}^{-3}$
 Location of largest difference peak near Br(24)

Table 1. Atomic coordinates ($\times 10^4$) and equivalent isotropic displacement parameters ($\text{\AA}^2 \times 10^4$). $U(\text{eq})$ is defined as one third of the trace of the orthogonalized U_{ij} tensor. E.s.ds are in parentheses.

	x	y	z	U(eq)
N(1)	3947(3)	3376.7(17)	3469(4)	220(9)
C(11)	2990(4)	3475(2)	1979(5)	194(10)
C(12)	2055(4)	3886(2)	1892(5)	221(11)
O(12)	2133(3)	4241.9(14)	3203(4)	214(7)
C(121)	1378(4)	4081(2)	4209(6)	249(11)
C(122)	16(4)	4230(3)	3387(6)	348(13)
C(123)	1914(5)	4473(2)	5653(6)	340(13)
C(124)	1513(5)	3437(2)	4668(6)	297(12)
C(13)	1091(4)	3969(2)	459(5)	217(10)
C(14)	1032(4)	3623(2)	-849(6)	248(11)
O(14)	96(3)	3664.1(16)	-2297(4)	328(9)
C(141)	-967(5)	4002(3)	-2356(6)	388(14)
C(15)	1940(4)	3209(2)	-764(5)	240(11)
C(16)	2913(4)	3139(2)	643(5)	248(11)
C(2)	4876(4)	3841(2)	4087(5)	233(11)
C(21)	5274(4)	3996(2)	5806(5)	210(10)
C(22)	5982(4)	4500(2)	6320(6)	243(11)
C(23)	6390(4)	4662(2)	7885(6)	274(12)
C(24)	6062(5)	4335(2)	9000(5)	280(12)
Br(24)	6582.0(5)	4547.0(3)	11181.6(6)	397(2)
C(25)	5332(4)	3813(2)	8540(6)	250(11)
C(26)	4969(4)	3659(2)	6942(6)	265(11)
C(3)	5184(4)	3263(2)	3437(5)	217(11)
C(31)	5902(4)	2795(2)	4539(6)	244(11)
O(31)	5509(3)	2486.3(15)	5372(4)	315(8)
O(32)	7054(3)	2766.6(15)	4475(4)	269(8)
C(33)	7842(5)	2305(3)	5473(7)	381(13)
C(34)	9111(5)	2395(3)	5383(7)	429(15)

Table 2. Molecular dimensions. Bond lengths are in Ångstroms, angles in degrees. E.s.ds are in parentheses.

N(1)-C(11)	1.434(5)	C(15)-C(16)	1.386(6)
N(1)-C(2)	1.465(6)	C(2)-C(21)	1.483(6)
N(1)-C(3)	1.439(6)	C(2)-C(3)	1.512(6)
C(11)-C(12)	1.396(6)	C(21)-C(22)	1.387(7)
C(11)-C(16)	1.383(6)	C(21)-C(26)	1.389(7)
C(12)-O(12)	1.390(5)	C(22)-C(23)	1.361(7)
C(12)-C(13)	1.400(6)	C(23)-C(24)	1.375(7)
O(12)-C(121)	1.466(5)	C(24)-Br(24)	1.890(5)
C(121)-C(122)	1.524(7)	C(24)-C(25)	1.425(7)
C(121)-C(123)	1.513(7)	C(25)-C(26)	1.384(6)
C(121)-C(124)	1.508(7)	C(3)-C(31)	1.493(7)
C(13)-C(14)	1.380(7)	C(31)-O(31)	1.200(6)
C(14)-O(14)	1.383(5)	C(31)-O(32)	1.331(5)
C(14)-C(15)	1.380(7)	O(32)-C(33)	1.472(6)
O(14)-C(141)	1.417(6)	C(33)-C(34)	1.485(7)
C(11)-N(1)-C(2)	118.6(4)	C(11)-C(16)-C(15)	121.3(4)
C(11)-N(1)-C(3)	118.1(4)	N(1)-C(2)-C(21)	120.0(4)
C(3)-N(1)-C(2)	62.7(3)	N(1)-C(2)-C(3)	57.8(3)
C(12)-C(11)-N(1)	119.7(4)	C(21)-C(2)-C(3)	124.2(4)
C(16)-C(11)-N(1)	121.5(4)	C(22)-C(21)-C(2)	119.1(4)
C(16)-C(11)-C(12)	118.6(4)	C(26)-C(21)-C(2)	123.1(4)
O(12)-C(12)-C(11)	119.6(4)	C(22)-C(21)-C(26)	117.9(4)
C(11)-C(12)-C(13)	120.2(4)	C(23)-C(22)-C(21)	121.8(5)
O(12)-C(12)-C(13)	120.0(4)	C(22)-C(23)-C(24)	120.1(5)
C(12)-O(12)-C(121)	117.9(3)	C(23)-C(24)-Br(24)	121.8(4)
O(12)-C(121)-C(122)	111.1(4)	C(23)-C(24)-C(25)	120.4(4)
O(12)-C(121)-C(123)	102.1(4)	C(25)-C(24)-Br(24)	117.8(4)
O(12)-C(121)-C(124)	111.9(4)	C(26)-C(25)-C(24)	117.2(4)
C(123)-C(121)-C(122)	110.4(4)	C(25)-C(26)-C(21)	122.5(5)
C(124)-C(121)-C(122)	110.0(4)	N(1)-C(3)-C(2)	59.5(3)
C(124)-C(121)-C(123)	111.1(4)	N(1)-C(3)-C(31)	116.7(4)
C(14)-C(13)-C(12)	119.8(4)	C(31)-C(3)-C(2)	120.6(4)
C(13)-C(14)-O(14)	123.7(4)	O(31)-C(31)-C(3)	125.4(4)
C(13)-C(14)-C(15)	120.3(4)	O(32)-C(31)-C(3)	110.4(4)
C(15)-C(14)-O(14)	116.0(4)	O(31)-C(31)-O(32)	124.2(4)
C(14)-O(14)-C(141)	117.8(4)	C(31)-O(32)-C(33)	115.4(4)
C(14)-C(15)-C(16)	119.8(4)	O(32)-C(33)-C(34)	106.8(4)

Table 3. Anisotropic displacement parameters ($\text{\AA}^2 \times 10^3$) for the expression: $\exp \{-2\pi^2(h^2a^2U_{11} + \dots + 2hka*b*U_{12})\}$
E.s.ds are in parentheses.

	U_{11}	U_{22}	U_{33}	U_{23}	U_{13}	U_{12}
N(1)	19(2)	22(2)	24(2)	-2.4(17)	5.8(17)	1.8(17)
C(11)	16(2)	23(3)	19(2)	2(2)	5.6(18)	-2(2)
C(12)	25(3)	22(3)	24(2)	-3(2)	14(2)	-3(2)
O(12)	22.8(16)	21.2(18)	23.7(17)	-3.2(14)	12.5(14)	-1.8(14)
C(121)	27(3)	26(3)	29(3)	-4(2)	19(2)	-1(2)
C(122)	27(3)	44(3)	41(3)	-1(3)	21(2)	3(3)
C(123)	34(3)	37(3)	34(3)	-9(2)	16(2)	-4(3)
C(124)	33(3)	31(3)	31(3)	1(2)	19(2)	-5(2)
C(13)	18(2)	23(3)	27(3)	1(2)	10(2)	6(2)
C(14)	17(2)	33(3)	25(3)	1(2)	8(2)	-3(2)
O(14)	23.0(18)	52(2)	22.8(18)	-1.0(17)	5.9(14)	7.3(17)
C(141)	30(3)	55(4)	28(3)	8(3)	4(2)	13(3)
C(15)	21(2)	32(3)	19(2)	-6(2)	8(2)	-2(2)
C(16)	21(2)	29(3)	28(3)	-1(2)	12(2)	5(2)
C(2)	22(2)	23(3)	25(3)	2(2)	8(2)	2(2)
C(21)	18(2)	20(3)	29(3)	3(2)	12(2)	8(2)
C(22)	20(2)	24(3)	32(3)	2(2)	13(2)	5(2)
C(23)	19(2)	17(3)	39(3)	3(2)	-1(2)	-6(2)
C(24)	35(3)	37(3)	14(2)	6(2)	10(2)	28(2)
Br(24)	43.6(3)	47.0(4)	24.3(3)	-10.2(3)	4.7(2)	-2.1(3)
C(25)	29(3)	24(3)	25(3)	3(2)	12(2)	0(2)
C(26)	28(3)	22(3)	28(3)	-6(2)	7(2)	-2(2)
C(3)	16(2)	27(3)	23(2)	4(2)	8.4(19)	2(2)
C(31)	21(3)	24(3)	29(3)	-4(2)	8(2)	1(2)
O(31)	29.9(19)	29(2)	40(2)	7.3(17)	17.1(17)	2.0(16)
O(32)	19.6(17)	34(2)	29.0(18)	9.5(16)	10.5(14)	6.9(15)
C(33)	30(3)	37(3)	41(3)	10(3)	3(2)	13(3)
C(34)	29(3)	50(4)	49(4)	10(3)	12(3)	13(3)

Table 4. Hydrogen coordinates ($\times 10^4$) and isotropic displacement parameters ($\text{\AA}^2 \times 10^3$). All hydrogen atoms were included in idealised positions with $U(\text{iso})$'s set at $1.2 \times U(\text{eq})$ or, for the methyl groups, $1.5 \times U(\text{eq})$ of the parent carbon atom.

	x	y	z	U(iso)
H(12A)	-306	3984	2461	52
H(12B)	-59	4638	3072	52
H(12C)	-444	4160	4111	52
H(12D)	2771	4375	6157	51
H(12E)	1465	4413	6394	51
H(12F)	1847	4880	5324	51
H(12G)	1156	3198	3736	44
H(12H)	1094	3360	5434	44
H(12I)	2377	3342	5126	44
H(13)	491	4257	389	26
H(14A)	-1538	3998	-3423	58
H(14B)	-725	4402	-2044	58
H(14C)	-1359	3834	-1640	58
H(15)	1900	2977	-1649	29
H(16)	3525	2860	691	30
H(2)	4799	4179	3370	28
H(22)	6185	4735	5575	29
H(23)	6891	4994	8201	33
H(25)	5110	3586	9282	30
H(26)	4503	3317	6616	32
H(3)	5301	3282	2386	26
H(33A)	7536	1916	5080	46
H(33B)	7845	2341	6568	46
H(34A)	9661	2106	6037	64
H(34B)	9395	2784	5756	64
H(34C)	9097	2351	4297	64

Table 5. Torsion angles, in degrees. E.s.ds are in parentheses.

C(3)-N(1)-C(11)-C(16)	41.4(6)
C(2)-N(1)-C(11)-C(16)	113.9(5)
C(3)-N(1)-C(11)-C(12)	-143.6(4)
C(2)-N(1)-C(11)-C(12)	-71.1(5)
C(16)-C(11)-C(12)-O(12)	-177.9(4)
N(1)-C(11)-C(12)-O(12)	6.9(6)
C(16)-C(11)-C(12)-C(13)	-2.4(7)
N(1)-C(11)-C(12)-C(13)	-177.6(4)
C(11)-C(12)-O(12)-C(121)	-101.5(5)
C(13)-C(12)-O(12)-C(121)	82.9(5)
C(12)-O(12)-C(121)-C(124)	49.2(5)
C(12)-O(12)-C(121)-C(123)	168.0(4)
C(12)-O(12)-C(121)-C(122)	-74.2(5)
O(12)-C(12)-C(13)-C(14)	178.6(4)
C(11)-C(12)-C(13)-C(14)	3.1(7)
C(12)-C(13)-C(14)-C(15)	-2.0(7)
C(12)-C(13)-C(14)-O(14)	178.2(4)
C(13)-C(14)-O(14)-C(141)	-11.6(7)
C(15)-C(14)-O(14)-C(141)	168.7(5)
C(13)-C(14)-C(15)-C(16)	0.3(7)
O(14)-C(14)-C(15)-C(16)	-180.0(4)
C(12)-C(11)-C(16)-C(15)	0.7(7)
N(1)-C(11)-C(16)-C(15)	175.8(4)
C(14)-C(15)-C(16)-C(11)	0.4(7)
C(11)-N(1)-C(2)-C(21)	137.4(4)
C(3)-N(1)-C(2)-C(21)	-113.8(5)
C(11)-N(1)-C(2)-C(3)	-108.8(4)
N(1)-C(2)-C(21)-C(22)	-168.8(4)
C(3)-C(2)-C(21)-C(22)	121.8(5)
N(1)-C(2)-C(21)-C(26)	11.1(7)
C(3)-C(2)-C(21)-C(26)	-58.3(6)
C(26)-C(21)-C(22)-C(23)	1.0(7)
C(2)-C(21)-C(22)-C(23)	-179.1(4)
C(21)-C(22)-C(23)-C(24)	-2.5(7)
C(22)-C(23)-C(24)-C(25)	2.3(7)
C(22)-C(23)-C(24)-Br(24)	-179.0(3)
C(23)-C(24)-C(25)-C(26)	-0.5(7)
Br(24)-C(24)-C(25)-C(26)	-179.3(3)
C(24)-C(25)-C(26)-C(21)	-1.0(7)
C(22)-C(21)-C(26)-C(25)	0.8(7)
C(2)-C(21)-C(26)-C(25)	-179.1(4)
C(11)-N(1)-C(3)-C(31)	-139.0(4)
C(2)-N(1)-C(3)-C(31)	111.4(5)
C(11)-N(1)-C(3)-C(2)	109.6(4)
C(21)-C(2)-C(3)-N(1)	106.6(5)
N(1)-C(2)-C(3)-C(31)	-104.9(5)
C(21)-C(2)-C(3)-C(31)	1.8(7)
N(1)-C(3)-C(31)-O(31)	4.5(7)
C(2)-C(3)-C(31)-O(31)	73.2(6)
N(1)-C(3)-C(31)-O(32)	-175.3(4)
C(2)-C(3)-C(31)-O(32)	-106.6(5)
O(31)-C(31)-O(32)-C(33)	2.2(7)
C(3)-C(31)-O(32)-C(33)	-178.0(4)
C(31)-O(32)-C(33)-C(34)	-173.4(4)

Crystal data: C₂₂H₂₆BrNO₄, M = 448.4. Monoclinic, space group P2₁/c (no. 14), a = 11.3776(5), b = 22.6095(11), c = 8.8388(4) Å, β = 108.569(5) °, V = 2155.34(17) Å³. Z = 4, D_c = 1.382 g cm⁻³, F(000) = 928, T = 140(1) K, μ(Mo-Kα) = 19.3 cm⁻¹, λ(Mo-Kα) = 0.71069 Å.

Crystals are colourless plates. One, ca 0.29 x 0.23 x 0.07 mm, was mounted in oil on a glass fibre and fixed in the cold nitrogen stream on an Oxford Diffraction Xcalibur-3/Sapphire3-CCD diffractometer, equipped with Mo-Kα radiation and graphite monochromator. Intensity data were measured by thin-slice ω- and φ-scans. Total no. of reflections recorded, to θ_{max} = 25°, was 27295 of which 3789 were unique (R_{int} = 0.053); 2607 were 'observed' with I > 2σ_I.

Data were processed using the CrysAlisPro-CCD and -RED (1) programs. The structure was determined by the direct methods routines in the SHELXS program (2A) and refined by full-matrix least-squares methods, on F²'s, in SHELXL (2B). The non-hydrogen atoms were refined with anisotropic thermal parameters. Hydrogen atoms were included in idealised positions and their U_{iso} values were set to ride on the U_{eq} values of the parent carbon atoms. At the conclusion of the refinement, wR₂ = 0.150 and R₁ = 0.082 (2B) for all 3789 reflections weighted $w = [\sigma^2(F_o^2) + (0.0787P)^2 + 2.09P]^{-1}$ with $P = (F_o^2 + 2F_c^2)/3$; for the 'observed' data only, R₁ = 0.056.

In the final difference map, the highest peak (ca 1.63 eÅ⁻³) was near Br(24).

Scattering factors for neutral atoms were taken from reference (3). Computer programs used in this analysis have been noted above, and were run through WinGX (4) on a Dell Precision 370 PC at the University of East Anglia.

References

- (1) Programs CrysAlisPro, Oxford Diffraction Ltd., Abingdon, UK (2010).
- (2) G. M. Sheldrick, SHELX-97 – Programs for crystal structure determination (SHELXS) and refinement (SHELXL), *Acta Cryst.* (2008) **A64**, 112-122.
- (3) *International Tables for X-ray Crystallography*, Kluwer Academic Publishers, Dordrecht (1992). Vol. C, pp. 500, 219 and 193.
- (4) L. J. Farrugia, *J. Appl. Cryst.*, (1999) **32**, 837-838 .

9.10.3: Appendix 3: Percentage Composition and Rate Calculation Data for the syntheses of rac-(342) catalysed by PyTf-h (279), or PyTf-d (345)

Substrate	Catalyst	Time (h)	Absolute Integral			Percentage Composition			Moles (mmol)			
			Aldehyde	Imine	Aziridine	Total	Aldehyde	Imine	Aziridine	Aldehyde	Imine	Aziridine
p-Br	PyTf-h	0	1770.71	5448.89	147.24	7366.84	24.04	73.97	2.00	0.078	0.240	0.006
"	"	1	817.38	1553.21	1172.47	3543.06	23.07	43.84	33.09	0.075	0.142	0.107
"	"	2	1475.11	2030.92	3659.51	7165.54	20.59	28.34	51.07	0.067	0.092	0.165
"	"	3	1329.87	1175.39	4044.02	6549.28	20.31	17.95	61.75	0.066	0.058	0.200
"	"	4	1632.41	1348.85	5910.58	8891.84	18.36	15.17	66.47	0.059	0.049	0.215
"	"	5	1523.47	1005.01	5162.27	7690.75	19.81	13.07	67.12	0.064	0.042	0.217
"	"	6	659.03	515.33	2620.48	3794.84	17.37	13.58	69.05	0.056	0.044	0.224
"	"	7	1480.73	1120.1	5508.6	8109.43	18.26	13.81	67.93	0.059	0.045	0.220

Moles of Aldehyde added = 0.324 mmol
Volume = 1.5 mL 0.0015 L

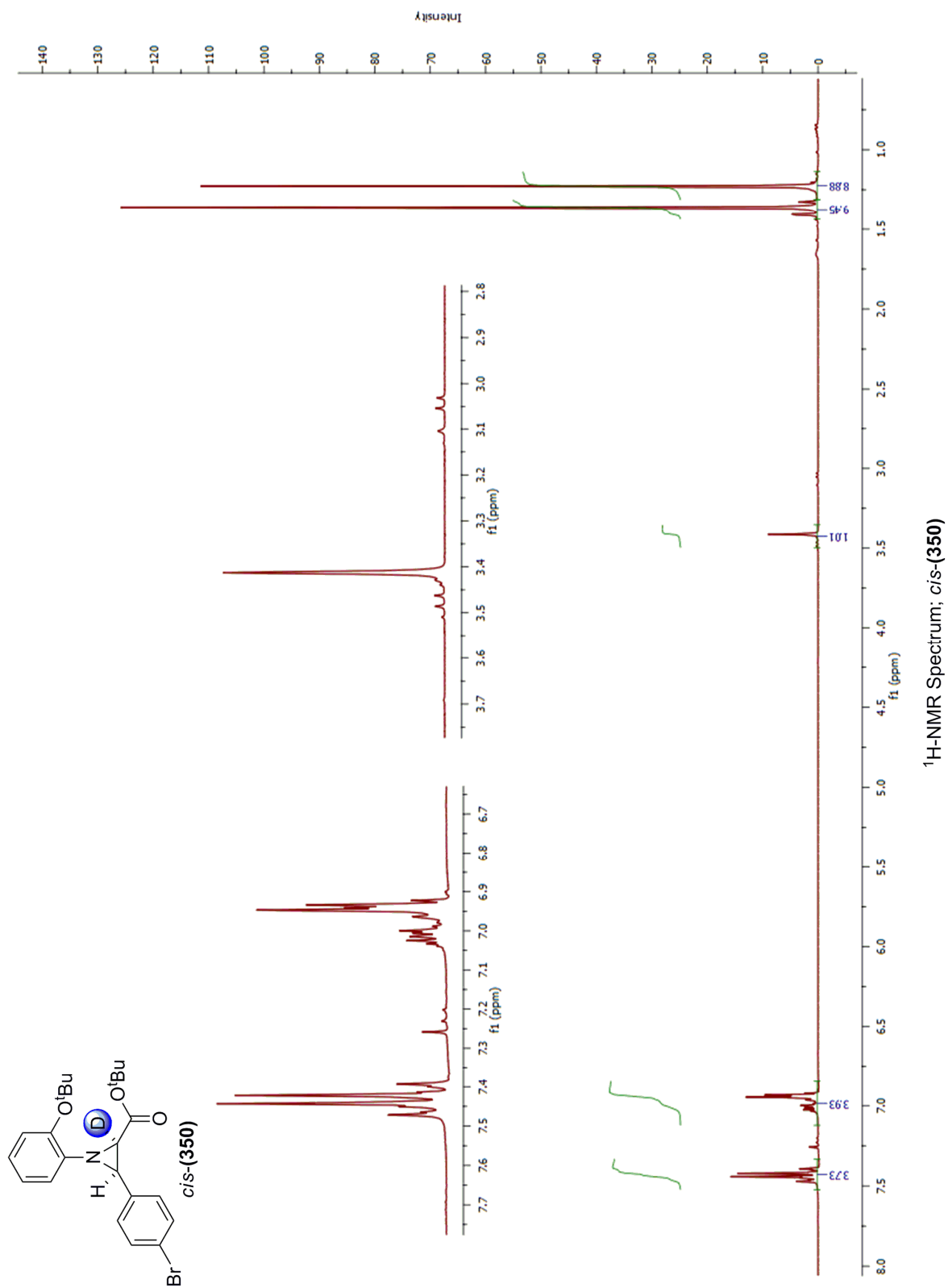
Substrate	Catalyst	Time (h)	Concentration (mol L ⁻¹)			1/concentration		
			Aldehyde	Imine	Aziridine	Aldehyde	Imine	Aziridine
p-Br	PyTf-h	0	5.192E-02	1.598E-01	4.317E-03	1.926E+01	6.259E+00	2.316E+02
"	"	1	4.983E-02	9.469E-02	7.148E-02	2.007E+01	1.056E+01	1.399E+01
"	"	2	4.447E-02	6.122E-02	1.103E-01	2.249E+01	1.633E+01	9.065E+00
"	"	3	4.386E-02	3.877E-02	1.334E-01	2.280E+01	2.580E+01	7.498E+00
"	"	4	3.965E-02	3.277E-02	1.436E-01	2.522E+01	3.052E+01	6.965E+00
"	"	5	4.279E-02	2.823E-02	1.450E-01	2.337E+01	3.543E+01	6.897E+00
"	"	6	3.751E-02	2.933E-02	1.492E-01	2.666E+01	3.409E+01	6.704E+00
"	"	7	3.944E-02	2.983E-02	1.467E-01	2.535E+01	3.352E+01	6.815E+00

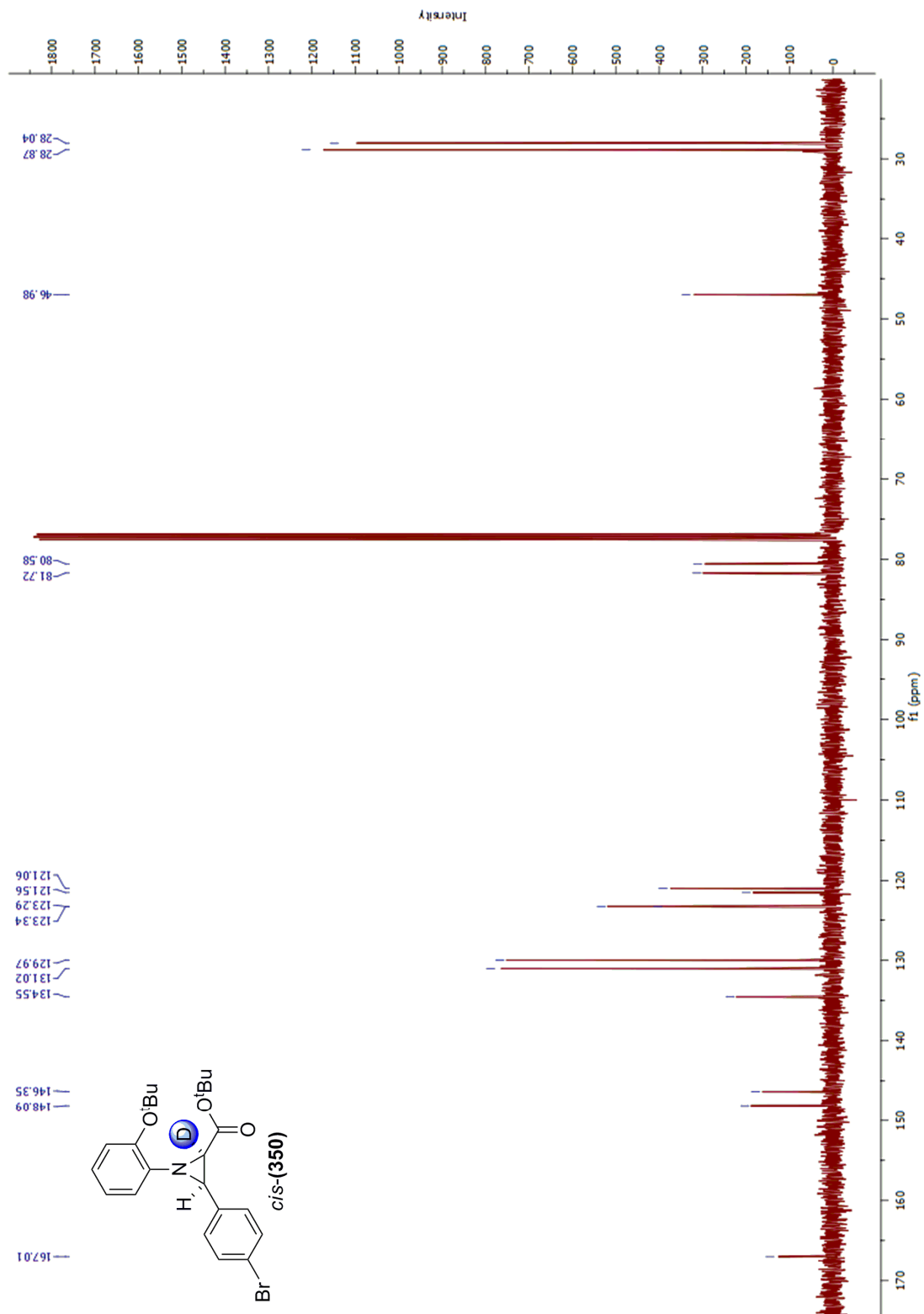
Substrate	Catalyst	Time (h)	Absolute Integral			Percentage Composition			Moles (mmol)			
			Aldehyde	Imine	Aziridine	Total	Aldehyde	Imine	Aziridine	Aldehyde	Imine	Aziridine
p-Br	PyTf-d	0	1843.08	6609.68	129.73	8582.49	21.47	77.01	1.51	0.070	0.250	0.005
"	"	1	999.78	4111.88	1062.02	6173.68	16.19	66.60	17.20	0.052	0.216	0.056
"	"	2	938.33	4759.59	2244.1	7942.02	11.81	59.93	28.26	0.038	0.194	0.092
"	"	3	729.55	3784.01	2462.03	6975.59	10.46	54.25	35.29	0.034	0.176	0.114
"	"	4	563.94	3747.94	2629.16	6941.04	8.12	54.00	37.88	0.026	0.175	0.123
"	"	5	429.4	3334.68	3013.36	6777.44	6.34	49.20	44.46	0.021	0.159	0.144
"	"	6	421.82	3176.44	2762.59	6360.85	6.63	49.94	43.43	0.021	0.162	0.141
"	"	7	675.33	4306.69	3596.67	8578.69	7.87	50.20	41.93	0.026	0.163	0.136

Moles of Aldehyde added = 0.324 mmol
Volume = 1.5 mL 0.0015 L

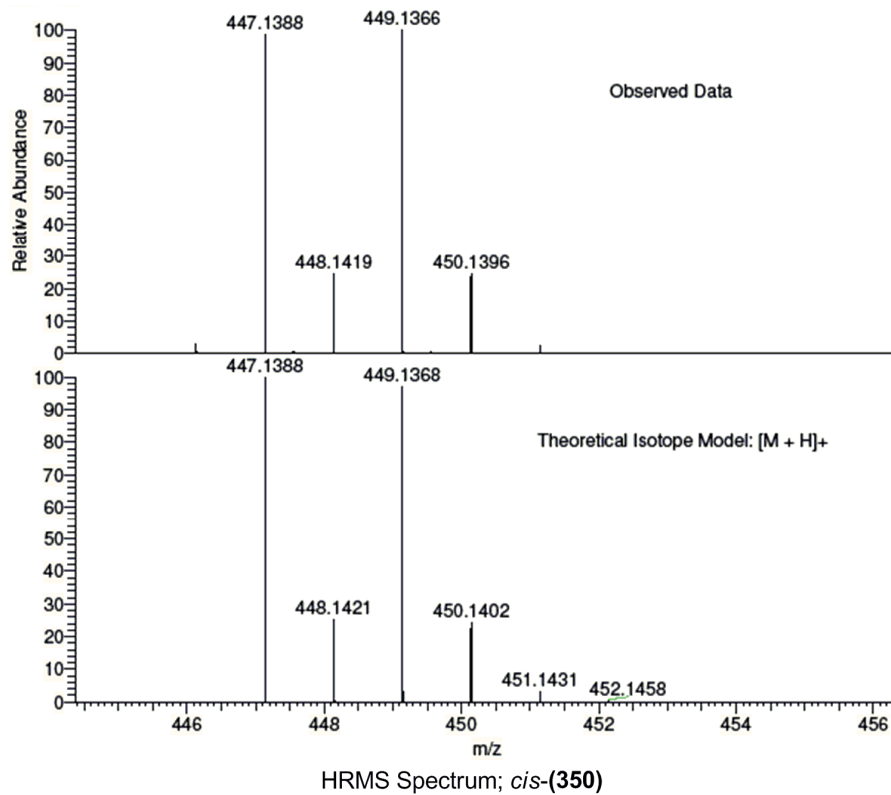
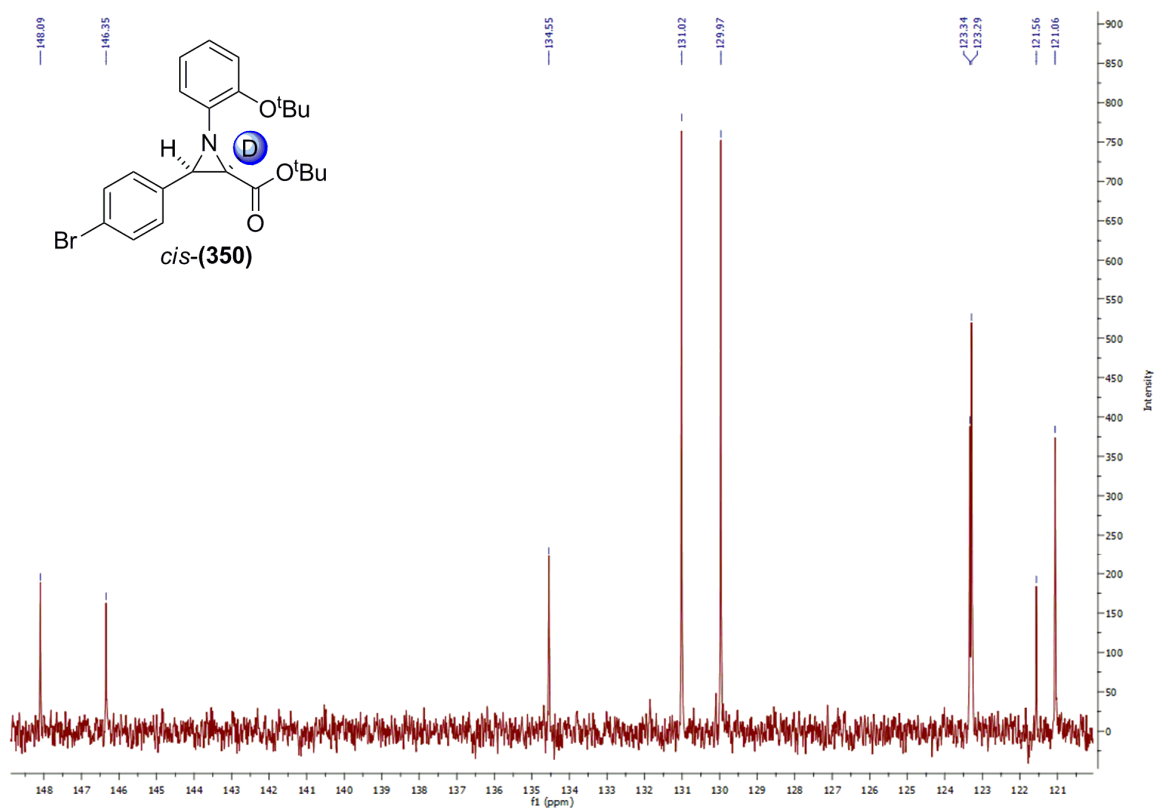
Substrate	Catalyst	Time (h)	Concentration (mol L ⁻¹)			1/concentration		
			Aldehyde	Imine	Aziridine	Aldehyde	Imine	Aziridine
p-Br	PyTf-d	0	4.639E-02	1.663E-01	3.265E-03	2.156E+01	6.011E+00	3.063E+02
"	"	1	3.498E-02	1.439E-01	3.716E-02	2.859E+01	6.951E+00	2.691E+01
"	"	2	2.552E-02	1.294E-01	6.103E-02	3.919E+01	7.725E+00	1.638E+01
"	"	3	2.259E-02	1.172E-01	7.624E-02	4.427E+01	8.534E+00	1.312E+01
"	"	4	1.755E-02	1.166E-01	8.182E-02	5.698E+01	8.574E+00	1.222E+01
"	"	5	1.369E-02	1.063E-01	9.604E-02	7.307E+01	9.409E+00	1.041E+01
"	"	6	1.432E-02	1.079E-01	9.381E-02	6.981E+01	9.271E+00	1.066E+01
"	"	7	1.700E-02	1.084E-01	9.056E-02	5.881E+01	9.222E+00	1.104E+01

9.10.4: Appendix 4: $^1\text{H-NMR}$ and $^{13}\text{C-NMR}$ spectra; and HRMS spectrum for compound *cis*-(350)





^{13}C -NMR Spectrum; *cis*-(350)



9.10.5: Appendix 5: Crystal Structure Data for compound cis-(356)

Table 1. Crystal data and structure refinement details.

Identification code	ST4006 (2010src1036)	
Empirical formula	C ₂₃ H ₂₈ N ₂ O ₅	
Formula weight	412.47	
Temperature	120(2) K	
Wavelength	0.71073 Å	
Crystal system	Monoclinic	
Space group	P21/n	
Unit cell dimensions	<i>a</i> = 11.8592(7) Å	$\alpha = 90^\circ$
	<i>b</i> = 10.7332(7) Å	$\beta = 96.588(3)^\circ$
	<i>c</i> = 17.2217(10) Å	$\gamma = 90^\circ$
Volume	2177.6(2) Å ³	
Z	4	
Density (calculated)	1.258 Mg / m ³	
Absorption coefficient	0.089 mm ⁻¹	
<i>F</i> (000)	880	
Crystal	Lath; light blue	
Crystal size	0.18 × 0.03 × 0.01 mm ³	
θ range for data collection	3.79 – 24.99°	
Index ranges	–14 ≤ <i>h</i> ≤ 14, –12 ≤ <i>k</i> ≤ 12, –20 ≤ <i>l</i> ≤ 20	
Reflections collected	17789	
Independent reflections	3799 [<i>R</i> _{int} = 0.0729]	
Completeness to $\theta = 24.99^\circ$	99.4 %	
Absorption correction	Semi-empirical from equivalents	
Max. and min. transmission	0.9991 and 0.9842	
Refinement method	Full-matrix least-squares on <i>F</i> ²	
Data / restraints / parameters	3799 / 0 / 277	
Goodness-of-fit on <i>F</i> ²	1.173	
Final <i>R</i> indices [<i>F</i> ² > 2σ(<i>F</i> ²)]	<i>R</i> 1 = 0.0673, <i>wR</i> 2 = 0.1139	
<i>R</i> indices (all data)	<i>R</i> 1 = 0.1286, <i>wR</i> 2 = 0.1414	
Largest diff. peak and hole	0.241 and –0.255 e Å ⁻³	

Diffraction: *Nonius KappaCCD* area detector (ϕ scans and ω scans to fill asymmetric unit). Cell determination: **DirAx** (Duisenberg, A.J.M.(1992). *J. Appl. Cryst.* **25**, 92-96.) Data collection: **Collect** (Collect: Data collection software, R. Hooft, Nonius B.V., 1998). Data reduction and cell refinement: **Denzo** (Z. Otwinowski & W. Minor, *Methods in Enzymology* (1997) Vol. 276: *Macromolecular Crystallography*, part A, pp. 307–326; C. W. Carter, Jr. & R. M. Sweet, Eds., Academic Press). Absorption correction: Sheldrick, G. M. SADABS - Bruker Nonius area detector scaling and absorption correction - V2.10 Structure solution: **SHELXS97** (G. M. Sheldrick, *Acta Cryst.* (1990) A46 467–473). Structure refinement: **SHELXL97** (G. M. Sheldrick (1997), University of Göttingen, Germany).

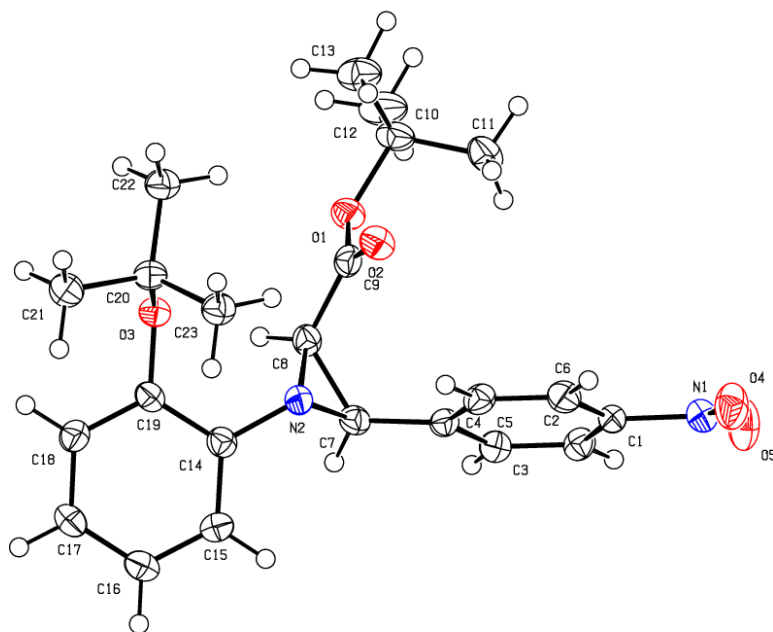


Figure 1. An Ortep representation of the crystal structure ST4006 (2010src1036). Thermal ellipsoids are drawn at 50% probability level

Table 2. Atomic coordinates [$\times 10^4$], equivalent isotropic displacement parameters [$\text{\AA}^2 \times 10^3$] and site occupancy factors. U_{eq} is defined as one third of the trace of the orthogonalized U^{ij} tensor.

Atom	x	y	z	U_{eq}	$S.o.f.$
O1	9072(2)	2006(2)	2479(1)	29(1)	1
O3	7034(2)	1628(2)	4262(1)	25(1)	1
O2	8294(2)	91(2)	2569(1)	30(1)	1
O4	6580(2)	-1909(3)	-850(2)	46(1)	1
O5	6784(3)	-146(3)	-1420(2)	49(1)	1
N2	6141(2)	1257(3)	2722(2)	25(1)	1
N1	6632(2)	-766(3)	-842(2)	33(1)	1
C12	10830(3)	2760(4)	2197(2)	45(1)	1
C22	8539(3)	354(3)	4770(2)	31(1)	1
C17	4186(3)	2953(3)	4317(2)	31(1)	1
C18	5287(3)	2570(3)	4560(2)	28(1)	1
C21	6796(3)	444(3)	5461(2)	32(1)	1
C4	6231(3)	1147(3)	1252(2)	24(1)	1
C5	6354(3)	-148(3)	1255(2)	27(1)	1
C3	6200(3)	1785(3)	546(2)	28(1)	1
C20	7247(3)	421(3)	4668(2)	26(1)	1
C14	5456(3)	1815(3)	3259(2)	25(1)	1
C8	7169(3)	1951(3)	2615(2)	25(1)	1
C1	6479(3)	-108(3)	-114(2)	25(1)	1
C10	10190(3)	1551(4)	2291(2)	32(1)	1
C2	6336(3)	1165(3)	-140(2)	28(1)	1
C13	10768(3)	789(4)	2965(2)	42(1)	1
C11	10024(3)	828(4)	1527(2)	42(1)	1
C7	6178(3)	1890(3)	1974(2)	26(1)	1
C16	3711(3)	2747(3)	3557(2)	32(1)	1
C15	4341(3)	2185(3)	3030(2)	29(1)	1
C19	5917(3)	1973(3)	4039(2)	25(1)	1
C9	8222(3)	1207(3)	2559(2)	27(1)	1
C23	6727(3)	-627(3)	4158(2)	30(1)	1
C6	6485(3)	-781(3)	569(2)	30(1)	1

Table 3. Bond lengths [\AA] and angles [$^\circ$].

O1–C9	1.344(4)
O1–C10	1.483(4)
O3–C19	1.387(4)
O3–C20	1.480(4)
O2–C9	1.200(4)
O4–N1	1.228(4)
O5–N1	1.227(4)
N2–C14	1.431(4)
N2–C8	1.458(4)
N2–C7	1.461(4)
N1–C1	1.469(4)
C12–C10	1.522(5)
C12–H12A	0.9800
C12–H12B	0.9800
C12–H12C	0.9800
C22–C20	1.524(5)
C22–H22A	0.9800
C22–H22B	0.9800
C22–H22C	0.9800
C17–C16	1.382(5)
C17–C18	1.388(5)
C17–H17	0.9500
C18–C19	1.387(5)
C18–H18	0.9500
C21–C20	1.522(5)
C21–H21A	0.9800
C21–H21B	0.9800
C21–H21C	0.9800
C4–C3	1.392(5)
C4–C5	1.397(5)
C4–C7	1.485(5)
C5–C6	1.387(5)
C5–H5	0.9500
C3–C2	1.380(5)
C3–H3	0.9500
C20–C23	1.515(5)
C14–C15	1.394(5)
C14–C19	1.401(5)
C8–C9	1.495(5)
C8–C7	1.518(5)
C8–H8	1.0000
C1–C2	1.377(5)
C1–C6	1.380(5)
C10–C13	1.518(5)
C10–C11	1.520(5)
C2–H2	0.9500
C13–H13A	0.9800
C13–H13B	0.9800
C13–H13C	0.9800
C11–H11A	0.9800
C11–H11B	0.9800
C11–H11C	0.9800
C7–H7	1.0000
C16–C15	1.379(5)
C16–H16	0.9500
C15–H15	0.9500
C23–H23A	0.9800
C23–H23B	0.9800
C23–H23C	0.9800
C6–H6	0.9500
C9–O1–C10	120.8(3)
C19–O3–C20	118.1(2)
C14–N2–C8	114.3(3)
C14–N2–C7	116.9(3)

C8-N2-C7	62.6(2)
O5-N1-O4	122.9(3)
O5-N1-C1	118.4(3)
O4-N1-C1	118.7(3)
C10-C12-H12A	109.5
C10-C12-H12B	109.5
H12A-C12-H12B	109.5
C10-C12-H12C	109.5
H12A-C12-H12C	109.5
H12B-C12-H12C	109.5
C20-C22-H22A	109.5
C20-C22-H22B	109.5
H22A-C22-H22B	109.5
C20-C22-H22C	109.5
H22A-C22-H22C	109.5
H22B-C22-H22C	109.5
C16-C17-C18	120.3(3)
C16-C17-H17	119.9
C18-C17-H17	119.9
C17-C18-C19	120.0(3)
C17-C18-H18	120.0
C19-C18-H18	120.0
C20-C21-H21A	109.5
C20-C21-H21B	109.5
H21A-C21-H21B	109.5
C20-C21-H21C	109.5
H21A-C21-H21C	109.5
H21B-C21-H21C	109.5
C3-C4-C5	119.1(3)
C3-C4-C7	117.9(3)
C5-C4-C7	123.0(3)
C6-C5-C4	120.3(3)
C6-C5-H5	119.8
C4-C5-H5	119.8
C2-C3-C4	121.0(3)
C2-C3-H3	119.5
C4-C3-H3	119.5
O3-C20-C23	109.9(3)
O3-C20-C21	110.6(3)
C23-C20-C21	111.7(3)
O3-C20-C22	102.2(3)
C23-C20-C22	111.6(3)
C21-C20-C22	110.5(3)
C15-C14-C19	119.3(3)
C15-C14-N2	121.8(3)
C19-C14-N2	118.9(3)
N2-C8-C9	116.8(3)
N2-C8-C7	58.8(2)
C9-C8-C7	120.8(3)
N2-C8-H8	116.0
C9-C8-H8	116.0
C7-C8-H8	116.0
C2-C1-C6	122.4(3)
C2-C1-N1	118.5(3)
C6-C1-N1	119.1(3)
O1-C10-C13	110.3(3)
O1-C10-C11	109.1(3)
C13-C10-C11	112.9(3)
O1-C10-C12	102.2(3)
C13-C10-C12	110.7(3)
C11-C10-C12	111.1(3)
C1-C2-C3	118.5(3)
C1-C2-H2	120.7
C3-C2-H2	120.7
C10-C13-H13A	109.5
C10-C13-H13B	109.5

H13A-C13-H13B	109.5
C10-C13-H13C	109.5
H13A-C13-H13C	109.5
H13B-C13-H13C	109.5
C10-C11-H11A	109.5
C10-C11-H11B	109.5
H11A-C11-H11B	109.5
C10-C11-H11C	109.5
H11A-C11-H11C	109.5
H11B-C11-H11C	109.5
N2-C7-C4	119.8(3)
N2-C7-C8	58.6(2)
C4-C7-C8	121.9(3)
N2-C7-H7	115.0
C4-C7-H7	115.0
C8-C7-H7	115.0
C15-C16-C17	120.1(3)
C15-C16-H16	120.0
C17-C16-H16	120.0
C16-C15-C14	120.4(3)
C16-C15-H15	119.8
C14-C15-H15	119.8
O3-C19-C18	120.8(3)
O3-C19-C14	119.2(3)
C18-C19-C14	119.8(3)
O2-C9-O1	125.8(3)
O2-C9-C8	126.3(3)
O1-C9-C8	107.9(3)
C20-C23-H23A	109.5
C20-C23-H23B	109.5
H23A-C23-H23B	109.5
C20-C23-H23C	109.5
H23A-C23-H23C	109.5
H23B-C23-H23C	109.5
C1-C6-C5	118.7(3)
C1-C6-H6	120.7
C5-C6-H6	120.7

Symmetry transformations used to generate equivalent atoms:

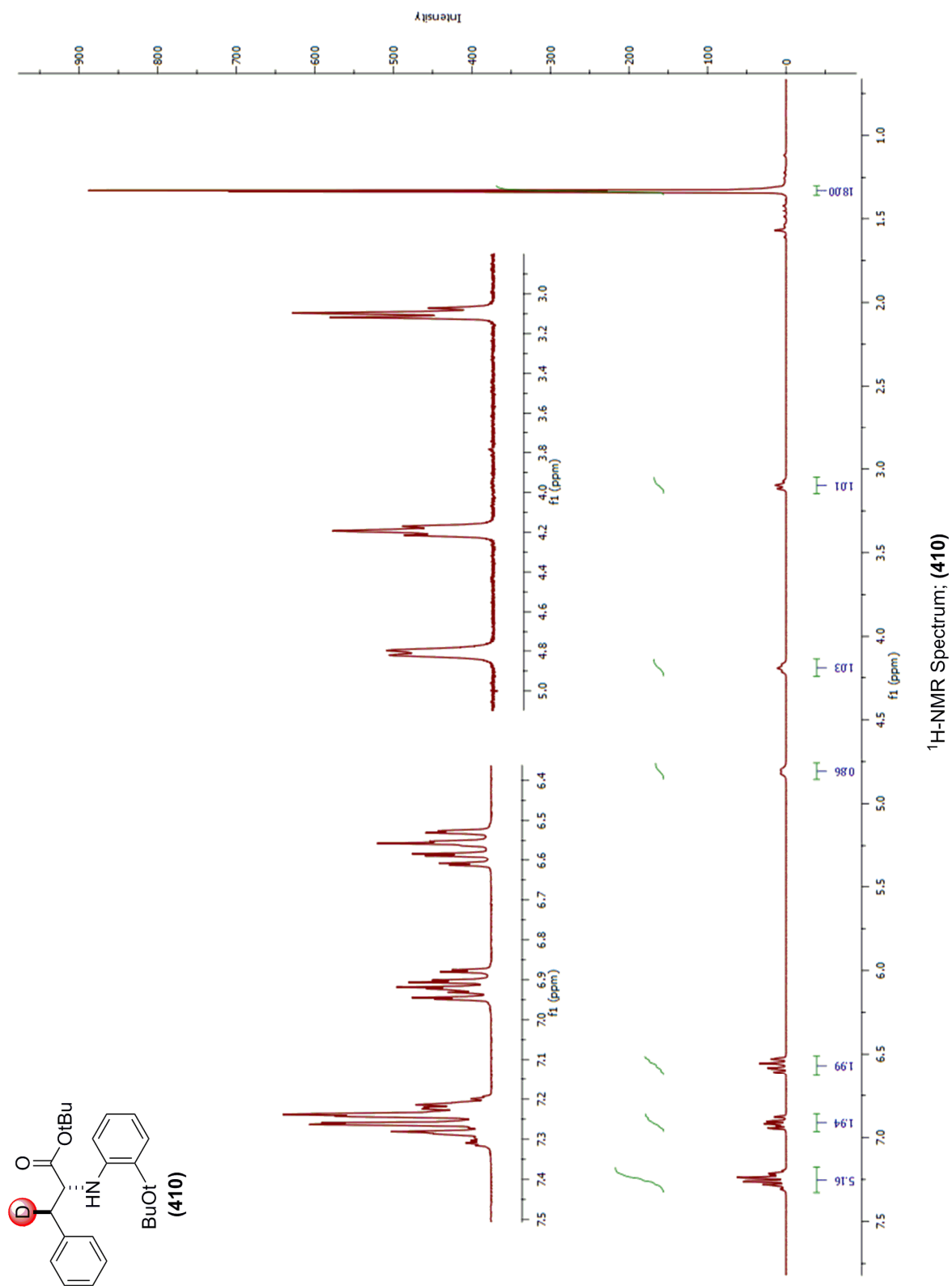
Table 4. Anisotropic displacement parameters [$\text{\AA}^2 \times 10^3$]. The anisotropic displacement factor exponent takes the form: $-2\pi^2[h^2a^{*2}U^{11} + \dots + 2hk a^* b^* U^{12}]$.

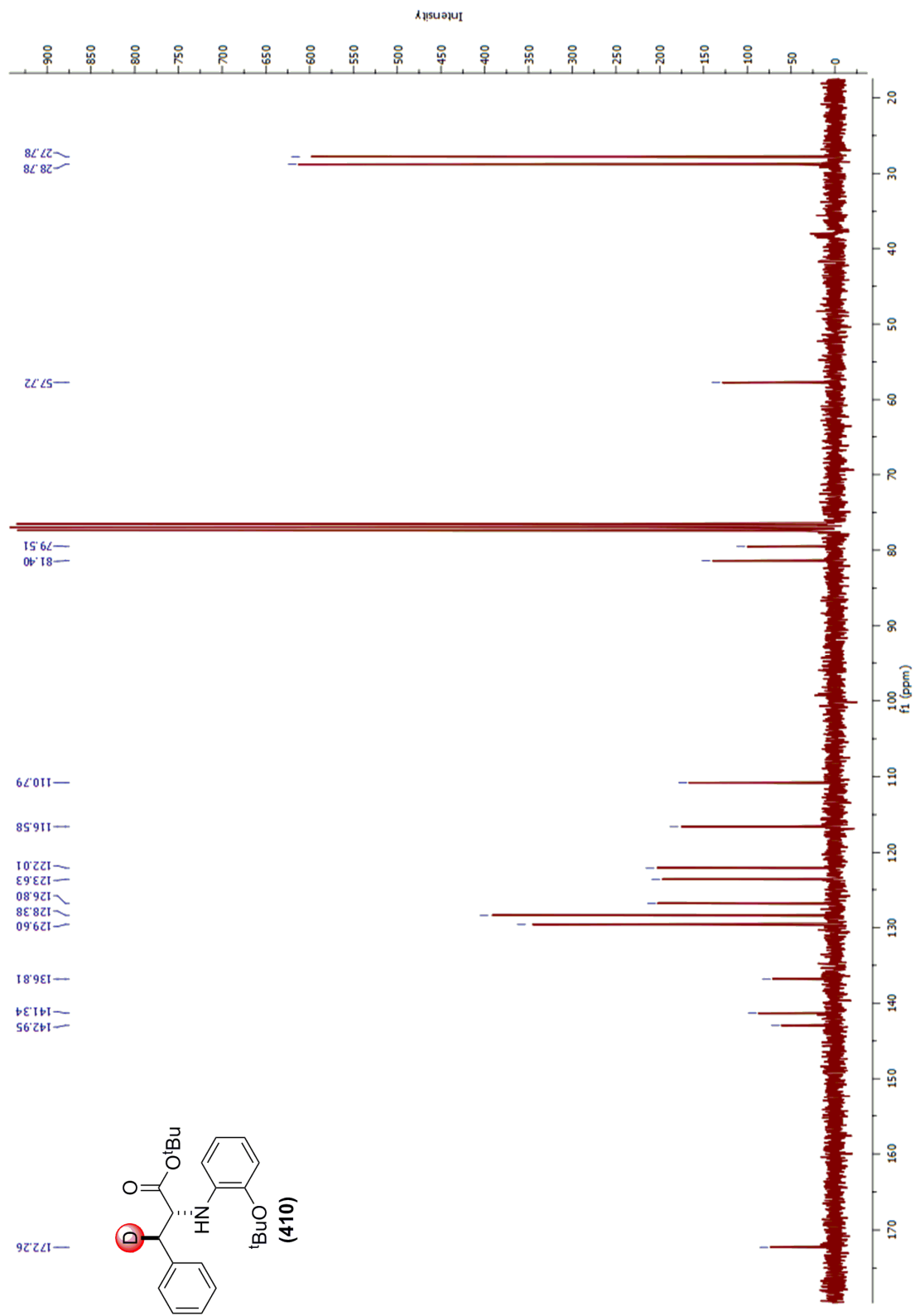
Atom	U^{11}	U^{22}	U^{33}	U^{23}	U^{13}	U^{12}
O1	24(1)	31(1)	33(1)	0(1)	7(1)	-2(1)
O3	23(1)	23(1)	28(1)	1(1)	2(1)	0(1)
O2	30(1)	24(1)	38(2)	-1(1)	6(1)	-1(1)
O4	68(2)	32(2)	36(2)	-6(1)	3(1)	14(1)
O5	68(2)	53(2)	30(2)	-5(1)	21(1)	-13(2)
N2	23(2)	29(2)	23(2)	-3(1)	4(1)	-1(1)
N1	29(2)	41(2)	30(2)	-6(2)	6(1)	2(2)
C12	29(2)	52(3)	54(3)	15(2)	2(2)	-4(2)
C22	27(2)	31(2)	34(2)	1(2)	1(2)	2(2)
C17	29(2)	31(2)	34(2)	-2(2)	9(2)	6(2)
C18	29(2)	32(2)	24(2)	0(2)	2(2)	0(2)
C21	31(2)	33(2)	34(2)	1(2)	6(2)	-2(2)
C4	21(2)	29(2)	22(2)	0(2)	2(1)	-1(2)
C5	29(2)	26(2)	26(2)	2(2)	-1(2)	2(2)
C3	28(2)	26(2)	29(2)	0(2)	3(2)	0(2)
C20	26(2)	23(2)	28(2)	5(2)	1(2)	3(2)
C14	25(2)	23(2)	28(2)	-3(2)	4(2)	-1(2)
C8	26(2)	24(2)	26(2)	-4(2)	5(2)	-3(2)
C1	21(2)	33(2)	23(2)	-5(2)	3(1)	0(2)
C10	22(2)	41(2)	34(2)	11(2)	6(2)	2(2)
C2	29(2)	31(2)	23(2)	4(2)	3(2)	-4(2)
C13	33(2)	48(3)	43(3)	14(2)	0(2)	2(2)
C11	35(2)	56(3)	37(2)	-1(2)	14(2)	6(2)
C7	26(2)	25(2)	27(2)	1(2)	3(2)	5(2)
C16	24(2)	34(2)	37(2)	-1(2)	6(2)	3(2)
C15	24(2)	31(2)	29(2)	1(2)	-1(2)	-1(2)
C19	23(2)	24(2)	28(2)	-2(2)	7(2)	0(2)
C9	28(2)	34(2)	20(2)	-1(2)	4(2)	-3(2)
C23	28(2)	28(2)	33(2)	0(2)	2(2)	-1(2)
C6	32(2)	26(2)	33(2)	0(2)	2(2)	6(2)

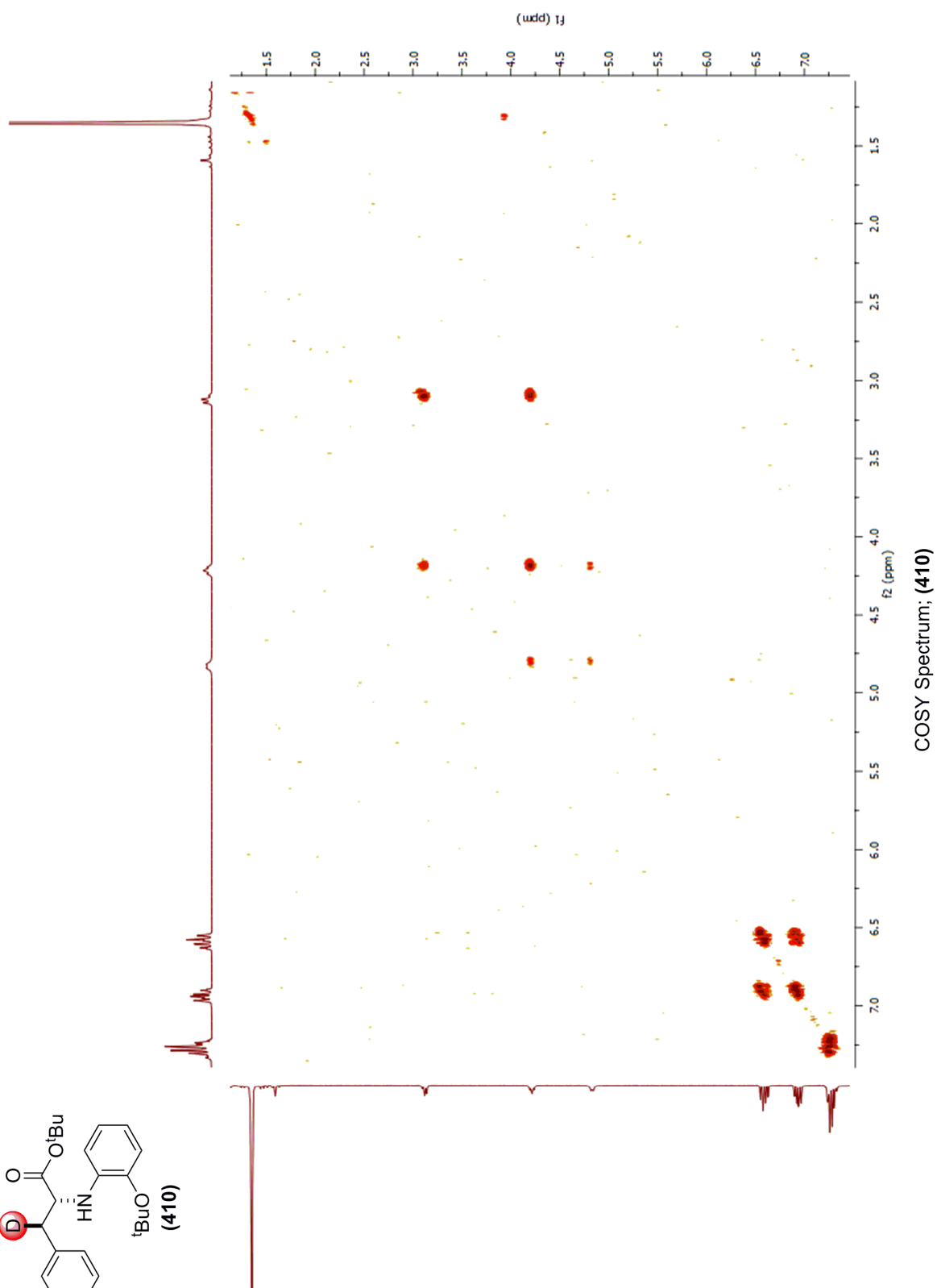
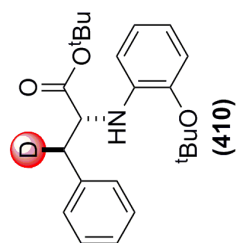
Table 5. Hydrogen coordinates [$\times 10^4$] and isotropic displacement parameters [$\text{\AA}^2 \times 10^3$].

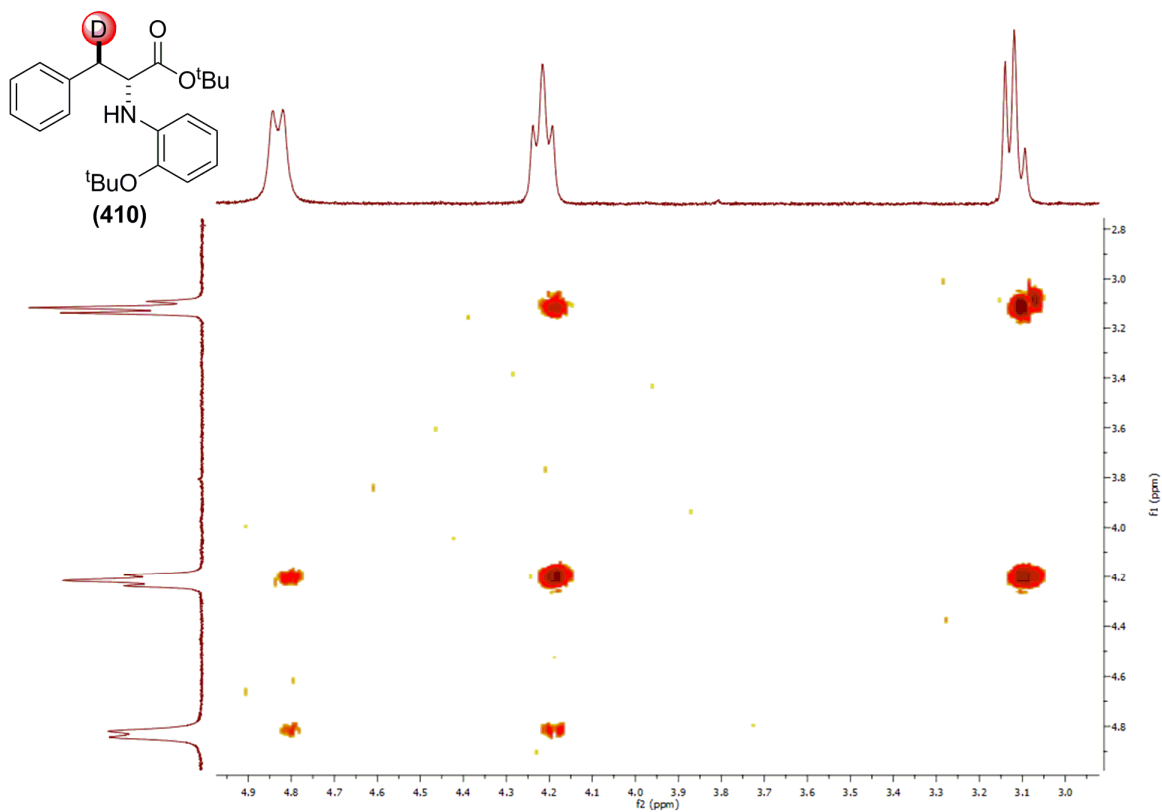
Atom	<i>x</i>	<i>y</i>	<i>z</i>	U_{eq}	<i>S.o.f.</i>
H12A	10420	3261	1780	68	1
H12B	11592	2571	2061	68	1
H12C	10891	3228	2689	68	1
H22A	8814	293	4255	46	1
H22B	8785	-380	5082	46	1
H22C	8849	1107	5037	46	1
H17	3756	3359	4676	37	1
H18	5611	2716	5082	34	1
H21A	7112	1163	5761	48	1
H21B	7019	-324	5746	48	1
H21C	5966	507	5386	48	1
H5	6347	-597	1730	33	1
H3	6084	2661	536	33	1
H8	7273	2760	2902	30	1
H2	6330	1607	-618	34	1
H13A	10790	1271	3450	62	1
H13B	11544	588	2864	62	1
H13C	10342	16	3016	62	1
H11A	9633	42	1608	63	1
H11B	10765	653	1352	63	1
H11C	9566	1323	1130	63	1
H7	5713	2667	1903	31	1
H16	2951	2993	3398	38	1
H15	4012	2049	2508	34	1
H23A	5902	-516	4069	45	1
H23B	6901	-1427	4420	45	1
H23C	7040	-618	3656	45	1
H6	6578	-1660	570	36	1

9.10.6: Appendix 6: $^1\text{H-NMR}$ and $^{13}\text{C-NMR}$ spectra; and COSY, and HSQC Correlation spectra for compound (410)

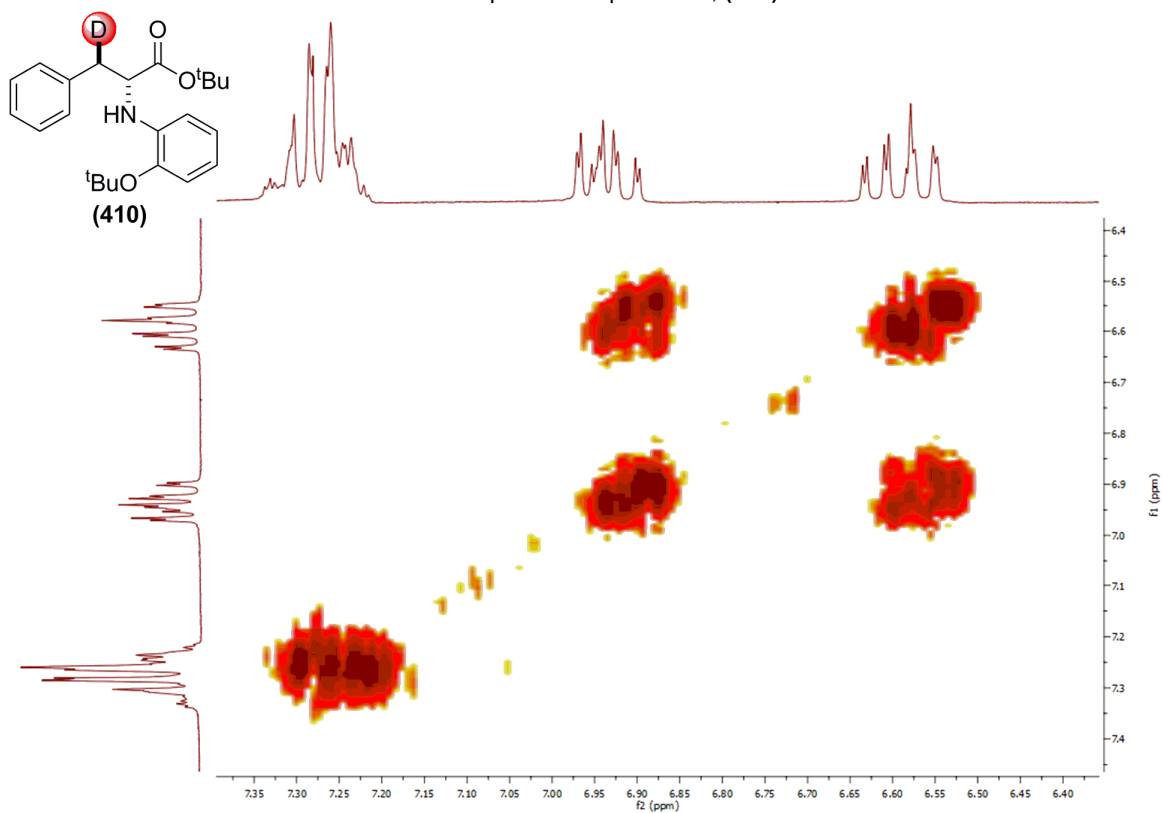




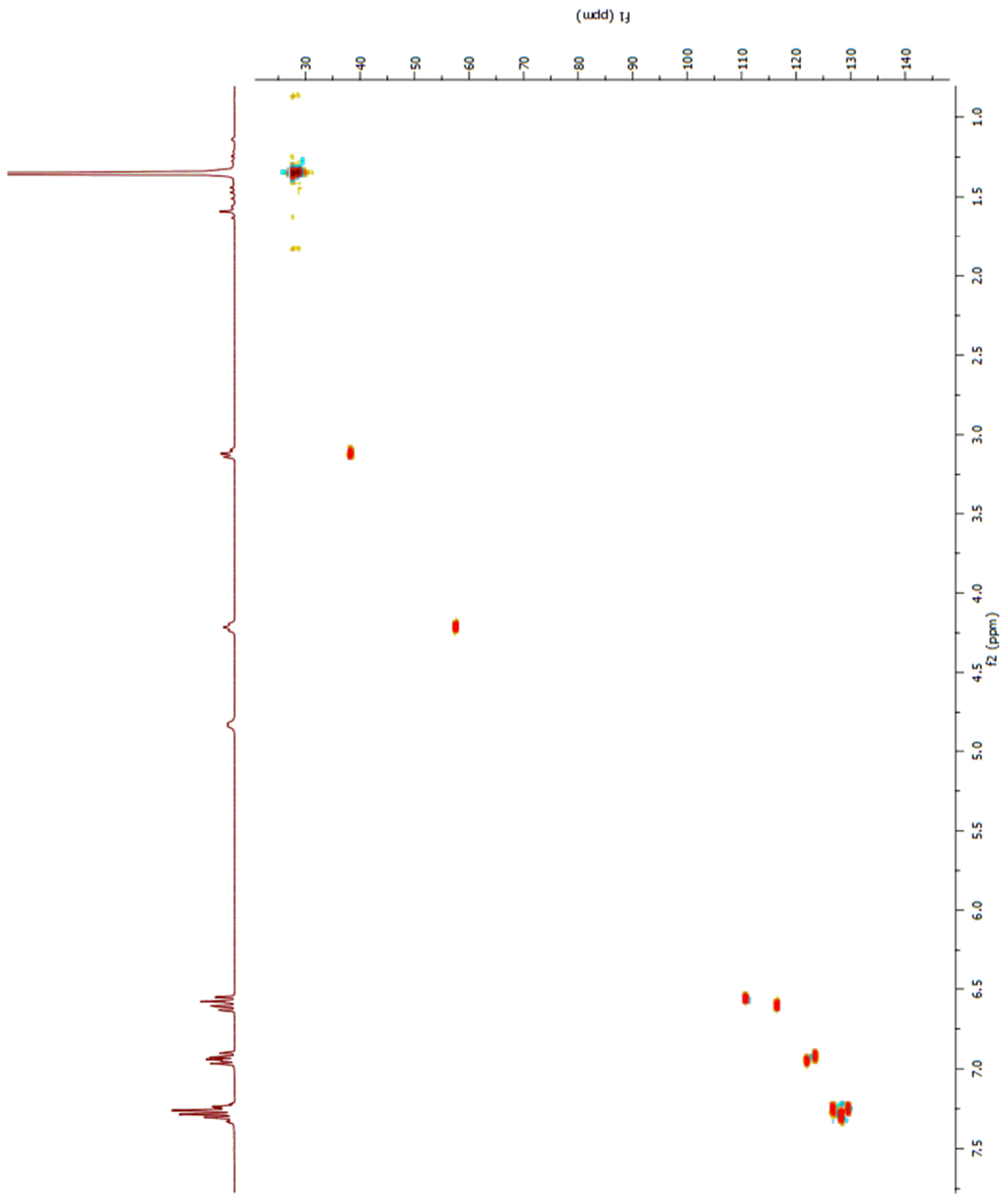
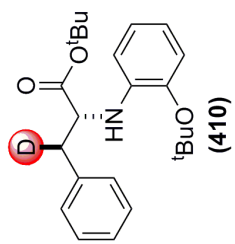




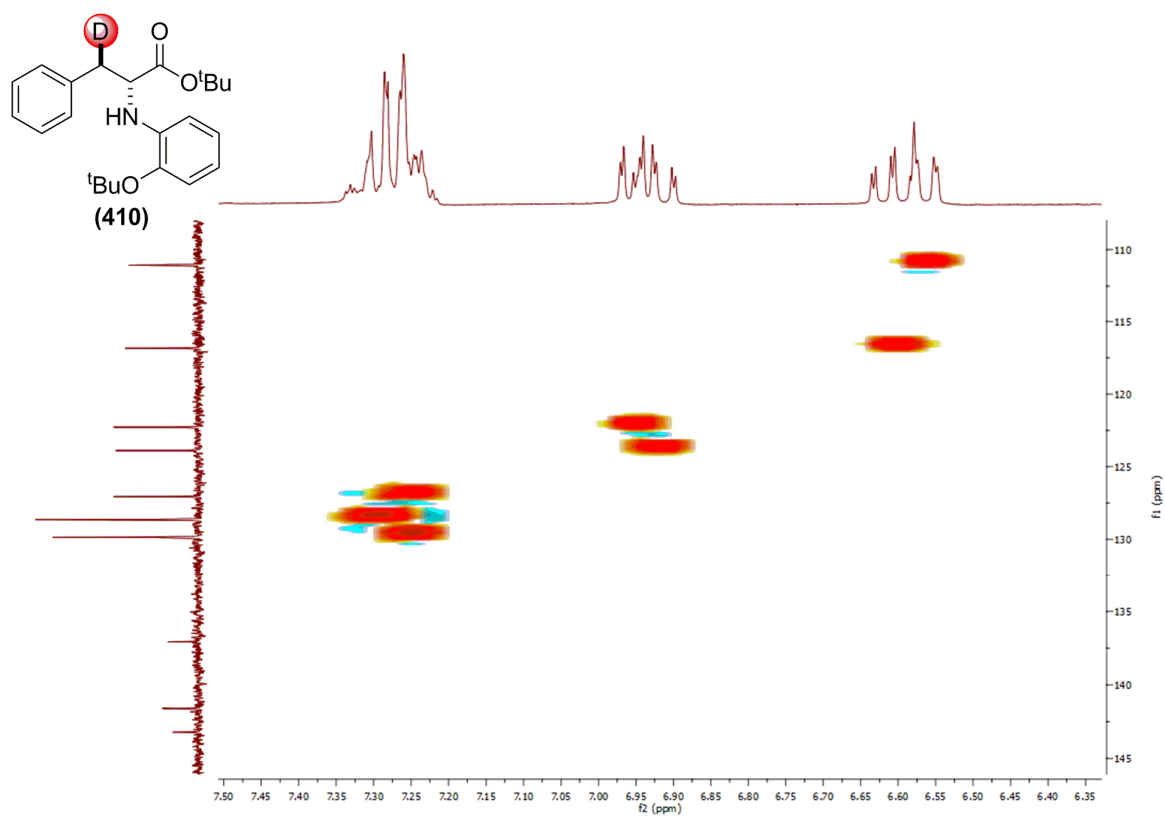
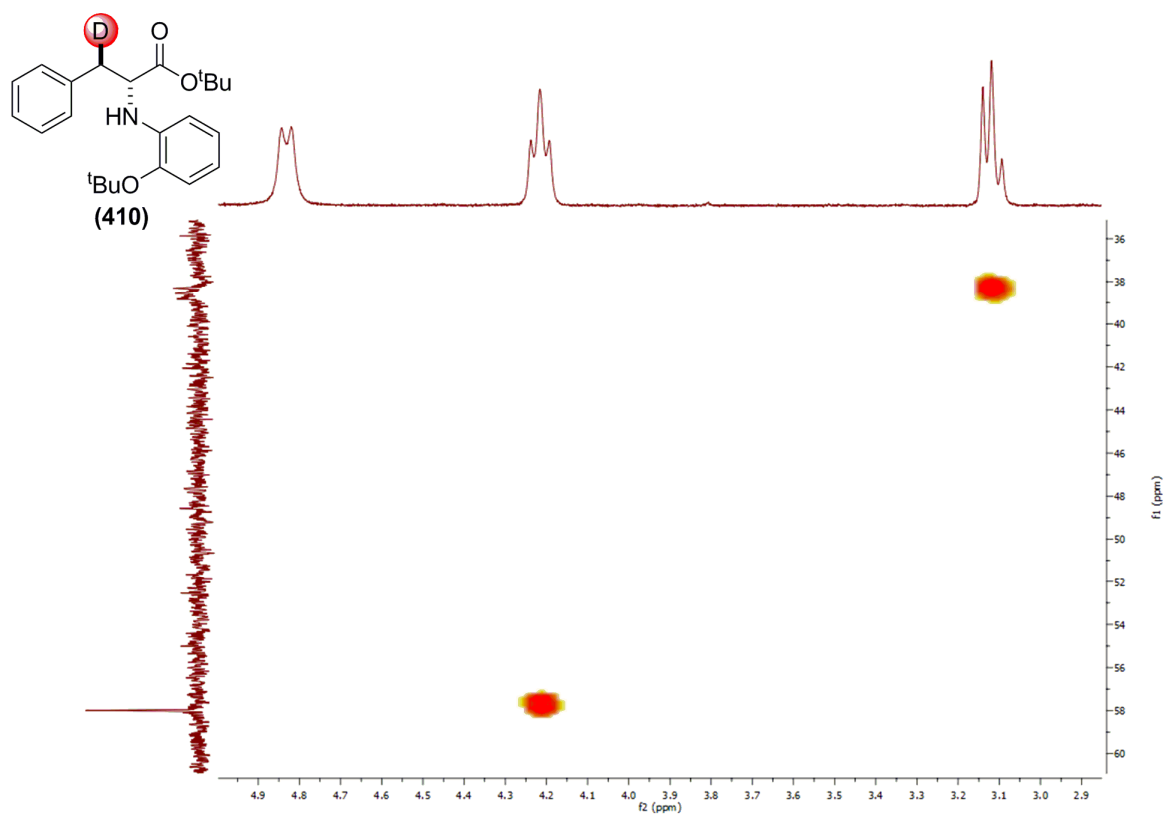
COSY Spectrum Expansion 1; (410)



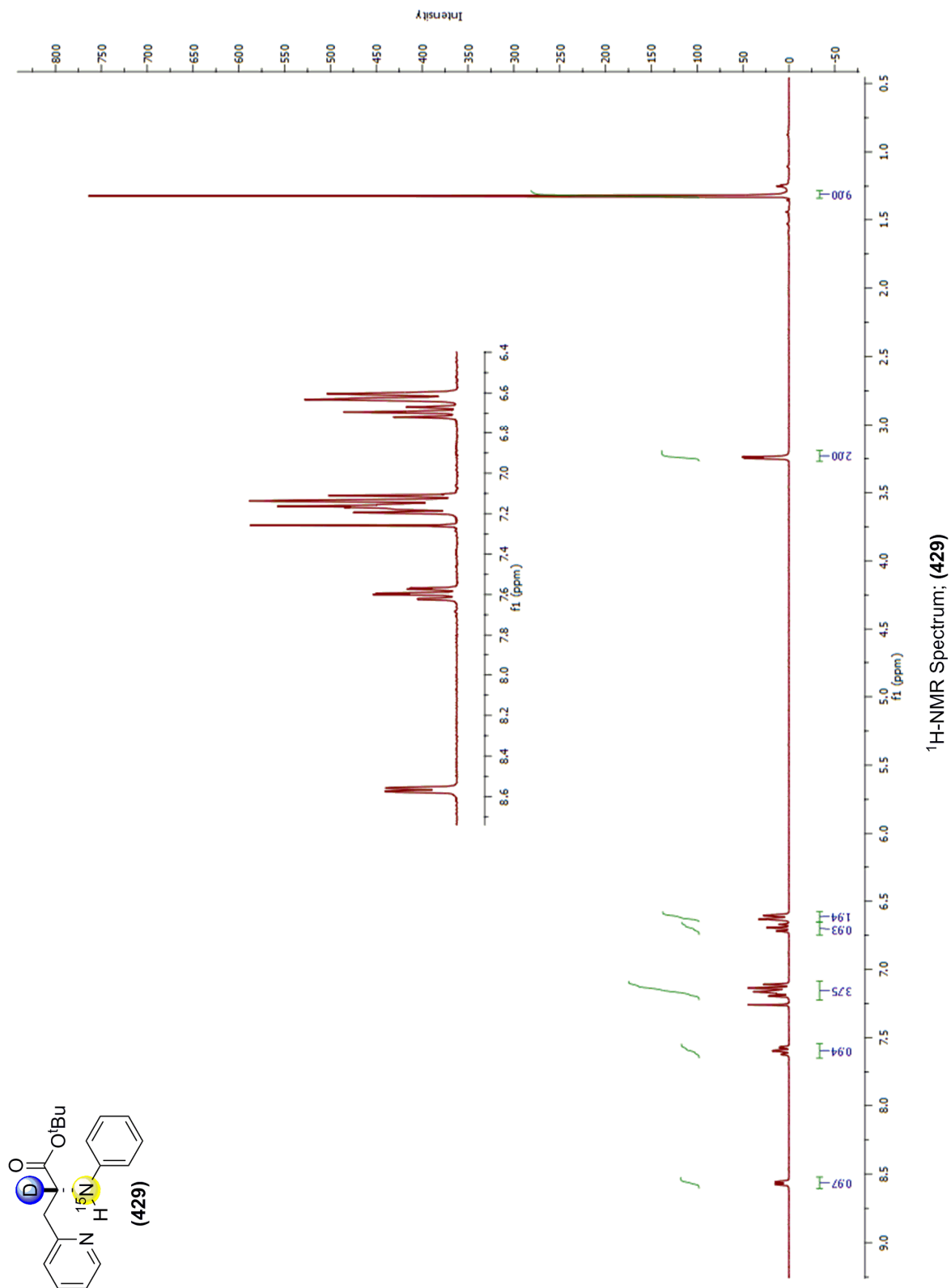
COSY Spectrum Expansion 2; (410)

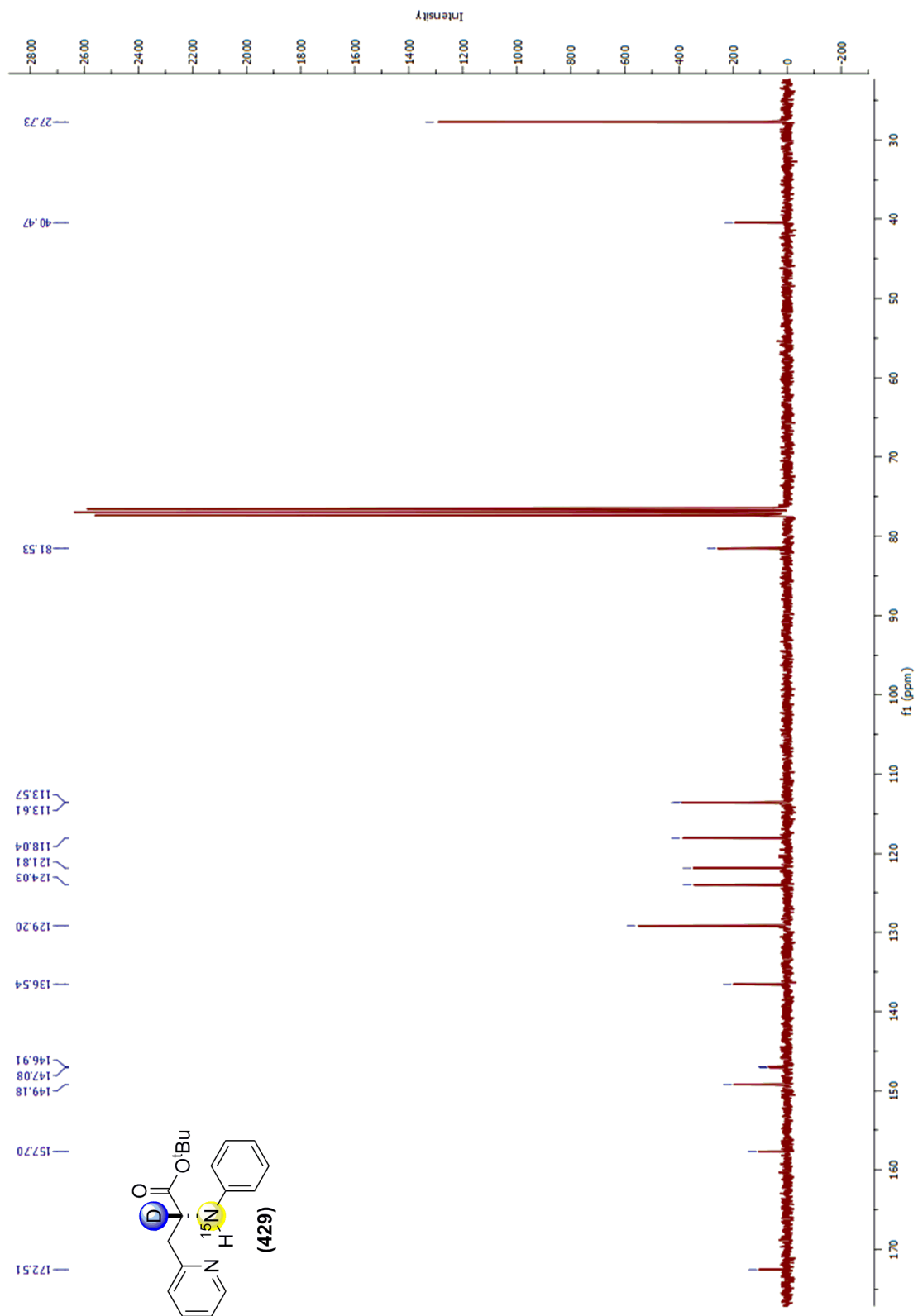


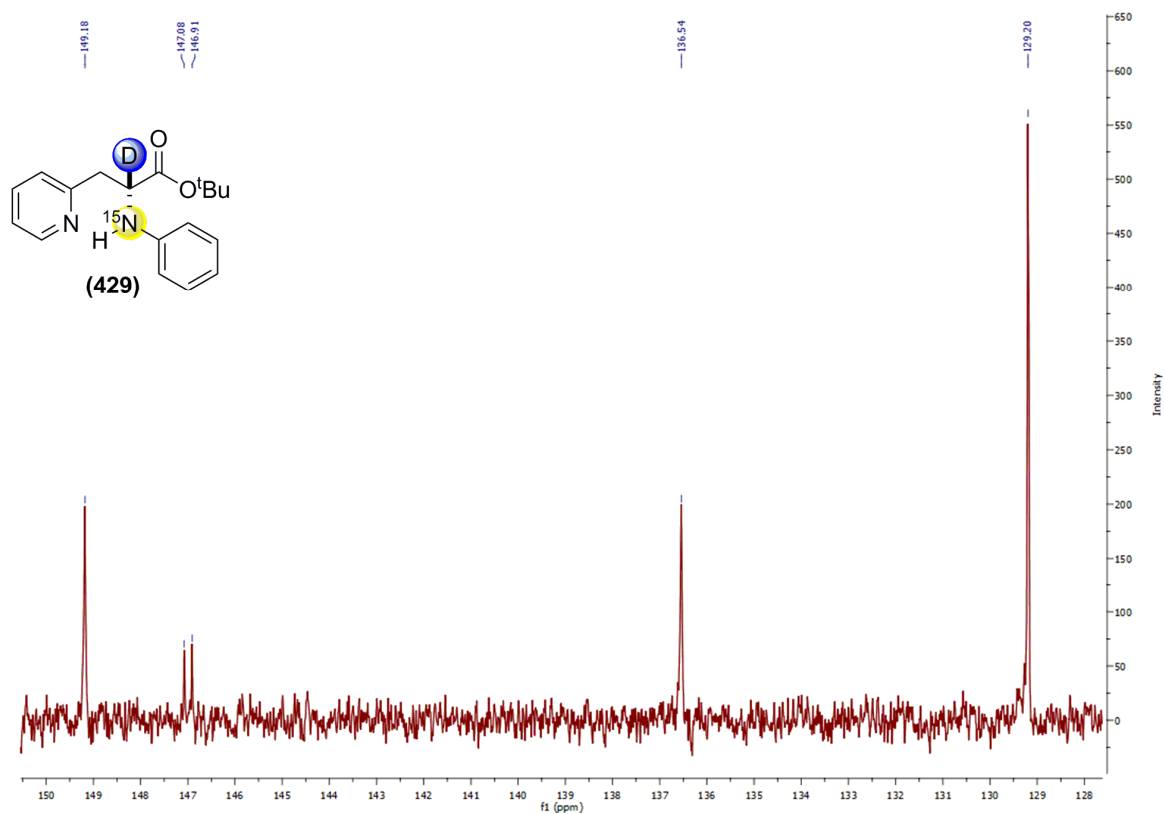
HSQC Spectrum; (410)



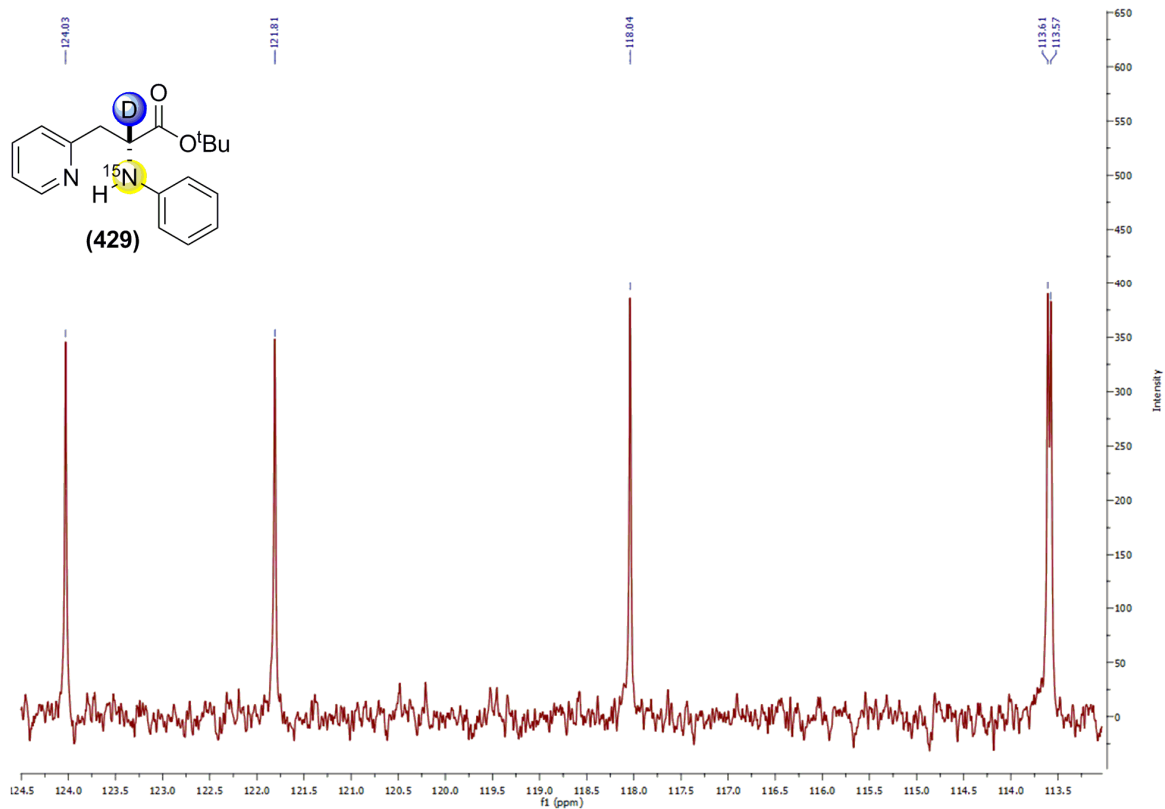
9.10.8: Appendix 8: $^1\text{H-NMR}$ and $^{13}\text{C-NMR}$ spectra; HSQC and $^{15}\text{N-}^1\text{H-}$ HMBC Correlation spectra for compound (429)



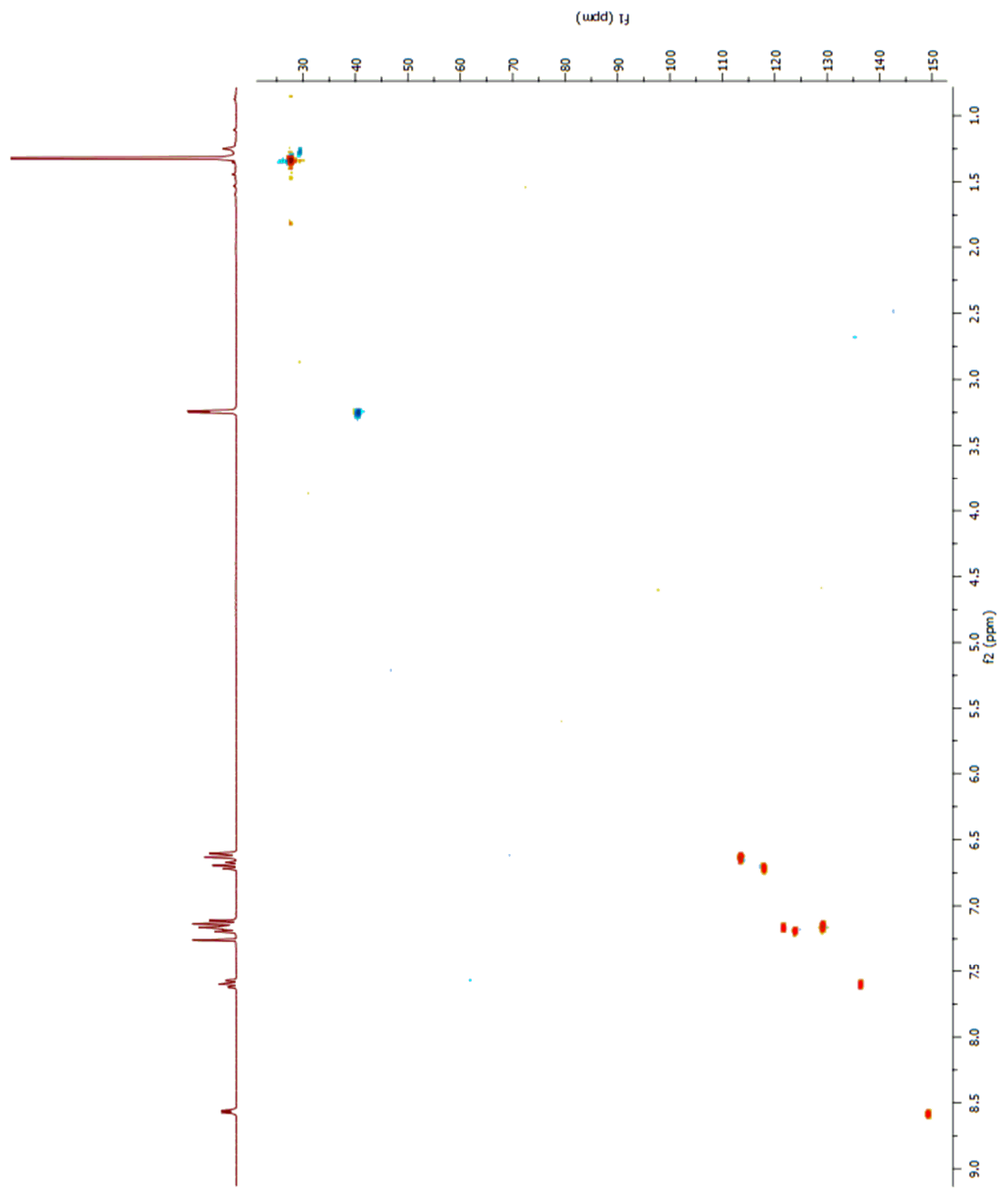
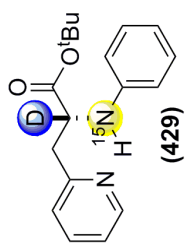


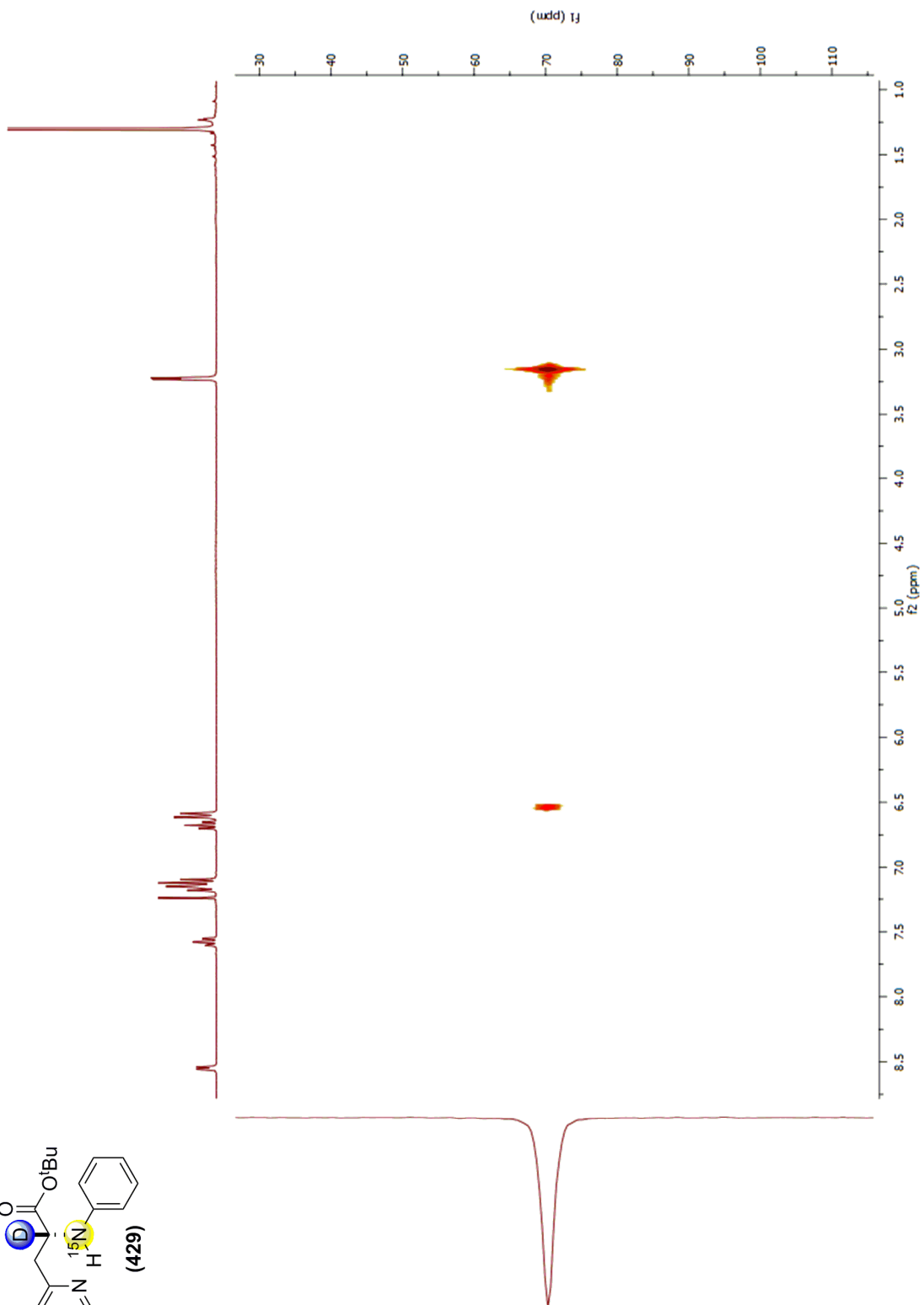


^{13}C -NMR Spectrum Expansion 1; (429)



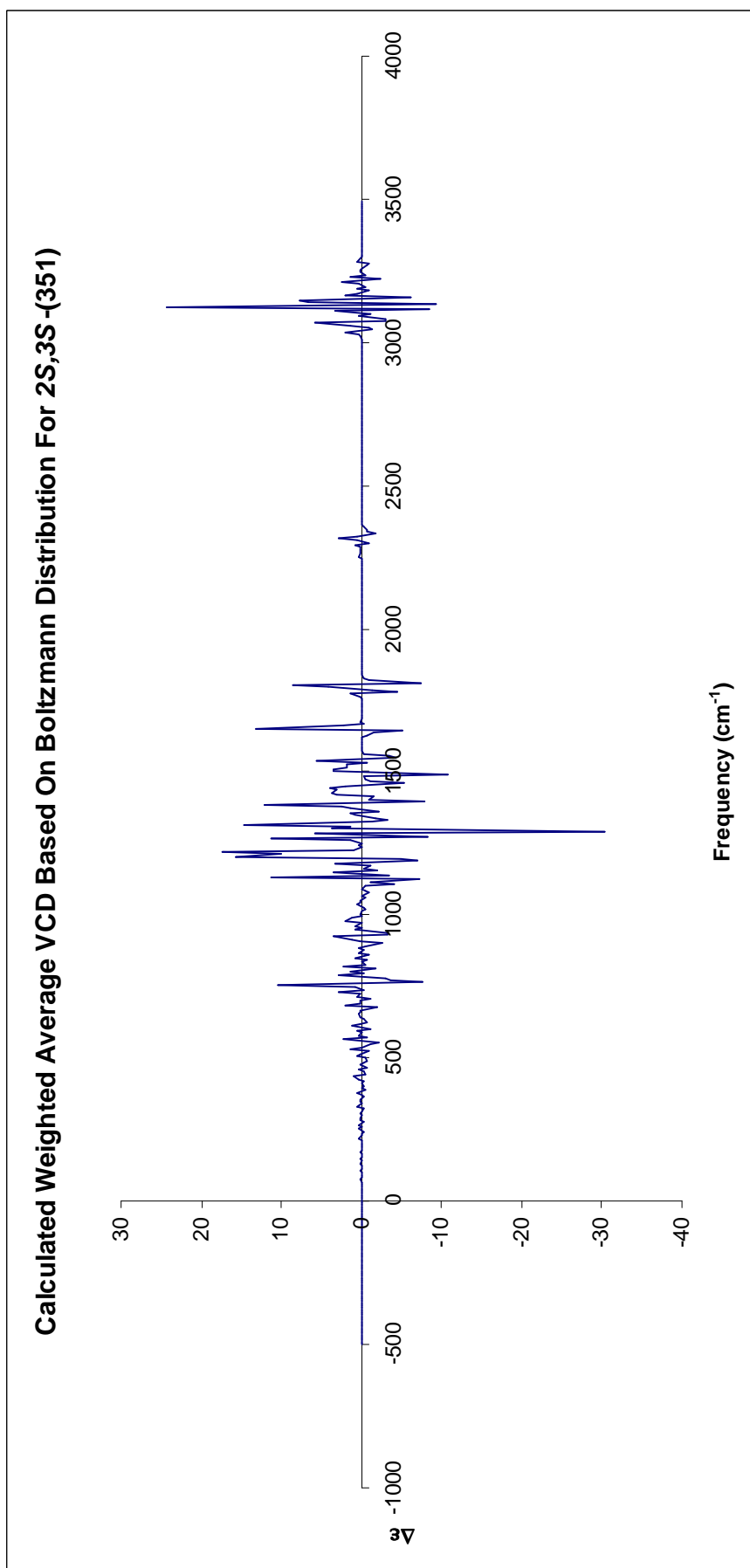
^{13}C -NMR Spectrum Expansion 2; (429)



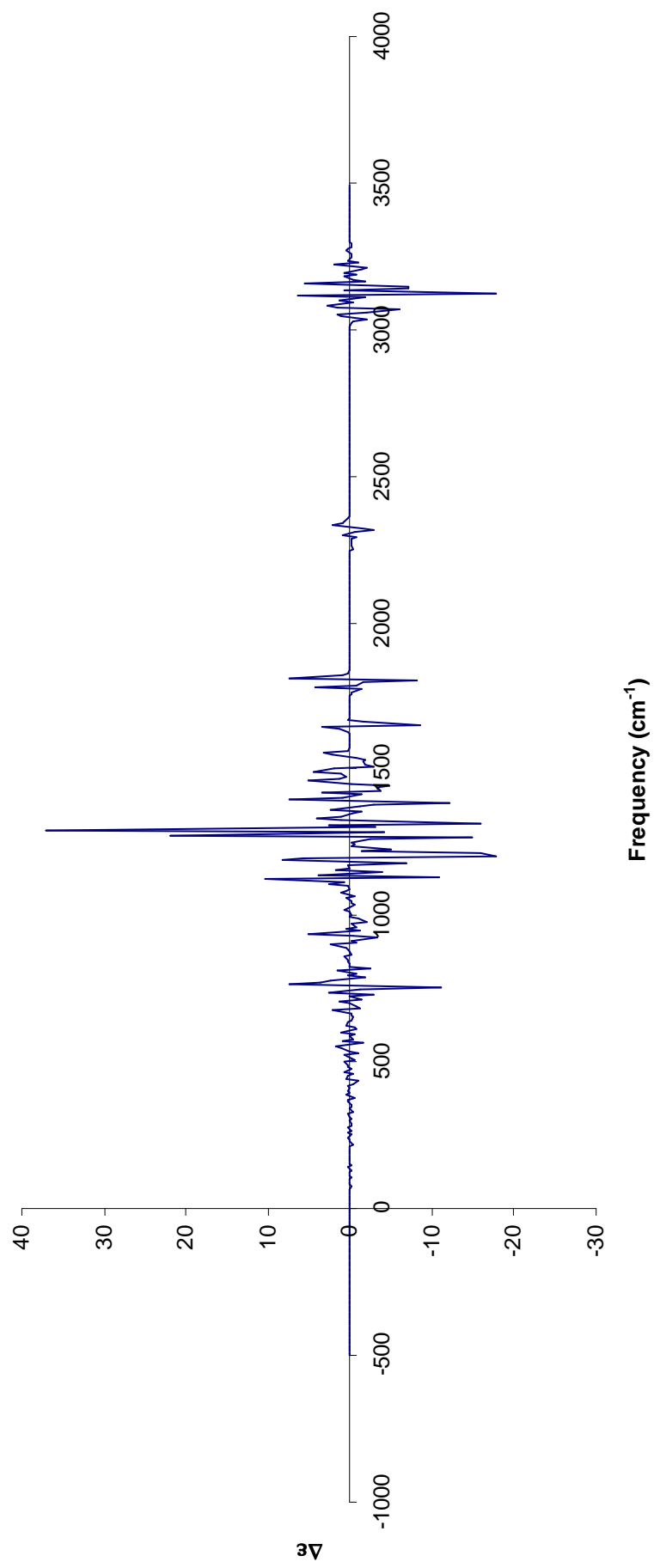


¹⁵N-, ¹H-, HMQC Spectrum; (429)

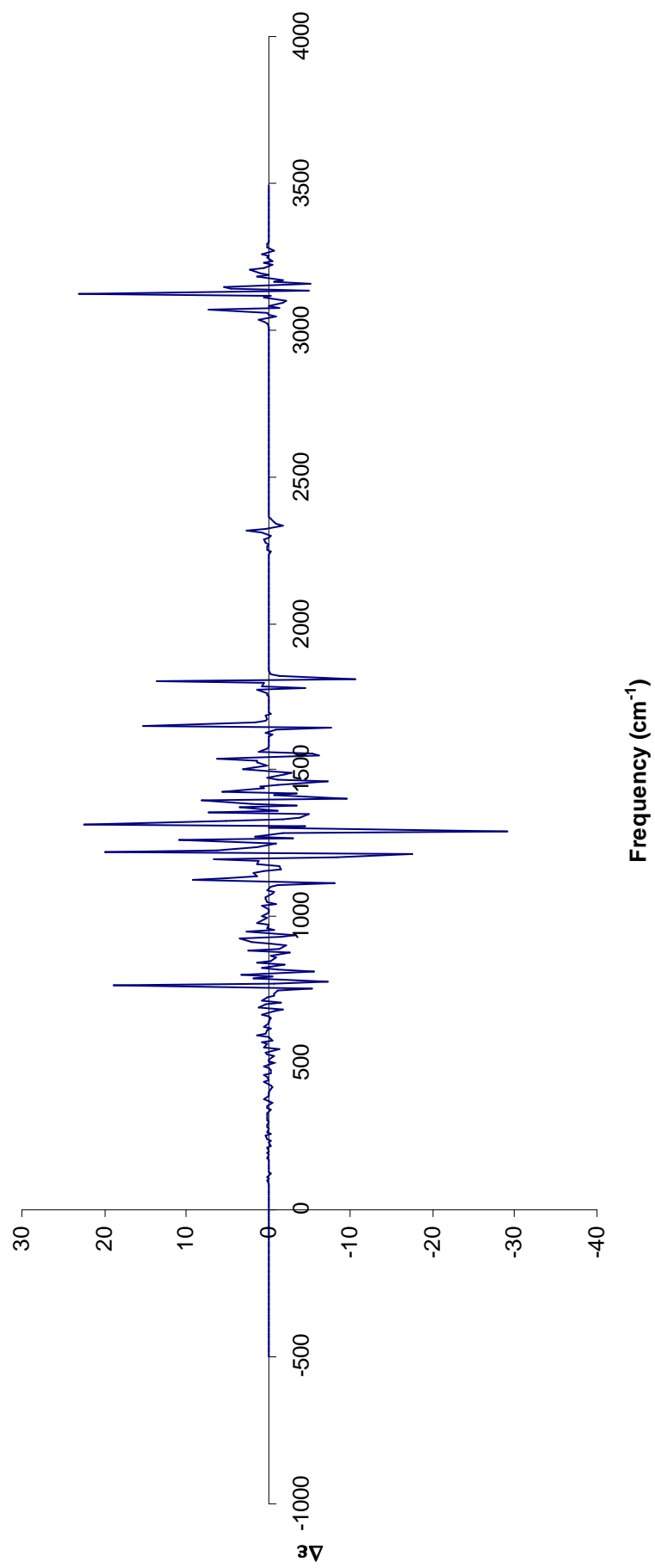
9.10.9: Appendix 9: VCD predictions for both *cis*-enantiomers of compounds *cis*-(351) and *cis*-(358); and sample Gaussian Input File for *cis*-(351), Conformer 1



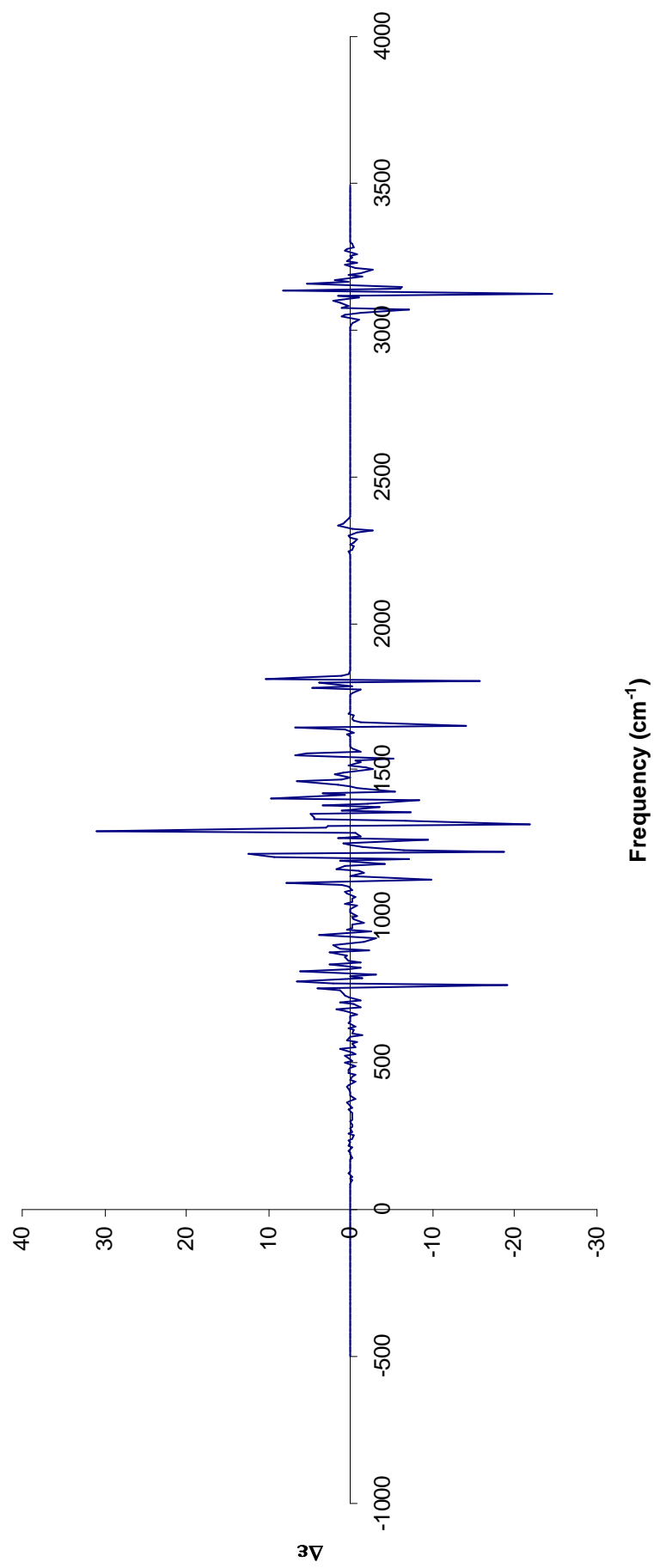
Weighted Average VCD Based On Boltzmann Distribution For 2R,3R-(351)



Calculated Weighted Average VCD Based On Boltzmann Distribution For 2S,3S-(358)



Calculated Weighted Average VCD Based On Boltzmann Distribution For 2*R*,3*R*-(358)



```

$Rungauss
%nproc=12
%chk=phenylenantiomer_conformer1.chk
#N b3lyp/6-31g* opt freq=(readiso,vcd) scf=tight test ginput

```

Phenyl Aziridine Enantiomer Conformer 1 With Frequency Check and VCD

```

0 1
C      -1.832498      0.738915      3.097539
C      -1.592311      0.781344      1.712424
C      -2.693858      0.983403      0.858557
C      -3.951254      1.295187      1.385180
C      -4.158266      1.290112      2.763333
C      -3.103103      0.992738      3.619560
N      -0.286726      0.535771      1.203732
C       0.850317      1.200190      1.860881
C       2.099262      0.384991      2.088907
C       2.046563     -0.973413      2.446310
C       3.209051     -1.716671      2.666809
C       4.455778     -1.112234      2.538003
C       4.538317      0.232429      2.189589
C       3.371960      0.970412      1.971059
O      -2.521234      1.025049     -0.500622
C      -2.886246     -0.167848     -1.236164
C      -2.259272     -1.458857     -0.687614
C       0.395783      1.601837      0.466182
C       1.273424      1.289453     -0.685169
O       2.087850      2.112375     -1.079835
O       1.073319      0.047005     -1.194386
C       1.941824     -0.478090     -2.227983
C       1.869786      0.354708     -3.512679
C       1.394977     -1.883253     -2.522604
C       3.381470     -0.612032     -1.718602
C      -2.335647      0.076991     -2.651019
C      -4.410140     -0.324995     -1.350885
H       0.597529      1.910977      2.643399
H      -0.165508      2.523344      0.369436
H       1.079339     -1.463454      2.544786
H       3.137023     -2.767104      2.935732
H       5.361410     -1.688598      2.706368
H       5.509027      0.709600      2.083235
H       3.458608      2.019437      1.692068
H      -4.774227      1.546724      0.723117
H      -5.142270      1.514678      3.166447
H      -3.263084      0.967885      4.694398
H      -1.022891      0.505617      3.784754
H      -2.479686     -2.313320     -1.337161
H      -2.639732     -1.699847      0.310777
H      -1.172495     -1.370749     -0.605314
H      -4.678377     -1.094069     -2.083817
H      -4.881069      0.617815     -1.650489
H      -4.856699     -0.622114     -0.396549
H      -2.534437     -0.766451     -3.320516
H      -1.255800      0.248502     -2.621779
H      -2.777313      0.979053     -3.090694
H       4.015391     -1.129755     -2.446453
H       3.409423     -1.170052     -0.776345
H       3.836439      0.362949     -1.519234
H       1.987413     -2.398966     -3.285612
H       0.355965     -1.833469     -2.867981
H       1.389129     -2.497432     -1.614431
H       2.393364     -0.141266     -4.337280
H       2.323980      1.341999     -3.387715
H       0.830420      0.522553     -3.813651

```


Bibliography

- (1) Krauss, L. M.; Scherrer, R. J.; *Scientific American*, *The End of Cosmology?*, 25th February 2008
- (2) McCracken, G.; Stott, P.; *Fusion*, 2nd ed., Academic Press: London, 2012.
- (3) Urey, H. C.; *Ind. Eng. Chem.*, **1933**, 26, 803 - 806.
- (4) Urey, H. C.; *Science*, **1933**, 78, 566 - 571.
- (5) Washburn, E. W.; Urey, H. C.; *Proc. N. A. S.*, **1932**, 496 - 498.
- (6) Lewis, G. N.; *J. Am. Chem. Soc.*, **1933**, 55, 1297 - 1298.
- (7) Urey, H. C.; Brickwedde, F. G.; Murphy, G. M.; *Science*, **1933**, 78, 602 - 603.
- (8) Urey, H. C.; Brickwedde, F. G.; Murphy, G. M.; *J. Chem. Phys.*, **1933**, 1, 512 - 513.
- (9) Urey, H. C.; Failla, G.; *Science*, **1935**, 273.
- (10) Waltham, C.; *An Early History of Heavy Water*, University of British Columbia, 1998.
(<http://cds.cern.ch/record/562098/files/0206076.pdf>).
- (11) Cohen, K.; *The Theory of Isotope Separation*, McGraw Hill: New York, 1951.
- (12) Ontario Power Generation, 'Bruce Heavy Water Plant Decommissioning', Canadian Nuclear Safety Commission, 2002.
http://www.globalsecurity.org/wmd/library/news/canada/01_e.pdf
- (13) NIST, *The NIST reference on Constants, Units, and Uncertainty*, 2011, (Accessed 7/7/2012), <http://physics.nist.gov/cgi-bin/cuu/Value?mmd>
- (14) Buckingham, A. D.; Fan-Chen, L.; *Int. Rev. Phys. Chem.*, **1981**, 1, 2153 - 2169.
- (15) Selwood, P. W.; Frost, A. A.; *J. Am. Chem. Soc.*, **1933**, 55, 4335 - 4336.
- (16) Lewis, G. N.; Macdonald, R. T.; *J. Am. Chem. Soc.*, **1933**, 55, 3057 - 3059.
- (17) Hardy, R. C.; Cottington, R. L.; *J. Chem. Phys.*, **1949**, 17, 509 - 510.
- (18) Claridge, T. D. W.; *High Resolution NMR Techniques in Organic Chemistry*, 2nd ed., Elsevier: Amsterdam, 2004.
- (19) Housecroft, C. E.; Constable, E. C.; *Chemistry*, 3rd ed.; Pearson Education Ltd: Harlow, 2006, p402.
- (20) Housecroft, C. E.; Constable, E. C.; *Chemistry*, 3rd ed.; Pearson Education Ltd: Harlow, 2006, p625.
- (21) Bell, R. P.; *Acids and Bases: Their Quantitative Behaviour*, Methuen: London, 1969.
- (22) Westheimer, F. H.; *Chem. Rev.*, **1960**, 61, 265 - 273.
- (23) Reitz, O.; *Z. Physik. Chem.*, **1939**, 184, 429.
- (24) Reitz, O.; *Z. Physik. Chem.*, **1936**, 176, 363.
- (25) Wynne-Jones, W. F. K.; *J. Chem. Phys.*, **1934**, 2, 381.
- (26) Trotman-Dickenson, A. F.; *Gas Kinetics*, Butterworths Scientific Publications: London, 1955.
- (27) Glad, S.; Jensen, F.; *J. Am. Chem. Soc.*, **1996**, 119, 227 - 232.
- (28) Davico, G. E.; Bierbaum, V. M.; *J. Am. Chem. Soc.*, **2000**, 122, 1740 - 1748.
- (29) Lee, I.; *Chem. Soc. Rev.*, **1995**, 223 - 229.
- (30) Poirier, R. A.; Wang, Y.; Westaway, K. C.; *J. Am. Chem. Soc.*, **1994**, 116, 2526 - 2533.
- (31) Boyd, R. J.; Kim, C.; Shi, Z.; Weinberg, N.; Wolfe, S.; *J. Am. Chem. Soc.*, **1993**, 115, 10147 - 10152.
- (32) Kim, C.; Wolfe, S.; *J. Am. Chem. Soc.*, **1991**, 113, 8056 - 8061.

- (33) Houk, K. N.; Gustafson, S. M.; Black, K. A.; *J. Am. Chem. Soc.*, **1992**, *114*, 8565 - 8572.
- (34) The range of deuterated synthesis materials available varies over time. However, the author has found Sigma-Aldrich to provide a range of deuterated materials as of the summer of 2010.
- (35) Coumbarides, G. S.; Dingjan, M.; Eames, J.; Flinn, A.; Northen, J.; *J. Label. Compd. Radiopharm.*, **2006**, *49*, 903 - 914.
- (36) Fournial, A.; Lebreton, J.; Mathe-Allainmat, M.; Ranaivondrambola, T.; Robins, R. J.; *Eur. J. Org. Chem.*, **2010**, 152 - 156.
- (37) Chapelle, M. R.; Kent, B. B.; Jones, J. R.; Shui-Yu, L.; Morgan, A. D.; *Tetrahedron. Lett.*, **2002**, *43*, 5117 - 5118.
- (38) Otley, K. D.; Saccomano, B. W.; McKee, S. A.; Nizialek, G. A.; Hamilton, D. S.; Sherrow, L. K.; Jones, C. Y.; Rosenstein, I. J.; *J. Label. Compd. Radiopharm.*, **2011**, *54*, 308 - 311.
- (39) Morgan, A. J.; Nguyen, S.; Uttamsingh, V.; Bridson, G.; Harbeson, S.; Tung, R.; Masse, C. E.; *J. Label. Compd. Radiopharm.*, **2011**, *54*, 613 - 624.
- (40) Li, S.; Pang, J.; Schroepfer, G. J.; Wilson, W. K.; *J. Label. Compd. Radiopharm.*, **1999**, *42*, 815 - 826.
- (41) Hawes, E. M.; Midha, K. K.; Mohannad, T.; *J. Label. Compd. Radiopharm.*, **1987**, *25*, 416.
- (42) Kelly, N. M.; Sutherland, A.; Willis, C. L.; *Nat. Prod. Rep.*, **1997**, 205 - 219.
- (43) Al-Qahtani, M. H.; Cleator, N.; Danks, T. N.; Garman, R. N.; Jones, J. R.; Stefaniak, S.; Morgan, A. D.; Simmonds, A. J.; *J. Chem. Res.*, **1998**, 400 - 401.
- (44) Kadai, T.; Werstiuk, N. H.; *Can. J. Chem.*, **1973**, *51*, 1485 - 1486.
- (45) Timmins, G.; Werstiuk, N. H.; *Can. J. Chem.*, **1981**, *59*, 3218 - 3219.
- (46) Kadai, T.; Werstiuk, N. H.; *Can. J. Chem.*, **1973**, *52*, 2169 - 2171.
- (47) Timmins, G.; Werstiuk, N. H.; *Can. J. Chem.*, **1984**, *63*, 530 - 533.
- (48) Baba, S.; Furuta, T.; Kasuya, Y.; Sasaki, Y.; *J. Label. Compd. Radiopharm.*, **1984**, *22*, 149 - 158.
- (49) Baba, S.; Sasaki, Y.; *Radioisotopes*, **1987**, *36*, 628 - 632.
- (50) Garnett, J. L.; Long, M. A.; Vining, R. F. W.; *J. Chem. Soc. Perkin. Trans. II*, **1975**, 1298 - 1303.
- (51) Garnett, J. L.; Long, M. A.; Vining, R. F. W.; *Tetrahedron. Lett.*, **1976**, *17*, 4531 - 4534.
- (52) Rasku, S.; Wahala, K.; *J. Label. Compd. Radiopharm.*, **2000**, *43*, 849 - 854.
- (53) Brewer, J. R.; Jones, J. R.; Lawrie, K. W. M.; Saunders, D.; Simmonds, A.; *J. Label. Compd. Radiopharm.*, **1994**, *34*, 391 - 400.
- (54) Boix, C.; Poliakoff, M.; *Tetrahedron. Lett.*, **1999**, *40*, 4433 - 4436.
- (55) Junk, T.; Catallo, W. J.; *Chem. Soc. Rev.*, **1997**, *26*, 401 - 406.
- (56) Junk, T.; Catallo, W. J.; USPIO, Ed. US, 1998; Vol. 5830763.
- (57) Nakahara, T.; USPIO, Ed. US, 1998; Vol. 5733984.
- (58) Evilia, R. F.; Yao, J.; *J. Am. Chem. Soc.*, **1994**, *116*, 11229 - 11233.
- (59) Junk, T.; Catallo, W. J.; *Tetrahedron. Lett.*, **1996**, *37*, 3445 - 3448.
- (60) Arnett, E. M.; Kuhlmann, B.; Siskin, M.; *J. Org. Chem.*, **1994**, *59*, 3098 - 3101.
- (61) Kerler, B.; Pol, J.; Hartonen, K.; Soderstrom, M.; Koskela, H.; Reikkola, M.; *J. Supercrit. Fluids.*, **2007**, *39*, 381 - 388.
- (62) Lockley, W. J. S.; Heys, J. R.; *J. Label. Compd. Radiopharm.*, **2010**, *53*, 635 - 644.
- (63) Weitkamp, A. W.; *J. Catal.*, **1966**, *6*, 431 - 457.

- (64) Garnett, J. L.; Sollich-Baumgartner, W. A.; *J. Phys. Chem.*, **1964**, *68*, 3177 - 3183.
- (65) Sajiki, H.; Ito, N.; Esaki, H.; Maesawa, T.; Maegawa, T.; Hirota, K.; *Tetrahedron. Lett.*, **2005**, *46*, 6995 - 6998.
- (66) Garnett, J. L.; Sollich, W. A.; *Aust. J. Chem.*, **1965**, *18*, 993 - 1002.
- (67) Blomberg, M. R. A.; Siegbahn, P. E. M.; Svensson, M.; *J. Phys. Chem.*, **1993**, *97*, 2564 - 2570.
- (68) Moebius, G.; Schaaf, G.; Office, E. P., Ed. 1990.
- (69) Matsubara, S.; Oshima, K.; Yokota, Y.; *Chem. Lett.*, **2004**, *33*, 294 - 295.
- (70) Matsubara, S.; Oshima, K.; Yamamoto, M.; *Heterocycles*, **2006**, *67*, 353 - 359.
- (71) Yamamoto, M.; Yokota, Y.; Oshima, K.; Matsubara, S.; *Chem. Commun.* **2004**, 1714 - 1715.
- (72) Aoki, F.; Hattori, K.; Hirota, K.; Sajiki, H.; Yasunaga, K.; *Synlett.*, **2002**, 1149 - 1151.
- (73) Sajiki, H.; Aoki, F.; Esaki, H.; Kato, M.; Maegawa, T.; Monguchi, Y.; Umemura, M.; *Chem. Eur. J.*, **2007**, *13*, 4052 - 4063.
- (74) Sajiki, H.; Akashi, A.; Aoki, F.; Esaki, H.; Hirota, K.; Maegawa, T.; *Synlett.*, **2005**, *5*, 845 - 847.
- (75) Derdau, V.; Atzrodt, J.; *Synlett.*, **2006**, *12*, 1918 - 1922.
- (76) Derdau, V.; Atzrodt, J.; Zimmermann, J.; Kroll, C.; Bruckner, F.; *Chem. Eur. J.*, **2009**, *15*, 10397 - 10404.
- (77) Sajiki, H.; Ito, N.; Maesawa, T.; Maegawa, T.; Watahiki, T.; *Adv. Synth. Catal.*, **2006**, *348*, 1025 - 1028.
- (78) Garnett, J. L.; Hodges, R. J.; *J. Am. Chem. Soc.*, **1967**, *89*, 4546 - 4547.
- (79) Garnett, J. L.; Hodges, R. J.; *J. Chem. Soc. Chem. Commun.*, **1967**, 1001 - 1003.
- (80) Garnett, J. L.; Long, M. A.; McLaren, A. B.; Peterson, K. B.; *J. Chem. Soc. Chem. Commun.*, **1973**, 749.
- (81) Golden, J. T.; Andersen, R. A.; Bergman, R. G.; *J. Am. Chem. Soc.*, **2001**, *123*, 5837 - 5838.
- (82) Bergman, R. G.; Klei, S. R.; Tilley, D.; *Organometallics*, **2002**, *21*, 4905 - 4911.
- (83) Bergman, R. G.; Skaddan, M. B.; Yung, C. M.; *Org. Lett.*, **2004**, *6*, 11 - 13.
- (84) Bergman, R. G.; Klei, S. R.; Golden, J. T.; Burger, P.; *J. Mol. Catal. A: Chem.*, **2002**, *189*, 79 - 94.
- (85) Peris, E.; Corberan, R.; Sanau, M.; *J. Am. Chem. Soc.*, **2006**, *128*, 3974 - 3979.
- (86) Salter, R.; *J. Label. Compd. Radiopharm.*, **2010**, *53*, 645 - 657.
- (87) Heys, J. R.; *Chem. Commun.*, **1992**, 680 - 681.
- (88) Heys, J. R.; Shu, A. Y. L.; Senderoff, S. G.; Phillips, N. M.; *J. Label. Compd. Radiopharm.*, **1993**, *33*, 431 - 438.
- (89) Crabtree, R. H.; Davis, M. W.; *J. Org. Chem.*, **1986**, *51*, 2655 - 2661.
- (90) Hesk, D.; Das, P. R.; Evans, B.; *J. Label. Compd. Radiopharm.*, **1995**, *36*, 497 - 502.
- (91) Heys, J. R.; Shu, A. Y. L.; Chen, W.; *J. Organometallic Chem.*, **1996**, *524*, 87 - 93.
- (92) Lockley, W. J. S.; *Tetrahedron. Lett.*, **2004**, *45*, 8621 - 8624.
- (93) Kerr, W. J.; Brown, J. A.; Irvine, S.; Kennedy, A. R.; Andersson, S.; Nilsson, G. N.; *Chem. Commun.*, **2008**, 1115 - 1117.
- (94) Powell, M. E.; Elmore, C. S.; Dorff, P. N.; Heys, R. J.; *J. Label. Compd. Radiopharm.*, **2007**, *50*, 523 - 525.

- (95) Kerr, W. J.; Nilsson, G. N.; *J. Label. Compd. Radiopharm.*, **2010**, *53*, 662 - 667.
- (96) Garnett, J. L.; Blake, M. R.; Gregor, I. K.; Hannan, W.; Hoa, K.; Long, M. A.; *J. Chem. Soc. Chem. Commun.*, **1975**, 930 - 932.
- (97) Lockley, W. J. S.; Hesk, D.; *J. Label. Compd. Radiopharm.*, **2010**, *53*, 704 - 715.
- (98) Otsuka, S.; Okano, T.; Saito, K.; Yoshida, T.; *Inorg. Chim. Acta.*, **1980**, *44*, L135 - L136.
- (99) Brookhart, M.; Lenges, C. P.; White, P. S.; *J. Am. Chem. Soc.*, **1999**, *121*, 4385 - 4396.
- (100) Regan, S.; *J. Org. Chem.*, **1974**, *39*, 260 - 261.
- (101) Bergman, R. G.; Bouwkamp, M. W.; Fulton, J. R.; Skienak, S.; *J. Am. Chem. Soc.*, **2002**, *124*, 4722 - 4737.
- (102) Choukroun, R.; Larsonneur, A.; *Organometallics*, **1993**, *12*, 3216 - 3224.
- (103) Jia, G.; Lam, W.; Lau, C.; Mak, C.; Ng, S.; Tsang, C.; *Organometallics*, **2003**, *22*, 641 - 651.
- (104) Jones, W. D.; Fan, M.; Perthulsot, C.; *Organometallics*, **1992**, *11*, 3622 - 3629.
- (105) Berry, D.H.; Carroll, P. J.; Djurovich, P. L.; *Organometallics*, **1994**, *13*, 2551 - 2553.
- (106) Gutsche, C. D.; *Calixarenes*; 2nd ed., RSC Publishing: Cambridge, 2008.
- (107) Mutlib, A. E.; Dickenson, P.; Chen, S.; Espina, R. J.; Daniels, J. S.; Gan, L.; *Chem. Res. Toxicol.*, **2002**, *15*, 1190 - 1207.
- (108) Mutlib, A. E.; Shockor, J.; Chen, S.; Espina, R.; Graciani, N.; Lin, J.; Prakash, S.; Gan, L.; *Drug. Metab. Dispos.*, **2000**, *29*, 1296 - 1306.
- (109) Mutlib, A. E.; Shockor, J.; Chen, S.; Espina, R.; Graciani, N.; Pinto, D.; Orwatt, M.; Prakash, S.; Gan, L.; *Chem. Res. Toxicol.*, **2002**, *15*, 48 - 62.
- (110) Mutlib, A. E.; Shockor, J.; Chen, S.; Espina, R.; Graciani, N.; Prakash, S.; *Chem. Res. Toxicol.*, **2002**, *15*, 63 - 75.
- (111) Wise, R.; Andrews, J. M.; *Antimicrobial Agents and Chemotherapy* **1984**, *25*, 612 - 617.
- (112) Jones, A. D.; Silverman, I. R.; Zelle, R. E.; WIPO, Ed. 2009.
- (113) Yarnell, A.; *Science & Technology*, 2009; Vol. 87, p 36 - 39.
- (114) Shao, L.; Abolin, C.; Hewitt, M. C.; Koch, P.; Varney, M.; *Med. Chem. Lett.*, **2006**, *16*, 691 - 694.
- (115) Bold, G.; *et al.*, *J. Med. Chem.*, **1998**, *41*, 3387 - 3401.
- (116) Zeldin, R.; Petruschke, R.; *J. Antimicrob. Chemother.*, **2004**, *53*, 4 - 9.
- (117) Harbeson, S.; WIPO, Ed. 2008.
- (118) Ghosh, A. K.; Dawson, Z.; Mitsuya, H.; *Bioorg. Med. Chem.*, **2007**, *15*, 7576 - 7580.
- (119) Armarego, W. L. F.; Li Lin Chai, C.; *Purification of Laboratory Chemicals*; 6th ed.; Butterworth-Heinemann: Oxford, 2009.
- (120) Hajos, Z. G.; Parrish, D. R.; *J. Org. Chem.*, **1973**, *39*, 1615 - 1621.
- (121) Houk, K. N.; Liu, J.; DeMello, N. C.; Condroski, K. R.; *J. Am. Chem. Soc.*, **1997**, *119*, 10147 - 10152.
- (122) Shi, Y.; Tu, Y.; Wang, Z.; *J. Am. Chem. Soc.*, **1996**, *118*, 9806 - 9807.
- (123) Yang, D.; Yip, Y.; Tang, M.; Wong, M.; Zheng, J.; Cheung, K.; *J. Am. Chem. Soc.*, **1996**, *118*, 491 - 492.
- (124) Denmark, S.; Wu, Z.; Crudden, C.; Matsushashi, H.; *J. Org. Chem.*, **1997**, *62*, 8288 - 8289.
- (125) Corey, E. J.; Grogan, M. J.; *Org. Lett.*, **1999**, *1*, 157.
- (126) Jacobsen, E. N.; Sigman, M. S.; *J. Am. Chem. Soc.*, **1998**, *120*, 4901 - 4902.

- (127) List, B.; Barbas, C. F.; Lerner, R. A.; *J. Am. Chem. Soc.*, **2000**, *122*, 2395 - 2396.
- (128) Ahrendt, K. A.; Borths, C. J.; MacMillan, D. W. C.; *J. Am. Chem. Soc.*, **2000**, *122*, 4243 - 4244.
- (129) Bahmanyar, S.; Houk, K. N.; Martin, H. J.; List, B.; *J. Am. Chem. Soc.*, **2003**, *125*.
- (130) Danishefski, S.; Cain, P.; *J. Am. Chem. Soc.*, **1976**, *98*, 4975 - 4984.
- (131) Agami, C.; Meyner, F.; Pascard, C.; *Tetrahedron*, **1984**, *40*, 1031 - 1038.
- (132) List, B.; Hoang, L.; Martin, H. J.; *Proc. Natl. Acad. Sci. U.S.A.*, **2004**, *101*, 5839 - 5842.
- (133) Houk, K. N.; Clemente, F. R.; *Angew. Chem. Int. Ed.*, **2004**, *43*, 5766 - 5768.
- (134) Houk, K. N.; Clemente, F. R.; *J. Am. Chem. Soc.*, **2005**, *127*, 11294 - 11302.
- (135) Kolb, H.; VanNieuwenhze, M.; Sharpless, K. B.; *Chem. Rev.*, **1994**, *94*, 2483 - 2547.
- (136) Notz, W.; List, B.; *J. Am. Chem. Soc.*, **2000**, *122*, 7386 - 7387.
- (137) Mahrwald, R.; Scheffler, U.; *Synlett.*, **2011**, *12*, 1660 - 1667.
- (138) Trost, B. M.; Brindle, C. S.; *Chem. Soc. Rev.*, **2010**, *39*, 1600 - 1632.
- (139) Zhao, C.; Bhanushali, M.; *Synlett.*, **2011**, *12*, 1815 - 1830.
- (140) Peng, L.; Zhang, T.; Zhang, F.; Mei, T.; Li, Y.; Li, Y.; *Tetrahedron. Lett.*, **2003**, *44*, 5107 - 5108.
- (141) Shan, Z.; Zhou, Y.; *J. Org. Chem.*, **2006**, *71*, 9510 - 9512.
- (142) Benaglia, M.; Celentano, G.; Cozzi, F.; *Adv. Synth. Catal.*, **2001**, *343*, 171 - 173.
- (143) Benaglia, M.; Cinquini, M.; Cozzi, F.; Puglisi, A.; Celentano, G.; *Adv. Synth. Catal.*, **2002**, *344*, 533 - 542.
- (144) Samanta, S.; Liu, J.; Dodda, R.; Zhao, C.; *Org. Lett.*, **2005**, *7*, 5321 - 5323.
- (145) Kano, T.; Takai, J.; Tokuda, O.; Maruoka, K.; *Angew. Chem. Int. Ed.*, **2005**, *44*, 3055 - 3057.
- (146) Kano, T.; Tokuda, O.; Maruoka, K.; *Tetrahedron. Lett.*, **2006**, *47*, 7423 - 7426.
- (147) List, B.; *J. Am. Chem. Soc.*, **2000**, *122*, 9336 - 9337.
- (148) List, B.; Pojarliev, P.; Biller, W.; Martin, H.; *J. Am. Chem. Soc.*, **2002**, *124*, 827 - 833.
- (149) Notz, W.; Tanaka, F.; Watanabe, S.; Chowdarj, N.; Turner, J.; Thayumanavan, R.; Barbas, C.; *J. Org. Chem.*, **2003**, *68*, 9624 - 9634.
- (150) Bøgevig, A.; Juhl, K.; Kumaragurubaran, N.; Zhuang, W.; Jørgensen, K. A.; *Angew. Chem. Int. Ed.*, **2002**, *41*, 1790 - 1793.
- (151) Kim, S.; Park, T.; Kim, B.; *Tetrahedron. Lett.*, **2006**, *47*, 6369 - 6372.
- (152) Hiyama, T.; Shimizu, M.; *Angew. Chem. Int. Ed.*, **2005**, *44*, 214 - 231.
- (153) Beeson, T.; MacMillan, D. W. C.; *J. Am. Chem. Soc.*, **2005**, *127*, 8826 - 8828.
- (154) Yuan, W.; Munoz, B.; Wong, C.; *J. Med. Chem.*, **1993**, *36*, 211 - 220.
- (155) Marigo, M.; Wabnitz, T. C.; Fielenback, D.; Jørgensen, K. A.; *Angew. Chem. Int. Ed.*, **2005**, *44*, 794 - 797.
- (156) Marigo, M.; Jørgensen, K. A.; *Chem. Commun.*, **2006**, *19*, 2001 - 2011.
- (157) Kinsman, A. C.; Kerr, M. A.; *J. Am. Chem. Soc.*, **2003**, *125*, 14120 - 14125.
- (158) Benaglia, M.; Celentano, G.; Cinquini, M.; Puglisi, A.; Cozzi, F.; *Adv. Synth. Catal.*, **2002**, *344*, 149 - 152.
- (159) Chu, Q.; Zhang, W.; Curran, D. P.; *Tetrahedron. Lett.*, **2006**, *47*, 9287.
- (160) Kano, T.; Tanaka, Y.; Maruoka, K.; *Org. Lett.*, **2006**, *8*, 2687 - 2689.

- (161) Yamaguchi, M.; Yokota, N.; Minami, T.; *J. Chem. Soc. Chem. Commun.*, **1991**, 1088 - 1089.
- (162) Holland, N.; Aburel, P. S.; Jørgensen, K. A.; *Angew. Chem. Int. Ed.*, **2003**, *42*, 661 - 664.
- (163) Brandau, S.; Landri, A.; Franzen, J.; Marigo, M.; Jørgensen, K. A.; *Angew. Chem. Int. Ed.*, **2006**, *45*, 4305 - 4309.
- (164) Bertelsen, S.; Diner, P.; Johansen, R. L.; Jørgensen, K. A.; *J. Am. Chem. Soc.*, **2007**, *129*, 1536 - 1537.
- (165) Diner, P.; Nielsen, M.; Marigo, M.; Jørgensen, K. A.; *Angew. Chem. Int. Ed.*, **2007**, *46*, 1983 - 1987.
- (166) Marigo, M.; Schulte, T.; Franzen, J.; Jørgensen, K. A.; *J. Am. Chem. Soc.*, **2005**, *127*, 15710 - 15711.
- (167) Yang, J. W.; Hechavarría Fonseca, M. T.; Vignola, N.; List, B.; *Angew. Chem. Int. Ed.*, **2005**, *44*, 108 - 110.
- (168) Erkkilä, A.; Majander, I.; Pihko, P. M.; *Chem. Rev.*, **2007**, *107*, 5416 - 5470.
- (169) Hine, J.; Linden, S.; Kanagasabapathy, V.; *J. Am. Chem. Soc.*, **1985**, *107*, 1082 - 1083.
- (170) Etter, M.; Lipkowska, Z.; Zia-Ebrahimi, M.; Pananto, T.; *J. Am. Chem. Soc.*, **1990**, *112*, 8415 - 8426.
- (171) Vachal, P.; Jacobsen, E.; *J. Am. Chem. Soc.*, **2002**, *124*, 10012 - 10014.
- (172) Wensel, A.; Lalonde, M.; Jacobsen, E. N.; *Synlett.*, **2003**, *12*, 1919 - 1922.
- (173) Wenzel, A. G.; Jacobsen, E. N.; *J. Am. Chem. Soc.*, **2002**, *124*, 12964 - 12965.
- (174) Yoon, T.; Jacobsen, E. N.; *Angew. Chem. Int. Ed.*, **2005**, *44*, 466 - 468.
- (175) Yoon, T.; Jacobsen, E. N.; *Science*, **2003**, *299*, 1691 - 1693.
- (176) Taylor, M.; Jacobsen, E. N.; *J. Am. Chem. Soc.*, **2004**, *126*, 10558 - 10559.
- (177) Fuerst, D.; Jacobsen, E. N.; *J. Am. Chem. Soc.*, **2005**, *127*, 8964 - 8965.
- (178) Joly, G.; Jacobsen, E. N.; *J. Am. Chem. Soc.*, **2004**, *126*, 4102 - 4103.
- (179) Beeson, T.; Mastracchio, A.; Hong, J.; Ashton, K.; MacMillan, D.; *Science*, **2007**, *316*, 582 - 585.
- (180) Beel, R.; Kobialka, S.; Schmidt, M.; Engeser, M.; *Chem. Commun.*, **2011**, *47*, 3293 - 3295.
- (181) Kim, H.; MacMillan, D.; *J. Am. Chem. Soc.*, **2008**, *130*, 398 - 399.
- (182) Jui, N.; Lee, C.; MacMillan, D.; *J. Am. Chem. Soc.*, **2010**, *132*.
- (183) Rendler, S.; MacMillan, D.; *J. Am. Chem. Soc.*, **2010**, *132*, 5027 - 5029.
- (184) Pham, P.; Ashton, K.; MacMillan, D.; *Chem. Sci.*, **2011**, *2*, 1470 - 1473.
- (185) Renaud, P.; Leong, P.; *Science*, **2008**, *322*, 55 - 56.
- (186) Mayer, S.; List, B.; *Angew. Chem. Int. Ed.*, **2006**, *45*, 4193 - 4195.
- (187) Mukherjee, S.; List, B.; *J. Am. Chem. Soc.*, **2007**, *129*, 11336 - 11337.
- (188) Raheem, I.; Thiara, P.; Peterson, E.; Jacobsen, E.; *J. Am. Chem. Soc.*, **2007**, *129*, 13404 - 13405.
- (189) Knowles, R.; Lin, S.; Jacobsen, E.; *J. Am. Chem. Soc.*, **2010**, *132*, 5030 - 5032.
- (190) Akiyama, T.; Itoh, J.; Yokota, K.; Fuchibe, K.; *Angew. Chem. Int. Ed.*, **2004**, *43*, 1566 - 1568.
- (191) Uraguchi, D.; Terada, M.; *J. Am. Chem. Soc.*, **2004**, *126*, 5356 - 5357.
- (192) Gridnev, I.; Kouchi, M.; Sorimachi, K.; Terada, M.; *Tetrahedron. Lett.*, **2007**, *48*, 497 - 500.
- (193) Akiyama, T.; Tamura, Y.; Utoh, J.; Morita, H.; Fuchibe, K.; *Synlett.*, **2006**, 141 - 143.
- (194) Uraguchi, D.; Sorimachi, K.; Terada, M.; *J. Am. Chem. Soc.*, **2005**, *127*, 9360 - 9361.

- (195) Itoh, J.; Fuchibe, K.; Akiyama, T.; *Angew. Chem. Int. Ed.*, **2006**, *45*, 4796 - 4798.
- (196) Nakashima, D.; Yamamoto, H.; *J. Am. Chem. Soc.*, **2006**, *128*, 9626 - 9627.
- (197) Rueping, M.; Nachtsheim, B. J.; Ieawuswan, W.; Atodiresei, I.; *Angew. Chem. Int. Ed.*, **2011**, *50*, 6706 - 6720.
- (198) Jiao, P.; Nakashima, D.; Yamamoto, H.; *Angew. Chem. Int. Ed.*, **2008**, *47*, 2411 - 2413.
- (199) Simonsen, K. B.; Bayon, P.; Hazell, R. G.; Gothelf, K. V.; Jørgensen, K. A.; *J. Am. Chem. Soc.*, **1999**, *121*, 3845 - 3853.
- (200) Rueping, M.; Ieawsuwan, W.; Antonchick, A.; Nachtsheim, B.; *Angew. Chem. Int. Ed.*, **2007**, *46*, 2097 - 2100.
- (201) Cheon, C.; Yamamoto, H.; *J. Am. Chem. Soc.*, **2008**, *130*, 9246 - 9247.
- (202) Rueping, M.; Ieawsuwan, W.; Atodiresei, I.; Nachtsheim, B.; *Angew. Chem. Int. Ed.*, **2011**, *50*, 6706 - 6720.
- (203) Akaiyama, T.; *Chem. Rev.*, **2007**, *107*, 5744 - 5758.
- (204) Zamfir, A.; Schenker, S.; Freund, M.; Tsogoeva, S.; *Org. Biomol. Chem.*, **2010**, *8*, 5262 - 5276.
- (205) Garcia, P.; Lay, F.; Garcia, P.; Rabalakos, C.; List, B.; *Angew. Chem. Int. Ed.*, **2009**, *48*, 4363 - 4366.
- (206) Treskow, M.; Neudorfl, J.; Giernoth, R.; *Eur. J. Org. Chem.*, **2009**, 3693 - 3697.
- (207) Padawa, A.; *Comprehensive Heterocyclic Chemistry III*; Katritzky, A., Ed.; Pergamon: Oxford, 2008, p 2 - 97.
- (208) Nakagawa, H.; Sei, Y.; Yamaguchi, K.; Nagano, T.; Higuchi, T.; *J. Mol. Catal. A.*, **2004**, *219*, 221 - 226.
- (209) Sun, L.; Can-Ping, D.; Qin, J.; You, J.; Yang, M.; Yu, X.; *J. Mol. Catal. A.*, **2005**, *234*, 29 - 34.
- (210) Takagi, S.; Takahashi, E.; Miyamoto, T.; Sasaki, Y.; *Chem. Lett.*, **1986**, 1275 - 1278.
- (211) Sweeney, J. B.; *Chem. Soc. Rev.*, **2002**, *31*, 247 - 258.
- (212) Evans, D.; Faul, M.; Bilodeau, M.; *J. Org. Chem.*, **1991**, *56*, 6744 - 6746.
- (213) Evans, D.; Faul, M.; Bilodeau, M.; Anderson, B.; Barnes, D.; *J. Am. Chem. Soc.*, **1993**, *115*, 5328 - 5329.
- (214) Li, Z.; Conser, K.; Jacobsen, E.; *J. Am. Chem. Soc.*, **1993**, *115*, 5326 - 5327.
- (215) Stang, P.; *Chem. Rev.*, **1996**, *96*, 1123 - 1178.
- (216) Dauban, P.; Saniere, L.; Tarrade, A.; Dodd, R.; *J. Am. Chem. Soc.*, **2001**, *123*, 7707 - 7708.
- (217) Di Chenna, P.; Robert-Peillard, F.; Dauban, P.; Dodd, R.; *Org. Lett.*, **2004**, *6*, 4503 - 4505.
- (218) Cardillo, G.; Gentilucci, L.; Tomasini, C.; Castejon-Bordas, M.; *Tetrahedron Asymm.*, **1996**, *7*, 755 - 762.
- (219) Barros, T.; Matias, P.; Maycock, C.; Ventura, M. R.; *Org. Lett.*, **2003**, *5*, 4321 - 4323.
- (220) D'hooghe, M.; Hofkens, A.; De Kimpe, N.; *Tetrahedron. Lett.*, **2003**, *44*, 1137 - 1139.
- (221) Boukhris, S.; Souizi, A.; *Tetrahedron. Lett.*, **2003**, *44*, 3259 - 3261.
- (222) Concellon, J.; Bernad, P.; Forcen-Acebal, A.; Riego, E.; Garcia-Granda, S.; *J. Org. Chem.*, **2001**, *66*, 2764 - 2768.
- (223) Sweeney, J.; *Eur. J. Org. Chem.*, **2009**, 4911 - 4919.
- (224) Bew, S. P.; Carrington, R.; Hughes, D.; Liddle, J.; Pesce, P.; *Adv. Synth. Catal.*, **2009**, *16*, 2579 - 2588.
- (225) Ochiai, M.; Kitagawa, Y.; *J. Org. Chem.*, **1999**, *64*, 3181 - 3189.
- (226) Gennari, C.; Vulpetti, A.; Pain, G.; *Tetrahedron*, **1997**, *53*, 5909 - 5924.

- (227) Kattuboina, A.; Guigen, L.; *Tetrahedron Lett.*, **2008**, *49*, 1573 - 1577.
- (228) Sweeney, J.; Cantrill, A.; Drew, M.; McLaren, A.; Thobhani, S.; *Tetrahedron*, **2006**, *62*, 3694 - 3703.
- (229) Deyrup, J. A.; *J. Org. Chem.*, **1969**, *34*, 2724.
- (230) Wartski, L.; *J. Chem. Soc. Chem. Commun.*, **1977**, 602 - 603.
- (231) Rasmussen, K.; Jørgensen, K.; *J. Chem. Soc. Chem. Commun.*, **1995**, 1401 - 1402.
- (232) Casarrubios, L.; Perez, J. A.; Brookhart, M.; Templeton, J.; *J. Org. Chem.*, **1996**, *61*, 8358 - 8359.
- (233) Rasmussen, K.; Juhl, K.; Hazell, R.; Jørgensen, K.; *J. Chem. Soc. Perkin. Trans. II*, **1998**, 1347 - 1350.
- (234) Rasmussen, K.; Jørgensen, K.; *J. Chem. Soc. Perkin. Trans. I*, **1997**, 1287 - 1291.
- (235) Mazumdar, A.; Xue, Z.; Mayer, M.; *Synlett.*, **2007**, *13*, 2025 - 2028.
- (236) Juhl, K.; Hazell, R.; Jørgensen, K.; *J. Chem. Soc. Perkin. Trans. I*, **1999**, 2293 - 2297.
- (237) Antilla, J.; Wulff, W.; *J. Am. Chem. Soc.*, **1999**, *121*, 5099 - 5100.
- (238) Zhang, Y.; Lu, Z.; Wulff, W.; *Synlett.*, **2009**, *17*, 2715 - 2739.
- (239) Hu, G.; Huang, L.; Huang, R.; Wulff, W.; *J. Am. Chem. Soc.*, **2009**, *131*, 15615 - 15617.
- (240) Williams, A.; Johnston, J.; *J. Am. Chem. Soc.*, **2004**, *126*, 1612 - 1613.
- (241) Hashimoto, T.; Nakatsu, H.; Watanabe, S.; Maruoka, K.; *Org. Lett.*, **2010**, *12*, 1668 - 1671.
- (242) Bew, S. P.; Fairhurst, S.; Hughes, D.; Legentil, L.; Liddle, J.; Pesce, P.; Nigudkar, S.; Wilson, M.; *Org. Lett.*, **2009**, *11*, 4552 - 4555.
- (243) Hashimoto, T.; Uchiyama, N.; Maruoka, K.; *J. Am. Chem. Soc.*, **2008**, *130*, 14380 - 14381.
- (244) Hashimoto, T.; Maruoka, K.; *J. Am. Chem. Soc.*, **2007**, *129*, 10054 - 10055.
- (245) pK_a values calculated using the JChem pK_a Calculator add-on for Marvin.
- (246) Akiyama, T.; Suzuki, T.; Mori, K.; *Org. Lett.*, **2009**, *11*, 2445 - 2447.
- (247) Hashimoto, T.; Nakatsu, H.; Yamamoto, K.; Maruoka, K.; *J. Am. Chem. Soc.*, **2011**, *133*, 9730 - 9733.
- (248) Hu, E. X.; *Tetrahedron*, **2004**, 2701 - 2743.
- (249) McCoull, W.; Davis, F.; *Synthesis*, **2000**, 1347 - 1365.
- (250) Ham, G. E.; *J. Org. Chem.*, **1964**, *29*, 3052 - 3054.
- (251) Nenajdenko, V.; Karpov, A.; Balenkova, E.; *Tetrahedron Asymm.*, **2001**, *12*, 2517 - 2527.
- (252) Gini, F.; Del Moro, F.; Macchia, F.; Pineschi, M.; *Tetrahedron Lett.*, **2003**, *44*, 8559 - 8562.
- (253) Farras, J.; Ginesta, X.; Sutton, P.; Taltavull, J.; Egeler, F.; Romea, P.; Urpi, F.; Vilarrasa, J.; *Tetrahedron*, **2001**, *57*, 7665 - 7674.
- (254) Chandrasekhar, S.; Narsihmulu, C.; Shameem Sultana, S.; *Tetrahedron. Lett.*, **2002**, 7361 - 7363.
- (255) Saha, B.; Nandy, J.; Shukla, S.; Siddiqui, I.; Iqbal, J.; *J. Org. Chem.*, **2002**, *67*, 7858 - 7860.
- (256) National Library of Medicine, 2009, (<http://toxnet.nlm.nih.gov/cgi-bin/sis/search/a?dbs+hsdb:@term+@DOCNO+5387>), Accessed 09/08/2012.
- (257) Petra, D.; Karner, P.; Spek, A.; Schoemaker, H.; van Leeuwen, P.; *J. Org. Chem.*, **2000**, *65*, 3010 - 3017.
- (258) Wu, J.; Hou, X.; Dai, L.; *J. Org. Chem.*, **2000**, *65*, 1344 - 1348.
- (259) Sim, T.; Kang, S.; Lee, K.; Lee, W.; *J. Org. Chem.*, **2003**, *68*, 104 - 108.

- (260) Park, C.; Kim, M.; Sim, T.; Pyun, D.; Lee, C.; Choi, D.; Lee, W.; *J. Org. Chem.*, **2003**, *68*, 43 - 49
- (261) Satoh, T.; Matsue, R.; Fujii, T.; Morikawa, S.; *Tetrahedron*, **2001**, *57*, 3891 - 3898.
- (262) Hwang, G.; Chung, J.; Lee, W.; *Tetrahedron*, **1996**, *52*, 12111 - 12116.
- (263) Lim, Y.; Lee, W.; *Tetrahedron. Lett.*, **1995**, *36*, 8431 - 8434.
- (264) Greenfield, H.; *J. Org. Chem.*, **1964**, *29*, 3082 - 3084.
- (265) Davis, F.; Deng, J.; Zhang, Y.; Haltiwanger, R.; *Tetrahedron*, **2002**, *58*, 7135 - 7143.
- (266) Bansal, R. K.; *Heterocyclic Chemistry*; 3rd ed.; New Age International Publishers: New Dehli, **2005**.
- (267) Reich, H. J.; 'Bordwell pKa Table', **2011**, Accessed 09/08/2012, <http://www.chem.wisc.edu/areas/reich/pkatable/kacont.htm>
- (268) Pesce, P.; 'Organocatalytic methods towards the synthesis of chiral racemic, and chiral non-racemic C2,3-difunctionalised N-alkyl and N-arylaziridines', Thesis (PhD), University of East Anglia, **2005**
- (269) Davis, F. A.; Zhou, P.; *Tetrahedron. Lett.*, **1994**, *35*, 7525 - 7528.
- (270) Gupta, A.; Mukherjee, M.; Wulff, W.; *Org. Lett.*, **2011**, *13*, 5866 - 5869.
- (271) Chiral Technologies Europe will provide an application guide for the Chiralpak AD-H column on CD. Available at http://www.chiral.fr/application_guide.asp (As of 09/08/2012)
- (272) Topczewski, J.; Neighbors, J.; Weimer, D.; *J. Org. Chem.*, **2009**, *74*, 6965 - 6972.
- (273) Sigma-Aldrich, 'Sigma-Aldrich Microreactor Explorer Kit', **2012**, Accessed 09/08/2012, <http://www.sigmaaldrich.com/catalog/product/aldrich/19979?lang=en®ion=GB>
- (274) Baumann, M.; Baxendale, I.; Martin, L.; Ley, S.; *Tetrahedron*, **2009**, *65*, 6611 - 6625.
- (275) Carter, C.; Baxendale, I.; Lange, H.; Ley, S.; Goodes, J.; Gaunt, N.; Willkamp, B.; *Org. Proc. Res. Dev.*, **2010**, *14*, 393 - 404.
- (276) Jacobsen, N. E.; *NMR Spectroscopy Explained*; 1st ed.; John Wiley & Sons Inc.: Hoboken, **2007**.
- (277) Dougherty, D.; Anslyn, E.; *Modern Physical Organic Chemistry*; 1st ed.; University Science Books: Herndon, **2005**.
- (278) Reich, H.; 'Integration of Proton NMR Spectra', **2012**, University of Winsconsin, <http://www.chem.wisc.edu/areas/reich/nmr/05-hmr-01-integration.htm>
- (279) Schultz, A.; *Neutron Scattering*, 1 ed., Price, S., Ed., Academic Press: London, **1986**, p 339 - 365.
- (280) Diamond Light Source Ltd., *Diamond Light Source*, 2012, Accessed 10/07/2012, <http://www.diamond.ac.uk/>
- (281) Tsang, W.; Richard, J.; *J. Am. Chem. Soc.*, **2009**, *131*, 13952 - 13962.
- (282) Tagore, D.; Sprinz, I.; Fletcher, S.; Jayawickamarajah, J.; Hamilton, A.; *Angew. Chem. Int. Ed.*, **2006**, *46*, 223 - 225.
- (283) Bachera, D.; Title undecided, Thesis (PhD), University of East Anglia, **2013**
- (284) Pozzi, M.; Gawandi, V.; Fitzpatrick, P.; *Biochemistry*, **2009**, *48*, 12305 - 12313.
- (285) Bennett, D.; Kirby, G. W.; Moss, V. A.; *J. Chem. Soc. C.*, **1970**, 2049 - 2051.
- (286) Chikashita, H.; Miyazaki, M.; Itoh, K.; *J. Chem. Soc. Perkin. Trans. 1*, **1987**, 699 - 706.
- (287) Barnett, D.; Panigot, M.; Curley, R.; *Tetrahedron. Asymm.*, **2002**, *13*, 1893 - 1900.

- (288) Nuijens, T.; Cusan, C.; Kruijtzter, J.; Rijkers, D.; Liskamp, R.; Quaedflieg, P., *J. Org. Chem.*, **2009**, *74*, 5145 - 5150.
- (289) Tillman, A. L.; Ye, J.; Dixon, D.; *Chem. Commun.*, **2006**, *11*, 1191 - 1193.
- (290) Yadav, J.; Balanarsaiah, E.; Raghavendra, S.; Satyanarayana, M.; *Tetrahedron. Lett.*, **2006**, *47*, 4921 - 4924.
- (291) Wu, Y.; Limburg, D.; Wilkinson, D.; Vaal, M.; Hamilton, G.; *Tetrahedron Lett.*, **2000**, *41*, 2847 - 2849.
- (292) Park, D.; Park, J.; *Bull. Korean. Chem. Soc.*, **2009**, *30*, 230 - 232.
- (293) Filali, E.; Lloyd-Jones, G.; Sale, D.; *Synlett.*, **2009**, *2*, 205 - 208.
- (294) Buchwald, S.; Chae, J.; *J. Org. Chem.*, **2004**, *69*, 3336 - 3339.
- (295) Wu, J.; Sun, X.; Sun, W.; Ye, S.; *Synlett.*, **2006**, 2489 - 2491.
- (296) Kobayashi, N.; Atsuya, A.; Mack, J.; *Circular Dichroism and Magnetic Circular Dichroism for Organic Chemists*; 1st ed.; RSC Publishing: Cambridge, 2012.
- (297) A.; Nafie, L.; *Vibrational Optical Activity*, Wiley: EBook, 2011.
- (298) Foresman, J. B.; Frisch, A.; *Exploring Chemistry with Electronic Structure Methods*; 2nd ed.; Gaussian Inc: Pittsburgh, 1996.
- (299) Wavefun Ltd., Conformational Analysis, 2006, Accessed 10/07/2012, http://www.wavefun.com/support/sp_compfaq/Conf_FAQ.html
- (300) Nicewicz, D. A.; Brétéché, G.; Johnson, J. S.; *Organic Syntheses*, **2008**, *85*, 278.
- (301) Hodgson *et al*; *Chem. Eur. J.*, **2007**, *13*, 3470 – 3479.
- (302) Saegusa, T.; Ito, Y.; Shimizu, T.; Kobayashi, S.; *Bull. Chem. Soc. Japan.*, **1969**, *42*, 3535-3538.
- (303) Bordwell, F. G.; Bausch, M. J.; Cheng, J.; Cripe, T. H.; Lynch, T.; Mueller, M. E.; *J. Org. Chem.*, **1990**, *55*, 58 - 63.
- (304) Bernardi, L.; Bonini, B. F.; Capitò, E.; Dessole, G.; Fochi, M.; Comes-Franchini, M.; Ricci, A.; *Synlett*, **2003**, *12*, 1778 - 1782.
- (305) Griesbeck, A. G.; Bondock, S.; Cygon, P.; *J. Am. Chem. Soc.*, **2003**, *125*, 9016 - 9017.
- (306) Wipf, P.; Jung, J.; *J. Org. Chem.*, **2000**, *65*, 6319.